



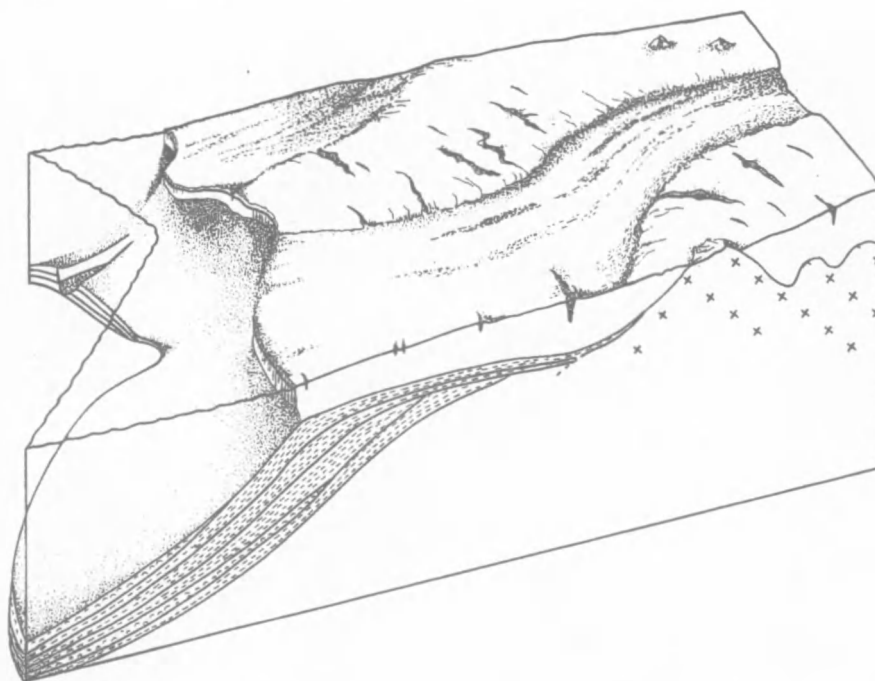
UNIVERSITEIT GENT

Faculteit Wetenschappen
Vakgroep Geologie en Bodemkunde

A comparative seismic stratigraphic study of major Plio-Pleistocene glaciogenic depocentres along the polar North Atlantic margins

**Vergelijkend seismostratigrafisch onderzoek van
grootschalige Plio-Pleistocene glacigene sedimentkegels
langs de randen van de polaire Noord-Atlantische Oceaan**

Kris Vanneste



Academiejaar 1994-1995

*Proefschrift voorgelegd voor het verkrijgen van de graad van
Doctor in de Wetenschappen (richting Geologie)*

*Promotor:
Prof. Jean-Pierre Henriët*



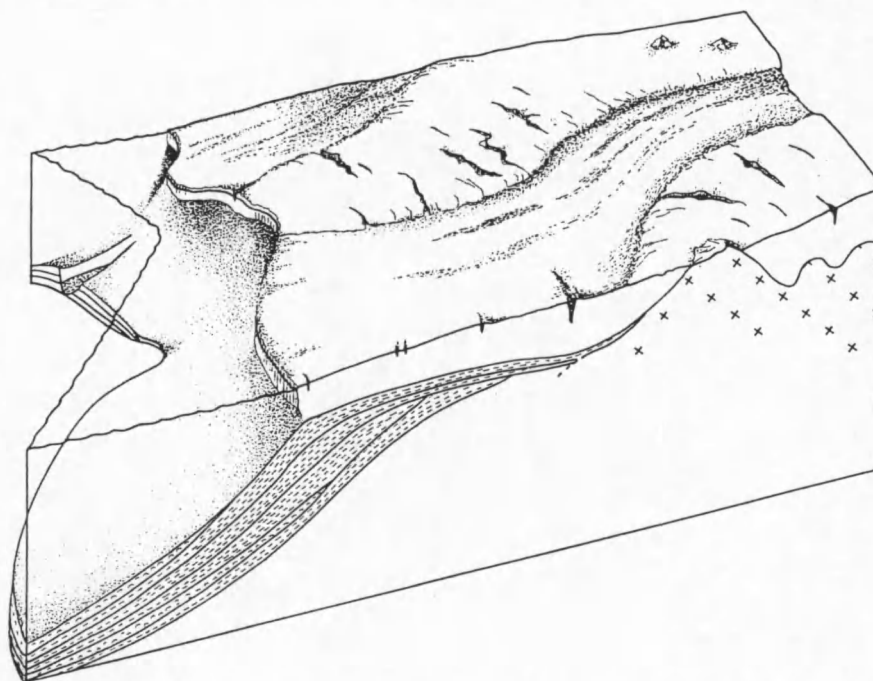
UNIVERSITEIT GENT

Faculteit Wetenschappen
Vakgroep Geologie en Bodemkunde

A comparative seismic stratigraphic study of major Plio-Pleistocene glaciogenic depocentres along the polar North Atlantic margins

Vergelijkend seismostratigrafisch onderzoek van
grootschalige Plio-Pleistocene glacigene sedimentkegels
langs de randen van de polaire Noord-Atlantische Oceaan

Kris Vanneste



Academiejaar 1994-1995

*Proefschrift voorgelegd voor het verkrijgen van de graad van
Doctor in de Wetenschappen (richting Geologie)*

*Promotor:
Prof. Jean-Pierre Henriët*

Thank You

[one] to express gratitude. 2. "to acknowledge", 3. to appreciate.
[4] To Be Thankful. [five] to give credit. "6". "to be grateful".
7. TO BE PLEASED WITH, 8. (to highly estimate). [9] to enjoy.
[ten] to cherish. 11. to appraise. twelve, TO BE INDEBTED.

In retrospect to these past five years of scientific research, I wish to express my earnest gratefulness to the following persons and institutions, without the dedication of whom this study would not have appeared in its present shape:

Prof. Jean-Pierre Henriët *FOR LAUNCHING ME INTO AN INTERNATIONAL PROJECT,
PROFESSIONAL MANAGEMENT, MOTIVATION AND SUPERVISION*

Ad INTERIM PROMOTORSHIP **Prof. Robert Maréchal**
& **Prof. William De Breuck**

FUNDING ME 4 YEARS AS RESEARCH ASSISTANT **Belgian National Fund for
Scientific Research (N.F.W.O.)**

Dr. Marc De Batist *CLOSE follow-up, CRITICAL READING AND DISCUSSION,
HELPFUL SUGGESTIONS, AND MANAGEMENT*

**Alfred Wegener Institut
Marine Geophysik Kiel
Norwegian Petroleum Directorate** *KIND RELEASE AND/OR SHARING OF DATA*

*FRUITFUL CO-OPERATION, CRITICAL READING,
AND OVERSEAS follow-up* **Prof. Jan Inge Faleide**
& **Dr. Anders Solheim**

Dr. Friedrich Theilen *FOR OPEN-MINDED CO-OPERATION,
AND HOSTING ME 1 YEAR AT THE INSTITUT FÜR GEOPHYSIK*

*FOR HIS ENTHUSIASTIC
CO-ORDINATION OF THE PONAM PROJECT* **Prof. Anders Elverhøi**

Prof. Heinz Miller *FOR MANY YEARS OF EXCELLENT CO-OPERATION, AND
SKILLFUL LEADING OF THE ARK-VIII/3b AND ANT-XII/3 SURVEYS*

*ADDITIONAL DATA PROCESSING
AND INTERESTING DISCUSSIONS* **Dagmar Matuschke**
& **Dr. Gabriele Uenzelmann-Neben**

**Berit Oline Hjelstuen
& Anne Fiedler** *FOR PLEASANT CO-OPERATION
AND SUPPLY OF INDISPENSABLE LITERATURE*

MINUTE DIGITISATION OF INTERPRETED SECTIONS **Anthony De Vos**

Jens Mouridsen *DATA PROCESSING ASSISTANCE
AND INITIAL INTERPRETATION OF SCORESBY SOUND DATA*

**Renard Centre
of Marine Geology**

EXTENSIVE logistical support

Additional printing facilities

Prof. Patric Jacobs & Erwin Sevens

Martien Bogaert

*ARTWORK, drawing ASSISTANCE,
AND MANY HOURS of dedicated WORKING OVERTIME*

*COMPUTER facilities
during MILITARY SERVICE*

**Beheerseenheid Mathematisch Model
Noordzee en Schelde-estuarium**

**Philip Bart
Lene Clausen
Dr. Berit Kuvaas
Dr. Jan Sverre Laberg
Pieter Van Rensbergen
Dr. Robert Whittington**

STIMULATING AND RELEVANT discussions

HARD- & SOFTWARE PROBLEM SOLVERS

Eric Maes & Wim Versteeg

DATA ACQUISITION ASSISTANCE

Erwin Van Heuverswyn

Bart De Corte

ADDITIONAL TRACKING of LITERATURE

*EFFICIENT AND MOTIVATED help
during SEVERAL SEISMIC SURVEYS*

**Captain and crew of research vessels
Polarstern, Belgica, Håkon Mosby, Poseidon**

**Everybody else at RCMG
(Annemie, Jean, Mark,
Pieter, Théo, Tine, Tom),
and former colleagues in Kiel
(Andreas, Ingo, Jörg, Lotte,
Sönke, Stefan, Wiho, ...)**

*FOR A PLEASANT WORKING ATMOSPHERE
THROUGHOUT THE PAST FIVE YEARS*

And the numerous persons I undoubtedly forgot ...

Gent, June 28th 1995,

Kris Nannede

Table of contents

NEDERLANDSE SAMENVATTING (DUTCH SUMMARY)

1. Inleiding	1
2. Scoresby Sund, centraal Oost-Groenland	3
Inleiding	3
Geologie van het substraat	3
Glaciale evolutie in Scoresby Sund	4
Sedimentaire opbouw en glaciatiegeschiedenis van de continentale shelf en helling	5
3. De westelijke rand van de Barents Zee t.h.v. Bereneiland Trog	7
Introductie	7
Structurele situering	8
Algemene stratigrafie	8
Gedetailleerd seismostratigrafisch onderzoek	9
Glaciale evolutie	11
4. Conclusie: de glaciale randen met elkaar vergeleken	13
Glaciale evolutie van de polaire Noord-Atlantische Oceaan	13
Naar een sequentiestratigrafisch model voor glaciale randen?	14
Toekomstperspectieven	16

CHAPTER I : SEDIMENTATION ALONG GLACIAL CONTINENTAL MARGINS

1. Glacial continental margins: definition and general characterisation	17
1.1. Definition	17
1.2. Physiographic characterisation	17
1.2.1. The continental shelf	17
1.2.2. The continental slope	19
2. Sedimentation processes acting on a glacial margin	21
2.1. Deposition by the direct action of ice	21
2.2. Other sedimentation mechanisms	23
2.3. Secondary sedimentation processes	24
3. Models for sedimentation along glacial continental margins	25
3.1. Limitations of the sequence stratigraphic model	25

3.2. A discussion of glacial sequence stratigraphic models	28
3.2.1. Model proposed by Larter & Barker (1989, 1991).....	28
3.2.2. Model proposed by Vorren et al. (1989).....	28
3.2.3. Model proposed by Boulton (1990).....	30
3.2.4. Model proposed by Kuvaas & Kristoffersen (1991).....	30
4. Recognising glacial sequences on low-resolution seismic records	34
5. This work's objectives	34
References cited	36

CHAPTER II : SEISMIC INVESTIGATION OF THE SCORESBY SUND FJORD SYSTEM AND THE ADJACENT CENTRAL EAST GREENLAND SHELF

1. Introduction	39
1.1. History of exploration.....	39
1.2. The ARK VII/3b expedition	39
1.3. Objectives	40
2. Data acquisition and processing	41
2.1. Data acquisition	41
2.2. The data set.....	41
[1] Shelf lines	42
[2] Scoresby Sund lines.....	42
[3] Higher-resolution lines	42
2.3. Data processing.....	47
3. Physiography of Scoresby Sund and the East Greenland shelf.....	50
3.1. The East Greenland continental shelf	50
3.2. The Scoresby Sund region	52
3.2.1. Topography and bathymetry	52
3.2.2. Ice cover.....	52
3.2.3. Water circulation.....	54
4. Geological evolution of Scoresby Sund and the East Greenland margin.....	55
4.1. Pre-glacial development of the Scoresby Sund region	55
4.1.1. Structural setting.....	55
[1] Tectonic window complexes	56
[2] Vestfjord - Hinks Land gneiss and schist zone	56
[3] Gåsefjord - Stauning Alper migmatite and granite zone.....	56
[4] the post-Caledonian sedimentary Jameson Land basin	56
[5] Liverpool Land - Canning Land	56
[6] Geikie Plateau	56
4.1.2. Geological history	58
Precambrian.....	58
Caledonian orogeny	58
Late Paleozoic - Mesozoic	59
Tertiary.....	59
Quaternary.....	60

4.2. Geology of the East Greenland shelf.....	60
4.2.1. The South-eastern Shelf (SEAS)	65
4.2.2. The Denmark Strait Ridge (Danmarks Stræde High).....	66
4.2.3. The Blossville Kyst Shelf (BLKS).....	66
4.2.4. The Liverpool Land Shelf (LILS)	67
4.2.5. The North-east Greenland Shelf (NEAS).....	69
4.3. Glacial history of Greenland and Scoresby Sund	69
4.3.1. Tertiary climatic deterioration	69
Paleogene	69
Neogene.....	71
4.3.2. Plio-Pleistocene development of the Greenland ice sheet	71
4.3.3. The terrestrial record of Quaternary glaciations	74
Extensive ?Saalian glaciation (c. 200 - 133 ka BP).....	75
Eemian interglacial (c. 133 - 114 ka BP).....	75
Weichselian (114 - 10 ka BP).....	75
Holocene deglaciation (< 10,300 a BP)	78
Recent situation	78
5. Bedrock geology of Scoresby Sund	79
5.1. Location of the data.....	79
5.2. Bathymetry	79
5.3. Bedrock geology.....	81
5.3.1. Unit A — Mesozoic sediments of the Jameson Land Basin.....	81
5.3.2. Unit B — Middle Proterozoic and Caledonian migmatites.....	84
5.3.3. Unit C — Caledonian intrusives.....	85
5.3.4. Unit D — Plateau basalts ?.....	86
5.3.5. The western boundary of the Jameson Land basin	86
5.4. The combined reflection/refraction lines in the inner fjords	92
5.5. Conclusions	94
6. Quaternary glacially-influenced deposits in Scoresby Sund.....	95
6.1. General distribution of unlithified sediments in Hall Bredning.....	95
6.1.1. Identification.....	95
6.1.2. Sediment distribution and origin	96
6.1.3. Glacial history.....	100
6.2. Glacial sediments in Vikingebugt — a small case study	101
6.2.1. Bathymetry and basement topography	101
6.2.2. Sediments within Vikingebugt	103
6.2.3. Reconstruction of the glacial history.....	107
6.3. Conclusions	109
7. The central East Greenland shelf and slope off Scoresby Sund	110
7.1. Location of the seismic data	110
7.2. Morphology of shelf and slope.....	110
7.3. Acoustic basement.....	113
7.3.1. General characteristics	113
7.3.2. Pseudo-escarpment.....	115

7.4. Sediment stratigraphy	116
Unit I (sequence 1).....	118
Unit II (sequences 2 - 5).....	118
Unit III (sequences 6 - 11).....	120
Comparison with other seismic lines	121
7.5. Geological and glacial history	123
7.5.1. Pre-glacial development	123
7.5.2. Glacial evolution	124
7.6. Conclusions	128
References cited	129

CHAPTER III : SEISMIC INVESTIGATION OF THE WESTERN BARENTS SEA MARGIN OFF BEAR ISLAND TROUGH

1. Introduction	133
2. Data properties.....	134
3. Physiography of the western Barents Sea - Svalbard margin.....	137
3.1. Bathymetry of shelf and slope.....	137
3.2. Water circulation	142
3.3. Ice cover	143
4. Structural setting and geo-tectonical evolution	144
4.1. Main structural elements	144
4.1.1. Oceanic basins	144
4.1.2. Continental margin and ocean-continent transition	146
Senja Fracture Zone	146
Hornsund Fault Zone	146
Central fault segment and associated marginal high.....	147
Free-air gravity field	147
4.1.3. Continental shelf.....	148
Barents shelf	148
Svalbard Platform	148
4.2. Plate tectonic evolution	150
4.2.1. History prior to break-up	150
4.2.2. Opening of the Norwegian-Greenland Sea.....	151
4.2.2.1. Opening of the Norwegian Sea (54 - 51 Ma)	153
4.2.2.2. Opening of the southern Greenland Sea (51 - 36 Ma).....	153
4.2.2.3. Opening of the northern Greenland Sea (36 Ma - present).....	154
5. Seismic stratigraphy	156
5.1. The Cenozoic sedimentary wedge: general aspects	156
5.2. Review of existing stratigraphic work.....	158
5.2.1. The Barents Sea margin (70° - 75° N).....	158
High-resolution studies of the outer shelf	164
5.2.2. The Svalbard margin (75° - 79° N)	165
5.2.3. A regional stratigraphic framework (70° - 77° N).....	166

5.2.4. Age constraints	168
5.2.4.1. The basal unconformity R7.....	168
5.2.4.2. The prominent erosional unconformity R5	170
5.2.4.3. The upper regional unconformity R1	172
5.2.5. Link to geological history	173
5.3. A detailed seismic stratigraphy of the northern half of Bear Island Cone	174
5.3.1. Introductory notes	174
5.3.2. Acoustic basement reflector (r0)	178
Oceanic crust	178
Vestbakken volcanic province (VVP).....	180
Continental crust	181
5.3.3. Megasequence G0 (r0 - r8).....	181
5.3.3.1. General characteristics	181
5.3.3.2. Description of individual reflectors and units	182
5.3.4. Megasequence GI (r8 - r15).....	184
5.3.4.1. Basal unconformity r8.....	184
5.3.4.2. Thickness distribution and description	185
5.3.4.3. Summary of GI.....	187
5.3.5. Megasequence GII (r15 - r30)	188
5.3.5.1. Basal unconformity r15	188
5.3.5.2. Thickness distribution	188
5.3.5.3. General seismic facies characteristics	189
5.3.5.4. Description of individual reflectors and units	192
5.3.5.5. Summary of GII	197
5.3.6. Megasequence GIII (r30 - seafloor)	197
5.3.6.1. Basal unconformity r30	197
5.3.6.2. Thickness distribution	200
5.3.6.3. General seismic facies characteristics	201
5.3.6.4. Description of individual reflectors and units	201
5.3.6.5. Summary of GIII	204
6. Sediment remobilisation processes on the Bear Island Cone	206
6.1. Introduction	206
6.2. Submarine mass movements — a short overview	207
6.3. The slide scar at the GII/GIII boundary	215
6.4. Seismic evidence for mass wasting in megasequence GII.....	220
6.5. Mass wasting styles in megasequence GIII	227
6.6. Causes behind mass wasting.....	229
6.7. The Bear Island Cone: a submarine fan?	233
7. Glacial evolution.....	237
7.1. General outline	237
Glacial lead-in phase	239
Glacial phase 1 (2.6 - 1.2/1.0 Ma).....	239
Glacial phase 2 (1.2/1.0 - 0.6 Ma).....	239
Glacial phase 3 (0.6 Ma - present)	239

7.2. GI : initial glacial advances (2.6 - ~1.2 Ma)	241
7.3. GII : intensified glaciations (~1.2 - ~0.6 Ma)	242
7.4. GIII : modern glacial conditions (~0.6 Ma - present).....	244
7.5. Conclusions	250
References cited	251

CHAPTER IV :COMPARING THE SEISMIC REFLECTION GEOMETRIES ON THE DIFFERENT GLACIAL MARGINS

1. Introduction	259
2. Glacial evolution of the polar North Atlantic.....	259
Glacial phase 1	262
Glacial phase 2	262
Glacial phase 3	262
Origin of late Pleistocene aggradation.....	263
3. Towards a sequence stratigraphic model for glaciated margins ?	267
3.1. Outer shelf and upper slope geometries	267
3.2. Lower slope and continental rise geometries.....	269
3.3. A tentative cyclic depositional model for glaciated margins.....	274
4. Future research scopes.....	276
References cited	277

LIST OF FREQUENTLY USED ABBREVIATIONS	279
LIST OF TABLES.....	281
LIST OF FIGURES	283

Nederlandse samenvatting

1. Inleiding

Het onderwerp van deze verhandeling is te situeren langs de randen van het noordelijkste, polaire deel van de Noord-Atlantische Oceaan, waar tijdens de opeenvolgende Plio- en Pleistocene glaciaties grote hoeveelheden sediment werden afgezet. De verdeling van deze glaciogene sedimenten langs de continentale randen is niet gelijkmatig, maar focust zich in verschillende kegelvormige accumulatiecentra ter hoogte van de meest actieve uitlaatkleppen van de ijskappen. Aan de hand van reflectie-eismische gegevens met een intermediaire tot lage resolutie (verticaal gemiddeld niet beter dan 10 m) werd de interne structuur onderzocht van twee dergelijke depocentra, min of meer aan tegenover elkaar gelegen zijden van de polaire Noord-Atlantische Oceaan: de centrale rand van Oost-Groenland ter hoogte van Scoresby Sund in het westen, en de westelijke rand van de Barents Zee voor de monding van de Bereneiland Trog aan de oostzijde. Beide continentaalranden kunnen worden bestempeld als zgn. glaciële randen, d.w.z. continentale randen waarop zich meermaals in de recente geologische geschiedenis ijskappen hebben uitgebreid, soms zelfs tot aan de shelfrand¹. Terwijl de Groenlandse ijskap tot op heden is blijven bestaan op het continent, is de ijskap in de Barents Zee, een exclusief mariene ijskap die ontstaat uit de convergentie van ijskappen in Fennoscandia en op omgevende eilanden, helemaal verdwenen tijdens de huidige Holocene interglaciële periode.

Het jongste decennium heeft de sequentiestratigrafie, een model dat de sedimentatie op een continentaalrand beschrijft in functie van (relatieve) schommelingen van het zeeniveau, sterk bijgedragen tot een beter inzicht in de cyclische opbouw van deze randen. Glaciële continentaalranden verschillen echter op een aantal essentiële punten van hun tegenhangers op meer gematigde breedten, op basis waarvan het sequentiestratigrafisch model in de eerste plaats werd geformuleerd. Vooreerst wordt het sediment er niet aangevoerd door rivieren, maar door gletsjers en ijsstromen, die niet alleen gekenmerkt worden door totaal verschillende erosie- en afzettingsmechanismen, maar bovendien ook niet noodzakelijk, en zeker niet op dezelfde manier, beïnvloed worden door zeespiegelschommelingen. Overigens laat de buitengewone diepte (meestal groter dan 300 m aan de shelfrand, tegenover de normale waarde van ca. 120 m) waarin de meeste glaciële shelveën zich althans heden ten dage bevinden, niet toe dat eustatische zeespiegelschommelingen, met een maximale amplitude van 120 m, de sedimentatiepatronen zouden bepalen. Een tijdelijke emersie gepaard met de vorming van een subaërisch erosie-oppervlak is dan ook in de meeste gevallen uitgesloten, zeker tijdens de recentste glaciële cycli. Tenslotte heeft de zeespiegel ook weinig of geen invloed op de accommodatieruimte op de shelf: tijdens glaciaties wordt deze namelijk sterk ingeperkt, of zelfs tot nul herleid, door de aanwezigheid van een ijskap, terwijl er tijdens interglaciële periodes dan weer veel te weinig sediment wordt aangevoerd om de ontstane

¹ Eng. "shelf edge"; de reguliere vertaling "continentaal plat" voor het Engelse "continental shelf" wordt in deze tekst niet aangehouden, wegens de mindere geschiktheid bij samenstellingen.

ruimte op te vullen. De sedimentatie op een glaciële continentaalrand wordt dus voornamelijk bepaald door oscillaties van het ijsfront, en niet — tenzij indirect — door zeespiegelvariaties, zodat het sequentiestratigrafisch model hier niet van toepassing kan zijn.

Anderzijds is sedimentatie op een glaciële continentaalrand wel degelijk cyclisch van aard, ingevolge de cycliciteit die inherent is aan klimaatschommelingen. Eén van de grote uitdagingen bestaat er daarom in een alternatief, zgn. "glaciaal" sequentiestratigrafisch model te ontwikkelen, waarbij de verschillende fasen van afzetting in verband worden gebracht met de afwisselende uitbreiding en contractie van ijskappen. De voorbije jaren hebben onderzoekers reeds enkele modellen voorgesteld op basis van regionale studies van een aantal specifieke, doch alleenstaande voorbeelden. Hieruit blijkt dat de meeste glaciële randen gedomineerd worden door een uitgesproken progradiatie voor de monding van belangrijke glaciële troggen op de buiten-shelf. Er bestaat een algemene consensus dat deze tot stand komt tijdens uitgebreide vergletsjeringen van de shelf, wanneer het ijs tot aan de shelfrand in contact is met de zeebodem², al bestaan er uiteenlopende visies over het precieze afzettingsmechanisme (glaciomariën of subglaciaal) dat de progradiatie teweegbrengt; tijdens interglaciële periodes, wanneer het ijs zich terugtrekt tot binnen de grenzen van het continent, zou de shelf dan grotendeels van sediment verstoken blijven. Met betrekking tot de sedimentatie lager op de continentale helling en glooiing³ daarentegen, lopen de opvattingen zeer sterk uiteen, zowel wat betreft de overheersende sedimentatieprocessen als de timing van deze processen binnen de glaciële cyclus. Zo zijn er voorbeelden van submariene waaiersystemen⁴ aan de voet van de continentale helling, van uitgestrekte puinkegels⁵ die zijn opgebouwd door grootschalige massaverschuivingen, en van hellingen waar enkel de gebruikelijke kleinschalige massabewegingen lijken op te treden.

De huidige studie biedt de mogelijkheid om een aantal analoog gesitueerde glaciële randen direct met elkaar te vergelijken. Het grootste deel van het onderzoek is gewijd aan een gedetailleerde stratigrafische en proces-georiënteerde analyse van de twee afzonderlijke glaciogene sedimentkegels langs de continentaalranden van centraal Oost-Groenland en de westelijke Barents Zee, voornamelijk aan de hand van geometrische lagenpatronen zoals deze zich op seismogrammen manifesteren.

Het is in de eerste plaats de bedoeling om uit een vergelijking van deze beide regionale studies een algemene glaciatiegeschiedenis te distilleren voor de polaire Noord-Atlantische Oceaan. Tot nog toe is deze, vooral dan de geschiedenis op langere termijn, grotendeels onbekend gebleven. De glaciële afzettingen op het land en in fjorden zijn namelijk zeer schaars en fragmentarisch; de meeste van deze afzettingen dateren bovendien niet verder terug dan de laatste glaciële/interglaciële cyclus. Sporen van oudere glaciële cycli zijn dan ook nog veel moeilijker te herkennen, daar hun afzettingen meestal door latere glaciaties zijn geërodeerd. De omvangrijke depocentra langs de continentaalranden tonen aan dat ijskappen de meeste van hun erosieproducten tot op de buiten-shelf transporteerden tijdens periodes van maximale uitbreiding. Het meest complete archief, zowel wat betreft continuïteit als tijdsduur, van de glaciële geschiedenis op langere termijn ligt dus vervat in de bestudeerde sedimentkegels, en kan het best bestudeerd worden aan de hand van reflectieseismische gegevens, bij voorkeur in combinatie met diepzeeboringen. Dit onderzoek werd geïnitieerd in het kader van het 5 jaar durende PONAM (Polar North Atlantic Margins) onderzoeksproject van de

² Eng. "ice sheet grounding". De term "grounding" is in het Nederlands moeilijk in één woord te vatten.

³ In het Engels respectievelijk "continental slope" en "continental rise".

⁴ Eng. "submarine fans".

⁵ Eng. "slope aprons", of meer algemeen "sediment cones".

European Science Foundation, waarbij de reconstructie van de lange-termijns glaciale geschiedenis van de polaire Noord-Atlantische Oceaan één van de drie hoofdoelstellingen vormt.

De tweede doelstelling van deze studie bestaat uit een vergelijkend onderzoek van de grootschalige sedimentatieprocessen die zich op beide sedimentkegels hebben afgespeeld. De aandacht gaat hierbij vooral uit naar het lagere gedeelte van de continentale helling en de continentale glooiing, gezien de bestaande modellen daar het sterkst uiteenlopen. Er wordt daarom ook een derde voorbeeld uit de zuidelijke hemisfeer, waarover in de onderzoeksgroep de voorbije jaren een rijke ervaring is opgebouwd, kort in het onderzoek betrokken: met name de Weddell Zee in Antarctica.

2. Scoresby Sund, centraal Oost-Groenland

Inleiding

Scoresby Sund is de verzamelnaam voor een uitgebreid fjordencomplex, zowat het grootste ter wereld, centraal langs de kust van Oost-Groenland. Tijdens de zomer van 1990 was de fjordregio het toneel van een omvangrijke seismische campagne met het meetschip "Polarstern". Hierbij werd een groot aantal profielen geschoten in de brede buitenste fjordarmen, alsook een lange traverse over de continentale shelf en helling, waarvan de opvallende zeewaartse uitbouw voor de fjordmonding de ligging verraaft van een depocentrum van vermoedelijk glaciale oorsprong.

Scoresby Sund bestaat uit een relatief ondiepe en brede buitenste fjordzone (Hall Bredning en Scoresby Sund s.s.) waarin een aantal smalle maar extreem diepe binnenfjorden uitmonden. Aan het landwaartse uiteinde van deze fjorden bevinden zich de termini van belangrijke gletsjers die rechtstreeks gevoed worden door het "Inlandijs" (de Groenlandse ijskap). De metingen in Scoresby Sund bleven grotendeels beperkt tot de buitenste fjordzone, meer bepaald tot Hall Bredning, waarin slechts een gering aantal, vooral kleinere gletsjers uitgeeft.

Geologie van het substraat

Het dicht gegevensnetwerk liet zonder probleem toe de pre-Kwartaire geologische eenheden van eerste orde die in de regio rondom Hall Bredning dagzomen, doorheen de fjord te traceren, wat een aanvulling op de geologische kaart inhoudt. Deze eenheden zijn: [1] metamorfe gesteenten gevormd tijdens de Caledonische orogenese, doorspekt met [2] intrusieven van dezelfde ouderdom, ten noorden en westen van Hall Bredning, [3] sedimentaire gesteenten afgezet in een Mesozoïsch riftbekken, dominant in het oosten, en [4] vroeg-Tertiaire plateaubazalten die tijdens een kortstondige fase van overvloedig hot-spot-gelieerd vulkanisme bij de initiële opening van de polaire Noord-Atlantische Oceaan zijn uitgevloeid, en nu de zuidkust van de fjord bedekken. Deze verschillende eenheden worden vooral onderscheiden op grond van hun uiteenlopende morfologische kenmerken, die op hun beurt een verschillende resistiviteit tegen (voornamelijk glaciale) erosie weerspiegelen. De verschillen komen het meest extreem tot uiting in de uitwendige morfologie van het fjordensysteem: zo blijkt dat de brede buitenfjorden geheel het resultaat zijn van een preferentiële erosie van de zachtere Mesozoïsche sedimenten langsheen het breuk-contact met de hardere kristallijne gesteenten van het Caledonisch massief.

Glaciale evolutie in Scoresby Sund

Wellicht het meest verrassende resultaat dat door het onderzoek aan het licht werd gebracht, houdt verband met de verspreiding van niet-geconsolideerd, glaciaal of glaciomariën afgezet materiaal binnen de fjord: slechts zeer geringe sedimentdiktes, in vele gevallen zelfs beneden de seismische resolutie, konden op de profielen worden waargenomen. Kwartaire afzettingen vormen een min of meer continue laag, minder dan 15 m dik, die over de oudere geologische eenheden gedrapeerd is; grotere accumulaties, tot 50 of maximaal 100 m, worden enkel aangetroffen in bepaalde topografische depressies, en voor de monding van gletsjers en kleine riviersystemen. Eén van deze lokale accumulaties (max. 160 m, het dikste sedimentpakket dat werd waargenomen) kon dankzij een aantal hogere-resolutie profielen meer in detail worden bestudeerd: het bevindt zich in Vikingebugt, een kleine, slechts 14 km lange inham langs de zuidkust van Scoresby Sund waar zich niet toevallig het grootste gletsjerfront (Bredegletscher) bevindt dat rechtstreeks in de buitenste fjordarm uitmondt. De opvulling van de Vikingebugt-vallei blijkt hoofdzakelijk te bestaan uit sterk waterhoudende glaciomariene sedimenten, die vermoedelijk grotendeels werden afgezet uit suspensiewolken van subglaciaal smeltwater, en in veel mindere mate door de bijdrage van materiaal dat vrijkomt uit afsmeltende ijsbergen⁶. Het aandeel van materiaal afgezet uit suspensie neemt echter sterk af met toenemende afstand tot het ijsfront, en het continue sedimentdek in Hall Bredning is dan ook in hoofdzaak toe te schrijven aan het afsmelten van de talloze ijsbergen die in de fjord ronddrijven.

Twee oorzaken liggen vermoedelijk aan de basis van de lage sedimentconcentraties: [1] een volledige uitschuring van de fjord tijdens de laatste glaciatie van het Laat-Weichseliaan, en [2] algemeen lage sedimentatiesnelheden tijdens het huidige Holoceen interglaciaal, ten gevolge van de distale positie die de buitenste fjordzone de hele tijd heeft ingenomen t.o.v. de belangrijkste gletsjerfronten. Het voorbeeld van Vikingebugt toont aan dat de grootste accumulaties diep in de binnenfjorden te verwachten zijn — helaas konden hier tengevolge van de barre ijscondities geen profielen worden opgenomen. Bovendien blijft ook veel sediment gevangen ter hoogte van de topografische barrières die binnen- en buitenfjorden van elkaar scheiden, doordat veel ijsbergen daar aan de grond lopen en er aldus vroegtijdig hun lading verliezen. De lage sedimentatiesnelheden in Hall Bredning impliceren ook dat de toevoer van sediment naar de continentale shelf nog veel geringer is, vanwege de nog veel grotere transportafstand. De continentale rand moet dan ook als overwegend sediment-deficiënt⁷ worden beschouwd tijdens interglaciale periodes.

De bevinding dat weinig of geen afzettingen uit voorgaande glaciale en interglaciale periodes bewaard gebleven zijn, houdt in dat de ijskap tijdens het Laat-Weichseliaan dik genoeg was om althans in Hall Bredning op de fjordbodem te rusten en aldus alle niet-geconsolideerde materiaal in haar loop mee te voeren. Voorheen werd nog aangenomen dat de ijskap grotendeels dreef, en pas op de continentale shelf voor de monding van Scoresby Sund aan de grond liep. Vermoed wordt dat de opvulling tijdens interglacialen en de daaropvolgende leegschuring tijdens glaciaties, een scenario vormen dat zich herhaaldelijk heeft afgespeeld tijdens de glaciale evolutie van Scoresby Sund. Het meeste sediment zou aldus van Holocene ouderdom zijn, zoals wordt bevestigd door andere studies op basis van ondiepe boorkernen, en het potentieel om uit de fjordafzettingen de glaciale geschiedenis te reconstrueren is navenant zeer laag. Al bij al zijn hiervoor in Vikingebugt nog de meeste aanwijzingen voorhanden. Dit is namelijk de enige locatie waar oudere afzettingen konden worden waargenomen die vermoedelijk dateren uit een eerdere glaciale of interglaciale periode. Deze

⁶ Voor het Engelse begrip "ice-rafted debris" (ook wel kortweg IRD) werd geen eenvoudige vertaling gevonden.

⁷ Eng. "sediment-starved".

afzettingen komen voor als een geïsoleerd pakket, gevat tussen twee duidelijke erosie-oppervlakken, wat dus zou wijzen op minstens twee glaciaties — al waren het er vermoedelijk veel meer. Voor de monding van Vikingebugt, aanleunend tegen een opwelling in het substraat die de vallei scheidt van de hoofdvallei van Scoresby Sund, werd een intern chaotische eenheid waargenomen, die hier wordt geïnterpreteerd als een laterale morene, gevormd waar Bredegletscher tijdens de glaciatie van het Laat-Weichseliaan werd afgebogen en meegevoerd in de van west naar oost bewegende fjordgletsjer. De belangrijkste opvullingsfase van de Vikingebugt-vallei had plaats na de terugtrekking van Bredegletscher, tijdens het Holoceen. Er zijn enkele aanwijzingen dat er tijdens deze periode een kortstondige heropmars van het gletsjerfront heeft plaatsgevonden, misschien gelijktijdig met een stagnatie van de terugschrijdende grotere gletsjerfronten ter hoogte van de respectievelijke mondingen van de binnenfjorden in Hall Bredning. Deze fase is gekend als het Rødefjord stadiaal (Jonger Dryas tot Preboreaal). Sindsdien is de opvulling van de Vikingebugt-vallei door glaciomariene sedimentatie gestaag verdergegaan, af en toe onderbroken door fases van catastrofale massaverschuivingen.

Sedimentaire opbouw en glaciatiegeschiedenis van de continentale shelf en helling

Voor de monding van Scoresby Sund reikt de shelf minstens 20 km verder in zee dan langs aanpalende delen van de continentaalrand. De lange seismische traverse die overheen de shelf en continentale helling werd geschoten, toont aan dat dit te wijten is aan een omvangrijke prograderende sedimentkegel die zich vanaf de buiten-shelf uitstrekt over de oceanische korst. Deze sedimenten bereiken een totale dikte van ca. 2000 m op de bovenste continentale helling, geleidelijk aan teruglopend tot ongeveer 500 m verder hellingafwaarts. De verschillende fasen in de geologische opbouw van de rand liggen vervat in de geometrische patronen in en tussen de sedimentlagen onderling. In een eerste benadering kunnen drie grootschalige afzettingseenheden (I - III, van oud naar jong) worden onderscheiden die getuigen van een wisselende relatieve invloed van twee brongebieden: de Scoresby Sund fjordregio in het noordwesten, en het IJsland Plateau in het zuidoosten. Gezien in het studiegebied geen boringen voorhanden zijn, vormen magnetische lineaties van de oceanische korst de enige indicatie voor de ouderdom van de geïdentificeerde eenheden.

Afzettingsreeks I is beperkt tot de voet van een vulkanisch plateau dat het zuidoostelijk uiteinde van het profiel domineert; dit plateau, dat kan beschouwd worden als de uitloper van het IJsland Plateau verder naar het zuiden, eindigt abrupt op een uitgesproken steilflank⁸ die verder niet structureel bepaald is (vandaar de benaming "pseudo-escarpment"). De interne opbouw en externe morfologie van het plateau suggereren dat deze structuur tot stand is gekomen tijdens een periode van verhoogde magma-injectie langs een subaërisch spreidende Kolbeinsey Rug, ongeveer 15 à 12 Ma geleden, in het Midden-Mioceen. Deze hypothese wordt grotendeels bevestigd door de geometrie der reflectoren in afzettingsreeks I, die aangeeft dat deze sedimenten vermoedelijk ongeveer gelijktijdig werden afgezet met de opbouw van het plateau, in een ondiepe flexurele depressie groeiend voor de rand van het plateau door de toenemende belasting van nieuw uitgestroomde lavas. De aanwezigheid van kleine prograderende lobben (delta-lobben?) bovenin de eenheid zou eveneens kunnen wijzen op afzetting in een kustnabije omgeving.

Sedimenten ouder dan afzettingsreeks I komen vrijwel zeker voor dichterbij het continent, maar worden aan de observatie onttrokken door storende meervoudige zeebodemreflecties. Deze afzettingen, tot zowat 23 Ma oud (Vroeg-Mioceen), werden vermoedelijk aangevoerd door een

⁸ Eng. "escarpment".

belangrijk rivierensysteem ter hoogte van het huidige Scoresby Sund. Het kleine depocentrum aan de voet van het vulkanisch plateau bleef blijkbaar geïsoleerd t.o.v. de aanvoer van het continent.

Afzettingsreeks II registreert de definitieve subsidentie van het vulkanisch plateau beneden de zeespiegel, in het laat Midden-Mioceen tussen 12 en 10 Ma. Als gevolg hiervan liep de bijdrage van klastisch materiaal afkomstig van deze structuur sterk terug, en werd ze vervangen door de aanvoer van sediment vanaf het immer subaërische IJsland Plateau verder zuidwaarts. Ondertussen progradeerden de sedimenten (nog steeds aangevoerd door rivieren) afkomstig van Oost-Groenland verder zuidoostwaarts, en kwam reeds vroeg tijdens de afzetting van afzettingsreeks II een connectie tot stand tussen beide depocentra, resulterend in sedimentatie over de gehele lengte van het profiel; dit ging gepaard met een complex patroon van interdigitatie⁹. Opvallend is verder dat binnen afzettingsreeks II sterke erosie wordt waargenomen aan de voet van de toenmalige continentale helling. Bodemwaterstromingen vormen hiervoor de meest waarschijnlijke verklaring. Mogelijk markeert deze erosiefase het ontstaan van de Noordwest-Atlantische bodemwaterstroming, die in dit gebied zuidwestwaarts convergeert naar een smalle doorgang over de transversale rug tussen Groenland en IJsland, en ook nu nog de sedimentatie op de lagere continentale helling beheerst. Dit zou betekenen dat de Arctische, en ook de polaire Noord-Atlantische Oceaan, in deze periode reeds gevoelig waren afgekoeld, in de aanloop naar de instelling van een volledig glaciële omgeving in het Plio-Pleistoceen. Een laatste waarneming i.v.m. afzettingsreeks II is dat de jongste sequenties een diktetrend vertonen die tegengesteld is aan die van de onderliggende lagen: deze sequenties bereiken nl. hun grootste dikte boven het vulkanisch plateau, en verdunnen enigszins op de continentale helling. Dit wijst op een relatief afgenomen sedimentaanvoer vanuit Oost-Groenland, misschien wel te wijten aan de graduele opbouw van een continentale ijskap, wat een algemene restrictie van sediment-transport naar de shelf voor gevolg zou gehad hebben, tot de ijskap voldoende omvangrijk was om rechtstreeks in zee uit te geven.

De overgang tussen afzettingsreeksen II en III markeert de meest uitgesproken verandering tijdens de sedimentatiegeschiedenis bestreken door het seismisch profiel. Een belangrijk erosie-oppervlak op de shelf vormt de basis van een reeks van sterk prograderende sequenties die een gezamenlijke dikte van ongeveer 1 km bereiken t.h.v. de shelfrand, maar opvallend verdunnen boven het vulkanisch plateau, wat een drastisch verhoogde relatieve invloed van het brongebied in Oost-Groenland impliceert. Deze waarnemingen leiden tot de karakterisatie van afzettingsreeks III als een hoofdzakelijk glaciaal afgezette eenheid. Het erosie-oppervlak kwam vermoedelijk tot stand wanneer de eerste grootschalige glaciatie van de shelf plaatsvond; de verhoogde toevoer van sediment naar de shelf en helling zou dan verklaard kunnen worden door een intensere erosie onder invloed van de groter wordende ijskap, en de opeenvolgende uitbreidingen van het ijs tot aan de shelfrand resulteerden in de overwegend prograderende geometrie van de lagen. Het is dan ook vooral tijdens deze laatste periode dat de laterale uitbouw (zo'n 45 km) van de continentaalrand plaatsvond. Hoewel recente boringen op de rand van Zuidoost-Groenland de aanwezigheid aangetoond hebben van een belangrijke ijskap reeds sedert 7 Ma, begonnen de grootschalige vergletsjeringen van de shelf waarschijnlijk later, misschien pas rond 2.6 Ma wanneer ook de overige ijskappen rond de polaire Noord-Atlantische Oceaan zich begonnen uit te breiden. Gezien de grote dikte van deze afzettingsreeks, is het ook duidelijk dat de hier begraven informatie over de glaciatiegeschiedenis van centraal Oost-Groenland veel verder teruggaat in de tijd, en ook vollediger is, dan de afzettingen die bewaard zijn gebleven op het land en in Scoresby Sund zelf.

⁹ Eng. "interfingering".

Gebaseerd op de variatie van progradationale en aggradationale componenten kan afzettingsreeks III verder worden verdeeld in drie sub-eenheden A-C, die op hun beurt elk nog eens uit twee sequenties bestaan. De onderste eenheid III-A geeft een eerder geringe progradatie aan van slechts 5 km; de middelste eenheid III-B wordt gekenmerkt door sterk toenemende progradatiehoeveelheden, waarbij de shelfrand in twee opeenvolgende stappen respectievelijk 15 en 23 km in zeewaartse richting is voortgeschreden. In scherpe tegenstelling tot III-A en III-B, is de bovenste eenheid III-C nagenoeg volledig aggradationeel, terwijl progradatie daarentegen beperkt blijft tot minder dan 5 km; opmerkelijk in dit verband is dat ook deze aggradationale sequenties geïnterpreteerd worden als zijnde afgezet tijdens glaciaties. Vermoedelijk weerspiegelen deze variaties de opeenvolging van verschillende fasen in de glaciële ontwikkeling van de regio. Initiële expansies van de ijskap op de shelf zouden aldus eerder bescheiden gebleven zijn (III-A). In een tweede fase (III-B) zou er een aanzienlijke intensifiëring zijn opgetreden van de glaciaties, met progressief groter wordende en langer aan de shelfrand gepositioneerde ijskappen. De finale ontwikkeling (III-C) tenslotte, lijkt gepaard te zijn gegaan met een sterk gereduceerde erosieve capaciteit van de ijskappen op de shelf. Deze trends zijn waarschijnlijk grotendeels gebonden aan wisselende afmetingen van de zich uitbreidende ijskappen, die worden bepaald door de algemene klimatologische evolutie in de polaire Noord-Atlantische Oceaan, al kunnen ook factoren zoals bv. de uitdieping¹⁰ van de shelf, invloed uitoefenen op de dynamiek van het ijs.

In totaal werden dus in afzettingsreeks III zes verschillende sequenties geïdentificeerd, wijzend op minstens evenzoveel expansies van het Inlandijs op de continentale shelf. Nochtans zijn uit globale zuurstofisotopencurves zeker meer dan 20 ijstijden gekend. Er bestaat echter niet noodzakelijk een één-op-één correlatie tussen de globale klimatologische evolutie en het gedrag van de Groenlandse ijskap; verder lijkt het ook aannemelijk dat slechts de sterkste glaciaties hun sporen nalieten in de lagenpatronen op de continentale shelf en helling. Door het ontbreken van boorgegevens kunnen de individuele sequenties dan ook niet met de gekende ijstijden worden gecorreleerd. Er zijn echter aanwijzingen dat de jongste sequentie werd afgezet tijdens het Saale glaciaal; sedertdien zou de centrale rand van Oost-Groenland dus geen noemenswaardige sedimentatie hebben gekend.

3. De westelijke rand van de Barents Zee t.h.v. Bereneiland Trog

Introductie

De westelijke rand van de Barents Zee strekt zich uit tussen Noorwegen en de arctische Svalbard Archipel, waarvan Spitsbergen het belangrijkste eiland uitmaakt. De continentaalrand vormt de begrenzing van de epicontinentale Barents Zee met de polaire Noord-Atlantische Oceaan. De morfologie van deze shelfzee wordt gedomineerd door twee brede en glaciaal uitgediepte transversale troggen, de Bereneiland Trog en noordelijk daarvan de Storfjorden Trog, van elkaar gescheiden door de ondiepe Spitsbergen Bank waarop zich Bereneiland bevindt. Zoals ter hoogte van Scoresby Sund in Oost-Groenland, wordt ook voor de monding van deze shelftroggen een opvallende uitbouw van de shelfrand waargenomen, die de contouren omschrijft van twee reusachtige sedimentkegels, respectievelijk de Bereneiland Conus en de Storfjorden Conus. Dit wordt toegeschreven aan de convergentie van ijsstromen, en het daaruit voortvloeiend preferentieel sediment-transport in de troggen tijdens voorbijgaande glaciaties van de Barents Zee.

¹⁰ Eng. "overdiepening".

De beschikbare seismische gegevens vormen een complementair netwerk van noord-zuid georiënteerde lijnen parallel met de shelfrand, en oost-west georiënteerde transversaallijnen; ze bestrijken de buiten-shelf en continentale helling over de noordelijke helft van de Bereneiland Conus en de zuidelijkste uitlopers van de Storfjorden Conus. In vergelijking met vroegere datasets reiken deze seismische profielen veel verder in de diepzee, waardoor ze een vollediger beeld geven van de opbouw van deze sedimentkegels dan voorheen.

Structurele situering

Tektonisch gezien omvat de Barents Zee een uitgestrekte zuidelijke provincie van bekkens en ruggen, gevormd tijdens verschillende laat-Paleozoïsche en Mesozoïsche riftfasen, en het meer noordelijk gelegen, structureel verheven Svalbard Platform. Naar het westen toe worden deze provincies afgebakend door een langgerekte breukzone waarlangs zich het oceanische Lofoten Bekken uitstrekt. Deze breukzone bestaat uit drie verschillende segmenten: de Senja Breukzone en de Hornsund Breukzone, respectievelijk in het zuiden en noorden, met elkaar verbonden door een tussenliggend segment (hier informeel aangeduid als “Centrale” Breukzone) dat een andere strekking heeft en geassocieerd is met de Vestbakken vulkanische provincie. Volgens de huidige geofysische modellen onderging de westelijke Barents Zee rand oorspronkelijk een hoofdzakelijk transforme beweging (t.o.v. Noordoost-Groenland) bij de initiële opening van de Noord-Atlantische Oceaan; rekbewegingen heersten er enkel langs de Centrale Breukzone, waar een kortstondige fase van exuberant subaërisch vulkanisme leidde tot het ontstaan van de Vestbakken vulkanische provincie. Na 51 Ma evolueerde de continentaalrand tot een riftende en later passief subsiderende rand, ten gevolge van de stapsgewijze noordwaartse propagatie van de spreidingsas, de Knipovich Rug.

Het bestudeerde gebied situeert zich volledig langs de Centrale Breukzone, en bestrijkt een tip van de continentale Barents Zee provincie, en grote delen van de Vestbakken vulkanische provincie en van het Lofoten Bekken. Deze drie provincies worden elk gekenmerkt door hun eigen sokkeltype, gemakkelijk van elkaar te onderscheiden door de sterk uiteenlopende akoestische eigenschappen. Het dominante sokkeltype bestaat uit oceanische korst, die een zeer onregelmatig verloop kent, vooral naar de actieve Knipovich Rug toe, met opwelvingen tot 1 km boven het omgevende substraat. Vermoed wordt dat deze opwelvingen gealigneerd zijn volgens de spreidingsrichting, naar analogie met bathymetrische lineamenten gekend aan de tegenoverliggende zijde van de spreidingsas.

Algemene stratigrafie

Cenozoïsche afzettingen vormen overal langs de rand westelijk van Svalbard en de Barents Zee een imposante prograderende wig die tot 7 km dik kan worden, en waarin de hierboven beschreven sedimentkegels grote individuele depocentra vertegenwoordigen. Deze sedimenten werden afgezet ingevolge de opheffing en erosie van de Barents Zee en Svalbard, en weerspiegelen vooral de tektonische, en bovenin de sectie ook de glaciële ontwikkeling van de rand. De voorbije jaren werden reeds verscheidene seismostratigrafische studies verricht op de sedimentwig. Deze waren echter sterk gelimiteerd door de geringe ouderdomscontrole, en door het uitblijven van een directe correlatie tussen de noordelijke en zuidelijke gedeelten van de continentaalrand. Twee recente ontwikkelingen gaven het onderzoek echter een nieuwe impuls. Vooreerst werden enkele nieuwe boringen uitgevoerd, waaruit blijkt dat een belangrijk deel van de wig veel jonger is dan voorheen werd aangenomen: zo wordt een oppervlak (R7, zie verder) waarboven de grote depocentra hun voornaamste groei kenden, nu gedateerd op ca. 2.5 Ma, terwijl deze grens eerder nog werd beschouwd als 10 tot 15 Ma oud; en voor een belangrijk discordantie-oppervlak op de shelf (de zgn. “upper regional unconformity” of

R1, zie verder), waarboven zeker 500 m sediment ligt, wordt een ouderdom van slechts 440 ka vooropgesteld. Ten tweede is men er aan de universiteit van Oslo in geslaagd de noord-zuid correlatie door te voeren. Het resultaat is een regionaal stratigrafisch referentiekader bestaande uit zeven seismische horizonten ("reflectoren") R7-R1, die over een afstand van ca. 1000 km traceerbaar zijn. Op basis van de relatieve belangrijkheid van deze reflectoren, wordt er een hiërarchie vooropgesteld van vier eenheden van hogere orde of "megasequenties": G0 (pre-R7), GI (R7-R5), GII (R5-R1) en GIII (post-R1). Ook deze studie heeft voor een bescheiden deel tot dit referentiekader bijgedragen, mede dankzij de cruciale ligging van de beschikbare dataset. Tegelijkertijd vormt dit werk een meer gedetailleerd stratigrafisch onderzoek dat de brug wil slaan tussen twee gelijkaardige detailstudies, van de zuidelijke Bereneiland Conus en de Storfjorden Conus, door collega's in Oslo.

Gedetailleerd seismostratigrafisch onderzoek

De stratigrafische opbouw van het studiegebied is zeer complex. In totaal werden 37 oppervlakken geïdentificeerd, r1-r37, die alle in meer of mindere mate een discordant karakter uitwijzen. Bepaalde van deze reflectoren zijn lokaal belangrijker dan sommige regionale reflectoren; de verdeling in vier megasequenties is evenwel ook hier onmiskenbaar. Op vele plaatsen wordt de gelaagdheid echter grondig verstoord door diverse vormen van massa-afzettingen.

Megasequentie G0, volumetrisch de meest belangrijke afzettingsreeks, overdekt de drie sokkeltypes over het grootste deel van het studiegebied, en vult op deze manier het onderliggende reliëf uit. Dit resulteert in zeer sterke diktevariëaties, waarbij een maximale dikte van meer dan 3 km wordt bereikt aan de voet van de Centrale Breukzone; naar het zuidwesten wigt de eenheid uit door de laterale beëindiging van haar bovengrens R7 (r8) tegen de oceanische korst van het Lofoten Bekken. Megasequentie G0 vertegenwoordigt de langste tijdsspanne in de afzettingsgeschiedenis van de continentaalrand, vanaf de opening van de oceaan in het Vroeg-Eoceen, tot laat in het Pliocene (ca. 2.5 Ma). De interne lagenpatronen registreren dan ook voornamelijk de tektonische evolutie van de rand. De grote depocentra voor de monding van de Bereneiland en Storfjorden Troggen kwamen daarentegen vooral tot ontwikkeling in de bovenliggende megasequenties GI-GIII.

Megasequentie GI is het best ontwikkeld op de lagere continentale helling, waar de dikte gemiddeld 500 à 750 m bedraagt, en wigt naar het westen uit tegen de hoogste pieken van de oceanische korst. Een maximale dikte van meer dan 1 km wordt in het uiterste noorden opgetekend, wat wijst op een relatief hogere toevoer vanuit het Storfjorden gebied. Bovendien worden de afzettingen op deze plaats gekenmerkt door een chaotisch seismisch faciës; dit wordt verondersteld voort te spruiten uit massatransport t.g.v. een belangrijke toename van de plaatselijke sedimentatiesnelheden. Op de bovenhelling neemt de dikte van de eenheid sterk af, behalve in een depocentrum voor de axiale monding van Bereneiland Trog. Individuele sequenties binnenin dit depocentrum vertonen een opvallende progradatie (in totaal 18 km), met steil hellende frontlagen¹¹ die naar boven toe getrunceerd worden door de basis van GIII (R1). De gegevens tonen echter aan dat deze prograderende eenheid slechts van zeer lokale aard is.

Megasequentie GII wordt onderaan begrensd door reflector R5 (r15), een over het hele gebied uitgesproken erosieve horizon die, zoals de basis van GI, zelf afgesneden wordt door de ondergrens van GIII in de buitenste Bereneiland Trog. In de Vestbakken vulkanische provincie vertoont R5

¹¹ Eng. "foresets".

lokaal een duidelijke opwelling, geassocieerd met breuken; samen met de complexe lagenbeëindigingspatronen waargenomen in de bovenliggende afzettingen vormt dit een sterke aanwijzing voor een tektonische opheffing van dit gebied. Op de isopachenkaart springen twee duidelijk gescheiden maxima in het oog: een kleiner depocentrum (max. 1 km dik) bovenaan de continentale helling in het Storfjorden gebied, en een omvangrijker depocentrum (> 1 km dik) dat zich uitstrekt over de benedenhelling en continentale glooiing in de zuidelijke helft van het gebied. Hellingopwaarts hiervan wigt GII echter nagenoeg volledig uit. Het meest frappante kenmerk van de megasequentie is het overwegend chaotisch tot transparant seismisch faciës, dat op sommige plaatsen zelfs over het volledige verticale bereik van het interval is ontwikkeld, ofwel een dikte tot 1 km. Meestal kunnen echter meerdere chaotische niveaus worden onderscheiden. Naar de Storfjorden Conus toe wordt het faciës geleidelijk, maar soms ook abrupt, gestratificeerd. De chaotische signatuur wordt toegeschreven aan een verstoring van de oorspronkelijke gelaagdheid, door toedoen van massabewegingen. Op basis van een minder uitgebreide dataset was men er tot voor kort van overtuigd dat de volledige chaotische eenheid het resultaat is van één enkele catastrofale gebeurtenis. Deze interpretatie kan niet langer weerhouden worden. Een gedetailleerde faciësanalyse en correlatie van reflectoren toont duidelijk aan dat er meerdere opeenvolgende fasen van instabiliteit zijn geweest, waarbij grote hoeveelheden sediment *en masse* hellingafwaarts werden verplaatst. Er wordt daarnaast ook een hogere mobiliteit geconstateerd dan eerder was vooropgesteld: vermoedelijk ging het om een combinatie van glijden en vloeien¹², in plaats van om een pure afschuiving¹³; de interne vervorming wordt ook groter met toenemende bewegingsafstand. Het merendeel van deze massabewegingen vond een oorsprong op de bovenste continentale helling voor de monding van Bereneiland Trog, waar verticale extensie van het chaotisch faciës het grootst, en interne deformatie minimaal zijn. De geremobiliseerde massa's strekken zich uit naar het noordwesten, in bepaalde gevallen zelfs tot op de Storfjorden Conus.

Megasequentie GIII is de jongste van de vier geïdentificeerde eenheden van eerste orde. De basis correspondeert met reflector R1 (r30), wellicht de meest opvallende seismische horizon die in het studiegebied werd geïdentificeerd. In het distale (buitenste) deel van Bereneiland Trog truncateert R1 alle zeewaarts hellende reflectoren van achtereenvolgens megasequenties GII en GI, een eigenschap waaraan het de benaming "upper regional unconformity" (kortweg URU) ontleent. Bovenliggende sedimenten zijn hoofdzakelijk horizontaal en parallel gelaagd. In het gebied omheen de Storfjorden Trog neemt het discordant karakter van R1 sterk af. Het meest opmerkelijke kenmerk van de GII/GIII grens betreft echter ongetwijfeld een enorme incisie in de bovenste continentale helling voor de monding van de Bereneiland Trog. Deze insnijding vormt een — naar de zee open — semi-circulaire depressie, omgeven door erosieve steilflanken tot max. 300 m hoog, en met een oppervlakte van om en bij de 9500 km². Het fenomeen wordt in zijn geheel geïnterpreteerd als een begraven "litteken"¹⁴ achtergelaten door een afschuiving van de toenmalige zeebodem. Zowel qua afmetingen en morfologische kenmerken vertoont het sterke overeenkomsten met een meer recente en beter gekende afglijdingsdepressie¹⁴ op de zuidelijke flank van de Bereneiland Conus, nog steeds zichtbaar in de bathymetrie nabij 72° N. Beide afschuivingen behoren tot de grootste zeebodeminstabiliteiten die tot op heden beschreven werden. Waarschijnlijk staan ze ook model voor de massabewegingen die de afzetting van de onderliggende megasequentie GII hebben overheerst.

¹² Eng. "flow-slide".

¹³ Eng. "slide" of "slump".

¹⁴ Eng. "slide scar".

De uitbreiding van GIII wordt gekenmerkt door één enkel depocentrum dat de volledige zuidelijke helft van het studiegebied domineert. De sedimentdikte bedraagt er meer dan 500 m, en loopt zelfs op tot meer dan 1 km over de hierboven beschreven insnijding. Opvallend is dat dit depocentrum een hogere positie inneemt op de continentale helling dan zijn voorloper in GII. In contrast met de vorige intervallen, is er in GIII dus geen depocentrum tot ontwikkeling gekomen ter hoogte van de Storfjorden Trog. Binnenin het zuidelijke depocentrum wordt er een duidelijke tweedeling van de samenstellende sequenties waargenomen. De oudere sequenties zijn voornamelijk gelimiteerd tot het insnijdingsgebied, en wiggen uit tegen de omgevende steilflanken of soms verder noordwestwaarts. Van deze sequenties vertegenwoordigt enkel de onderste sequentie het materiaal dat werd geremobiliseerd bij de catastrofale hellingsafglijding; deze afzettingen zijn gemiddeld niet meer dan 80 m dik, en spreiden zich uit in een brede lob vanuit de afglijdingsdepressie. De overige sequenties corresponderen dan met een fase van preferentiële opvulling van het achtergebleven "litteken". Het bovenste deel van GIII strekt zich uit overheen de grenzen van het insnijdingsgebied. De individuele sequenties worden gekenmerkt door opvallende progradatie (meer dan 30 km voor de monding van Bereneiland Trog), maar ook door aggradatie, waardoor het de enige sequenties zijn binnen GI-GIII die in dit gebied tot op de shelf reiken. Het seismisch faciës tenslotte van de GIII-afzettingen kan worden omschreven als semi-chaotisch, duidelijk te onderscheiden van het onmiskenbaar chaotisch faciës van GII. Het wordt eveneens geacht te wijzen op een verstoring van de gelaagdheid, ingevolge het optreden van massabewegingen, maar dan wel kleinschaliger dan in GII. Puinstromen¹⁵ vormden waarschijnlijk het overheersende afzettingsmechanisme, wat trouwens bevestigd wordt door recent hoger-resolutie onderzoek.

Glaciale evolutie

Aan de hand van de geobserveerde lagenpatronen is het mogelijk de geologische, en in het bijzonder de glaciale, evolutie van de westelijke rand van de Barents Zee te reconstrueren. In totaal werden de afzettingen langs de continentaalrand onderverdeeld in vier eenheden van eerste orde, nl. megasequenties G0-GIII. Hun begrenzingen markeren telkens een belangrijke ommekeer qua afzettingsstijl. De basis van megasequentie GI wordt gecorreleerd met het optreden van de eerste grootschalige glaciaties in het Laat-Pliocene, op grond van een recente absolute datering op 2.3 Ma, en van de continue aanwezigheid van door ijsbergen afgezet materiaal (IRD) in boorkernen boven deze horizon. De megasequenties GI-GIII zouden aldus een hoofdzakelijk glaciale oorsprong hebben, terwijl G0 als preglaciaal beschouwd wordt. Blijkbaar leidden de glaciaties tot de afzetting van gigantische hoeveelheden sediment (tot meer dan 3 km!) in een relatief kleine tijdsspanne, en resulteerden ze in de differentiatie van de Storfjorden en Bereneiland Coni. Variaties in de geometrie der lagen, sedimentatiesnelheden, relatieve activiteit van de twee depocentra, en afzettingsprocessen (vooral dan de grootteorde van de dominerende massabewegingen) tussen de verschillende megasequenties, weerspiegelen waarschijnlijk opeenvolgende fasen in de glaciale geschiedenis. De transities tussen deze verschillende fasen blijven essentieel ongedateerd, hoewel de GII/GIII grens recent op de continentale shelf werd aangeboord. Afzettingen net boven deze discordantie werden gedateerd op ca. 440 ka; de huidige studie toont echter aan dat een tot 300 m dik interval (nl. het pakket dat de afglijdingsdepressie invult) volledig uitwigt naar de boorlocatie toe, zodat deze grens vermoedelijk ietwat ouder is.

¹⁵ Eng. "debris flows".

Megasequentie GI kwam vermoedelijk tot stand tijdens een initiële glaciële fase waarbij de eerste ijskappen zich vanuit de bergachtige Svalbard Archipel uitbreidden tot op de shelf, terwijl zich op het vlakke, en toen nog subaërische, Barents Zee platform daarentegen nog geen volgroeide ijskap kon ontwikkelen. Ter hoogte van de Storfjorden Trog, die zich rechtstreeks vanuit Svalbard lijkt te projecteren, werden door de ijskappen grote hoeveelheden erosiemateriaal aangevoerd. De verhoogde sedimentatiesnelheden gaven aanleiding tot omvangrijke massabewegingen en de accumulatie van een omvangrijk depocentrum beneden op de continentale helling. Zuidelijker langs de continentaalrand was dit veel minder het geval. Een lokaal progradatiecentrum ten zuiden van Bereneiland, op de plaats waar zich de monding van de huidige Bereneiland Trog bevindt, reflecteert de invloed van een puntbron, vermoedelijk een proglaciaal rivierensysteem drainerend van een meer oostwaarts gelokaliseerde ijskap in de Barents Zee.

Megasequentie GII documenteert een tweede glaciëtfase waarbij het ijs nu ook in de Barents Zee meermaals de shelfrand bereikte. Deze periode wordt gekenmerkt door de coëxistentie van twee individuele depocentra, de Storfjorden Conus en de Bereneiland Conus. De sedimentatiesnelheden gingen gevoelig de hoogte in, wat vooral op de Bereneiland Conus resulteerde in zeer grootschalige massabewegingsprocessen. De destabilisatie werd mogelijk verhoogd door een lokale tektonische opheffing in de Vestbakken vulkanische provincie, die zich onder de sedimentkegel voor Bereneiland Trog uitstrekt. Door deze massale sedimentremobilisatie werd het accumulatiecentrum sterk hellingafwaarts verschoven, zodat de progradatie van de continentaalrand op langere termijn nagenoeg tot stilstand kwam. Deze massabewegingen traden zo veelvuldig op, en waren zo grootschalig dat de resulterende afzettingen op bepaalde plaatsen zijn samengesmolten tot één gigantische chaotische massa die tot 1 km dik kan worden.

Megasequentie GIII tenslotte, werd afgezet in de loop van een laatste fase in de glaciële evolutie. Deze periode wordt bepaald door de wegwijzing van het Storfjorden depocentrum, terwijl voor de monding van Bereneiland Trog de shelfrand verder is uitgebouwd dan ooit tevoren. De gemiddelde sedimentatiesnelheden zakten terug tot ongeveer het niveau van GI, wat zich ook weerspiegelt in een schaalverkleining van de overheersende massabewegingen op de Bereneiland Conus. Er wordt gespeculeerd dat dit alles te wijten is aan een gewijzigde ijsstromingsdynamiek, misschien veroorzaakt door de erosie van het Barents Zee platform tot beneden de zeespiegel tijdens voorafgaande glaciaties, en/of door de graduele uitdieping van de Bereneiland Trog. Waarnemingen m.b.t. de situatie tijdens de laatste volledige vergletsjering van het Laat-Weichseliaan, suggereren dat ijsstromen pas laat in de glaciële cyclus de shelfrand konden bereiken, en daar slechts een relatief korte tijd verbleven. Het erosief vermogen van deze ijsstromen was bijgevolg sterk gereduceerd, waardoor aggradatie kon optreden van sedimentlagen in het buitendeel van de trog. Correlatie met een gedateerde hoge-resolutie seismische sectie geeft aan dat de jongste vier sequenties elk ruwweg overeenstemmen met een tijdsspanne van 100 ka, i.e. de duur van één glaciële cyclus.

4. Conclusie: de glaciale randen met elkaar vergeleken

Glaciale evolutie van de polaire Noord-Atlantische Oceaan

De bestudeerde depocentra langs de randen van centraal Oost-Groenland en de westelijke Barents Zee blijken allebei een logboek te bevatten van lokale ijskap-expansies op de shelf. Door een vergelijking van de stratigrafische opbouw van deze aan weerszijden van de oceaan gelegen glacigene depocentra, is het mogelijk de langere-termijns glaciale evolutie van de polaire Noord-Atlantische regio te reconstrueren. Onze kennis daaromtrent is tot nog toe beperkt tot de puntwaarnemingen van een aantal diepe ODP-boringen op het Vøring Plateau, langs de centrale continentaalrand van Noorwegen. De seismische gegevens blijken een opvallend parallelle ontwikkeling aan te geven aan weerszijden van de polaire Noord-Atlantische Oceaan tijdens het Plio-Pleistoceen. Op basis van de variatie van geometrische lagenpatronen werd voor beide studiegebieden een glaciale evolutie in drie fasen voorgesteld. Hoewel ook duidelijke verschillen werden vastgesteld, stemmen deze drie fasen in grote lijnen overeen; dergelijke onderverdeling vertoont bovendien sterke gelijkenissen met de paleoceanografische reconstructies op basis van de boven vermelde diepzeeboringen, al dient opgemerkt dat deze hoofdzakelijk de evolutie weerspiegelen van de Fennoscandische ijskap. Het algemene model voor de glaciale evolutie van de polaire Noord-Atlantische Oceaan ziet er als volgt uit:

Glaciale fase 1 vertegenwoordigt een initiële glaciatiefase waarbij middelgrote ijskappen gevormd werden. Hoewel continentale ijskappen naar alle waarschijnlijkheid reeds eerder ontstaan waren, vonden de eerste grootschalige vergletsjeringen van de shelf pas plaats rond 2.6 Ma. Dit blijkt onder meer uit zuurstofisotopencurves en uit een verhoging van de IRD-afzetting met meerdere grootteordes. Ijskappen die zich vanuit alpiene gebieden zoals Groenland en Svalbard uitbreidden, waren in staat de smallere gedeelten van de omgevende continentaalrand te traverseren, en aldus de eerste glacigene depocentra te initiëren. In vergelijking met de daaropvolgende periodes bleef de toevoer van IRD al bij al nog betrekkelijk laag.

Glaciale fase 2 duidt op een aanzienlijke intensifiëring van de glaciaties: een toenemend sterke progradiatie in centraal Oost-Groenland, en het ontstaan van grootschalige massabewegingsprocessen op de Bereneiland Conus, houden beide verband met een verhoogde aanvoer van sediment naar de shelf, en bijgevolg met een toegenomen activiteit van ijskappen. Deze waarneming wordt in verband gebracht met een beduidende toename van de IRD-gehaltes bij 1.2 Ma. Er wordt aangenomen dat progressief grotere ijskappen zich van dan af herhaaldelijk tot aan de shelfrand uitbreidden, overal langs Oost-Groenland en de westelijke rand van de Barents Zee en Svalbard.

Glaciale fase 3 lijkt in beide locaties, maar ook op andere glaciale continentaalranden in de wereld, gepaard te gaan met een opvallende aggradiatie van shelf-afzettingen. Op de Bereneiland Conus valt deze samen met een forse progradiatie; in vergelijking met centraal Oost-Groenland komt de voornaamste progradiatiefase dus beduidend later, wat vermoedelijk te wijten is aan een sterk verschillende hellingsstabiliteit tijdens de voorafgaande periode van verhoogde sedimentatie, en dus niet aan een klimatologische factor. De oorzaak voor de toegenomen aggradiatie is nog niet ten volle begrepen. Paleoceanografische gegevens wijzen op een finale fase in de glaciale evolutie die bij ca. 0.6 Ma een aanvang nam, en waarin de moderne glaciale condities werden ingesteld. Deze kenmerken zich door een sterker contrast tussen koudere glaciale, en warmere interglaciale periodes, door een dominantie van langere glaciale cycli (100 i.p.v. 40 ka), en door globaal grotere ijsvolumes. Deze laatste factor weerspiegelt echter vooral de expansie van de ijskappen tot in meer gematigde

breedtes, en dus niet noodzakelijk een vergroting van de polaire ijsmassa's zelf; de enigszins terugvallende sedimentatiesnelheden lijken inderdaad eerder het tegendeel aan te geven. Dunnere ijskappen zouden naar de buiten-shelf toe aanleiding kunnen gegeven hebben tot een verminderde erosie, en daaruit voortvloeiend een verhoogde aggradatie. Vermoedelijk speelde de progressieve uitdieping van vooral de shelftroggen tijdens voorgaande glaciaties hierbij ook een cruciale rol: hierdoor werd de druk die door het ijs op de onderliggende sedimenten wordt uitgeoefend, immers fel gereduceerd. Zoals onder meer blijkt uit het ongelijke aantal sequenties dat langs beide continentaalranden kon worden geïdentificeerd, bestond er tijdens glaciële fase 3 de hele tijd lang vermoedelijk een asymmetrische situatie met een eerder stabiele Groenlandse ijskap in het westen, en een sterk fluctuerende mariene ijskap in de Barents Zee, aan de oostzijde van de oceaan.

Naar een sequentiestratigrafisch model voor glaciële randen?

Tot slot van deze studie werd een onderzoek verricht naar de variatie van de geometrische lagenpatronen langs glaciële randen, en hun eventuele oorzaak en timing binnen een cyclisch afzettingsmodel. Hiertoe werd een bijkomend profiel geanalyseerd, afkomstig van een derde glaciële continentaalrand: de Weddell Zee in Antarctica.

Buiten-shelf en bovenhelling blijken in de drie gevallen gedomineerd te worden door een sterk prograderende geometrie. Dergelijke progradering, het meest uitgesproken ter hoogte van glaciële shelftroggen, werd reeds door verschillende onderzoekers vastgesteld. Ze wordt toegeschreven aan de expansie tot aan de shelfrand van een met de zeebodem contact houdende ijskap tijdens het glaciëel maximum. De studie toont echter aan dat glaciële sequenties ook een aanzienlijke aggradationale component kunnen vertonen, vooral dan op de buiten-shelf. Er zijn aanwijzingen dat dergelijke sequenties eveneens afgezet zijn tijdens volledige glaciaties van de shelf. Mogelijk vertegenwoordigen ze een situatie waarbij ijskappen minder dik werden en/of een kortere tijd aan de shelfrand gepositioneerd waren.

Lager op de continentale helling en glooiing blijken de geometrieën bij lange niet zo consistent te zijn. De continentale helling voor centraal Oost-Groenland wordt gekenmerkt door zich continu tot op de benedenhelling uitstrekkende prograderende frontlagen; enkel in de jongste twee sequenties komen aan de voet van de continentale helling individuele eenheden voor, waarbovenop de frontlagen uitwijken. De helling ten westen van de Barents Zee wordt daarentegen volledig overheerst door grootschalige massa-afzettingen die de stratigrafie in sterke mate verstoren. Individuele massa-afzettingen worden echter zelden herkend, maar zijn meestal versmolten tot één grotere chaotische eenheid. In beide gebieden is er dus geen sprake van een submariene waaier, zoals eerder werd gesuggereerd door het "trough mouth fan" concept. In dit concept worden de depocentra aan de monding van glaciële shelftroggen beschouwd als de tegenhangers van de gekende, door rivieren gevoede, submariene waaiers langs niet-polaire continentaalranden. Deze glaciogene depocentra vertonen echter in veel gevallen geen enkel kenmerk van de karakteristieke fan-sedimentatie. In de Weddell Zee is dit bijvoorbeeld wel het geval: daar heeft zich aan de voet van de continentale helling de Crary Fan ontwikkeld, een reusachtig waaiersysteem gekenmerkt door typische kanaal- en oeverwal-afzettingen. Uit een vergelijking met andere voorbeelden uit de literatuur komt naar voren dat de drie bestudeerde voorbeelden beschouwd kunnen worden als representatief voor drie categorieën waarin alle gekende glaciële randen kunnen gegroepeerd worden, op basis van de overheersende afzettingsstijl op de lagere continentale helling en glooiing: [1] "macroscopisch" stabiele randen zoals centraal Oost-Groenland, [2] opvallend onstabiele randen zoals de westelijke Barents Zee, en [3] fan-gedomineerde randen zoals in de Weddell Zee.

Er is geen éénduidige oorzaak aan te duiden die bepaalt welk sedimentatieproces dominant is op de continentale helling en glooiing van een gegeven glaciële rand. Vermoedelijk dragen verschillende factoren daartoe bij, zoals bv. de aard van het geërodeerde hinterland (sedimentair of kristallijn), de morfologie van de shelf (diepte, aan- of afwezigheid van een shelftrog), het karakter (gedeeltelijk of volledig marien) en basaal regime (nat of droog) van de ijskap, de steilte van de continentale helling, de manier van terugtrekking van de ijskap (gradueel afsmelten of catastrofaal opbreken), etc. Vaak zijn deze factoren niet van elkaar los te koppelen. Alle lijken ze, direct of indirect, invloed uit te oefenen op de stabiliteit van de sedimenten die tijdens glaciaties op de bovenste continentale helling worden afgezet. Mogelijk verklaren ze ook ten dele de sterk uiteenlopende glaciële sedimentdiktes in de depocentra van centraal Oost-Groenland (1 km) en de westelijke Barents Zee (3 km). Grootschalige massabewegingen treden bij voorkeur op waar hoge accumulatiesnelheden heersen, sedimenten fijnkorrelig en water-verzadigd zijn, en de continentale helling niet al te steil is (ca. 1°). De voorwaarden waaronder een submariene waaier tot ontwikkeling komt, worden minder goed begrepen. Het regelmatig optreden van gekanaliseerde turbidietstromingen vereist waarschijnlijk een hoger zandpercentage in de glaciaal afgezette sedimenten, evenals een relatief steile helling (ca. 3° of meer), en de eventuele aanwezigheid vooraf van canyons of kanalen die de continentale helling traverseren. Mogelijk spelen specifieke afzettingsprocessen hierbij ook een belangrijke rol, zoals bv. onderstromingen¹⁶ van dichte smeltwatersuspensies die direct aanleiding zouden geven tot turbidietstromingen.

Informatie m.b.t. de timing van accumulatie onderaan de continentale helling volgt uit de geometrische relatie tussen deze afzettingen met de prograderende lagen bovenaan de helling. Ten gevolge van de grootscheepse verstoring van de stratigrafie is deze relatie niet of nauwelijks na te gaan op de Bereneiland Conus. Waarnemingen van de continentale hellingen van centraal Oost-Groenland en de Weddell Zee lijken er echter op te wijzen dat zowel massabewegingen als fan-depositie grotendeels gedefaseerd optreden ten opzichte van de hoofdfase van progradatie, en dus ten opzichte van het glaciaal maximum. Theoretische beschouwingen, vooral omtrent de stabiliteit van de bovenste continentale helling, suggereren dat beide processen bij voorkeur, maar niet exclusief, optreden naar het einde van het glaciaal maximum toe, en tijdens de initiële terugtrekking van de ijskap.

Om af te sluiten wordt het volgende, nog grotendeels tentatieve, cyclisch afzettingsmodel naar voren geschoven voor glaciële continentaalranden:

- tijdens de uitbreiding van een ijskap blijft de sedimentatie beperkt tot een proximale zone voor het voortschrijdende ijsfront, terwijl op de binnen-shelf vooral erosie optreedt; sedimenten die op de buiten-shelf zijn afgezet, worden bij verdere uitbreiding door de ijskap overreden en sterk vervormd;
- tijdens het glaciaal maximum, wanneer de ijskap tot aan de shelfrand aan de zeebodem is gekoppeld, focust de sedimentatie zich op de bovenste continentale helling voor de monding van brede glaciële shelftrokken, waarbij de karakteristieke progradatie tot stand komt. Afhankelijk van de dynamiek van de ijsstromen kan er ook een belangrijke aggradatie plaatsvinden in het distale deel van deze trokken;

¹⁶ Eng. "underflows".

- tegen het eind van het glaciaal maximum, en tijdens de initiële deglaciatie, streeft de destabilisatie van de bovenste continentale helling naar een maximum, waardoor de hellingafwaartse remobilisatie, hetzij door onbegrensde¹⁷ massabewegingen, hetzij door gekanaliseerde turbidietstromingen, in een hoofdfase treedt. Op de shelf worden ondertussen discontinue sedimentpakketten afgezet op plaatsen waar het terugschrijdend ijsfront tijdelijk halt houdt, terwijl afgekalfde ijsbergen het sediment op de zeebodem grondig herwerken;
- tijdens interglaciale periodes heeft het ijs zich teruggetrokken tot op de binnen-shelf of zelfs tot op het land. De meeste sedimenten blijven gevangen in diepe bekkens op de binnen-shelf of in fjorden, terwijl de buiten-shelf, en de continentale helling en glooiing, grotendeels sediment-deficiënt worden, op een beperkte herwerking na die wordt geïnduceerd door oceanische en thermohaliene stromingen.

Toekomstperspectieven

Gezien de beperkte beschikbaarheid van gegevens op de centrale rand van Oost-Groenland, helt dit onderzoek ongetwijfeld sterk over naar de oostzijde van de polaire Noord-Atlantische Oceaan. Toekomstig werk zou zich daarom moeten richten op het verzamelen van nieuwe seismische profielen van intermediaire resolutie langs de Oost-Groenland rand, in een poging een correlatie tot stand te brengen met het beter gekende shelfgebied van Zuidoost-Groenland, waar recent ook enkele ODP-boringen werden uitgevoerd. Op deze manier zou misschien een regionaal stratigrafisch kader kunnen worden opgesteld voor de gehele continentaalrand, zoals dit reeds bestaat voor de rand westelijk van de Barents Zee en Svalbard; ook zou de laterale variabiliteit langs de rand beter aan het licht komen.

Aan de overkant van de oceaan wordt deze zomer nog een ODP-boring voorgenomen ten westen van Spitsbergen. Indien succesvol, zou deze boring moeten leiden tot een nieuwe doorbraak in de ontwikkeling van een chronostratigrafisch referentiekader, geldig over de volledige lengte van de continentaalrand. Hiermee kunnen de boorresultaten gemakkelijk naar de Storfjorden en Bereneiland Coni worden geëxtrapoleerd, zodat de hier geïdentificeerde belangrijke veranderingen in afzettingstijl uiteindelijk gedateerd kunnen worden, en in verband gebracht met variaties in de glaciële evolutie.

Tot slot vergt de verdere ontwikkeling van een glaciaal sequentiestratigrafisch model in elk geval bijkomende gegevens, van meer diverse locaties. Aanvullend hoger-resolutie onderzoek is verder onontbeerlijk om beter te begrijpen wat de rol is van de verschillende afzettingsprocessen die zich op een glaciële rand afspelen, en welke factoren deze processen controleren.

¹⁷ Eng. "unconfined".

CHAPTER I

Sedimentation along glacial continental margins

1. Glacial continental margins: definition and general characterisation

1.1. Definition

Glacial continental margins are defined here as “*continental margins influenced by large ice sheets which at regular intervals were grounded onto the continental shelf, or even to the shelf break*”. Present-day examples (Fig. 1) include the East Greenland and the Barents Sea - Svalbard margins in the polar North Atlantic, the Canadian/Alaskan margins, the margins encircling the Arctic Ocean, and in the southern hemisphere the entire Antarctic continental margin. During interglacials like the present Holocene period the ice sheets may remain marine-based, as along parts of the Antarctic margin, retreat back to the continent, as in Greenland, or disappear entirely, as in the Barents Sea region or in Canada. The presence of ice at the present day is therefore not a prerequisite for the identification of a glacial continental margin. Synonyms used throughout this work are: glacial margin, glaciated margin, polar margin and high-latitude margin.

1.2. Physiographic characterisation

1.2.1. The continental shelf

The continental shelves of glacial margins often display greater depths than normally observed on continental margins. For example, the average water depth of the Barents Sea is about 230 m (Elverhøi et al. 1989), with the shelf break lying in water depths of about 400 m. The East Greenland shelf shows water depths in the range of 250 to 350 m (Johnson et al. 1990). And the southern Weddell Sea continental shelf in Antarctica terminates in water depths of about 500 m (cf. map of Haugland et al. 1985). In contrast, typical values for shelf break water depths in non-glaciated settings are e.g. 140 ± 50 m for the U.S. Pacific margin and 120 ± 100 m for the U.S. Atlantic margin, while the global average is about 130 m (Shepard 1973). Overdeepening of the continental shelf thus seems to be characteristic of polar margins, and is probably mainly related to severe erosion during repeated ice sheet advances.

The morphology of most glacial shelves is characterised by broad transverse troughs in which even larger water depths are recorded (Fig. 2). These are glacially eroded and overdeepened troughs which most likely were shaped by converging ice streams during periods when the ice sheet advanced onto



Fig. I.1 - Distribution of present-day glacially-influenced continental margins in the world.

the continental shelf (Anderson 1989; Vorren et al. 1989). Commonly, these troughs exhibit a foredeepened profile, i.e. their floor slopes landward and reaches maximum depths on the inner shelf; this is attributed to a stronger erosive power of ice streams in their upstream portions, and net deposition in their outer segments (ten Brink & Cooper 1992). In Antarctica, deeply eroded glacial troughs extend seaward from virtually every major ice stream (Anderson 1989). One of the largest of those is Crary Trough, extending beyond the Filchner Ice Shelf in the Weddell Sea: the trough has a maximum observed water depth of 1140 m near the ice shelf, and a depth of about 630 m at the shelf edge (Haugland et al. 1985). Another such glacial trough is the Laurentian Channel, a 700 km long and 80 km wide depression that crosses the Canadian Atlantic margin and has been excavated some 300 m below the regional depth of the shelf (Piper et al. 1985). The shelf break at the mouth of the channel lies in a water depth of c. 400 m. The Barents shelf in the polar NE Atlantic is dominated by the Bear Island Trough, a 720 km long and 170 km wide glacial trough cutting the continental shelf down to water depths of over 400 m (Perry 1986); the trough is thought to be located in the converging area of the Weichselian Barents Sea and Fennoscandian Ice Sheets (Vorren et al. 1989).

1.2.2. *The continental slope*

The continental slope beyond the mouth of a glacial trough usually shows a higher degree of progradation than the adjacent portions of the margin (Fig. 2), because the troughs represent the preferential glacial outlets, and thus the main sediment discharge routes. The glaciomarine sediments that thus have been supplied to the margin build large depocentres below the outer shelf and upper slope, evident as prominent seaward-convex bulges in the bathymetry off the trough mouths. These depocentres usually have a somewhat oblate shape rather than the radial or elongate form observed in front of river deltas on low-latitude margins, because the grounded ice sheet from which they are deposited represents a short line source rather than a point source (Larter & Cunningham 1993).

Major depocentres of prograding sediments, located below the outer shelf/upper slope and spreading out from the mouth of glacial shelf troughs, have been referred to as "trough mouth fans" (TMF's) by Vorren et al. (1988). Although they have the morphological appearance of a fan, they should not be confused with submarine fans, a term which has a rather strict sedimentological connotation (cf. specific volumes on this subject, edited by Bouma et al. 1985 and by Weimer & Link 1991). The term submarine fan is understood here as "*a radial to elongate cone of sediment deposited on the basin floor by channelised turbidity currents*", a definition which was slightly modified from Nelson & Nilson (1984). The block diagram in Fig. 3 schematically outlines some of the essential features of a submarine fan: [i] submarine fans are usually cone- or fan-shaped sediment bodies hugging the foot of the continental slope, [ii] they are associated with a path leading across the outer shelf and upper slope, typically a large river or submarine canyon, that provides a fixed point source (Mitchum 1985), [iii] most of the sediment is deposited by turbidity currents (Mitchum 1985; Posamentier et al. 1991), flowing within the confines of a large fan valley that divides further downslope into several distributary channels as the flows gradually loose confinement; overbank flow results in development of pronounced levees along the fan valley (Normark 1978), [iv] the presence of lobe (or sheet sand) deposits is essential (Shanmugam & Muiola 1988).

Some major glacial depocentres may be associated, however, with a submarine fan further downslope, which may have added to the considerable confusion presently existing. The best known examples of such a configuration are probably the Laurentian Fan on the Canadian Atlantic margin (Stow et al. 1981; Normark et al. 1983; Piper et al. 1985), and the Crary Fan in the SE Weddell Sea, Antarctica (Kuvaas & Kristoffersen 1991; Moons et al. 1992).

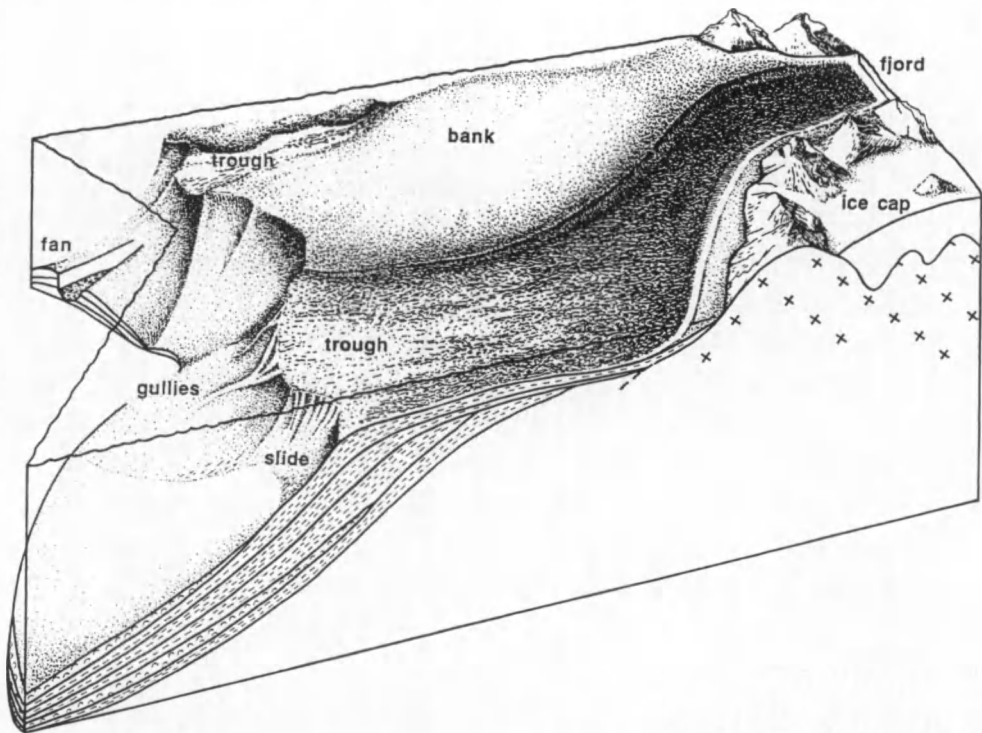


Fig. I.2 - Conceptual sketch model of an idealised glacial continental margin, showing prograding upper slope depocentres at the mouth of broad transverse shelf troughs. Upper slope depocentres may be associated with a submarine fan lower on the slope.

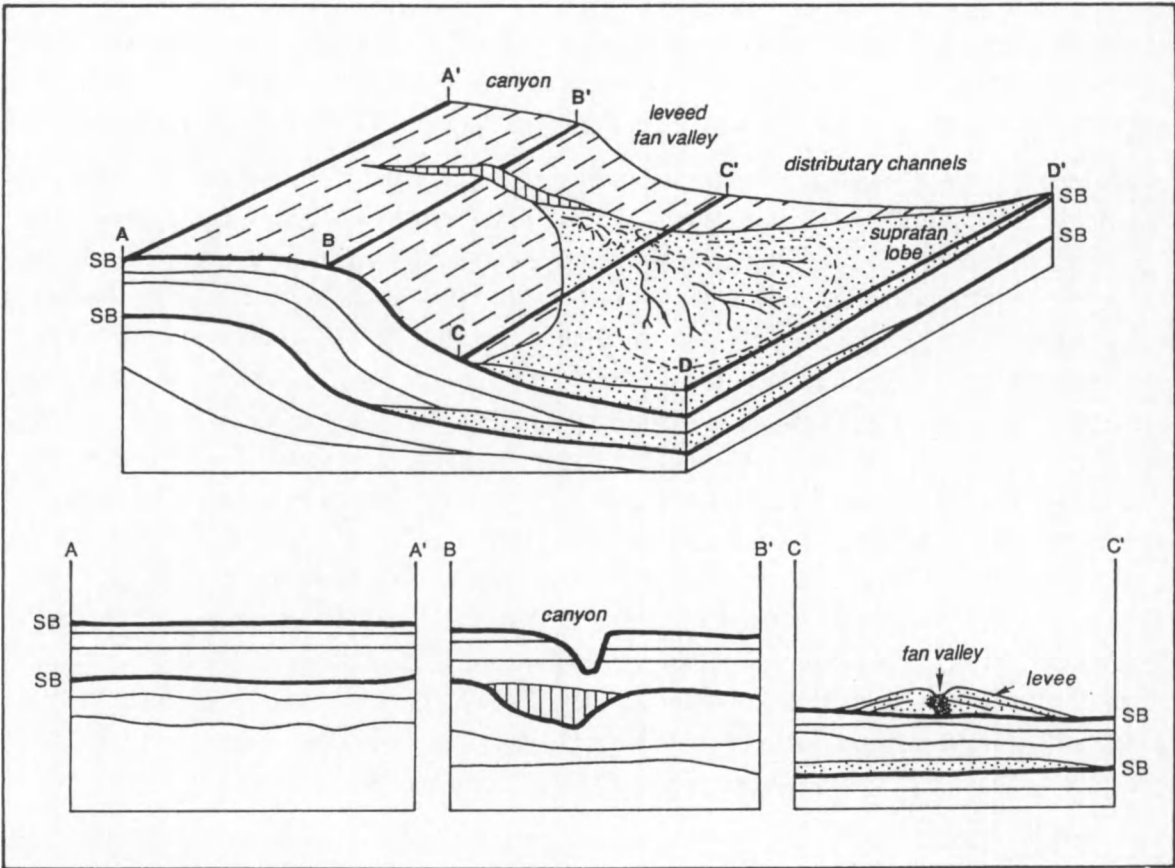


Fig. I.3 - Conceptual sketch model of a submarine fan at the foot of the continental slope (from Weimer & Link 1991). The upper fan is characterised by a leveed fan valley which divides into numerous distributary channels on the middle fan. The middle fan usually has a convex-upward profile and lobate shape (suprafan lobe).

2. Sedimentation processes acting on a glacial margin

2.1. Deposition by the direct action of ice

The residence of ice caps on a continental margin results in a depositional environment strongly differing from the “normal” (= low-latitude) setting. Debris transported within large glaciers was introduced to the outer shelf / upper slope system during repeated glacial advances, in sufficiently large quantities to produce the observed prograding depocentres. Deposition of sediment from ice sheets mainly occurs by the following glacial (1, 2 and 3) and glaciomarine (4 and 5) processes (Fig. 4):

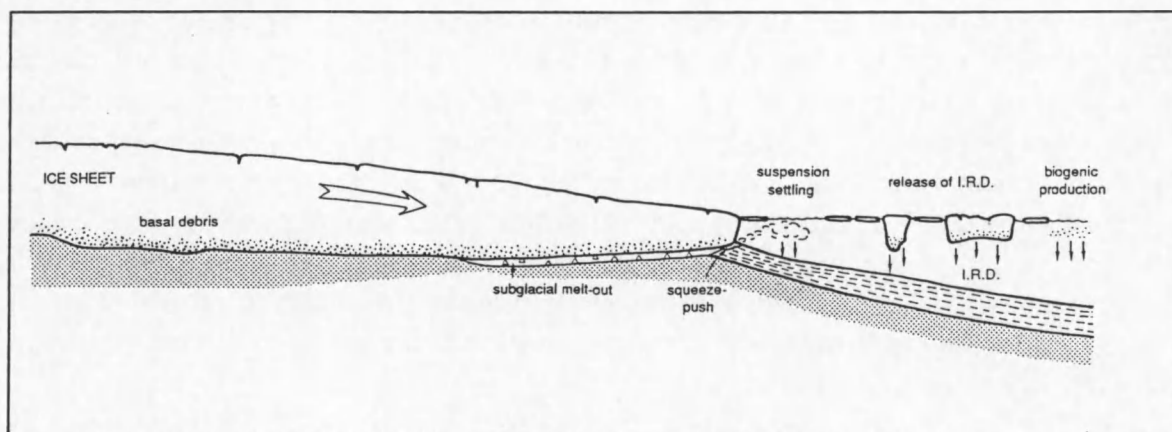


Fig. 1.4 - First-order depositional processes on a glaciated margin: subglacial melt-out, squeeze and push, settling from meltwater plumes, and release of ice-rafted debris; also indicated is the accumulation of biogenic products.

[1] Basal melt-out of entrained debris

The bulk of the sediment transported within grounded ice is entrained in thick layers close to the bed. Part of this basal debris is released underway by subglacial melt-out or “lodgement”, from ice in direct contact with the sea bed (King et al. 1987). The resulting deposit is till, a very poorly sorted deposit lacking stratification, and often showing evidence of overconsolidation (King et al. 1987).

[2] Deformation of basal till

The rapid advance of an ice stream or outlet glacier to the edge of the continental shelf can be lubricated by deformation of a several metres thick, water-saturated till (consisting of lodgement till and remoulded glaciomarine mud). Only recently, such a deforming subglacial till layer has been directly observed, beneath Ice Stream B on the Ross Sea Ice Shelf (Alley et al. 1989). In this situation, subglacial meltwater is thought to be distributed in a thin, pressurised basal film effectuating the ice-till coupling, rather than in subglacial channels. Contrasting views exist regarding the erosional capacity of a deforming till layer: according to Boulton & Jones (1979) it does not, or only slightly, erode the underlying sediments, whereas Alley et al. (1989) argue that the mobile layer results in an erosional unconformity. A deforming basal till would imply the possibility of a sediment flux at least an order of magnitude greater than the maximum estimates of sediment flux resulting from any other glacial transport mechanism. Large volumes of unsorted, water-saturated and unconsolidated sediment would thus be deposited at the mouth of an ice stream,

producing a deltaic feature with a small surface slope (c. 1°) all along the grounding line (see Fig. 11b). Such till-fed deltas can be tens of kilometres long and tens of metres thick.

[3] Squeeze and push

An advancing ice mass can exert large horizontal pressure on the seafloor sediments lying in front. As a result, these sediments are squeezed up into ridges or push moraines of highly consolidated material, in which thrust planes can sometimes be recognised. Push moraines commonly exhibit a seaward-convex external shape, and can reach a thickness of a few tens of metres. Best preserved are those push moraines marking the maximum extent of the ice sheet, e.g. at the shelf edge.

[4] Release of ice-rafted debris (IRD)

Icebergs calving from an ice front commonly contain sediments not previously melted out. The debris content of icebergs depends on the type of ice front they calve from: most ice shelves don't produce bergs containing significant amounts of basal debris, while rapidly calving outlet glaciers appear to be the dominant source of debris-rich sediments (Drewry 1986). Sea ice may also transport a significant quantity of sediment. Release of sediment from drifting ice can occur as gradual melt-out, but also as dumping when the ice abruptly turns over. The ice-rafted debris contributes as dropstones to the glaciomarine sediment that is deposited beyond the grounding line; when sediment rain is dominated by IRD a heterogeneous clast-rich diamicton tends to form (Boulton 1990). The importance of this sedimentation process lies in the delayed release of the enclosed debris, which is dispersed over considerable distances. The spatial distribution of IRD can vary strongly depending on bathymetry and circulation of wind and surface water, factors controlling the preferred ice trajectories (Boulton 1990).

[5] Settling from subglacial meltwater streams

Whether a glacier is drained by subglacial meltwater depends on its basal thermal regime, which is controlled by climate (Powell & Molnia 1989): temperate glaciers are wet-based and slide rapidly over their bed; large discharge of meltwater near the grounding line results in extremely high sedimentation rates. In contrast, cold polar glaciers are dry and frozen to the substrate; they move by internal deformation — an order of magnitude slower than temperate glaciers — and produce little meltwater. Subpolar glaciers, having bases with complex freezing/thawing zones, primarily result in thick basal debris accumulations.

Meltwater streams entering the sea through tunnels in or beneath the ice experience a dramatic velocity drop; as a result coarse-grained sediment is deposited in stream-fed fans or deltas close to the grounding line, while fine-grained sediment goes into suspension (Powell & Molnia 1989). Depending on the density of the suspensions and on the sea water density stratification, overflows or interflows (causing turbid meltwater plumes) or — in rare cases — underflows (resulting directly in turbidity currents retaining bed contact; Henrich 1991) will be initiated. Settling from meltwater plumes results in deposition of underconsolidated glaciomarine mud (Boulton 1990). The rates of sedimentation from suspension can be very high close to the glacier front, but fall off logarithmically with distance. In the glacier-proximal zone (10 - 25 km) suspension settling overwhelms contribution from IRD, whereas the iceberg-dropped component becomes important in the distal zone (Fig. 5, Boulton 1990). Meltwater plumes can reach 50 to 100 km from the ice margin.

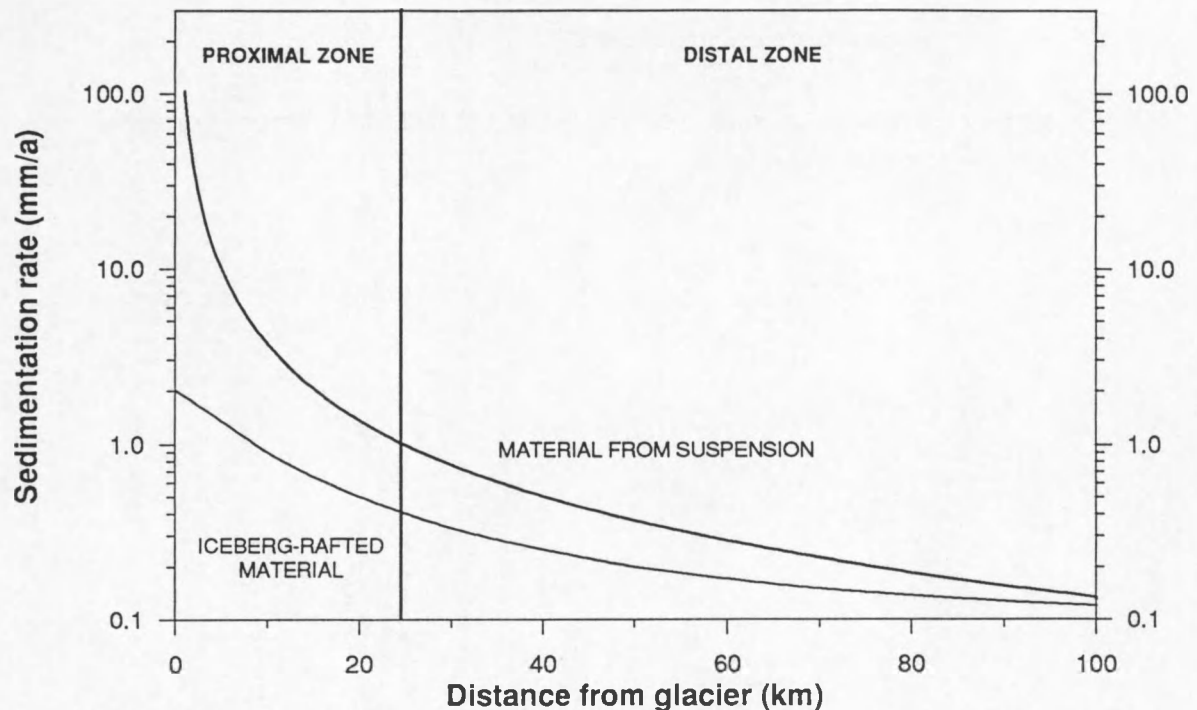


Fig. 1.5 - Relationship between sedimentation rate and distance from the glacier for suspension settling and iceberg rafting (Boulton 1990).

2.2. Other sedimentation mechanisms

Of the marine sedimentation processes that also take place on a normal continental margin, biogenic sedimentation is probably the most important process in a glacial setting. Fluvial discharge in contrast is mostly limited: the rivers that develop when the ice sheets have retreated back to the continent are too small to significantly contribute to sedimentation on the continental shelf and slope. Only when the ice sheet disappears completely, major river systems can develop, leaving their imprint on the margin as they do on lower-latitude margins.

Pelagic sedimentation

The contribution of biogenic material is regulated by sea ice: biogenic production is near zero under a perennial ice cover, but can be abundant where the ice cover is seasonal. In polynyas, continuously ice-free regions produced under the influence of e.g. katabatic winds, productivity can exist throughout the year. Upwelling of deep water along the continental slope can result in enhanced nutrient supply sustaining high rates of biological productivity (Anderson et al. 1984). The resulting biogenic ooze is usually thin and well stratified, and occurs in a distal position with respect to the ice front (Anderson et al. 1991).

2.3. Secondary sedimentation processes

Remobilisation of previously deposited sediment can be effectuated by various processes, some of them unique to the glacial setting (Fig. 6):

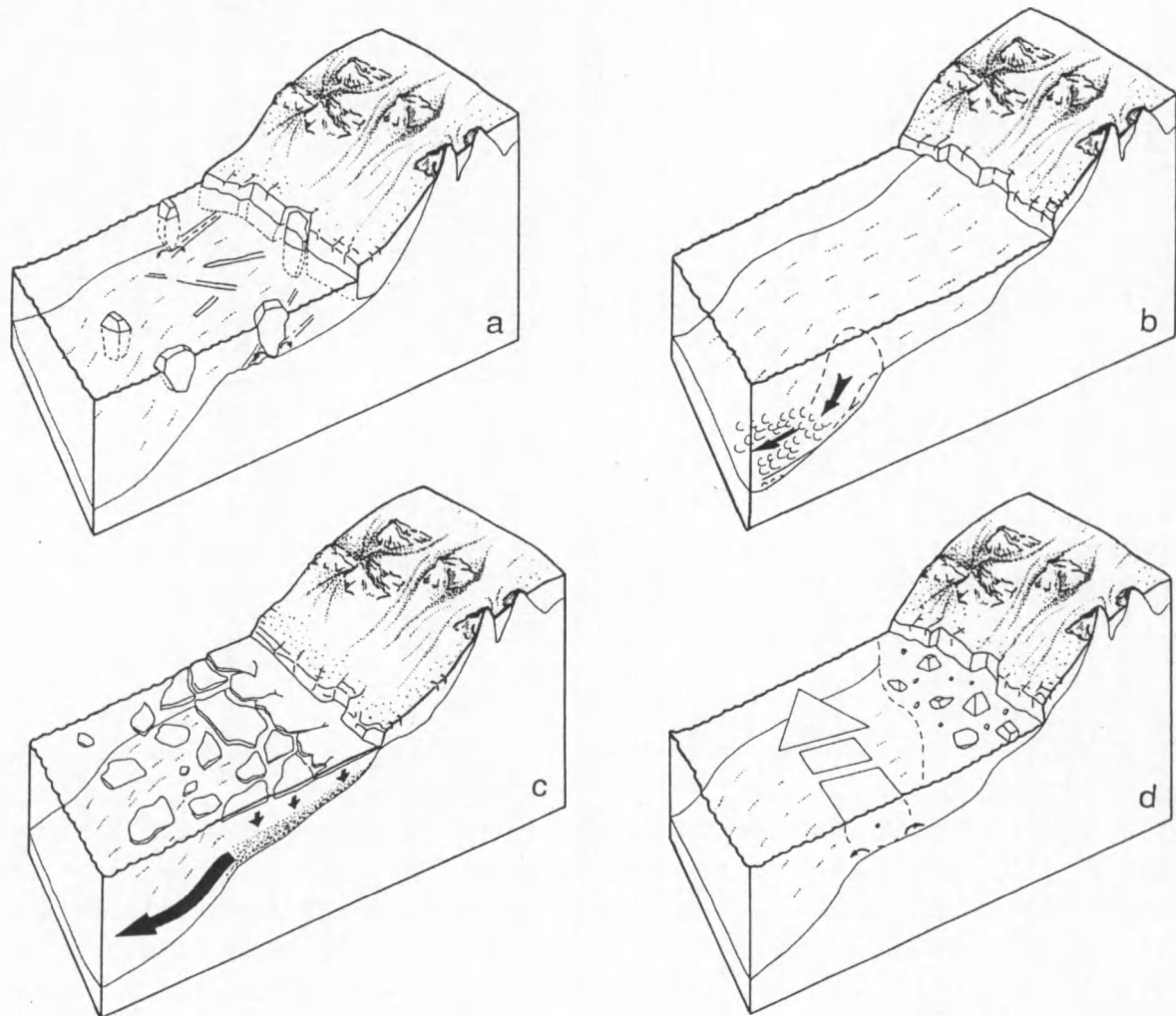


Fig. 1.6 - Secondary sedimentation processes on a glacial margin: [a] iceberg scouring, [b] gravitational mass transport, [c] downslope thermohaline circulation, and [d] winnowing by long-shelf currents. Partly adopted from Henrich et al. (1989). Not to scale.

[1] Iceberg ploughing

Scouring by iceberg keels severely disturbs the seafloor sediments on the shelf down to water depths of about 300 m on average. Sediment reworking involves the resuspension and selective removal of the fine-grained fraction, and the resulting deposit is termed an iceberg turbate (Vorren et al. 1983; Josenhans & Fader 1989).

[2] Mass movements

Seafloor failure and subsequent gravitational transport frequently occur on most continental slopes; these mass movements commonly occur as slides or slumps grading downslope into debris flows and further into turbidites. Totally unsorted tillite becomes gradually sorted in downslope direction by this process (J.B. Anderson, Erasmus intensive course 1993). More importantly, thick masses of glacially-influenced sediment can thus accumulate on the lower slope, at large distances from an ice margin (Syvitski 1994).

[3] Downslope thermohaline currents

Dense shelf water masses, generated by salt rejection during seasonal formation of sea ice, result in episodic currents flowing down the continental slope (Elverhøi et al. 1989). These thermohaline currents can erode gullies on the upper continental slope (Vorren et al. 1989) and carry significant amounts of fine-grained sediment with them. This transport ceases at a depth where the cold water meets equally dense deep-sea water and forms an interflow, hereby loosing bed contact (Vorren et al. 1989). Dense shelf water formation ceases during complete glaciations of the shelf.

[4] Along-shelf currents

During interglacials, when the outer shelf and upper slope are free again from ice, the strong long-shelf surface water currents related to global oceanic circulation patterns, are re-established, causing sediment reworking and winnowing down to considerable depth. As a result, sandy and gravelly lag horizons are formed on the shelf (Vorren et al. 1988; Boulton 1990).

3. Models for sedimentation along glacial continental margins

3.1. Limitations of the sequence stratigraphic model

Our knowledge about sedimentation along continental margins has greatly expanded the past few years by the concept of sequence stratigraphy (Posamentier et al. 1988; Posamentier & Vail 1988). The model was originally formulated for non-glaciated margins, where sediment is supplied to the margin mainly by river systems. It explains the geometry of the marginal deposits in terms of changes in relative sea level, and has been successfully applied to a number of continental margins all over the world. In the absence of major vertical tectonic movements, as is the case on most mature passive margins, relative sea level more or less coincides with the global eustatic cycle, the high-frequency components of which are glacially driven: eustatic sea level changes of 3rd or higher order are associated with changes in ocean water volume caused by fluctuations in climate and ice volume, and are therefore referred to as glacio-eustatic sea level changes (Vail & Hardenbol 1979).

The sequence stratigraphic model essentially predicts (Fig. 7) that when sea level drops beneath the shelf edge (contemporaneous with the expansion of major ice sheets), canyons are incised in the outer shelf and upper slope, guiding the passage of mass flows that lead to the deposition of a lowstand fan on the basin floor. This is followed by the deposition of a progradational lowstand wedge on the slope at the time of eustatic minimum (glacial maximum). During the subsequent sea level rise (break-up of major ice sheets) a backstepping transgressive systems tract of relatively small volumetric importance is deposited, mainly on the shelf. At times of high sea level stand (interglacials), first aggradation and later progradation of shelfal sediments takes place.

Along polar margins large amounts of ocean water are trapped in expanding ice sheets during glacial periods and released again during interglacial phases. As polar margins thus are the loci where the processes take place governing eustatic sea level, and consequently global sedimentation patterns, one could be tempted to conclude that the same depositional architecture will develop here, contemporaneously.

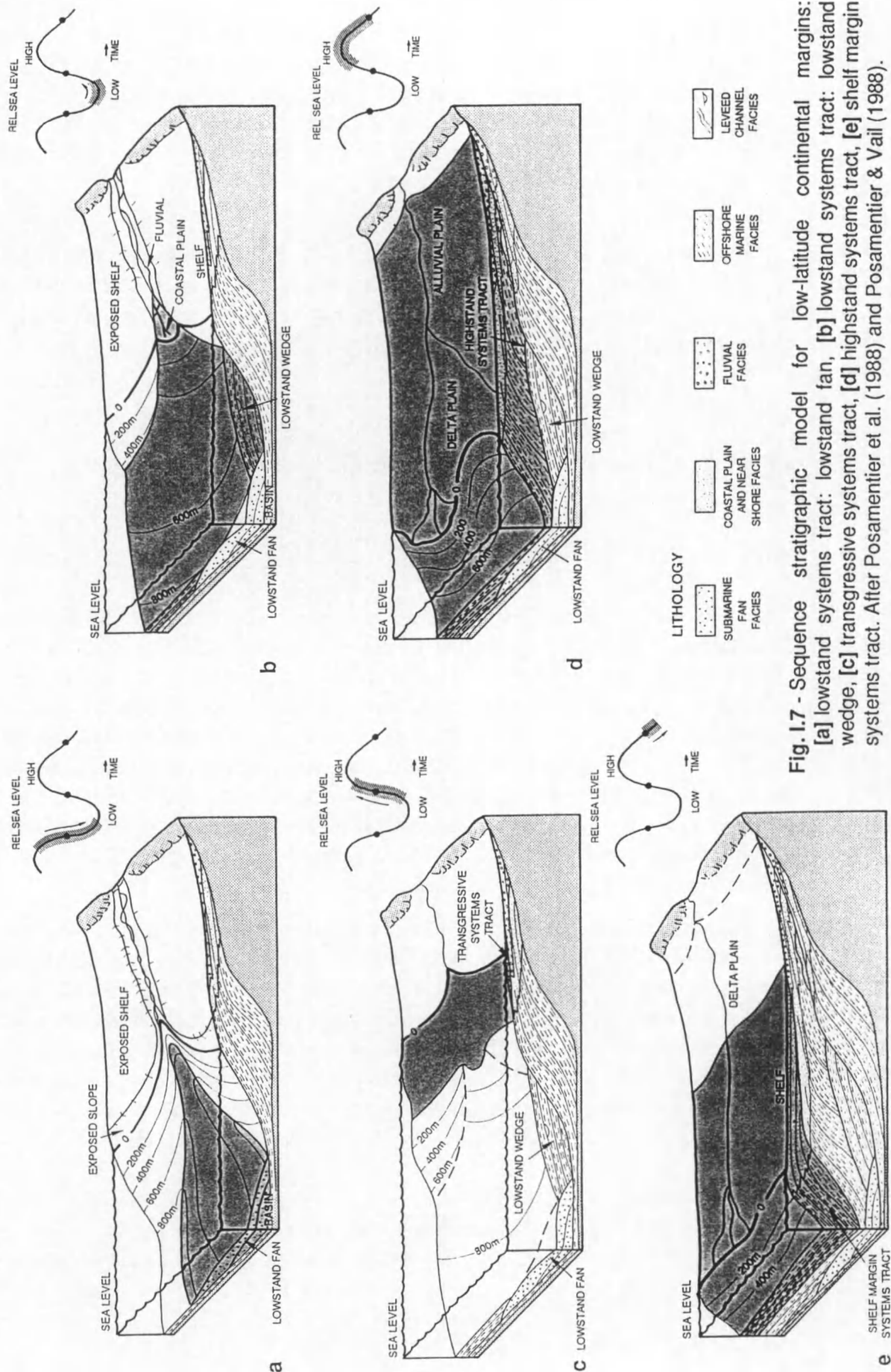


Fig. 1.7 - Sequence stratigraphic model for low-latitude continental margins: [a] lowstand systems tract: lowstand fan, [b] lowstand systems tract: lowstand wedge, [c] transgressive systems tract, [d] highstand systems tract, [e] shelf margin systems tract. After Posamentier et al. (1988) and Posamentier & Vail (1988).

There are a few additional factors to consider, however:

- In sharp contrast to lower-latitude margins, there are no rivers involved in the supply of sediment to a polar margin. Sediment erosion and deposition is effectuated by glacial processes (see previous section) which are quite different from the processes considered in the sequence stratigraphic model. Another major difference is the fact that glaciers and ice sheets don't adjust to varying sea level the same way rivers do. Sea level represents a base level for rivers: when sea level drops, rivers incise into the shelf delivering their load to the outer shelf and upper slope; during sea level rise sediment is deposited on the alluvial plain and near to the coast (Posamentier et al. 1988; Posamentier & Vail 1988). The shift in depocentre is thus caused directly by a change in relative sea level. On polar margins ice caps build and expand on the continental shelf during the larger glacials; sediment transported within the ice is then deposited near the shelf break. During interglacials the ice retreats, and the depocentre correspondingly shifts landward. This shift in depocentre thus occurs in response to the movement of ice sheets, which is not necessarily in phase with the global glacio-eustatic cycle (cf. Boulton 1990).
- During glacial advances the accommodation space on the shelf is limited by the ice sheet rather than by sea level, whereas during interglacials not enough sediment is supplied to fill in the freed accommodation space.
- Along glaciated margins, vertical movements can occur due to the isostatic effects of expanding ice sheets. Such glacio-isostatic movements can have amplitudes comparable to glacio-eustatic sea level fluctuations (but noticeably decreasing towards the shelf break), and therefore have implications for relative sea level. During ice sheet expansion, the lithosphere under the continental shelf and upper slope is isostatically depressed; rebound takes place after retreat of the ice sheet. Due to the large viscosity of the accommodating flow in the asthenosphere, isostatic movements display a certain lag behind the glacial cycle, in contrast to the eustatic effect which is immediate. Boulton (1990) calculated the resulting complex pattern of relative sea level change in space and time (see Fig. 10): at the shelf break e.g., relative sea level is seen to drop before glacier advance to this position, to rise during glacial maximum, and to drop again during deglaciation.
- Most present glacial shelves are overdeepened, and several researchers (Cooper et al. 1991; J.B. Anderson, Erasmus intensive course 1993) have already pointed out that these depths (generally over 300 m) by far exceed the combined amplitude of glacio-eustatic sea level fluctuations and glacio-isostatic vertical movements, indicating that relative sea level changes have virtually no direct control on the sedimentation patterns in such a setting. Most glacial shelves could for instance not have been exposed at any time during the glacial cycle, at least not during the most recent cycles.

In summary, sedimentation along glacial margins is not directly related to relative sea level fluctuations, but occurs in response to the expansion and retreat of ice sheets onto the continental shelf — which may itself in some cases be influenced by sea level, however. This doesn't mean, though, that the whole concept of sequence stratigraphy should be abandoned: sedimentation on a glacially influenced margin is clearly cyclic in nature, and all sediments deposited during one glacial cycle can therefore be regarded as a depositional sequence. The erosional surfaces created on the shelf during glacial advances could be regarded as sequence boundaries; likewise, the boundary till/glaciomarine sediments, reflecting glacial retreat, would correspond to the maximum flooding

surface in sequence stratigraphic terminology (J.B. Anderson, Erasmus intensive course 1993). The latter boundary is easily defined in sediment cores, but is probably hard to image seismically. Sedimentation mechanisms unique to the glacial environment will cause the systems tracts deposited along polar margins to differ from those deposited along lower-latitude margins during corresponding periods of time, or even corresponding levels of relative sea level. Finally, caution should be exerted when correlating glacial sequences to the global sequence cycle chart of Haq et al. (1987), as ice sheets can behave very differently: the larger northern hemisphere ice sheets (e.g. the Laurentide Ice Sheet) are known to dominate the high-frequency eustatic cycles of the Plio-Pleistocene (J.B. Anderson, Erasmus intensive course 1993); growth and decay of smaller ice caps can lead or lag the eustatic cycle (Boulton 1990), though a phase-relationship may still exist between the sequences deposited along their margins and those on a lower-latitude margin. The Antarctic ice sheets, on the other hand, respond passively to the eustatic cycle, but not in a very sensitive way: large parts of the Antarctic ice sheets are still marine-based under the present interglacial conditions.

3.2. A discussion of glacial sequence stratigraphic models

Authors working on glaciated margins have advanced several cyclic sedimentation models the past few years, relating the observed stratal geometries to alternating periods of glaciation and ice-free conditions. These models have in common that they are still relatively simplistic and lack detail, as they are to a large extent based on low-resolution multi-channel seismic (MCS) data. Four selected models illustrate the current views.

3.2.1. Model proposed by Larter & Barker (1989, 1991)

The model for deposition of glacial margin sequences proposed by Larter & Barker (1989 and 1991) is largely based on MCS profiles from the Pacific margin of the Antarctic Peninsula. This model is illustrated in Fig. 8. A sequence begins, and ends, at the start of glacial recession. During interglacials, an “intergrounding subsequence” (IGS) of unconsolidated glaciomarine and pelagic sediment is deposited on the shelf and slope [a]. During the next phase of cooling an advancing ice sheet grounds on the shelf [b]. Depending on such factors as ice sheet thickness, basal temperature and sediment supply, the grounded ice sheet erodes part of the IGS or deposits a basal till above it. When at glacial maximum the ice sheet is grounded out to the shelf edge, unsorted material is transported in a basal debris zone to the outer shelf and upper slope to form a “grounding subsequence” (GS), steepening the slope [c]. The prograding slope, largely consisting of unsorted glaciomarine diamicton, is quite stable and shows no evidence of major failure. This stability is attributed to the textural composition of the slope sediments (unsorted mixture of sand and gravel) and to overcompaction of the sediment near the shelf break. Deposition of the next IGS starts when the ice sheet decouples, or shortly beforehand if a thinning but still grounded ice sheet becomes everywhere depositional [d].

Note that this model relates all shelf aggradation to interglacial periods.

3.2.2. Model proposed by Vorren et al. (1989)

The glacial depositional model of Vorren et al. (1989), depicted in Fig. 9, mainly derives from seismic observations from the southwestern Barents Sea margin. During glacials [a] advancing ice

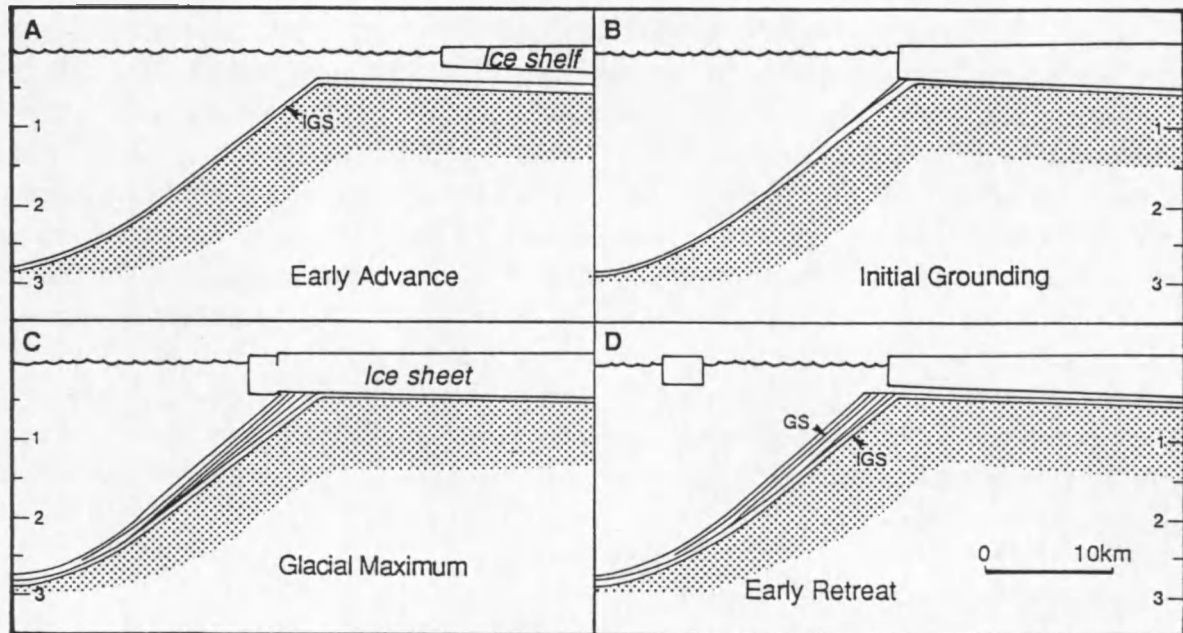


Fig. 1.8 - Model for the development of a glacial margin sequence, proposed by Larter & Barker (1989): [a] early stage of ice sheet advance: deposition of an intergrounding subsequence (IGS) on shelf and slope, [b] initial grounding, [c] glacial maximum: ice sheet is eroding and compacting shelf sediments and is depositing a grounding subsequence (GS) on the slope, [d] early stage of glacial retreat: hiatus on outer shelf ends and deposition of next IGS begins.

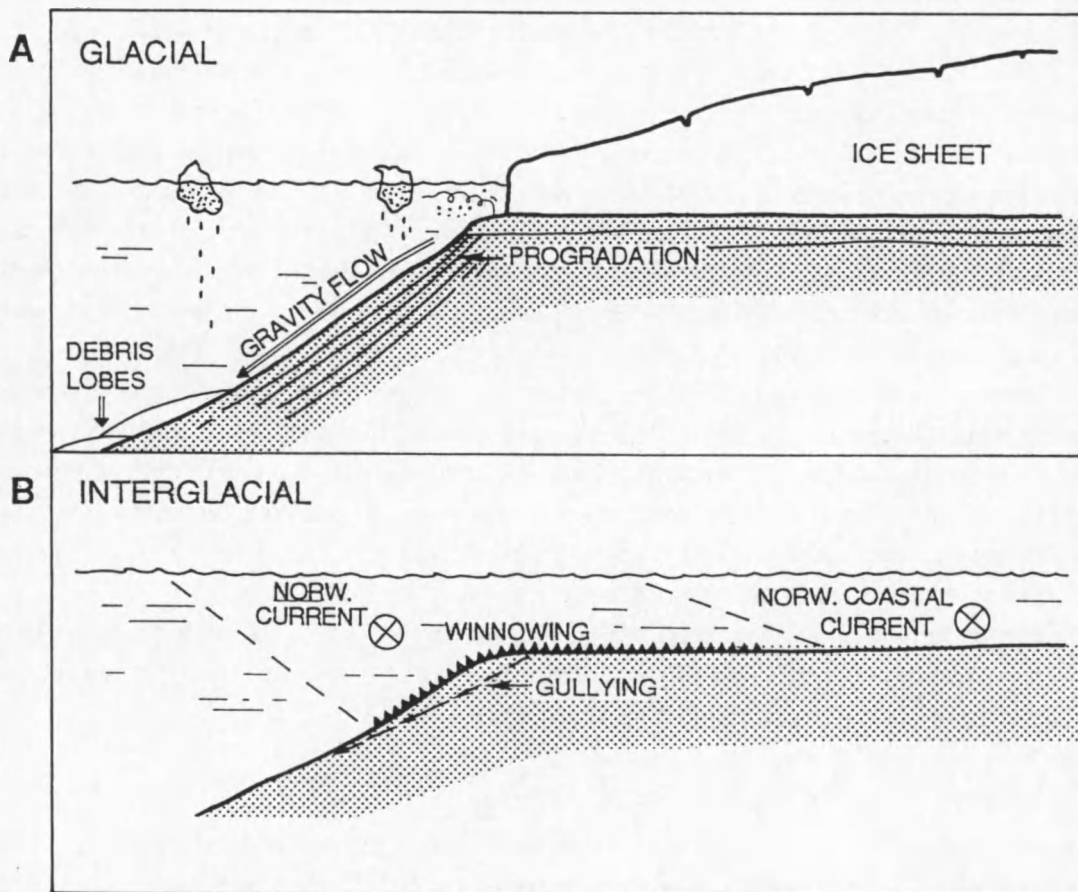


Fig. 1.9 - Schematic model of the main sedimentary processes on the outer shelf and upper slope during glacial and interglacials, proposed by Vorren et al. (1989).

sheets create erosional surfaces that extend all the way to the shelf break. Most of the sediment above this unconformity on the shelf is probably deposited by direct basal melt-out. If the glacier is wet-based, glaciofluvial deposits may also be present. Sedimentation on the upper slope is determined by meltwater plumes (most of which probably escaped at the mouth of glacial troughs) and calving icebergs; part of the prograding deposits may also be deposited as tills. The high input of sediment during glacial phases tends to oversteepen the upper slope, which becomes unstable. Failing of the rapidly deposited sediments generates various types of sediment gravity flows, resulting in accumulation of debris lobes on the lower slope. During interglacials [b] only very small amounts of clastic sediment are introduced to the slope as most of it settles in the fjord basins. Redistribution does occur, however, both by horizontal shelf currents and downslope thermohaline circulation. Note that the intermittent progradation and downslope remobilisation within a single glacial phase predicted by this model, should produce a complex pattern of interfingering slope-attached strata and lower slope units.

3.2.3. Model proposed by Boulton (1990)

Fig. 10 shows the model of glacial margin architecture put forward by Boulton (1990) on the basis of intermediate-resolution seismic data from the western Svalbard margin. An ice sheet advancing onto the continental shelf deposits glaciomarine sediment ahead of its glacial front; when subsequently these deposits are overridden by the ice, they are remoulded into a deformation till which adds to the till deposited by basal melt-out. When the ice sheet has brought the proximal zone of meltwater-plume dominated sedimentation to the outer shelf region, the resulting large discharge of sediment over the shelf edge leads to active shelf progradation. On glacier withdrawal, the outer shelf region becomes relatively starved of a primary sediment supply, and outbuilding of the margin consequently comes to a halt. Relative sea level at the location of the shelf edge drops due to isostatic rebound, leading to collapse of the glacially oversteepened upper slope: sediments deposited during glacial maximum undergo a period of extensive mass wasting, to produce thick sediment accumulations onlapping the middle and lower slope. As the proximal zone of high sedimentation continues to shift landward, the inner continental shelf becomes the site of glaciomarine deposition. When the glaciers have retreated from the shelf, surface water currents are re-established, producing long-shelf sediment dispersion.

There is considerable contrast in the facies architecture between the mouths of glaciated troughs and the shelf edge adjacent to intervening bank areas. In the trough mouths, till is overlain by relatively thick glaciomarine mud units, probably deposited during the early stages of retreat. These thick inter-till units are absent from the bank regions, which is ascribed to their relative shallowness: strong bottom current activity and/or iceberg scouring during glacier retreat remove glaciomarine mud units or rework them in iceberg turbates.

This model is important for two aspects: [i] significant aggradation of the shelf during early glacial and late glacial phases, and [ii] out-of-phase accumulation on the upper and lower slope, reflected by an alternation of prograding units and base-of-slope units.

3.2.4. Model proposed by Kuvaas & Kristoffersen (1991)

Kuvaas & Kristoffersen (1991) based their model (no figure available) on MCS data from the southern Weddell Sea margin, where a large submarine fan system, the Cray Fan, is associated with a major prograding glacial depocentre in front of Cray Trough. Glacial periods are characterised by the advance of ice sheets eroding underlying sediments; truncation of slope foresets may be inhibited,

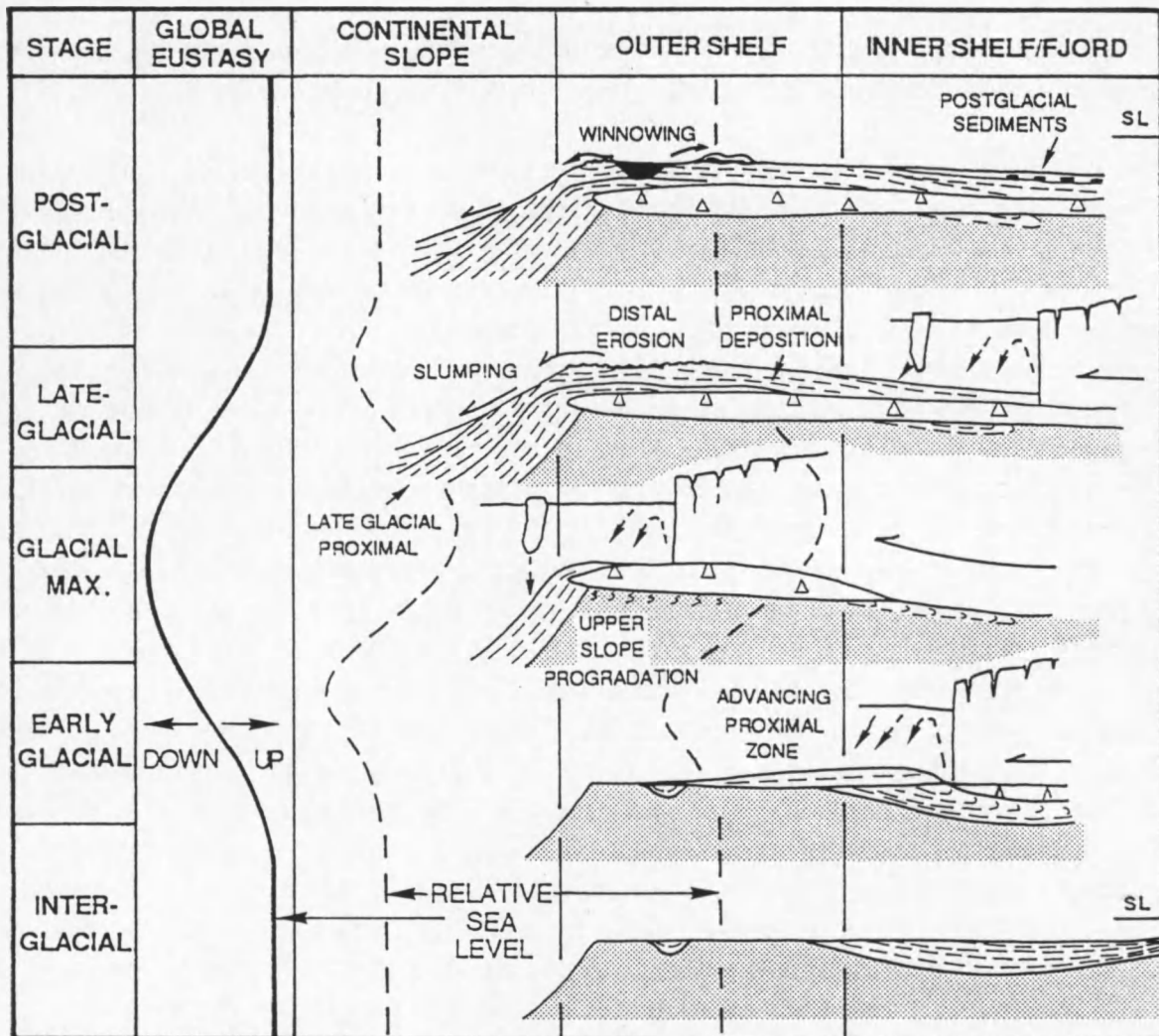


Fig. I.10 - A model of glaciomarine facies architecture for different portions of the continental margin through one glacial cycle, proposed by Boulton (1990). The relative sea level changes appropriate to each zone are shown as well.

however, if considerable amounts of sediment were deposited during the previous glacial retreat. Deposition occurs of basal till, and of dropstone diamictos beneath the floating ice shelf. When the ice sheet is positioned at the shelf edge, large amounts of sediment build out the upper slope. Slumping of rapidly deposited sediments at the grounding line generates mass flows resulting in lens-shaped deposits on the lower slope, while turbidity currents generated by underflow from subglacial meltwater streams, supply sediment directly to the channels feeding the fan, giving rise to widespread channel-levee deposition on the continental slope and abyssal plain. During interglacials, sediment supply to the outer shelf and upper slope is greatly reduced, and the fan becomes essentially sediment-starved. Downslope thermohaline currents develop, but they have low concentrations of suspended matter, and their contribution to deposition on the fan is considered minor. During less extensive glaciations, when the ice sheet did not advance far enough to reach the shelf edge, the continental shelf acted as the main depositional area. The result is aggradation of the shelf, terminating in moraine ridges on the outer shelf, without progradation.

The model of Kuvaas & Kristoffersen (1991) is the only model discussed here involving submarine fan deposition in a glacial setting. The authors suggest that development of channel-levee systems requires meltwater suspensions, and thus a wet-based ice sheet. They also favour a scenario in which

outbuilding of the margin and accumulation on the lower slope, both by slumping and channelised turbidity flows, occur more or less simultaneously, namely during glacial maximum.

The four models reviewed here demonstrate that the grounded ice sheet model is a widely accepted concept amongst researchers studying glacial margins. Most investigators (e.g. Vorren et al. 1988, 1989; Larter & Barker 1989; Boulton 1990; Kuvaas & Kristoffersen 1991; Bartek et al. 1991; Cooper et al. 1991; Anderson & Bartek 1992) indeed support the idea that the thick prograding wedges observed along polar margins have been produced mainly by the action of ice sheets grounded out to the shelf edge at times of glacial maximum. The amount of progradation is seen to vary strongly in a lateral direction along the margin: it is most pronounced in front of the large transverse shelf troughs described above (section 1.2.1), but only minor off the inter-trough areas; this reflects the position of major ice streams. Regarding the origin of this progradation two views can be discerned: on the one hand (Fig. 11a), King & Fader (1986) and King et al. (1987) pointed out that glacial till, forming the “topset beds” of glacial sequences on the continental shelf, is deposited by subglacial melt-out of debris from ice in direct contact with the seabed, whereas seaward of the grounding line stratified glaciomarine sediments (the “foreset beds”) are deposited by settling of debris raining out from the lower surface of a floating ice shelf, as well as from turbid meltwater plumes generated at the grounding line. Small variations in the position of the grounding line would produce the features known as “till tongues” near the edge of the continental shelf. This suggests a wet-based ice sheet. On the other hand (Fig. 11b), observations by Alley et al. (1989) have revealed that fast-moving polar ice streams in Antarctica can move by basal shear deformation of unconsolidated sediments, thus dragging debris along the base of the ice stream. At the grounding line this debris is released beneath a floating ice shelf into a subglacial delta with geometries comparable to those observed near the shelf edge in prograding glacial sequences (cf. Cooper et al. 1991). The topsets of these features consist of deformed till, the fore- and bottomsets of mass flows and some glaciomarine sediments. Erosion of the head of the delta and subsequent recycling allow progradation of the delta and advance of the grounding line; this mechanism is known as “conveyor belt” recycling. Deforming till layers were also inferred to exist beneath some temperate ice sheets (Boulton & Jones 1979), and it is not clear whether their existence precludes the presence of channelised subglacial meltwater — temporarily or continuously.

In contrast to the overall agreement regarding the timing of margin outbuilding, notorious variations are noted among the models outlined above with respect to the timing and mode of sediment accumulation on the lower continental slope. In the model of Larter & Barker (1989) no significant phase of lower slope accumulation is considered: downslope redeposition by small-scale mass movements more or less takes place continuously. Vorren et al. (1989) and Kuvaas & Kristoffersen (1991) propose that sediment bodies on the lower slope develop during glacial maximum (i.e. simultaneously with the main phase of progradation of the margin), whereas Boulton (1990) favours a model in which debris lobes are deposited on the lower slope during glacial retreat. In addition to the often considered process of slumping, the model of Kuvaas & Kristoffersen (1991) is the only one to describe submarine fan deposition through channelised turbidity currents.

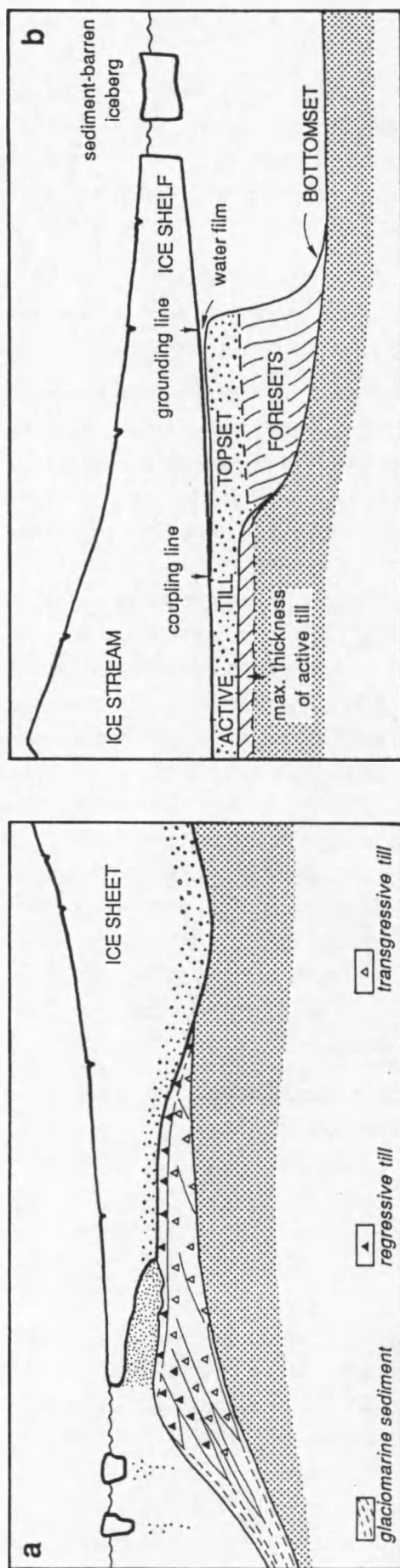


Fig. 1.11 - Two views regarding the origin of shelf edge progradation: [a] in the till tongue model of King & Fader (1986) and King et al. (1987) lodgement till deposited at the base of a grounded ice sheet forms the topset beds of a glacial sequence, whereas glaciomarine sediment deposited below a floating ice shelf build the foresets; [b] in the deformable till layer concept of Alley et al. (1989) remoulded till is dragged along by the movement of the overlying ice, and where the ice becomes gradually decoupled from the till by a mm thick film of water, a till delta develops. The active till layer and the delta are on the order of a few metres and a few tens of metres thick, respectively. Vertical scales in a and b are different.

4. Recognising glacial sequences on low-resolution seismic records

Glacial sequences have geometric features that are commonly observed on polar margins, but that are atypical of low-latitude, non-glaciated margins. Cooper et al. (1991) have proposed the label “type IA” for these specific sequences, as opposed to “type IIA” sequences displaying the more classical geometries described for normal continental margins. The distinction between type IA and type IIA may sometimes be subtle, however.

Type IA sequences, deposited principally by grounded ice sheets, can display the following acoustic characteristics; though each of those characteristics by itself cannot be regarded as a diagnostic criterion for identifying glacial sequences, the combined appearance of several of them probably is:

- strong outward building of the margin by extensive progradation, combined with relatively minor aggradation of the paleo-continental shelf (Cooper et al. 1991);
- horizons of shallow shelf strata with high seismic velocities (2.0 - 2.6 km/s), reflecting overcompaction by ice sheet loading (Larter & Barker 1989; Solheim et al. 1991);
- presence of erosional unconformities extending to the shelf edge below presently overdeepened continental shelves (Larter & Barker 1989). In analogy to the present shelf morphology, these erosional unconformities usually have a foredeepened profile, if the dip has not been reversed already by the load of overlying sediments on the outer shelf; they are furthermore associated with broad glacial troughs (tens to several hundreds of km wide, over 100 m deep) marking the position of former ice streams, and with smaller U-shaped glacially-carved channels which have a width/depth ratio (about 10 km wide and hundreds of m deep) distinctly different from that of fluvially incised valleys (V-shaped, 1 km wide, only tens of m deep) (J.B. Anderson, Erasmus intensive course 1993); because of their orientation normal to the shelf edge, these troughs are best observed on strike-oriented lines;
- presence of major oblate (elongated in transverse direction) depocentres at the mouth of broad glacial troughs, indicating deposition from a short line source at the shelf edge, such as the front of an ice stream, rather than from a point source such as a submarine canyon (Haugland et al. 1985; Larter & Cunningham 1993);
- presence of small ridge-like features near the paleo-shelf edge, interpreted as grounding-line moraines or lift-off moraines (King & Fader 1986).

Identification of a glacial sequence may of course be aided if an ice sheet is present on the margin up to the present day, but is less obvious for older sequences.

5. This work's objectives

The present study will focus on two major northern hemisphere prograding depocentres of supposedly glacial origin, located along geographically opposite margins of the polar North Atlantic Ocean: one on the central East Greenland margin off Scoresby Sund, and the other on the western Barents Sea margin off Bear Island Trough (Fig. 12). The architecture and stratigraphy of the respective margins will be investigated by observing the stratal geometries revealed by seismic reflection records of intermediate to low resolution. The aim is to identify the onset of extensive glacial advances on the shelf, to reconstruct the long-term history of glaciation, and to examine the

applicability of the large-scale glacial sequence stratigraphic models discussed above. Attention will focus on the sedimentation processes governing accumulation on the lower continental slope, as that is the point where current models are diverging at most.

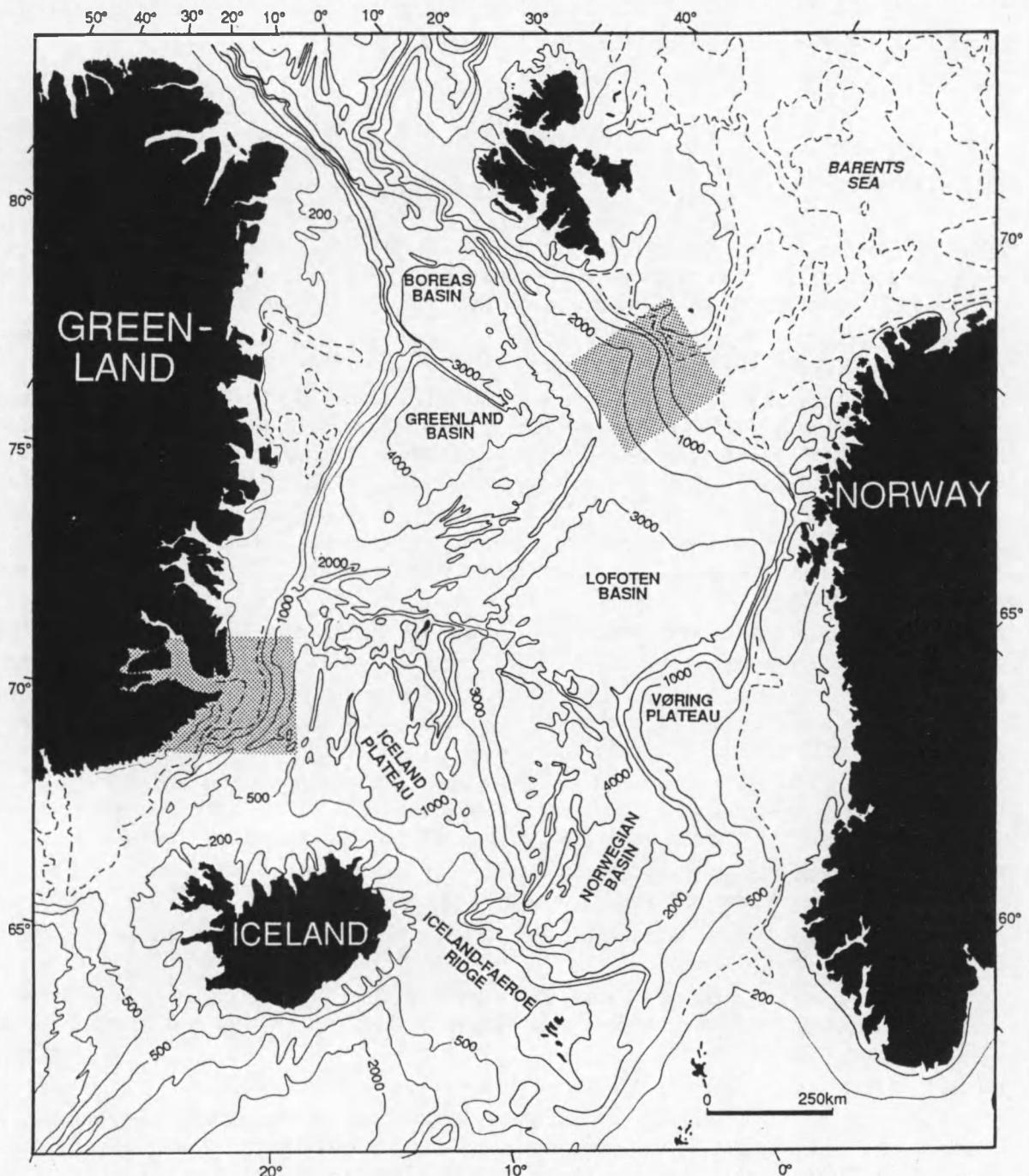


Fig. I.12 - Bathymetry map of the polar North Atlantic Ocean (from Perry 1986), outlining the location of the two different study areas: the central East Greenland margin off Scoresby Sund, and the western Barents Sea margin off Bear Island Trough.

Chapter II is dedicated to the depocentre located on the central East Greenland margin off Scoresby Sund, and includes a seismic study of the Scoresby Sund fjord system itself, while chapter III presents a more detailed investigation of the depocentre located at the mouth of Bear Island Trough on the western Barents Sea margin. In the concluding chapter IV the observations from both margins

will be compared, in order to line up the most striking contrasts and affinities. In addition, the scope will be broadened to a southern hemisphere glacial margin — the SE Weddell Sea margin in Antarctica — as in this area a substantial amount of work has already been carried out by colleagues (PhD. thesis of A. Moons 1992). The main challenge is to isolate the factors determining the varying depositional styles observed on these three glacial continental margins.

References cited

- Alley R.B., Blankenship D.D., Rooney S.T. & Bentley C.R. (1989) — Sedimentation beneath ice shelves : The view from Ice Stream B. In: Powell R.D. & Elverhøi A. (Eds.), *Modern Glacimarine Environments: Glacial and Marine Controls of Modern Lithofacies and Biofacies*. Marine Geology, 85, pp. 101-120.
- Anderson J.B. (1989) — Antarctica's glacial setting. In: Anderson J.B. & Molnia B.F. (Eds.), *Glacial-marine Sedimentation*. Short course, 9, American Geophysical Union, Washington, D.C., pp. 11-57.
- Anderson J.B. & Bartek L.R. (1992) — Cenozoic glacial history of the Ross Sea revealed by intermediate resolution seismic reflection data combined with drill site information. In: Kennett J.P. & Warnke D.A. (Eds.), *The Antarctic Paleoenvironment: A Perspective on Global Change (Part one)*. Antarctic Research Series, 56, American Geophysical Union, Washington, D.C., pp. 231-263.
- Anderson J.B., Bartek L.R. & Thomas M.A. (1991) — Seismic and sedimentological record of glacial events on the Antarctic Peninsula shelf. In: Thomson M.R.A., Crame J.A. & Thomson J.W. (Eds.), *Geological Evolution of Antarctica*. World and regional geology series, 1, Cambridge University Press, Cambridge, pp. 687-691.
- Anderson J.B., Brake C.F. & Myers N.C. (1984) — Sedimentation on the Ross Sea continental shelf, Antarctica. Marine Geology, 57, pp. 295-333.
- Bartek L.R., Vail P.R., Anderson J.B., Emmet P.A. & Wu S. (1991) — Effect of Cenozoic ice sheet fluctuations in Antarctica on the stratigraphic signature of the Neogene. *Journal of Geophysical Research*, 96, pp. 6753-6778.
- Boulton G.S. (1990) — Sedimentary and sea level changes during glacial cycles and their control on glacimarine facies architecture. In: Dowdeswell J.A. & Scourse J.D. (Eds.), *Glacimarine Environments: Processes and Sediments*. Special Publication, 53, The Geological Society, London, pp. 15-52.
- Boulton G.S. & Jones A.S. (1979) — Stability of temperate ice caps and ice sheets resting on beds of deformable sediment. *Journal of Glaciology*, 24, pp. 29-43.
- Bouma A.H., Normark W.R. & Barnes N.E. (Eds.) (1985) — *Submarine Fans and Related Turbidite Systems*. Springer-Verlag, New York.
- Cooper A.K., Barrett P.J., Hinz K., Traube V., Leitchenkov G. & Stagg H.M.J. (1991) — Cenozoic prograding sequences of the Antarctic continental margin : A record of glacio-eustatic and tectonic events. *Marine Geology*, 102, pp. 175-213.
- Drewry D. (1986) — *Glacial Geologic Processes*. Edward Arnold Publishers, London, 276 pp.
- Elverhøi A., Pfirman S.L., Solheim A. & Larssen B.B. (1989) — Glaciomarine sedimentation in epicontinental seas exemplified by the northern Barents Sea. In: Powell R.D. & Elverhøi A. (Eds.), *Modern Glacimarine Environments: Glacial and Marine Controls of Modern Lithofacies and Biofacies*. Marine Geology, 85, pp. 225-250.
- Haq B.U., Hardenbol J. & Vail P.R. (1987) — Chronology of fluctuating sea levels since the Triassic. *Science*, 235, pp. 1156-1167.
- Haugland K., Kristoffersen Y. & Velde A. (1985) — Seismic investigations in the Weddell Sea Embayment. *Tectonophysics*, 114, pp. 293-313.
- Henrich R. (1991) — Cycles, rhythms, and events on high input and low input glaciated continental margins. In: Einsele G., Ricken W. & Seilacher A. (Eds.), *Cycles and Events in Stratigraphy*. Springer-Verlag, Berlin, pp. 751-772.

- Henrich R., Kassens H., Vogelsang E. & Thiede J. (1989) — Sedimentary facies of glacial-interglacial cycles in the Norwegian Sea during the last 350 ka. *Marine Geology*, 86, pp. 283-319.
- Johnson G.L., Grantz A. & Weber J.R. (1990) — Bathymetry and physiography. In: Grantz A., Johnson L. & Sweeney J.F. (Eds.), *The Arctic Ocean Region. The Geology of North America*, Vol. L, The Geological Society of America, Boulder, Colorado, pp. 63-77.
- Josenhans H.W. & Fader G.B.J. (1989) — A comparison of models of glacial sedimentation along the eastern Canadian margin. In: Powell R.D. & Elverhøi A. (Eds.), *Modern Glacimarine Environments: Glacial and Marine Controls of Modern Lithofacies and Biofacies*. *Marine Geology*, 85, pp. 273-300.
- King L.H. & Fader G. (1986) — Wisconsinan glaciation of the continental shelf : Southeast Atlantic Canada. *Geological Society of Canada Bulletin*, 363, 72 pp.
- King L.H., Rokoengen K. & Gunleiksrud T. (1987) — Quaternary seismostratigraphy of the Mid Norwegian Shelf, 65° - 67°30' N : A till tongue stratigraphy. Publication, no. 114, Continental Shelf and Petroleum Technology Research Institute IKU, 58 pp.
- Kuvaas B. & Kristoffersen Y. (1991) — The Crary Fan : A trough-mouth fan on the Weddell Sea continental margin, Antarctica. *Marine Geology*, 97, pp. 345-362.
- Larter R.D. & Barker P.F. (1989) — Seismic stratigraphy of the Antarctic Peninsula Pacific margin : A record of Pliocene-Pleistocene ice volume and paleoclimate. *Geology*, 17, pp. 731-734.
- Larter R.D. & Barker P.F. (1991) — Neogene interaction of tectonic and glacial processes at the Pacific margin of the Antarctic Peninsula. In: Macdonald D.I.M. (Ed.), *Sedimentation, Tectonics and Eustasy: Sea-level Changes at Active Margins*. International Association of Sedimentologists Special Publication, 12, Blackwell Scientific Publications, Oxford, pp. 165-186.
- Larter R.D. & Cunningham A.P. (1993) — The depositional pattern and distribution of glacial-interglacial sequences on the Antarctic Peninsula Pacific margin. *Marine Geology*, 109, pp. 203-219.
- Mitchum R.M. Jr. (1985) — Seismic stratigraphic expression of submarine fans. In: Berg O.R. & Woolverton D.G. (Eds.), *Seismic Stratigraphy II : An Integrated Approach to Hydrocarbon Exploration*. Special Publication, 39, American Association of Petroleum Geologists, Tulsa, Oklahoma, pp. 117-136.
- Moons A. (1992) — Gedetailleerde seismo- en sequentiestratigrafische studie van de Crary Fan, zuidoostelijke Weddell Zee, Antarctica. Unpublished Ph. D. thesis, Universiteit Gent, 174 pp.
- Moons A., De Batist M., Henriot J.-P. & Miller H. (1992) — Sequence stratigraphy of the Crary Fan, Southeastern Weddell Sea. In: Yoshida Y., Kaminuma K. & Shiraishi K. (Eds.), *Recent Progress in Antarctic Earth Science*. Terra Scientific Publishing Company, Tokyo, pp. 613-618.
- Nelson C.H. & Nilson T.H. (1984) — Modern and ancient deep sea-fan sedimentation. Short Course, no. 14, Society of Economic Paleontologists and Mineralogists, Tulsa, Oklahoma, 404 pp.
- Normark W.R. (1978) — Fan valleys, channels, and depositional lobes on modern submarine fans : Characters for recognition of sandy turbidite environments. *American Association of Petroleum Geologists Bulletin*, 62, pp. 912-931.
- Normark W.R., Piper D.J.W. & Stow D.A.V. (1983) — Quaternary development of channels, levees, and lobes on Middle Laurentian Fan. *American Association of Petroleum Geologists Bulletin*, 67(9), pp. 1400-1409.
- Perry R.K. (1986) — Bathymetry. In: Hurdle B.G. (Ed.), *The Nordic Seas*. Springer-Verlag, New York, pp. 211-234.
- Piper D.J.W., Stow D.A.V. & Normark W.R. (1985) — Laurentian Fan, Atlantic Ocean. In: Bouma A.H., Normark W.R. & Barnes N.E. (Eds.), *Submarine Fans and Related Turbidite Systems*. Springer-Verlag, New York, pp. 137-142.
- Posamentier H.W., Erskine R.D. & Mitchum R.M. Jr. (1991) — Models for submarine-fan deposition within a sequence-stratigraphic framework. In: Weimer P. & Link M.H. (Eds.), *Seismic Facies and Sedimentary Processes of Submarine Fans and Turbidite Systems*. Springer-Verlag, New York, pp. 127-136.
- Posamentier H.W., Jervey M.T. & Vail P.R. (1988) — Eustatic controls on clastic deposition I : Conceptual framework. In: Wilgus C.K., Hastings B.S., Kendall C.G.St.C., Posamentier H.W., Ross C.A. & Van Wagoner J.C. (Eds.), *Sea Level Changes: An Integrated Approach*. Special Publication, 42, Society of Economic Paleontologists and Mineralogists, Tulsa, Oklahoma, pp. 109-124.

- Posamentier H.W. & Vail P.R. (1988) — Eustatic controls on clastic deposition II : Sequence and systems tract models. In: Wilgus C.K., Hastings B.S., Kendall C.G.St.C., Posamentier H.W., Ross C.A. & Van Wagoner J.C. (Eds.), *Sea Level Changes : An Integrated Approach*. Special Publication, 42, Society of Economic Paleontologists and Mineralogists, Tulsa, Oklahoma, pp. 125-154.
- Powell R.D. & Molnia B.F. (1989) — Glacimarine sedimentary processes, facies and morphology of the south-southeast Alaska shelf and fjords. In: Powell R.D. & Elverhøi A. (Eds.), *Modern Glacimarine Environments: Glacial and Marine Controls of Modern Lithofacies and Biofacies*. Marine Geology, 85, pp. 359-390.
- Shanmugam G. & Molia R.J. (1988) — Submarine fans : Characteristics, models, classification, and reservoir potential. *Earth-Science Reviews*, 24, pp. 383-428.
- Shepard F.P. (1973) — *Submarine Geology*. Harper & Row, New York, 551 pp.
- Solheim A., Forsberg C.F. & Pittenger A. (1991) — A stepwise consolidation record for the glacial sediments of Prydz Bay and its relationship to the glacial history of East Antarctica. *Proceedings of the Ocean Drilling Program, Scientific Results*, 119, pp. 169-184.
- Stow D.A.V. (1981) — Laurentian Fan : Morphology, sediments, processes, and growth pattern. *American Association of Petroleum Geologists Bulletin*, 65, pp. 375-393.
- Syvitski J. (1994) — Glacial sedimentation processes. *Terra Antarctica*, 1(2), pp. 251-253.
- ten Brink U.S. & Cooper A.K. (1992) — Modeling the bathymetry of the Antarctic continental shelf. In: Yoshida Y., Kaminuma K. & Shiraishi K. (Eds.), *Recent Progress in Antarctic Earth Science*. Terra Scientific Publishing Company, Tokyo, pp. 763-771.
- Vail P.R. & Hardenbol J. (1979) — Sea-level changes during the Tertiary. *Oceanus*, 22, pp. 71-79.
- Vorren T.O., Hald M., Edvardsen M., & Lind-Hansen, O.W. (1983) — Glacigenic sediments and sedimentary environments on continental shelves : General principles with a case study from the Norwegian shelf. In: Ehlers J. (Ed.), *Glacial Deposits in North-West Europe*. A.A. Balkema, Rotterdam, pp. 61-73.
- Vorren T.O., Hald M. & Lebesbye E. (1988) — Late Cenozoic environments in the Barents Sea. *Paleoceanography*, 3(5), pp. 601-612.
- Vorren T.O., Lebesbye E., Andreassen K. & Larsen K.-B. (1989) — Glacigenic sediments on a passive continental margin as exemplified by the Barents Sea. In: Powell R.D. & Elverhøi A. (Eds.), *Modern Glacimarine Environments: Glacial and Marine Controls of Modern Lithofacies and Biofacies*. Marine Geology, 85, pp. 251-272.
- Weimer P. & Link M.H. (Eds.) (1991) — *Seismic Facies and Sedimentary Processes of Submarine Fans and Turbidite Systems*. Springer-Verlag, New York.

CHAPTER II

Seismic investigation of the Scoresby Sund fjord system and the adjacent central East Greenland shelf

1. Introduction

1.1. History of exploration

The Scoresby Sund fjord region — one of the world's largest fjord systems, situated on the east coast of Greenland between 70° and 72° N (Fig. 1) — was discovered in 1822 by the Scottish whaling captain William Scoresby. Systematic geological mapping of the East Greenland coast was undertaken by various Danish expeditions during the first half of this century, and was continued by expeditions of the GGU (Grønlands Geologiske Undersøgelse) between 1968 and 1972; in that period the terrestrial glacial record of the Scoresby Sund region was examined for the first time in detail. Geophysical investigations of the East Greenland shelf, between 63° and 66° N, started with the surveys of the GGU in 1974 and 1975. It was followed by other seismic studies of the structure of the East Greenland margin, conducted jointly by the Lamont-Doherty Geological Observatory and the German BGR (Bundesanstalt für Geowissenschaften und Rohstoffe) in the late seventies (Hinz & Schlüter 1980). GGU's efforts continued with the DANA 79 project (B. Larsen 1980); during this survey some seismic reflection lines were shot in Scoresby Sund as well. The DANA 79 project was succeeded by the NAD-project, a deep seismic reflection survey which was carried out from 1980 to 1983, and covered the East Greenland shelf up to 74° N (H.C. Larsen 1984, 1985, 1990). Again limited attention was paid to the Scoresby Sund fjord system. In 1988 finally, R.V. "Polarstern" undertook a first seismic reflection survey (ARK V/3) on the East Greenland shelf; during this cruise MCS profiles were recorded for the first time as far north as 80° N (Hinz et al. 1991).

1.2. The ARK VII/3b expedition

In the late summer of 1990 the Scoresby Sund fjord system was the subject of a thorough seismic investigation during the ARK VII/3b expedition with the German ice-breaking research vessel "Polarstern". ARK VII/3b took place from August 28 (Longyearbyen) to October 3 (Bremerhaven), and was a project organised by the German Alfred-Wegener-Institut für Polar- und Meeresforschung, in co-operation with a number of German and international partners, including the Renard Centre of Marine Geology of the University of Gent. A total of 64 seismic reflection profiles was recorded during this survey, with a cumulative length of about 4000 km.

1.3. Objectives

Most of the earlier seismic surveys had in common that they were strongly biased towards the deeper structure of the East Greenland margin; their attention primarily focused on the delineation of the basement and of large-scale sedimentary basins on the shelf.

The principal objectives of the ARK VII/3b survey on the contrary were dual: to image the deep crustal structure of part of the East Greenland margin on one hand, and on the other hand to investigate the imprint of alternating glaciations in the sedimentary record on the continental shelf and in a fjord setting. The latter objective was framing within the PONAM (Polar North Atlantic Margins) programme initiated by the European Science Foundation. This programme has been running from mid 1989 with the intention "to investigate major climatic changes as well as their mechanisms and effect on the sedimentary environment along the polar North Atlantic margins". The programme's objectives are approached by three different themes:

- [a] the late Cenozoic long-term record of climatic changes and their effect on the continental margin sedimentary environment;
- [b] the latest glacial/interglacial cycle;
- [c] the present-day interglacial environment.

All three of these themes were to a greater or lesser extent addressed by the ARK VII/3b expedition, though the long-term aspect has certainly received most attention.

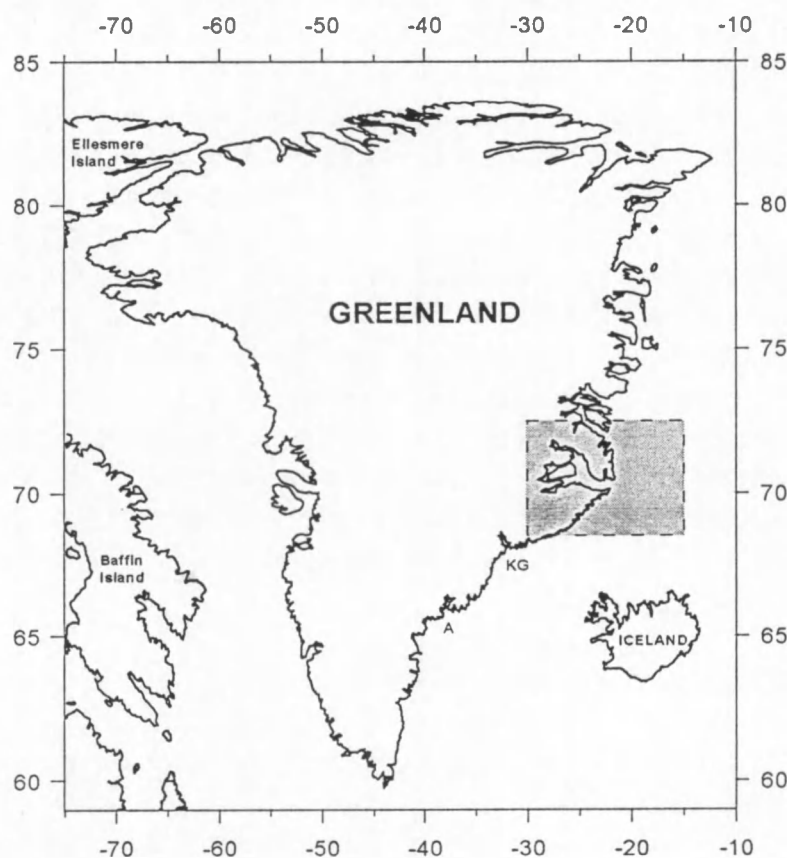


Fig. II.1 - Location of the study area around Scoresby Sund (shaded box) in Greenland. KG = Kangerdlugssuaq fjord, A = Angmagssalik fjord.

2. Data acquisition and processing

2.1. Data acquisition

The following acoustic sources were used for the seismic reflection work during ARK VII/3b:

- a 32 l airgun;
- a big tuned airgun array (total volume 20.2 l);
- a small airgun array (total volume c. 6 l);
- individual airguns ranging from 0.3 to 3 l);
- a 0.25 l watergun;
- a 3.5 kJ sparker.

These sources have very different characteristics. The main frequency of the tuned airgun array peaked around 70 Hz, which would theoretically¹ result in a vertical resolution of 7 - 11 m for seismic velocities of 2000 m/s to 3000 m/s in the traversed medium. The shot distance for this source was approximately 37 m. The resolution of the 32 l airgun was somewhere around 15 m. The 0.25 l watergun emits higher frequencies (around 140 Hz), however, and therefore obtains a theoretical resolution of about 3 m in soft sediments having a seismic velocity around 1700 m/s. The shot distance was close to 7.5 m.

Higher resolution implies a loss in penetration, however. It follows that at all times a trade-off had to be sought between higher resolution and deeper penetration, with regard to the dual objectives that were to be achieved (section 1.3).

Two streamers were used to detect the reflected signals: a 24-channel streamer with an active length of 600 m was generally deployed in combination with the big tuned airgun array; a 12-channel streamer with an active length of 100 m was used together with the lower-volume sources, and also during the refraction work with the 32 l airgun.

The recording of the signals was controlled by an EG&G ES2420 seismograph, equipped for 24 channels. The data were stored on magnetic tapes, while 2 different EPC-recorders provided analogue monitoring.

Navigation of RV "Polarstern" relied on the GPS positioning system, assisted by the on-board INDAS (Transit Satellite) system.

2.2. The data set

Depending on the geological setting, different seismic sources were deployed with different penetration and resolution characteristics: the study of tectonic structures in the basement requires good penetration and hence large-volume guns, while the revelation of Quaternary glacial deposits in the fjords requires a good resolution.

¹ The vertical resolution of a seismic wave can be approximated as $\lambda/4$ (Sheriff & Geldart 1983) or, substituting for the wavelength, as $v/4v$, where v is the seismic velocity and v the frequency.

As a result, the data can be divided into three sets of different quality, roughly corresponding to three different physiographic areas where a different geological problem was to be addressed. More details are given in Table 1.

[1] Shelf lines

Two lines were shot on the East Greenland continental shelf and slope (Fig. 2) in order to investigate the Cenozoic wedge of sediments that accumulated along this margin. Because a large sediment thickness was expected in this setting, the big tuned airgun array was favoured as acoustic source. Line 90500 runs from E to W at about 75° N, while line 90600 runs from the mouth of Scoresby Sund in SE-ward direction towards the Icelandic insular plateau.

[2] Scoresby Sund lines

Most of the seismic survey was focused on the Scoresby Sund fjord system, where the investigation of the structure of a Mesozoic rift basin and older geological units represented an important scientific goal. The second aim was to reveal the general distribution of glacial sediments within the fjord system. Lower-resolution sources were chosen to serve both purposes simultaneously, which — in particular regarding the study of glacial sediments — didn't always yield the desired results. For instance, the large tow depth of source and receiver (c. 10 m), needed for the refraction work, has resulted in a pronounced ghost signal badly affecting the data quality. The majority of the seismic lines inside Scoresby Sund is situated in the broad outer fjord region; in the narrow inner fjords only refraction lines were recorded (Fig. 3):

- a large seismic grid covers Hall Bredning and the south-western arm of Scoresby Sund: lines 90510-90512 and 90530-90536 were shot with the small airgun array, lines 90537-90546 and 90557-90558 with the 32 l airgun and lines 90547-90556 with the big tuned airgun array;
- combined refraction/reflection profiles were shot with the 32 l airgun, mainly to explore the narrow inner fjords (lines 90300-90380) and the eastern part of the fjord region (lines 90400-90430).

[3] Higher-resolution lines

In a few cases where larger accumulations of glacial sediments were expected, preference was given to the use of higher-resolution sources (Fig. 4):

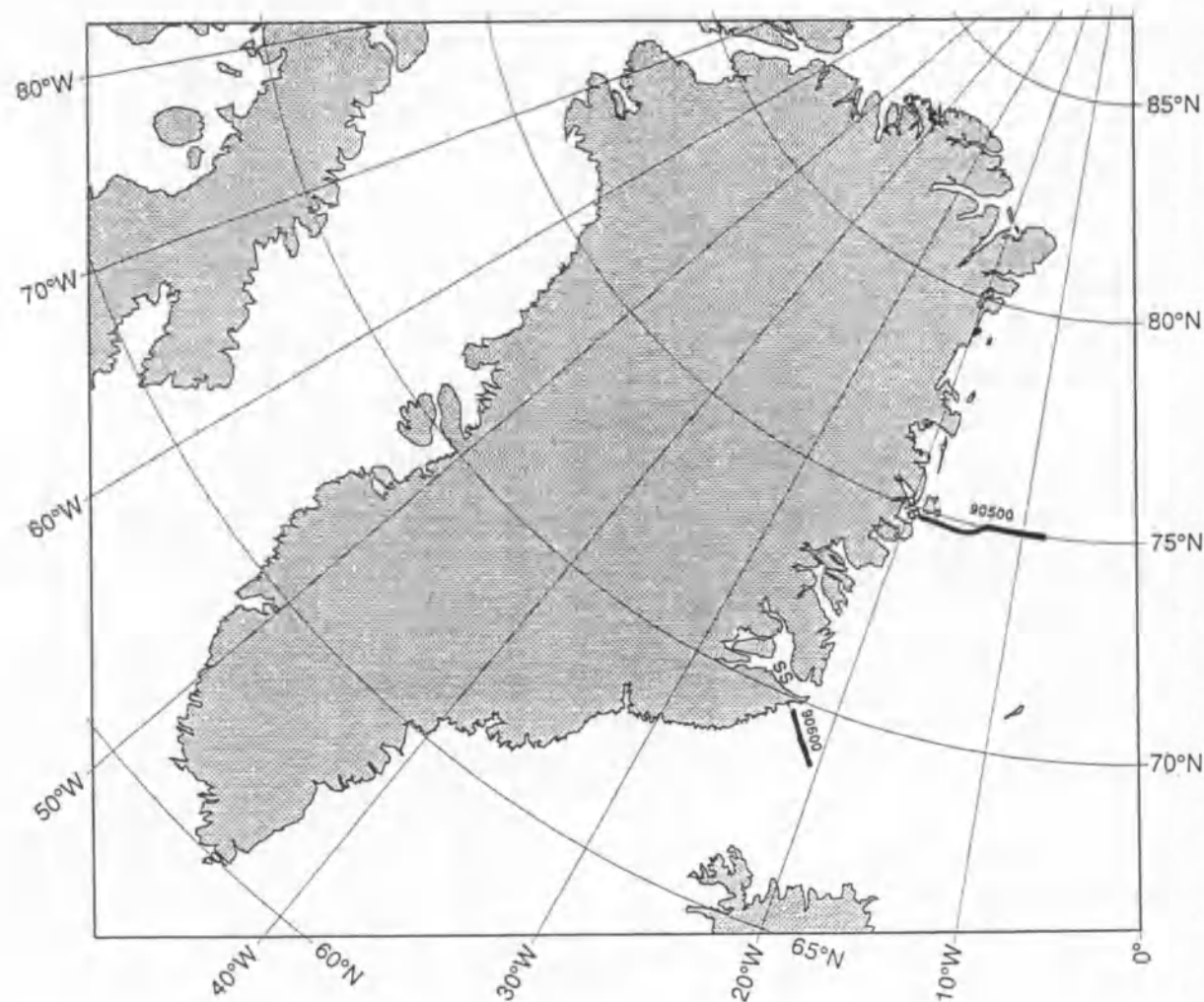
- first attempts to shoot higher-resolution profiles in Gåsefjord (lines 90311 and 90520) and Fønfjord (lines 90521) were unsuccessful due to the harsh ice conditions, with the exception perhaps of line 90300, where it was attempted to fire the watergun (shot interval: 3s) in between the 32 l airgun (shot interval: 30 s);
- lines 90560-90577 are higher-resolution seismic profiles shot with the watergun in Vikingebugt (the largest inlet along the southern coast of Scoresby Sund), across Scoresby Sund, and in front of the SW coast of Jameson Land. Lines 90578a-e were shot in shallow water even closer to the coast with the aid of the small emergency vessel "Polarfuchs";
- lines 90580 and 90590, finally, were shot with a single airgun (chamber volume 1.2 l) along the southern Jameson Land coast and inside Hurry Inlet.

Of the higher-resolution lines only the lines in Vikingebugt resolve a significant accumulation of post-Mesozoic sediments of presumable glacial origin. This justifies the treatment of Vikingebugt as a third separate region, whereas the other higher-resolution lines are only briefly discussed.

	LOCATION	SEISMIC SOURCE	STREAMER LENGTH	NO. OF CHANNELS	STATUS OF DATA AT RCMG
SHELF LINES (499 km)					
90500	outside Hochsetter Bugt (75° N)	big tuned airgun array	600 m	24 ch.	analog + digital 1 ch.
90600/601	outside Scoresby Sund (69° N)	big tuned airgun array	600 m	24 ch.	analog + digital 1 ch.
SCORESBY SUND					
REFRACTION LINES (1276 km)					
90300/310	Gåsefjord - Scoresby Sund	32 l airgun/watergun	100 m	12 ch.	analog + digital 8 ch.
90320/340	Fønifjord - Scoresby Sund	32 l airgun	100 m	12 ch.	analog only
90360	Rødefjord - Snæsund	32 l airgun	100 m	12 ch.	analog only
90380	Nordvestfjord	32 l airgun	100 m	12 ch.	analog only
90400	Hurry Inlet	32 l airgun	100 m	12 ch.	analog only
90420/430	Volquart Boon Kyst	32 l airgun	100 m	12 ch.	analog only
COMBINED REFLECTION / REFRACTION LINES (1589 km)					
90510-512	Hall Bredning - Scoresby Sund	small airgun array	600 m	24 ch.	analog only
90530-536	Hall Bredning - Scoresby Sund	small airgun array	600 m	24 ch.	analog only
90537-546	Hall Bredning - Scoresby Sund	32 l airgun	600 m	24 ch.	analog only
90547-556	Hall Bredning - Scoresby Sund	big tuned airgun array	600 m	24 ch.	analog only
90557-558	Hall Bredning - Scoresby Sund	32 l airgun	600 m	24 ch.	analog only
HIGHER-RESOLUTION LINES (340 km)					
90300	Gåsefjord - Scoresby Sund	0.25 l watergun	100 m	12 ch.	analog + digital 8 ch.
90311	Gåsefjord	3.5 kJ sparker	100 m	12 ch.	analog only
90520	Gåsefjord	3.5 kJ sparker	100 m	12 ch.	analog only
90521	Fønifjord	0.25 l watergun	100 m	12 ch.	analog only
90560-577	Vikingebugt + SW coast of Jameson Land	0.25 l watergun	100 m	12 ch.	analog + digital 12 ch.
90578a-e	Langelandseelv	0.25 l watergun	100 m	8 ch.	analog + digital 8 ch.
90580/590	Hurry Inlet	1.2 l airgun	100 m	12 ch.	analog + digital 12 ch.

Table II.1 - Overview of seismic lines shot during the ARK VII/3b survey.

Fig. II.2 - Location of the seismic lines 90500 and 90600 on the East Greenland continental shelf.
HB = Hochstetter Bugt, SS = Scoresby Sund.



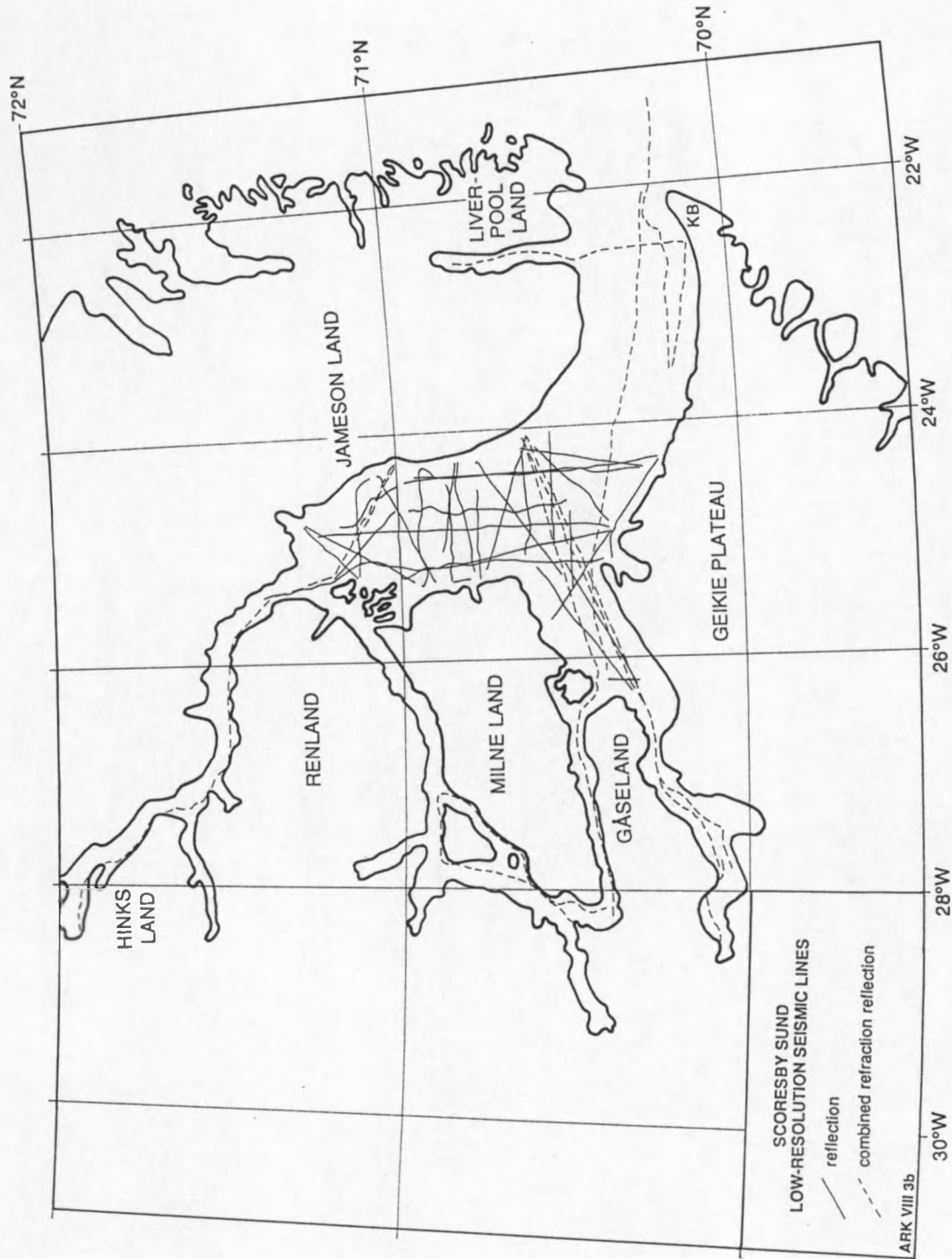


Fig. II.3 - Location of low-resolution seismic profiles in Scoresby Sund. KB = Kap Brewster.

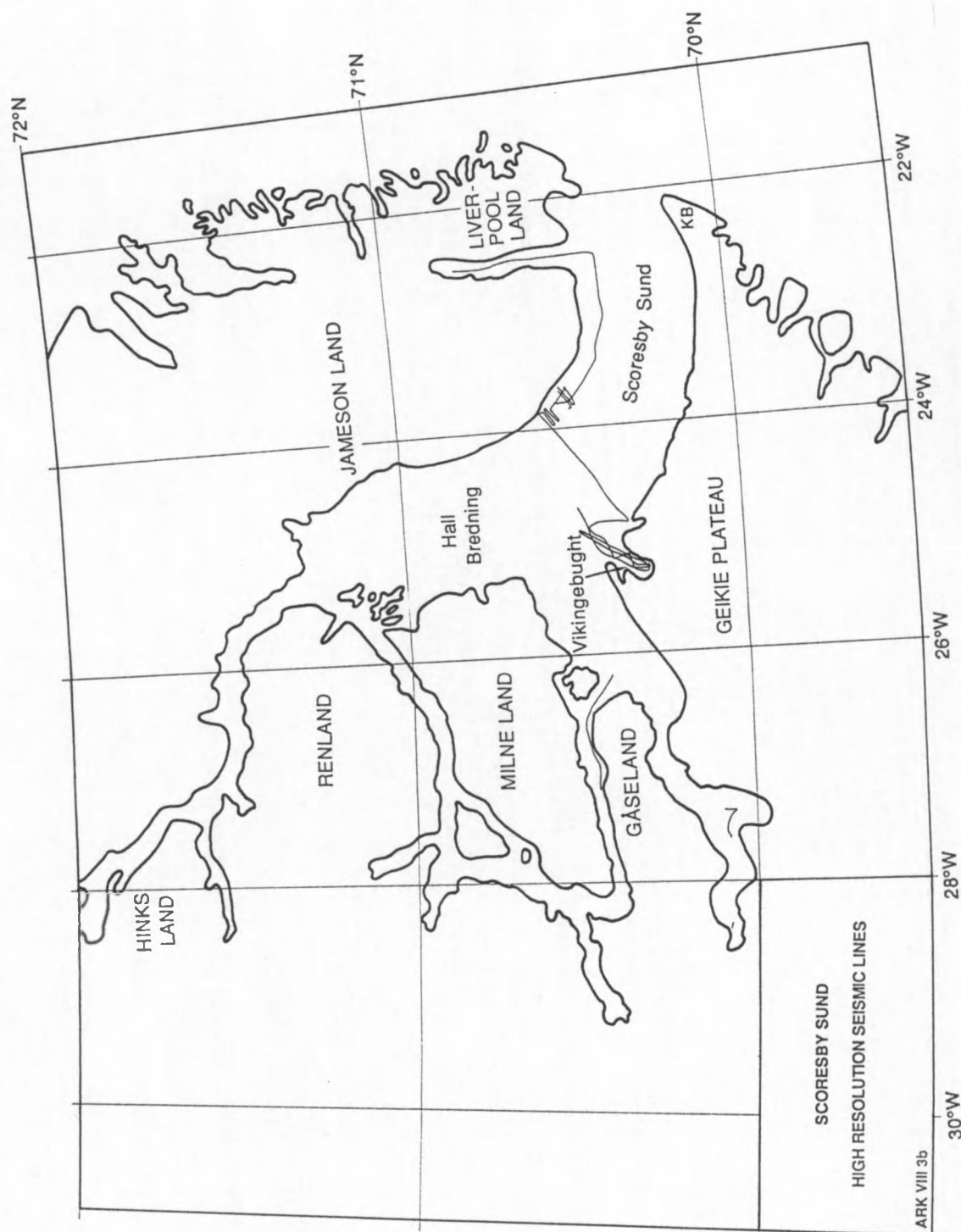


Fig. II.4 - Location of higher-resolution lines in the outer fjord region of Scoresby Sund. KB = Kap Brewster.

2.3. Data processing

All data were recorded on 6250 BPI tapes in the SEG-D format. Processing was already started on board, but had to be abandoned due to the breakdown of the CONVEX computer. The tapes were subsequently demultiplexed and thereby transferred to the DISCO tape format at the Alfred-Wegener Institute.

Copies were made of the shelf lines and of the higher-resolution lines shot with the watergun onto 1650 BPI tapes in the SEG-Y format, for further digital processing with RCMG's own PHOENIX VECTOR 5.0 software on a SUN 370 Spark Workstation.

Of the shelf lines 90500 and 90600 only one of the available 24 channels was copied on tape. All 12 channels were copied of the watergun lines (lines 90300 and 90560-90577) and of the 2 lines shot with a single airgun (lines 90580 and 90590). The other profiles shot in Scoresby Sund were only available as analogue monitoring recordings for the present study.

The recording parameters of the digital profiles available at RCMG are summarised in Table 2. Processing of the seismic data occurred with the assistance of Jens Mouridsen. Fig. 5 displays the processing flows for the different profiles. Additional processing to suppress the seismic multiple on line 90600 was performed by Dr. Gabriele Uenzelmann-Neben at the AWI, using an adaptive filter developed by Rosenberger (1992).

	SEISMIC SOURCE	SHOT INTERVAL	RECORD LENGTH	SAMPLE INTERVAL	NO. OF CHANNELS	NO. OF TAPES
SHELF LINES						
90500	big airgun array	14 s	10 s	2 ms	24 (1)	5
90600	big airgun array	15 s	10 s	2 ms	24 (1)	2
HIGH-RESOLUTION LINES						
90300	watergun	3 s	1.5 s	1 ms	12 (8)	15
90560-577	watergun	3 s	1.5 s	1 ms	12	74
90580/590	1.2 l airgun	5 s	3 s	2 ms	12	20

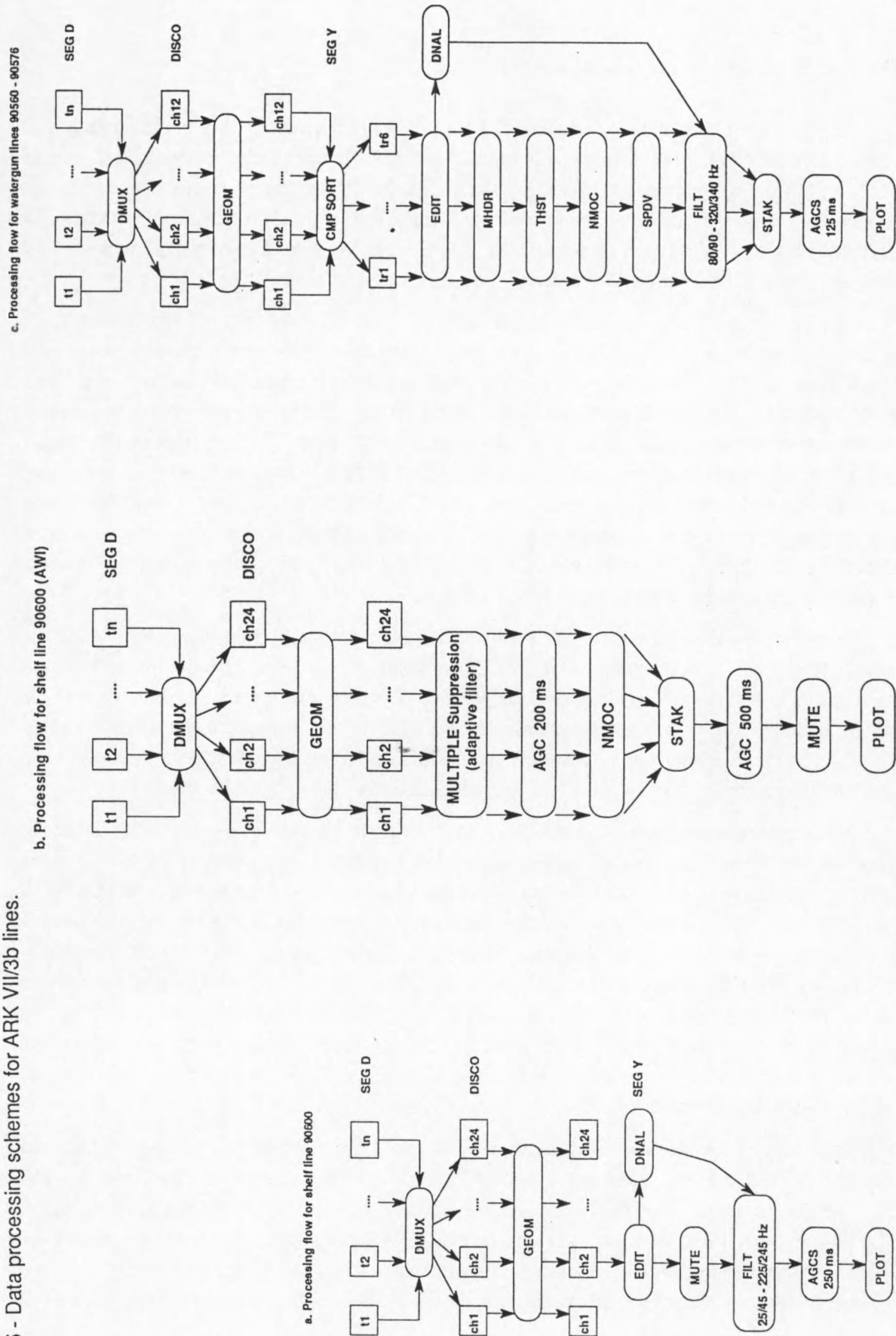
Table II.2 - Recording parameters of digitally recorded profiles.

Only the basic steps of digital data processing were applied to the data. Of the many functions available in both DISCO and PHOENIX VECTOR only a few were used. These are listed below, more or less in order of application:

- DMUX Demultiplexing: the first step of each processing cycle. The signals, stored on tape as successive samples of the different channels, are reorganised into separate channels.
- GEOM Geometry definition: geometrical parameters such as the relative position and tow depth of source and receiver and the ship's speed are necessary to calculate the fold of multi-channel data and the position of the common mid-point (CMP). Geometry definition occurs at an early stage.

MHDR	Modify header: used to correct for consistent errors in the header of the data. An error occurred in the floating point header format due to the incompatibility of the computer systems on which the data were processed originally (CONVEX) and in a later phase (SUN). This error had only implications for the calculation of the NMO correction (NMOC).
THST	Trace header statistics: used to correct for a consistent error in the arrival time of certain traces due to a malfunction of the recording equipment. Traces can be shifted upwards or downwards in time.
EDIT	Edit: is used to select or deselect certain channels or traces.
DNAL	Frequency analysis: on base of Fourier's theorem the recorded signal — a time series — can be described by the spectrum of the amplitudes of all its constituting frequency components. This is used to determine to which frequency band most of the signal is confined.
FILT	Filter, usually band-pass filter: allows to eliminate unwanted frequencies that represent a signal/noise ratio that is too low. This process is based on the results of a frequency analysis (DNAL).
MUTE	Mute: wipes the signal down to a certain time. This is used for aesthetic reasons only — to clear noise from the water column section of the profile — and doesn't influence the quality of the data.
SPDV	Spherical divergence: corrects for the loss of amplitude due to the spherical propagation of the compressional sound wave.
SORT	Sorts the traces of the different shots in groups with a common mid-point (CMP gathers). The calculation is based on the geometry definition (GEOM). The traces in a CMP gather are corrected for normal move-out (NMOC), and stacked (STAK).
NMOC	Normal move-out correction: the signals of each trace in a CMP-gather have travelled successively longer paths from source to receiver; this is known as move-out. It is corrected for in NMOC under the assumption that the reflecting surface is more or less horizontal (i.e. normal incidence). This process normally requires information about the seismic velocity between the different reflectors. For the Vikingebugt lines only the velocity in the water column was taken into account, as only the uppermost sediment interval was considered important.
STAK	Stacking: sums the traces of a CMP-gather after normal move-out correction (NMOC). This usually results in an enhanced signal/noise ratio, and partly suppresses multiple reflections.
SUMS	Summation: simply sums traces in a shot- or CMP-gather without any move-out correction. This simplification is justified when the water-depth is greater than the length of the streamer, so that the difference in arrival between traces in a CMP-gather can be considered negligible.
AGCS	Automatic gain control: calculates the required gain by averaging the energy in a sliding window and applying it to the middle of this window; depending on the length of the window the contrast between weak and powerful reflectors can be suppressed or enhanced.
PLOT	Plot: enables to plot the profile on the desired scale and in the desired direction.

Fig. II.5 - Data processing schemes for ARK VII/3b lines.



3. Physiography of Scoresby Sund and the East Greenland shelf

3.1. The East Greenland continental shelf

In general, the East Greenland shelf exhibits rather large water depths typically in the range of 250 to 350 m. The morphology of the sea bed is irregular where basement is exposed (in general close to the coast), but the sedimentary shelf is fairly flat with only slight changes in water depth (Fig. 6). The monotony is only disturbed by broad and mainly transverse channels originating from the major fjords and reaching water depths between 400 and 600 m, and by a number of banks, often situated at the outer shelf, with water depths around 200 m (H.C. Larsen 1984).

The two available shelf lines are located southward of Scoresby Sund and off Hochstetter Bugt, 500 km north of Scoresby Sund. Beyond the fjord entrance of Scoresby Sund the bathymetric contour lines display a clear bulge where the continental shelf extends farther eastward (over 100 km) than on adjacent portions of the margin (about 80 km). The shelf width gradually increases in northward direction to a maximum of c. 300 km between 77° and 79° N. In front of Hochstetter Bugt at 75° N the shelf width amounts to about 200 km. The shelf in front of Scoresby Sund is deep and fairly flat, and terminates in a water depth of 375 m. In front of Hochstetter Bugt the largest depth (about 340 m) is reached on the inner part of the shelf where older rocks outcrop; the outer sedimentary shelf is generally shallower than 300 m and in large areas even less than 225 m deep; the shelf break is found in a water depth of about 265 m.

The main hydrographic element on the East Greenland shelf is the southward flowing East Greenland Current (Fig. 6) which constitutes the main surface water outflow of cold polar water from the Arctic Ocean. Off southern East Greenland the polar water is mixed with warm Atlantic water of the Iminger Current, and the mixture flows around the southern tip of Greenland and northwards into Baffin Bay as the relatively warm West Greenland Current; the water circulates in Baffin Bay and eventually travels further southwards in the Labrador Current (The Open University 1989).

Polar pack ice originating from the Arctic Ocean is carried southward by the East Greenland Current. A belt of pack ice is omnipresent along the East Greenland coast down to 70° N throughout most of an average year, and blocks the entrance of the Scoresby Sund fjord system from October to May. The pack ice reaches its maximum extension in April/May before it starts retreating northward; the period from early August to mid September is normally the most ice-free period (H.C. Larsen 1985). Extreme situations do however occur with either very little (no massive pack ice south of 74° N) or very heavy ice (with pack ice remaining all summer as southerly as 68° N). A significant portion of the icebergs calved from fast-flowing outlet glaciers in the East Greenland fjords (at least as far N as 76° N, Reeh 1985) is able to leave the fjords and to join the polar pack ice in its southward drift in the East Greenland Current (Dowdeswell et al. 1993).

The East Greenland continental slope is affected by another current, the North-West Atlantic Bottom Water (NWABW) current. Deep water formed by cooling water masses in the Norwegian and Greenland Seas is prevented to flow freely into the North Atlantic by the Greenland-Scotland Ridge, which presents a major topographic barrier. The NWABW intermittently overflows this submarine ridge, and enters the North Atlantic Ocean through Denmark Strait. Southward of Scoresby Sund the current becomes very focused on the continental slope, as it is perched between the broad shelves of Greenland and Iceland (Fig. 6).

Fig. II.6 - Physiographic map of the East Greenland shelf, showing sea floor morphology in 500 m intervals (from IHO/IOC/CHS 1984), oceanic current patterns (The Open University 1989), and thickness contours of the Greenland Ice Sheet; small arrows represent the most important outlet glaciers (after Reeh 1985). Accentuated 500 m contour marks approximate position of the shelf edge. EGC = East Greenland Current, HB = Hochstetter Bugt, IC = Irminger Current, LC = Labrador Current, NWABW = North-West Atlantic Bottom Water, SS = Scoresby Sund, WGC = West Greenland Current.



3.2. The Scoresby Sund region

The Scoresby Sund fjord complex is situated along the central East Greenland coast, between 70° - 72° N latitude and 22° - 29° W longitude. It is composed of many larger and smaller fjords (Fig. 7) which jointly make up the world's most extensive fjord system, and displays the following characteristics — which are considered typical of the NE Greenland fjord province (Funder 1989):

- the fjord complex is strongly branched, separating a number of peninsulae (Hinks Land, Renland, Gåseland) or even islands (Milne Land) from the main land interior (Charcot Land and Stauning Alper);
- it extends deep into the continent, with a distance of 350 km between the head of the inner fjords and the main fjord mouth;
- there is a remarkable contrast between an overdeepened inner zone of narrow fjords (Nordvestfjord, Rødefjord, Øfjord, Fønfjord, Vestfjord and Gåsefjord: < 6 km wide) and a shallower outer zone with broad fjord arms (Hall Bredning and Scoresby Sund s.s.: up to 50 km wide);
- a pronounced sill (elevation) at the fjord entrance is absent.

3.2.1. Topography and bathymetry

The topography of the entire fjord region, both subaerially and submarine, is the result of severe glacial erosion, but is strongly controlled by the composition of the substrate (Henriksen 1986).

The inner and central fjord zone, outermost Liverpool Land and the Geikie Plateau south of the fjord region, all consisting of crystalline rock complexes (see section 4.1.1), are characterised by a rugged alpine topography. The average summit levels in the central fjord zone are 1500 - 2000 m and reach 2000 - 2500 m in the inner fjord zone and in the Stauning Alper (north of Hall Bredning). The inner fjords are correspondingly extremely deep, with depths over 1000 m, locally reaching 1200 - 1600 m. The height difference between the mountain summits and the bottom of the deepest fjords indicates a total topographic relief of 3000 - 4000 m.

In contrast to the rugged topography in the crystalline areas, the sedimentary Jameson Land area is characterised by an undulating, rounded topography with heights generally less than 1000 m (Henriksen 1986). Hall Bredning and Scoresby Sund s.s. — the two outer fjord arms — are 40 km broad in average and are characterised by an asymmetric bathymetry: water depths vary gradually from very shallow along the gentle Jameson Land shore to more than 600 m close to the western and southern opposite shores which are consequently much steeper (Dowdeswell et al. 1993). In places along the W coast of Hall Bredning and the S coast of Scoresby Sund s.s. troughs are evident.

3.2.2. Ice cover

The inner and central fjord zones are covered by local ice caps and numerous glaciers (Fig. 7). Large glaciers terminate in water at the head of most of the narrow inner fjords. They are fast-flowing outlet glaciers draining directly from the Inland Ice which has its margin just west of the Scoresby Sund region. The most impressive glaciers are the Daugaard-Jensen Gletscher and the Vestfjord Gletscher, at the heads of Nordvestfjord and Vestfjord respectively. They are characterised by high calving rates; Daugaard-Jensen Gletscher for instance is estimated to produce 10 km³ of icebergs per year, this is more than half of the 18 km³ of icebergs which are calved into the entire fjord system annually (Olesen & Reeh 1969).

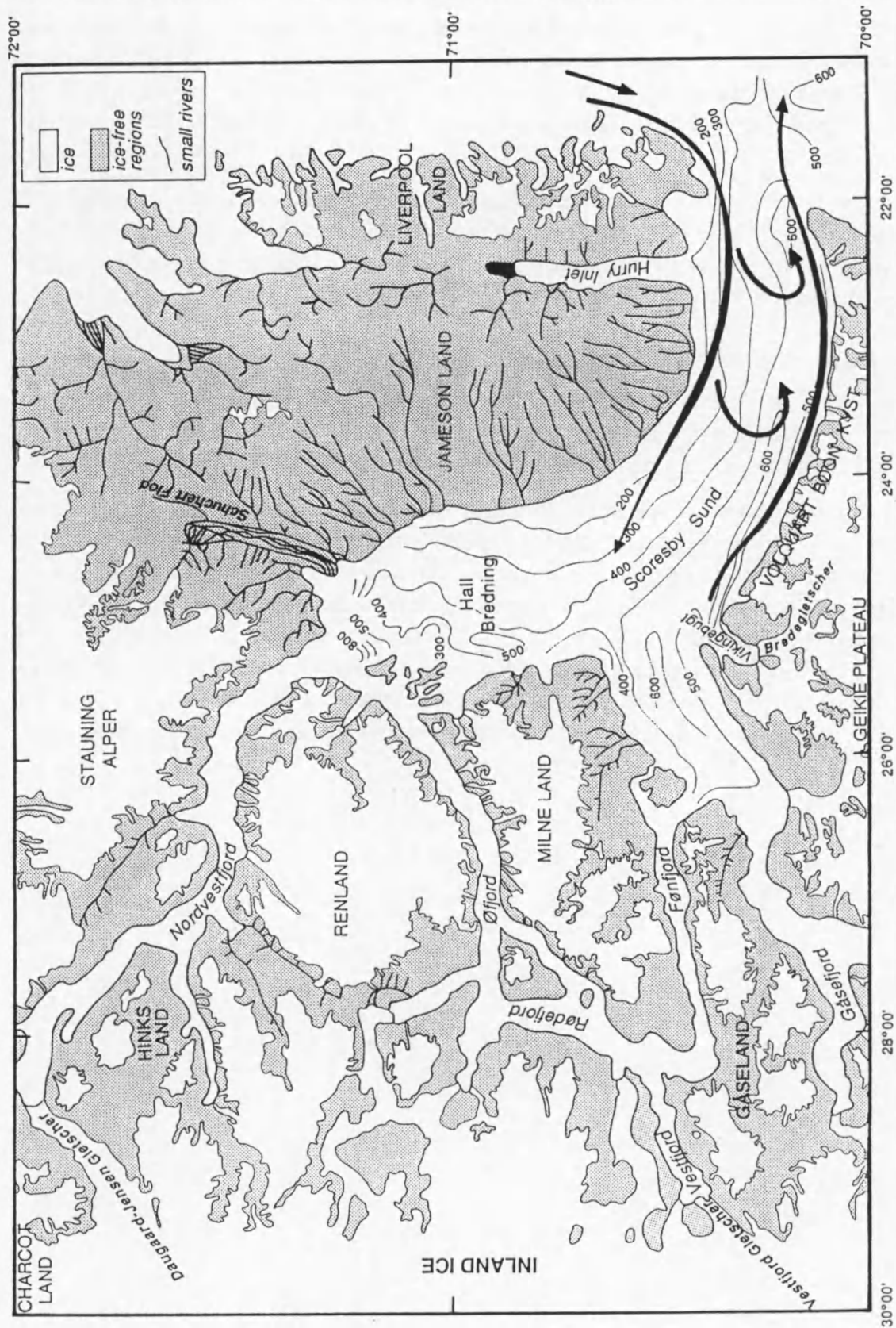


Fig. II.7 - Physiographic map of the Scoresby Sund fjord region, showing distribution of ice and rivers (after Henriksen 1986), and summer surface water circulation (from Koch 1945).

Along the margin of the Inland Ice a wide zone of nunataks occurs, bordering the inner fjord zone of the Scoresby Sund region. Renland, Milne Land and Gåseland in the central fjord zone and the Geikie Plateau to the S are covered by small local ice caps feeding several smaller tidewater glaciers. The glaciers draining from the local Geikie Plateau ice cap in the small inlets along the southern Volquart Boon Kyst are presently the only glaciers directly entering into Scoresby Sund. The most important of these glaciers is Bredegletscher at the mouth of Vikingebugt, the largest inlet along the southern coast.

In contrast to this, Jameson Land and Liverpool Land are largely ice-free; as a result numerous small river systems (Fig. 7) have developed flowing into Hall Bredning, Scoresby Sund s.s. and Hurry Inlet, the fjord arm separating Jameson Land from Liverpool Land. Schuchert Flod to the north of Hall Bredning appears to be the most extensive of these river systems.

3.2.3. Water circulation

The absence of a pronounced topographic barrier at the fjord mouth allows for a complete water exchange between fjord and marine environment: underneath a surface layer of about 50 m of fresh water the water column entirely consists of marine water (Marienfeld 1991).

Fjords normally experience a seasonally alternating in- and outflow of water. But because of the broad entrance of Scoresby Sund (more than 25 km) a surface water gyre develops during the summer, between July and the beginning of October (Koch 1945; Marienfeld 1991): marine water flows from the fjord mouth in westward direction along the northern edge of Scoresby Sund, while at the same time fjord water flows towards the fjord mouth along the southern coast (Fig. 7). As a result most icebergs drift along the southern coast towards the east, and eventually leave the fjord on its southern side. Throughout the winter period, between about October and the end of June, the presence of (shore)fast sea ice impedes drift of icebergs within the fjord system (Dowdeswell et al. 1992).

4. Geological evolution of Scoresby Sund and the East Greenland margin

4.1. Pre-glacial development of the Scoresby Sund region

4.1.1. Structural setting

In a first approximation (Fig. 8) the East Greenland margin can be divided into two geologically different regions (H.C. Larsen 1984). In general, the southern half of the East Greenland margin is made up of Precambrian basement rocks of Archaean and early Proterozoic age. The northern half of the margin comprises a coast-parallel belt of Caledonian age cut by Paleozoic to Mesozoic basins with the same trend. At the conjunction between these two geologically different regions, vast volumes of early Tertiary volcanics have flooded the margin and fringe the coast for several hundreds of kilometres. Important intrusive and tectonic activity of the same age is evident in even wider regions.

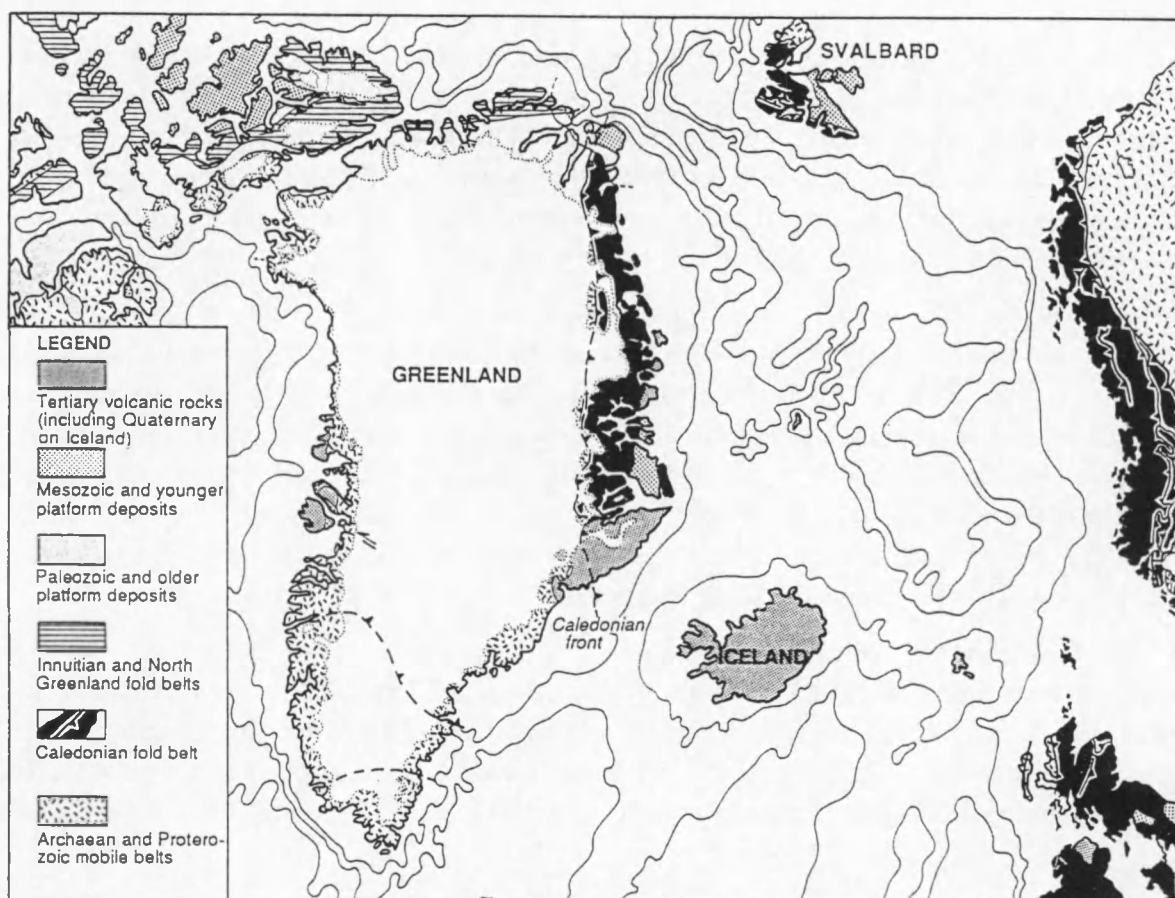


Fig. II.8 - Rough outline of the main geological units recognised in Greenland and surrounding land areas (from Escher & Watt 1976).

All of these elements can be recognised in the Scoresby Sund region, which occupies a central position along the East Greenland margin. On a simplified geological map of the area (Fig. 9) the following units are distinguished (Henriksen 1986):

[1] Tectonic window complexes

These are exposed in the western part of the region, along the margin of the Inland Ice; the largest areas of exposure are Charcot Land and western Gåseland. The rocks include Archaean to early Proterozoic gneisses and granites, which are interpreted as parts of the Greenland shield area, representing the Caledonian foreland outcropping in tectonic windows beneath Caledonian thrust sheets.

[2] Vestfjord - Hinks Land gneiss and schist zone

This is a 60 - 100 km wide zone in the inner fjord region, bordered to the W by the Caledonian front, and to the east by a major N-S trending thrust or reverse fault of probably Caledonian age. The outcropping rocks consist of an Archaean gneiss basement (Flyverfjord infracrustal complex) and an overlying unit of Middle Proterozoic metasediments (Krummedal supracrustal sequence). The zone is essentially made up of major Caledonian thrust units or nappes, which have been displaced in westward direction for distances of more than 100 km over and above the Precambrian foreland areas.

[3] Gåsefjord - Stauning Alper migmatite and granite zone

This 75 - 100 km wide zone, located in the central fjord region, is largely made up of migmatites and intrusions of Middle Proterozoic and Caledonian age. The zone constitutes the inner, basal portion or core of the Caledonian fold belt, and is bordered to the east by a N-S trending main boundary fault of post-Caledonian age, separating the crystalline rocks of the granite and migmatite zone from the sedimentary Jameson Land basin. This fault system is proposed to extend into Hall Bredning, and to connect with a fault line in eastern Milne Land which offsets Middle Jurassic sediments of the Milne Land fault block from the main granite and migmatite zone.

[4] the post-Caledonian sedimentary Jameson Land basin

The Jameson Land basin is a 125 km wide N-S trending sedimentary basin between Caledonian crystalline regions to the west and to the east. It was filled with a c. 4000 m thick sequence of sediments covering a time span of about 150 Ma (Devonian to Lower Cretaceous). The Jameson Land basin constitutes the southern part of a continuous sedimentary rift basin which stretches for more than 600 km towards the north (Fig. 10). It continues beneath the waters of Scoresby Sund, and an outlier of the basin is found in the SE part of Milne Land. Scattered evidence (L.M. Larsen et al. 1986) suggests that it continues southward beneath the basalt cover of the Geikie Plateau.

[5] Liverpool Land - Canning Land

This zone is a coast-parallel, horst-like zone bordering the North Atlantic Ocean. The rocks comprise pre-Caledonian gneiss complexes and Caledonian migmatites and plutonic intrusions, comparable to those of the Gåsefjord - Stauning Alper zone. The basement of Liverpool Land extends as a complicated block-faulted ridge across the entrance of Scoresby Sund (B. Larsen 1980).

[6] Geikie Plateau

The southern part of the Scoresby Sund region is covered by a thick pile of early Tertiary plateau basalts, forming part of the East Greenland Tertiary magmatic province. The volcanic province south of Scoresby Sund covers an area of at least 80,000 km³ and reaches a thickness maximum of more than 2000 m along the southern coast of the fjord system (Volquart Boon Kyst). The total stratigraphic thickness amounts to more than 3000 m. North of the main basalt outcrops, basalt patches of 300 to 800 m thick occur in Gåseland and Milne Land, suggesting that the basalt cover most likely extended further north across the Scoresby Sund fjord and covered large parts of the Jameson Land basin (H.C. Larsen 1985).

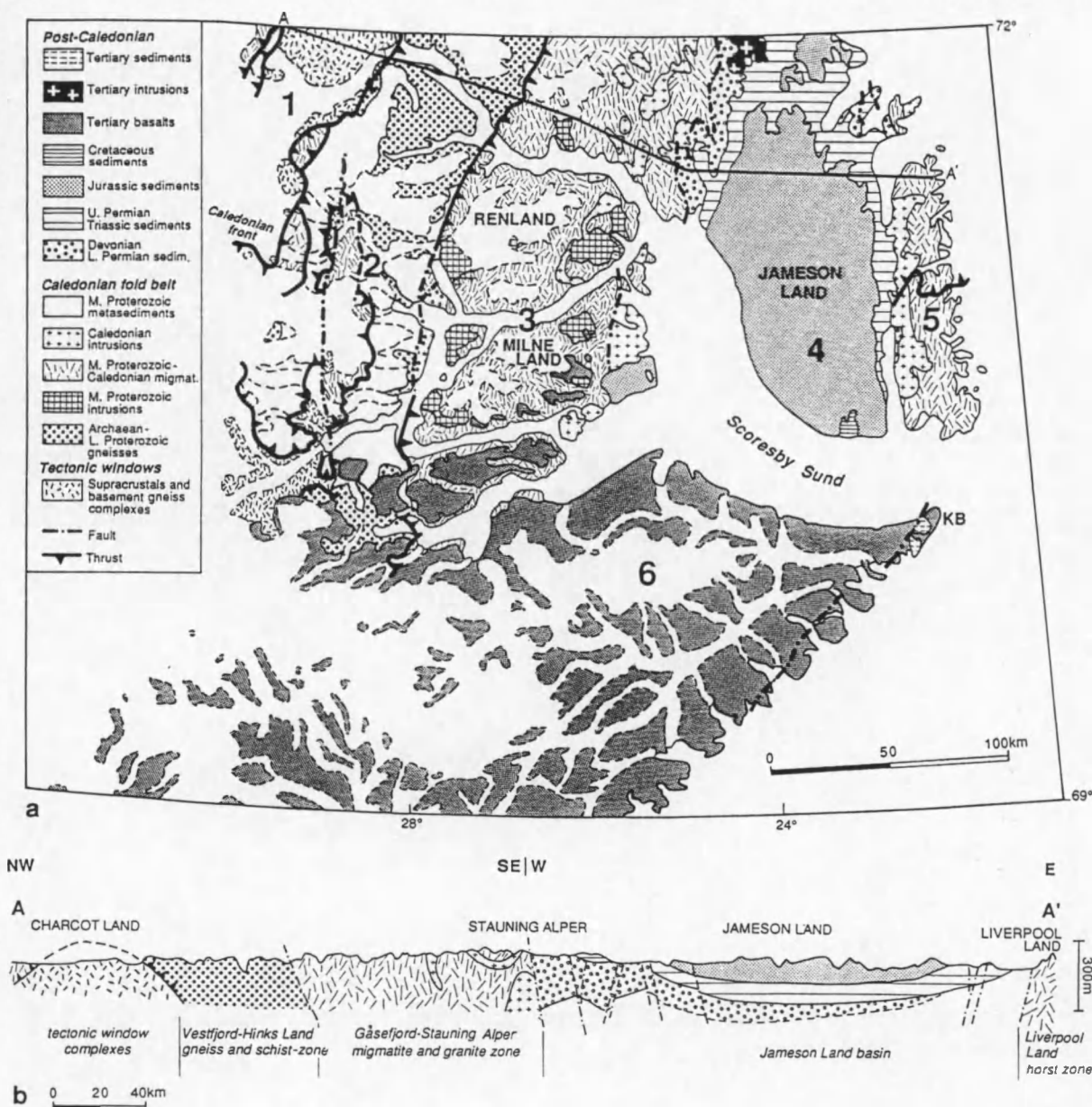
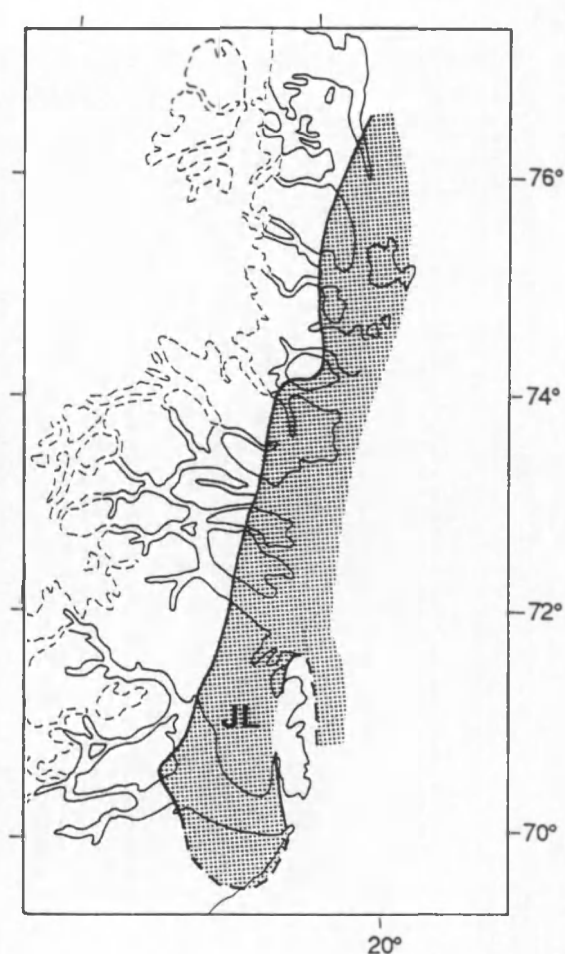


Fig. 11.9 - [a] Simplified geological map of the Scoresby Sund area (after Henriksen 1986). Numbers represent the zonation described in the text: (1) tectonic window complexes, (2) Vestfjord - Hinks Land gneiss and schist zone, (3) Gåsefjord - Stauning Alper migmatite and granite zone, (4) Jameson Land basin, (5) Liverpool Land, (6) Geikie Plateau. KB = Kap Brewster. **[b]** Geological cross-section through the northern part of the region (after Henriksen 1989).

Zone 1 thus belongs to the Precambrian Greenland shield, zones 2, 3 and 5 include the southernmost part of the East Greenland Caledonian fold belt, zone 4 represents the southern part of a major coast-parallel sedimentary basin of Paleozoic to Mesozoic age, while zone 6 constitutes the northern end of the East Greenland Tertiary magmatic province. The Tertiary basalt sequence conceals the southward continuation of the Caledonian fold belt and of the Jameson Land basin.

Fig. II.10 - The Jameson Land (JL) basin as the southernmost part of a larger Mesozoic sedimentary basin in central East Greenland (after Henriksen 1989).



4.1.2. Geological history

The following geological evolution has been reconstructed from the build-up of the Scoresby Sund region (Henriksen 1986, 1989):

Precambrian

During the Precambrian the Scoresby Sund area was an integrated part of the Greenland baserock shield, and has been submitted to the same series of events as the rest of the continent. Even though most of the rocks found around Scoresby Sund have been influenced by the Caledonian orogeny, it is possible to identify three earlier phases of deformation, in the Archaean, Early Proterozoic and Middle Proterozoic, respectively. Step by step, elements from the first three orogenic periods have been welded, to form a consolidated complex of primarily granites and gneisses — the baserock shield of Greenland. Rocks of Precambrian age are dominant in zones 1, 2, 3 and 5.

Caledonian orogeny

The Caledonian orogeny between the Late Ordovician and Silurian (450 - 400 Ma) represents the youngest, and for Scoresby Sund the most important orogeny. Along the east coast of Greenland a N-S oriented mountain range was created, stretching 1200 km from Scoresby Sund to the north of Greenland, and in continuity with the Caledonian fold belt of Norway. The main part of the Scoresby Sund area was affected in this process. Pre-existing Precambrian rocks were strongly folded and

metamorphosed, while renewed subduction created Caledonian granites and migmatites which are not easily distinguished from the older rocks. The western boundary of the Caledonian fold belt is found in the border zone near the Inland Ice, where pre-Caledonian foreland crops out in tectonic windows beneath westward directed Caledonian thrust units. The Caledonian complex comprises two zones with different lithologies: a western zone of nappes which were thrust towards the west over undeformed Precambrian rocks belonging to the Greenland shield (Vestfjord - Hinks Land), and a central zone constituting the core of the Caledonian fold belt (Gåsefjord - Stauning Alper).

Late Paleozoic - Mesozoic

Uplift and erosion of the Caledonian mountain belt started in the Devonian. From Carboniferous times onwards the region was subjected to an E-W oriented extension as a prelude to the opening of the North Atlantic Ocean. Block faulting and tilting shaped limited basins in which the erosional products of the Caledonian mountain belt accumulated: from the Devonian to the Early Permian mainly continental conglomerates and sandstones of fluvial origin were deposited, parts of which crop out along the western margin of the Jameson Land basin. The total stratigraphic thickness of these continental deposits in East Greenland is thought to amount to about 20 km.

The continental period ends in the Late Permian; at this time the rifted basins form a large and steadily subsiding N-S oriented depression, which develops into a continuous failed-rift basin. The first marine transgression takes place in the Late Permian from the NE. A thick succession of mainly marine shallow-water sediments of Late Permian to Early Cretaceous age was deposited (the Jameson Land Group). The marine sedimentation is interrupted by a phase of relative uplift in the Triassic during which again continental sediments are deposited. The youngest exposed sequence in Jameson Land is of Early Cretaceous age, but marine deposition probably continued into the Late Cretaceous (a small outcrop is observed below Tertiary basalts at Kap Brewster).

In the Milne Land area first deposition took place in the Middle Jurassic and continued into the Early Cretaceous.

Tertiary

The final opening of the polar North Atlantic Ocean determines the Tertiary evolution of the Scoresby Sund region. Under the influence of the Icelandic hot spot the initiation of seafloor spreading in the Greenland-Norwegian Sea at the Paleocene/Eocene transition is accompanied by the massive and widespread extrusion of plateau basalts onto the edges of the separated continents. In East Greenland an extensive area between Kangerdlugssuaq and Scoresby Sund was flooded by basalts. The basalts rest with a major angular unconformity on crystalline rocks of Caledonian or older age (Gåseland and Milne Land) or on Mesozoic sediments (Milne Land). They erupted over a relatively short period of a few million years in the latest Paleocene and earliest Eocene (between magnetic anomalies 25 and 24, i.e. 56 - 53 Ma) (L.M. Larsen & Watt 1985).

The basalts have been divided into a lower series and an upper series, each consisting of three different formations (L.M. Larsen & Watt 1985). These two regional basalt series were formed during different episodes of volcanic activity. Eruption sites for the first episode are inferred to have been centred in the inner fjord region, while those for the second episode seem to have been situated mainly to the east of the present Atlantic coast. A younger basaltic sequence of only local extension was produced during a third volcanic episode and was apparently fed by a dense coastal dyke swarm cutting the basalts in a 30 km wide zone south of Scoresby Sund. These three volcanic episodes can be correlated to different stages in the inception of seafloor spreading in the polar North Atlantic (L.M. Larsen & Watt 1985).

The basalt sequence has a general inclination of $0.5 - 1^\circ$ towards the SE, which is very near the observed dip of the Mesozoic sediments. This indicates that most of the tilting post-dates the basalts (B. Larsen 1980).

Much of the later Tertiary evolution is characterised by the formation of a crustal flexure or escarpment near the ocean/continent boundary along most of the southern and central East Greenland margin. This so-called East Greenland Escarpment accommodated strong differential vertical post-rift movements: a downthrow of more than 6 km is inferred (H.C. Larsen 1984). While the oceanic region east of the escarpment sank, the continent was uplifted and subjected to erosion. The Scoresby Sund region was tilted towards the SW, as indicated by the dip of the Mesozoic and basaltic layers, and most of the erosion took place north of the Geikie Plateau: in Jameson Land the complete early Tertiary lava cover (0 - 2 km) was removed, along with a fairly complete and thick Cretaceous section and large parts of the Jurassic section; in northernmost Jameson Land even Triassic and Permian strata were eroded (H.C. Larsen 1985). The erosion was effectuated by a major eastward flowing river system which in Neogene times took up the position of the present-day Scoresby Sund fjord. Drainage by river systems within the volcanic plateau was probably of minor importance (H.C. Larsen 1985).

The erosional products, mainly sands and clays, were all deposited in the waxing oceanic basin east of the East Greenland Escarpment, below the present-day continental shelf. The Tertiary sediments offshore of the Scoresby Sund region are approximately 5 - 6 km thick (H.C. Larsen 1984, 1985). A more detailed description follows in section 4.2. Marginal exposures of the extensive Tertiary basin are preserved in downfaulted areas on land at Kap Dalton and Kap Brewster (both along the Atlantic coast south of Scoresby Sund); the Kap Dalton Formation is of Eocene to Oligocene age, while the Kap Brewster Formation is probably Miocene in age.

Quaternary

The last 2 Ma a glacial environment was established and the Scoresby Sund region has been dominated by the erosional force of ice during the subsequent glaciations. Tertiary river valleys were taken in by glaciers and further eroded. Erosion was strongly amplified, and deposition must have continued on the continental shelf and slope. A substantial part of the erosional relief seen today is of glacial and Quaternary origin, at least in the basalts of the Geikie Plateau, where the zeolite zonation indicates that the present-day exposed top of the lava sequence comes close to the original top of the sequence (H.C. Larsen 1985).

The glacial evolution will be discussed in more detail in section 4.3.

4.2. Geology of the East Greenland shelf

The East Greenland shelf has been intensively investigated in the early eighties by the Geological Survey of Greenland (GGU) in the NAD project, which integrated aeromagnetic and seismic methods. The results of this project were described by H.C. Larsen (1984, 1985, 1990).

The East Greenland shelf has been divided into five different geological provinces, separated by four transverse zones (Fig. 11). These transverse zones mark boundaries across which important structural and stratigraphic changes take place, and are believed to roughly correspond to the landward projection of oceanic fracture zones. The five geological provinces went through a different

tectonic evolution during the opening of the Greenland-Norwegian Sea, which is reflected in differences in crustal type, amount of subsidence, basement tectonics etc. An overview of the main characteristics of each of the shelf provinces is summarised in Table 3, while representative cross-sections can be found in Fig. 12. Fig. 13 sketches the opening history of the Greenland-Norwegian Sea.

From north to south these structural elements are:

North-east Greenland shelf	
————— <i>Kong Oscar Fjord "Fracture Zone"</i>	(proj. of proto - Jan Mayen Fracture Zone)
Liverpool Land shelf	
————— <i>Scoresby Sund "Fracture Zone"</i>	(proj. of Spar Fracture Zone)
Blosseville Kyst shelf	
————— <i>Kangerdlugssuaq Escarpment Zone</i>	(proj. of Tjörnes FZ north of Iceland)
Denmark Strait Ridge	
————— <i>Denmark Strait Escarpment Zone</i>	(proj. of FZ south of Iceland)
South-east Greenland shelf	

The East Greenland shelf is generally characterised by strong vertical post-rift movements of the lithosphere. Along the southern half of the margin these differential vertical movements were concentrated in a narrow zone near the ocean/continent transition (OCT). The continental crust in this region consists of Precambrian cratonic basement that underwent limited rifting prior to Cenozoic seafloor spreading and resisted major down-flexuring by the adjacent cooling and subsiding oceanic lithosphere ("lithospheric flexuring"): this resulted in the formation of a mainly coast-parallel narrow flexure zone, which is most intensely developed as a huge escarpment (relief of 5 to 8 km) in the Blosseville Kyst and Liverpool Land shelf regions: the East Greenland Escarpment. Along the flexure zone or escarpment oceanic lithosphere thermally subsided while the continental lithosphere was uplifted: the two types of lithosphere were thus effectively decoupled. The location of this feature near the coast implies that the southern shelf is floored by oceanic crust and that no pre-rift sediments are present in that area; the Tertiary post-rift sediments are concentrated in narrow basins in front of the escarpment. A further characteristic of the southern provinces is the almost continuous presence of a zone of so-called "seaward-dipping reflectors" associated with the OCT. Such features have been discussed by a.o. Hinz (1981) and Mutter (1985), and are generally believed to reflect a period of subaerial spreading (Fig. 14). Eventually they grade seaward into pillow lavas erupted under submarine conditions, and having a more hummocky reflection pattern.

The continental crust along the northern half of the East Greenland margin consists of Caledonian basement that underwent extensive late Paleozoic and Mesozoic rifting before the initiation of seafloor spreading. Between the attenuated (and less buoyant) continental lithosphere and the oceanic lithosphere a good coupling developed, so that differential vertical movements were spread over a much broader zone, more like in a typical passive margin setting. The inner portion of the northern shelf therefore experienced almost no subsidence, while substantial parts of the outer continental shelf, comprising Paleozoic to Mesozoic basins, subsided along with the adjacent oceanic lithosphere. These basins are covered by a relatively thin (or even absent) layer of Tertiary post-rift sediments, which were more widely distributed over the broad continental shelf.

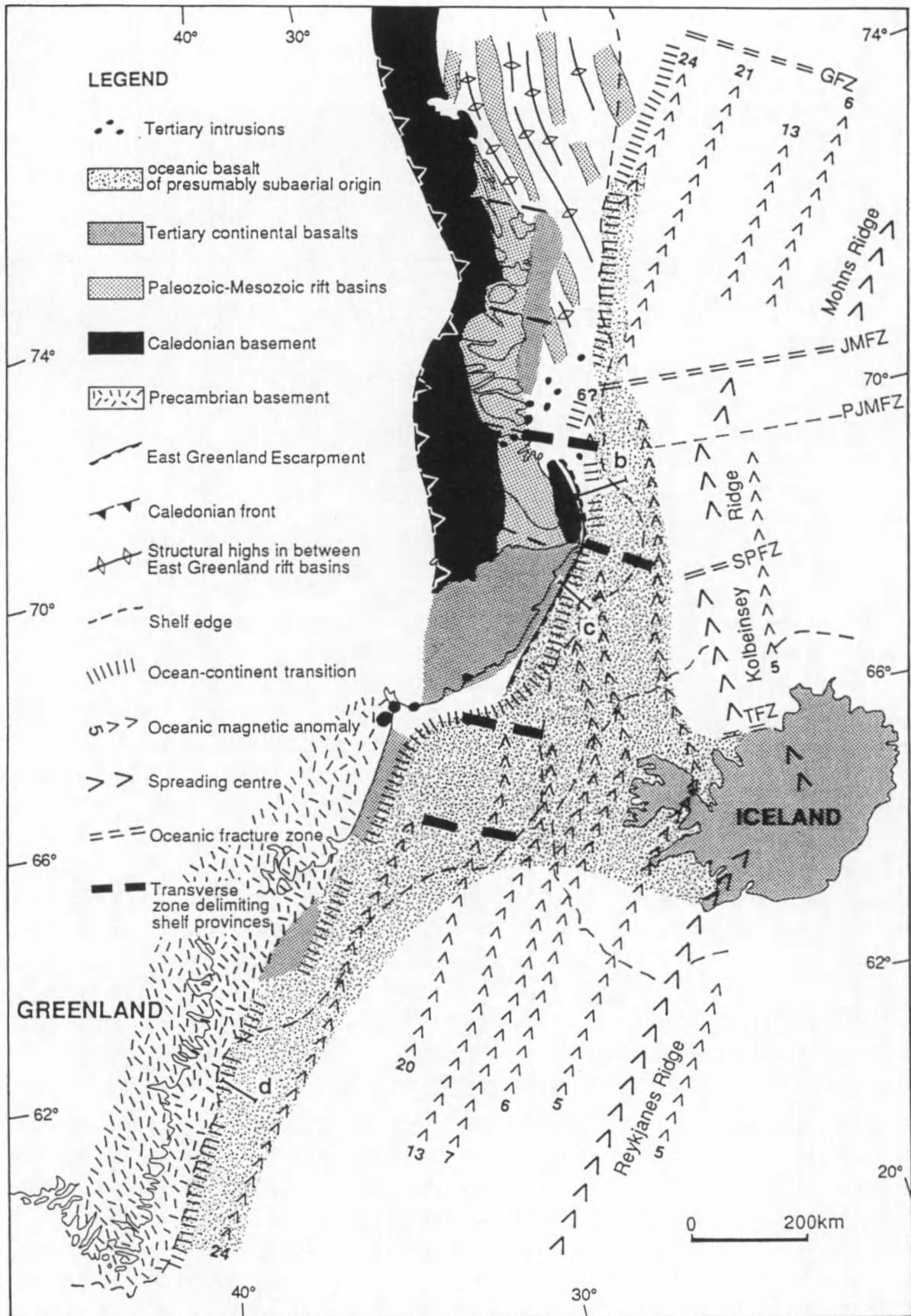


Fig. II.11 - Geological and tectonic map of the East Greenland margin, showing the location of the different shelf provinces (after H.C. Larsen 1990). GFZ = Greenland Fracture Zone, JMFZ = Jan Mayen Fracture Zone, SPFZ = Spar Fracture Zone, TFZ = Tjörnes Fracture Zone; b-d mark location of cross-sections presented in Fig. II.12.

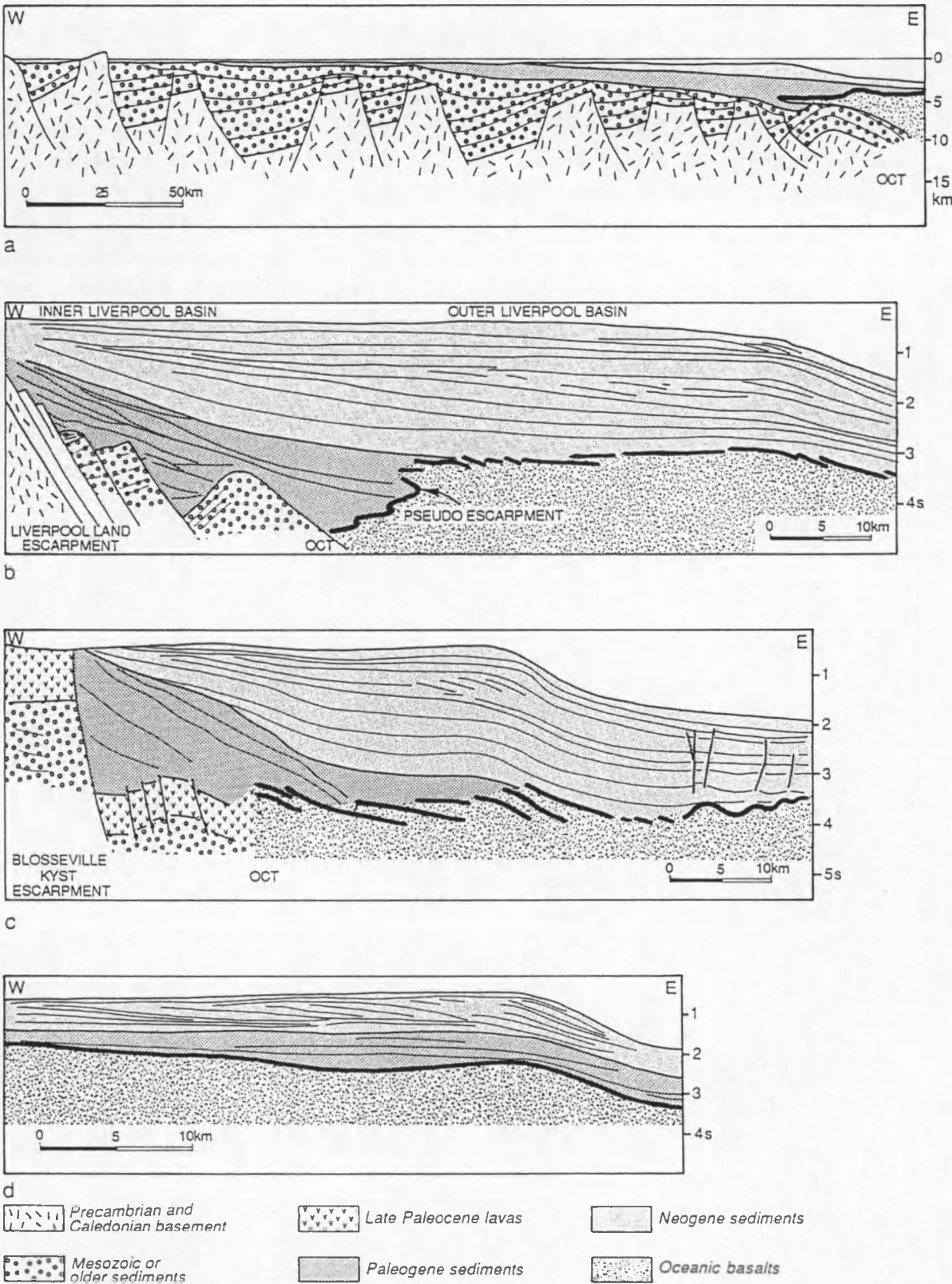


Fig. II.12 - Cross-sections through different shelf provinces (from north to south). Location is indicated in Fig. II.11. [a] North-East Greenland shelf at 76° N (hypothetical), [b] Liverpool Land shelf, [c] Blosseville Kyst shelf, and [d] South-East Greenland shelf. After H.C. Larsen 1984 (d), 1985 (a-c).

Superimposed on the tectonic inhomogeneity along the line of opening, the seafloor spreading process itself was strongly variable along the margin: the spreading axis is subdivided into three segments (Fig. 13). The southern (Reykjanes Ridge) and northern (Mohns Ridge) segments, along which regular seafloor spreading took place since late Paleocene times, correlate closely with the South-east Greenland shelf / Denmark Strait Ridge and the North-East Greenland shelf provinces, respectively. The middle segment, between Iceland and the Jan Mayen Fracture Zone, comprises two paired spreading axes (the Aegir Axis and the Kolbeinsey Ridge) and correlates with the transition zone of the Blosseville Kyst and Liverpool Land shelf regions. The spreading history here is much more complex: spreading initiated along the now extinct Aegir Axis in the late Paleocene, but shifted westward to the Kolbeinsey Ridge during the Oligocene, as a result of which the Jan Mayen Ridge was split from the Greenland continent (Talwani & Eldholm 1977; Nunns 1983; H.C. Larsen 1988).

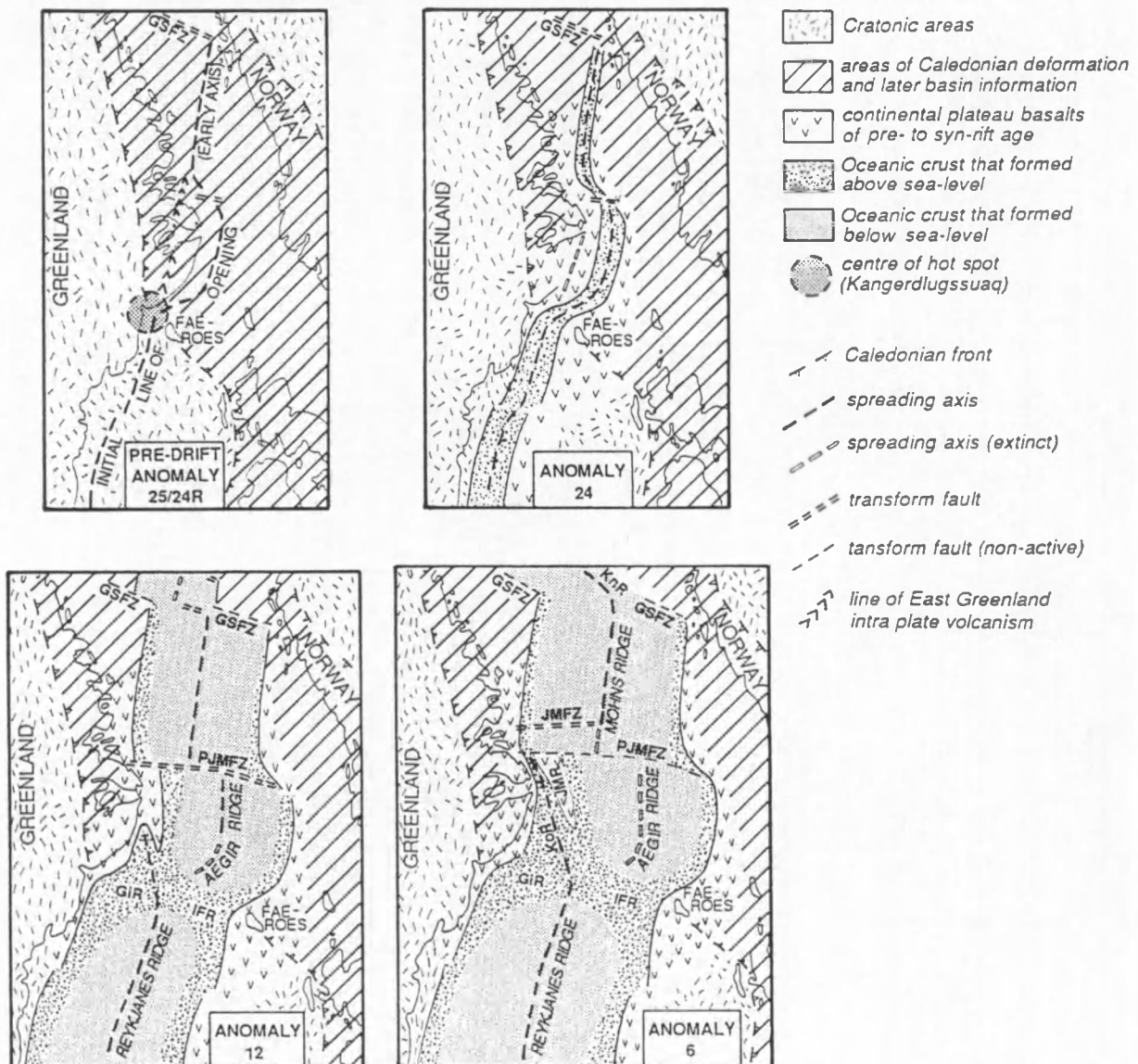


Fig. 11.13 - Four steps in the sea floor spreading history of the NE Atlantic (H.C. Larsen 1988).

GIR = Greenland-Iceland Ridge, GSFZ = Greenland-Senja Fracture Zone, IFR = Iceland-Faeroe Ridge, JMFZ = Jan Mayen Fracture Zone, JMR = Jan Mayen Ridge, KnR = Knipovich Ridge, KoR = Kolbeinsey Ridge, P.JMFZ = proto - Jan Mayen Fracture Zone.

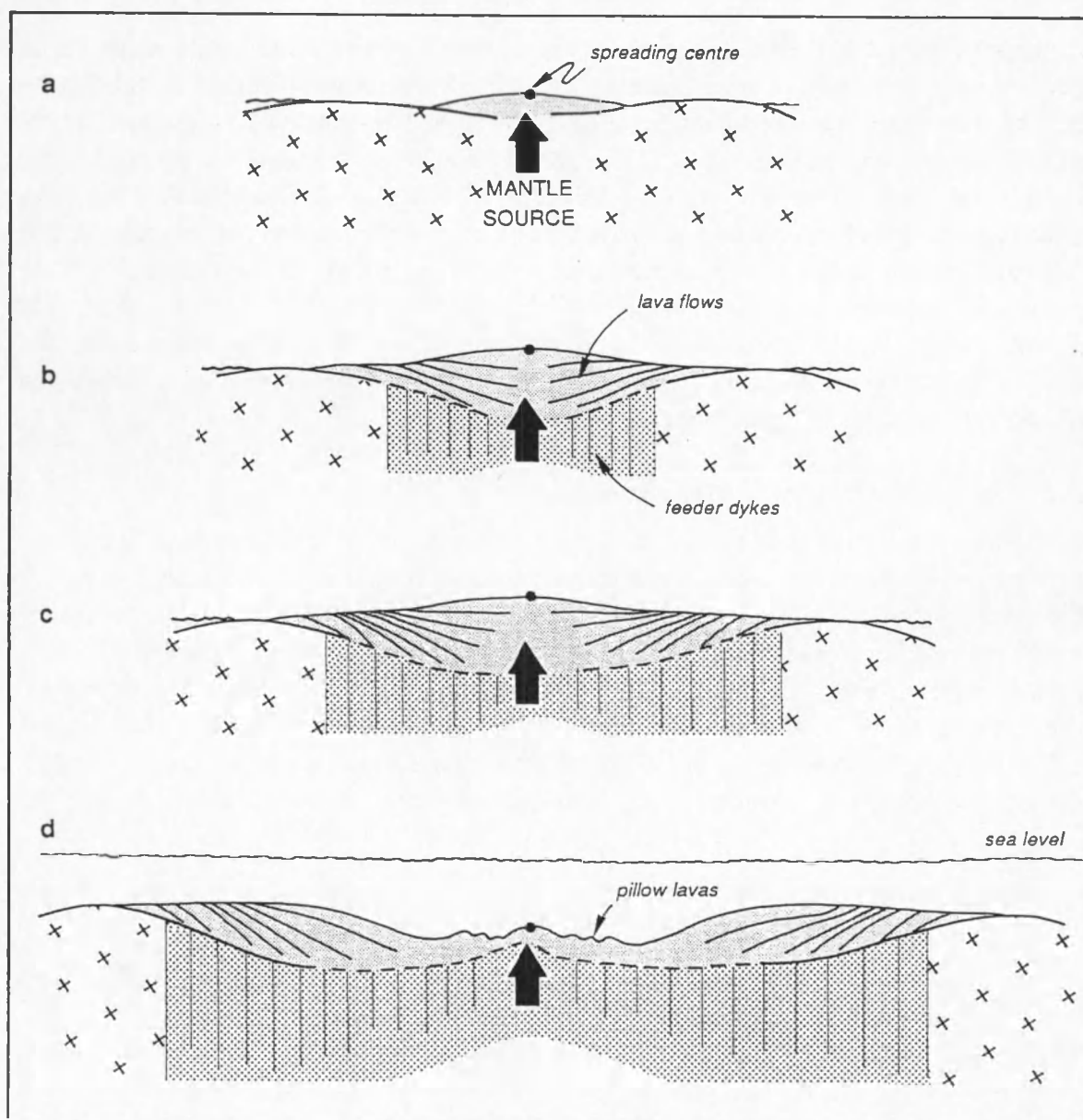


Fig. 11.14 - Schematic evolution of wedges of seaward dipping reflectors, formed by extensive volcanism along a subaerial spreading axis. The dip of lava flows towards the spreading centre is post-depositional, acquired through rapid differential subsidence under the weight of younger flows in the central rift zone [a-c]. When the spreading centre drops below sea level, the lava flow lengths dramatically reduce, and the normal chaotic structure of the upper oceanic crust is created [d]. Modified from Mutter (1985).

4.2.1. The South-eastern Shelf (SEAS)

Seafloor spreading along the South-eastern Shelf started under subaerial conditions along the Reykjanes Ridge in the late Paleocene, during the period of reverse magnetic anomaly 24R (Fig. 13). The oldest recognised anomaly is 24 A/B (H.C. Larsen 1980; H.C. Larsen & Jakobsdóttir 1988). The coast-parallel crustal flexure zone associated with the OCT follows the shelf edge in the southern part of the SEAS, but approaches the coast in the north. On the southern shelf, which is quite narrow (75 km), Precambrian basement is therefore exposed, while the northern shelf, widening to 175 km, is floored by subsided oceanic crust displaying seaward-dipping reflectors (Fig. 12d).

Sedimentation started in the latest Paleocene in a depression formed on subsiding oceanic crust between the incipient marginal flexure zone in the west and the subaerial Reykjanes Ridge in the east. The embayment was flooded from the south. With the subsidence below sea level of the Reykjanes Ridge during the Eocene (H.C. Larsen & Jakobsdóttir 1988) a seaway was established to the east. In the course of the Paleogene the sediment supply from East Greenland became restricted, and the basin developed into a deep-water basin: the depocentre consequently shifted seaward. Due to increased crustal flexuring, a new pattern of basin filling started in the Neogene with the deposition of a strongly progradational clastic wedge, which makes up most of the present-day sedimentary shelf (Fig. 12d). The progradation amounted to only 5 to 20 km in the south, and between 50 and 70 km in the centre and north. The general thickness of the post-rift sediments within the SEAS is less than 2 km. Pre-rift sediments are virtually absent.

4.2.2. The Denmark Strait Ridge (Danmarks Stræde High)

The Denmark Strait area builds a basement ridge between Iceland and Greenland, exclusively floored by anomalously thick oceanic crust displaying seaward-dipping reflectors (H.C. Larsen & Jakobsdóttir 1988). This is the result of prolonged subaerial seafloor spreading in the trail of the Icelandic hot spot from about anomaly 24 onward (Fig. 13). The Denmark Strait Ridge most likely remained emergent during large parts of the Tertiary, up to late Middle Miocene times, and underwent a relatively small amount of subsidence (< 1 km). The coast-parallel flexure zone is therefore only weakly developed in this region. Another consequence is that the Blosseville Kyst basin and the South-east Greenland basin remained completely separated during most of the Tertiary.

The oldest sediments on top of the ridge are of late Middle Miocene or younger age. The total sediment thickness varies from less than 800 m to 1200 m.

4.2.3. The Blosseville Kyst Shelf (BLKS)

The Blosseville Kyst shelf stretches along the East Greenland continental basalt province, which is found to continue below part of the inner shelf (Fig. 12c). The coast-parallel monoclinical flexure is a prominent feature, most intensely developed as an escarpment in the northern part of the BLKS. It is responsible for a much larger subsidence and consequently greater sediment thickness than in the SEAS. The OCT is thought to be located slightly seaward of the flexure zone, which means that part of the shelf is actually floored by attenuated continental crust. The larger part of the shelf is underlain by oceanic crust showing no clear evidence of seaward-dipping reflectors, however. The magnetic lineations terminate obliquely towards the flexure zone (Fig. 11), indicating that generation of oceanic crust along the Kolbeinsey Ridge propagated from Iceland northward between anomalies 20 and 6 (Fig. 13). Seafloor spreading started above sea level and was quite voluminous: the WNW sloping volcanic basement surface of the Icelandic insular plateau partly extends below the present-day continental slope and outer shelf.

The sedimentary section is exclusively of Tertiary age, 5 - 7 km thick and up to 10 km in stratigraphical thickness (Fig. 12c). Deposition started in the Eocene in a very deep and narrow half-graben, formed in front of the coastal flexure and escarpment zone, which was initiated just after initial rifting and was mainly established prior to sedimentation. The half-graben basin was restricted by an emerged proto-Icelandic plateau to the east and by the Denmark Strait ridge to the south, but probably had a narrow connection to the north through the Liverpool Land basin. The half-graben

was filled during the Paleogene. By Late Oligocene time, the Kolbeinsey Ridge had propagated along the eastern flank of the half-graben, thus enabling a seawards expansion of the Blosseville Kyst basin onto the newly formed oceanic crust. As the basin remained bounded to the east by the subaerial Kolbeinsey Ridge, however, the Early and Middle Miocene are characterised by mainly vertical shelf aggradation. In the late Middle Miocene the spreading axis subsided below sea level, and the basin became a wider and open shelf basin in which up to 4.5 km of Neogene and Quaternary sediments accumulated. During the Late Miocene and the Plio-Pleistocene increasing fluctuations in sea level, together with an increased input of sediments, led to episodes of strong shelf progradation (between 10 and 30 km), alternating with more aggradational periods.

4.2.4. *The Liverpool Land Shelf (LILS)*

The Liverpool Land shelf extends from just south of the mouth of Scoresby Sund northward to the entrance of Kong Oscar fjord (Fig. 11). The shelf is structurally divided into two coast-parallel entities of equal width, the Inner Liverpool Land basin and the Outer Liverpool Land basin. The inner basin is bounded towards the Liverpool Land crystalline basement in the west by the northern continuation of the East Greenland Escarpment. It is the broader equivalent of the Paleogene half-graben in the Blosseville Kyst area, with this difference that it contains a fairly thick (about 4 km) sequence of pre-rift sediments of presumed late Paleozoic to Mesozoic age. Extensive syn-rift volcanics seem to be absent. The two Liverpool Land basins are separated by a west-facing pseudo-escarpment, formed by the landward termination of the oceanic basement flooring the outer basin, and consisting of interdigitating volcanics and sediments (Fig. 12b). This pseudo-escarpment approximately represents the OCT. The outer shelf basin developed from anomaly 6 onward (Fig. 13), and locally displays seaward-dipping reflectors. It can be compared with the Neogene basin development of the Blosseville Kyst shelf. Here also the spreading started subaerially. The outer basin is bounded to the east by the west-sloping volcanic basement surface of the Icelandic insular plateau.

As in the Blosseville Kyst shelf region, the main tectonic episode of block-faulting and escarpment formation is probably of early to middle Eocene age. A deep tectonic depression was created which was most likely contiguous with the Jan Mayen Ridge to the east, and in which deep marine sedimentation took place throughout the Paleogene. Seafloor spreading at that time occurred along the now extinct Aegir axis east of the Jan Mayen Ridge (Fig. 13). This scenario changed during the Oligocene, when a volcanic ridge started to form between the inner Liverpool Land shelf and the Jan Mayen Ridge as a result of a northward propagation of the Kolbeinsey Ridge. The western flank of this volcanic ridge constitutes the present pseudo-escarpment. During the early part of the Neogene, the LILS was a shallow to moderately deep marine embayment with a limited marine opening to the north. When the Kolbeinsey Ridge became permanently submarine around anomaly 5 to 5A, increasingly open marine conditions developed. As in the BLKS area, vertical aggradation dominated throughout the Early and Middle Miocene, whereas the Late Miocene and the Plio-Pleistocene are characterised by progradation (Fig. 12b). Most important for the Neogene evolution, however, is the development of a striking depocentre in front of the mouth of Scoresby Sund. As much as 6000 m of mid-Miocene to recent sediments — the thickest section along the East Greenland margin — were deposited here within only 18 Ma. The large and rapid subsidence within this area, averaging up to 300 m/Ma is ascribed to cooling of the young oceanic lithosphere in combination with strong loading by the large volumes of sediment supplied by the Scoresby Sund river system (see section 4.1.2).

	Southeastern shelf	Denmark Strait	Blosseville Kyst shelf	Liverpool Land shelf	Northeastern shelf
N-S extension	60° - 66° N	66° - 67°30' N	67°30' - 69°30' N	69°30' - 72° N	72° - 80° N
Shelf width	75 km (S) - 175 km (N)	175 - 200 km	200 km (S) - 100 km (N)	100 - 125 km	125 km (S) - 300 km (N)
Onshore geology	Precambrian shield	Precambrian shield	Tertiary plateau basalts	Caledonian fold belt, late Paleozoic to Mesozoic basins, local Tertiary plutons	Caledonian fold belt, late Paleozoic to Mesozoic basins
Major structural elements	coast-parallel monoclinical crustal flexure	basement ridge; weakly developed flexure zone	crustal flexure zone, developing into the East Greenland Escarpment	near-coastal East Greenland Escarpment; seaward pseudo-escarpment	no coastal flexuring or escarpment, but gentle seaward downflexuring
Location of OCT	associated with flexure zone	associated with flexure zone	slightly seaward of East Greenland Escarpment	just seaward of the pseudo-escarpment	near the shelf edge, much more seaward than to the S
Floored by	oceanic crust (N); Precambrian basement (S)	oceanic crust	oceanic crust; thinned continental crust near the escarpment	thinned continental crust (inner shelf); oceanic crust (outer shelf)	continental crust with late Paleozoic to Mesozoic grabens; Tertiary plutons in S
Seaward dipping reflectors	widespread	everywhere present	no obvious sign	locally developed (outer shelf)	not present
Pre-rift sediments	absent	absent	only near the escarpment	on the inner shelf	omnipresent
Start of oceanic spreading	at anomaly 24 R	after anomaly 24	between anomalies 23 and 6	at anomaly 6	between anomalies 24 and 21
Submergence of spreading ridge	during the Eocene	spreading emergent up to present	late Middle Miocene	between anomaly 5 and 5A	from the start
Start of post-rift deposition	latest Paleocene	late Middle Miocene or later	early Eocene	Eocene (inner shelf); late Middle Miocene (outer shelf)	post-Paleocene
Tertiary sediment thickness	generally less than 2 km	generally less than 1 km	5 - 7 km	3 - 6 km	< 1 km or absent (inner shelf); up to 3 km (outer shelf)

Table II.3 - Comparison of the main characteristics of the East Greenland shelf provinces (compiled from H.C. Larsen 1984, 1985, 1990).

4.2.5. The North-east Greenland Shelf (NEAS)

The North-east Greenland shelf stretches for about 800 km from 72° to 80° N, terminating against the Greenland Fracture Zone. The shelf is 125 km wide in the south, but widens to as much as 300 km towards the north (Fig. 11). The North-east Greenland shelf differs markedly from the southern provinces by its more gentle seawards downflexuring of the shelf after rifting time (as opposed to the strong flexuring of the lithosphere along a coastal hinge line), and by the much more seaward position of the OCT. The result is a much wider continental shelf with a limited cover of post-rift sediments: Tertiary sediments are thin (< 1 km) or locally absent on the inner shelf, but increase to 3 km on the outer shelf (Fig. 12a). The history of seafloor spreading in the adjacent oceanic basin is much less complicated than in the LILS or BLKS areas, and took a start between anomalies 24 and 21 under predominantly submarine conditions (Fig. 13).

The NEAS can be divided into a southern part affected by tectonism and volcanism of presumed mid-Tertiary age (72° to 75° N), and a northern, nonvolcanic part (75° to 80° N). The northern region seems to be dominated by a number of very long, coast-parallel graben-ridge systems (Figs. 11, 12a), which can be correlated with basins onshore North-east Greenland (H.C. Larsen 1980; Surlyk et al. 1981) and in the SW part of the Barents Sea (Rønnevik & Jacobsen 1984). In the graben areas as much as 8 to 10 km of late Paleozoic to Mesozoic sediments may be present.

4.3. Glacial history of Greenland and Scoresby Sund

Greenland is presently covered by the only ice sheet in the northern hemisphere, known as the "Inland Ice". The ice sheet has so wide an extent that — in contrast to glaciers — it moves largely independently from the topography of the substratum. The Inland Ice is a lens-shaped body of firm and ice covering the interior of the Greenland continent: 81 % of the total surface of Greenland is covered by the Inland Ice or by local ice patches, while only 19 % is ice free (Fig. 15a), and an almost continuous ice coverage occurs as far southward as 60° N (Weidick 1976). The Inland Ice obtains a maximal thickness of 3.4 km. Total disappearance of the Inland Ice would result in a global sea level rise of 6 - 7 m (Weidick 1976). The summit of the Greenland ice sheet is located at an altitude of 3240 m. The crust is strongly depressed by loading of the ice, and the centre of the continent presently lies below sea level (Fig. 15b).

4.3.1. Tertiary climatic deterioration

Since rifting of the North Atlantic in Cretaceous times Greenland has been free of other continents and was surrounded by deep ocean basins. Tertiary Greenland can therefore be envisaged as an island similar to its present situation; the tendency towards colder conditions appears to have existed already in the Mesozoic, but intensified during the Tertiary, and culminated in the strongly marked Plio-Pleistocene ice ages (Weidick 1976).

Paleogene

Fossil plants in the Lower Paleocene beds in West Greenland indicate a warm temperate climate and a depositional environment of big river systems deriving their material from areas presently under the Inland Ice (Koch 1964).

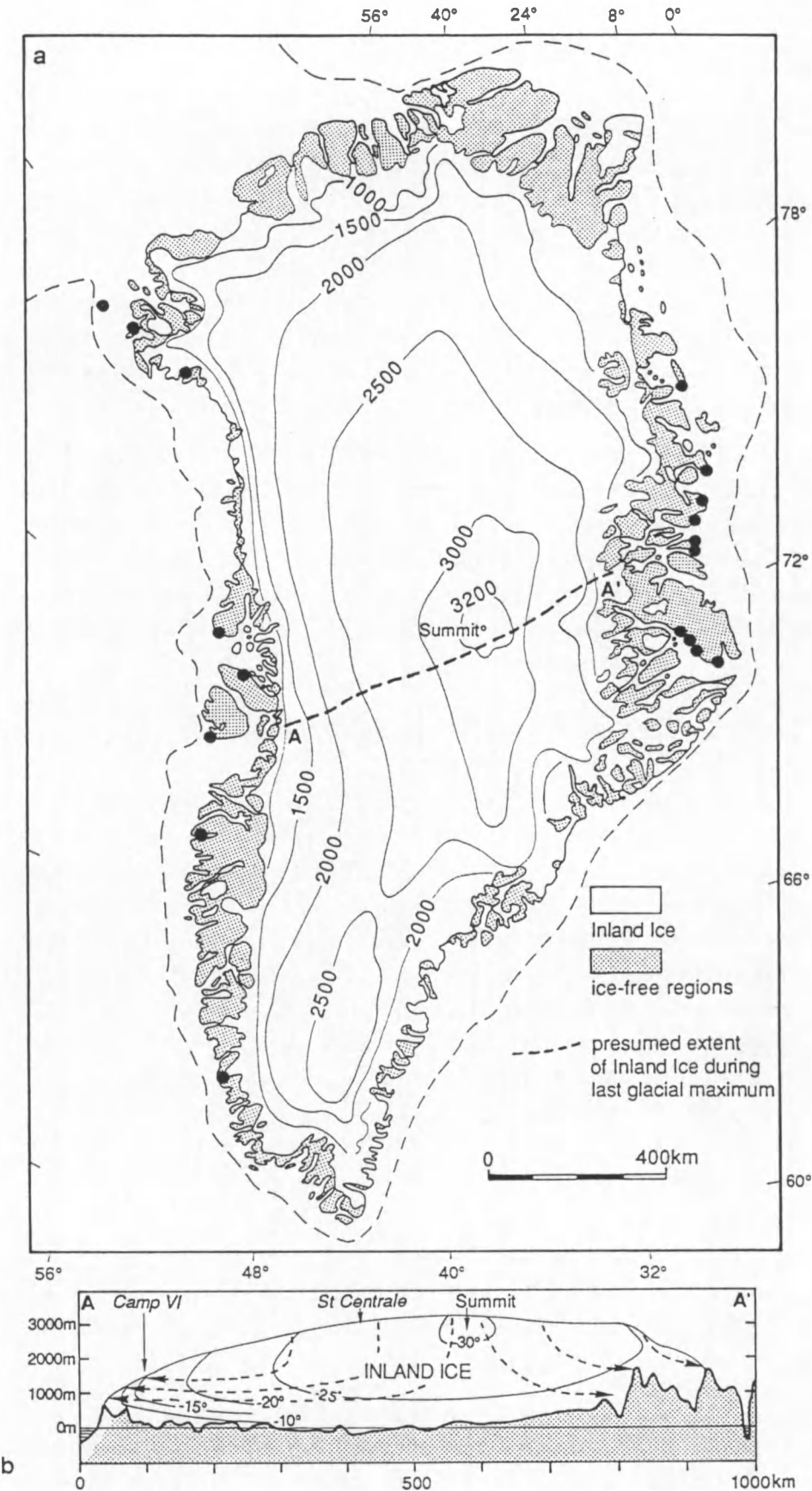


Fig. II.15 - [a] Thickness contour map of the Greenland Ice Sheet (from Weidick 1976), with black dots indicating known sites of pre-Holocene glacial sediment (Funder 1984). [b] Cross-section and temperature profile through the central part of the Inland Ice. Arrows indicate general ice flow direction. From Weidick (1976).

Neogene

No deposits from this period are known on Greenland. The Miocene climate of Greenland was similar to that of present-day southern Europe, with a glaciation limit at least at 2000 m above sea level near the coast (presently 500 - 700 m) and increasing to 3000 m in the interior of Greenland (presently 1500 - 1700 m). With the present altitudes (taking into account the isostatic correction for the loading of the Inland Ice) only small local glaciers could have existed in the highest areas (Weidick 1976).

4.3.2. Plio-Pleistocene development of the Greenland ice sheet

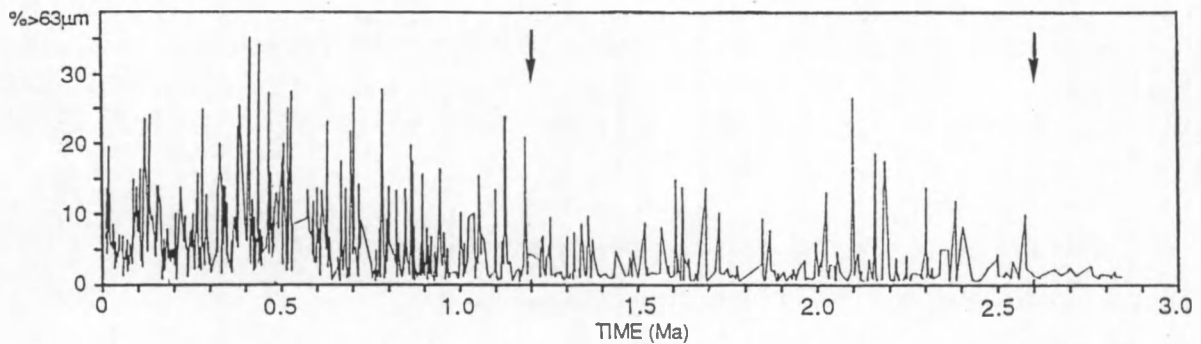
The time by which the Greenland ice sheet came into existence is still very speculative. Glaciation of the Greenlandic interior probably started with small local glaciers in the mountains. Once the mountain glaciers had spread sufficiently to form piedmont glaciers, development of the main ice sheet would be rapid because of the autocatalysis of glaciation (Weidick 1976).

The land record of glaciation on Greenland is discontinuous and fragmentary, and very sparse. Pre-Holocene glacial sediments occur only in sites at the outer coasts (Fig. 12a), at great distances from the present Inland Ice margins (Funder 1984). Repeated glaciations of the outer coast are evident from these sites, indicating phases when the Inland Ice reached beyond the present coast line (Funder 1984). The majority of the sites are attributed to the last glacial/interglacial cycle (Funder 1984). The individual imprint of older ice ages, in contrast, is very difficult to recognise as most evidence has been obliterated by later glaciations. In southern West Greenland no deposits have been observed at all, which must be indicative of intensive glacial erosion (Funder 1984). With the exception of the Lodin Elv Formation which was observed in the Scoresby Sund area and may originate from the Plio-Pleistocene transition (Feyling-Hansen et al. 1983; see section 4.3.3), the oldest glacial deposits in Greenland are thought not to date back beyond the Saale glaciation. Little is known about the preceding glaciations, however.

Due to the sparsity of land data we have to rely on evidence from the deep sea to reconstruct the entire history of glaciation. Jansen et al. (1990) discussed records of ice rafted detritus (IRD) and of benthic oxygen isotopes in ODP drillholes from the Vøring Plateau in the Norwegian Sea. These provide evidence for the late Cenozoic glacial evolution of the polar North Atlantic (Fig. 16):

- the earliest clear documentation of IRD input into the Norwegian Sea took place at 5.45 Ma. These peaks are minor, but significant, and indicate the existence of glaciers or ice sheets of sizeable proportions in the northern hemisphere as far back as the late Miocene. The glaciers or ice sheets had to be large enough to reach coastal areas;
- a major IRD peak at 2.57 Ma marks a dramatic change with the onset of repetitive glacial events. It corresponds to the most pronounced environmental change that affected the Norwegian Sea during the Plio-Pleistocene. At this time significant northern hemisphere ice sheets began to form. A continuous glacial environment was established, with interglacials less warm than at present (Jansen et al. 1988);
- after 1.2 Ma a further amplification took place: IRD peaks become progressively larger and more frequent. Large ice sheets to a much larger degree expanded out onto the continental shelves. This is probably also the time when ice sheets were beginning to expand to the more southern latitudes of northern Europe;
- by about 0.6 Ma climatic variation had developed through a final transitional period into a scenario with more severe glacials and warmer interglacials (Jansen et al. 1988).

Fig. II.16 - Coarse-fraction record for the last 3 Ma in ODP Site 644A on the Vøring Plateau (Jansen et al. 1988).



Late in 1993 the Ocean Drilling Program drilled a transect of six sites (914 - 919) on the continental shelf and slope south of Angmagssalik fjord during Leg 152 (Fig. 17). The results (H.C. Larsen et al. 1994) show that substantial glaciation in Greenland began already in the Late Miocene, following a relatively mild climate during the Middle Miocene. Cooling most likely started shortly after 10 Ma within the early Late Miocene. Glaciation nucleated in southern Greenland, and full glacial conditions in SE Greenland — with glaciers extending to the coastline or beyond and with the production of icebergs at a similar (or higher) level than at present — were established around 7 Ma in the middle Late Miocene. The Late Miocene and Pliocene climate was variable, and during interglacials the glaciers onshore Greenland retreated from coastal areas or perhaps even disappeared entirely. Glaciers advanced to the sea during several intervals in the Pliocene and Pleistocene. The other North Atlantic ice sheets probably started to form later (between 5.7 and 4.5 Ma) and were fully established around 2.5 Ma.

The Greenland ice sheet thus seems to have been formed well before the Plio-Pleistocene transition. It remains a question however whether the Inland Ice has been in existence continuously, or disappeared intermittently during interglacial periods. A retreat of 100 km beyond the present limits would bring the Inland Ice close to its threshold of existence, beyond which it would disappear as did the other ice sheets in the northern hemisphere (Weidick 1976). Since the Inland Ice receded in places 20 km behind its present position during the Holocene climatic optimum, a total disappearance could be expected during a long and warm interglacial period. Estimates for the length of time required for the renewed build-up of an ice sheet range from 100,000 a to as little as 5,000 to 10,000 a (references in Weidick 1976); recent results from thermomechanical modelling suggest a span of several 10,000 a (Huybrechts & T'siobbel, in press).

Recently the European Greenland Ice-core Project (GRIP) drilled an ice core in Summit in central Greenland at the very top of the Greenland Ice sheet (3238 m a.s.l.), reaching bedrock at a depth of 3029 m. According to the calculated timescale (partly based on ice flow modelling) the record extends over the past 160 ka (into the Saalian) and possibly even over the past 250 ka, into the Holsteinian (Fig. 18, Dansgaard et al. 1993). If these estimates are correct, this would suggest that the Inland Ice has been continuously in existence since the Elster glaciation, the glacial phase preceding the Holsteinian interglacial. An earlier total disappearance of the ice sheet prior to 250 ka is not excluded by the findings of the GRIP ice core, however.

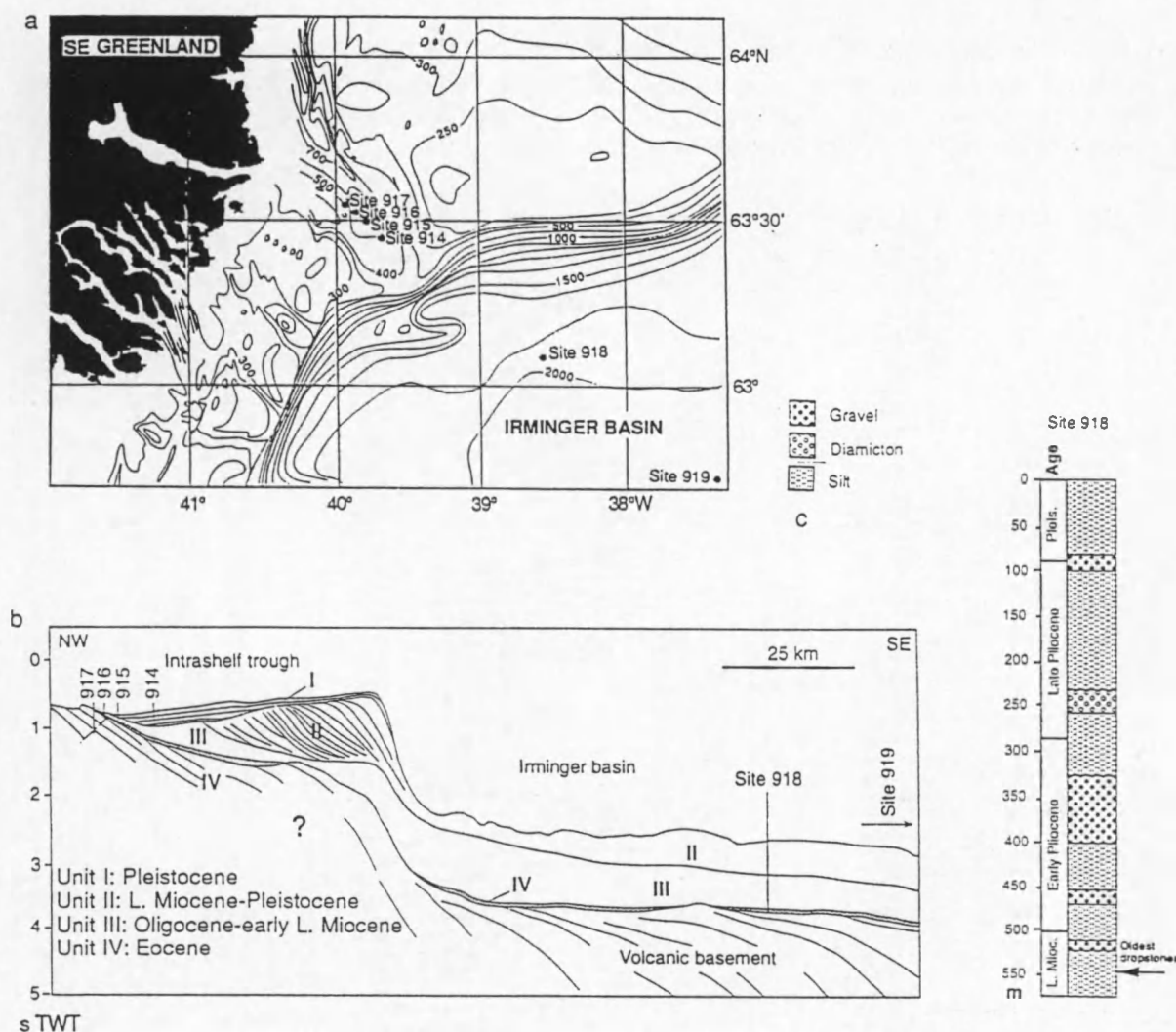
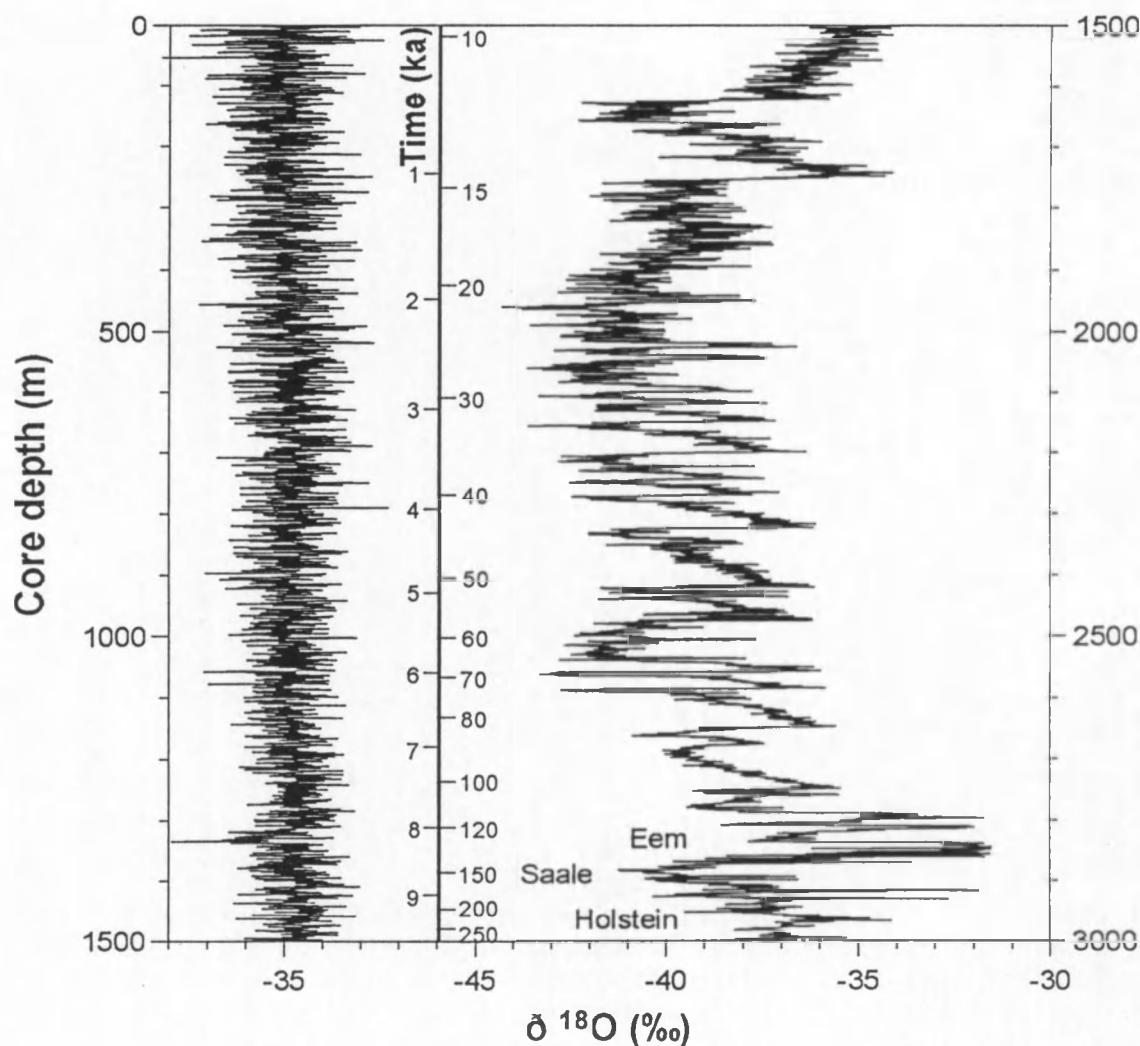


Fig. 11.17 - Results of ODP Leg 152. **[a]** Location of ODP Sites 914, 915, 916 and 917 in the transverse trough on the SE Greenland shelf south of Angmagssalik, and Sites 918 and 919 in the oceanic Irminger Basin. **[b]** Interpreted line drawing of seismic profile connecting the drill sites. **[c]** Simplified lithologic log of the most complete Miocene - Pleistocene record, obtained at Site 918. From H.C. Larsen et al. (1994).

The Greenland ice sheet has clearly shown a greater stability in its response to climatic change (at least over the past 130 ka) compared to other ice sheets in the northern hemisphere (e.g. the Fennoscandian, Spitsbergen and Laurentide ice sheets) (Funder 1984). On the other hand, the conditions are more critical than those in Antarctica, probably because Greenland is not centrally located with respect to the pole and because it extends to much lower latitudes (Emiliani 1969), but also because of the influence of rapid circulation changes in the adjacent North Atlantic ocean (Dansgaard et al. 1993). This is documented by a general pre-Holocene climate instability inferred from violent oxygen isotope shifts in the Summit ice core, in comparison to the less pronounced shifts recorded in the Vostok ice core from East Antarctica (Dansgaard et al. 1993).

Fig. II.18 - The continuous $\delta^{18}\text{O}$ record of the GRIP ice core in Summit (location in Fig. II.15a), plotted linearly in function of core depth (note the two sections). The non-linear scale in the middle is a time scale based on counting of annual layers back to 14.5 ka BP, and on ice flow modelling beyond that. From Dansgaard et al. (1993).



4.3.3. The terrestrial record of Quaternary glaciations

One of the key areas to the history of Quaternary glaciations in Greenland is Jameson Land, located in Scoresby Sund, East Greenland: unconsolidated marine, fluvial and glaciogenic sediments, recording mostly ice-free periods, form a continuous belt along the SW coast and constitute the most complete Quaternary record found in Greenland (Funder 1984). Thick Quaternary deposits, mainly glacial in origin, are also found on the high plateau building the interior of Jameson Land. The Quaternary deposits of Jameson Land have been studied intensively on a terrestrial field work survey in the summer of 1990, framing in the PONAM programme. The results were summarised by Funder et al. (1991). Earlier overviews for the whole of Greenland were given by Weidick (1976) and by Funder (1984). A compilation of this work is shown in Table 4.

The earliest trace of glaciation in Scoresby Sund, and probably in entire Greenland, is represented by the Lodin Elv Formation, found in some places along the west coast of Jameson Land and probably recording the Plio-Pleistocene transition (Feyling-Hansen et al. 1983). The presence of Pacific molluscs in the contemporaneous Tjörnes deposits on the north coast of Iceland indicates a still

relatively warm Arctic Ocean and an open Bering Strait during this period of time (late Pliocene - early Pleistocene) (Einarsson et al. 1967).

Extensive ?Saalian glaciation (c. 200 - 133 ka BP)

Both in East and West Greenland there is evidence of a pre-Eemian period of extensive glaciation when even mountain summits and offlying islands were covered by an ice sheet; this period is thought to correlate to the Saale glaciation around 200 ka BP. In Scoresby Sund this is known as the Scoresby Sund glaciation (formerly Kap McKenzie glaciation, Funder & Hjort 1973) during which the Inland Ice overrode the entire region and extended onto the shelf (Fig. 19a). Recently an older glacial event, the Lollandselv glaciation, which may be of Elsterian age ($\pm 300 - 250$ ka), has been recognised in deposits on the Jameson Land plateau (Funder, communication on PONAM workshop, 1993).

Eemian interglacial (c. 133 - 114 ka BP)

The Eemian interglacial period is known from deposits in which marine faunas indicate that subarctic water masses along the coasts of both East and West Greenland penetrated further north than presently, which resulted in higher summer temperatures than known during the Holocene (Funder 1984). The GRIP ice core largely confirms this, but also shows that the period was interrupted by a series of colder periods with more mid-glacial conditions (GRIP Members 1993). The Eemian is in the Scoresby Sund region represented by sediments of the Langelandselv Interglacial, found along the SW coast of Jameson Land. This period is firmly correlated to marine isotope substage 5e (Funder et al. 1991).

Weichselian (114 - 10 ka BP)

A threefold division of the Weichselian glacial period into Early, Middle and Late (Flint 1971) is generally accepted for Greenland, the Middle Weichselian representing a relatively warm period between the colder periods of Early and Late Weichselian.

Early Weichselian (> 75 ka BP)

In West Greenland there is no evidence of the extent of the Inland Ice in the Early Weichselian (Weidick 1976). In Scoresby Sund the Early Weichselian is known as the Jameson Land marine episode (Fig. 19b), which in fact consisted of two periods during which a fjord glacier extended in Scoresby Sund but not onto the shelf, each followed by a period of arctic marine conditions preserved in marine and delta deposits on Jameson Land (Funder et al. 1991). The glacial intervals are presently referred to as the Aucellaelv stade (115 - 107 ka) and the Jyllandselv stade (95 - 85 ka), whereas the warmer periods are known as the Hugin sø interstade (107 - 95 ka) and the Mønselv interstade (85 - 75 ka) respectively (Funder, PONAM communication 1993). The Jameson Land marine episode corresponds to marine isotope substages 5a - 5d (Hansen & Jørgensen 1993).

Middle Weichselian (75 - 20 ka BP)

A long hiatus follows the Jameson Land marine episode, so that the Middle Weichselian remains largely unknown in the Scoresby Sund area (Funder et al. 1991). In West Greenland a retreat of the ice sheet has been inferred. According to ice core studies by Dansgaard et al. (1982) a phase of rapid accumulation between 40 and 30 ka gradually moved the ice margins back towards the outer coasts, a process which culminated in the Late Weichselian glaciation.

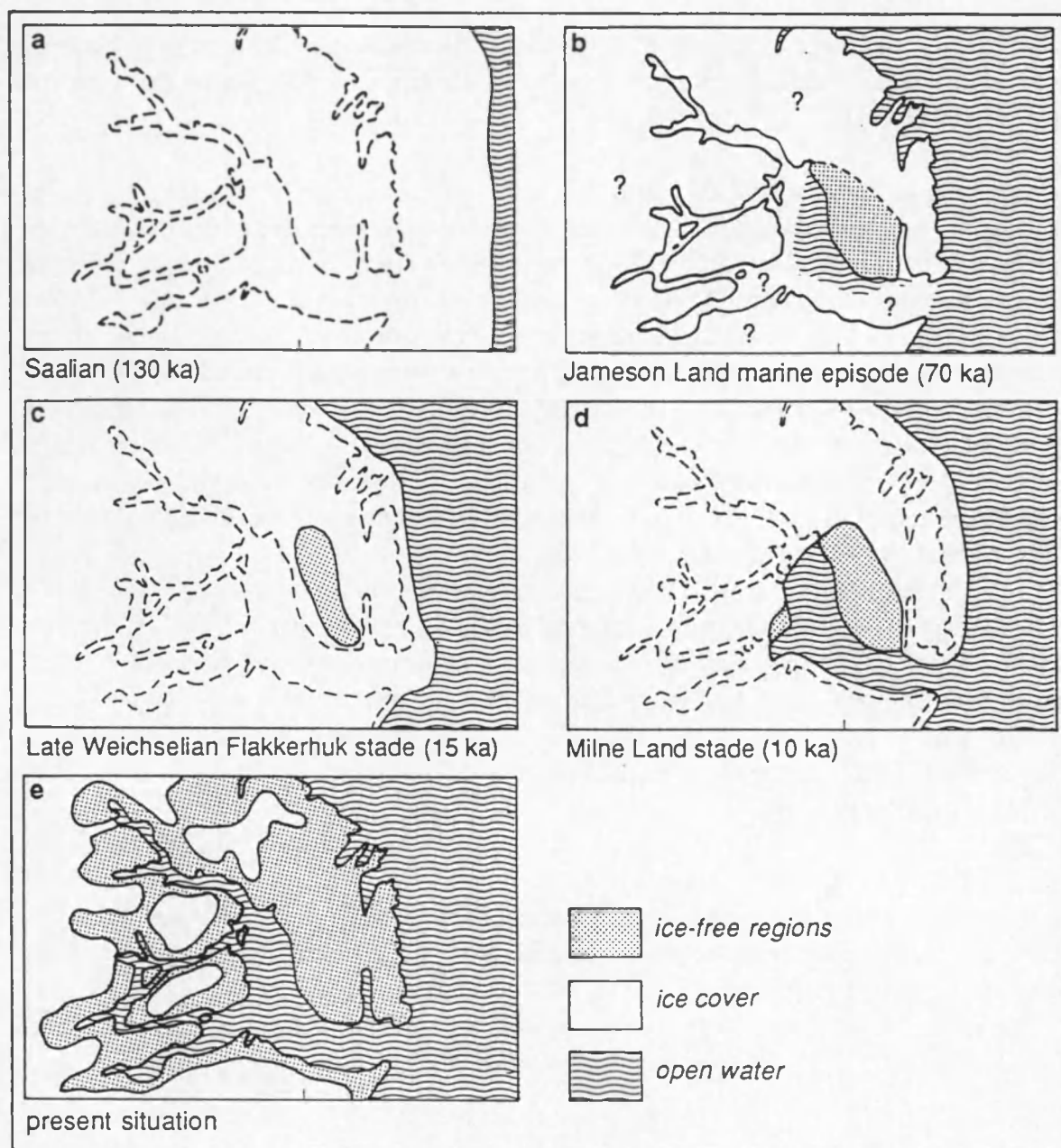


Fig. II.19 - Past and present ice cover in Scoresby Sund (from Henriksen 1989).

Late Weichselian (20 - 10 ka BP)

The Late Weichselian (isotope stage 2) witnessed the last advance of the Inland Ice in West and East Greenland. According to the latest views (Funder, PONAM comm. 1993) the Late Weichselian glaciation in the Scoresby Sund region is represented by the Flakkerhuk stade (Fig. 19c), which has earlier been temporarily regarded as Early Weichselian (Funder et al. 1991). The Flakkerhuk stade probably marked the maximum extent of the Weichselian Inland Ice (Funder 1984), and was responsible for a 50 km long glacial margin deposit, previously interpreted as a lateral moraine (Funder 1972), along the south coast of Jameson Land. Possibly the glacier floated in the fjord itself, and settled only on the shallow shelf (Funder 1989). The Flakkerhuk stade ended 14 - 15 ka ago.

All Weichselian glaciations are considered to be fjord glaciations, with ice advancing into Scoresby Sund and covering the coastal area of Jameson Land, which remained largely ice-free otherwise (Lyså & Landvik 1993).

Holocene deglaciation (< 10,300 a BP)

Following the last glaciation of the Late Weichselian the Inland Ice retreated both in East and West Greenland. Initial deglaciation began in South Greenland (Weidick 1976). In Scoresby Sund the Holocene retreat of the ice front was halted a first time during the Milne Land stade (10,300 - 9,500 a BP, Hjort 1979). The Milne Land stade, covering part of the Younger Dryas and the Preboreal represents a phase during which fjord glaciers terminated at the mouths of the narrow inner fjords (Øfjord, Fønfjord, Gåsefjord) into Hall Bredning and Scoresby Sund s.s. (Fig. 19d). Most of the Holocene ice recession in Greenland took place during the subsequent period. After a continuous retreat the glacier fronts came to a new standstill in Rødefjord during the early Atlantic: the Rødefjord stade (7,500 - 6,700 a BP) (Funder 1971). At the end of the Rødefjord stade the glaciers covered about the same area as today.

After the Rødefjord stade a short period of climate warmer than today was achieved (climatic optimum), lasting until about 5,000 a BP (Hjort & Funder 1974; Funder 1978). Overall recession in Greenland went $\pm 10 - 20$ km beyond the present limits of the Inland Ice just before or at 6,000 a BP, but was thereupon brought back to its present position. A subsequent shift towards more arctic vegetation (Funder 1978; Henriksen & Higgins 1988) and the extinction of subarctic mollusc species (Hjort & Funder 1974) documents a renewed lowering of the temperature in the Scoresby Sund region during the last millennia.

Recent situation (Fig. 19e)

The Inland Ice and local glaciers advanced as a result of the climatic deterioration up to the 17th century, and maintained an expanded position until the period 1900 - 1920. The improvement of the climate in the present century with a rise in mean annual temperature by 2° C caused a mean recession of land-based glacier lobes of 2 km, and of up to 20 km or more for calving ice lobes (Weidick 1976).

5. Bedrock geology of Scoresby Sund

5.1. Location of the data

The seismic reflection lines inside the Scoresby Sund fjord system are situated in the broad and relatively shallow outer fjord region. A more or less uniformly spaced grid covers most of Hall Bredning, and some lines extend into the south-western arm of Scoresby Sund s.s.; one line even enters the mouth of Nordvestfjord. The lines were shot with either the small airgun array, the large airgun array or the 32 l airgun. In addition, combined reflection/refraction profiles were shot with the 32 l airgun in some of the narrow inner fjords: Gåsefjord, Fønfjord, Rødefjord and Nordvestfjord.

5.2. Bathymetry

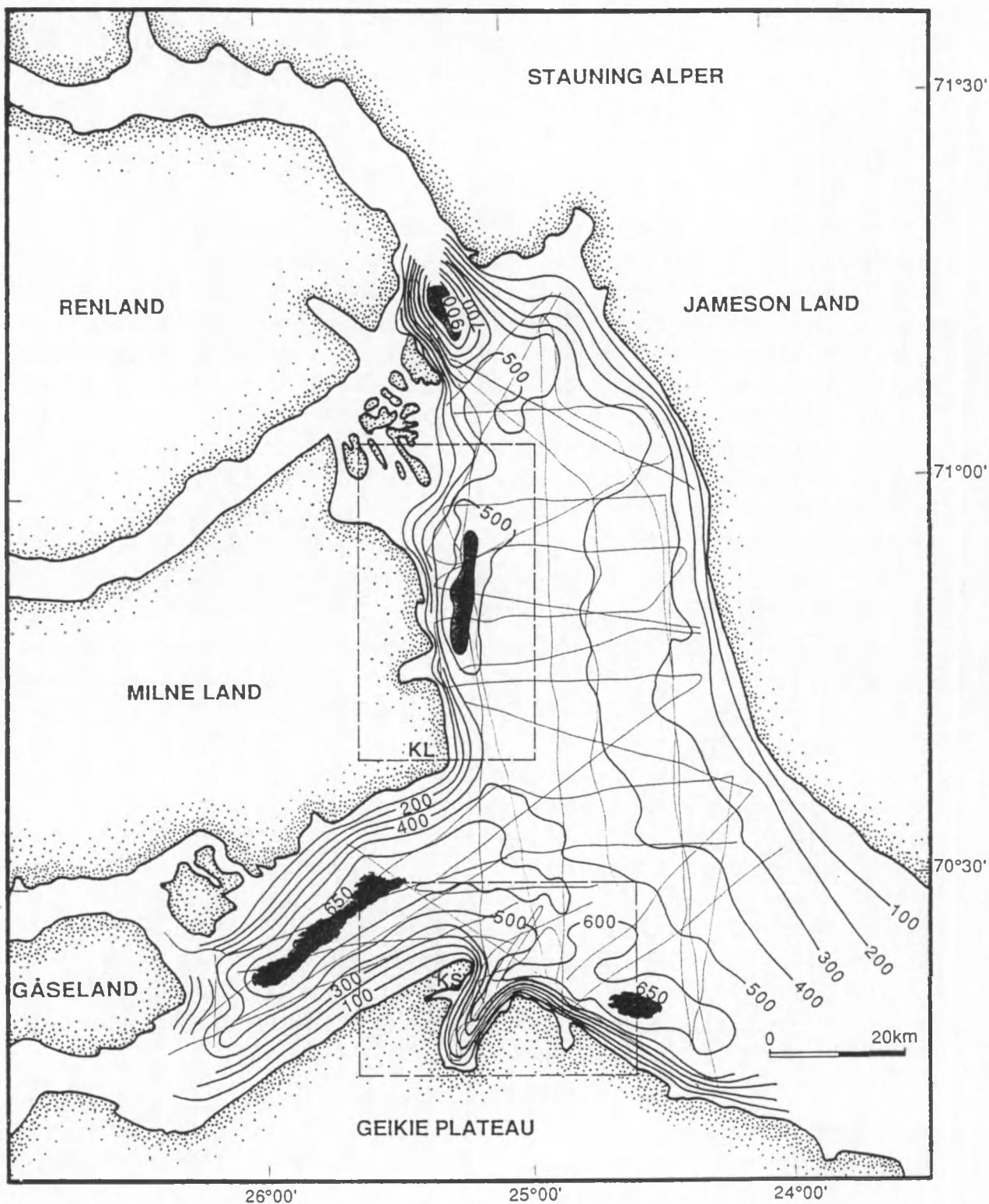
The bathymetric map constructed from the available lines (Fig. 20) confirms the general bathymetric trends outlined in section 3.2.1. Most of the study area essentially represents the continuation of the onshore Jameson Land basin, with a fjord floor that dips gently and uniformly from the smooth shores of Jameson Land in a transverse direction towards the much steeper opposite coasts. Water depths in Hall Bredning generally amount to about 450 m, but deep troughs with water depths exceeding 600 m are evident along the Milne Land coast in the west, and in front of Volquart Boon Kyst in the south; more detailed maps of these features are shown later on in Figs. 29 and 39, respectively. The largest depths (over 900 m) are recorded in the extreme N of the area, near the entrance of Nordvestfjord and Øfjord into Hall Bredning. The SW arm of Scoresby Sund is distinctly deeper than Hall Bredning, and the transition between both reaches occurs with a steeper-than-average gradient, along which the fjord floor falls from about 500 m to 650 m. A broad elevation with about 150 m relief and extending from Kap Stevenson, separates the main fjord valley from the above-mentioned trough emerging from Vikingebugt along Volquart Boon Kyst.

The fjord topography is clearly erosional in nature, and has been carved during several extensive glaciations in the Plio-Pleistocene. Glacial erosion was most intense along the western and southern shores of Hall Bredning, and in the SW arm of Scoresby Sund; this is most probably largely related to the orientation of major glacial outlets as Nordvestfjord and Gåsefjord/Fønfjord. As only negligible amounts of sediment have been deposited since the last glaciation, the bathymetry is strongly dependent on the lithology of the rocks subcropping the fjord floor: these have resisted quite differently to glacial abrasion. Mesozoic strata underlie large parts of the outer fjord region, which accounts for the generally smooth relief of this domain. The western limits of the study area are characterised by a more irregular topography, which can be ascribed to a change in the nature of the basement: Caledonian metamorphics and intrusives make up the floor in this part of the fjord. These rocks are more resistant to erosion, which resulted in the observed steep relief with magnitudes over 100 m. In general, the relief over the Caledonian intrusives is of lower amplitude and larger wavelength than over the metamorphics. Caledonian rocks usually stand in relief where they are in contact with Mesozoic sediments.

In front of the mouth of Gåsefjord, and especially of Nordvestfjord, the topography is very rugged and of large magnitude, as in the inner fjord regions. In both places changes in relief of up to 300 m can be observed which are probably to a large extent tectonically controlled. The elongated trough

along the Milne Land coast, located at the edge of a Caledonian intrusion, seems to be fault-controlled as well, and is probably only partly related to glacial erosion. The southern limit of this trough, however, connects with a smaller, but clearly erosional depression, which is carved into the softer Mesozoic sediments.

Fig. II.20 - Interpolated bathymetric contour map of Hall Bredning. Contour interval is 100 m. Shaded areas represent local minima. Dashed boxes surround areas for which more detailed maps were drawn (Figs. II.29 and II.39). KS = Kap Stevenson, KL = Kap Leslie.



5.3. Bedrock geology

Although the Scoresby Sund lines are generally of low resolution (10 - 20 m) and limited penetration (generally less than 200 ms), the data are suited enough for correlation with the geology of the surrounding land area. Hall Bredning is essentially bordered by the following geological entities (refer to section 4.1.1):

- migmatites of Middle Proterozoic and Caledonian age, specked by Caledonian intrusions, occupy the larger part of the western shore;
- Mesozoic sediments crop out along the entire shore of Jameson Land, as well as in eastern Milne Land (the Milne Land block);
- early Tertiary plateau basalts completely cover the south coast.

Except for the Milne Land block, the region to the west of Hall Bredning belongs to the Caledonian fold belt. The region to the east is part of the Jameson Land basin, a Mesozoic failed-rift basin. The contact between the two provinces is marked by a major fault system. The plateau basalts in the south are thought to conceal the southward continuation of both provinces.

On the seismic sections four different laterally-confined units (A-D) were discerned on the basis of seismic facies characteristics and surface morphology, which is strongly related to different resistance to (glacial) erosion. These seismic units can be correlated with the above mentioned geological units through extrapolation from the landward side of each profile towards the shore. This way an extension was established to the geological map of the area (Fig. 21).

5.3.1. Unit A — Mesozoic sediments of the Jameson Land Basin

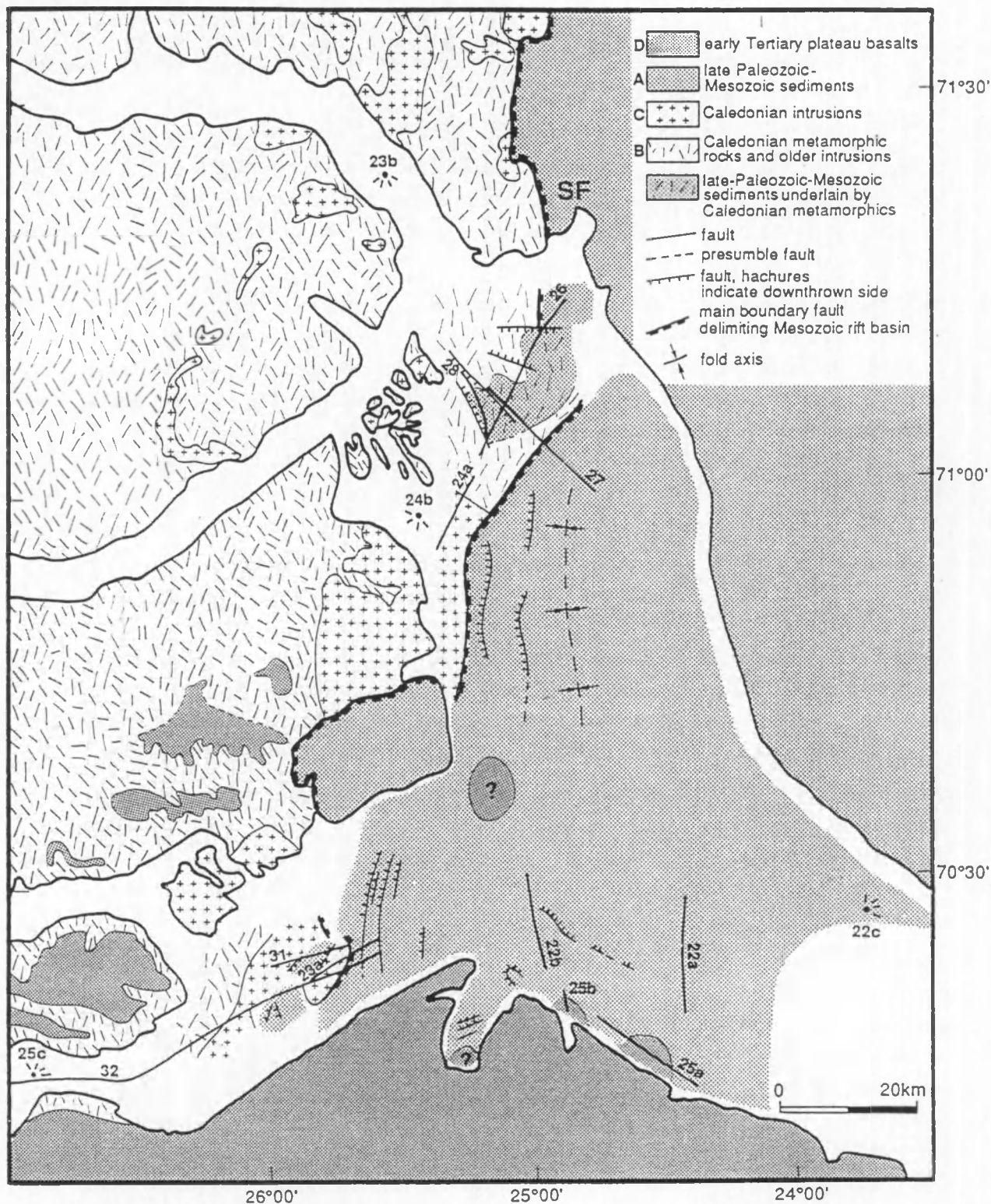
Unit A (Fig. 22 and also Fig. 33) is characterised by rather weak parallel to subparallel internal reflectors with a south-westward dipping trend. The internal reflectors are truncated by a prominent erosional surface which usually coincides with the seafloor and has little pronounced relief. This top reflector is marked by a powerful signal, limiting the seismic penetration to generally less than 200 ms. In some instances, no internal reflectors are obvious at all. All this suggests that the unit consists of rather hard, consolidated material, and that impedance contrasts within it are small. Even with a high energy source a base reflector could not be resolved, except for a small area in the north of Hall Bredning, where Caledonian basement underlies a thin patch of unit A (see Fig. 27).

The layered and mostly undisturbed internal reflection pattern leaves no doubt that unit A is sedimentary in origin. The unit constitutes the dominant basement type on the profiles, and crops out all along the eastern side of Hall Bredning, which renders correlation with the Mesozoic sediments of the Jameson Land basin straightforward. The Mesozoic sediments in Hall Bredning are probably mainly of Jurassic age (cf. B. Larsen 1980).

The Mesozoic sediments are altogether undisturbed, but some faults occur in the W and SW, near the contact with Caledonian terrain (Fig. 23); their apparent throw direction is towards the contact. Presumably most of the faults are oriented N-S, parallel to the contact zone. Additional faults can be observed within and in front of Vikingebugt along the south coast. All faults are reflected in the sea bed morphology, which may be the result of reactivation since the last erosional event, or more probably of preferential erosion along the fault planes. As a result, the real throw of the faults cannot be established with certainty. Other deformations are quite rare: there is evidence of some disturbance of the layering in the SW, and along most of the western limits of the Jameson Land

basin the dip of the strata has been inverted by a synclinal fold (see Fig. 30b) which runs along the axis of Hall Bredning (Fig. 21).

Fig. II.21 - Bedrock geology and structural map of Hall Bredning, constructed from the available seismic data. Location is indicated of seismic sections presented in the corresponding figure numbers. SF = Schuchert Flod.



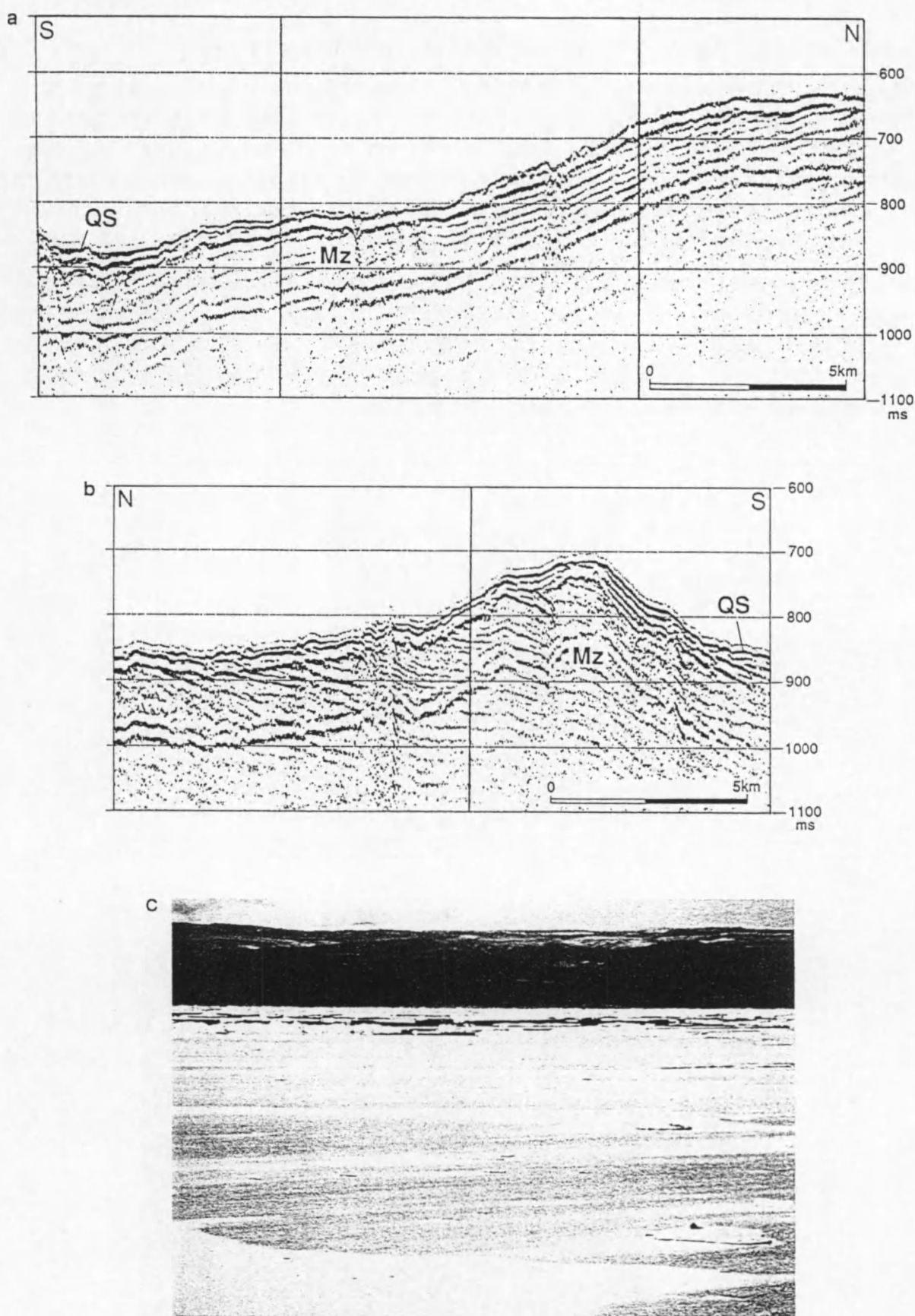


Fig. 11.22 - [a, b] Seismic signature and morphology of Mesozoic sediments in the southern part of Hall Bredning (location of profiles in Fig. 11.21), compared to an outcrop photograph from the southern Jameson Land coast [c]. The elevation on b is the subaqueous extension of Kap Stevenson. Mz = Mesozoic strata, QS = Quaternary sediments.

5.3.2. Unit B — Middle Proterozoic and Caledonian migmatites

Unit B (Fig. 23) is observed in the NW part of Hall Bredning and in the SW arm, close to terrestrial outcrops of Caledonian and older Middle Proterozoic migmatites which were welded during the Caledonian orogeny; in the discussion below they are denoted by the term “Caledonian metamorphics”, whereas the term “Caledonian terrain” includes both the Caledonian metamorphics and intrusives, together making up the Caledonian fold belt. In a small area in the north (see previous section), unit B is seen to underlie the Mesozoic sediments of unit A, which dates it as pre-Mesozoic.

Apart from an equally strong top reflection, unit B has distinctively different seismic characteristics compared to the Mesozoic unit. It shows no internal reflectors, only a dark noisy facies owing to a strong scattering of seismic energy. This suggests that layering is absent, which would confirm the non-sedimentary nature of the unit. Its surface morphology (Fig. 23) is rather irregular, showing rounded hummocks of relatively large magnitude (over 100 m).

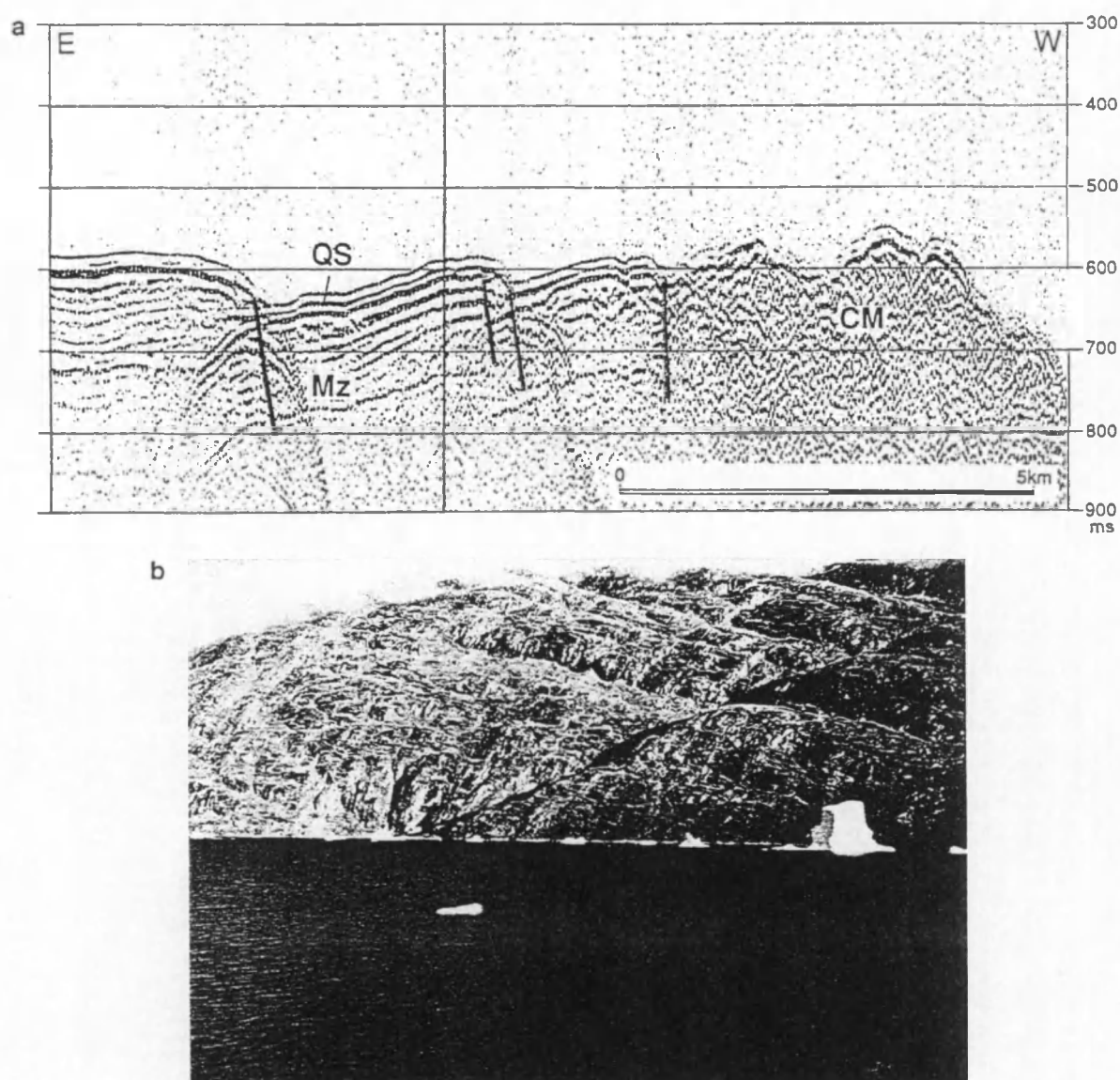


Fig. II.23 - [a] Seismic signature and morphology of Caledonian metamorphics in the SW part of Hall Bredning (location of seismic line in Fig. II.21), compared to an outcrop photograph from Nordvestfjord [b]. Note the faulted nature of the Mesozoic sediments close to the contact. CM = Caledonian metamorphics, Mz = Mesozoic strata, QS = Quaternary sediments.

5.3.3. Unit C — Caledonian intrusives

Intrusions of Caledonian age border the study area at two sites: on Danmark Ø in the SW arm, and along the NE coast of Milne Land. Near these areas a unit C was identified on the seismic lines with an appearance rather similar to the Caledonian metamorphic unit, with which it is in contact. As is the case for the metamorphic unit, unit C displays no internal reflectors or diffractions, which is not surprising for a crystalline body. It can be distinguished from the metamorphic unit by a less coarse and almost transparent facies, by a distinctly weaker top reflection, and by a different surface morphology (Fig. 24): the Caledonian intrusion is more deeply eroded than the metamorphic rocks, and the topography of its surface is more rugged, with irregularities of smaller amplitude but higher frequency compared to the metamorphics. The different relief characteristics are most spectacular east of Milne Land.

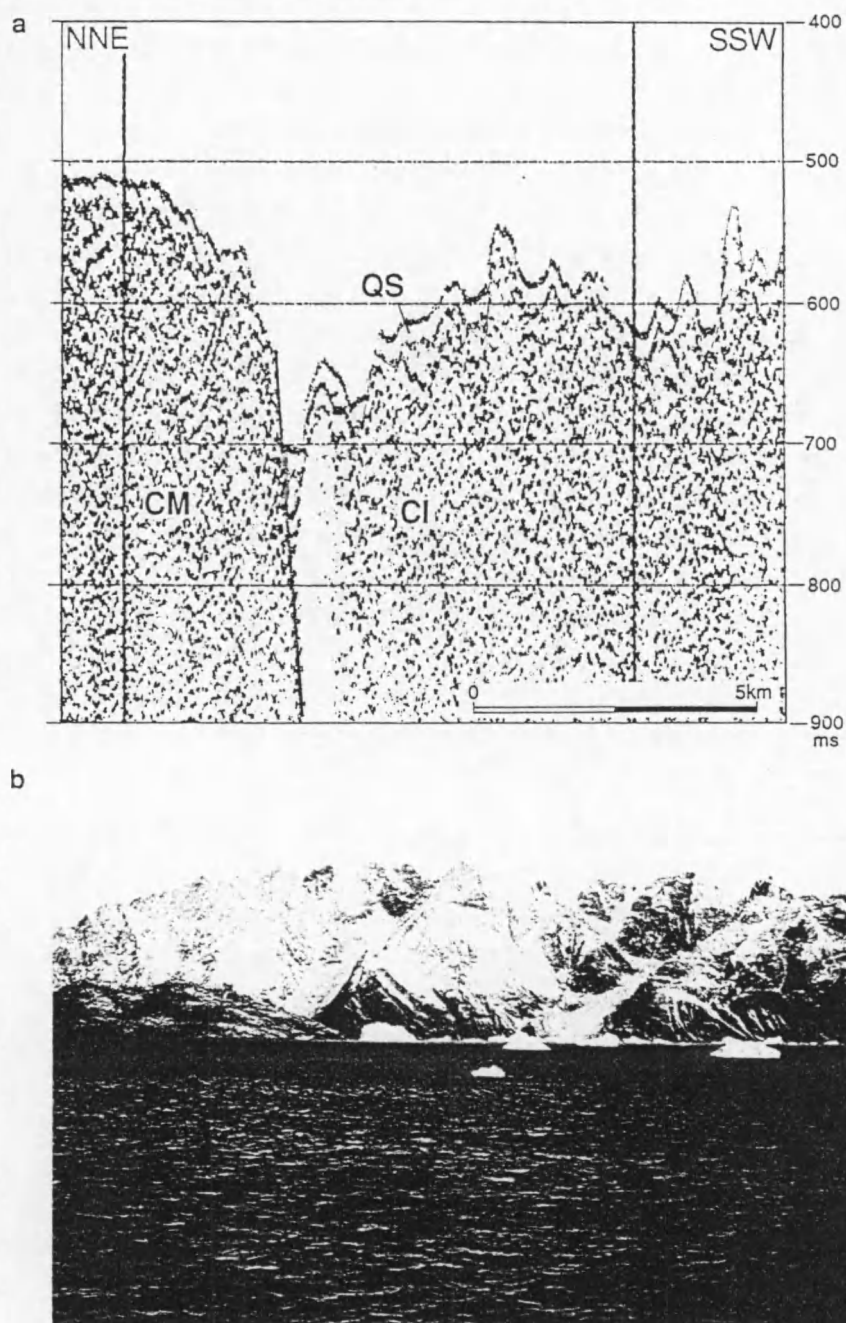


Fig. 11.24 - [a] Seismic signature and morphology of Caledonian intrusives close to the NE coast of Milne Land (location in Fig. 11.21), compared to an outcrop photograph from the same area [b]. Note the differences in character with respect to the adjacent Caledonian metamorphics. CI = Caledonian intrusives, CM = Caledonian metamorphics, QS = Quaternary sediments.

5.3.4. Unit D — Plateau basalts ?

Plateau basalts cover the entire Volquart Boon Kyst, the southern coast of the Scoresby Sund fjord system. They are thought to overlie the Mesozoic and Caledonian rocks which occur more northward. The presence of Mesozoic sediments close to the coast, and the identification of Mesozoic basement in Vikingebugt, the largest inlet along Volquart Boon Kyst, is indeed an indication that the Jameson Land basin simply continues southward beneath the plateau basalts. Because of the strong resistance properties of basalt against erosion, the basaltic coast has a very steep profile. As a consequence, basaltic units can only be observed on seismic profiles very near to the coast, and identification of the contact with underlying units — which occurs below sea level — is very difficult.

Observation of seismic units of possible basaltic nature is limited to a few occurrences. In front of Volquart Boon Kyst a local patch (the easternmost one on the map of Fig. 21) is observed with characteristics very different from the adjacent Mesozoic sediments of unit A (Fig. 25a): the top reflector is very diffuse, due to the rugged and erratic relief; no internal reflectors are evident, and the facies consists of scattered noise only. The unit has a relief of 100 to 150 m with respect to the surrounding terrain. At a first glance the contact with the Mesozoic unit appears to be intrusive; closer inspection reveals, however, that Mesozoic strata continue underneath the unit, their reflection energy being almost completely scattered and masked by the overlying unit. On ground of its seismic and topographic characteristics, and of the location close to the Geikie Plateau, the patch is interpreted as a thin outlier of early Tertiary plateau basalt overlying Mesozoic sediments of the Jameson Land basin. On the higher-resolution lines shot with the watergun two more basalt occurrences could be interpreted, one at the head of Vikingebugt (Fig. 25b) and one in front of a smaller inlet along the coast. The interpretation is based on relief characteristics and is rather tentative, due to the steepness of the seafloor. The base of the basalts varies in depth between 500 - 590 m below sea level for the easternmost occurrence, 640 m in the centre, and c. 580 m in the inner part of Vikingebugt; in front of Vikingebugt it must be less than 450 m, as Mesozoic sediments still crop out at this depth. These values are more or less in accordance with the estimate of B. Larsen (1980) that just off Vikingebugt the base of the basalts is situated between 400 m water depth and sea level, and with the observation by Watt (1970) that the basalts are inclined c. 2.5° towards the south in the Vikingebugt area, which is very near the apparent dip of the underlying Mesozoic sediments.

South-east of the Milne Land block another unit with very similar reflection characteristics and a relief of 75 m occurs amid Mesozoic sediments. Although two crossing profiles show no evidence of underlying reflectors, giving the unit the appearance of an intrusion as described above, it is interpreted as an isolated speck of basalt — similar to those presently occurring this far north in Milne Land.

5.3.5. The western boundary of the Jameson Land basin

On land the contact between the Caledonian fold belt and the Mesozoic Jameson Land basin is controlled by a N-S trending extensional boundary fault which has been identified slightly west of Schuchert Flod in the northern fjord area. This fault is postulated to extend southward into Hall Bredning, connecting with the fault bounding the Milne Land fault block (Henriksen 1989).

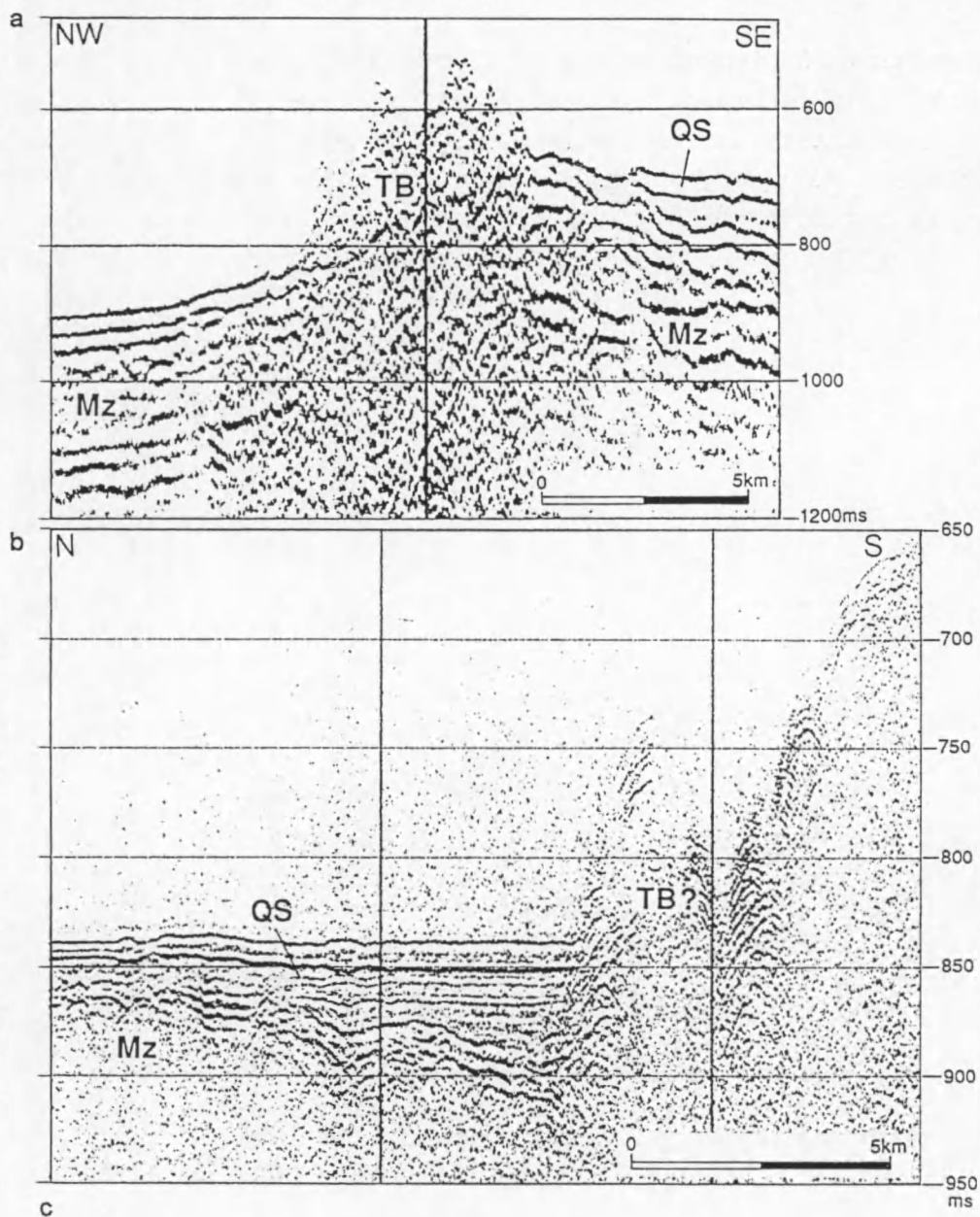


Fig. II.25 - Seismic signature and morphology of facies units of supposedly basaltic nature along Volquart Boon Kyst [a] and at the mouth of Vikingebugt [b], compared to an outcrop photograph from Gåsefjord [c]. Location of seismic lines in Fig. II.21. Mz = Mesozoic strata, QS = Quaternary sediments, TB = Tertiary basalts.

The seismic lines in Hall Bredning demonstrate the rather complex and variable trajectory of the western boundary of the Jameson Land basin. In the NW of Hall Bredning, near the immediate southward projection of the fault, Mesozoic sediments are in contact with Caledonian metamorphics. The fault itself is not actually displayed on the records. In the prolongation of the mouth of Nordvestfjord the boundary seems to be offset to the east, as it is affected by a WNW trending graben system which probably also exerts structural control on the mouth of Nordvestfjord (Fig. 26).

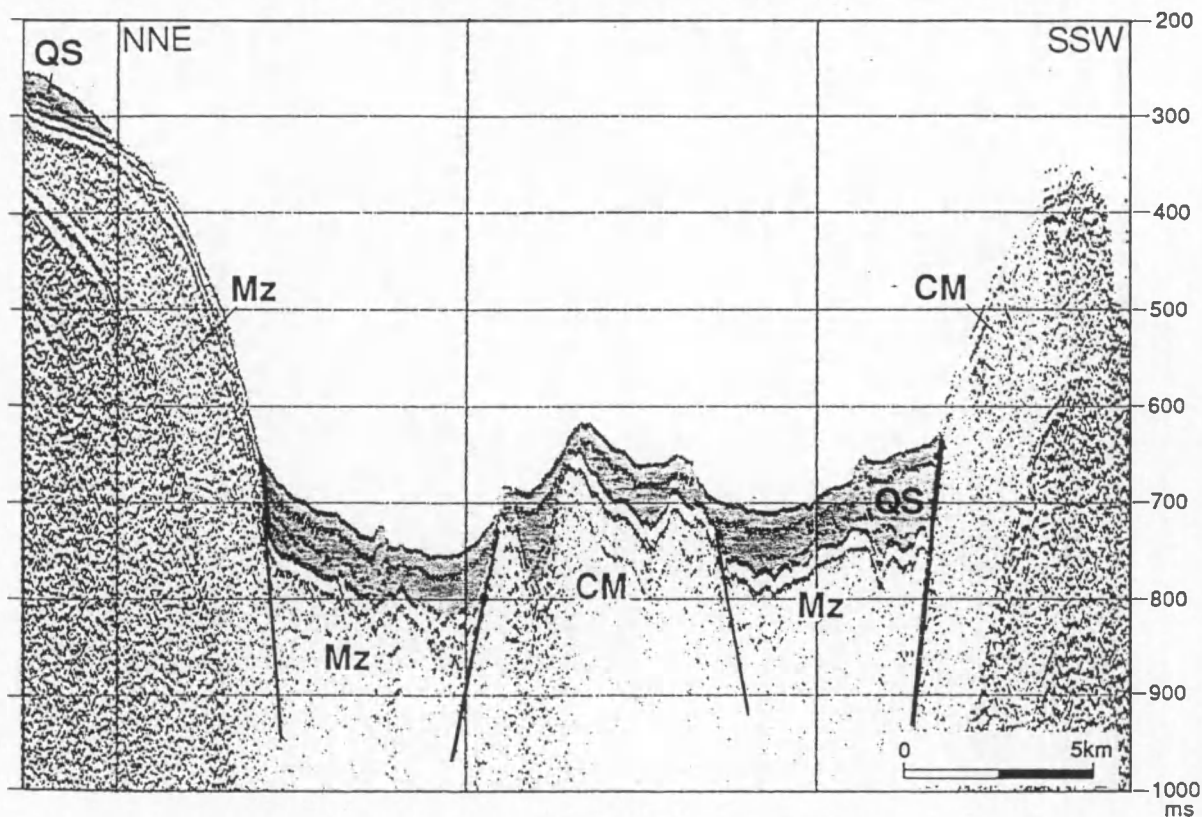


Fig. II.26 - Graben system near the entrance of Nordvestfjord into Hall Bredning. Location of line in Fig. II.21. Symbolic notations follow the conventions used in Figs. II.22 - II.25.

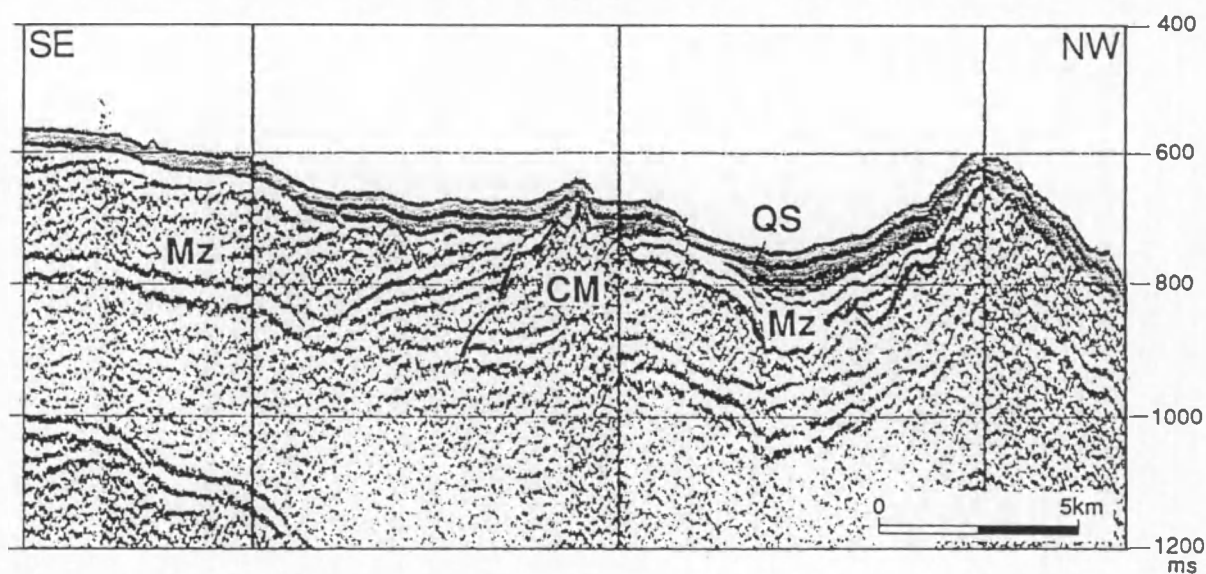


Fig. II.27 - Seismic profile showing the small area in the northern part of Hall Bredning where Caledonian metamorphics underlie a thin layer of Mesozoic strata. Location of line is given in Fig. II.21. Symbolic notations follow the conventions used in Figs. II.22 - II.25.

The graben system consists of two pronounced but smooth shoulders, between which the fjord floor is downfaulted by as much as 375 m, and a smaller axial horst structure. The graben floor is composed of metamorphic rocks, overlain by a thin layer of Mesozoic strata, and covered by up to 100 m of Quaternary sediments. The graben system defines a small area where Caledonian metamorphic basement is actually seen to unconformably underlie a thin layer of Mesozoic sediment (Fig. 27); this probably implies that the structure was initiated at some time during the Mesozoic, whereupon new sediments were spilled over the border fault into the graben. Along the westernmost graben fault, Mesozoic strata are deformed into what resembles a positive flower structure (Fig. 28), which would suggest that the graben faults are associated with a significant strike-slip component, and that the faults were still active (or were reactivated?) in post-Mesozoic times.

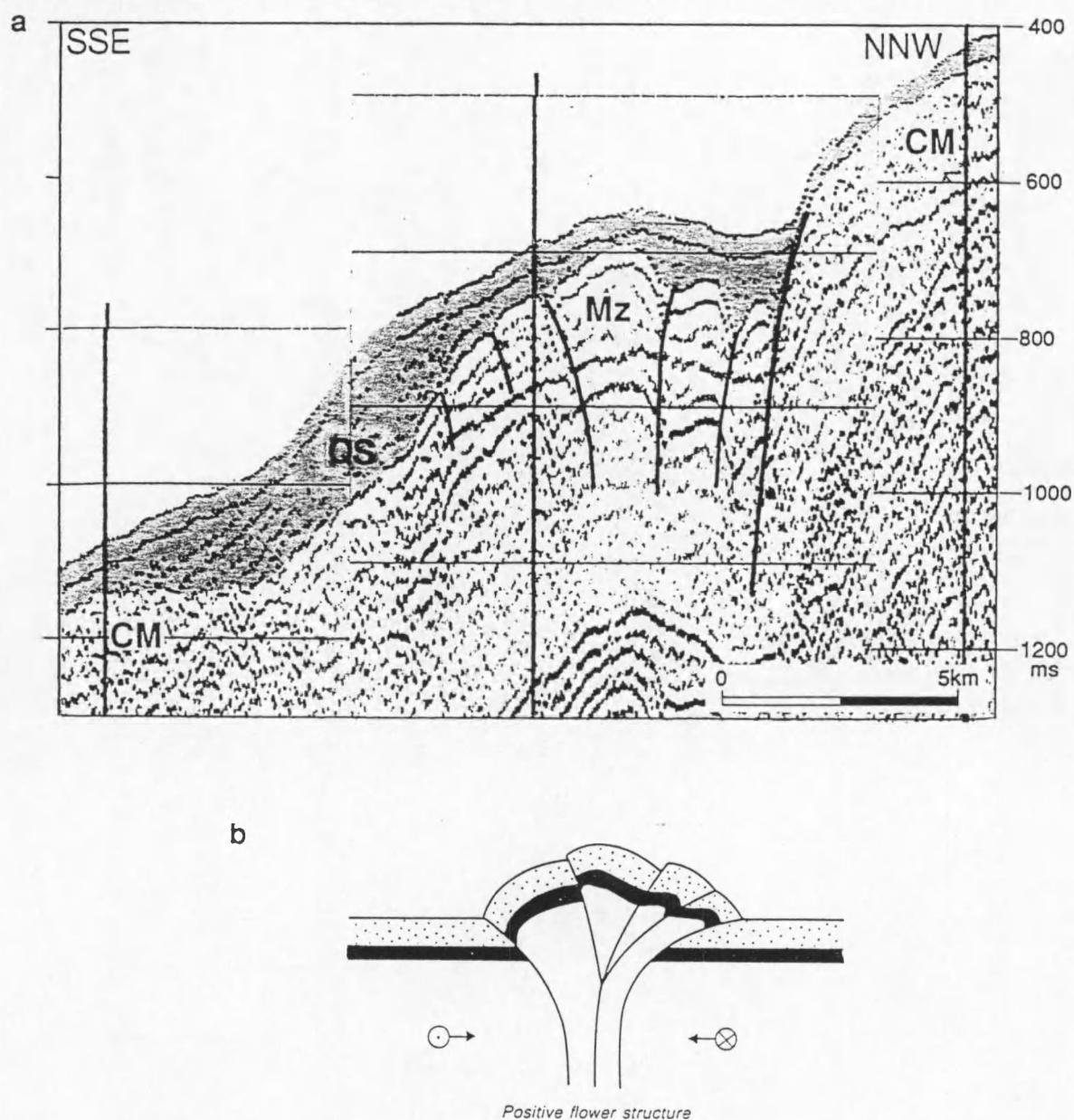


Fig. 11.28 - [a] Positive flower structure identified west of the graben system depicted in Fig. 11.26, compared to a schematic representation [b]. Location of line in Fig. 11.21. Symbolic notations follow the conventions used in Figs. 11.22 - 11.25.

In the west of the study area, in front of Milne Land, Caledonian intrusives replace the metamorphics along the boundary of the Jameson Land basin. Along most of its length the contact is associated with an elongated trough, about 5 km wide (500 m isobath) and extending southward to the mouth of Charcot Bugt (Fig. 29). The trough is probably fault-controlled (Fig. 30a, b): its bottom appears to be downfaulted along the landward flank. Bottom and landward shoulder of the trough are occupied by the Caledonian intrusives, whereas the eastern shoulder consists of Mesozoic sediments that have been uplifted, as indicated by an inversion of the regional dip of these strata (cf. section 5.3.1).

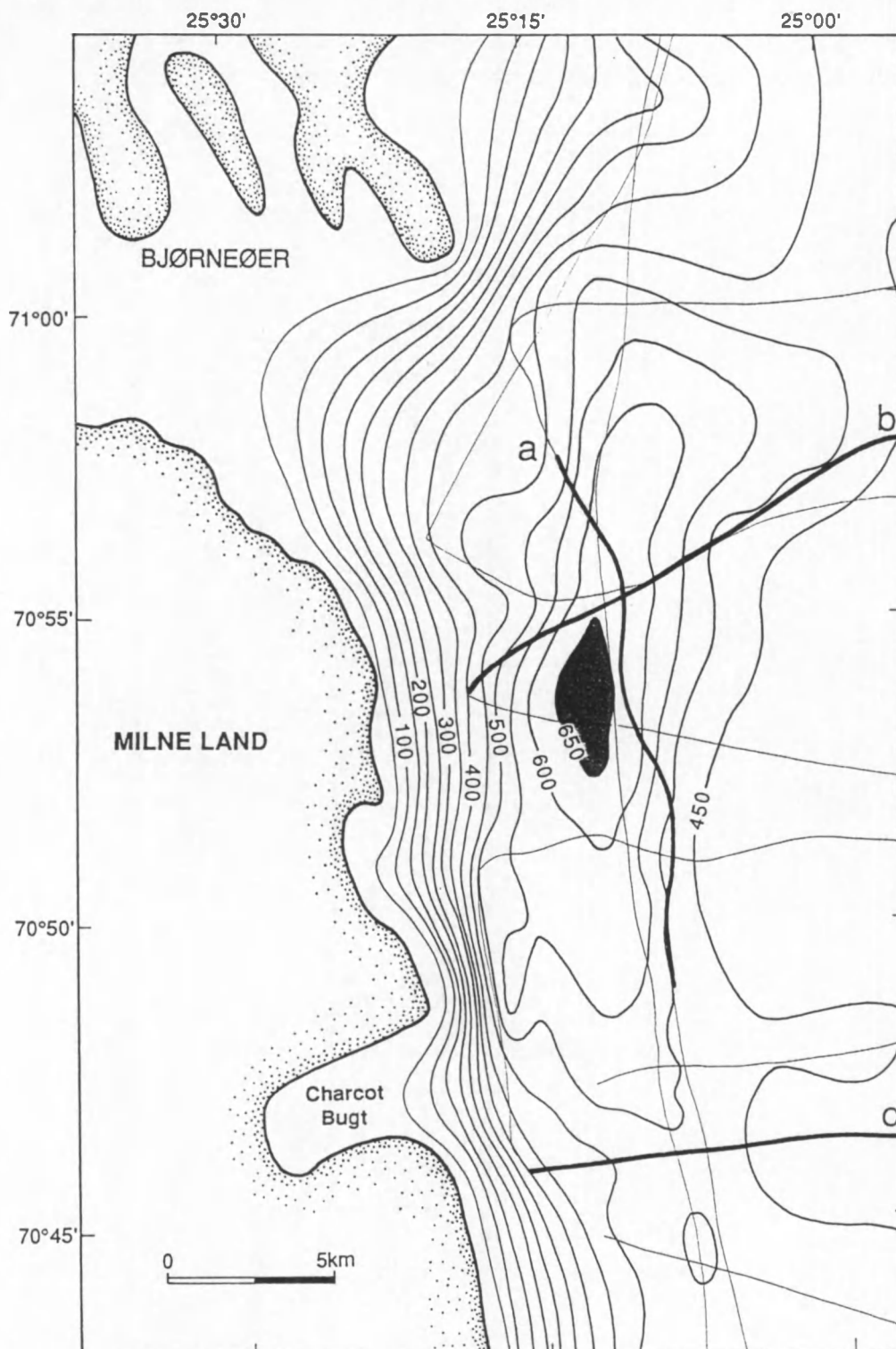


Fig. II.29 - Detailed bathymetry map delineating the elongated trough along the Milne Land coast. Contour interval is 50 m. Shaded area represents maximum depression.

The northern and southern limits of the trough are defined by a rising of the intrusive mass, probably by faults; Caledonian and Mesozoic rocks are almost at the same level here. The southern end of the trough continues into a smaller depression that is eroded in the softer Mesozoic sediments (Fig. 30c).

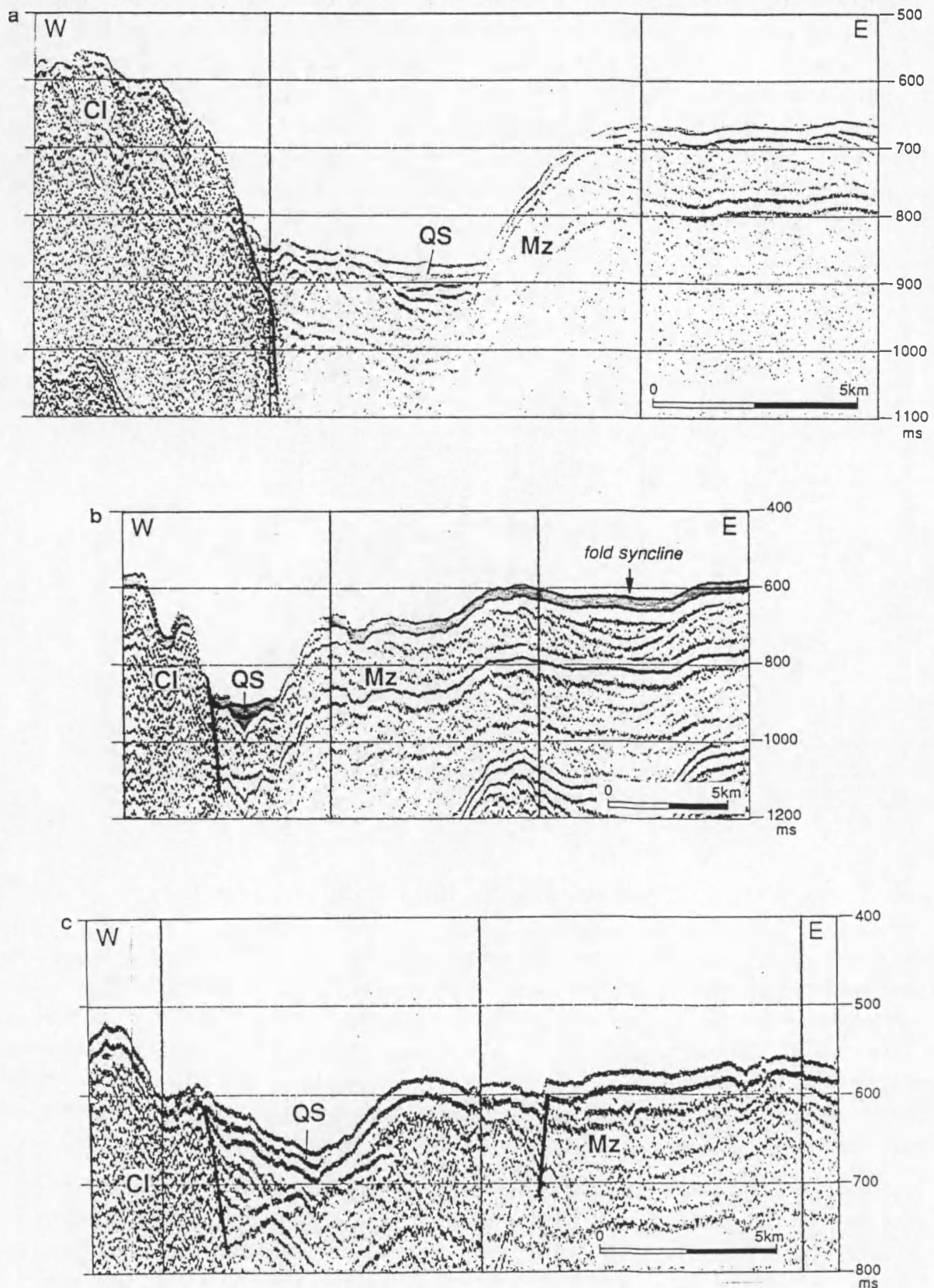


Fig. 11.30 - Three different cross-sections through the elongated fault-controlled trough along the Milne Land coast: [a] N-S section, [b] E-W section, [c] E-W section crossing a smaller depression carved in Mesozoic sediments in the southern continuation of the trough. Location of lines in Fig. 11.29. Symbolic notations follow the conventions used in Figs. 11.22 - 11.25.

South of this feature, the Caledonian/Mesozoic contact is inferred to bend landward by 90°, to separate Jurassic sediments of the Milne Land fault block from the Caledonian granite and migmatite zone (Henriksen 1986). Where the boundary enters the SW arm of Scoresby Sund again, its trajectory is poorly constrained by the seismic data. In the centre of the fjord arm Mesozoic sediments are interpreted to be in contact with another intrusion of Caledonian age. Near the contact, the sediments are deformed and affected by faults, which are thought to run parallel to the main boundary fault. The Caledonian intrusion centre is cut by a small but distinct graben structure, in which Mesozoic sediments seem to be preserved (Fig. 31). The further continuation of the boundary of the Jameson Land basin towards the Geikie Plateau is only partially documented by the seismic lines, but appears to occur way west of Kap Stevenson; this is significantly farther westward than indicated on the schematic map of Henriksen (1989) (see Fig. 10).

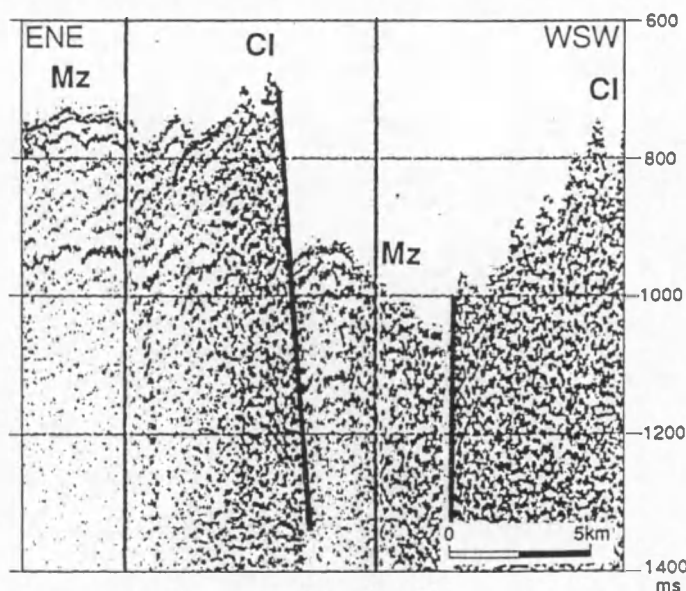


Fig. II.31 - Small graben structure cutting Caledonian intrusives in the SW arm of Scoresby Sund. Location in Fig. II.21. Symbolic notations follow conventions used in Figs. II.22 - II.25.

5.4. The combined reflection/refraction lines in the inner fjords

The combined reflection/refraction lines which were recorded in some of the inner fjords have a very poor horizontal and vertical resolution, permitting only a rough estimate of basement nature and relief, and of sedimentary fill. The inner fjords are very deeply eroded, and commonly reach depths of over 1000 m. Typically a topographic elevation is present at the entrance of the inner fjord arms into Hall Bredning. As the fjords are cut entirely into Caledonian terrain, the relief of the fjord floor is very irregular and rugged with a close alternation of basement highs and lows. This affects the quality of the seismic image in a bad way.

One profile (90300), which was as a kind of experiment shot with two different (high and low resolution) seismic sources simultaneously, is able to resolve some more detail: it shows the transition from Caledonian basement into Mesozoic sediments, at the entrance of Gåsefjord into Hall Bredning, and a limited basin, containing up to 125 m of unconsolidated Quaternary sediments, at the foot of the topographic barrier between both fjords (Fig. 32).

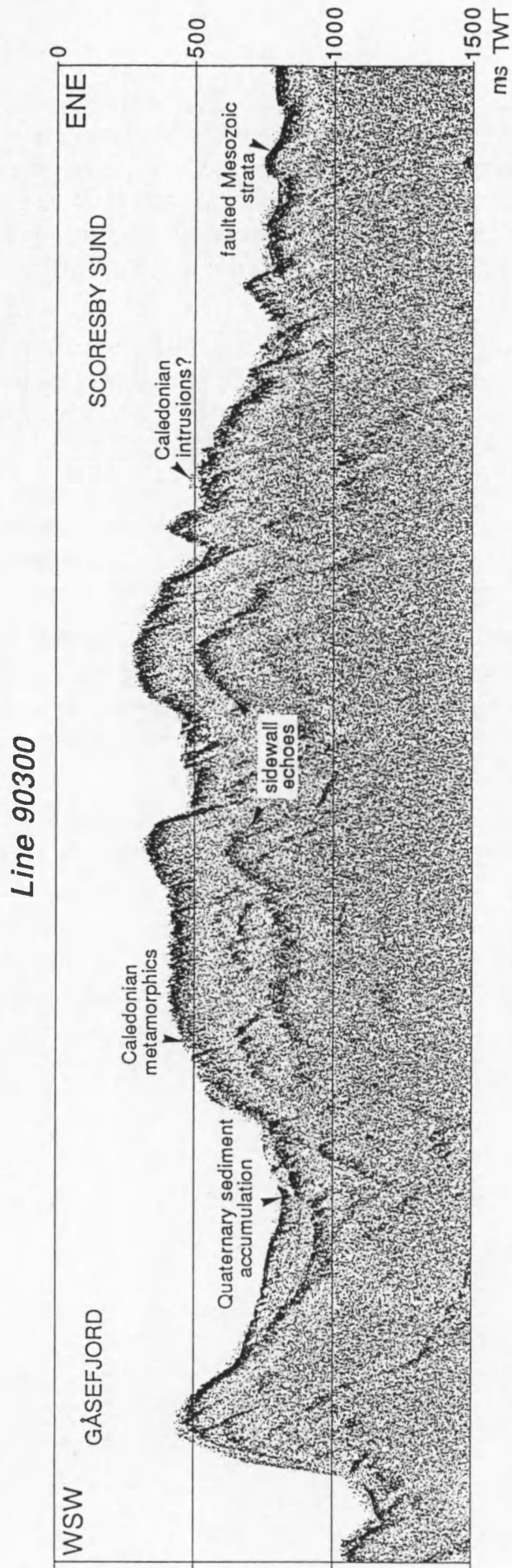


Fig. II.32 - Watergun line 90300 showing the contact zone between Mesozoic sediments and Caledonian terrain near the entrance of Gåsefjord.
Location indicated in Fig. II.21.

5.5. Conclusions

- The fjord topography shows that the Scoresby Sund region has been extensively eroded during the successive Plio-Pleistocene glaciations; the topography of the fjord floor is strongly dependent on the lithology of the subcropping basement rocks: stratified Mesozoic sediments are more easily and more uniformly eroded than the crystalline rocks of the Caledonian fold belt. Hall Bredning, which is Danish for “widening of the hall”, is a broad and relatively smooth glacially eroded valley which essentially formed by enhanced erosion at the transition between resistant Caledonian rocks and the weaker Mesozoic sediments.
- On the basis of seismic and topographic characteristics it has been possible to identify the regional lithological units indicated on the geological map (namely Mesozoic sediments, Caledonian metamorphics, Caledonian intrusives and early Tertiary plateau basalts) in the submerged Hall Bredning area.
- Stratified Mesozoic sediments of the Jameson Land basin constitute the dominant basement type throughout most of Hall Bredning; the strata are topped by a smooth truncating surface resulting from uniform erosion. The SW-ward dip of internal reflectors indicates that the region has been tilted towards the SW during Cenozoic times.
- The major fault defining the western boundary of the Jameson Land basin onshore can be traced in Hall Bredning and the SW arm of Scoresby Sund, bending on land in between these two ranges to connect with the fault delimiting the Milne Land block. Its trajectory is complex, intersected by a graben structure in front of the mouth of Nordvestfjord, and associated with a deep elongated trough along the coast of Milne Land.
- Caledonian metamorphics and intrusives border the western side of Hall Bredning; their irregular relief and noisy seismic facies readily allow to distinguish them from the adjacent Mesozoic sediments.
- Mesozoic sediments continue southward below the plateau basalts of the Geikie Plateau. Basalts overlying the Mesozoic substrate are only identified close to the southern shore, except for a patch to the SW of Milne Land, which may be akin to the basaltic outliers of similar dimensions found onshore.

6. Quaternary glacially-influenced deposits in Scoresby Sund

6.1. General distribution of unlithified sediments in Hall Bredning

6.1.1. Identification

The bedrock in Hall Bredning is in most places covered by a sediment unit which generally assumes the shape of a thin drape (Fig. 33). The thickness of this unit is most often between 5 and 15 m, but may drop below the seismic resolution. Except perhaps for some steep slopes, the unit is more or less omnipresent within the entire study area, as is also suggested by Parasound echo sounder recordings run simultaneously with the seismic reflection profiling (Marienfeld 1991). In some isolated locations, however, thicker deposits occur, reaching thicknesses of up to 160 m (200 ms).

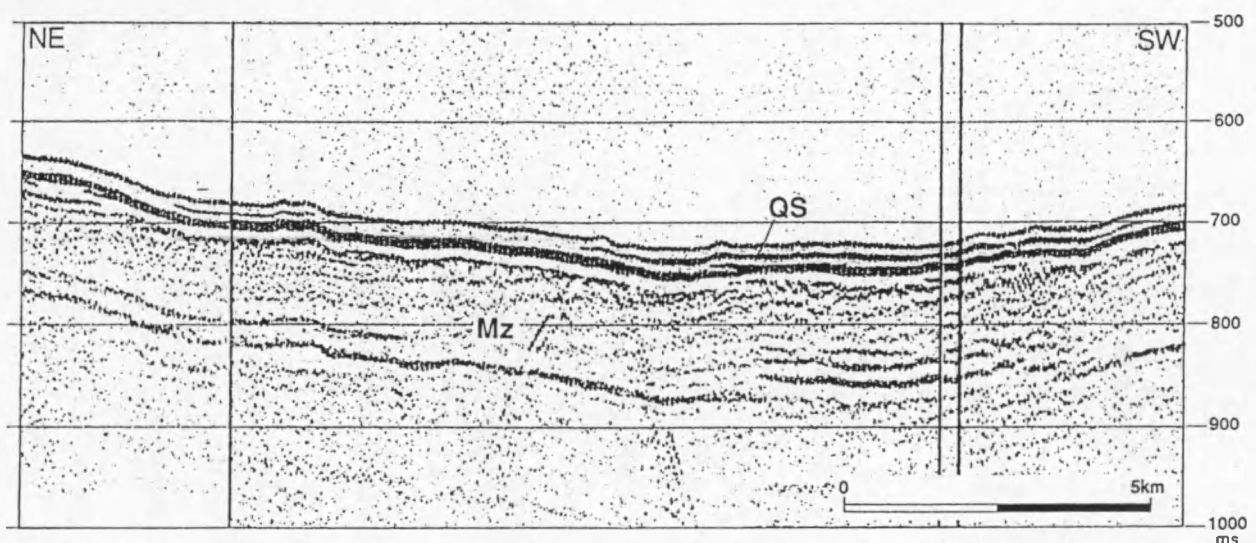


Fig. II.33 - Typical appearance of the thin unconsolidated sediment drape in Hall Bredning. Location of line in Fig. II.34. Symbolic notations conform to Fig. II.22.

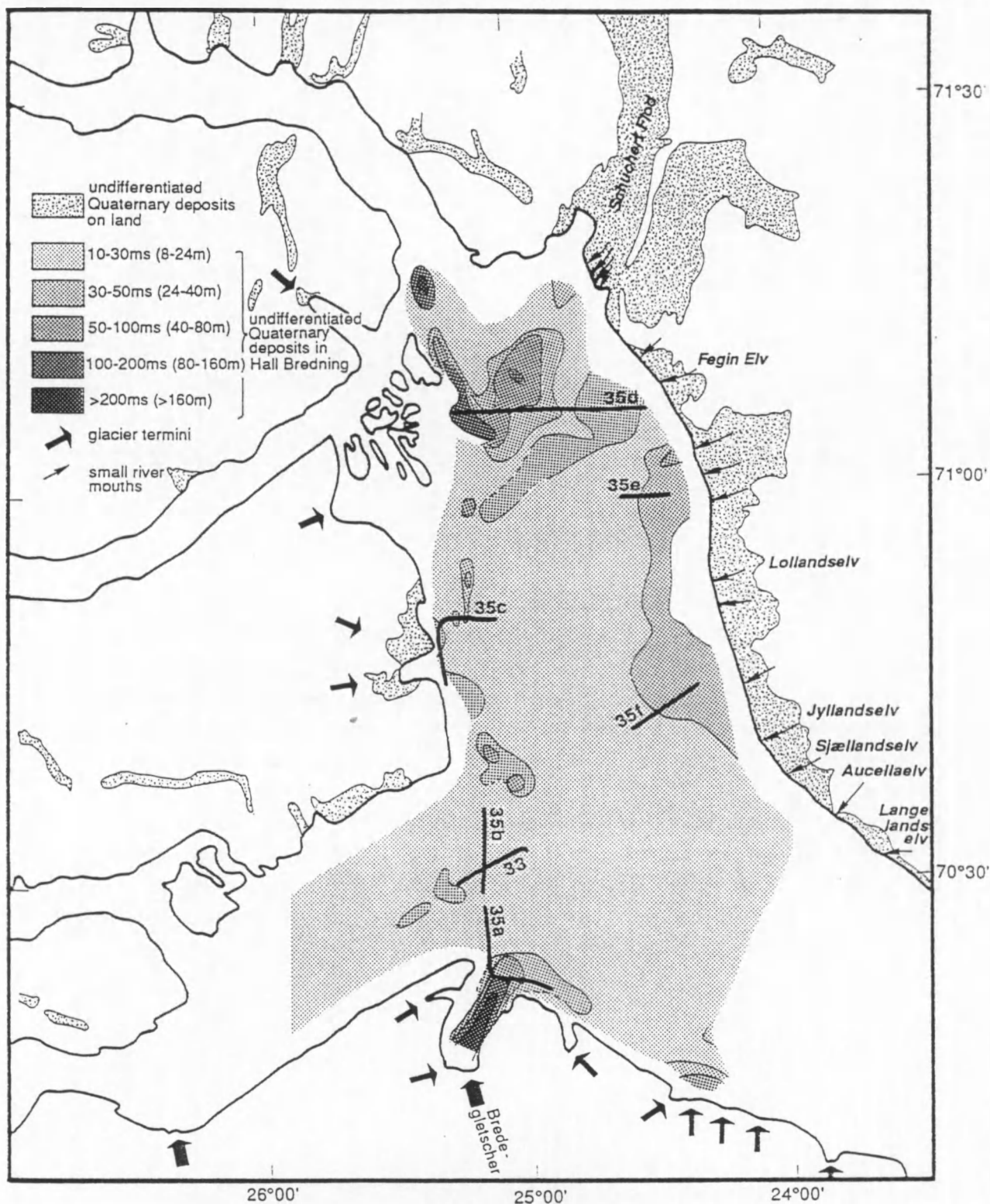
The draping unit is generally characterised by a relatively weak top reflection, running parallel to the underlying substrate, or more or less horizontal where the unit is filling up larger depressions. The weak top reflection is indicative of loose, unconsolidated sediments of rather recent origin. The acoustic character is more or less homogeneous; internal reflectors are weak and are only observed where the unit is sufficiently thick. The deposits of this unit are interpreted as Quaternary glaciomarine sediment; proper glacial deposits in the form of moraines or tills were only rarely observed.

Gravity cores collected at a number of positions in the outer fjord system confirm the glaciomarine nature of the sediment (Marienfeld 1991). Almost 90 % of the core material consists of a massive, non-stratified and heterogeneous diamicton, interpreted to be formed by the release of ice-rafted debris and subsequent reworking by iceberg keels (Dowdeswell et al. 1991, 1994); it can therefore be classified as an iceberg turbate (cf. Vorren et al. 1983).

6.1.2. Sediment distribution and origin

One of the first reconnaissance surveys by the Danish Geological Survey already found Quaternary deposits to be surprisingly thin in the Scoresby Sund fjord system (B. Larsen 1980); this result can now be extended to the whole of Hall Bredning. Using all available seismic data, a sediment distribution map was constructed, shown in Fig. 34. Comparison with the bathymetric map in Fig. 20 learns that there is no strict relation between sediment thickness and water depth, such as has been suggested by Uenzelmann-Neben (1993).

Fig. II.34 - Distribution map of Quaternary sediments in and around Hall Bredning. Thicknesses are calculated using a seismic velocity of 1.6 km/s. Distribution on land is from Henriksen (1986). Position is indicated of seismic sections presented in the corresponding figure numbers.



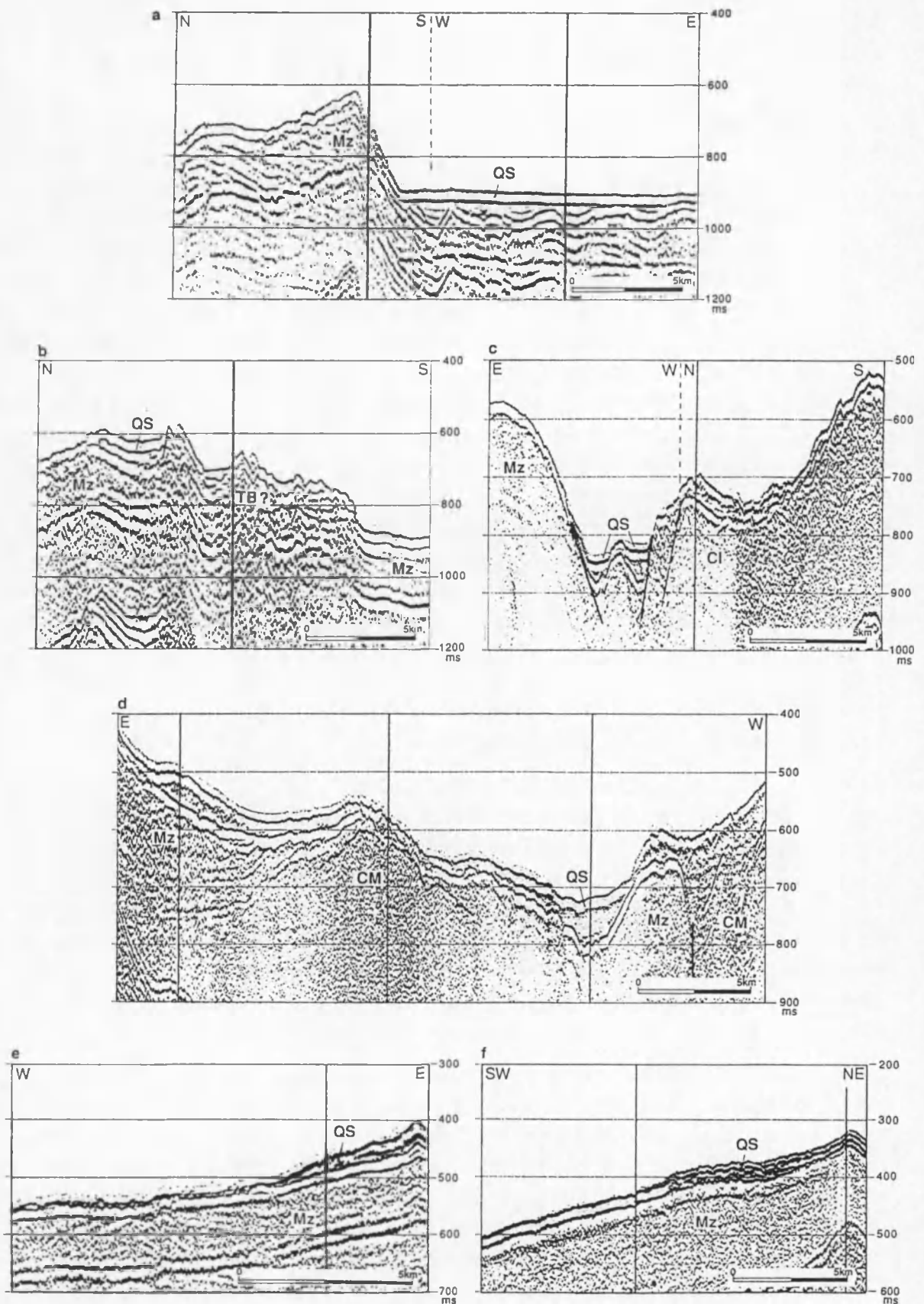


Fig. II.35 - Some examples of local sediment accumulations in Hall Bredning: [a] along Volquart Boon Kyst, at the mouth of Vikingebugt, [b] along the rims of a presumed basaltic outlier SW of Milne Land, [c] in the trough along the Milne Land coast, [d] in a large basinal area in the north of Hall Bredning and [e, f] in front of some river mounds along the Jameson Land coast. Location of seismic lines is indicated in Fig. II.34. Symbolic notations follow the conventions used in Figs. II.22 - II.25.

Local accumulations of loose sediment with thicknesses exceeding the average are observed in the following locations:

- in front of the Geikie Plateau: up to 160 m of sediment covers the floor of the Vikingebugt valley, thinning in SE-ward direction in the connecting depression along Volquart Boon Kyst (Fig. 35a); a second sediment accumulation of more than 75 m occurs further SE-ward, in front of a smaller inlet which is not named on maps of the area;
- in several depressions of predominantly erosional nature along the western side of Hall Bredning: two localised depocentres with sediment thicknesses exceeding 40 m cover the bottom of the long fault-controlled trough in front of Milne Land (Fig. 35c). A narrow erosional trough bordering the northern and eastern rims of the presumed basaltic patch in front of the Milne Land block is equally filled with up to 75 m of sediment (Fig. 35b);
- in front of some river mouths along the coast of Jameson Land: small lobes, no more than 40 m thick, are piled upon the Mesozoic substrate in front of Schuchert Flod (Fig. 26) and in front of a small unnamed river between Fegin Elv and Lollandselv (Fig. 35e and f), both in the NE of Hall Bredning;
- a large basinal area defined by the graben system in front of the mouth of Nordvestfjord (see section 5.3.5) is covered by more than 100 m of sediment (Figs. 26 and 35d), and a localised depression slightly further northward contains over 160 m of sediment; similar basins of restricted areal extent were observed in the inner fjords.

Mariénfeld (1991) listed the following processes as the main sedimentation processes presently taking place in Scoresby Sund. These are thought to have been important throughout the Holocene, and adequately explain the observed sediment distribution:

[1] rafting of debris contained within icebergs (IRD)

This process (Fig. 36) is of importance over the entire outer fjord region, and takes place during summer when free drift of icebergs is not impeded by fast ice. Icebergs calving from the large glacier fronts in the inner fjords often ground at the bathymetric elevations marking the entrance of the inner fjords in the outer fjord region. Most sediment remains trapped within the inner fjords that way, but the sediment introduced to the outer fjord region by icebergs able to pass this topographic barrier is still sufficient to account for the bulk of the observed sediment drape (Dowdeswell et al. 1991, 1994). Bathymetric lows in front of Milne Land, located along the preferential pathway of icebergs emerging from Nordvestfjord, apparently received more sediment than average.

[2] basal melt-out and suspension settling of turbid meltwater near glacial fronts

This is an important factor only in the southern part of the study area, as the various small and medium-sized glaciers descending from the Geikie Plateau are about the only glaciers presently entering the outer fjord region. Turbid surface meltwater plumes feeding from these glaciers have been imaged by satellites (Fig. 37, Dowdeswell et al. 1994). Most of the sediment transported within the glaciers is deposited proximal to the glacier front, in depressions along the coast eroded during earlier glacial advances. Depocentres are found in Vikingebugt, the largest inlet along Volquart Boon Kyst and terminus of Bredegletscher, and more eastward, in front of a much smaller inlet where several small glaciers seem to converge. Rockfalls from the steep basaltic shoreface may contribute additional sediment to these depocentres.

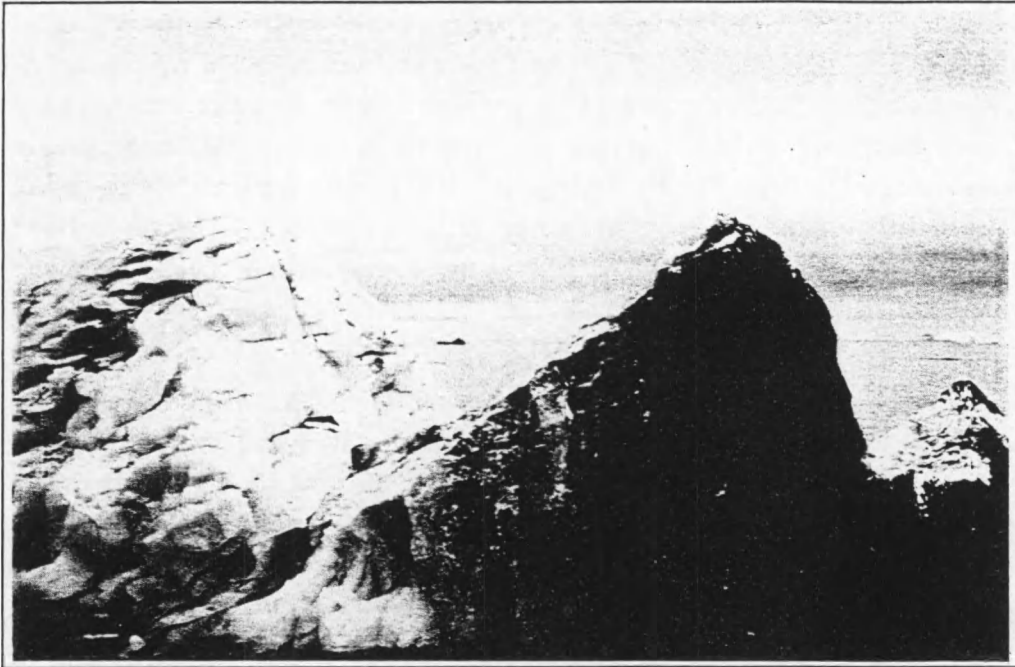


Fig. II.36 - Floating iceberg containing basal debris layers, photographed during ARK VII/3b survey in 1990.

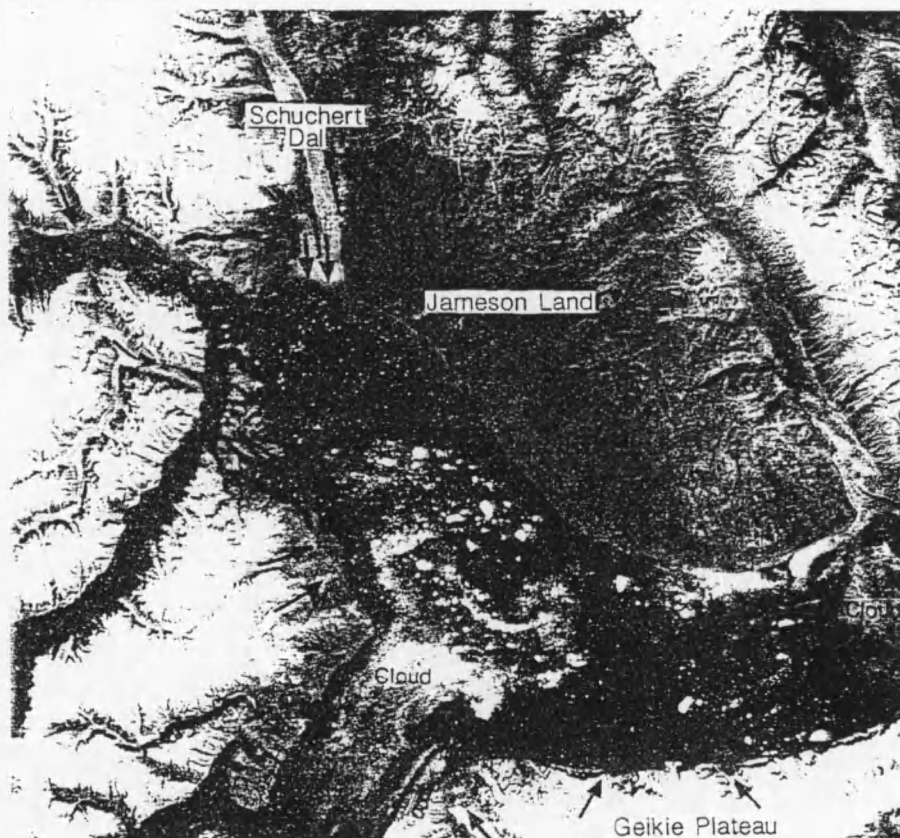


Fig. II.37 - 1985 Landsat image of the outer fjord region, showing turbid meltwater plumes discharged from glacier fronts and rivers (from Dowdeswell et al. 1994).

[3] deposition of fluvial sediments in front of river mouths along the Jameson Land coast

This process can only take place during the short summer, when the small rivers are not frozen. Increased accumulation of sediment is obvious more or less along the entire Jameson Land coast; sediment lobes interpreted as deltaic deposits are observed in front of Schuchert Flod, the most extensive river system on Jameson Land and the only one draining from an ice cap (the Stauning Alper ice cap), and in front of another river system draining into NE Hall Bredning. However, in front of Aucellaelv and Langelandselv, two river systems along the SW coast of Jameson Land where Quaternary deltas have been identified on land during the 1990 PONAM field season (Landvik & Lyså 1991), deltaic lobes could not at all be observed.

[4] secondary reworking and redistribution of sediment by the action of iceberg keels

Grounded icebergs leave scours in the soft fjord floor sediments, reworking the material to a depth of several m and bringing it in suspension, which enables the fine fraction to be selectively carried away. As the mean iceberg keel depth measured in Hall Bredning is between 300 and 400 m (Dowdeswell et al. 1993), this process is very important within a radius of 25 - 30 km around the Jameson Land coast.

6.1.3. Glacial history

The modest overall thickness, the homogeneous character and the absence of true glacial deposits all suggest that the sediments draping bedrock in Hall Bredning were deposited after the last extension of the Inland Ice into the outer fjord system, which according to Funder et al. (1991) took place during the late Weichselian (Flakkerhuk stade). A moraine ridge identified offshore from Kap Brewster (Dowdeswell et al. 1991), just outside the mouth of Scoresby Sund, may mark the maximum extension of this ice mass. The observation that even in the topographic depressions along the Milne Land coast and in the SW arm of Scoresby Sund s.s. so little sediment is preserved, may further imply that most previously deposited sediments were effectively removed from the entire outer fjord by grounded ice (cf. Uenzelmann-Neben et al., 1991), which contradicts earlier views (Funder 1989) that the Late Weichselian fjord glacier was floating in the outer fjord region and only settled onto the shallow shelf. Most of the observed sediments are therefore thought to be of post-Weichselian age. Gravity cores indeed recovered only Holocene sediments, without in most cases reaching bedrock, however (Marienfeld 1991). From these cores a mean sedimentation rate of 0.2 - 0.3 m/ka was calculated over the last 10 ka, which is considered quite low for a glaciomarine environment. Apparently the outer region of the Scoresby Sund fjord system has throughout the Holocene been located in too distal a position (> 100 km) with respect to the large outlet glaciers draining the Greenland ice sheet. Most sediment supplied by these glaciers is probably trapped in deep basins within the inner fjords. An exception is the large volume of sediment found in a large basinal area in the north of Hall Bredning; this accumulation was interpreted by Dowdeswell et al. (1991) as the result of proximal sedimentation from ice grounded in relatively shallow (300 - 400 m) water near the mouth of Nordvestfjord, supposedly during a standstill of retreating glacier fronts during the Milne Land stade, though there is no firm evidence to support this.

6.2. Glacial sediments in Vikingebugt — a small case study

With the small grid of higher-resolution watergun profiles shot within the confines of Vikingebugt, it has been possible to study this small glacial subsystem in greater detail (compare e.g. the lines presented later on in Figs. 43 and 44 with the 32 l gun profile in Fig. 35a). Vikingebugt is the largest of a series of small inlets along Volquart Boon Kyst. It measures 14 km from head to mouth and is c. 6 km wide. A medium-sized glacier, Bredegletscher, drains from the small ice cap on the Geikie Plateau into the head of the inlet (Fig. 38). The data density was sufficient to allow the construction of rough contour maps for the bathymetry, basement depth and sediment thickness.

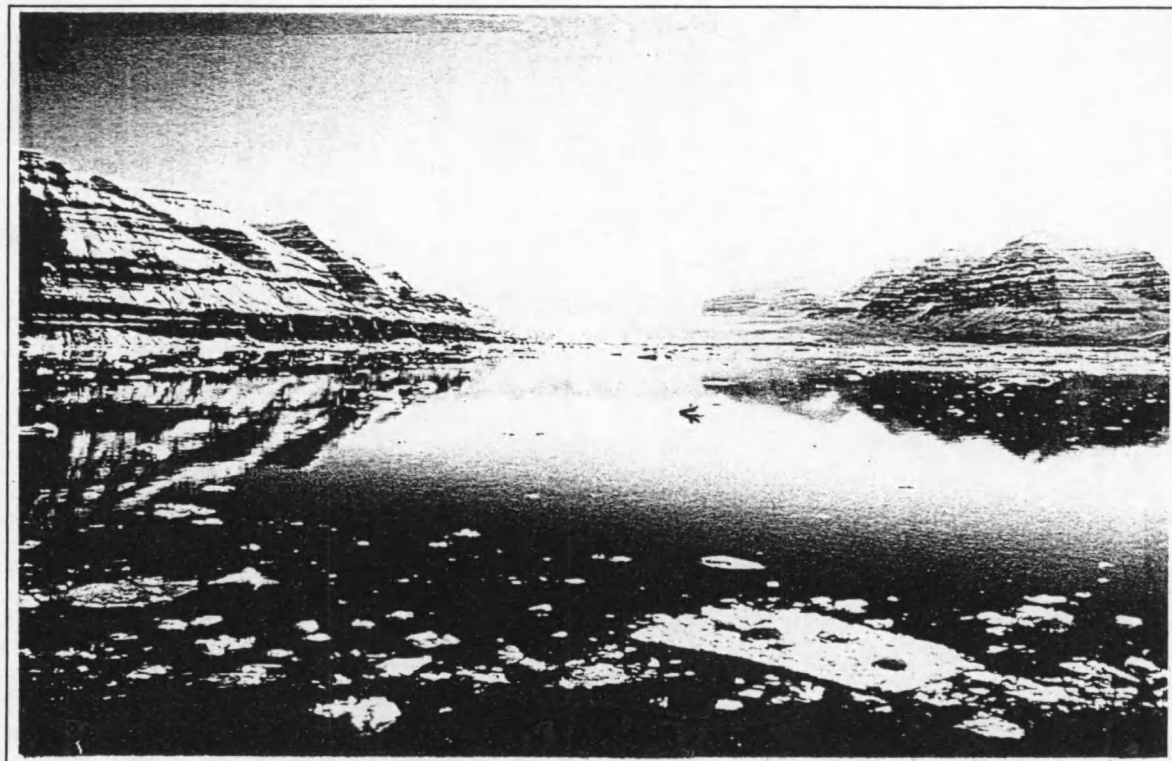


Fig. 11.38 - Vikingebugt — view towards Bredegletscher.

6.2.1. Bathymetry and basement topography

Vikingebugt has the typical shape of a glacial valley (Fig. 39), deeply cut into the basaltic rocks of the Geikie Plateau and in the underlying Mesozoic strata. The larger part of the bedrock could be identified as Mesozoic sediments on the seismic records; basaltic rocks were only observed at the head of the inlet, and even there their identification is debatable (cf. section 5.3.4). The morphology map of the eroded substrate (Fig. 40) shows that the valley has been eroded to a depth of more than 750 m below sea level, significantly deeper than the main fjord valley of Scoresby Sund which is about 600 m deep. The largest depths are reached along the axis of the valley. The western and eastern flanks are very steep, whereas the head of the valley has a slightly gentler gradient. It should be noted here that the apparent lateral asymmetry is probably due to inaccuracy of the existing maps and/or of the positioning.

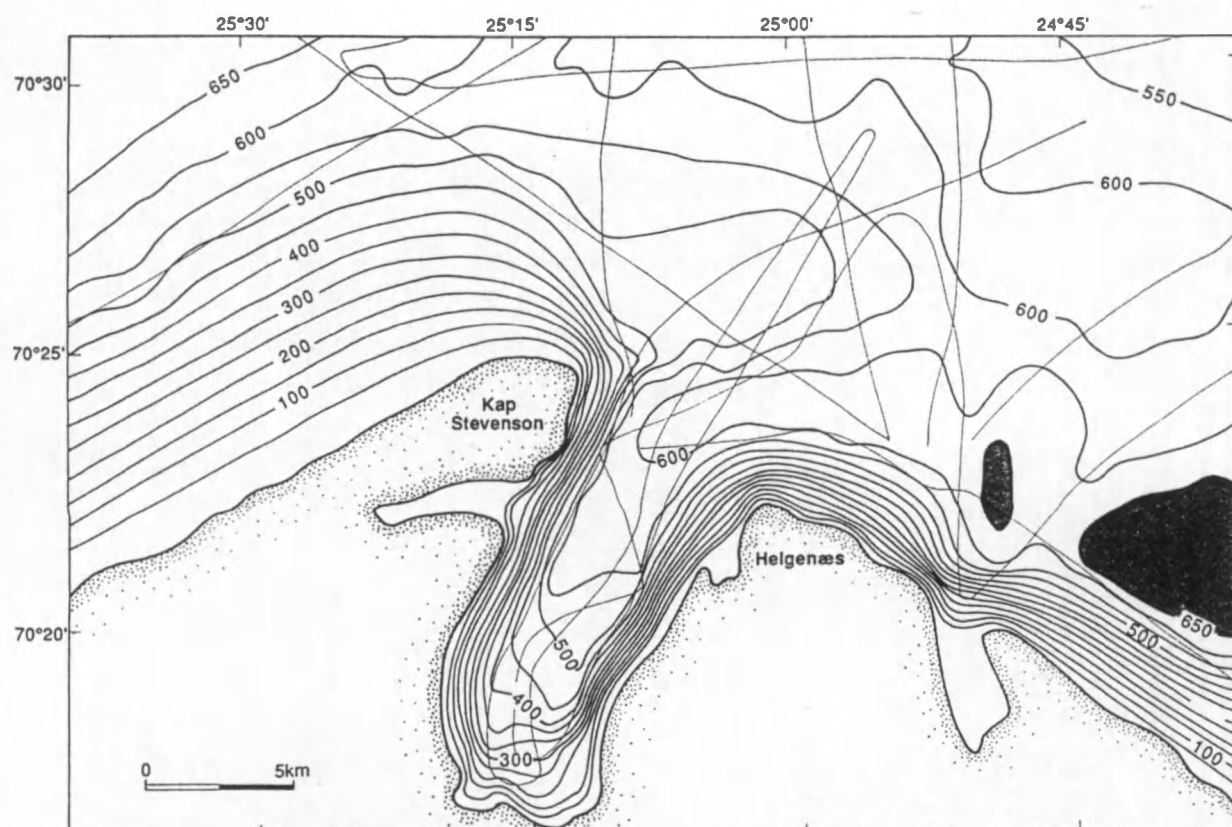


Fig. II.39 - Detailed bathymetry map of the area around Vikingebugt. Contour interval is 50 m.

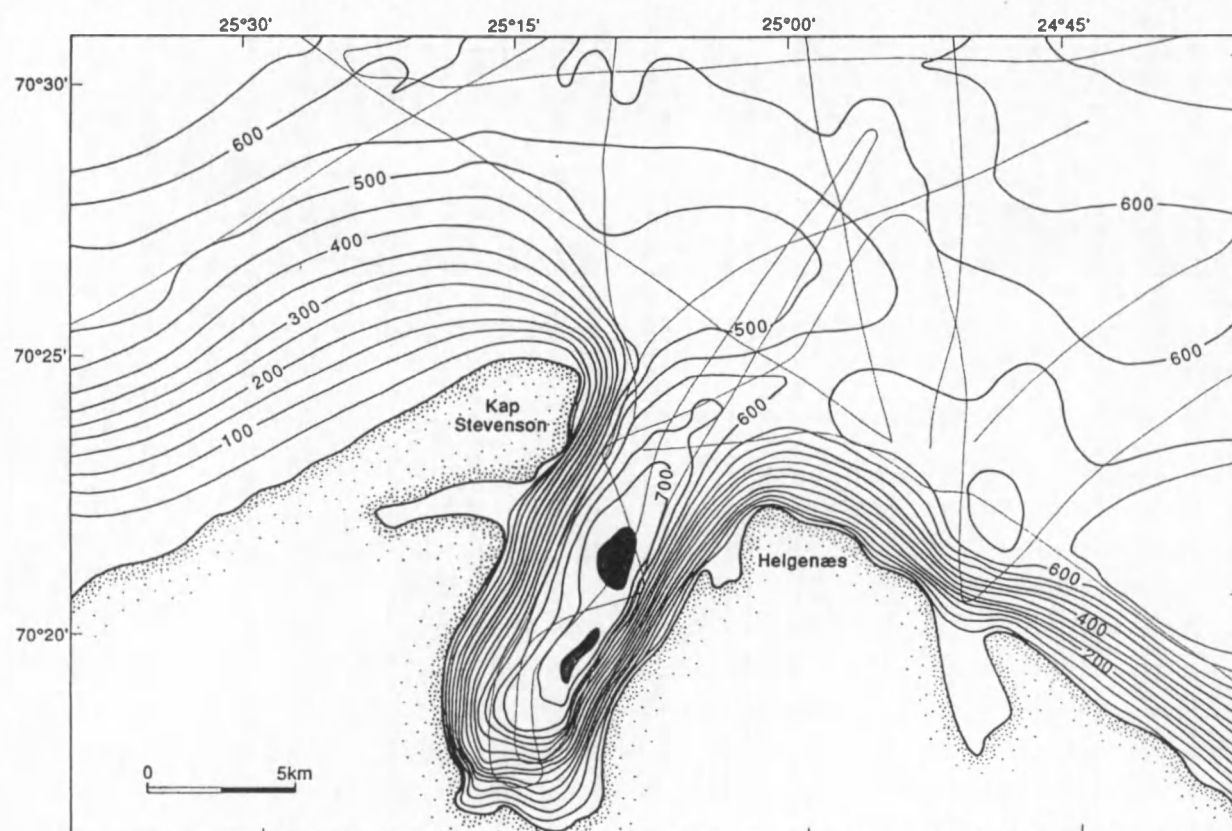


Fig. II.40 - Morphology of the glacially eroded bedrock surface in Vikingebugt, calculated using seismic velocities of 1.46 km/s in the water column and 1.6 km/s for the Quaternary sediments. Contour interval is 50 m.

As is typical for fjords, the mouth of the valley is characterised by a pronounced barrier or sill that is determined by a broad elevation of the Mesozoic substrate extending from Kap Stevenson. The trough emanating from Vikingebugt is seen to bend eastward in front of this topographic barrier, to merge with the main Scoresby Sund valley. This is interpreted to indicate that glaciers coming forth from Vikingebugt were generally deflected and entrained within the main fjord glacier moving from west to east (Fig. 41).

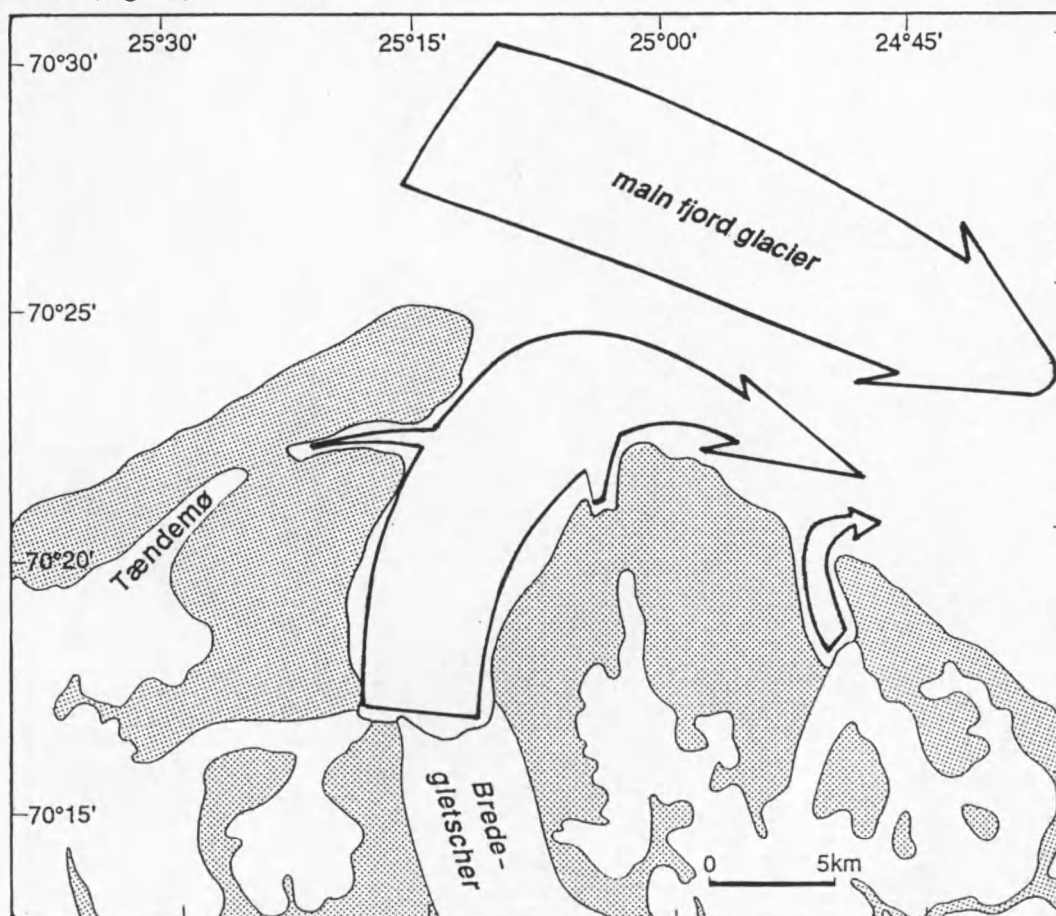


Fig. II.41 - Inferred deflection of Bredegletscher by the main eastward moving fjord glacier during the last glacial maximum.

6.2.2. Sediments within Vikingebugt

Comparing the maps of bathymetry (Fig. 39) and basement depth (Fig. 40) clearly demonstrates that sediments have smoothened out the relief of the glacially eroded bedrock surface, and have partially filled in the Vikingebugt valley. The sediment distribution map (Fig. 42) shows the thickness of these sediments, varying between more than 280 m at the head of the inlet and about 50 m at the mouth and along the flanks, to be strongly determined by the morphology of the valley and by the distance to the present ice front.

Five different facies units have been identified: [1] an isolated and unconformity-bound unit of acoustically stratified sediments in the proximal part of the basin, [2] a chaotic unit sitting on the flank of a broad basement mound in front of Vikingebugt, [3] a transparent lens-shaped unit occurring close to the head of the Bugt, [4a] a transparent unit at the bottom of the distal part of the

basin, and [4b] an acoustically stratified unit constituting the main basin fill. Most of the features discussed below can be observed on line 90561 (Fig. 43), a representative longitudinal section through Vikingebugt, as well as on the three oblique sections 90563-90565 (Fig. 44).

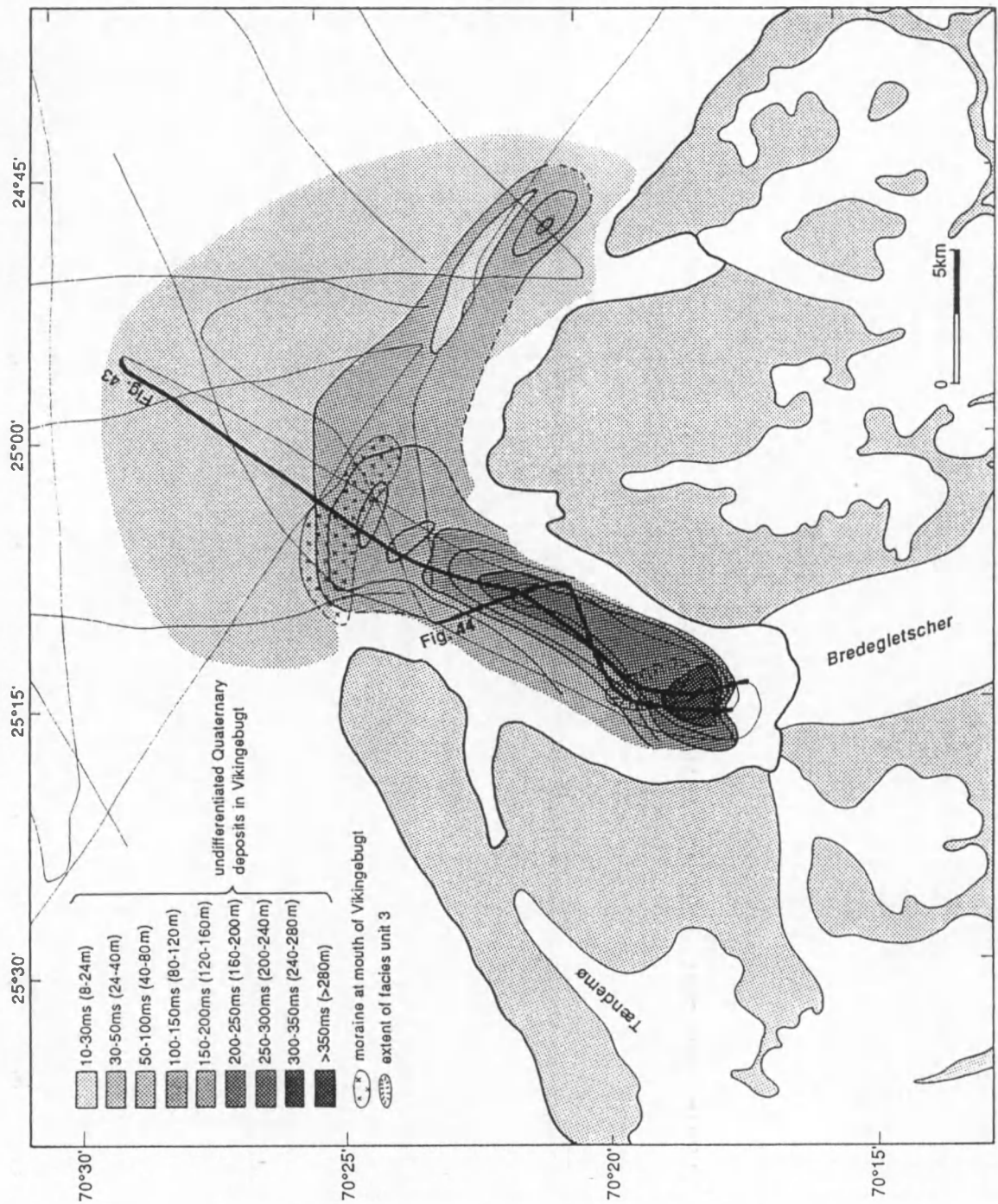


Fig. II.42 - Distribution map of Quaternary sediments in and around Vikingebugt. Sediment thicknesses are based on a seismic velocity of 1.6 km/s. Location is indicated of seismic sections presented in the corresponding figure numbers.

[1] Facies unit 1 consists of an isolated patch of stratified sediments, up to 70 m thick and limited in extent. It is located next to a small elevation of the underlying Mesozoic substrate in the proximal part of the valley. Internal reflectors appear to be cut by an erosional surface which in either direction merges with the glacially eroded Mesozoic substrate. The unit is interpreted as an erosional remnant consisting of older glacial deposits, although it cannot be entirely ruled out that it makes part of the Mesozoic substrate, from which it hardly differs in character.

VIKINGEBUGT Lines 90563 - 565

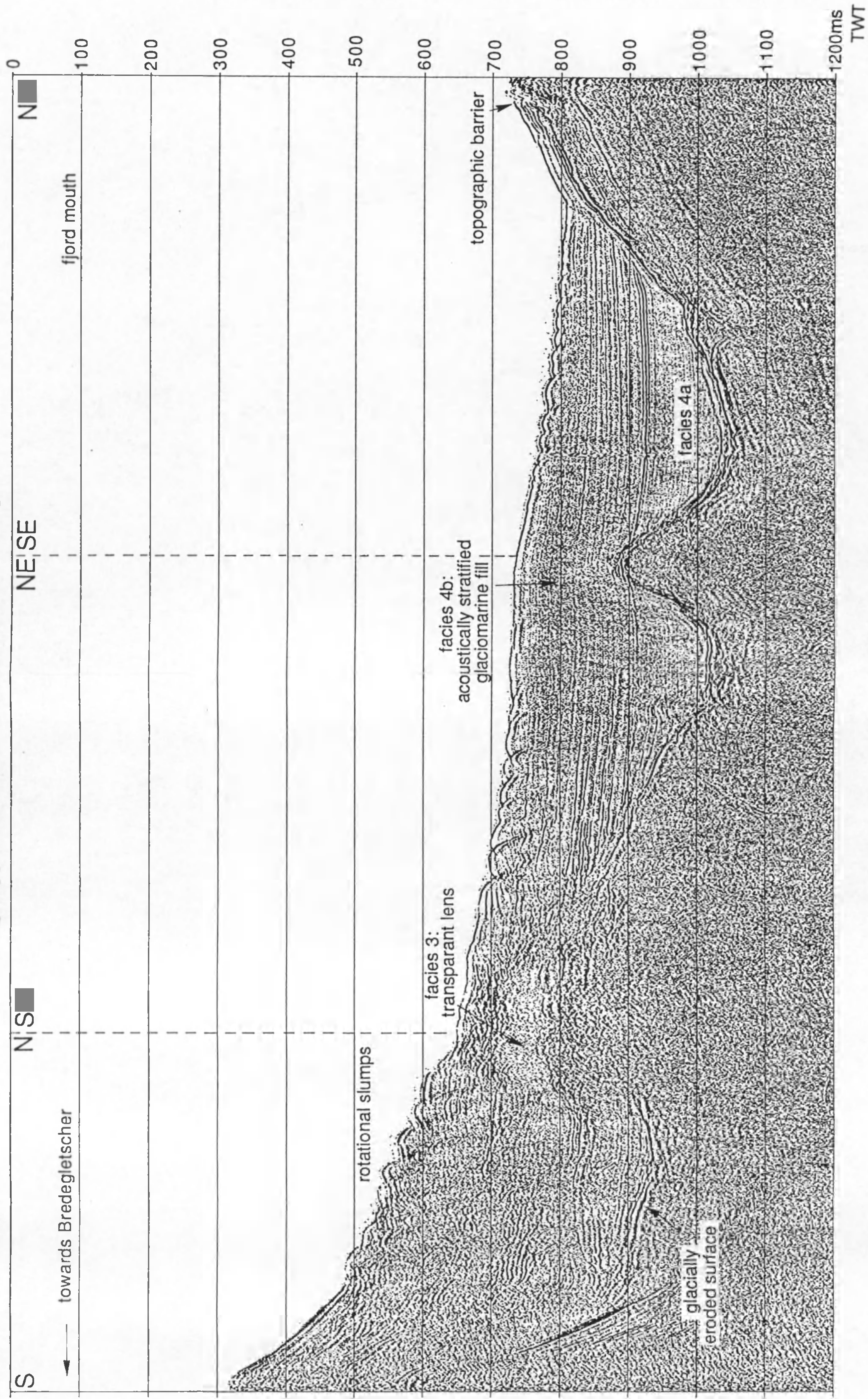


Fig. II.44 - Watergun lines 90563 - 90565, crossing Vikingebugt obliquely. Indicated are facies units and features discussed in text. Note that deformation of the seafloor sediments is much less pronounced above the lens-shaped transparent deposit. Location in Fig. II.42.

■ KINGEBUGT Line 90561

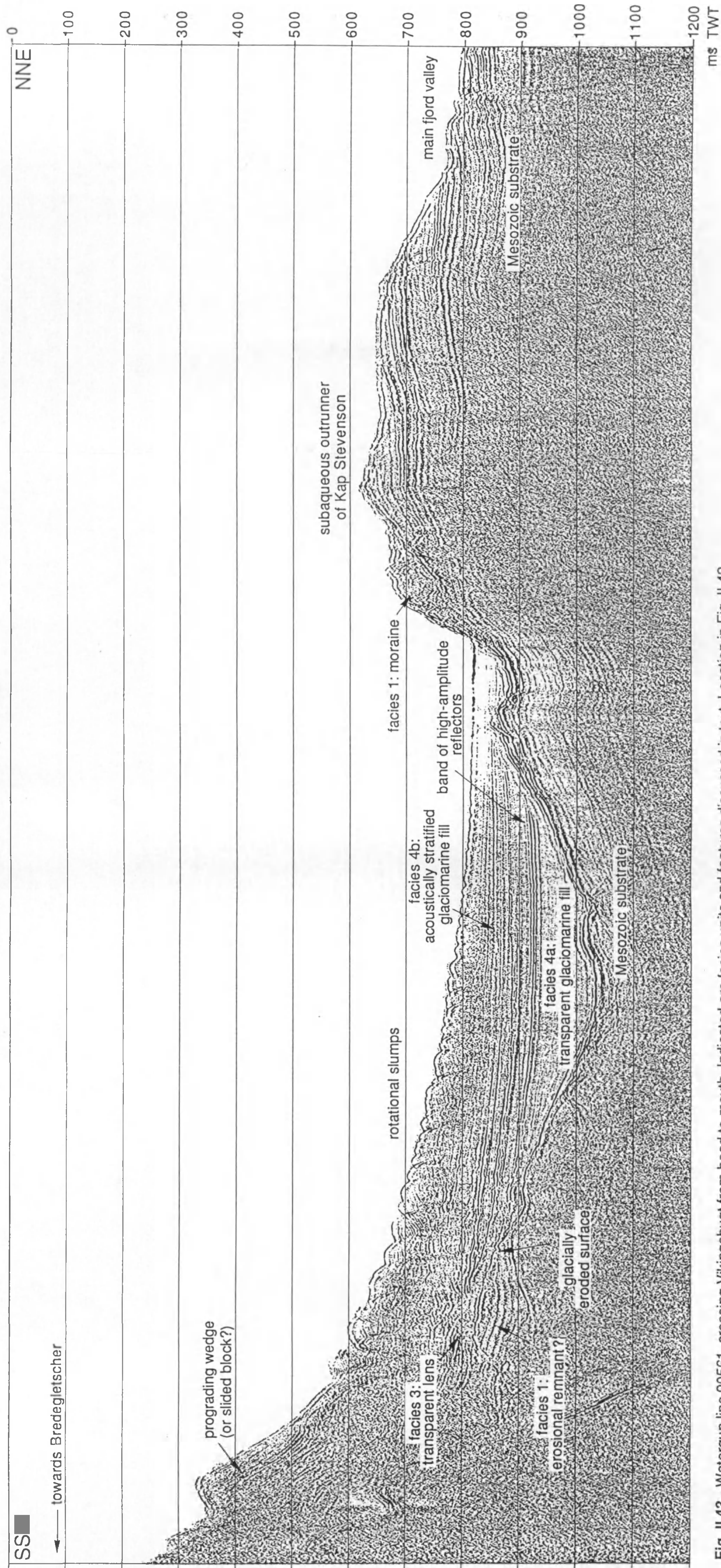


Fig. II.43 - Watergun line 90561, crossing Vikingebugt from head to mouth. Indicated are facies units and features discussed in text. Location in Fig. II.42.

[2] Facies unit 2 is a roughly wedge-shaped deposit of max. 80 m thick; the chaotic facies, associated with diffraction hyperbolae, probably indicates heavily disturbed sediments. The unit seems to be perched on the flank of the topographic barrier in front of Vikingebugt. Its foot is just barely overlapped by the uppermost reflectors of the stratified sediments of facies unit 4b. The shape, disturbed facies, distal location with respect to the glacier, and the high position on the flank of the mound all suggest that this facies unit constitutes a moraine deposit.

[3] The third facies unit consists of a transparent lens-shaped deposit, up to 60 m thick, which is entirely contained within the stratified facies unit 4b. The boundary of the lens is not recognised as an individual reflector, but shows up as an envelope of high-amplitude reflector terminations. The unit seems to be typically located on top of the highest elevation of the substrate in the proximal part of the valley. Facies unit 3 might represent a stack of buried slump masses similar to the sediments presently underlying the seafloor, or as an isolated ice contact deposit — the interpretation favoured here.

[4a] The sediments composing unit 4a display a rather transparent seismic facies, in which a few faint reflections can still be recognized, however. These sediments constitute the lower third (up to 85 m) of the basin fill deposits in the distal part of the valley. Their nature is most likely glaciomarine.

[4b] The basin fill deposits of facies unit 4b appear rather featureless in the proximal part of the basin, but generally show more distinct reflections in a distal direction. A characteristic band of high-amplitude reflectors separates the unit from the underlying unit 4a, the transparent facies of which makes for a strong contrast. Individual reflectors are curved more or less logarithmically: steeply dipping near the glacial front, and gradually downlevelling to horizontal towards the fjord mouth. They lap out against the Mesozoic substrate near the edges of the valley, or against facies units 1 and 3 more centrally in the basin. Unconformities within the unit are very little pronounced, and distinct erosional surfaces were not observed. The top of unit 4b is affected by a set of small rotational faults, which are still expressed in the sea bed morphology as a series of wavy hummocks with amplitude and wavelength decreasing in downslope direction. These features are interpreted as slumps, probably caused by oversteepening close to the glacial front. The wedge-shaped deposit near the fjord head might represent a sediment slab that slid down from the glacial front, though this kind of rigid behaviour is considered unlikely in the highly water-saturated sediment masses that are thought to be deposited in this environment (see below); there are some indications that the slumps presently appearing at the seafloor further downslope, continue as a disturbance below this wedge, making it more probable that it is a unit that has prograded over the slump mass.

6.2.3. Reconstruction of the glacial history

The Vikingebugt valley has been shaped during at least two, and probably much more glaciations. Two erosional surfaces can be identified, the lower one constituting the top of Mesozoic bedrock. The stratified sediments of facies unit 1 perched between both unconformities, are believed to be the oldest sediments recognised on the seismic records, and probably date back to an older (maybe the previous) interglacial. Other fjord sediments apparently have not survived the periods of glacial erosion.

The moraine deposit at the head of Vikingebugt (Fig. 42) is thought to document the last major advance of Bredegletscher, which is supposed to have taken place during the Late Weichselian, concurrently with the last extension of the Inland Ice into Scoresby Sund (Funder et al. 1991; see

section 4.3.3). This advance created the youngest erosional unconformity, hereby finally shaping the glacial valley. The data available do not allow to determine whether this sediment body is a terminal moraine, or a lateral moraine deposited where the glacier was forced eastward by the topographic barrier blocking the entrance of Vikingebugt (cf. Fig. 41). More recent observations reveal, however, that the moraine continues along the western flank of the valley, thus supporting the latter interpretation (R. Whittington, pers. comm. 1995). The onlapping relationship of stratified basin fill deposits against the base of the moraine (Fig. 43), together with the absence of further erosional surfaces within these deposits, suggests that the entire basin fill (facies units 3 and 4) post-dates the moraine deposit and is thus probably of Holocene age. Using an age of 14 ka for the Late Weichselian deglaciation (Funder 1984), accumulation rates of 3.5 to max. 20 m/ka are calculated for the Holocene; this strongly contrasts with the low sedimentation rates (0.2 - 0.3 m/ka) reported for most of the outer fjord region (Marienfeld 1991).

As the age relationship of facies unit 3 with respect to the units 4a and 4b is highly uncertain, several scenarios are possible for the evolution following the last glacial maximum. It is considered most likely that deposition of facies unit 3 took place between deposition of units 4a and 4b. An older (pre-dating or contemporaneously with unit 4a) or even younger (contemporaneously with the lower part of unit 4b) cannot be excluded, however. Following this interpretation, the retreat of Bredegletscher after the last glacial maximum probably occurred dramatically and all the way to the head of the inlet, as no typical ice-contact deposits are observed which can be ascribed to a longer residence or even a halt of the glacier front in the valley. After the glaciomarine sediments of unit 4a had been infilling the basin for some time, a small re-advance of Bredegletscher may have taken place in the proximal part of the basin. The ice would have grounded on a relatively elevated part of the fjord floor, but may have been floating in the rest of the valley. The transparent lens on top of this elevation could in this context be interpreted as a coarse-grained grounding line delta that was built during the standstill of the glacier front following the re-advance of Bredegletscher. There is evidence (see below) that this deposit is more consolidated than the overlying sediments of the stratified facies unit 4b. This phase is tentatively correlated with the Milne Land stade (around 10,000 a BP), a period when the large fjord glaciers in Scoresby Sund during their retreat halted some time at the mouths of the inner fjord arms (Hjort 1979). The outer fjord region was at this time probably covered by closed sea ice which stabilised the glacier fronts and impeded the drift of icebergs; this resulted in a drop of the sedimentation rate and in the fjord-wide deposition of a thin layer (< 1 m) of laminated sediments, void of IRD (Marienfeld 1991). The characteristic band of high-amplitude reflectors covering facies unit 4a in the distal part of Vikingebugt may well be related to this phase of non-deposition.

After the final retreat of the glacier, more or less to its present position, infilling of the basin was resumed. The stratified basin fill deposits of unit 4b seem to consist of poorly consolidated material, probably glaciomarine mud with a high water content. Suspension settling from turbid plumes of subglacial meltwater is therefore thought to be the dominant sedimentation process acting in Vikingebugt, characterised by a typical logarithmic fall of sedimentation rate with distance to the ice front (cf. Fig. I.5; Boulton 1990). Although debris-containing icebergs have been observed during the survey in Vikingebugt, the contribution from ice-rafted debris is probably of minor importance, as the travel distance (14 km) is far too small for any significant melting of icebergs to take place. Some larger icebergs may be trapped by the topographic barrier at the mouth of the inlet, but this is not reflected in significant accumulation of sediment at that location. Most of the sediment transported by icebergs is thus carried off and released outside Vikingebugt. Reworking of sediment

by scouring of iceberg keels is equally unimportant, as the present fjord floor is way deeper than the icebergs calving from Bredegletscher.

In the recent geological past a catastrophic mass wasting event affected the upper portion of the glaciomarine basin fill, probably as a result of oversteepening of the slope by the rather high sedimentation rates near the glacial front. The poorly consolidated, water-rich sediments of unit 4b were easily displaced; deformation is much less pronounced, however, where the lens-shaped deposit of unit 3 is underlying the fjord floor (Fig. 44), which indicates a better internal coherence for this deposit with respect to the overlying muds. Recent progradation seems to have obscured the proximal part of these slump deposits.

6.3. Conclusions

- The fjord topography shows that the outer fjord region has been extensively eroded during the successive Plio-Pleistocene glaciations. The present relief is essentially a relic from the last, probably Late Weichselian, glaciation.
- With the exception of a few local accumulations, the sediment cover — which is probably entirely of Holocene age — is very thin. This suggests that the outer fjord region was wiped clear of any previously deposited sediments by grounded ice during the last glacial maximum, and that sedimentation rates have been low since, due to the distal position the region has been occupying with respect to the large glacier fronts. Sediment distribution is not dependent on bathymetry alone; larger accumulations are primarily found in the proximity of glacier and river mouths. The glacial record in Scoresby Sund is correspondingly very limited.
- A more detailed study of a small ice-proximal basin, Vikingebugt, shows the same trends for the glacial history: the Late Weichselian ice advance extended to the head of the inlet, and removed all but one limited occurrence of older deposits from the system. There is some evidence for a less extensive re-advance of the glacier during the Younger Dryas. Sedimentation is thought to occur primarily by suspension settling from meltwater plumes, and the sedimentation rate drops rapidly with increasing distance from the glacier front.
- Apart from the infill (up to 100 m) of certain narrow depressions, Quaternary sediments are still surprisingly sparse in the inner fjords. It is thought that, in analogy to the Vikingebugt case, most sediment is occurring in deep troughs in front of the glacier fronts, where no seismic data have been gathered, however.
- The storage of unconsolidated deposits in Scoresby Sund during interglacial periods, and subsequent removal during large glaciations is a scenario that probably applied to most earlier major glacial advances. Sediments removed from the fjord system were delivered to the shelf, where they contributed to outbuilding of the margin, as is suggested by the broad seaward-convex bathymetric bulge in front of Scoresby Sund.

7. The central East Greenland shelf and slope off Scoresby Sund

7.1. Location of the seismic data

Line 90600 is a long seismic transect located just southward of the entrance to the Scoresby Sund fjord system. It starts about 8 km outside the East Greenland coast and extends for about 150 km in approximately SE-ward direction towards the Kolbeinsey Ridge (Fig. 45). The line covers the continental shelf and slope of the East Greenland margin, and the north-western edge of the Icelandic insular plateau.

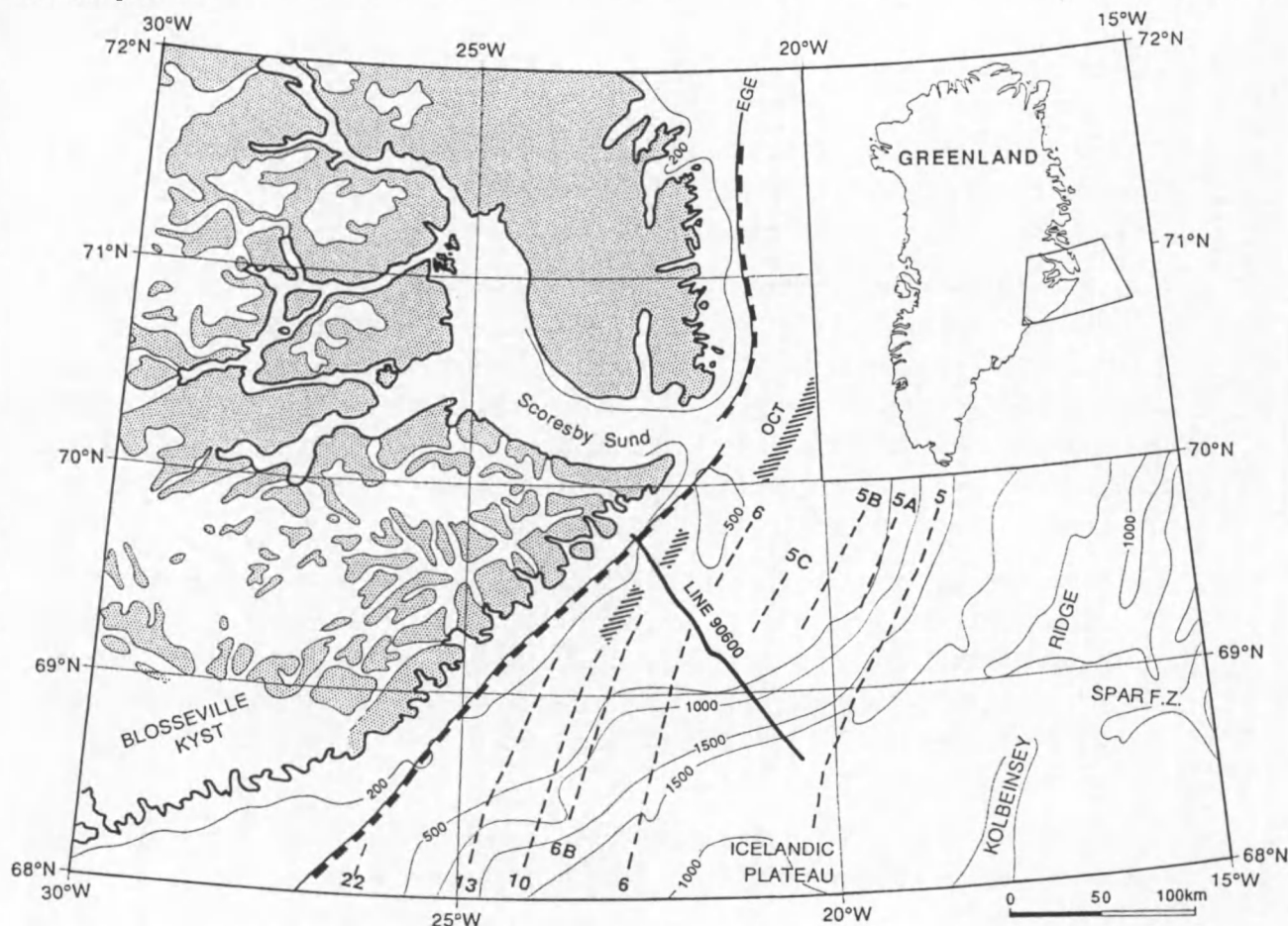
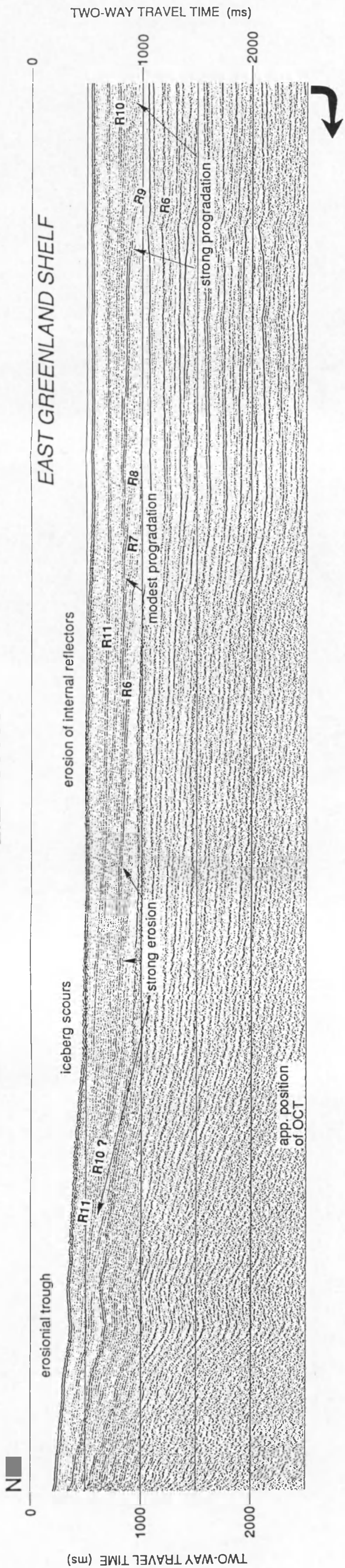


Fig. II.45 - Location of line 90600 on the East Greenland shelf in front of Scoresby Sund. Bathymetric contours (solid lines) are superposed on a tectonic sketch map of the region, showing location of the East Greenland Escarpment (EGE), ocean-continent transition (OCT), and magnetic anomaly lineations (dashed lines). The 500 m isobath approximately represents the shelf break. Adapted from H.C. Larsen (1990). Bathymetry from IHO/IOC/CHS 1984.

7.2. Morphology of shelf and slope

The continental shelf gradually deepens to 375 m (500 ms TWT) about 30 km outside the coast, but remains fairly horizontal over the remaining 70 km towards the shelf edge, which is found in a water depth of 410 m (Fig. 46). The shelf — almost exclusively underlain by sediments over the length of the profile — is thus fairly flat and rather deep. This is true for most of the East Greenland shelf,

LINE 90600



CONTINENTAL SLOPE

ICELANDIC PLATEAU EDGE

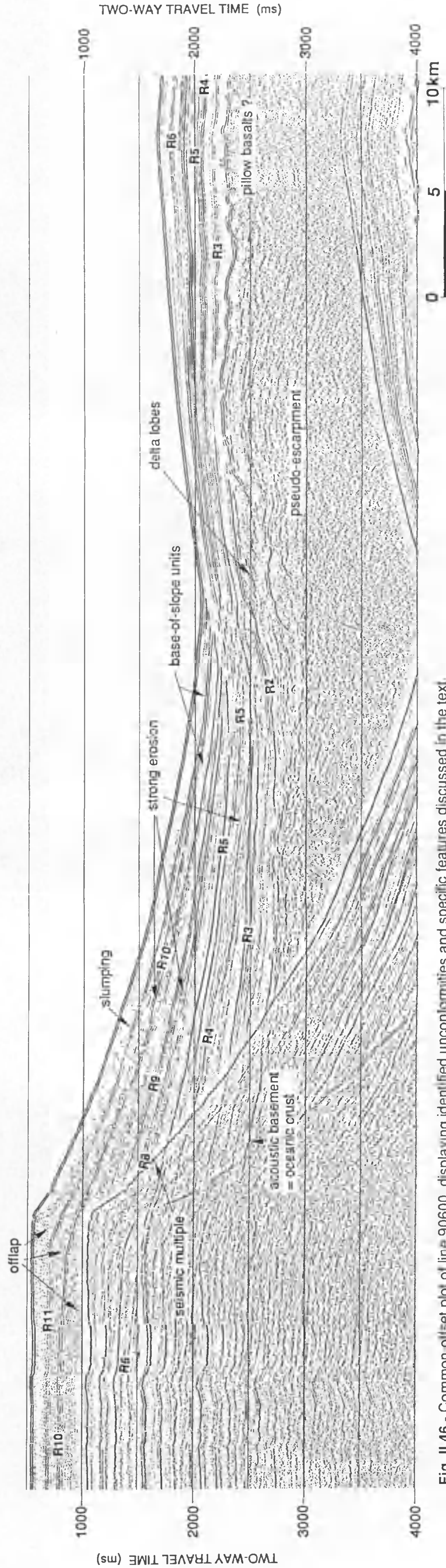


Fig. II.46 - Common offset plot of line 90600, displaying identified unconformities and specific features discussed in the text. Note that seismogram is in two sections.

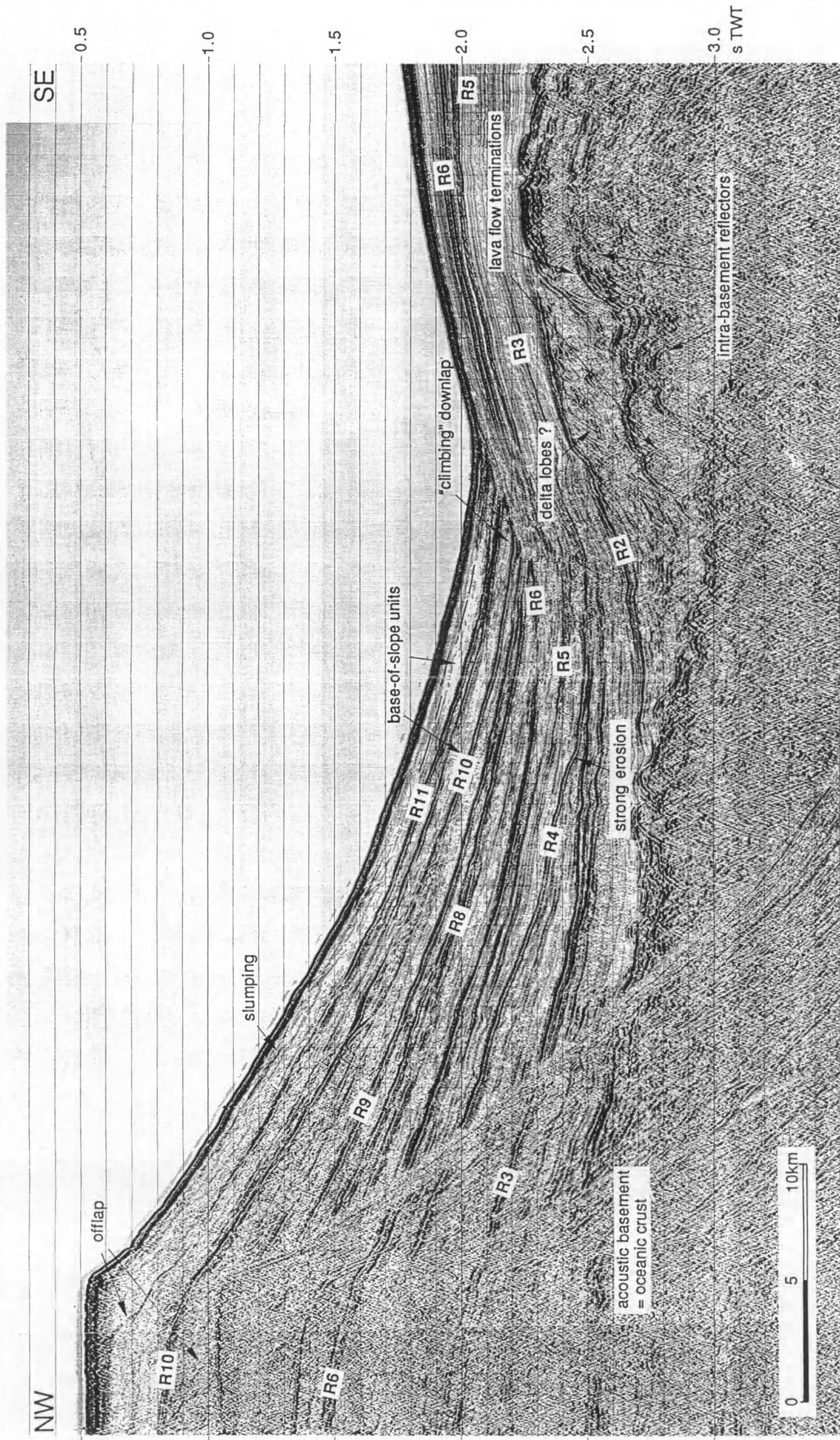


Fig. II.47 - Stacked seismic section, outlining in more detail the sediment wedge on the continental slope and pseudo-escarpment. Note how suppression of the seismic multiple improved the continuity of reflectors R3 and R6 and of the acoustic basement.

which displays water depths in the range of 250 to 350 m (Johnson et al. 1990), and more generally seems to be typical of most polar shelves. According to H.C. Larsen (1990) the present depth of the shelf outside Scoresby Sund may be of fairly recent (Pleistocene?) origin; the strongly reduced vertical sediment aggradation is probably the result of isostatic depression and erosion during repeated ice sheet advances (cf. Anderson & Bartek 1992). A pronounced transverse shelf trough, typical of many large glacial outlets, seems not to extend from the fjord system, however. Foredeepening of the shelf is not observed either.

Over two thirds of the shelf the sea bottom reflector displays a rather irregular character, accompanied by diffraction hyperbolae (Fig. 46). This is attributed to intensive scouring by iceberg keels. Beyond this reach the shelf slightly deepens (by about 35 m) and the sea bottom reflector appears less disturbed; the diffractions remain, however. A more detailed study of Parasound echo sounder and Hydrosweep swath bathymetry records by Dowdeswell et al. (1993) revealed that this outer shelf portion is still affected by scours of intermediate intensity. The plough marks are produced by large icebergs carried southward by the East Greenland current. Considering the relatively small number of icebergs presently observed (Dowdeswell et al. 1992, 1993), the intensity of scouring suggests that at least some of the marks are relict and date back to the last glaciation, i.e. the Late Weichselian.

The continental slope stretching beyond the sharply defined shelf break is fairly narrow and steep: on the upper 5 km of the slope a gradient of about 3.8° was measured.

7.3. Acoustic basement

7.3.1. General characteristics

Line 90600 is located on the very boundary between the Blosseville Kyst and the Liverpool Land shelf provinces, as defined by H.C. Larsen (1990) (see section 4.2). This boundary, sometimes denoted as the Scoresby Sund "Fracture Zone", is somewhat arbitrary; it builds a NW-SE striking basement ridge, approximately in the prolongation of the Spar Fracture Zone north of Iceland.

On the SE part of the profile and below the continental slope an acoustic basement reflector (Figs. 46 and 47) is imaged, which disappears in the strong seafloor multiple of the shelf. The strong reflectivity, rough topography and hyperbolic character of this reflector favour its interpretation as the top of the basaltic oceanic crust. According to maps published by H.C. Larsen (1990) the ocean/continent transition (OCT) is located only a few tens of km outside the coast, implying that the larger part of the continental shelf is underlain by oceanic crust as well. Magnetic anomalies (Fig. 45) indicate that along line 90600 the age of the oceanic crust ranges from 23 - 20 Ma (anomalies 6B - 6) near the OCT, to 10 Ma, the age of anomaly 5 which extends just SE-ward of the line. Still following H.C. Larsen (1990) the oceanic crust is almost entirely of subaerial origin.

Oceanic crust is normally found at increasing depths as one moves away from the spreading axis, because of thermal contraction and the consequent density increase with age. The rather opposite trend shown by the volcanic basement on profile 90600 may be ascribed to two different factors: [i] loading by younger lava flows building the volcanic plateau observed on the SE part of the profile, and [ii] velocity pull-up caused by the considerable increase of the sediment cover along the continental slope.

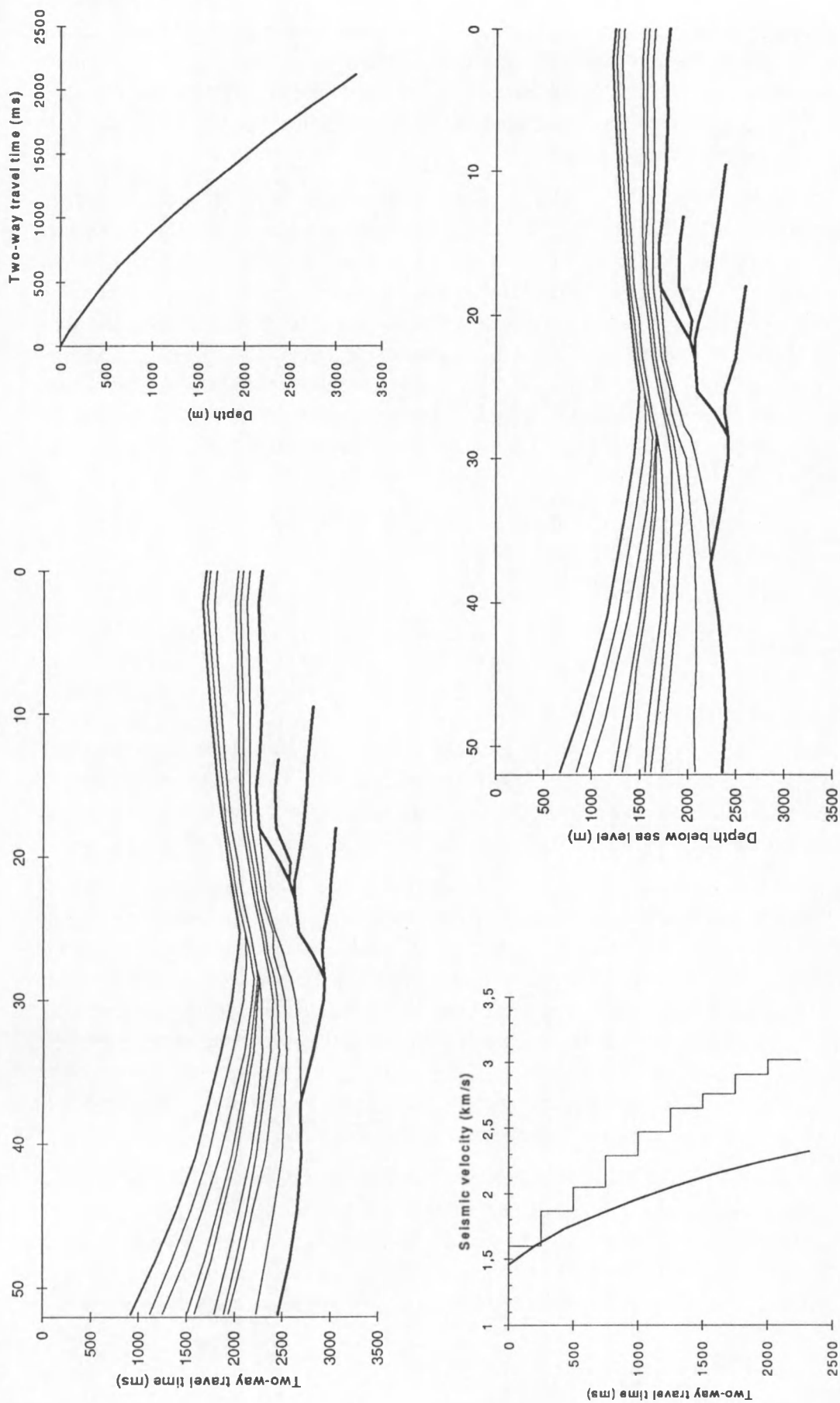


Fig. II.48 - Removal of the velocity pull-up effect: [a] original time section, [b] time/depth conversion curve published by H.C. Larsen (1985) for the Bløseville Kyst shelf region, [c] interval velocities (thin line) and average velocity (thick line) calculated from b, [d] depth section resulting from the application of the interval velocities in c.

The velocity pull-up effect has been removed by applying an appropriate time/depth conversion curve — published for this region by H.C. Larsen (1985) — to the time section of line 90600. From the resulting depth section (Fig. 48d) it appears that below the continental slope the basement indeed dips towards the continent. A map of H.C. Larsen (1985) indicates that the basement reflector reaches a depth of over 4600 m near the OCT. Loading by the volcanic plateau in the SE has caused an inversion of the original inclination of the basement there. In between both reaches the basement is relatively elevated; this may be an artefact due to the discontinuous application of the time/depth function, but could also be explained as a forebulge which usually occurs in front of a flexural depression.

7.3.2. *Pseudo-escarpment*

The most striking feature concerning the oceanic basement is the occurrence in the SE part of the profile of a steep west-facing ramp (Fig. 47) with a total relief of c. 900 m (700 ms) and a horizontal extent of about 10 km. The volcanic basement surface at that location leads up to a volcanic plateau which probably merges with the Icelandic insular plateau further SE-ward. On a magnetic map of Nunns et al. (1983) the ramp could be correlated with large positive magnetic anomalies superimposed on magnetic lineation 5A. The isolated nature of the magnetic anomaly and a comparison with nearby located seismic lines published in literature (see below) suggest that it is of limited extent. Features like this have been described by H.C. Larsen (1985, 1990) as “pseudo-escarpments”, and occur in a few places in the Blosseville Kyst shelf province. The pseudo-escarpment consists of three to five distinct levels, each bounded by intra-basement reflectors, which would suggest that it is a stack of several packages of lava flows which have flooded the older volcanic basement. By analogy with the interpretation of similar features in the Faeroe-Rockall area in the NE Atlantic (Wood et al. 1987, 1988) the pseudo-escarpment is thought to mark the position of a paleo-shoreline where repeated subaerial lava flows came in contact with water, cooled rapidly and ceased to flow (Fig. 49). The lava flow terminations, which are characterised by a weaker seismic facies, probably include sediments as a result of coexisting sedimentation and volcanism near the shoreline. The geometry and internal stratification of the sediment body deposited in front of the pseudo-escarpment indicates a near-coastal environment as well (see next section).

All this adds support to the concept of H.C. Larsen (1990) that most of the oceanic crust in this region was generated along a subaerial spreading axis. The stacking pattern of the lava flow packages suggests that they were emplaced during a period of increased magma production along an already subaerially spreading Kolbeinsey Ridge, in the interval between magnetic anomalies 5B and 5A (15 - 12 Ma), or possibly in an even shorter time span. Loading by subsequently younger basalt flows, extruded from a progressively more distal location, has caused the older flows to be inclined eastward, towards the spreading centre (Fig. 49). The pseudo-escarpment is therefore considered a small-scale analogue to the so-called “seaward-dipping” reflector sequences (cf. Fig. 14) which are associated with the OCT at volcanic passive margins and are formed during initial subaerial seafloor spreading (Hinz 1981; Mutter 1985; White & McKenzie 1989). In contrast to the subaerial origin of the pseudo-escarpment, the more hummocky reflection pattern of the basement at the far end of the plateau (Fig. 46) may be indicative of pillow basalts, thus marking the time (between 12 and 10 Ma) when the entire seafloor spreading process became submarine.

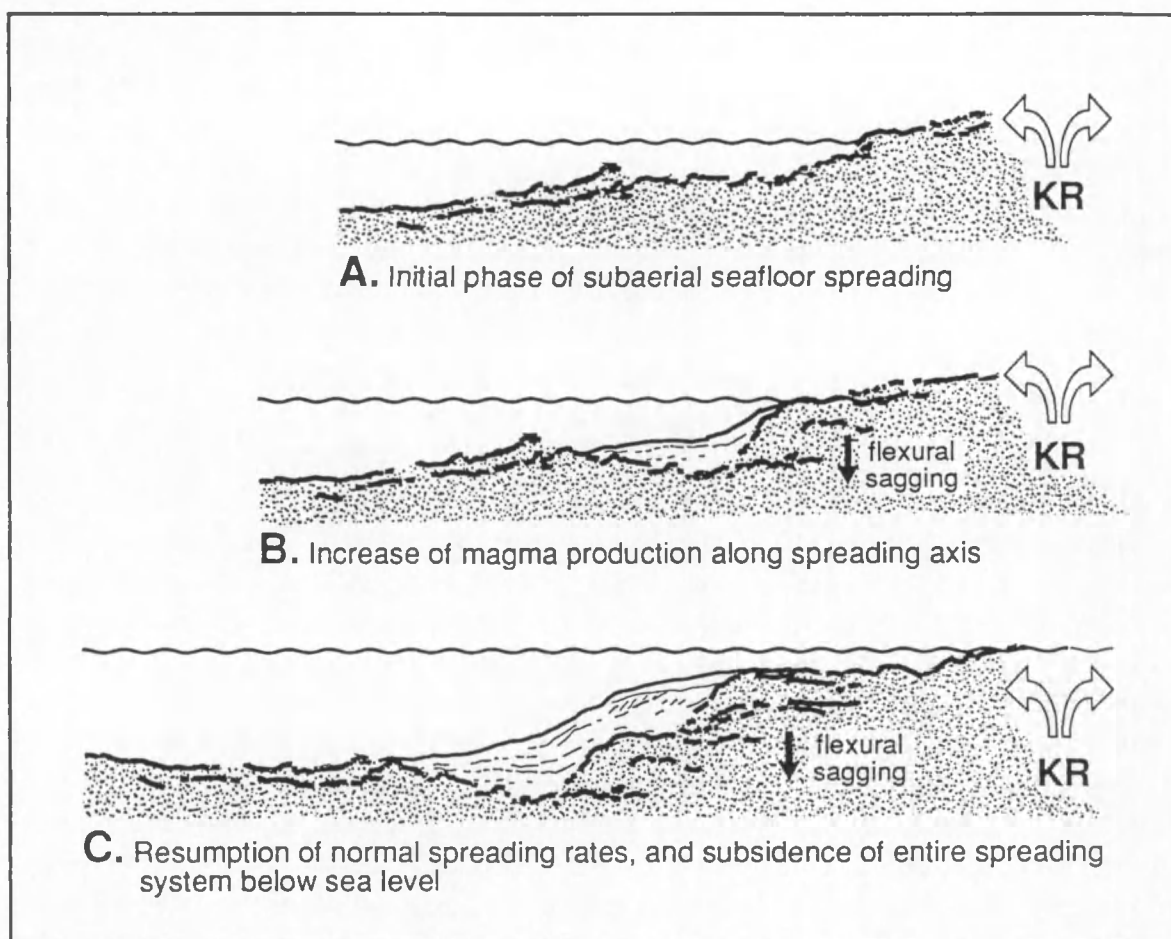


Fig. II.49 - Three-step model for the evolution of the pseudo-escarpment along the subaerially spreading Knipovich Ridge (KR).

7.4. Sediment stratigraphy

The oceanic crust on line 90600 is covered by a sedimentary wedge varying in thickness between 2000 m on the upper continental slope and about 500 m over the volcanic plateau in the SE of the profile. In a first approximation the sediments can be divided into three large-scale units (Fig. 50), witnessing the varying relative influence of two different source areas: the Scoresby Sund fjord region in the NW, and the Icelandic insular plateau to the SE. The lowermost unit I is solely derived from the edge of the volcanic plateau; the middle unit II records rather uniform sediment input from both source areas; the upper unit III extends over the entire shelf and slope, but strongly thins above the edge of the Icelandic insular plateau, implying a drastic change in the relative importance of the two source areas.

The Greenland side of the seismic line is more or less parallel to the main transport direction of sediment from the Scoresby Sund area, whereas the absence of pronounced unconformities in the section overlying the volcanic plateau in the SE suggests that the profile here cuts the direction of sediment input from the Icelandic insular plateau at an oblique angle. Strata dip from both sides of the profile towards a kind of "depositional minimum", characterised by a complex pattern of interfingering. This minimum thus represents the divide between both spheres of influence, but is at the same time the site of the North-West Atlantic Bottom Water current (NWABW) converging to Denmark Strait in the SW.

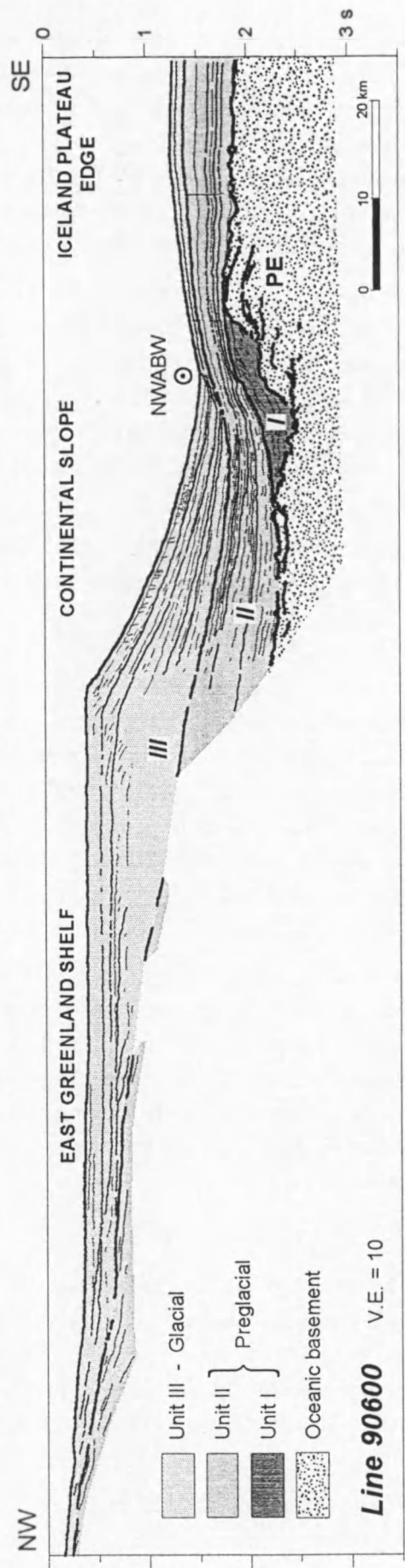


Fig. II.50 - Water-depth corrected line drawing of line 90600, illustrating the first-order division of the sediment wedge into three units.
NWABW = North-West Atlantic Bottom Water, PE = pseudo-escarpment.

In a more detailed approach a total of ten erosional unconformities was identified below the continental shelf and slope, defining eleven “sequences” (Figs. 46 and 47). It is suspected, however, that these entities do not strictly correspond to sequences in the sense of Posamentier et al. (1988): in the lower units I and II the resolution is generally not sufficient to recognise the different systems tracts usually composing such a sequence, whereas the upper unit III is believed to have been deposited in a glacial environment, which strongly differs from the “normal”, lower-latitude passive margin setting for which the sequence stratigraphic model was originally developed (see chapter I).

The sequences were numbered from oldest to youngest, the number of the respective sequence boundary (R_n) corresponding to that of the overlying sequence; reflector 1 represents the oceanic basement reflector. Though the continental slope is separated from the volcanic plateau by a zone of complex interfingering, some of the identified sequence boundaries could be traced onto the plateau. These reflectors may not have a sequence stratigraphic connotation here; they are merely the time-correlative counterparts of the sequence boundaries identified below the shelf and slope.

The section below gives a brief description of the geometrical relationships observed between the identified sequences, and the interpreted geological significance. A more detailed summary of the stratal geometries and thickness variations of each individual sequence can be found in Table 5.

Unit I (sequence 1)

The lowermost unit is restricted to the foot of the volcanic pseudo-escarpment. The internal geometry shows evidence of several subunits, their top reflector onlapping at subsequently higher levels against the pseudo-escarpment; this seems to indicate that the unit was deposited in several steps, associated with the successive phases of lava extrusion. The presence of small progradational bodies (possibly deltaic lobes) in its upper part (Fig. 47) is an indication for deposition in a near-coastal environment. Thus, the sediments composing unit I were probably derived from erosion of the volcanic plateau at a time when it was still subaerial, and filled the flexural depression which was growing in front of the pseudo-escarpment as a result of the progressive loading by lava flows.

The deposits of unit I are clearly the oldest sediments observed on line 90600; their age is confined by onlap of the top reflector onto the crest of the pseudo-escarpment, which is of anomaly 5A age (± 12 Ma). The more landward location of the ocean/continent transition — where the oceanic crust has an age between 23 and 20 Ma (H.C. Larsen 1990) — implies, however, that strata up to Early Miocene in age lie hidden below the seismic multiple on the continental shelf. According to H.C. Larsen (1985, 1990) sediments of even older age are present in a narrow halfgraben-like structure in front of the East Greenland Escarpment.

Unit II (sequences 2 - 5)

The middle unit is observed below the continental slope and over the edge of the Icelandic insular plateau; the continuation on the shelf is completely masked by the seismic multiple. Four sequences can be recognised, the lower two quite thick and the upper two much thinner. For reasons that have been outlined above, correlation of these sequences with the global sequence cycle chart of Haq et al. (1987) is not evident, and in particular the lower two sequences may actually comprise multiple sequences sensu Posamentier et al. (1988).

Draping of the lowermost sequence 2 over the pseudo-escarpment indicates that the volcanic plateau had mostly subsided below sea level before deposition of unit II commenced. Input of erosional

	INNER SHELF	OUTER SHELF	SHELF EDGE	SLOPE	ICELANDIC PLATEAU EDGE	Sea floor	GEOLOGICAL EVENT	TENTATIVE AGE CORRELATION
Sequence 11 Ref. 11	erosion 0 ms	175 ms	toplap 230 ms	parallel ? downlap (→SE)	130 ms (NW←) onlap	Sequence 11 Ref. 11	last extensive glaciation reaching to the shelf edge	Saale? (0.2 Ma)
Sequence 10 Ref. 10	erosion 0 ms	100 ms	toplap 170 ms	parallel ? (NW←) onlap	90 ms "climbing" downlap (→SE)	Sequence 10 Ref. 10	shift to aggradational depositional style	0.6 Ma ?
Sequence 9 Ref. 9	erosion 80-200 ms	100 ms	toplap 280 ms	erosion "climbing" downlap (→SE)	55 ms 30 ms	Sequence 9 Ref. 9		
Sequence 8 Ref. 8	erosion 0 ms	120 ms	100 ms	parallel ? downlap (→SE)	40 ms <10 ms	Sequence 8 Ref. 8	further amplification of the glaciations	1.2 Ma
Sequence 7 Ref. 7	erosion 0 ms	125 ms	200 ms	erosion	110 ms <10 ms			
Sequence 6 Ref. 6	erosion 0 ms	50 ms		"climbing" downlap (→SE)	erosion ? 120 ms downlap (→SE)	Sequence 6 Ref. 6	onset of large-scale glaciations of the continental shelf	2.5 Ma
	erosion	erosion		100 ms	130 ms	Sequence 5 Ref. 5		
				erosion 50 ms (NW←) onlap	100 ms 70 ms	Sequence 4 Ref. 4	first passage of NWABW "	± 6 Ma ?
				280 ms (NW←) onlap	erosion 80 ms 50 ms	Sequence 3 Ref. 3		> 10 Ma
				320 ms	erosion 140 - 70 ms onlap (→SE)	Sequence 2 Ref. 2	subsidence of oceanic crust below sea level	12 Ma
				0 ms downlap (→SE)	erosion (?) 250 - 350 ms (NW←) downlap onlap (→SE)	Sequence 1 Basement		

Table II.5 - Sequence stratigraphic correlation table for line 90600, summarising reflector configurations and thickness variations for each individual sequence, along with a tentative age correlation and interpreted geological significance.

products from this structure consequently dropped, and new sediment input proceeded from a direction oblique to the profile, most likely from the Icelandic insular plateau more to the south. Sediments derived from East Greenland are evident as continental slope reflectors, lapping out onto the underlying unit I in the lower part of sequence 2; further up-sequence they merge with the strata on the volcanic plateau, resulting in continuous sedimentation all over the profile. As the top of sequence 2 is not seen to terminate against the oceanic crust anywhere on the profile, it is estimated to have an age somewhat younger than 10 Ma, the age of the youngest magnetic anomaly identified along the profile (section 7.3.1).

Sequence 3 constitutes a thick package that more or less displays the same trends as the underlying sequence. A most conspicuous observation is that the sequence is severely eroded at the foot of the continental slope; bottom currents are considered the most likely mechanism capable of such erosion. Sequences 2 and 3 reach a combined thickness of 830 m below the continental slope, thinning to 110 m over the volcanic plateau. The thickness maximum is probably located below the outer shelf, but cannot be observed due to the multiple.

The two upper sequences 4 and 5 are much thinner than the older sequences within unit II. Their combined thickness totals 170 m below the continental slope, but increases to 210 m towards the SE. This remarkable thickening over the volcanic plateau, which is particularly striking within sequence 5, indicates that sediment input from East Greenland relatively lost importance during this interval, as is also expressed by a clear NW-ward shift of the depositional minimum.

Unit III (sequences 6 - 11)

The upper unit, extending over the entire continental shelf and slope, is the part of the sedimentary section that is best observed on line 90600. The most conspicuous characteristic of unit III is the strong thickness contrast between the East Greenland and the Icelandic sides of the profile: the thickness is generally about 275 m on the shelf, reaches a maximum of 1000 m below the outer shelf and upper slope, but thins to less than 140 m over the volcanic plateau. The thinning takes place at all levels within the unit, resulting in a reflection pattern that could be described as "climbing" downlap (Fig. 47). This stratal termination pattern is caused by the thinning of the individual strata below the seismic resolution as they climb up the pseudo-escarpment. A drastic increase of the sediment input from the Scoresby Sund region is inferred. The base of unit III, reflector 6, is tentatively correlated with a prominent erosional surface on the continental shelf which is thought to reflect the first advance of an ice sheet onto the continental shelf. Mainly on these two grounds, unit III is interpreted as being entirely glacial in origin.

Within unit III, five more erosional unconformities are identified as sequence boundaries on the continental shelf, the present seafloor being erosional as well. In addition, reflectors 7 and 9 show significant erosion on the slope, probably as an effect of bottom current activity. Unit III thus comprises at least 6 sequences, each corresponding to a phase of extensive ice sheet grounding. It appears that the observed stratal patterns are quite different from those predicted by the sequence stratigraphic model of Posamentier & Vail (1988) and Posamentier et al. (1988) applicable to most non-glaciated continental margins. The overall depositional style is one of strong progradation. Aggradation is markedly reduced, except for the two upper sequences. Internal reflectors are more or less horizontal and parallel on the continental shelf, but turn into distinct offlap near the shelf edge.

Further downslope, reflectors terminate by downlap onto the underlying sequence boundary or, as observed in the upper sequences 10 and 11, against a surface which constitutes the top of a base-of-slope wedge (Fig. 47). Finally, the youngest sequence 11 is affected by slumping on the continental slope. Apart perhaps from the base-of-slope units identified in the two youngest sequences, there is no evidence of extensive submarine fan deposits, nor is there any on other seismic profiles published for this region (see below). In contrast to earlier suggestions, there is thus probably no such thing as a "Scoresby Sund fan".

On the basis of stratal geometry patterns unit III can be subdivided into three different subunits of two sequences each (Fig. 51). The lower subunit III-A (sequences 6 and 7) is characterised by minor seaward progradation of the shelf margin by only 5 km. The second subunit III-B (sequences 8 and 9) is marked by increasingly strong shelf margin progradation: in two subsequent steps the shelf edge moved seaward by amounts of 15 km and 23 km, respectively. Both III-A and III-B are characterised by rather small amounts (130 m total) of vertical shelf aggradation. In contrast, the uppermost subunit III-C (sequences 10 and 11) is almost purely aggradational (over 260 m), whereas progradation is reduced to less than 5 km.

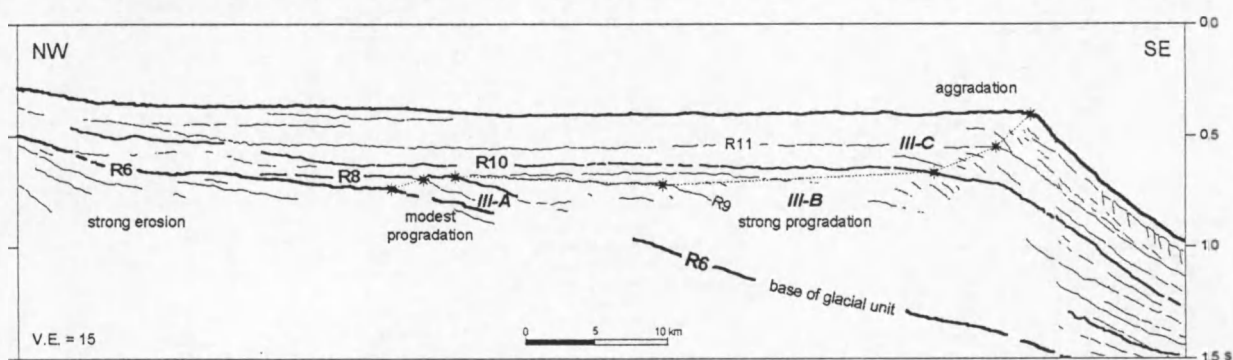


Fig. 11.51 - Detailed, water-depth corrected line drawing illustrating the stratal geometries on the continental shelf. Based on the variation of progradational and aggradational components, glacial unit III can further be divided into three subunits A-C.

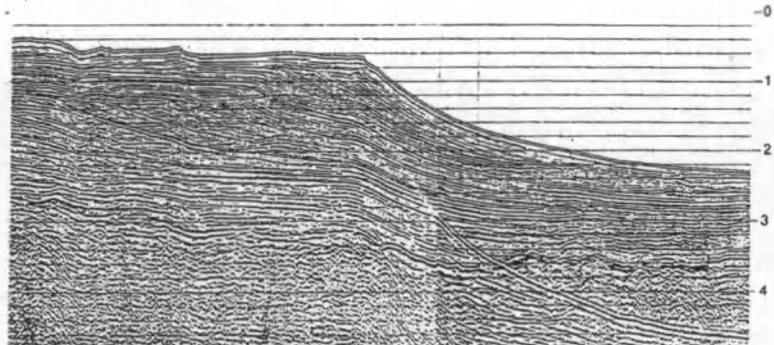
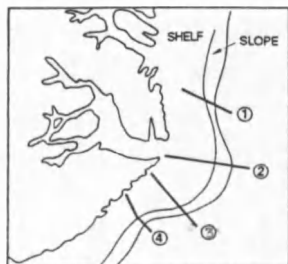
Comparison with other seismic lines

Fig. 52 shows a series of earlier published seismic lines that are located in the vicinity of line 90600. Due to the low resolution and reduced scale of these industrial-quality data it is very hard to make a correlation with the stratigraphy described above. The profiles are located at varying distances from the mouth of Scoresby Sund, which acts as the main supplier of sediment: line GGU 82-12 is located centrally on the glacial depocentre in front of Scoresby Sund; line BGR 76-11 covers the northern edge of the depocentre, whereas line GGU 82-28 is located to the south of the depocentre, on a portion of the margin receiving far less sediment. A marked lateral variability is evident along the margin. The seismic reflection geometries of line 90600 are most resemblant to those of line BGR 76-11, which occupies a similar position, but on the opposite side of the glacial depocentre. The BGR-line shows the same general trends as outlined above: strong progradation of the sequences underlying the outer continental shelf and distinct aggradation of the youngest sequences; submarine fan deposits seem not to have developed, but a large mass flow deposit is apparent below the foot of the continental slope.

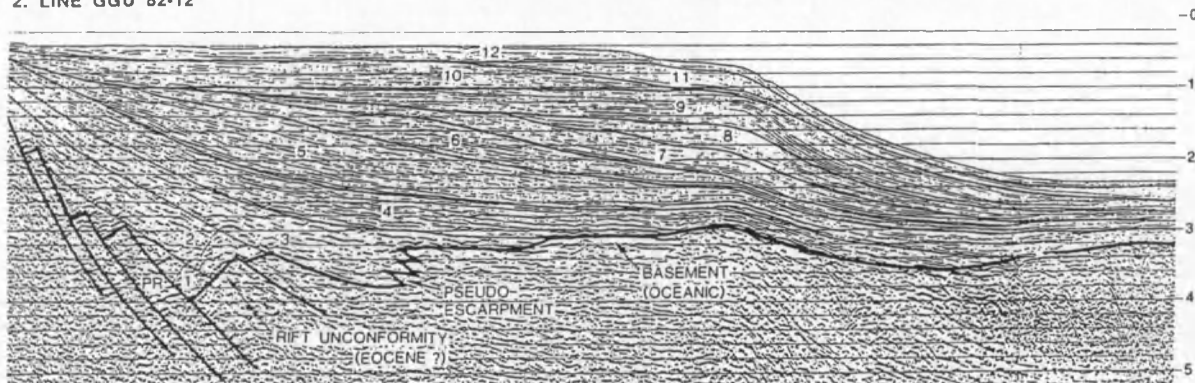
W

E

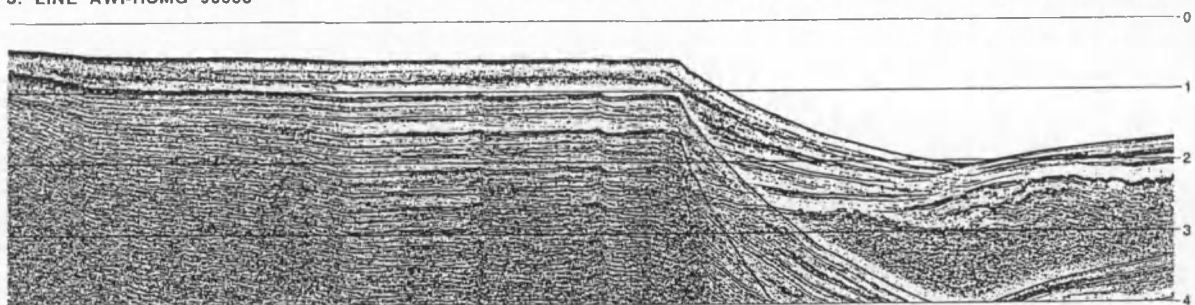
1. LINE BGR 76-11



2. LINE GGU 82-12



3. LINE AWI-RCMG 90600



4. LINE GGU 82-28

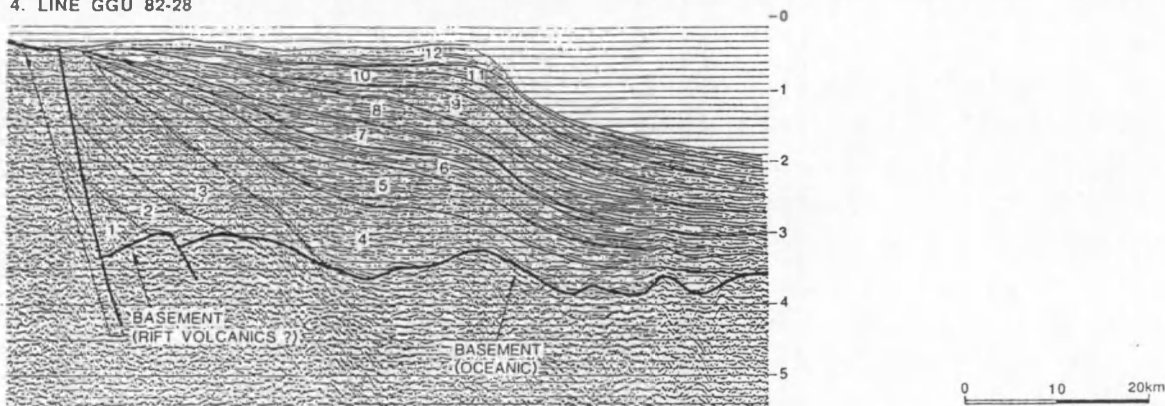


Fig. II.52 - Line 90600 compared to three other seismic sections published for the surrounding area: [a] line BGR 76-11 (from Hinz & Schlüter 1980), [b] line GGU 82-12 (from H.C. Larsen 1990), [c] line AWI-RCMG 90600, and [d] line GGU 82-28 (from H.C. Larsen 1990). BGR = Bundesanstalt für Geowissenschaften und Rohstoffe, GGU = Grønlands Geologiske Undersøgelse.

7.5. Geological and glacial history

The following section gives an account of the geological and glacial history of the East Greenland margin adjacent to Scoresby Sund, reconstructed from the seismic reflection geometries discussed in the preceding section. In the absence of “ground-truth” evidence such as deep drill holes, the only age estimates are provided by the magnetic anomaly lineations of the oceanic crust discussed in section 7.3.1: the termination of a reflector onto oceanic crust of known age yields a maximum age for this reflector. Therefore, the reconstruction necessarily remains rather approximate. A step-by-step reconstruction through time of line 90600 is shown in Fig. 53.

7.5.1. Pre-glacial development

After the initiation of seafloor spreading in the Early Miocene, sediments delivered by a major river system occupying the position of the present-day Scoresby Sund fjord area (cf. H.C. Larsen 1985), were deposited onto the newly formed oceanic crust, and started to build out the continental margin. In the Middle Miocene, between 15 and 12 Ma, a pseudo-escarpment came into existence as a result of increased magma production along the subaerially spreading Kolbeinsey Ridge. Sediments derived from this volcanic edifice were contemporaneously deposited in front of the structure (Unit I), while progradation of the East Greenland margin went on. The small depocentre in front of the pseudo-escarpment apparently remained isolated from the sediment supply from the continent.

Between 12 and 10 Ma, in the late Middle Miocene, the volcanic plateau and pseudo-escarpment subsided below sea level; probably the entire seafloor spreading process became submarine at that time. Input of erosional products from the volcanic plateau consequently came to a halt, and was replaced by sediment input from the still emergent Icelandic insular plateau more to the south. In the mean time, sediments derived from the continent had been prograding further SE-ward, and soon a link was established between both areas of deposition, resulting in continuous sedimentation all over the profile (sequence 2). The contribution of sediment from East Greenland still proceeded by river systems. For a long period of time sediment input from the two source areas remained fairly uniform (sequences 2 and 3). Following the deposition of sequence 3, significant erosion occurred at the base of the continental slope, perhaps by the action of a bottom current. In view of the present oceanographic setting (section 3.1), it is speculated that this event documents the development of the NWABW current, which would indicate that the Arctic and polar North Atlantic oceans had significantly cooled by that time, announcing the instalment of a full glacial environment in the Plio-Pleistocene. The exact timing of this event is not known, but carbon and oxygen isotope studies of Jansen et al. (1990) suggest that cold deep waters were being formed within the Arctic Ocean and Greenland-Norwegian Sea throughout most of the last 6 Ma. During ensuing deposition of sequences 4 and 5 sediment input from the Scoresby Sund region noticeably decreased. Transport of sediment towards the shelf may well have been restricted for a while during the gradual build-up of a continental ice sheet, until the ice sheet was large enough to reach coastal areas. Recent ODP drilling on the East Greenland shelf (H.C. Larsen et al. 1994) has traced IRD in sediments as old as 7 Ma, implying the existence of sizeable ice masses giving way to the ocean from at least that time on.

7.5.2. Glacial evolution

The transition from unit II to unit III marks the most pronounced depositional change within the geological record revealed by line 90600, and is interpreted to reflect the onset of extensive glaciations characterised by repeated grounding of ice beyond the coastline. The Greenland ice sheet had been gradually built up until large outlet glaciers were filling the former river valleys in the Scoresby Sund area. Erosion on the continent intensified, which probably accounts for the increased delivery of sediment to the shelf and slope system throughout unit III time. A major erosional surface (reflector 6) was carved on the continental shelf when the Inland Ice for the first time grounded to the shelf edge. Oxygen isotope and IRD evidence for the onset of repetitive large-scale northern hemisphere glaciations goes back to the Late Pliocene, around 2.6 Ma (Shackleton et al. 1984; Jansen et al. 1988). According to Jansen et al. (1990) this time corresponds to the most pronounced environmental change that affected the polar North Atlantic region during the late Cenozoic. The resulting glacio-eustatic sea level fall is likely to have affected sedimentation on continental margins world-wide, since the global sequence cycle chart of Haq et al. (1987) indicates a sequence boundary at that time too. Although recent ODP drilling (H.C. Larsen et al. 1994) has shown that glaciation in Greenland began as early as 7 Ma, extensive glacial advances onto the continental shelf probably started later, perhaps around 2.5 Ma when the other North Atlantic ice sheets were fully established. As has been observed on many other glaciated margins (see chapter I), the action of successive glacial advances to the shelf edge at times of glacial maximum shifted sedimentation in a strongly progradational mode. The East Greenland margin south of Scoresby Sund has prograded no less than 45 km since the first glacial advance. During interglacials, in contrast, most sediment was probably trapped inside Scoresby Sund, and only minor amounts were input to the shelf and slope (cf. Stein et al. 1993).

The changing amounts of progradation and aggradation of the three subunits recognised within unit III probably reflect successive phases in the glacial evolution of the region. Small amounts of progradation indicate that the initial glacial advances were still of fairly modest magnitude. A shift to stronger progradation during the second glacial episode is probably indicative of progressively larger and longer-lasting ice sheets, building the shelf margin ever further out. Despite the lack of good age constraints, such an interpretation runs markedly parallel to the findings of IRD and oxygen isotope studies of ODP drill holes on the Vøring Plateau in the Norwegian Sea, published by Jansen et al. (1990) (Fig. 54). These authors inferred that, following the establishment of a continuous glacial environment, repetitive advances of medium-sized ice sheets took place; after 1.2 Ma, however, a strong amplification of the glaciations occurred. In sharp contrast to the two earlier intervals, the latest glacial episode is characterised by aggradational shelf development. This recentmost change in depositional style is poorly understood, but may again be related to another variation of climatic conditions. A possible candidate is the shift of climatic cyclicity from a 41 ka rhythm (response to orbital obliquity) into a dominant 100 ka rhythm (response to eccentricity) (Ruddiman et al. 1986), which was more or less completed by 0.6 Ma (Jansen et al. 1988), but this remains rather speculative. An important aspect is that these two upper aggradational shelf sequences were most likely deposited during glacial advances as well; this is supported by the erosional nature of their basal unconformities, by the offlapping internal reflector patterns which can just barely be discerned, and by the low present-day interglacial sedimentation rates on the shelf (Marienfeld 1991; Stein et al. 1993).

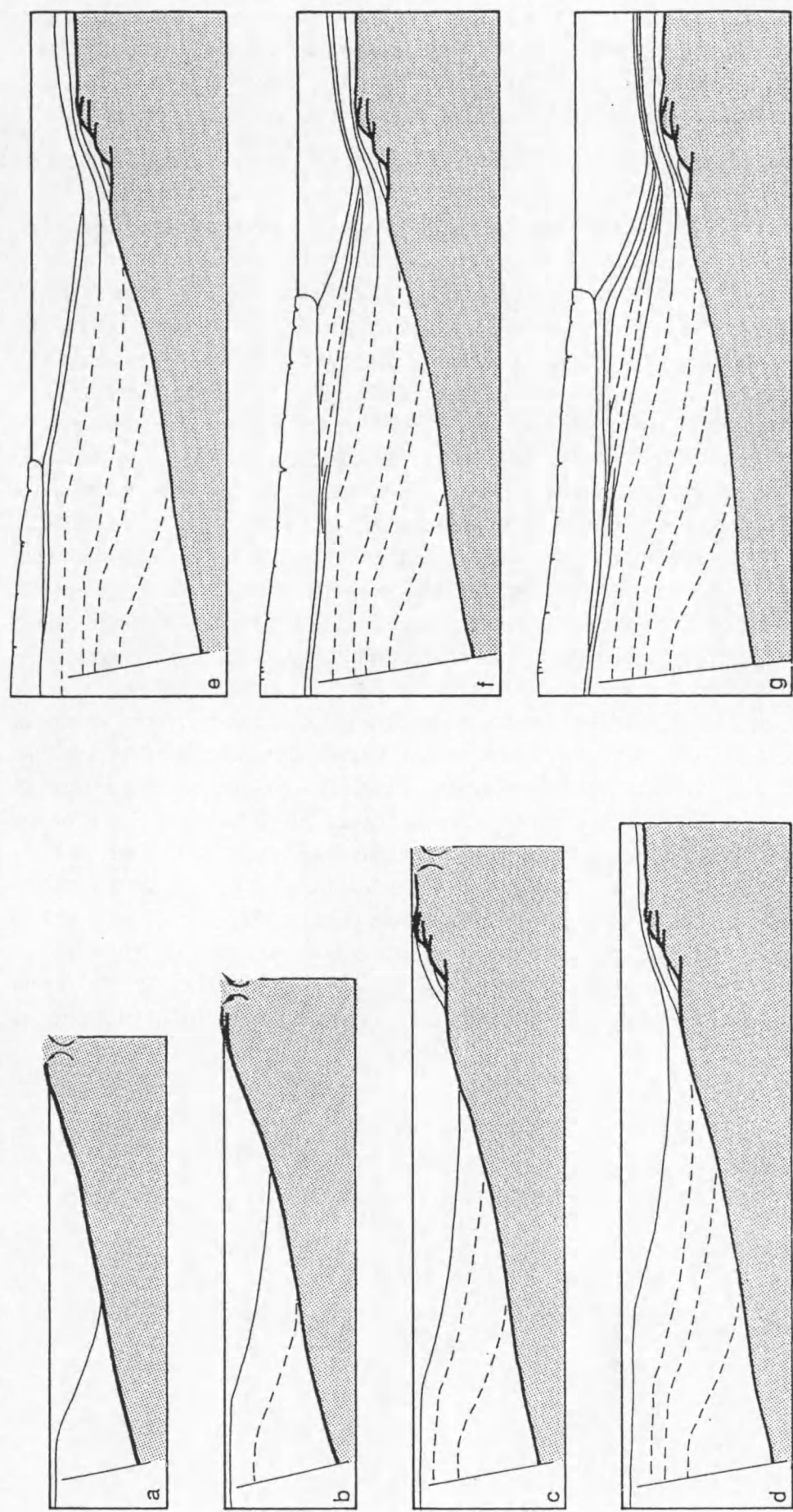


Fig. II.53 - Cartoon showing evolution of line 90600 in 7 stages. [a] Initial phase of subaerial spreading, sediment input from E Greenland proceeds by rivers. [b] increase of magma production along subaerial spreading ridge, leading to the formation of a pseudo-escarpment. [c] submergence of spreading ridge below sea level. [d] two depocentres coalesce, resulting in sedimentation all over the profile. [e] initial moderate glaciations of the continental shelf. [f] intensification of glaciation, resulting in strong progradation and deepening of the shelf. [g] latest glacial phase of aggradational development. Basement depth in g partly taken from maps of H.C. Larsen (1985).

The aggradational development seems to imply a significant reduction of the erosional force of the advancing ice sheets compared to preceding glaciations. This may be related to a variety of mechanisms, including less prolonged residence of the ice sheet at the shelf edge, thinner ice sheets, reduced loading effect by overdeepening of the shelf, etc. The role of passive margin subsidence is considered minor, however, in view of the relatively short time spans involved here.

Whereas the correlation of changes in depositional style with general trends in northern hemisphere glacial evolution appears relatively good, a closer correlation of the individual sequences is hard to establish without additional information from deep drill holes on the margin itself. The oxygen isotope record indicates that more than 20 ice ages occurred during the Pleistocene, and more so in the late Neogene (Mix 1987), whereas only 6 sequences were identified within the glacial unit. It thus appears that not all glaciations have left detectable traces in the stratal geometry on the central East Greenland continental shelf and slope. It is important to realise that the ice ages did not occur in a discrete manner, but with various periods and amplitudes (Mix 1987). Some glaciations may thus not have been extensive enough to reach far beyond the coastline, whereas the sequences deposited by other advances may have been obliterated by later grounding events. This is in particular illustrated by the uppermost glacial sequence 11. Erosion of internal reflectors by the seafloor on the inner shelf (Fig. 46) suggests that deposition of this sequence was followed by other glacial advances of lesser extent. As the different Weichselian glaciations are generally thought to have had a rather small extent (Funder et al. 1991) — and thus probably didn't reach all the way to the shelf edge — it seems more likely that the uppermost glacial sequence dates back to the extensive Saale glaciation (oxygen isotope 6), which represents the maximum of recorded glaciation on land (Weidick 1976; Funder et al. 1991). The erosive character of the seafloor near the coast may in that case represent the extension of the ice during the last glacial maximum. This interpretation is in good agreement with results of Marienfeld (1991), who concluded from gravity cores outside Scoresby Sund that the Late Weichselian ice sheet extended only a short distance from the coast on the continental shelf. In addition, Dowdeswell et al. (1991) identified a moraine ridge extending offshore from Kap Brewster which probably represents the limits of that ice sheet. From a study of the literature, Berry & Piper (1993) have ranked oxygen isotope stages 6 and 12 as the most severe late Pleistocene glaciations. Extrapolating the correlation of sequence 11 down the section, it seems likely that stages 8 and 10 have no major expression in the depositional record either, so that the underlying aggradational sequence 10 probably corresponds to isotope stage 12 (D.J.W. Piper, pers. comm. 1995). Though speculative, this independent reasoning supports the more general correlation of subunits, as indicated in Fig. 54.

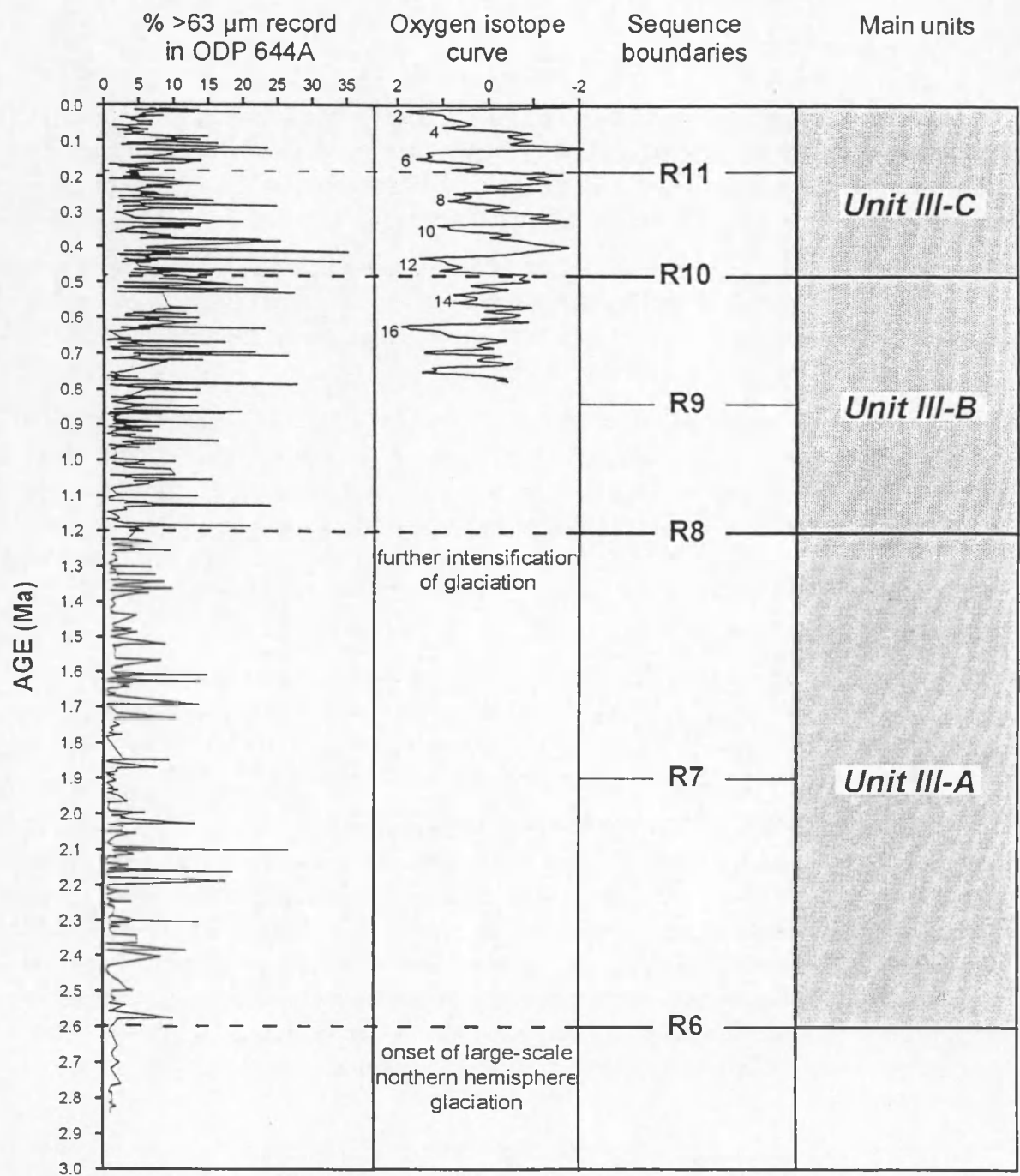


Fig. II.54 - Proposed correlation of the seismic stratigraphy with oxygen isotope stages (Imbrie et al. 1989), coarse fraction record of ODP Site 644A, and general northern hemisphere glacial evolution (Jansen et al. 1988).

7.6. Conclusions

- Due to its ideal location off one of the major outlets of the Inland Ice along the central East Greenland margin, the information provided by line 90600 on the long-term history of glaciation reaches much farther back in time than the terrestrial record (cf. section 4.3.3) or the seismic data recorded in the Scoresby Sund fjord system itself (cf. section 6).
- The seismic reflection line records the transition from a non-glacial environment into a fully glacial setting characterised by increased sedimentation rates and strong shelf margin progradation. A pronounced erosional surface is interpreted to witness the first ice grounding event on the continental shelf outside Scoresby Sund.
- The successive Plio-Pleistocene glacial advances drastically augmented the input of sediment from the continent to the outer shelf/upper slope system. A large depocentre — evident in the bathymetry as a pronounced seaward-convex bulge — underlying the outer shelf and upper slope indicates that the continental margin has been strongly built out by grounded ice sheets: along line 90600 the shelf edge has prograded by an amount of 45 km; in front of Scoresby Sund this value is probably even higher. This glacial depocentre seems not to be associated with a submarine fan system further downslope.
- At least 6 glacial advances out to the shelf edge are evident by as many erosional surfaces and sequences. It is suspected that only the strongest glaciations left detectable traces in the stratal geometry patterns, however. Sequences deposited by less extensive glacial advances are either too thin to be observed, or were obliterated by subsequent stronger glaciations.
- The individual sequences could not be assigned to known ice ages, but varying amounts of progradation and aggradation within the glacial unit seem to correlate with different phases of the glacial evolution in the polar North Atlantic, deduced from ODP drill holes distally located in the Norwegian Sea: minor amounts of progradation suggest that the first glacial advances were still of rather modest magnitude; increased progradation within a second interval indicate a strong amplification of the glaciations, with progressively larger ice sheets building the continental margin ever further out; the youngest interval is remarkably characterised by aggradation rather than progradation, which may probably be attributed to thinner ice sheets with a reduced erosional force.
- The youngest sequence recognised on line 90600 was probably deposited during the Saale glaciation; the central East Greenland continental margin would thus have been essentially sediment-starved since.

References cited

- Anderson J.B. & Bartek L.R. (1992) — Cenozoic glacial history of the Ross Sea revealed by intermediate resolution seismic reflection data combined with drill site information. In: Kennett J.P. & Warnke D.A. (Eds.), *The Antarctic Paleoenvironment: A Perspective on Global Change* (Part one). Antarctic Research Series, 56, American Geophysical Union, Washington, D.C., pp. 231-263.
- Berry J.A. & Piper D.J.W. (1983) — Seismic stratigraphy of the central Scotian Rise : A record of continental margin glaciation. *Geo-Marine Letters*, 13, pp. 197-206.
- Boulton G.S. (1990) — Sedimentary and sea level changes during glacial cycles and their control on glacial marine facies architecture. In: Dowdeswell J.A. & Scourse J.D. (Eds.), *Glacial Marine Environments: Processes and Sediments*. Special Publication, 53, The Geological Society, London, pp. 15-52.
- Dansgaard W., Clausen H.B., Gundestrup N., Hammer C.U., Johnson S.F., Kristinsdottir P.M. & Reeh N. (1982) — A new Greenland deep ice core. *Science*, 218, pp. 1273-1277.
- Dansgaard W., Johnsen S.J., Clausen H.B., Dahl-Jensen D., Gundestrup N.S., Hammer C.U., Hvidberg C.S., Steffensen J.P., Sveinbjörnsdottir A.E., Jouzel J. & Bond G. (1993) — Evidence for general instability of past climate from a 250-kyr ice-core record. *Nature*, 364(6434), pp. 218-220.
- Dowdeswell J.A., Villinger H., Whittington R.J. & Marienfeld P. (1991) — The Quaternary marine record in the Scoresby Sund fjord system, East Greenland : Preliminary results and interpretation. In: Möller P., Hjort C. & Ingólfsson Ó. (Eds.), *The Last Interglacial-Glacial Cycle: Preliminary Report on the PONAM Fieldwork in Jameson Land and Scoresby Sund, East Greenland*. Lundqua Report, 33, pp. 149-155.
- Dowdeswell, J.A., Villinger H., Whittington R.J. & Marienfeld P. (1993) — Iceberg scouring in Scoresby Sund and on the East Greenland continental shelf. *Marine Geology*, 111, pp. 37-53.
- Dowdeswell J.A., Whittington R.J. & Hodgkins R. (1992) — The sizes, frequencies and freeboards of East Greenland icebergs observed using ship radar and sextant. *Journal of Geophysical Research*, 97, pp. 3515-3528.
- Dowdeswell J.A., Whittington R.J. & Marienfeld P. (1994) — The origin of massive diamicton facies by iceberg rafting and scouring, Scoresby Sund, East Greenland. *Sedimentology*, 41, pp. 21-35.
- Einarsson T., Hopkins D.M. & Doell R.R. (1967) — The stratigraphy of Tjörnes, northern Iceland, and the history of the Bering Land Bridge. In: Hopkins D.M. (Ed.), *The Bering Land Bridge*. Stanford University Press, pp. 312-325.
- Emiliani C. (1969) — Interglacial high sea levels and the control of Greenland ice by the precession of the equinoxes. *Science*, 166, pp. 1503-1504.
- Escher A. & Watt W.S. (Eds.) (1976) — *Geology of Greenland*. The Geological Survey of Greenland, Copenhagen.
- Feyling-Hansen R.W., Funder S. & Petersen K.S. (1983) — The Lodin Elv Formation : A Plio-Pleistocene occurrence in Greenland. *Bulletin of the Geological Society of Denmark*, 31, pp. 81-106.
- Flint R.F. (1971) — *Glacial Geology and Quaternary Geology*. Wiley & Sons, New York, 892 pp.
- Funder S. (1971) — Observations on the Quaternary geology of the Rødefjord region, Scoresby Sund, East Greenland. *Rapp. Grønlands Geologiske Undersøgelse*, 48, pp. 51-55.
- Funder S. (1972) — Remarks on the Quaternary geology of Jameson Land and adjacent areas, Scoresby Sund, East Greenland. *Rapp. Grønlands Geologiske Undersøgelse*, 48, pp. 93-98.
- Funder S. (1978) — Holocene stratigraphy and vegetation history in the Scoresby Sund area, East Greenland. *Bull. Grønlands Geologiske Undersøgelse*, 129, pp. 1-66.
- Funder S. (1984) — Chronology of the last interglacial/glacial cycle in Greenland : First approximation. In: Mahaney W.C. (Ed.), *Correlation of Quaternary Chronologies*. GeoBooks, Norwich, pp. 261-279.
- Funder S. (1989) — Quaternary geology of the ice-free areas and adjacent shelves of Greenland. In: Fulton R.J. (Ed.), *Quaternary Geology of Canada and Greenland*. *Geology of Canada*, Vol. 1, The Geological Survey of Canada, pp. 743-792.
- Funder S. & Hjort C. (1973) — Aspects of the Weichselian chronology in central East Greenland. *Boreas*, 2, pp. 69-84.

- Funder S., Hjort C. & Landvik J.Y. (1991) — Quaternary stratigraphy of Jameson Land : A first approximation. In: Möller P., Hjort C. & Ingólfsson Ó. (Eds.), *The Last Interglacial-Glacial Cycle: Preliminary Report on the PONAM Fieldwork in Jameson Land and Scoresby Sund, East Greenland*. Lundqua Report, 33, pp. 171-175.
- Greenland Ice-core Project (GRIP) Members (1993) — Climate instability during the last interglacial period recorded in the GRIP ice core. *Nature*, 364(6434), pp. 203-207.
- Hansen L.A. & Jørgensen M.E. (1993) — Late Pleistocene stratigraphy and depositional environments of the Fynselv area, Jameson Land, East Greenland. Abstract volume of the Fourth annual workshop on the Polar North Atlantic Margins (PONAM) programme, Cambridge.
- Haq B.U., Hardenbol J. & Vail P.R. (1987) — Chronology of fluctuating sea levels since the Triassic. *Science*, 235, pp. 1156-1167.
- Henriksen N. (1986) — Descriptive text to the geological map of Greenland 1:500000, sheet 12 Scoresby Sund. The Geological Survey of Greenland, Copenhagen, 27 pp.
- Henriksen N. (1989) — Scoresby Sund områdets geologi: geologisk beskrivelse og kort 1:500000. Grønlands Geologiske Undersøgelse, Copenhagen, 40 pp.
- Henriksen N. & Higgins A.K. (1988) — The geological map of Greenland 1:100000, Rødefjord 70°0.3 Nord and Kap Leslie 70°0.2 Nord. The Geological Survey of Greenland, Copenhagen, 34 pp.
- Hinz K. (1981) — A hypothesis on terrestrial catastrophes : Wedges of very thick oceanward dipping layers beneath passive continental margins. *Geologisches Jahrbuch, Reihe E*, 22, pp. 3-28.
- Hinz K., Meyer H. & Miller H. (1991) — North-east Greenland shelf north of 79° N : Results of a reflection seismic experiment in sea ice. *Marine and Petroleum Geology*, 8, pp. 461-467.
- Hinz K. & Schlüter H.U. (1980) — Continental margin off East Greenland. In: *Proceedings of the Tenth World Petroleum Congress, September 1979, Bucharest. Vol. 2*, Heyden, London, pp. 405-418.
- Hjort C. (1979) — Glaciation in northern East Greenland during the Late Weichselian and Early Flandrian. *Boreas*, 8, pp. 281-296.
- Hjort C. & Funder S. (1974) — The subfossil occurrence of *Mytilus edulis* L. in central East Greenland. *Boreas*, 3, pp. 23-33.
- Huybrechts P. & Tsiobbel S. (in press) — Thermomechanical modelling of northern hemisphere ice sheets with a two-level mass-balance parameterisation. *Annals of Glaciology*, 21.
- IHO/IOC/CHS (1984) — GEBCO : General Bathymetric Chart of the Oceans (5th Edition). International Hydrographic Organization / Intergovernmental Oceanographic Commission / Canadian Hydrographic Service, Ottawa, Canada, 74 pp. + 18 maps.
- Imbrie J., McIntyre A. & Mix A.C. (1989) — Oceanic response to orbital forcing in the late Quaternary : Observational and experimental strategies. In: Berger A.L., Schneider S.H. & Duplessy J.-C. (Eds.), *Climate and Geo-sciences: A Challenge for Science and Society in the 21st Century*. Kluwer Academic Publishers, Boston, pp. 121-164.
- Jansen E., Bleil U., Henrich R., Kringstad L. & Slettemark B. (1988) — Paleoenvironmental changes in the Norwegian Sea and the Northeast Atlantic during the last 2.8 Ma : DSDP/ODP Sites 610, 642, 643 and 644. *Paleoceanography*, 3(5), pp. 563-581.
- Jansen E., Sjøholm J., Bleil U. & Erichsen J.A. (1990) — Neogene and Pleistocene glaciations in the northern hemisphere and late Miocene - Pliocene global ice volume fluctuations : Evidence from the Norwegian Sea. In: Bleil U. & Thiede J. (Eds.), *Geological History of the Polar Oceans: Arctic versus Antarctic*. NATO ASI Series C, Mathematical and Physical Sciences, 308, Kluwer Academic Publishers, Dordrecht, pp. 677-705.
- Johnson G.L., Grantz A. & Weber J.R. (1990) — Bathymetry and physiography. In: Grantz A., Johnson L. & Sweeney J.F. (Eds.), *The Arctic Ocean Region. The Geology of North America, Vol. L, The Geological Society of America, Boulder, Colorado*, pp. 63-77.
- Koch B.E. (1964) — Review of fossil floras and nonmarine deposits of West Greenland. *Bulletin of the Geological Society of America*, 75, pp. 535-548.
- Koch L. (1945) — The East Greenland Ice. *Meddelelser om Grønland*, 130(3), pp. 1-374.

- Landvik J.Y. & Lyså A. (1991) — Depositional history and regional implications of the Eemian and Weichselian sequences in the Aucellaelv-Langelandselv area, southern Jameson Land, East Greenland. In: Möller P., Hjort C. & Ingólfsson Ó. (Eds.), *The Last Interglacial-Glacial Cycle: Preliminary Report on the PONAM Fieldwork in Jameson Land and Scoresby Sund, East Greenland*. Lundqua Report, 33, pp. 27-52.
- Larsen B. (1980) — Project "DANA 79" : A marine geophysical survey of the continental shelf of East Greenland 60° N - 71° N. Preliminary report, The Geological Survey of Greenland, Copenhagen, 30 pp.
- Larsen H.C. (1980) — Geological perspective of the East Greenland continental margin. *Geological Society of Denmark Bulletin*, 29, pp. 77-101.
- Larsen H.C. (1984) — Project NAD East Greenland : An integrated aeromagnetic and marine geophysical project off the east coast of Greenland. Pre-final report, The Geological Survey of Greenland, Copenhagen, 44 pp.
- Larsen H.C. (1985) — Project NAD East Greenland : Petroleum geological assesment of the East Greenland shelf. Final report, The Geological Survey of Greenland, Copenhagen, 78 pp.
- Larsen H.C. (1988) — A multiple and propagating rift model for the NE Atlantic. In: Morton A.C. & Parson L.M. (Eds.), *Early Tertiary Volcanism and the Opening of the NE Atlantic*. Geological Society of London Special Publication, 39, Blackwell Scientific Publications, Oxford, pp. 157-158.
- Larsen H.C. (1990) — The East Greenland Shelf. In: Grantz A., Johnson L. & Sweeney J.F. (Eds.), *The Arctic Ocean Region. The Geology of North America, Vol. L*, The Geological Society of America, Boulder, Colorado, pp. 185-210.
- Larsen H.C. & Jakobsdóttir S.J. (1988) — Distribution, crustal properties, and significance of seawards-dipping sub-basement reflectors off East Greenland. In: Morton A.C. & Parson L.M. (Eds.), *Early Tertiary Volcanism and the Opening of the NE Atlantic*. Geological Society of London Special Publication, 39, Blackwell Scientific Publishers, Oxford, pp. 95-114.
- Larsen H.C., Saunders A.D., Clift P.D., Beget J., Wei W., Spezzaferri S. & ODP Leg 152 Scientific Party (1994) — Seven million years of glaciation in Greenland. *Science*, 264(13 May 1994), pp. 952-955.
- Larsen L.M. & Watt W.S. (1985) — Episodic volcanism during break-up of the North Atlantic : Evidence from the East Greenland plateau basalts. *Earth and Planetary Science Letters*, 73, pp. 105-116.
- Larsen L.M., Watt W.S. & Watt M. (1986) — Volcanic history of the lower Tertiary plateau basalts in the Scoresby Sund region, East Greenland. *Rapp. Grønlands Geologiske Undersøgelse*, 128, pp. 147-146.
- Lyså A. & Landvik J.Y. (1993) — The Late Pleistocene stratigraphy on SW coastal Jameson Land (East Greenland) : An improved chronology. Abstract volume of the Fourth annual workshop on the Polar North Atlantic Margins (PONAM) programme, Cambridge.
- Marienfeld P. (1991) — Holozäne Sedimentationsentwicklung im Scoresby Sund, Ost-Grönland. *Berichte zur Polarforschung*, no. 96, Alfred-Wegener Institut für Polar- und Meeresforschung, Bremerhaven, 162 pp.
- Mix A.C. (1987) — The oxygen-isotope record of glaciation. In: Ruddiman W.F. & Wright H.E. Jr. (Eds.), *North America and Adjacent Oceans During the Last Deglaciation. The Geology of North America, Vol. K3*, The Geological Society of America, Boulder, Colorado, pp. 111-135.
- Mutter J.C. (1985) — Seaward dipping reflectors and the continent-ocean boundary at passive continental margins. *Tectonophysics*, 114, pp. 117-131.
- Nunns A.G. (1983) — Plate tectonic evolution of the Greenland-Scotland Ridge and surrounding regions. In: Bott M.H.P., Saxov S., Talwani M. & Thiede J. (Eds.), *Structure and Development of the Greenland-Scotland Ridge*. NATO Conference Series, IV : Marine Sciences, Plenum Press, New York, pp. 11-30.
- Nunns A.G., Talwani M., Lorentzen, G.R., Vogt P.R., Sigurgeirsson T., Kristjansson L., Larsen H.C. & Voppel D. (1983) — Magnetic anomalies over Iceland and surrounding seas. In: Bott M.H.P., Saxov S., Talwani M. & Thiede J. (Eds.), *Structure and Development of the Greenland-Scotland Ridge*. NATO Conference Series, IV : Marine Sciences, Plenum Press, New York, pp. 661-678 + map.
- Olesen O.B. & Reeh N. (1969) — Preliminary report on glacier observations in Nordvestfjord, East Greenland. *Rapp. Grønlands Geologiske Undersøgelse*, 21, pp. 41-53.
- The Open University (1989) — *Ocean Circulation*. Pergamon Press, Oxford, 238 pp.
- Posamentier H.W., Jervey M.T. & Vail P.R. (1988) — Eustatic controls on clastic deposition I : Conceptual framework. In: Wilgus C.K., Hastings B.S., Kendall C.G.St.C., Posamentier H.W., Ross C.A. & Van Wagoner J.C. (Eds.), *Sea Level Changes: An Integrated Approach*. Special Publication, 42, Society of Economic Paleontologists and Mineralogists, Tulsa, Oklahoma, pp. 109-124.

- Posamentier H.W. & Vail P.R. (1988) — Eustatic controls on clastic deposition II : Sequence and systems tract models. In: Wilgus C.K., Hastings B.S., Kendall C.G.St.C., Posamentier H.W., Ross C.A. & Van Wagoner J.C. (Eds.), *Sea Level Changes : An Integrated Approach*. Special Publication, 42, Society of Economic Paleontologists and Mineralogists, Tulsa, Oklahoma, pp. 125-154.
- Reeh N. (1985) — Greenland ice-sheet mass balance and sea-level change. In: *Glaciers, Ice Sheets and Sea Level: Effect of a CO₂-induced Climatic Change*. U.S. Department of Energy, Washington, D.C., pp. 155-171.
- Rønnevik H.C. & Jacobsen H.-P. (1984) — Structural highs and basins in the western Barents Sea. In: Spencer A.M. et al. (Eds.), *Petroleum Geology of the North European Margin*. Graham & Trotman for the Norwegian Petroleum Society, London, pp. 19-32.
- Rosenberger A. (1992) — Mehrkanalige adaptive Filter für die Unterdrückung von multiplen Reflexionen in Verbindung mit der freien Oberfläche in marinen seismogrammen. *Berichte zur Polarforschung*, no. 104, Alfred-Wegener Institut für Polar- und Meeresforschung, Bremerhaven, 108 pp.
- Ruddiman W.F., Raymo M. & McIntyre A. (1986) — Matuyama 41,000-year cycles : North Atlantic Ocean and northern hemisphere ice sheets. *Earth and Planetary Science Letters*, 80, pp. 117-129.
- Shackleton N.J., Backman J. & Shipboard Scientific Party (1984) — Oxygen isotope calibration of the onset of ice rafting and history of glaciation in the North Atlantic region. *Nature*, 307, pp. 620-623.
- Sherrif R.E. & Geldart L.P. (1983) — *Exploration Seismology Volume 2 : Data-processing and Interpretation*. Cambridge University Press, Cambridge, 221 pp.
- Stein R., Grobe H., Hubberten H., Marienfeld P. & Nam S. (1993) — Latest Pleistocene to Holocene changes in glaciomarine sedimentation in Scoresby Sund and along the adjacent East Greenland continental margin: preliminary results. *Geo-Marine Letters*, 13, pp. 9-16.
- Surlyk F., Clemmensen L.B. & Larsen H.C. (1981) — Post-Paleozoic evolution of the East Greenland continental margin. In: Kerr J.S. & Fergusson A.J. (Eds.), *Geology of the North Atlantic Borderlands*. Memoir, 7, Canadian Society of Petroleum Geology, pp. 611-645.
- Talwani M. & Eldholm O. (1977) — Evolution of the Norwegian-Greenland Sea. *Geological Society of America Bulletin*, 88, pp. 969-999.
- Uenzelmann-Neben G. (1993) — Scoresby Sund, East Greenland : Structure and distribution of sedimentary rocks. *Polarforschung*, 62(1), pp. 1-9.
- Uenzelmann-Neben G., Jokat W. & Vanneste K. (1991) — Quaternary sediments in Scoresby Sund, East Greenland : Their distribution as revealed by reflection seismic data. In: Möller P., Hjort C. & Ingólfsson Ó. (Eds.), *The Last Interglacial-Glacial Cycle: Preliminary Report on the PONAM Fieldwork in Jameson Land and Scoresby Sund, East Greenland*. Lundqua Report, 33, pp. 139-148.
- Vorren T.O., Hald M., Edvardsen M., & Lind-Hansen, O.W. (1983) — Glacigenic sediments and sedimentary environments on continental shelves : General principles with a case study from the Norwegian shelf. In: Ehlers J. (Ed.), *Glacial Deposits in North-West Europe*. A.A. Balkema, Rotterdam, pp. 61-73.
- Watt W.S. (1970) — Preliminary report of the mapping of the Basalt area, South of Scoresby Sund. *Rapp. Grønlands Geologiske Undersøgelse*, 30, pp. 30-37.
- Weidick A. (1976) — Glaciation and the Quaternary of Greenland. In: Escher A. & Watt W.S. (Eds.), *Geology of Greenland*. The Geological Survey of Greenland, Copenhagen, pp. 430-458.
- White R. & McKenzie D.P. (1989) — Volcanism at rifts. *Scientific American*, (July 1989), pp. 44-55.
- Wood M.V., Hall J. & Doody J.J. (1988) — Distribution of early Tertiary lavas in the NE Rockall Trough. In: Morton A.C. & Parson L.M. (Eds.), *Early Tertiary Volcanism and the Opening of the NE Atlantic*. Geological Society of London Special Publication, 39, Blackwell Scientific Publishers, Oxford, pp. 283-292.
- Wood M.V., Hall J. & Van Hoorn B. (1987) — Post-Mesozoic differential subsidence in the north-east Rockall Trough related to volcanicity and sedimentation. In: Brooks J. & Glennie K. (Eds.), *Petroleum Geology of North West Europe*, 2. Graham & Trotman, London, pp. 677-685.

CHAPTER III

Seismic investigation of the western Barents Sea margin off Bear Island Trough

1. Introduction

More favourable ice conditions in the eastern half of the polar North Atlantic have advantaged the exploration of the western Barents Sea margin, compared to the East Greenland margin at the opposite side of the ocean. Most of the Barents Sea was mapped in the years 1594 - 1597 by the Dutch sailor Willem Barentsz, who also discovered the small island (178 km²) *Bereneiland* (Bear Island); this is more than two centuries before the discovery of the Scoresby Sund fjord system in East Greenland. Scientific reconnaissance began already at the turn of the century, with the pioneer work of Fridtjof Nansen. A large asymmetry in data coverage between the two margins persists to the present day: whereas large parts of the East Greenland margin remain essentially unexplored, the western Barents Sea margin is almost completely covered by an extensive grid of seismic lines. Most of the research occurred during the past two decades, and during this time geological reasoning went through a considerable evolution, as will be demonstrated at some points in the text.

The present study focuses on the evolution of the major depocentres that accumulated through geological time along the western Barents Sea margin, and in particular on the northern portion of Bear Island Cone. These depocentres are thought to hold an important archive of glaciation, more complete and reaching farther back in time than the sparsely preserved records on land and in fjords. The seismic reflection data used for this research were acquired in July 1988 by the Marine Geophysics group of the University of Kiel (Germany), on board of the research vessel "Meteor". This survey was framing in the joint research project Sonderforschungsbereich 313 "*Veränderungen der Umwelt: der nördliche Nord-Atlantik*", supported by the German Science Foundation (DFG). Additional data were released by the Norwegian Petroleum Directorate as part of a data exchange project with the University of Oslo.

The main objectives of this chapter are three-fold: [i] to establish a consistent and detailed stratigraphy for the northern portion of Bear Island Cone, fitting in a more general seismic stratigraphic framework valid for the entire western Barents Sea - Svalbard margin, [ii] to find clues for the reconstruction of the long-term glacial evolution of the margin, in the light of new and exciting dating results in cores from the continental shelf, and [iii] to examine the depositional processes that have built up the cones. The second, and to some extent also the third aspect, is related to Theme I (Late Cenozoic record of climatic changes and effects on the continental margin sedimentary environment) of the now ending PONAM (Polar North Atlantic Margins) programme initiated by the European Science Foundation.

2. Data properties

Two different sets of multi-channel seismic reflection data were available to this study: a group of 6 lines acquired by the Marine Geophysics department of the University of Kiel in Germany (MGK), and a set of 4 lines from the extensive data base of the Norwegian Petroleum Directorate (NPD). These lines form a complementary network of E-W oriented (transversal or “dip”-oriented) and N-S oriented (longitudinal or “strike”-oriented) transects along the western Barents Sea margin (Fig. 1). The grid spans a total length of c. 1900 km in a roughly square area, to the west and south-west of Bear Island, and measuring 200 by 200 km. The grid spacing is variable. The length of the individual profiles is listed in Table 1.

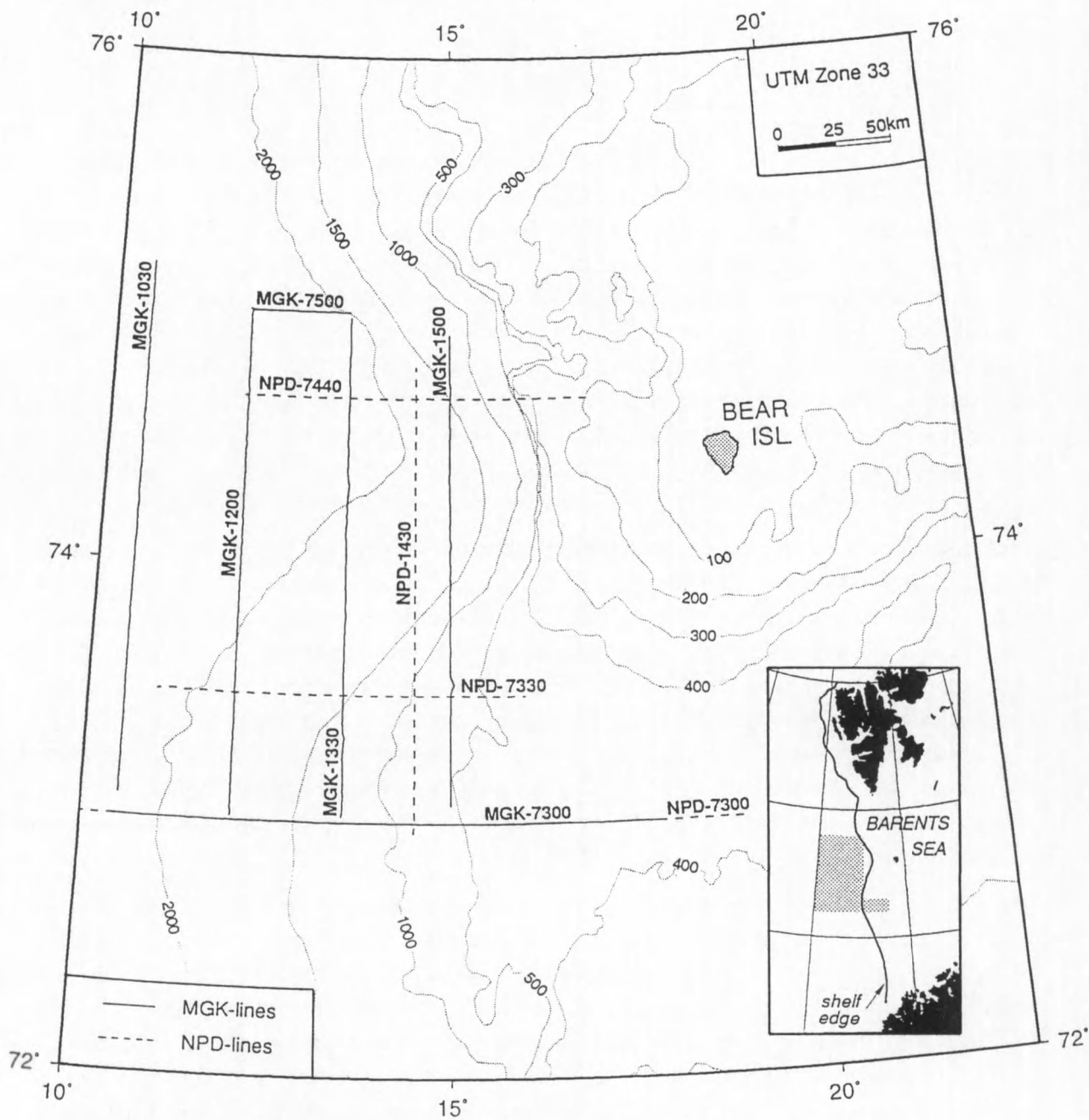


Fig. III.1 - Location of the available seismic grid along the western Barents Sea margin.

DIP LINES		STRIKE LINES	
Profile ID	Length (km)	Profile ID	(Length (km))
MGK-7300 (BEAR-I)	210	MGK-1030 (BEAR-II)	222
NPD-7300-75	250	MGK-1200 (BEAR-VII)	222
NPD-7330-77	160	MGK-1330 (BEAR-V)	222
NPD-7440-77	148	NPD-1430-77	215
MGK-7500 (BEAR-VI)	43	MGK-1500 (BEAR-III)	208
TOTAL	810	TOTAL	1090

Table III.1 - Length of individual seismic profiles.

The two data sets have somewhat different characteristics and quality. The NPD-lines were shot in 1975 and 1977 by industrial contractors, and meet the standards of the petroleum industry at that time. With a main frequency around 35 Hz, these data are characterised by low vertical resolution (c. 14 m for seismic velocities of 2000 m/s) and large penetration (up to 4 s), while data processing has successfully removed the water bottom multiple. The structural basement, whether of oceanic or continental origin, is therefore easily imaged on these lines. The main frequency content of the MGK-lines is contained between 50 and 60 Hz, resulting in a more intermediate vertical resolution of < 10 m. Due to the limited source energy, the depth of penetration is much less (max. 2.5 s), however. In addition, the lower limit of observation is most often defined by the water bottom multiple, which could not be sufficiently attenuated because the length of the receiver array was too small compared to the water depth. As a consequence, the oceanic basement can only be detected on the westernmost lines, where it considerably shoals and water depths increase. An additional drawback of the MGK-lines is the long signal train that follows the seafloor reflection: this strongly hampers the tracing of reflectors in the upper 100 ms of the section.

The most important acquisition and recording parameters of both data sets are summarised in Table 2. Comparison between the two data sets is pretty straightforward, due to the significant frequency overlap, and is aided even further by the identical location of lines MGK-7300 and NPD-7300.

	MGK-lines	NPD-lines
SEISMIC SOURCE	airgun array totalling c. 4 l	32 x 2 l airgun array, or 20 x 1.2 l array (line NPD-7300)
STREAMER LENGTH (m)	600	2400
NO. OF CHANNELS	24	48
SHOT DISTANCE (m)	25 / 50	50
RECORD LENGTH (s)	4 - 7	6 - 7
SAMPLE INTERVAL (ms)	4	4

Table III.2 - Key acquisition and recording parameters of the two data sets.

Most of the Meteor-data were processed in co-operation with Dagmar Matuschke during a one-year stay at the Institut für Geophysik of the University of Kiel, framing in the European student exchange programme ERASMUS. The idealised process flow is schematically drawn in Fig. 2. For an explanation of the abbreviations, the reader is referred to section 2 of the preceding chapter. The NPD-data, available as paper plots only, were already in processed form when obtained.

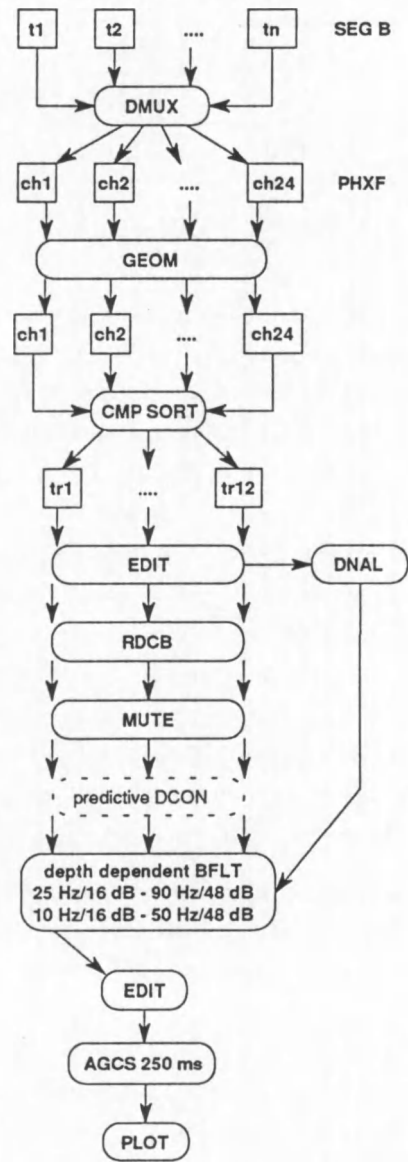


Fig. III.2 - Idealised process flow for MGK-lines.

3. Physiography of the western Barents Sea - Svalbard margin

3.1. Bathymetry of shelf and slope

The Barents Sea shelf, covering an area of app. 1.2 million km², represents one of the largest epicontinental seas in the world. It is enclosed between the land masses of Norway and the Kola Peninsula in the south, the Svalbard archipelago with the main island Spitsbergen to the north-west, Franz Josef Land to the north-east, and Nova Zembla in the east (Fig. 3). Towards the west and north the Barents Sea is bounded by passive continental margins, passing into the deep Lofoten and Eurasia Basins, respectively.

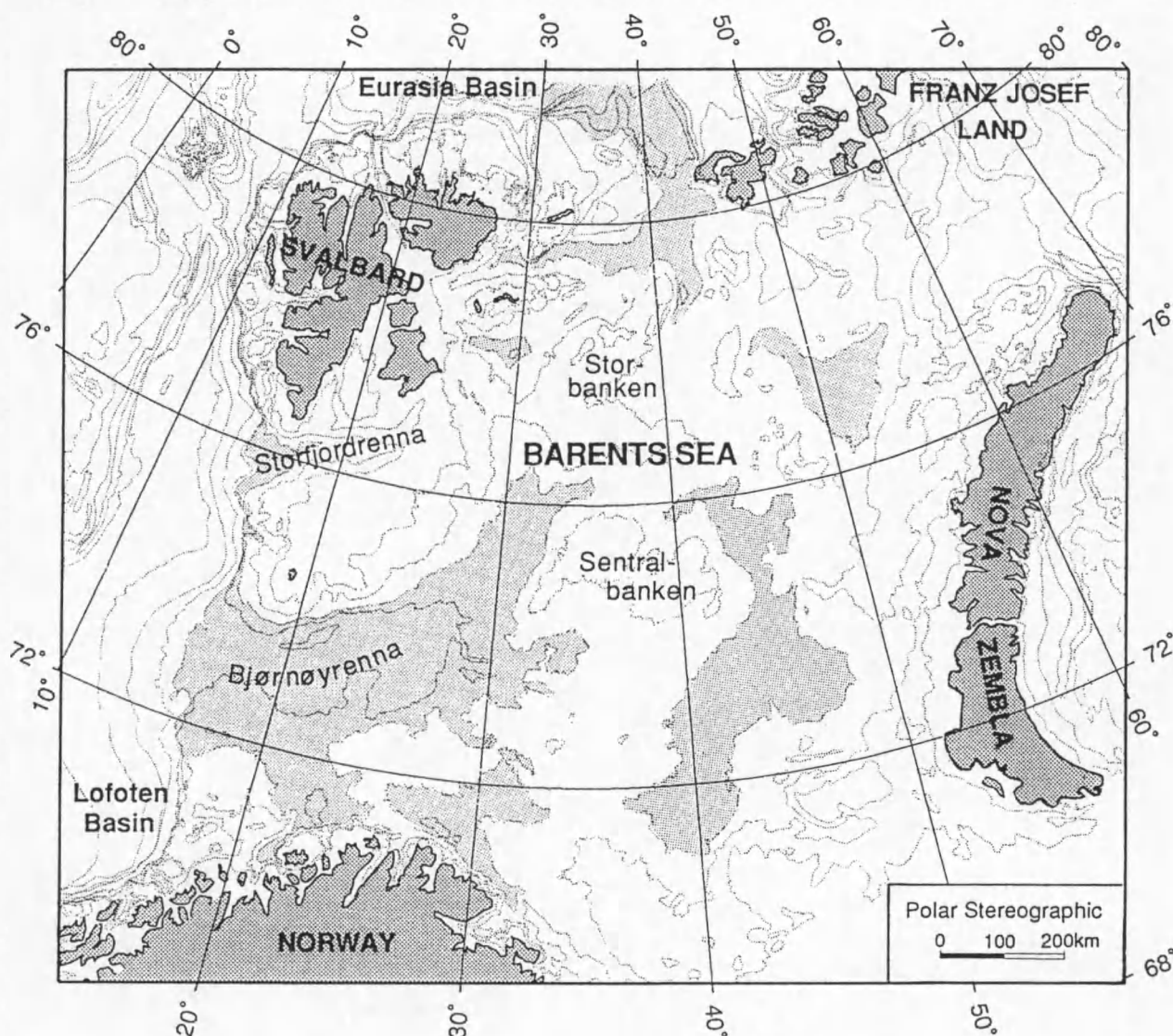


Fig. III.3 - Location and generalised bathymetry of the Barents Sea. Shaded areas represent shelf depressions deeper than 300 m.

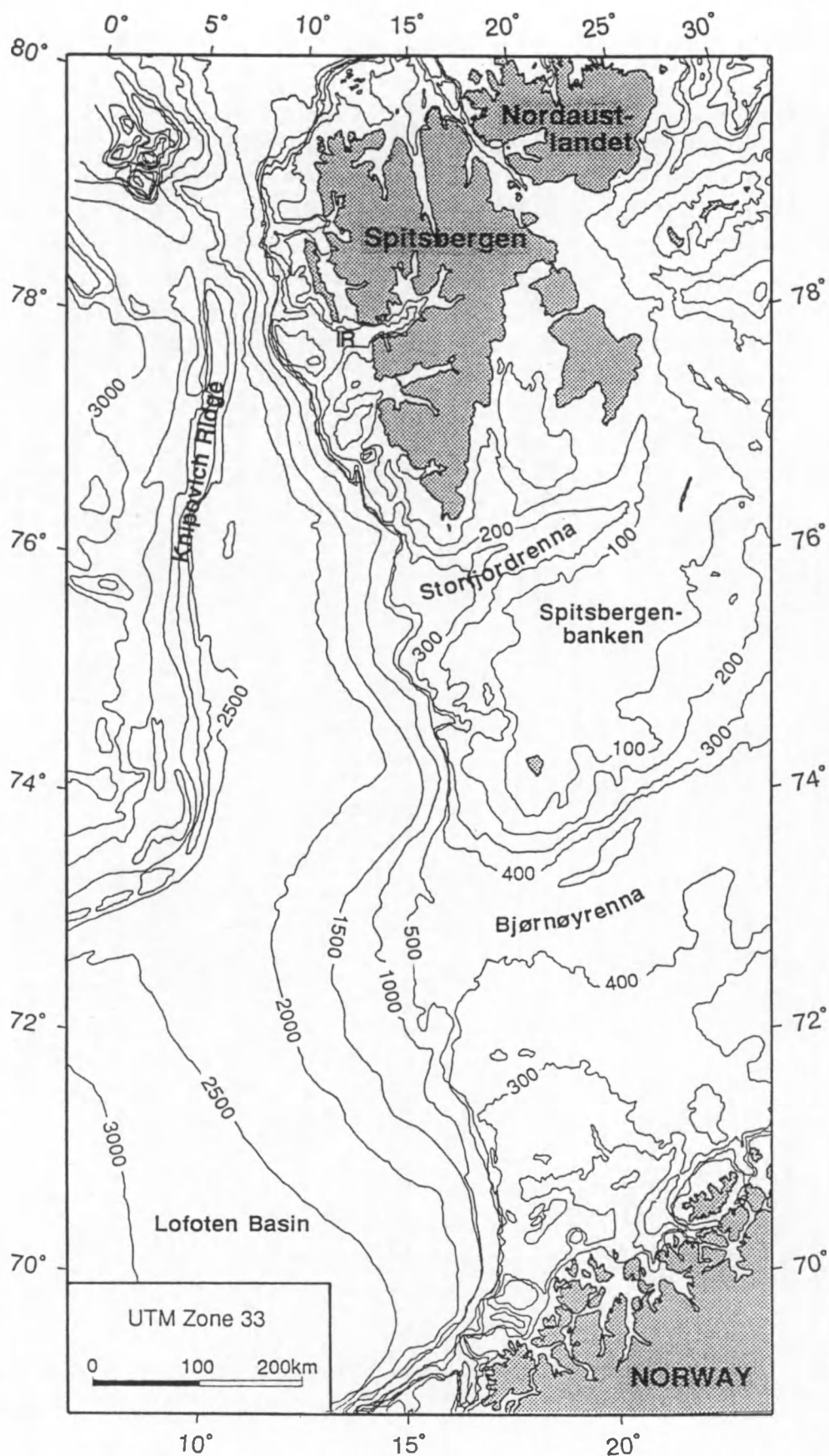


Fig. III.4 - Generalised bathymetry of the western Barents Sea margin. Contour interval is 100 m on the shelf, and 500 m on the slope and in the deep-sea.

With an average water depth of about 230 m (Elverhøi et al. 1989), the Barents Sea is also relatively deep. There are many localised banks and depressions, however, reflecting the action of grounded ice on the shelf during the last few million years (e.g. Solheim & Kristoffersen 1984). Particularly, the morphology of the western half of the Barents Sea (Fig. 4) is dominated by two broad transverse troughs, Bjørnøyrenna and Storfjordrenna, separated from each other by Spitsbergenbanken, on which the island Bjørnøya (Bear Island) is located. Both troughs are east-west oriented at their mouth near the shelf edge, but bend to a north-eastern trend inward; outside these troughs the shelf is generally less than 300 m deep. Bjørnøyrenna (or Bear Island Trough¹), occupying the entire central part of the shelf, is by far the largest trough, extending for some 720 km and reaching depths of about 500 m in one portion south of Bear Island, and at the shelf edge. This trough has a general dip to the west, and lacks a threshold which is typically found at the mouth of smaller glacial troughs (Vorren et al. 1990). Storfjordrenna (Storfjorden Trough), extending between Svalbard and Spitsbergenbanken (Spitsbergen Bank), seems to have a more typical foredeepened profile; its depth amounts to 350 m. Between these two major troughs Spitsbergenbanken is intersected by Kveitehola, a much narrower trough with depths exceeding 300 m (Fig. 5). More northward, the narrow shelf west of Svalbard is likewise intersected by transverse troughs which appear to extend from the main fjord systems (Myhre & Eldholm 1988). The largest trough here is Isfjordrenna (Isfjorden Trough), which is 200 to 300 m deep, whereas the adjacent shoals are less than 100 m deep.

The shelf edge varies in depth between 250 m and 400 m (mouth of Storfjordrenna) or even 500 m (mouth of Bjørnøyrenna). The western continental slope is characterised by seaward-convex bathymetry outlining major cone-shaped depocentres at the mouth of the largest troughs (Figs. 5 and 6). From south to north, and also in order of decreasing size, the Bear Island Cone, Storfjorden Cone and Isfjorden Cone can be discerned. The Bear Island Cone extends over 280 km beyond the shelf edge into the Lofoten Basin and is characterised by a very low gradient of max. 1.2° (Perry 1986); the cone is 220 km wide at its proximal part and 400 km at a depth of 2000 m (Vorren et al. 1989). The morphology of the cone is very smooth, except for a NE-SW striking indentation in the bathymetric contours on its southern flank, near 72° N, representing the scar of a large slope failure (Kristoffersen et al. 1978). Submarine canyons and channels are conspicuously absent (Vorren et al. 1989). The continental slope is generally steeper off the inter-trough areas, and the gradient also increases systematically from south to north: the slope is between 1 and 2° on the Storfjorden Cone (Laberg 1994), and 4 to 5° along the Svalbard margin (Andersen et al. 1994). To the west the continental slope of the Barents Sea margin gradually passes into the continental rise and further into the flat-lying deep-sea floor at depths of 2000 to 2500 m. But north of 77° N the slope extends directly onto the axial rift mountains of the Knipovich spreading ridge (Myhre & Eldholm 1988).

¹ Though the geographic features are introduced here by their Norwegian names, the English translations will be used throughout the coming sections.

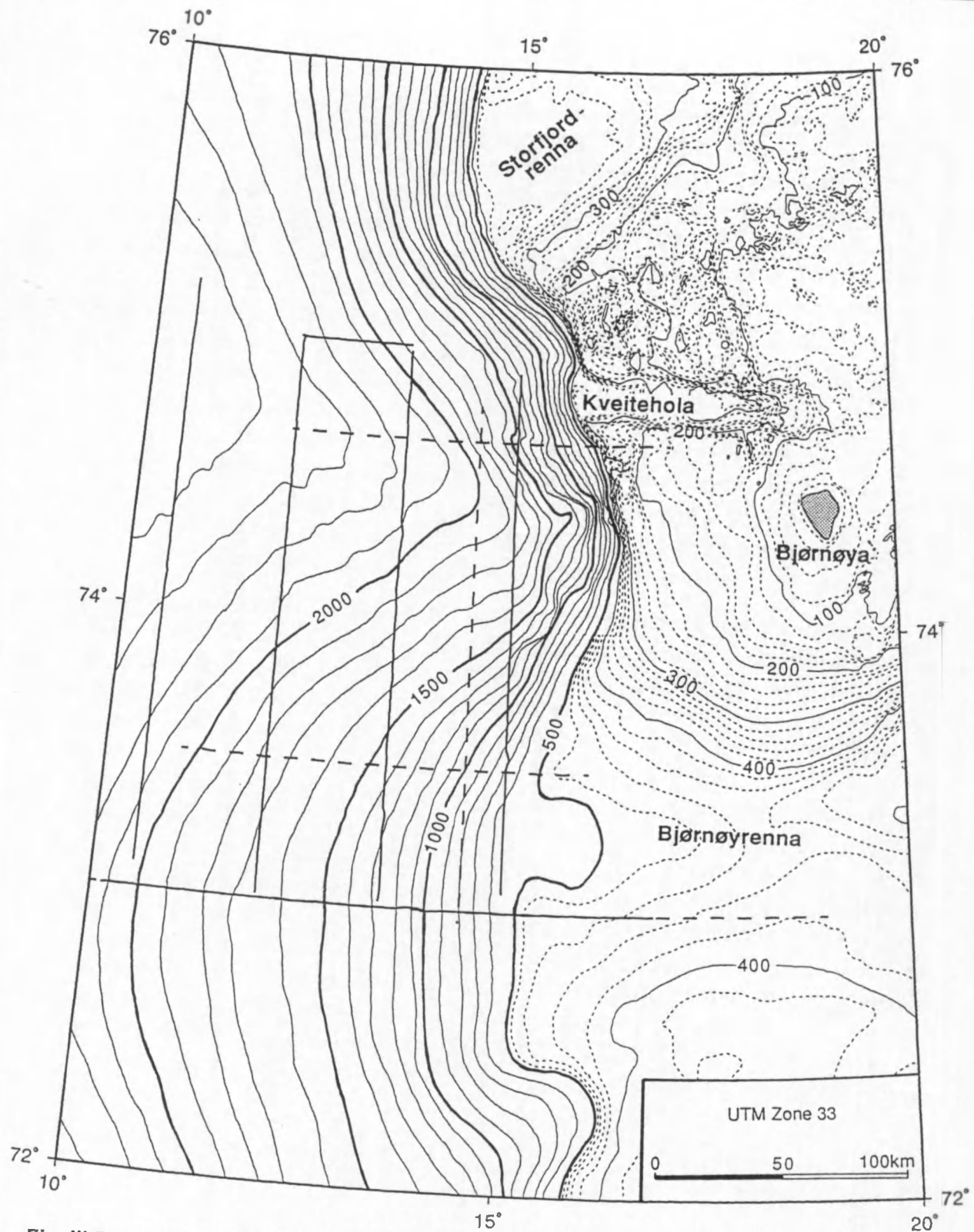


Fig. III.5 - Detailed bathymetry in the area of investigation. Contour interval is 100 m (full lines), and 20 m on the shelf (dashed lines). Bathymetric data courtesy of Norsk Polarinstitutt (the Norwegian Polar Institute).

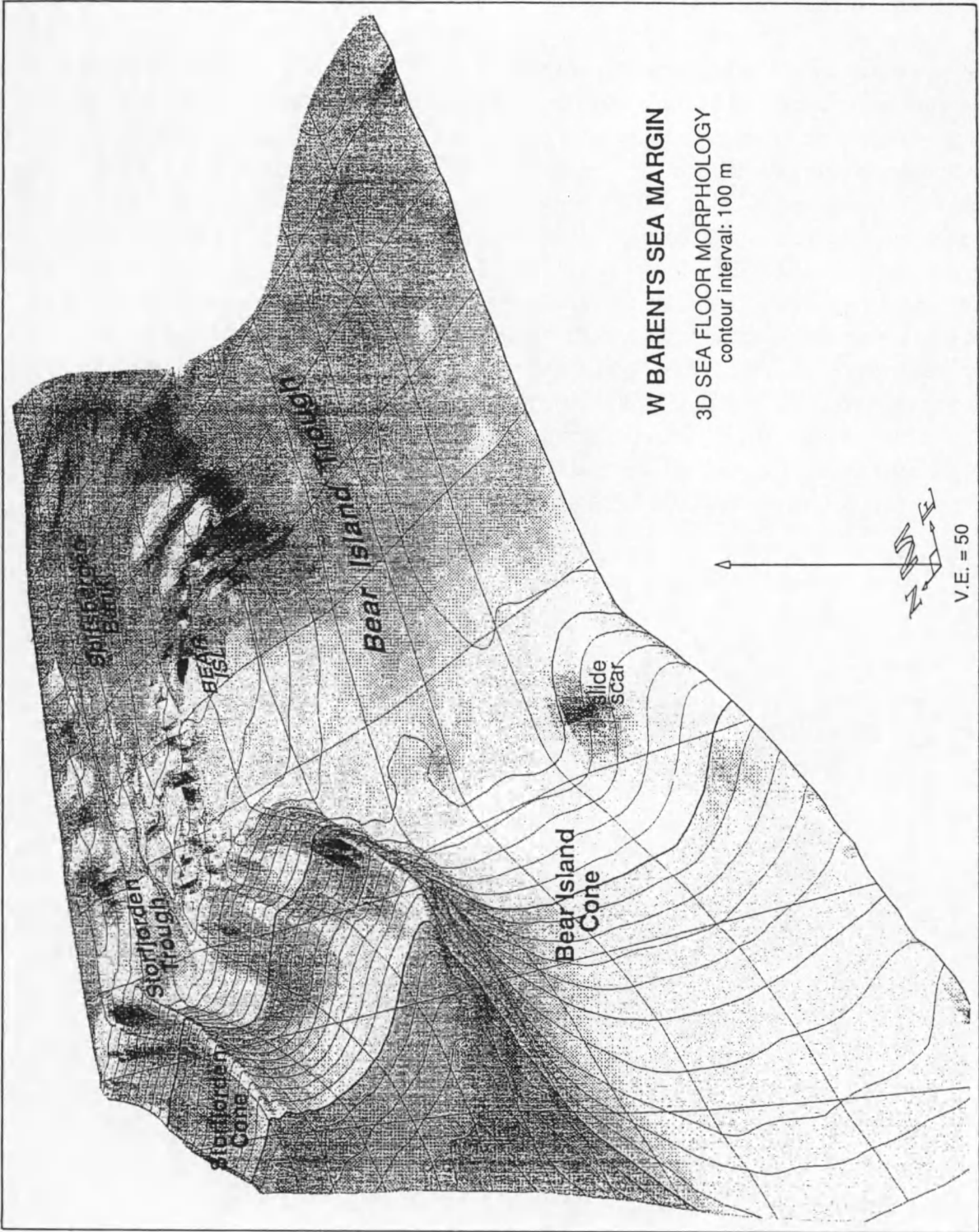


Fig. III.6 - 3D seafloor morphology visualising the major cone-shaped depocentres at the mouth of deep shelf troughs along the western Barents Sea margin. Based on bathymetric data from the Norwegian Polar Institute. Gridded using Geofox (Verschuren 1992).

3.2. Water circulation

The surface current system along the Barents Sea - Svalbard margin (Fig. 7) is dominated by warm and saline water introduced by the Norwegian Atlantic Current, an extension of the North Atlantic Current hugging the upper continental slope off Norway, and by the Norwegian Coastal Current, which is originating from the brackish outflow from the Baltic Sea as well as from runoff from the Norwegian fjords, and is flowing all along the Norwegian Coast (Johannessen 1986). Part of this combined surface water current continues to follow the outer shelf and upper slope northward, thus contributing to the West Spitsbergen Current, while another part branches off into the Barents Sea as the Nordkapp Current. The generally NE flowing Nordkapp Current constitutes the main inflow into the Barents Sea. In addition, cold Arctic water enters the sea from the north (Mosby 1968), and is transported SW-ward in the East Spitsbergen and Persey Currents (Elverhøi et al. 1989). Outflow of cold water takes place along the south-eastern flank of Spitsbergenbanken and between Bjørnøya and Spitsbergen, as the Bjørnøya Current and the East Spitsbergen Current respectively (Johannessen 1986). The cold and warm surface water masses in the Barents Sea are separated by the east-west trending oceanic Polar Front at app. 74-75° N (Elverhøi et al. 1989).

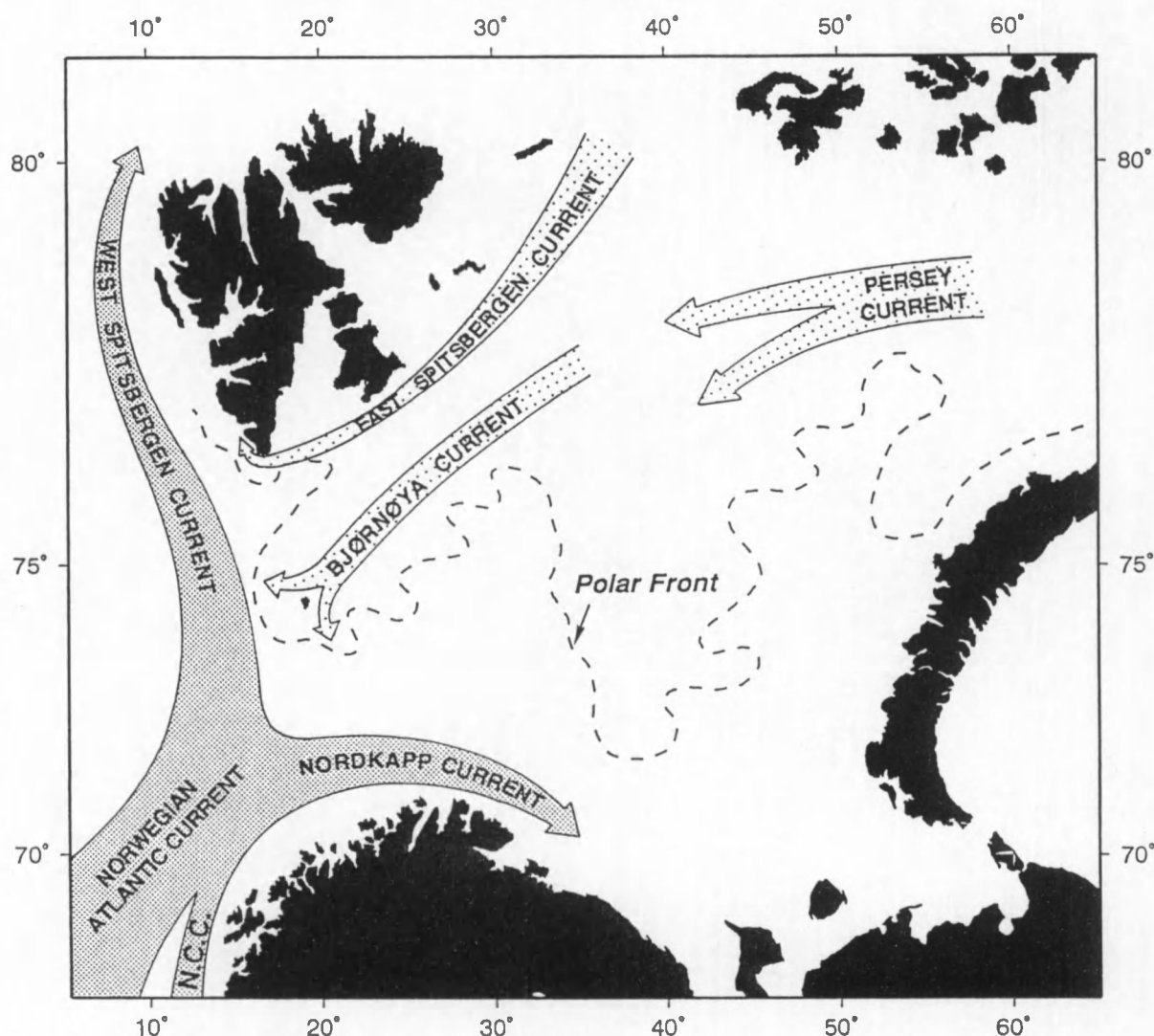


Fig. III.7 - Location of polar front and main surface water currents in the Barents Sea. From Johannessen (1986). NCC = Norwegian Coastal Current.

Cold saline water originating as a residue from the formation of sea ice, flows off the banks into the deeper troughs in the Barents Sea, where it forms dense water masses (Elverhøi et al. 1989). These water masses continue their way out of the Barents Sea, especially along the northern flank of Bjørnøya, giving rise to thermohaline currents cascading downslope into intermediate depths (500-800 m) in the Norwegian Sea (Blindheim 1989). This process exhibits large seasonal and annual variations (Elverhøi et al. 1989).

The motion of deep water in the Norwegian-Greenland Sea is otherwise rather small (Coachman & Aagaard 1974). Bottom water from the Arctic Ocean enters the area through Fram Strait, which is up to 2600 m deep, whereas deep water is also being formed in the Greenland Sea (GSDW), and to a lesser extent in the Norwegian Sea (NSDW) by cooling of the mixed surface layer and deep-reaching convection (Johannessen 1986). The deep water flows southward into the North Atlantic through Denmark Strait (cf. chapter II, section 3.1), the Faeroe-Shetland Channel, and in places across the Iceland-Faeroe Ridge.

3.3. Ice cover

Large glaciers in the Barents Sea area are restricted to the bordering islands in the north and east. They blanket most of Spitsbergen, Franz Josef Land and the northern part of Nova Zembla; Nordaustlandet, the second largest island of the Svalbard archipelago, even is covered by an ice cap, the Austfonna Ice Cap (8000 km²).

Approximately two thirds of the Barents Sea is influenced by sea ice and icebergs. The volume of sea ice input into the Barents Sea is estimated at about 550 km³ per year; icebergs, calving from glaciers on Svalbard and Franz Josef Land, are quantitatively of minor importance (Elverhøi et al. 1989). The icebergs are delivered mainly during late summer; their predominant trajectory follows the main surface water flow at this time of the year, towards the south-west (Vinje 1985). The highest concentrations of icebergs are observed over the shallow bank areas during spring (Elverhøi et al. 1989). Most of the sea ice cover in the Barents Sea is formed locally and increases to the north, where sea ice is present ten months of the year. The southern drift ice limit is close to the oceanic Polar Front (Fig. 7) during winter, but may retreat rapidly during the melt season of June to August, from app. 76° to 82° N (Vinje 1985). Large parts of the Barents Sea thus remain open, even during winter, resulting in large heat losses (Swift 1986). Dominant south-westerly winds drive the ice into the Arctic Ocean during the winter, while in summer the flow direction impelled by surface water currents is re-established, with net influx of sea ice into the Barents Sea, mainly through the strait between Franz Josef Land and Nova Zembla (Vinje 1985).

The western Barents Sea - Svalbard margin is profoundly influenced by the influx of warm Atlantic water, which carries enough heat to block sea ice formation in the Norwegian Sea, even during winter (Swift 1986). Ice is transported around Sørkapp, the southern tip of Spitsbergen, by the East Spitsbergen Current. The survival of this ice is severely hampered by the warm West Spitsbergen Current, which sweeps the west coast of Svalbard and keeps it clear of ice during all summers and many winters (Wadhams 1986).

4. Structural setting and geo-tectonical evolution

4.1. Main structural elements

The western Barents Sea - Svalbard margin contains the following first-order geological provinces (Fig. 8):

- two oceanic basins, formed during the Cenozoic opening of the polar North Atlantic Ocean (a.k.a. the Norwegian-Greenland Sea²), extend everywhere west of the margin: the Lofoten Basin, generated along the eastern flank of the Mohns Ridge, and an as yet unnamed basin east of the Knipovich Ridge;
- a continental province constituting the north-western corner of the Eurasian continent, and comprising the south-western Barents shelf province of basins and ridges, and the elevated Svalbard Platform, both of late Paleozoic to Mesozoic age;
- both provinces are separated by a major fault zone, which evolved during the early Tertiary in relation to the opening of the Norwegian-Greenland Sea, and consists of three main segments: [i] the Senja Fracture Zone south of 73° N, [ii] the Hornsund Fault Zone north of 75°30' N, both trending N-NW, and [iii] a complex intermediate fault zone linking the two other segments and offsetting the margin towards the north-east. This central segment is associated with the Vestbakken volcanic province, a marginal high of subaerial extrusives emplaced during initial opening along this margin segment.

4.1.1. Oceanic basins

The Norwegian-Greenland Sea west of the Barents Sea - Svalbard margin is transected by a continuous spreading ridge which describes a pronounced curve of over 50° near 73°30' N. The north-east-trending southern part is named the Mohns Ridge, while the north-trending northern part is known as the Knipovich Ridge. The axial rift valleys of both ridges appear to continue without major offsets into each other (Talwani & Eldholm 1977). A description of the entire plate boundary has been given by Eldholm et al. (1990).

The Mohns Ridge, extending south-westward to the Jan Mayen Fracture Zone, is located centrally in the ocean, thus separating the equidimensional Greenland and Lofoten Basins. The rift valley is associated with a central positive magnetic anomaly, and is flanked on either side by linear magnetic lineations.

The Knipovich Ridge occupies an asymmetric position in the ocean, approaching the Svalbard margin towards the north. At 78° N the spreading centre lies as close as 80 km to the coastline of Spitsbergen, and actually underlies the lower continental slope (Myhre & Eldholm 1988). The oceanic basin west of the Knipovich Ridge is known as the Boreas Basin; its much smaller and shallower eastern counterpart remains unnamed (essentially because it lacks the typical bathymetric expression of an oceanic basin, and merges with the continental rise and slope), but will in this text be referred to as the "anti-Boreas" Basin.

² Geographically, the Greenland Sea and the Norwegian Sea refer to the western and eastern halves of the polar North Atlantic, respectively. Several workers (e.g. Talwani & Eldholm 1977; Myhre et al. 1982) have in a geological sense narrowed the term "Greenland Sea" down to the oceanic basins formed along the Knipovich Ridge, and bounded by the Greenland-Senja and Spitsbergen Fracture Zones.

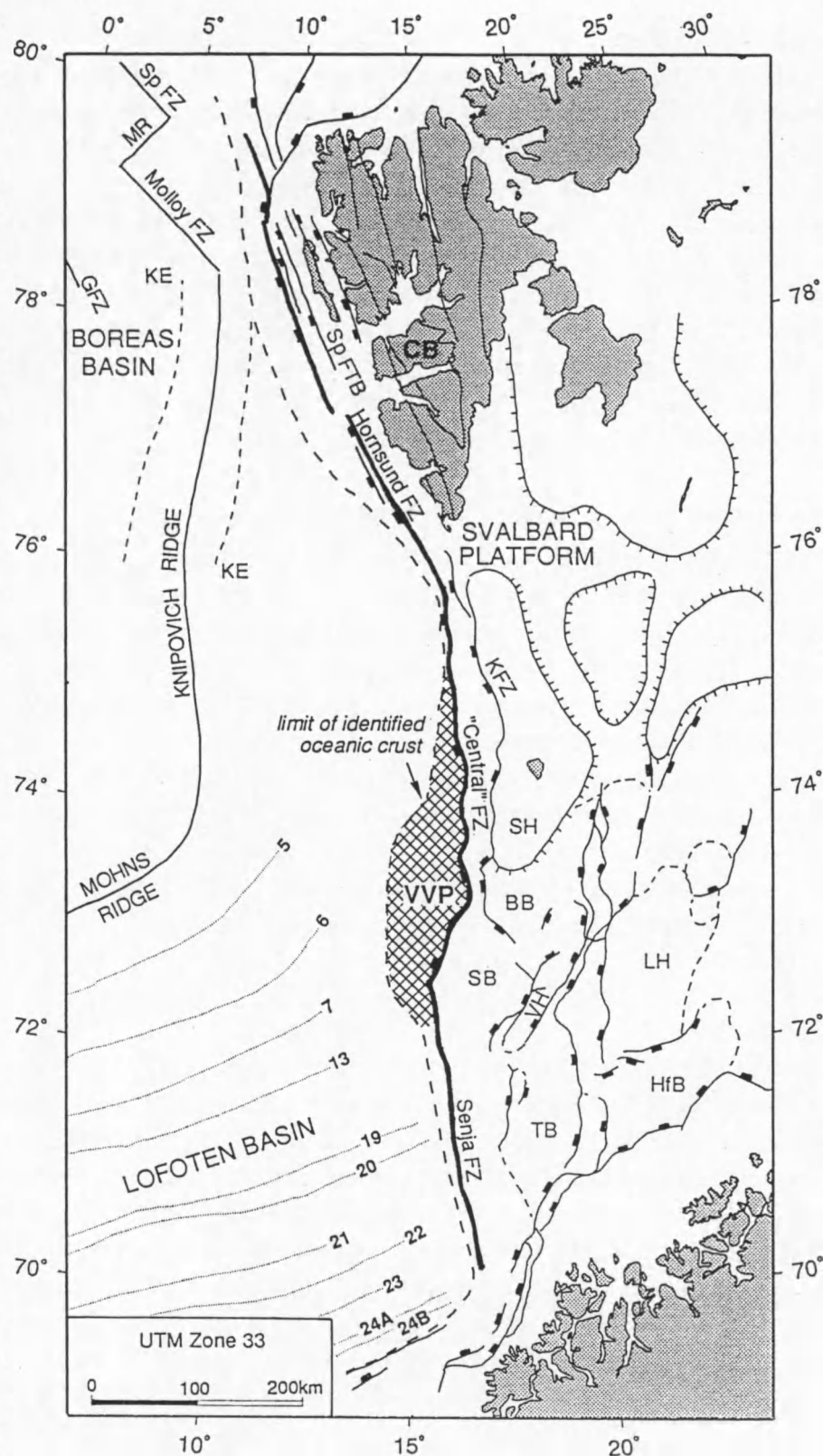


Fig. III.8 - Structural setting of the western Barents Sea margin. BB = Bjørnøya Basin, CB = Central Basin, GFZ = Greenland Fracture Zone, HB = Harstad Basin, HfB = Hammerfest Basin, KE = Knipovich Escarpment, KFZ = Knølegga Fracture Zone, LH = Loppa High, MR = Molloy Ridge, SB = Sørvestsnaget Basin, SH = Stappen High, SpFTB = Spitsbergen Fold and Thrust Belt, Sp FZ = Spitsbergen Fracture Zone, TB = Tromsø Basin, VH = Veslemøy High, VVP = Vestbakken volcanic province. Dotted lines represent magnetic anomaly lineations. From Myhre & Eldholm (1988) and Faleide et al. (1993).

The Knipovich Ridge is characterised by a rather prominent rift valley, narrow and V-shaped at the transition with the Mohns Ridge, but becoming progressively more U-shaped and wider (up to 10 km) towards the termination at the Molloy Fracture Zone in the north. As is the case for the Mohns Ridge, the axial mountains rise higher on the western side of the valley. Eldholm et al. (1990) ascribe this difference in elevation in part to a larger load of sediments burying the eastern flank of the ridge (see section 5.1). An elevated crustal block on either side of the rift valley is bounded by small but continuous basement escarpments: the western and eastern Knipovich Escarpments (Sundvor & Eldholm 1979). Bathymetric lineaments east and west of the ridge, and striking app. along the inferred flow lines, may represent small fossil and active transform offsets of the plate boundary. The central magnetic anomaly is of very small amplitude or locally even non-existent; in the adjacent oceanic basins too, the magnetic field is remarkably quiet, and typical seafloor spreading anomalies have not been identified (Myhre et al. 1982).

4.1.2. Continental margin and ocean-continent transition

The three fault segments of the Hornsund Fault Zone, the Senja Fracture Zone and the connecting fault define a major continental boundary fault truncating the Barents shelf and Svalbard Platform (Fig. 8). They represent rifted and sheared margin segments, directly related to the stepwise opening of the Norwegian-Greenland Sea (Myhre et al. 1982). The Senja Fracture Zone and Hornsund Fault Zone are sheared, and sheared-rifted margin segments, respectively; these two regional shear systems are linked by a NE-trending predominantly rifted margin complex south-west of Bear Island, associated with a marginal high (Myhre & Eldholm 1988; Faleide et al. 1988). Oceanic crust has been traced to, or close to, these boundaries (Myhre et al. 1982), suggesting that they essentially demarcate the ocean-continent transition. At the central rifted margin complex the OCT is masked by a marginal high with associated volcanism, the Vestbakken volcanic province. All these features presently appear beneath a thick wedge of Cenozoic clastics (see section 5) that has accumulated all along the continental margin.

Senja Fracture Zone

The Senja Fracture Zone was originally discovered as an elongated gravity high (Fig. 9), which was thought to mirror the Greenland Fracture Zone (associated with a positive gravity anomaly as well) on the western side of the Mohns Ridge (Talwani & Eldholm 1977). Later multi-channel seismic data have confirmed the existence of the fracture zone as a narrow fault zone beneath the landward flank of the gravity anomaly and with a throw of about 2.5 s TWT (Eldholm et al. 1987). The Senja FZ does not appear to bend into the ocean as the gravity anomaly suggests however. The Greenland-Senja FZ lacks definition in the vicinity of the spreading ridge, indicating that it is not a typical fracture zone associated with an offset ridge crest, but related to the transcurrent movement of Greenland past Svalbard (Talwani & Eldholm 1977). Oceanic basement is seen to extend to the location of the gravity anomaly (Eldholm et al. 1984).

Hornsund Fault Zone

The Hornsund Fault was first described as a continuous N-NW trending feature on the central shelf between Bear Island and app. 79° N (Sundvor & Eldholm 1979). Myhre et al. (1982) pointed out that it is composed of three separate and subparallel segments, and therefore proposed the term Hornsund Fault Zone. They further noted that the central fault segment, between 75° and 76°30', is shifted to the east. Additional seismic studies (Myhre & Eldholm 1988) confirmed the complex

nature of the fault zone as a series of subparallel blocks downfaulted towards the west, rather than a main boundary fault; the throw can amount to more than 3–4 s. The Hornsund Fault Zone forms a transition between oceanic crust and an older continental platform on the inner shelf, which is an extension of the Svalbard Platform. Between 74° and 76° N, where the fault zone is narrow, oceanic crust can be traced to less than 10 km from the outer fault, whereas further north the zone of unidentified crust widens to 10–30 km (Myhre & Eldholm 1988). Recent maps (e.g. Faleide et al. 1993) show that the part of the Hornsund Fault Zone south of about 75°30' N can actually be reckoned to the rifted margin segment. South of 78° N the fault zone is associated with a prominent elongate gravity maximum (Myhre et al. 1982).

Central fault segment and associated marginal high

The Senja Fracture Zone and the Hornsund Fault Zone are connected by an irregular continental boundary fault, informally denoted as the “Central Fault Zone” by Sættem et al. (1994). It offsets a region of elevated (with respect to adjacent oceanic crust) basement from the continental Stappen High and Sørvestsnaget Basin on the landward side. The Central Fault Zone seems to consist of several short north-east trending segments, intersected by lineaments subparallel to the Senja Fracture Zone and the Hornsund Fault Zone; these are interpreted as rifted margin segments offset by shear zones (Myhre & Eldholm 1988).

The region of elevated basement forms a roughly triangular-shaped marginal high south-west of Bear Island: the Vestbakken volcanic province (formerly known as the Bjørnøya Marginal High). The feature, which was described by Faleide et al. (1988) and by Myhre & Eldholm (1988), is bounded by the Central Fault Zone towards the south-east, but its outer boundary is poorly defined. Though the typical seaward-dipping reflector sequences have not been identified (Myhre & Eldholm 1988), the high is believed to be analogous to other volcanic rifted margins in the Norwegian-Greenland Sea (like e.g. the Vøring Plateau and large portions of the East Greenland margin), formed by massive extrusion of lavas during an initial subaerial phase of seafloor spreading (cf. Hinz 1981; Mutter 1985; see also Fig. II.14). The area is characterised by a smooth acoustic basement reflector, which can be traced to a short distance of the fault zone and is interpreted to represent the top of a series of lava flows; some sub-basement reflectors can be observed below the inner high (Myhre & Eldholm 1988; Faleide et al. 1988). The volcanic extrusives may hide thinned continental crust extending a short distance seaward of the Central Fault Zone (Eldholm et al. 1987). Locally, volcanics are observed landward of the main boundary fault, indicating that vertical movements along this fault post-date the main volcanic event; downfaulting exceeds 2 km west of the Stappen High, but diminishes towards the south-west (Faleide et al. 1988). Two buried basement peaks, each having a relief of more than 1 km, penetrate the acoustic basement surface and the oldest sediments at the inner flank of the high; the geometry suggests that they are younger than the adjacent volcanics (Faleide et al. 1988).

Free-air gravity field

Both the Senja Fracture Zone and the Hornsund Fault Zone are associated with positive free-air gravity anomaly belts (Fig. 9), peaking to maximum amplitudes in the Senja Fracture Zone Anomaly and the Hornsund Anomaly; in between the two anomalies, another well-defined but less pronounced positive gravity belt is observed over the marginal high: the Bjørnøya Anomaly (Myhre & Eldholm 1988). The latter feature seems to be similar in magnitude and shape to gravity anomalies observed over other volcanic rifted margins; this and the lower amplitude suggest that it is genetically different

from the two main anomalies (Eldholm et al. 1987), the origin of which has not yet been satisfactorily explained. The observation of abnormally high seismic velocities near the top of the oceanic basement led Eldholm et al. (1987) to suggest that the large gravity anomalies west of the Senja and the southern Hornsund fault zones are produced by the presence of isolated high-density crustal bodies at these locations. Sobczak (1975) on the other hand proposed a correlation of the free-air gravity highs with major sediment accumulations: the Senja Fracture Zone Anomaly is located over the bathymetric bulge in front of Bear Island Trough, and the Hornsund Anomaly at the mouth of Storfjorden Trough; smaller oval gravity anomalies occur in front of glacially incised troughs on the Svalbard margin. Particularly on Storfjorden Cone, the close resemblance of gravimetric and sediment thickness contours is striking.

4.1.3. Continental shelf

South of 73°30' the continental shelf contains the regional basin province of the south-western Barents shelf, whereas the stratigraphically elevated Svalbard Platform and its southern protrusion, the Stappen High, cover the area to the north.

Barents shelf

The regional geology of the Barents shelf is very complex (Fig. 8). The south-western Barents Sea accommodates a series of deep Mesozoic basins (the Harstad, Tromsø, Bjørnøya and Sørvestsnaget Basins) and inter-basinal highs (the Senja Ridge and Veslemøy High) (Rønnevik & Jacobsen 1984; Faleide et al. 1993). The deep Mesozoic basins are separated from an eastern platform province of less pronounced basins and highs between 20 and 25° E (comprising amongst others the Hammerfest Basin and Loppa High) by an intensively tectonised Jurassic-Cretaceous hinge zone, consisting of several interconnected fault complexes (Faleide et al. 1993). Sediments on the Barents shelf range in age from late Paleozoic (Late Devonian to Early Carboniferous according to Rønnevik & Jacobsen 1984) to Cretaceous, and attain max. thicknesses of 10-12 km. In the south-western basins Jurassic, Cretaceous and locally Paleocene strata have accumulated (Faleide et al. 1993). The Tromsø Basin is bounded in the west by the Senja Ridge and in the east by the complex hinge zone separating it from the Hammerfest Basin. The Bjørnøya Basin is located south-west of Bear Island, and continues into a still deeper basin, the Sørvestsnaget Basin, at the margin (Eldholm et al. 1984). The Veslemøy High occurs northward of the Senja Ridge, in between the Sørvestsnaget and Tromsø Basins. The basins developed by rapid early Cretaceous subsidence following mid-Kimmerian block faulting in the Jurassic. The Senja Ridge, actually a buried sedimentary high bounded by faults, was part of the early Cretaceous depocentre, but was inverted by late Cretaceous to early Tertiary tectonism (Faleide et al. 1988). The area east of 20° E has not experienced the pronounced Cretaceous subsidence (Faleide et al. 1993). The Sørvestsnaget Basin was additionally affected by major structural deformation during the early Tertiary opening of an oceanic basin along the margin (Faleide et al., 1993).

Svalbard Platform

The Svalbard Platform is underlain by a thick, relatively flat-lying succession of late Paleozoic and Jurassic-Triassic strata (Faleide et al. 1984). The Stappen High, which protrudes from the platform and surrounds Bear Island, was part of a north-south trending elevation from late Paleozoic to Jurassic times; its southern flank was formed by early Tertiary inversion of part of the Bjørnøya Basin (Faleide et al. 1993).

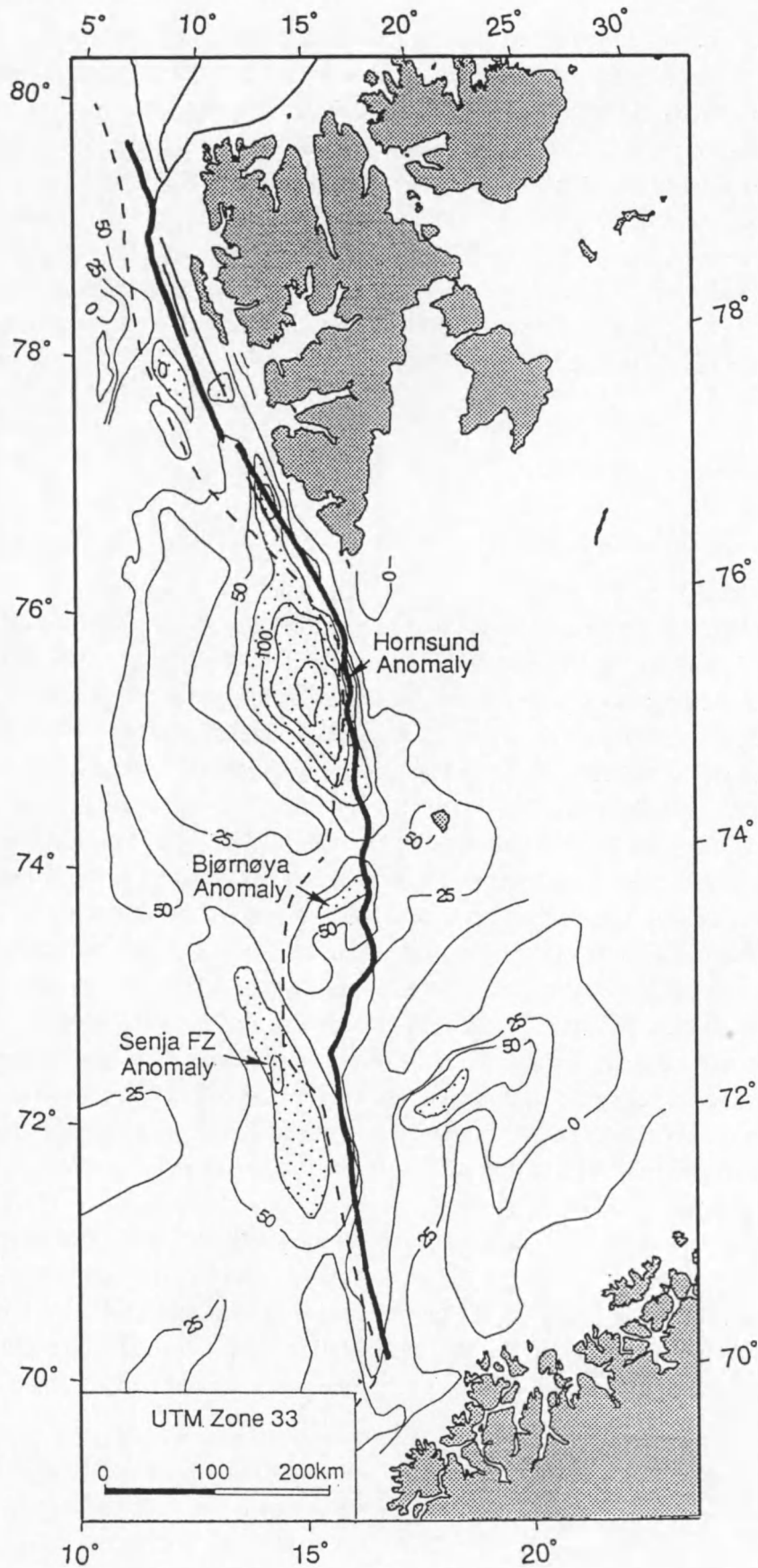


Fig. III.9 - Free-air gravity map of the western Barents Sea margin. Contour interval is 25 mgal, shaded areas mark gravity maxima > 75 mgal. From Myhre & Eldholm (1988).

The inner shelf off western Svalbard appears to be a continuation of the Svalbard Platform (Myhre et al. 1982), but is located within the early Tertiary fold and thrust belt of western Spitsbergen (Faleide et al. 1988). This orogenic belt is a distinct regional zone of elevated pre-Devonian basement along the western margin of the island (Fig. 8), and terminating north of Bear Island; it is flanked by the Central Basin, a foreland basin in Spitsbergen which is filled with up to 2500 m of Cenozoic clastic deposits (Steel et al. 1985). The inner shelf is further transected by the Knølegga Fault Zone (former Bjørmøya-Sørkapp Fault Zone), which trends parallel to regional structures on Svalbard and seems to have acted as a hinge line for the Cenozoic post-opening marginal subsidence south of Spitsbergen; like the Homsund Fault Zone, it is probably an older structural element that has been reactivated (Myhre & Eldholm 1988).

4.2. Plate tectonic evolution

4.2.1. History prior to break-up

The Barents shelf is an extension of the prominent sedimentary basin that extended north of the North Sea between Greenland and Norway prior to the early Tertiary opening of the Norwegian-Greenland Sea (Eldholm & Talwani 1977); more particularly the region was continuous with the North-eastern Shelf province in Greenland (Larsen 1990, see chapter II, section 4.2). Following the Caledonian orogeny the region developed as an epicontinental platform on which a series of marine transgressions and regressions occurred (Eldholm & Talwani 1977), and which was subjected to three rift phases: Late Devonian (?) - Early Carboniferous, Middle Jurassic - Early Cretaceous, and finally early Tertiary; the Svalbard Platform on the contrary has, apart from epeirogenic movements, been largely stable since late Paleozoic times, unaffected by extension (Faleide et al. 1993). Deposition has taken place since at least the Carboniferous period (Rønnevik & Jacobsen 1984). These sediments were deposited in fault-bounded basins, created during the late Paleozoic tectonic phase. Subsequently, the whole area underwent epeirogenic subsidence as one basin in the Late Carboniferous and Early Permian, with sedimentation gradually smoothing the relief. During the Mesozoic the area between Greenland and Norway has been subjected to several tensional phases, without complete crustal break-up however. The main phase of extension took place in mid- to late Jurassic times (Kimmerian), creating a system of basins and highs all over the Barents Sea platform (Rønnevik & Jacobsen 1984); in the south-western Barents Sea the deep Tromsø and Bjørmøya Basins were initiated (Faleide et al. 1988). In the early Cretaceous a new rift system developed (Fig. 10), probably as the northward continuation of the short-lived ocean that started to form in the southern Rockall Trough (Hanisch 1984). During this phase the south-western basins were decoupled from the eastern platform region, which remained mostly unaffected and experienced no additional large subsidence (Faleide et al. 1993). Marine sedimentation in the south-western Barents Sea succeeded during the Cretaceous and into the Paleocene, smoothing the relief once again.

In relation with the Cretaceous crustal extension a regime of wrench tectonics was established between the Svalbard - Barents shelf region and North-east Greenland (Eldholm et al. 1987). Regional shear took place along N-NW trending faults in a broad zone bounded by the Ringvassøy-Loppa, Knølegga and Homsund Fault Zones in the east and the Senja Fracture Zone and the

Trolleland Fault Zone in NE Greenland to the west. This continental mega-shear zone is referred to as the De Geer Zone (Harland 1965) (Fig. 11a). This plate tectonic movement induced transpressional folding of western Spitsbergen (Hanisch 1984), whereas complex structuring gave rise to the first phase of inversion in the south-western Barents Sea (Faleide et al. 1988).

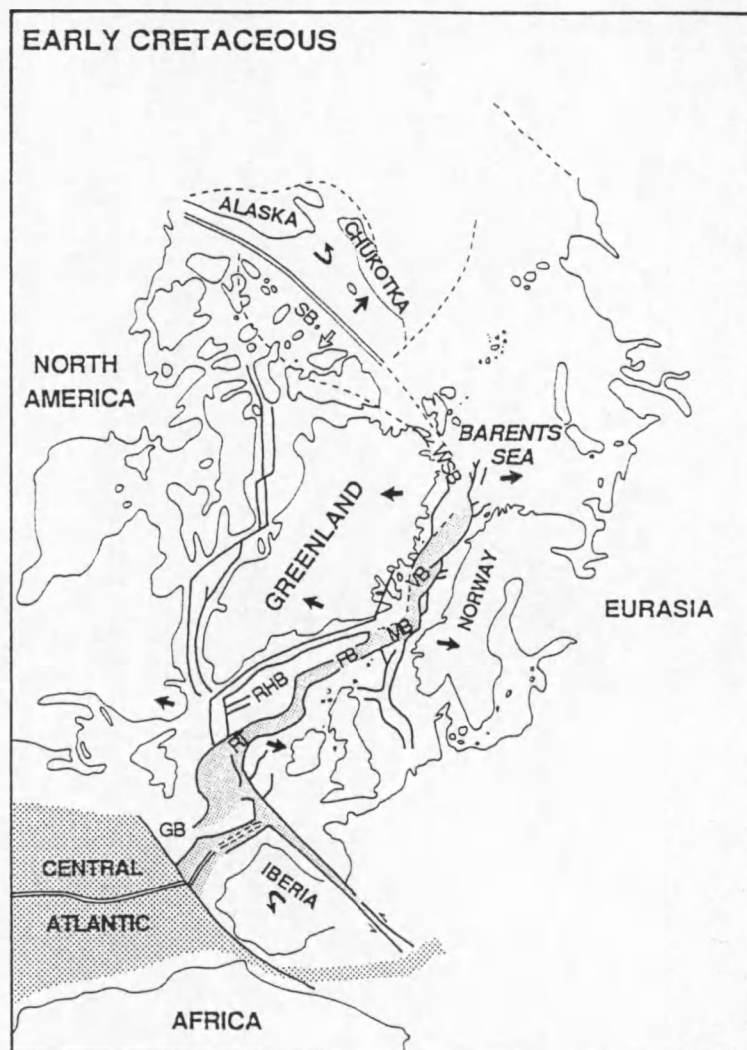


Fig. III.10 - Early Cretaceous plate reconstruction prior to opening of the North Atlantic ocean. FB = Faeroe Basin, GB = Grand Banks, MB = Møre Basin, RHB = Rockall-Hatton Basin, RT = Rockall Trough, VB = Vøring Basin. From Faleide et al. (1993b).

4.2.2. Opening of the Norwegian-Greenland Sea

The opening history of the Norwegian-Greenland Sea was originally proposed as a 2-stage model by Talwani & Eldholm (1977), and further developed into a 3-step model by Myhre et al. (1982). Further refinements were made by Eldholm et al. (1987) and Faleide et al. (1988). The simplified plate tectonic evolution is depicted in Fig. 11a through 11d.

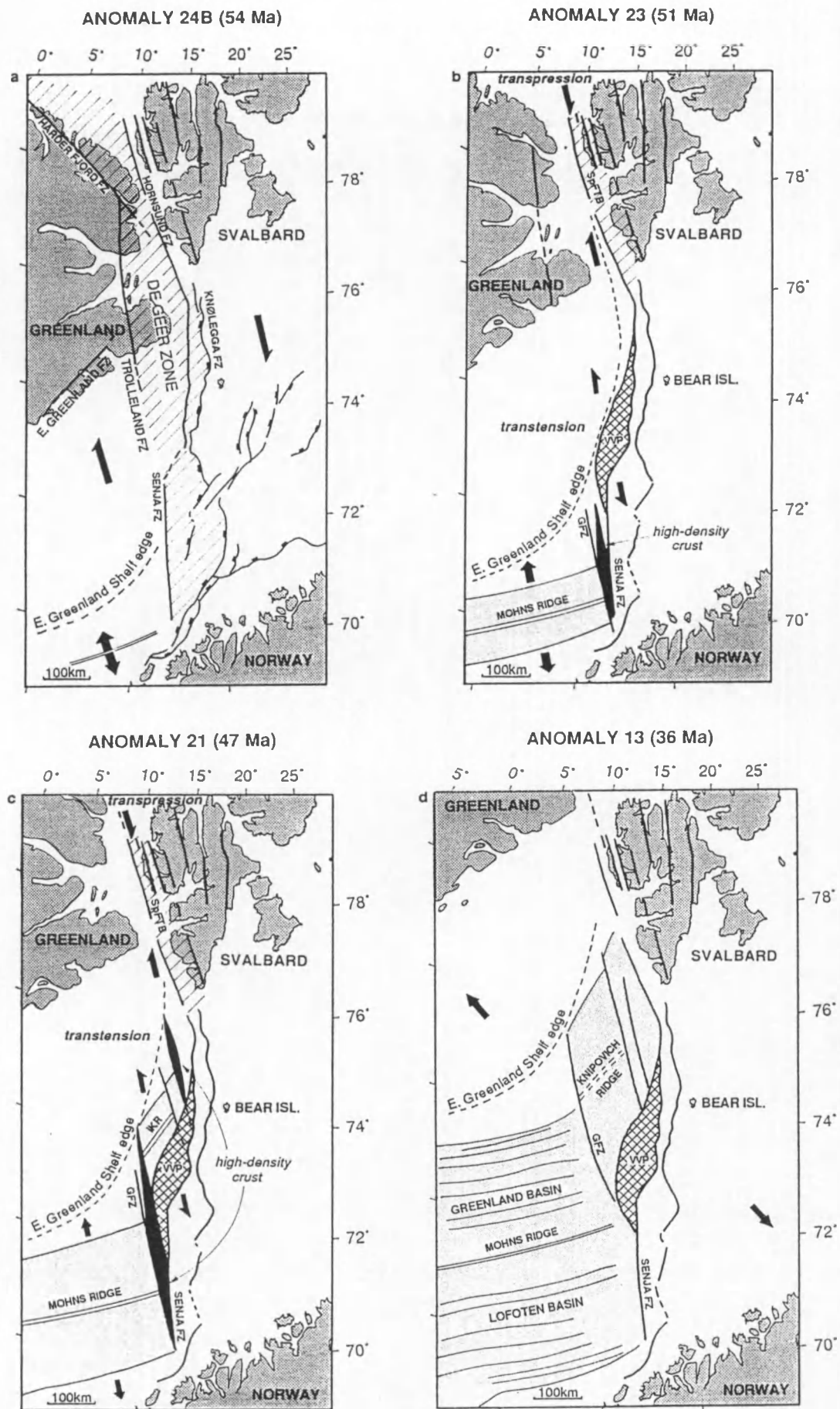


Fig. III.11 - Plate tectonic evolution of the western Barents Sea margin during the early Tertiary. Simplified from Eldholm et al. (1987) and Faleide et al (1993b).

4.2.2.1. Opening of the Norwegian Sea (54 - 51 Ma)

In earliest Tertiary times the crust between Greenland and Norway was being thinned a third time, which finally resulted in the initiation of seafloor spreading during the time period between magnetic anomalies 25 and 24B (Fig. 11b; Eldholm et al. 1984), at the Paleocene-Eocene transition (c. 55 - 53 Ma). The termination of linear magnetic anomalies towards the Senja Fracture Zone indicates that the first phase of spreading was limited to the Norwegian Sea, while regional shear movements were continued within the De Geer Zone, which was offsetting the nascent Lofoten and Greenland Basins from the Eurasia Basin in the Arctic Ocean. All of the western Barents Sea - Svalbard margin was subjected to dextral strike-slip as north-east Greenland slid past. Eldholm et al. (1987) have noticed that the direction of early opening makes a small but significant angle with the sheared Senja Fracture Zone and Hornsund Fault Zone, suggesting non-ideal transform movements (or oblique shear) with compressional and extensional components. Transpression caused folding and thrusting in western Spitsbergen (the Spitsbergen Orogeny, Steel et al. 1985), and local inversion of the Senja Ridge and the Stappen High. At the same time the Senja Fracture Zone may have developed as a "leaky" transform due to transtension. This would have allowed intrusion of asthenospheric material from levels deeper than normal, in a rhomboid-shaped depression along the transform boundary (Fig. 12); the resulting high-density crust would thus represent the oldest oceanic crust along the margin segment. This process might explain the observed high seismic velocities and prominent positive gravity anomalies. The central margin segment, which was being formed between the two regional shear systems of the Senja Fracture Zone and the Hornsund Fault Zone, was subject to rifting and volcanism, resulting in the emplacement under subaerial conditions of the Vestbakken volcanic province (Faleide et al. 1988).

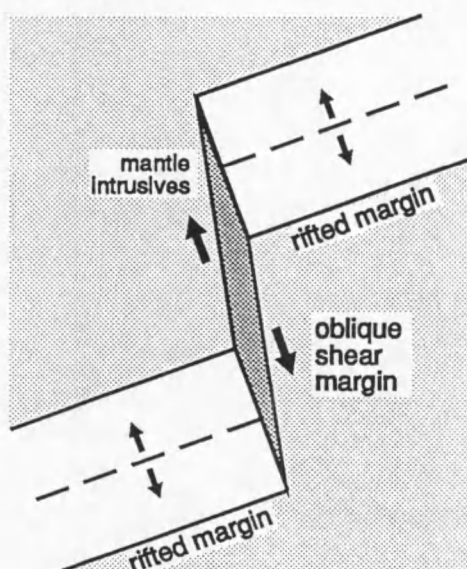


Fig. III.12 - Schematic model for the development of a "leaky" fracture zone along an oblique shear margin (Eldholm et al. 1987).

4.2.2.2. Opening of the southern Greenland Sea (51 - 36 Ma)

Myhre et al. (1982) were the first to recognise the stepwise opening of the Greenland Sea. The southern Greenland Sea, immediately north-east of the Senja Fracture Zone, opened up first (Fig. 11c). Lacking identifiable magnetic anomalies in the Greenland Sea, and structural and geophysical data from the conjugate Greenland margin, the authors tentatively suggested that along the central margin segment south-west of Bear Island oceanic crust was being generated from anomaly 21 time (Middle Eocene, c. 47 Ma) onward. More recent reconstructions indicate anomaly

23 time (Early Eocene, c. 51 Ma) for this event, this is 2 - 4 Ma later than the opening of the Norwegian Sea (Eldholm et al. 1987). As the anomalies in question are not observed to curve westward like the present rift axis, the incipient Knipovich Ridge must have been offset over a large distance from the Mohns Ridge by the Greenland-Senja Fracture Zone (Talwani & Eldholm 1977). The general configuration of the central margin segment consisting of short rifted and sheared segments is thought to reflect an oblique spreading system of *en échelon* ridges and transforms (Myhre et al. 1982). This in turn may indicate that opening of the southern Greenland Sea occurred by a step-wise north-eastward propagation of the spreading axis towards the southern Hornsund Fault Zone (Eldholm et al. 1987; Myhre & Eldholm 1988).

The initiation of seafloor spreading in the southern Greenland Sea was accompanied by faulting in a pull-apart setting along the Central Fault Zone, responsible for downfaulting of the Vestbakken volcanic province (Faleide et al. 1988) and deepening of the wide northern part of the Sørvestsnaget Basin (Faleide et al. 1993). The southern part of the Hornsund Fault Zone probably developed as a leaky transform, in a similar fashion to the Senja Fracture Zone earlier. Further north transpressional movements continued along the Hornsund Fault, which now became the main regional transform to the Eurasia Basin (Myhre & Eldholm 1988), and on Spitsbergen a foreland basin was filled with erosional products from the uplifted orogenic belt to the west (Steel et al. 1985).

4.2.2.3. Opening of the northern Greenland Sea (36 Ma - present)

The cessation of seafloor spreading in the Labrador Sea, west of Greenland, brought about a major plate reorganisation in the polar North Atlantic around the time of magnetic anomaly 13 (earliest Oligocene, c. 36 Ma); as Greenland thus became part of the North American plate, the relative direction of plate movement between Greenland and Eurasia changed from north-west to west-north-west (Talwani & Eldholm 1977). As a direct consequence an overall tensional setting was established, allowing the spreading axis to propagate further northward. The northern Greenland Sea thus opened as well (Fig. 11d; Myhre et al. 1982); the Hornsund Fault Zone developed from a sheared margin into a rifted margin (Myhre & Eldholm 1988). Since anomaly 13 time spreading has thus taken place along the entire Svalbard - Barents Sea margin, which was uplifted and remained mostly emergent during the Tertiary (Faleide et al. 1993). In the Vestbakken volcanic province the early Oligocene plate reorganisation was probably associated with a rejuvenation of volcanism which created the huge volcanic peaks observed there (Faleide et al. 1988).

The present asymmetric position of the Knipovich Ridge in the Greenland Sea prompted Talwani & Eldholm (1977) to suggest that the spreading axis has migrated eastward since its inception at anomaly 13 time. Sundvor & Eldholm (1979) took the presence of escarpments on both sides of the axial block as evidence for a recent (5 - 6 Ma) shift in the location of the plate boundary. The plate tectonic evolution might have been more complex however: the presence of numerous, but small inactive and active transforms, and the fact that the Knipovich Ridge seems to be spreading obliquely (the flow-lines are not normally oriented to the axis) seems to indicate an ongoing process of plate boundary adjustment (Eldholm et al. 1990). As the ocean matured, it appears that the entire plate boundary along the Mohns and Knipovich Ridges has gradually become more continuous (Myhre & Eldholm 1988).

Based on heat flow measurements and building on a concept outlined by Bonatti & Crane (1984) for the Central Atlantic, Crane et al. (1988) put forward the idea of a spreading centre trapped within the confines of an older continental shear zone. The oblique impact of the propagating rift axis with the Senja-Hornsund lineament (Fig. 13) created a stress regime of compression within the acute angle of impact (the south-east) and extension on the opposite side (the north-west). This caused faster spreading rates to the north-west than to the south-east, and resulted in the progressive westward migration of the spreading centre along a series of transform faults, bounding small *en échelon* oriented spreading centres. The process would also account for the chaotic nature of the magnetic anomalies in the Greenland Sea.

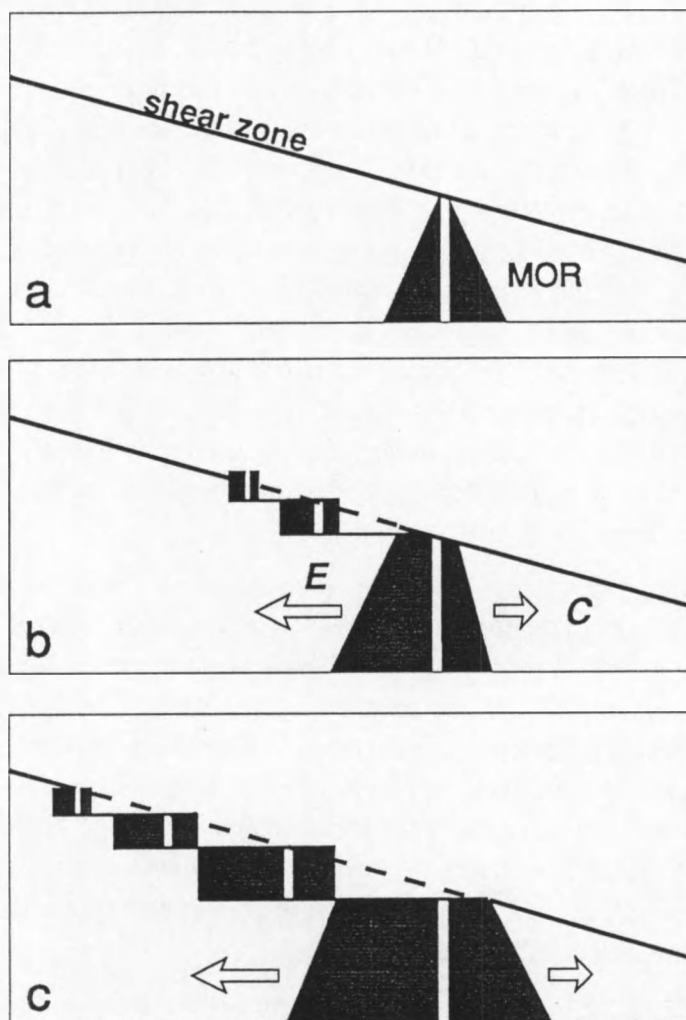


Fig. III.13 - Schematic model for the development of an asymmetric spreading centre by oblique impact with a pre-existing continental shear zone (Crane et al. 1988).

E = extension, C = compression.

5. Seismic stratigraphy

5.1. The Cenozoic sedimentary wedge: general aspects

The western Barents Sea - Svalbard margin extends some 1000 km in N-S direction, from 70° N to 79° N. A thick wedge of mainly prograding Cenozoic sediments has accumulated along its entire length, attaining a thickness of more than 7 km (5 s TWT) opposite to the Hornsund Fault Zone (Myhre et al. 1982). The sediment wedge was deposited in association with uplift and erosion of the western Barents shelf and Svalbard, thus providing a record of Cenozoic sedimentation which is not observed on land. The wedge generally overlies oceanic crust to the west and faulted continental crust (including pre-Tertiary sediments) to the east, and is everywhere most thickly developed on the edge of the oceanic crust (Spencer et al. 1984). To the west the basin is dammed by the mid-oceanic spreading centres of the Mohns Ridge and the Knipovich Ridge, but in the extreme north sediments have overspilled the Knipovich Ridge and were deposited in the present rift valley (Myhre et al. 1982). To the east the thickness of the wedge becomes greatly restricted on the continental shelf, beyond the Senja Fracture Zone and the Hornsund Fault Zone. The thickness of the wedge varies strongly along the margin: three depocentres are evident seaward of large E-W trending draining systems such as shelf depressions or fjord systems (cf. Myhre & Eldholm 1988). From north to south, they are located off Spitsbergen (mainly off Isfjorden), off Storfjorden Trough and off Bear Island Trough (Fig. 14). In contrast to common usage, and for reasons that will be outlined later (refer to section 6.7), these individual depocentres will not be denoted as "fans", but instead the more general morphological term "cones" will be used hereafter.

The general character of the clastic wedge is relatively simple: mostly parallel layering on the continental shelf, prograding clinoforms below the slope, and again parallel bedding on the basin floor (cf. Fiedler & Faleide, in press). Especially the upper half of the section reveals continuous westward (seaward) progradation of the shelf edge. Progradation is also most prominent at the location of the above-mentioned depocentres. The sediments within the wedge are described as well stratified, with reflectors that can be traced regionally; locally, however, extensive chaotic intervals have developed, indicating strong disturbance of the original stratigraphy. Tectonic deformation, on the other hand, is very limited. Low seismic velocities (1.8 - 2.4 km/s, Eldholm & Talwani 1977; less than 3 km/s, Schlüter & Hinz 1978) characterise the entire wedge, suggesting that it is composed of unconsolidated to semi-consolidated material.

The margin is traditionally divided into two regions: [i] the Barents Sea margin forming the boundary of the epicontinental Barents shelf south of 75° N, and terminated to the south by the Senja FZ, and [ii] the Svalbard margin bounding the Svalbard Platform north of 75° N and bordered by the Hornsund Fault Zone. Myhre et al. (1982) have noted a pronounced change in the seismic velocity gradient at about 74.5° N: the Svalbard margin is characterised by a gradient of 0.72 s⁻¹, whereas the typical value for the Barents Sea margin is 0.30 s⁻¹. A low-velocity gradient like that of the Barents Sea margin falls within the range reported for major delta deposits (Houtz & Windisch 1977), and is more generally indicative of rapid sediment accumulation. This is supported by the prominent positive gravity anomalies that occur over the Storfjorden and Bear Island Cones and which may in part be related to incompletely compensated, rapidly deposited sediments (Sobczak 1975).

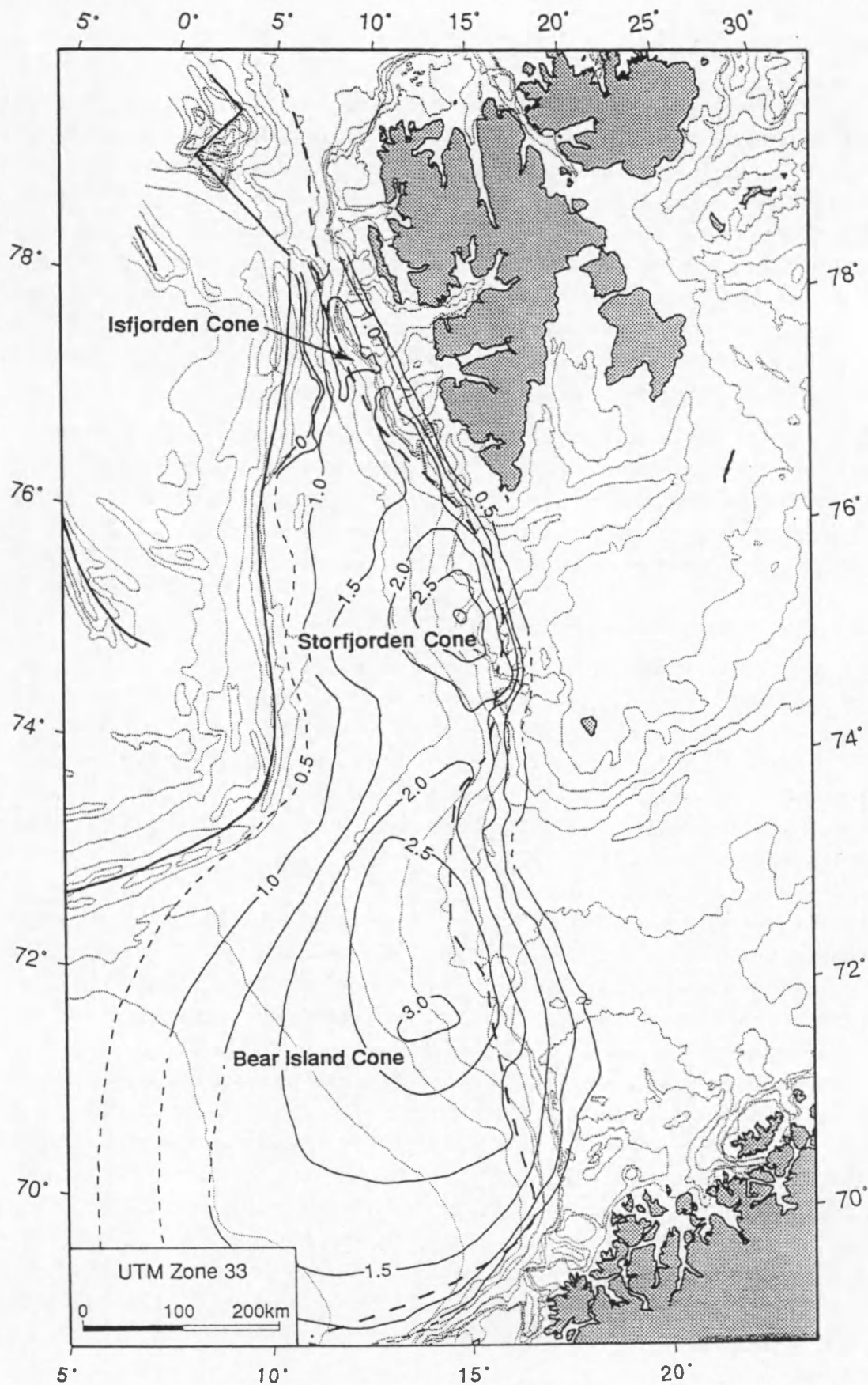


Fig. III.14 - Location of main depocentres along the western Barents Sea margin. The sediment thickness contours refer to the glacial part of the wedge only. From Faleide et al. (in press).

5.2. Review of existing stratigraphic work

Since the first seismic investigations on the Barents Sea and Svalbard margins in the late seventies, a substantial volume of work has been published that cannot be ignored when conducting a new stratigraphic study. Common to most of these studies is that they mainly concentrated on the continental shelf and on the shallowest part of the slope. In spite of the large amount of multi- and single-channel seismic reflection profiles acquired throughout the years, a detailed and well-constrained seismic stratigraphic analysis of the entire wedge has not been presented so far. The few depositional units and unconformities that were identified have been given not only a variety of names, but also strongly diverging ages. This can be ascribed mainly to the lack of reliable chronostratigraphic tie points such as deep drillholes, and to the difficulties encountered in correlating between the northern and southern portions of the margin.

Below a review will be made of previous seismic stratigraphic studies on the Barents Sea and Svalbard margins, respectively, concluded by a regional stratigraphic framework that was recently proposed for the entire margin — and in which the present study represents a small part. The chronology will be discussed separately. The general correlation table of Fig. 15, and the representative cross-sections in Fig. 16 summarise this discussion.

5.2.1. The Barents Sea margin (70° - 75° N)

Whereas the earliest studies (Rønnevik 1981; Faleide et al. 1984) were largely restricted to the lower parts of the wedge, the basis for the seismic stratigraphy of the Cenozoic wedge along the Barents Sea part of the margin was laid by Spencer et al. (1984). Their work was further updated by Vorren et al. (1990, 1991) and Richardsen et al. (1991). More detailed studies of two specific intervals within the wedge were presented by Richardsen et al. (1992) and Knutsen et al. (1992). The youngest part of the wedge, covering the Barents shelf, was described by Solheim & Kristoffersen (1984) and by Sættem et al. (1991, 1992).

[1] Rønnevik (1981) and Faleide et al. (1984) discerned three seismic horizons, labeled A (youngest) to C (oldest) in the SW Barents Sea (Fig. 16d). Horizon C is generally the deepest reflector that can be identified east of the OCT and south of the Stappen High. The B-C section is rather thin in the Mesozoic basins on the Barents shelf, but is more widespread and obtains a fairly uniform thickness further west on the margin. The sediments seem to have prograded from the north under fairly stable tectonic conditions. Horizon B is a local unconformity marking the timing of block faulting. The overlying A-B section is restricted to a narrow NNW-trending zone near the shelf edge, and was probably truncated near the present OCT by a phase of uplift around A time. The unit was deposited onto rotational fault blocks. The internal beds show a complex geometry, with evidence of initial progradation, erosional channels and several unconformities. Reflector A forms a pronounced angular unconformity in the east, but becomes less clearly defined toward the ocean, where it appears to be the strongest reflector near the base of the sediment wedge. Most faulting apparently ended prior to the creation of reflector A. The post-A section forms an undisturbed wedge of prograding terrigenous sediments derived from an emergent Barents shelf and deposited on a subsiding margin.

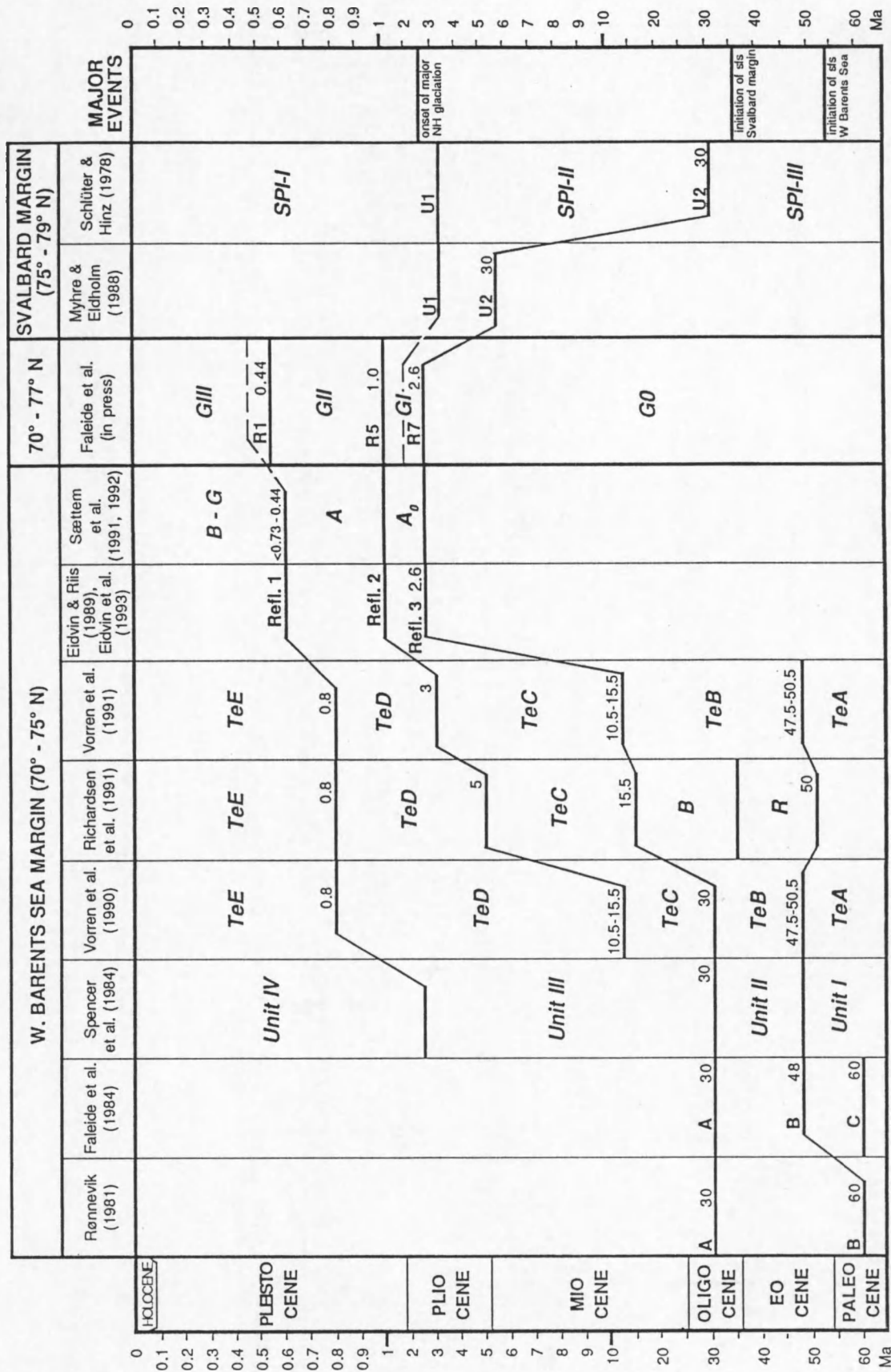


Fig. III.15 - General correlation table of important stratigraphic boundaries on the western Barents Sea and Svalbard margins. Abbreviations used: NH = Northern Hemisphere, sfs = seafloor spreading.

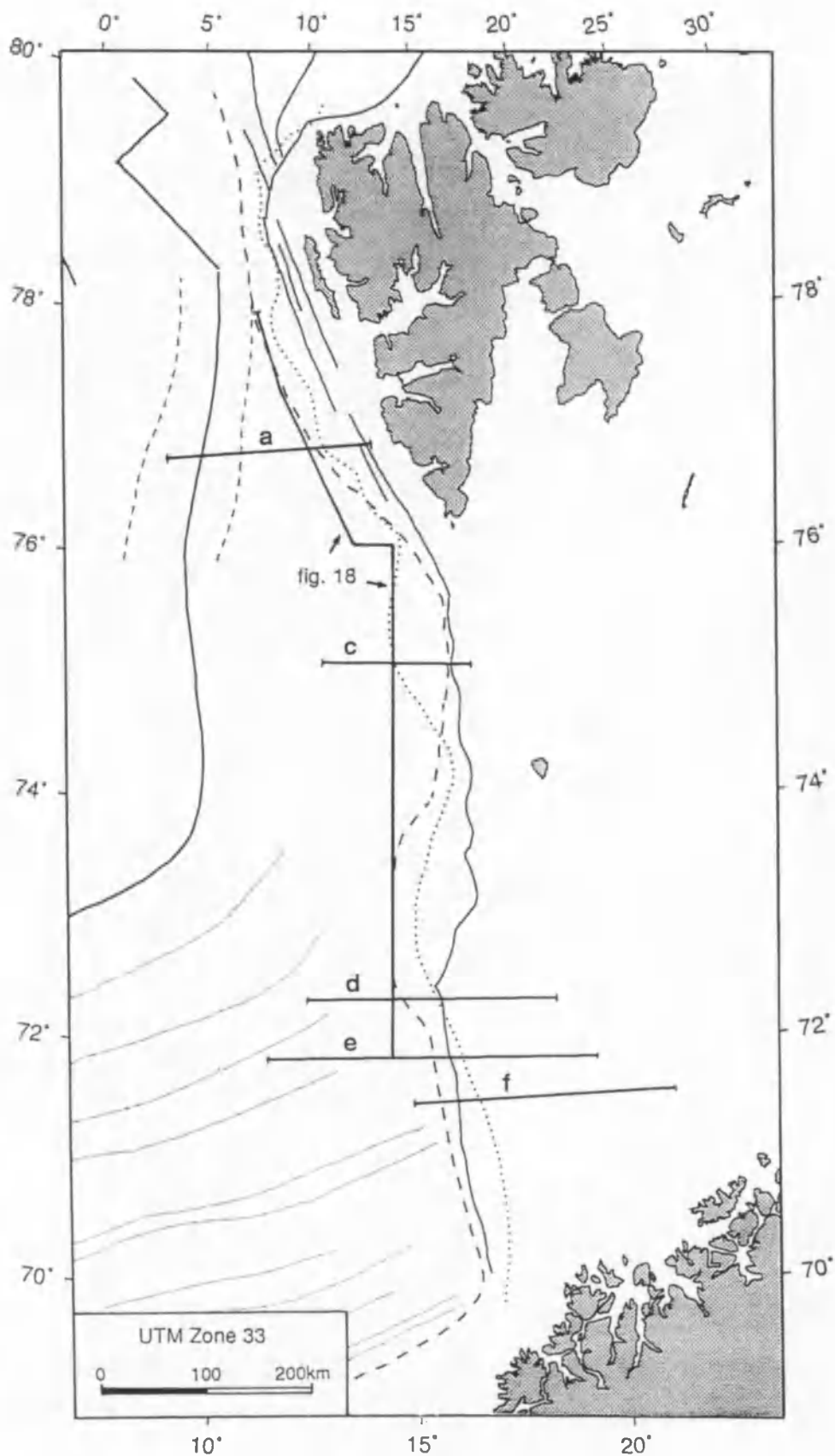
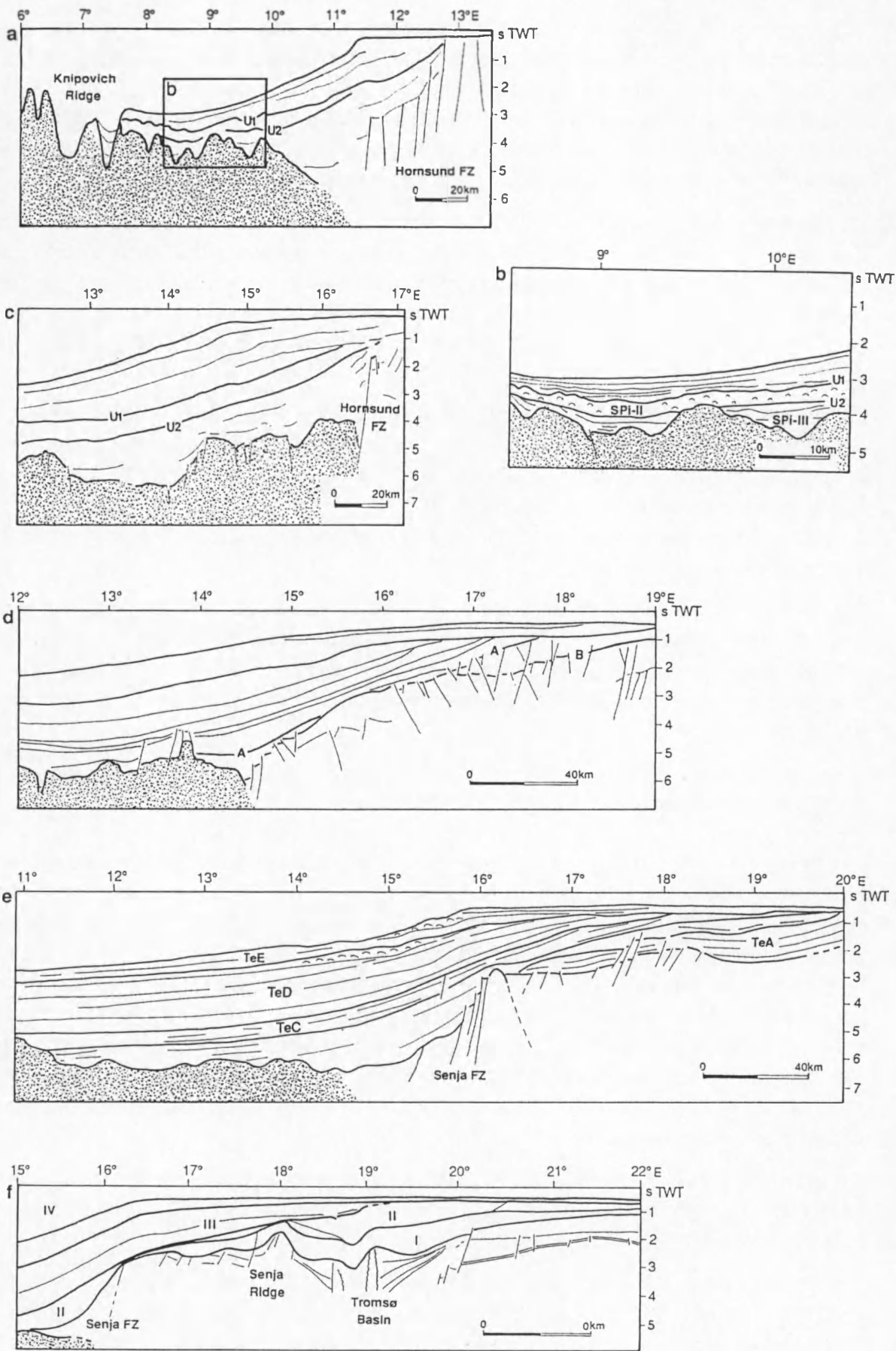


Fig. III.16 - Representative cross-sections through the western Barents Sea margin, illustrating the build-up of the margin, and the widely diverging stratigraphies used by different authors; [a,c] from Myhre & Eldholm (1988), [b] from Schlüter & Hinz (1978), [d] from Rønnevik (1981), [e] from Vorren et al. (1990), [f] from Spencer et al. (1984).



[2] Spencer et al. (1984) have recognised four main units within the Cenozoic wedge in the southernmost Troms area of the Barents Sea margin (Fig. 16f). The units were labeled I - IV (from the oldest upwards), and are separated by major regional discontinuities. The units rest unconformably on a suite of pre-Tertiary fault blocks developed between the Senja Ridge and the present shelf break. The basal unconformity is interpreted as a major hiatus, associated with the erosion of older sediments resulting from uplift along the margin.

The lowermost unit I (correlative to the B-C section of Faleide et al. 1984) has a widespread occurrence below the Barents shelf: it consists of bathyal sediments that accumulated in the Mesozoic basins underlying the shelf, and extended westwards to the present shelf edge; the Senja Ridge in the east was overstepped during the early stages of deposition. Internally, the unit is characterised by parallel, low-amplitude reflections which can be followed laterally over long distances.

Unit II (A-B section of Faleide et al. 1984) has a more restricted distribution, and is composed of two parts: a lower subunit (IIA) that is restricted to the area east of the Senja Ridge, and an upper subunit (IIB) that is most thickly (exceeding 1 s TWT) developed in the Tromsø Basin but is also present west of the Senja Ridge. Subunit IIB consists of westwards prograding shelf sediments characterised by a transparent seismic facies. Its upper boundary dips to the west, where the erosional character shows up more clearly.

Unit III extends westwards from the Senja Ridge beneath the present outer shelf and continental slope. The unit constitutes the main clastic wedge, consisting of westwards dipping and prograding shelf and slope clastics, which up-dip onlap the tilted upper surface of unit II. Unit III thus corresponds to a major change in depositional regime, ascribed to the regional tilting of the shelf towards the west.

Deposition of unit IV appears to have continued the pattern initiated during unit III, except that unit IV sediments extend over much of the Barents shelf as well.

[3] Vorren et al. (1990, 1991) and Richardsen et al. (1991) mainly built further upon the results of Spencer et al. (1984) in a more northerly region centred around 72° N. They divided the Cenozoic wedge into five units, labeled TeA (oldest) to TeE (youngest) (Fig. 16e). The unit boundaries generally correspond to angular unconformities separating eroded strata below from onlapping and downlapping strata above. The unconformities are attributed to periods of low relative sea level. Erosion was most intensive on the paleo-continental shelf and upper slope; the boundaries become conformable downslope. On a first-order scale the Cenozoic sedimentary wedge can be divided into a lower faulted part, comprising units TeA and TeB, and an upper tectonically undisturbed part, containing units TeC, TeD and TeE. It is the upper part that constitutes the characteristic prograding succession of the Cenozoic wedge.

The lowermost unit TeA, which is correlated to unit I of Spencer et al. (1984), can be mapped beneath the prograding wedge. This interval is truncated by the base-TeB reflector in the east and wedges out towards the west near the ocean-continent transition.

Unit TeB is a very complex unit with several internal unconformities and subunits, corresponding to unit II of Spencer et al. (1984). The sediments may exceed a thickness of 2 - 3 s TWT, and were to a large extent eroded from the Senja FZ and the Stappen High. Richardsen et al. (1991) further

subdivided unit TeB into a lower unit R and an upper unit B. Unit R is volumetrically the most important unit within the wedge, with thicknesses sometimes over 2 s TWT. Its base is represented by volcanic flows in the Vestbakken volcanic province west of the Stappen High, and corresponds to the top of faulted blocks south of the Stappen High. Unit R was deposited in a deep rift basin, offset from the Stappen High by major faults that already exhibited substantial relief. Initial sedimentation into the basin was probably dominated by mass movements; the upper parts of unit R are more indicative of a slowly subsiding basin. Unit B represents syntectonically deposited sediments related to a second period of extension and faulting. Deposition was concentrated in half-grabens adjacent to the major fault zone west of the Stappen High. The base of unit B truncates the upper parts of the underlying unit R.

Base-TeC (equivalent to base-unit III of Spencer et al. 1984) represents the base of the prograding part of the Cenozoic wedge. The thickness of unit TeC generally does not exceed 1 s TWT. The lower part of the unit is largely restricted to the lower continental slope and rise west of the Stappen High, and was probably transported through a large submarine canyon at the western edge of this structure. Overlying strata show eastward onlap onto the continental slope. The last phase of sedimentation is marked by progradation along the entire margin and shelf edge migration of about 20-40 km from near the Senja Ridge towards the west. Richardsen et al. (1992) have identified 6 sequences s.s. within TeC, C1-C6, which they related to the 3rd-order cycles of eustatic sea level on the Haq et al. (1987) chart.

Base-TeD is in most places identified as the strongest of a set of parallel reflectors. Unit TeD is a prograding succession deposited over the entire margin; during this interval the paleo-shelf edge prograded 10-25 km to the west. In contrast to the older units TeB and TeC, which have their depocentres west of the Stappen High, the thickness maximum (more than 2 s TWT) occurs southwest of the Stappen High. This is interpreted to indicate uplift of the shelf and adjacent land areas in this area. The unit is characterised by a chaotic reflection pattern, which is probably indicative of extensive slumping on the lower paleo-continental slope and rise, perhaps as a result of the increased sedimentation rates inferred for this unit. A detailed sequence stratigraphic analysis by Knutsen et al. (1992) discerned 9 sequences s.s. within TeD, D1-D9. All these sequences are truncated by a pronounced erosional surface interpreted as a huge slide scar, overlain by a more than 500 ms thick chaotic unit (facies A) and an almost equally thick acoustically stratified unit (facies B). This has been interpreted as a single large-scale slide/slump event, with facies A representing slid blocks and associated debris or mud flows, and facies B representing later turbidites which have filled in most of the slide scar.

The uppermost unit TeE is equivalent to unit IV of Spencer et al. (1984). The base-TeE reflector corresponds to the so-called upper regional unconformity or URU (see below) on the Barents shelf, where it is associated with overdeepened, glacially eroded troughs (Vorren et al. 1989). The thickness of unit TeE varies between 0 and 300 ms TWT on the shelf, but increases to a maximum of about 900 ms TWT in an oblong depocentre located below the present shelf break. The unit consists of 4 subunits showing a stepwise seaward progradation of the shelf edge towards its present position; the total progradation amounts to 30 km. There is abundant evidence of mass movements in this unit, as exemplified by a large slide scar — still evident in the bathymetry — on the southern flank of the Bear Island Cone.

High-resolution studies of the outer shelf

[1] Solheim & Kristoffersen (1984) have described the sedimentary succession overlying a regional angular unconformity known as URU in Bear Island Trough on the Barents shelf. URU separates an upper horizontally stratified or transparent section from underlying dipping and well stratified strata. This boundary is everywhere clearly defined, except on Spitsbergenbanken. At least three erosional surfaces (α , β and γ) were identified, extending from the inner part of the shelf to the shelf break, and delimiting four seismic sequences (I - IV, from the youngest downwards) above the upper regional unconformity. The entire section corresponds to the youngest unit IV or TeE described by Spencer et al. (1984) and Vorren et al. (1990, 1991), respectively.

[2] Sættem et al. (1991, 1992) have defined informal, local seismic units, named A_0 (oldest) to G (youngest), in the outer Bear Island Trough (Fig. 17a). These units are interpreted to mainly consist of continental shelf and upper slope deposits bounded by erosional surfaces which gradually become conformable to the west. The angular unconformity forming the base of unit A_0 corresponds to the base of what the authors call "the main clastic wedge" (which is in fact the prograding part of the wedge, or the Bear Island Cone proper), whereas the base of unit B is identical to URU. It follows that units A_0 and A correspond to unit III of Spencer et al. (1984) or to the combined units TeC and TeD of Vorren et al. (1990, 1991), and the younger units B-G to unit IV or unit TeE (Fig. 15).

Unit A_0 is characterised by internal reflectors which downlap westwards on the basal unconformity. Conspicuous observations include a number of ridges, with internal reflections resembling climbing megaripples, and large channels that were cut into the unit during several phases and partly re-excavated in unit A time. These channels have the form of deep broad valleys, cutting about 150 ms below the plane defined by the base- A_0 unconformity; they are interpreted as glacial troughs instead of submarine canyons, as was suggested (see above) by Vorren et al. (1990) and Richardsen et al. (1992). The channel infill is mainly well stratified, though complex.

Unit A includes the acoustically transparent or chaotic infill of the broad channels cut into the A_0 /A boundary; the rest of the unit is characterised by irregular, discontinuous reflections.

Unit B is mostly acoustically structureless. Paleo-shelf breaks with a similar transition from flatlying shelf deposits to dipping slope deposits with slump features as seen on the present-day sea bed are preserved both at the base and top of this unit.

Units C and D comprise a rather thick interval on the outer shelf and upper slope. Chaotic reflections are observed on the outer paleo-continental shelf / upper slope transition at the base of unit C. Otherwise, the seismic facies is mostly transparent, except for a high-amplitude reflector within unit D separating the two subunits D_1 (lower) and D_2 (upper).

Unit E displays a well developed and coherent internal acoustic stratification, which strongly contrasts to the facies of the units above and below. The seismic unit is in places more than 60 ms thick. Incised channels locally cut into the upper surface, and in the north the unit is truncated by the base of unit F.

Unit F is acoustically transparent or has faint, irregular and discontinuous reflections. The F/G boundary is commonly irregular and diffuse.

Unit G covers the entire trough area and is mostly acoustically transparent, though faint, irregular, discontinuous internal reflectors are sometimes observed. An exception to this is formed by the chaotic subunit G_1 , the surface of which exhibits considerable relief. Unit G is affected by gravity-induced collapse of the upper slope, in a water depth of about 500 m.

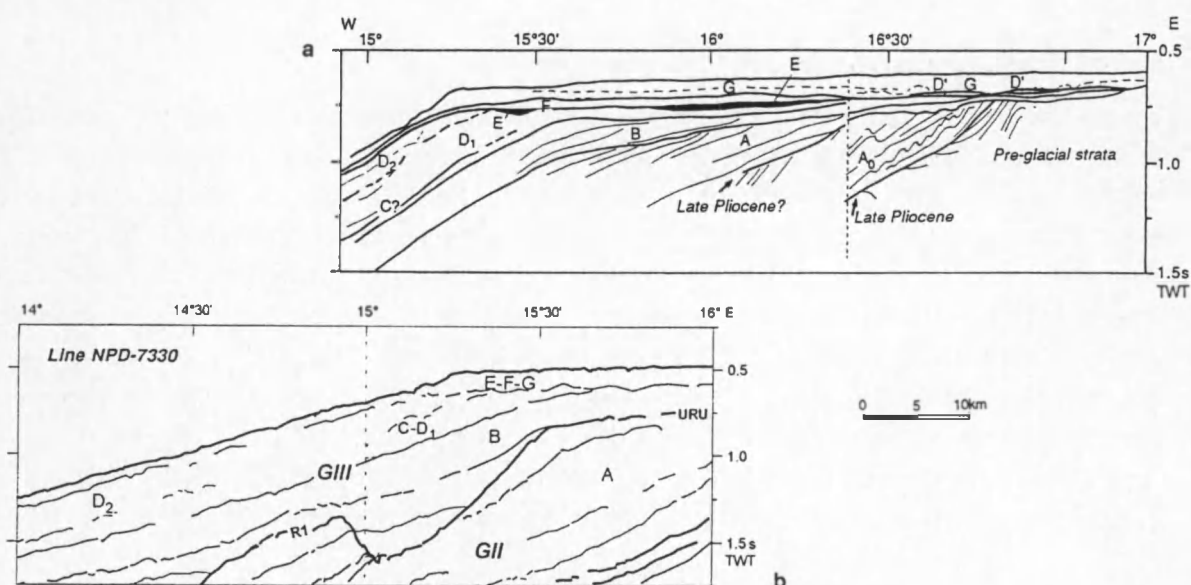


Fig. III.17 - [a] Cross-section of outer Bear Island Trough along 73°30' N, outlining the stratigraphic units identified by Sættem et al. (1991, 1992). **[b]** Line drawing of low-resolution seismic profile NPD-7330 along the same latitude, illustrating the eastward pinch-out of a significant interval against URU.

5.2.2. The Svalbard margin (75° - 79° N)

The clastic wedge underlying the continental shelf and slope off western Spitsbergen has received far less attention than its southern counterpart. The work of Schlüter & Hinz (1978) still forms the basis for most of the stratigraphic work on this part of the margin. These authors have determined three depositional units off central Spitsbergen: SPI-I to SPI-III (from the seafloor downwards), separated by the westward dipping regional unconformities U1 and U2 (Fig. 16b). This partition was extended to the remainder of the margin (Fig. 16a and c) by Myhre et al. (1982) and Myhre & Eldholm (1988). An identical division has been put forward by Vogt et al. (1978), who termed their boundaries X (~ U1) and Y (~ U2), however.

The oldest unit SPI-III is comprised between reflector U2 and the oceanic basement. Its thickness exceeds 2 s TWT below the continental slope, pinching out towards the Knipovich Ridge where U2 terminates against the axial mountains (Myhre & Eldholm 1988). The reflection pattern just seaward of the Homsund Fault Zone indicates a very rapid history of deposition: the sediments were probably dumped into a young immature rift basin. Further downslope several reflecting horizons are evident terminating westwards onto the igneous oceanic crust (Myhre et al. 1982).

Unit SPI-II varies in thickness between 0.1 and 0.5 s TWT, again pinching out on the basement highs near the Knipovich Ridge (Myhre & Eldholm 1988). A chaotic internal reflection pattern renders this unit its rather typical appearance. This pattern is thought to be indicative of slump deposits; the hummocky nature of the overlying unconformity U1 supports this interpretation.

The uppermost unit SPI-I forms a prograding wedge beneath the outer shelf and slope, showing seawards migration of the shelf edge by up to several tens of kilometres. The maximum thickness is almost 2 s, slightly decreasing to the north. The unit locally blankets the eastern axial mountains of the spreading ridge, and even partly fills the rift valley itself (Myhre & Eldholm 1988). SPI-I exhibits divergent to sub-parallel seismic reflections, but the pattern becomes more complex beneath the inner shelf. Within the area of the Knipovich Ridge, the unit is locally contorted and faulted.

5.2.3. A regional stratigraphic framework (70° - 77° N)

The absence of good tie lines has long prevented a direct correlation of the regional reflectors of the northern Svalbard margin and those recognised in the SW Barents Sea. The three units of Schlüter & Hinz (1978) are best developed north of about 76° N. Further south the seismic character of units SPI-II and III changes and their boundary (U2) becomes less pronounced; in particular unit SPI-II loses its characteristic chaotic facies and becomes more stratified than off Svalbard (Myhre & Eldholm 1988). From the opposite side, reflector A is recognised on the Barents Sea margin at least as far north as southernmost Svalbard (Faleide et al. 1984), but has not been identified along the Svalbard margin. A tie between both stratigraphies was not established, however. The dating proposed by Schlüter & Hinz (1978) for their reflector U2 (refer to section 5.2.4.1) suggested a correspondence to reflector A, whereas according to Myhre & Eldholm (1988) unit SPI-I, and perhaps SPI-II as well, lies within the uppermost unit IV of Spencer et al. (1984).

Recently however, Faleide et al. (in press), using a more extensive data base and inspired by new chronostratigraphic evidence (see section 5.2.4), established a direct tie between the stratigraphies developed for both parts of the margin. They proposed a stratigraphic framework of seven regionally-significant reflectors, R1 (youngest) to R7 (oldest), for the entire Barents Sea - Svalbard margin (Fig. 18). The seismic character of some reflectors and units can show considerable variation along-strike of the margin, however.

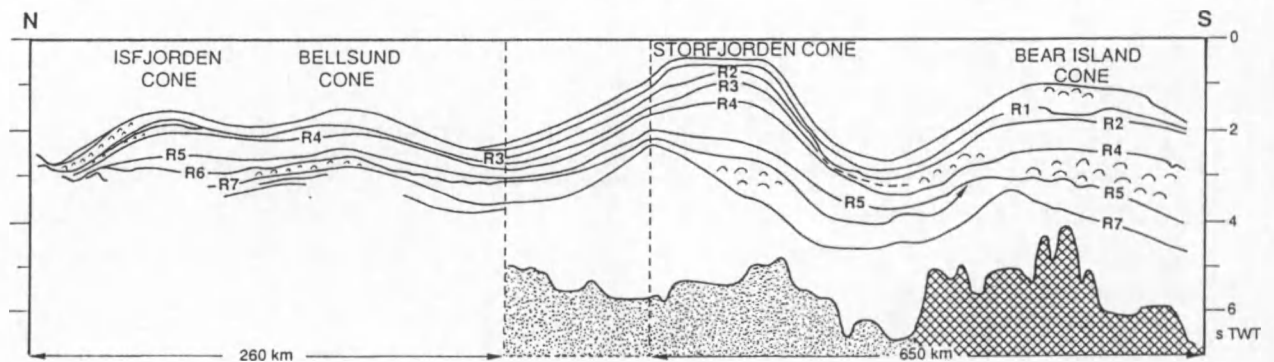


Fig. III.18 - Long seismic transect parallel to the western Barents Sea - Svalbard margin, demonstrating the regional stratigraphic framework developed by Faleide et al. (in press), and chaotic facies occurrences.

The lowermost reflectors R7 and R6 correspond to Schlüter & Hinz's (1978) reflectors U2 and U1, respectively. The sediment interval in between, corresponding to unit SPI-II, is characterised by a distinct chaotic reflection pattern lacking continuous internal reflectors in the type locality off central Spitsbergen (section 5.2.2). This signature was attributed to the action of extensive mass wasting processes. The unit is seen to change character towards the south however, becoming more stratified (cf. Myhre & Eldholm 1988). In the depocentre off Storfjorden Trough the chaotic pattern reappears, in app. 200 ms thick intervals bounded by continuous reflectors (Hjelstuen et al., in press); in the Bear Island Cone further south the interval is again stratified. While R7 remains a prominent boundary all along the transect, R6 gradually loses distinction and is eventually eroded by R5 on the northern flank of the Bear Island Cone. R7 in this area defines the base of the prograding part of the sedimentary wedge, and thus correlates with Rønnevik's (1981) and Faleide et al.'s (1984) reflector A, and with base-unit III of Spencer et al. (1984) and base-TeC of Vorren et al. (1990, 1991).

R5 probably is the most conspicuous seismic horizon along the entire margin. The reflector was defined in the Storfjorden region, where it constitutes a prominent erosional surface, truncating R6 and locally even R7 on the upper paleo-continental slope (Hjelstuen 1993; Hjelstuen et al., in press). On the shelf along the Svalbard margin R5 represents the upper regional unconformity (Solheim et al., in press), and on the Barents shelf R5 deeply erodes into Paleogene strata east of the Senja Ridge; the erosional channels reported by Sættem et al. (1992) (see section 5.2.1) at their A_0/A boundary in the outer Bear Island Trough probably occur at the same horizon. Truncation of R6 on the northern flank of the Bear Island Cone indicates that R5 represents an important erosional event in the deep sea as well. In most places R5 is identified as the top of a set of high-amplitude reflectors. In addition, the reflector defines the lower limit of a very thick and extensive chaotic unit in the Bear Island Cone. The base of this chaotic interval jumps to progressively higher stratigraphic levels towards the north, however. R5 corresponds to base-TeD of Vorren et al. (1990, 1991).

The facies of the chaotic unit, characterised by numerous diffraction hyperbolae, is not entirely identical to that observed between R7 and R6 adjacent to Svalbard, but it too is inferred to result from mass movements. These mass movements took place during several phases and have strongly disturbed the original stratigraphy on the middle and lower slope south of the Storfjorden Cone, thus strongly hampering the N-S correlation of especially reflectors R2 - R4. The major correlation barrier seems to be located at app. $73^{\circ}30'$ latitude, where a striking lateral transition occurs from an apparently stratified facies in the north, containing the reflectors R2 - R4, to the chaotic facies in the south.

Reflector R4 is an important unconformity on the Svalbard margin, characterised by a basinward shift of facies and onlap of overlying strata (Andersen et al. 1994). The boundary defines the initiation of two individual depocentres, off Isfjorden and off Bellsund. The significance of R4 decreases towards the south however, before it entirely disappears in the chaotic interval. R4 has not been identified on the Bear Island Cone.

Reflectors R3 and R2 delimit the base and the top, respectively, of a thin (about 200 ms TWT) but rather conspicuous chaotic interval at the foot of the continental slope in the Storfjorden Cone (Hjelstuen 1993). This interval represents an outlier of the much thicker chaotic interval on the Bear Island Cone. The development of the chaotic interval will be dealt with in more detail later (section 6.4). Both R3 and R2 are truncated by R1 north of $73^{\circ}30'$ N.

The uppermost reflector R1 is easily recognised as the second most important surface on the western Barents Sea margin. It is a high-amplitude reflector defining the upper limit of the chaotic interval described above. Where the reflector effectively bounds this interval, it has a hummocky character. R1 also exhibits a striking erosional ramp — interpreted as the edge of a buried slide scar — on the southernmost part of the margin, near $73^{\circ}30'$ N. Additionally, R1 is the lateral (downslope) equivalent of the reflector defined as URU in Bear Island Trough (Solheim & Kristoffersen 1984). R1 is not identical to base-TeE of Vorren et al. (1990, 1991) though; this boundary is interpreted to terminate against R1 by simple onlap (infilling the relief of the slide scar), not truncating this reflector. The post-R1 unit is thus somewhat thicker than unit IV of Spencer et al. (1984) and unit TeE of Vorren et al. (1990, 1991). This youngest unit is generally well stratified, with internal reflectors of relatively great lateral continuity; its seismic character is more or less uniform along the whole margin. There is still some evidence of mass wasting, but on a smaller scale than before, as has been confirmed by higher-resolution seismic data from the Svalbard margin (Andersen et al. 1994) and from the Storfjorden and Bear Island Cones (Laberg 1994).

Based on the relative importance of the regional reflectors, Faleide et al. (in press) put forward a hierarchy, consisting of four higher-order units or informal “megasequences”: *G0* (pre-R7), *G1* (R7-R5), *GII* (R5-R1) and *GIII* (post-R1). The megasequences *G1*-*GIII* were related to the glacial history of the margin, which will be discussed later (section 7). *G1* is the first unit showing strong progradation. A significant change in depositional pattern is indicated above the *G1*/*GII* boundary, as *GII* is characterised by large-scale mass wasting processes. *G1* and *GII* pinch out eastwards, due to truncation by the upper regional unconformity, and westwards by termination onto oceanic crust. The *GII*/*GIII* boundary marks another transition of depositional style to smaller-scale mass movements. *GIII* has developed a thickness maximum below the present shelf edge, thinning eastwards on the shelf and westwards downslope.

5.2.4. Age constraints

Age control of the identified horizons has long remained — and in part still is — very poor, a fact which has strongly handicapped seismic stratigraphic studies of the Barents Sea - Svalbard margin. Early datings had to rely on correlation to one single drillhole: DSDP Site 344, located on the eastern flank of the Knipovich Ridge (Talwani, Udintsev et al. 1976). Some years later the results became available of a deep exploration well (7117/9-1) on the Senja Ridge in the Barents Sea (Spencer et al. 1984). Additional information had to be obtained indirectly, by tracing reflectors until termination onto oceanic crust of known age³, by relating depositional events to the general opening history of the Norwegian-Greenland Sea (cf. section 4), and by comparison with the eustatic sea level cycle chart, first published by Vail et al. (1977) and later updated by Haq et al. (1987). Seismic stratigraphic correlations published in literature were strongly biased by the latter approach, in which important angular unconformities are linked to major drops of global sea level, and in particular by the search for the pronounced mid-Oligocene sea level fall. Some authors even managed to recognise all sea level cycles since the Middle Miocene in their stratigraphy. However, redating of the exploration wells on the Senja Ridge (Eidvin & Riis 1989, Eidvin et al. 1993) and recent results from shallow drillholes on the Barents shelf SW of Bear Island (Sættem et al. 1991, 1992, 1994; Mørk & Duncan 1993) have provided exciting new constraints on the chronological framework for the sedimentary wedge, quite contrasting to earlier notions. The position of all available wells is indicated in Table 3 and Fig. 19. The following is a line-up — in chronological order — of the most significant evidence presented so far for the important boundaries defined in this study. A summary is included in the general correlation table of Fig. 15.

5.2.4.1. The basal unconformity R7

On the Svalbard margin, reflector U2 was not cored in DSDP Site 344, which is located on the distal parts of the Storfjorden Cone, about 16 km short of the actual spreading axis of the Knipovich Ridge. This implies that the unconformity is older than about 5-7 Ma, the age of the oldest sediments recovered in the drillhole (Talwani, Udintsev et al. 1976). Schlüter & Hinz (1978) therefore proposed a correlation with the mid-Oligocene sea level drop at 30 Ma. This dating was questioned by Myhre et al. (1982) however, who noted that the U2 horizon extends onto the young axial mountains on the eastern flank of the Knipovich Ridge, where oceanic crust is probably as young as 5-6 Ma old. Hence, Myhre & Eldholm (1988) inferred that the Messinian sea level low stand (5.5 Ma) is the oldest event that could have created this unconformity.

³ Bearing in mind, however, that the magnetic field in the northern Greenland Sea is anomalously quiet, and that no magnetic anomalies have been identified north of the Greenland-Senja FZ (Myhre et al. 1982).

Dating of reflector A on the Barents Sea margin evolved through a rather analogue series of steps. Rønnevik (1981) observed reflector A lapping out onto oceanic crust between magnetic anomalies 5 and 13, which would date the boundary as somewhere between 10 and 35 Ma old. The author again favoured correlation with the global eustatic break at 30 Ma, herein followed by Faleide et al. (1984). On the basis of biostratigraphic dating in exploration well 7117/9-1 on the Senja Ridge Spencer et al. (1984) independently made the same correlation. In the well a major hiatus was recorded between units II and III, from intra-Oligocene to possibly Miocene. On ground of its onlapping geometry, unit III is inferred to become older down-dip to the west and may thus extend well into the Oligocene. Vorren et al. (1990) traced their Base-TeC reflector until downlap against oceanic crust in an area between magnetic anomalies 7 and 13, a slightly smaller time window than indicated by Rønnevik (1981). They correlated the reflector to the 30 Ma sea level fall as well. In a later publication, Vorren et al. (1991) revoked this correlation to the intra-Miocene global eustatic lowstand in the period 15.5 - 10.5 Ma. More recently, however, Fiedler (1992) has shown the same horizon, reflector R7, to terminate in the Lofoten Basin against oceanic basement with a maximum inferred age of 4.8 - 5.4 Ma. Large uncertainties linked to increasing basement relief in the proximity of the spreading axis make that R7 may even be younger. The maximum age of R7 was therefore set to 5.2 Ma, i.e. early Pliocene.

Some years ago Eidvin & Riis (1989) and Eidvin et al. (1993) redated the exploration wells 7117/9-1 and 7117/9-2 on the Senja Ridge. They noted that a lot of microfossils are severely reworked, and that the earlier age assignments by Spencer et al. (1984) are most likely wrong. Based on biostratigraphic and Sr-isotope analyses of material interpreted as in situ, they concluded that sediments immediately overlying the hiatus corresponding to the unconformity defining the base of the Bear Island Cone (R7), were deposited after the Early/Late Pliocene boundary (3.4 Ma; Berggren et al. 1985), but before 2.3 Ma. Taking into account paleoclimatic indicators such as IRD- and oxygen isotope records from the Norwegian Sea (Jansen & Sjøholm 1991) a most likely age of 2.6 Ma, coeval with the onset of large-scale glaciations in the northern hemisphere (see section 7.1), was put forward for this boundary. The Bear Island Cone would thus have been deposited essentially during the Plio-Pleistocene. Though Vorren et al. (1990, 1991) agreed with these new well datings, they disputed the correlation to the stratigraphy further downslope, and in particular the implications for the age of base of the Bear Island Cone. The eastward-onlapping geometry of reflectors within unit TeC indicates that the lower parts of the cone are not represented in the wells on the Senja Ridge; according to Vorren et al. (1991) unit TeC is entirely lacking or at most represented by its very youngest part in well 7117/9-1, thus implying that the cone contains much sediments older than Plio-Pleistocene. Recent $^{40}\text{Ar}/^{39}\text{Ar}$ dating of 2 volcanic clasts in a shallow drillhole (7316/03-U-01) SW of Bear Island (Mørk & Duncan 1993) indicates, however, that most of the cone is indeed contained within the two exploration wells; the volcanoclastic material is inferred to be positioned immediately *below* the basal unconformity, and yielded a crystallisation age of c. 2.3 Ma. This is probably the most convincing evidence presented so far for the young age of R7, though its conclusiveness may be somewhat attenuated by the resolution of the seismic record, the accuracy of the seismic correlation, and the uncertainty imposed by the conversion of reflection time to metres below sea floor.

The new data clearly demonstrate that the major depocentres along the Barents Sea - Svalbard margin are considerably younger than previously assumed. An age of 2.6 Ma for their basal unconformity will be used hereafter.

Drillsite ID	Position	Core depth	Operating institution	References
Site 344	76° 08.98' N 07° 52.52' E	414 m	DSDP	Talwani, Udintsev et al. (1976)
7117/9-1	± 71° 24.60' N ± 17° 57.00' E	1180 m	Consortium of oil companies	Spencer et al. (1984); Eidvin & Riis (1989); Eidvin et al. (1993)
7117/9-2	± 71° 28.20' N ± 17° 54.60' E	1120 m	Consortium of oil companies	Eidvin & Riis (1989); Eidvin et al. (1993)
7119/7-1	± 71° 26.40' N ± 19° 40.80' E	± 950 m	Consortium of oil companies	
7316/5-1	73° 31' N 16° 26' E	4027 m	Consortium of oil companies	Eidvin et al. (1993)
7316/03-U-01	73° 52.93' N 16° 54.48' E	193 m	IKU	Mørk & Duncan (1993); Sættem et al. (1991, 1992, 1994)
7316/06-U-01	73° 33.27' N 16° 49.98' E	108 m	IKU	Sættem et al. (1991, 1992, 1994)
7316/06-U-02	73° 34.12' N 16° 50.02' E	200 m		
7317/10-U-01	73° 08.98' N 17° 16.22' E	225 m		
7317/02-U-01	73° 49.18' N 17° 22.08' E	57 m		
7317/02-U-02	73° 47.13' N 17° 23.60' E	± 50 m		

Table III.3 - Key data for drillholes available on the western Barents Sea - Svalbard margin.
DSDP = Deep Sea Drilling Project, IKU = Institutt for Kontinentalsokkelundersøkelser.

5.2.4.2. The prominent erosional unconformity R5

The age of R5 is far less constrained than the other major boundaries R7 and R1. DSDP Site 344 (Talwani, Udintsev et al. 1976) has yielded only indirect information. This site was originally intended to core through reflector U1 (~ R6), which separates an upper thin section of acoustically stratified sediments from a thicker transparent to chaotic unit below (cf. sections 5.2.2 and 5.2.3). The uniform lithology of the recovered sediments suggests however that the entire succession at the drill site corresponds to the transparent unit, and that the overlying unit is very thin or even entirely pinched out at this location. Biostratigraphic age control in the upper part of the sediment column is quite poor, but nannofossils suggest that the Plio-Pleistocene boundary is recorded some 125 m below the seafloor. This would imply that reflector R6, and consequently also reflector R5, is younger than 1.8 Ma.

On the southern part of the margin Vorren et al. (1990) observed that the basal reflector of unit TeD downlaps onto oceanic crust just east of magnetic anomaly 5, dating back to between 19 and 9 Ma. Correlation was therefore suggested with the intra-Miocene sea level low between 15.5 and 10.5 Ma.

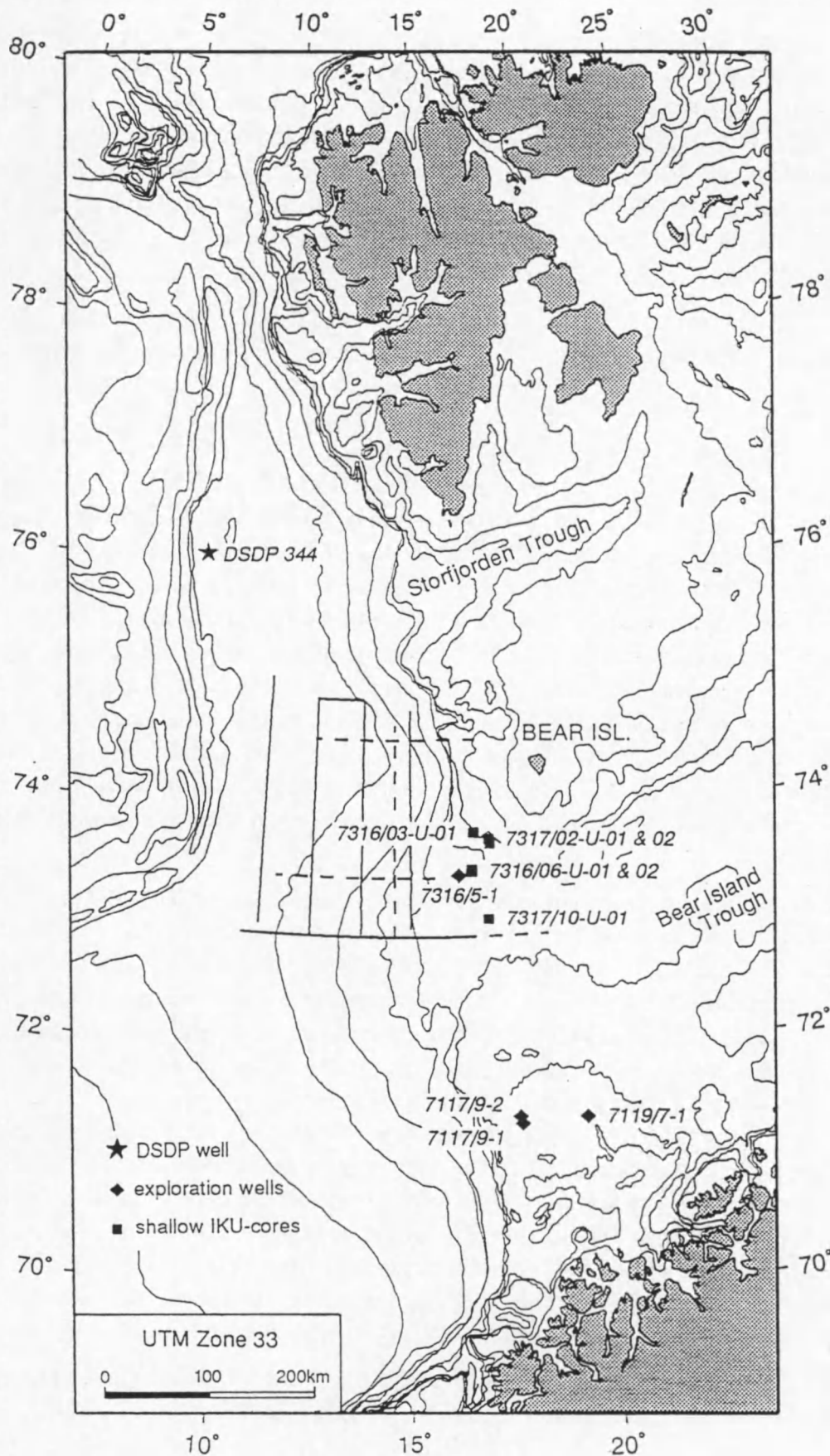


Fig. III.19 - Location of drillholes along the western Barents Sea - Svalbard margin, relative to the available seismic grid.

Considering the new evidence presented by Eidvin & Riis (1989) for the Senja Ridge wells, but modulated to their own observations (base-TeC gets older seaward of the drill site, and base-TeD comes close to the basal part of the Neogene section in one of the wells), Vorren et al. (1991) subsequently placed the boundary at c. 3 Ma. Although the unconformity R5 is indeed penetrated by the drillholes on the Senja Ridge, the age of this reflector (their Reflector 2) was not commented upon by Eidvin & Riis (1989) or Eidvin et al. (1993). But according to one of their figures (Fig. 13 of Eidvin et al. 1993) Sr-isotope datings of 0.55 and 1.3 Ma were obtained for sediments overlying the unconformity, and an age of 2.05 Ma for sediments below.

Faleide et al. (in press), finally, have tentatively linked R5 to the intensification of glaciations witnessed by Norwegian Sea oxygen isotope records (Jansen & Sjøholm 1991) around 1 Ma (see section 7.1).

5.2.4.3. The upper regional unconformity R1

The only other regional boundary with seismic tie to well information is R1. The upper regional unconformity is interpreted as a buried glacial erosional surface (Solheim & Kristoffersen 1984). The age of this surface is therefore related to the glaciation history of the Barents Sea. Solheim & Kristoffersen (1984) originally suggested a mid-Pliocene age for this boundary. This is more or less in accordance with the results of Spencer et al. (1984), who noted that in well 7117/9-1 URU is overlain by glaciomarine sediments and therefore assigned it an age of late Pliocene. Eidvin et al. (1993) on the other hand find that the biostratigraphic resolution in the Senja Ridge wells is not sufficient to accurately date URU. Vorren et al. (1988) have suggested that glaciation of the Barents shelf proper did probably not start before app. 0.8 Ma, when a change occurred in northern hemisphere glaciations to larger ice volumes and lower frequencies, from 41 to 100 ka cycles (Ruddiman et al. 1986). This would probably be the time when URU was created (Vorren et al. 1990, 1991).

R1 can also be traced to the shallow (few tens of metres) boreholes cored by IKU in the outer Bear Island Trough, near the eastern limit of the Plio-Pleistocene sediment cone. Recovery of this section was best for holes 7316/06-U-01 (21 %) and 7317/10-U-01 (9 %). Sediments overlying the unconformity (their A/B boundary) were dated by magnetopolarity and amino acid analyses (Sættem et al. 1991, 1992). Magnetostratigraphy indicates that all these sediments were deposited during the current Brunhes normal polarity epoch, yielding a maximum age of 730 ka, the time when the Brunhes epoch started (Berggren et al. 1985). From amino acid measurements on shell fragments and foraminifera an age of 440 ka is indicated. The youngest part of the underlying unit remains undated, however, and an older age for the unconformity can thus not be excluded. In particular, the seismic data used in the present study show that an up to 300 ms thick sediment interval, perched between R1 and a younger reflector (base-TeE of Vorren et al. 1990, 1991) formerly interpreted as the lateral equivalent of URU, pinches out towards the shelf (Fig. 17b); R1 thus represents a significant hiatus in the drillholes. As the ages determined by Sættem et al. (1991, 1992) are maximum ages, however, an age bracketed between 440 and 730 ka will further be assumed here.

In addition, Sættem et al. (1991, 1992) were able to date some of their younger unit boundaries as well. The following ages were inferred: 330 ka (B/D), 200 ka (D_1/D_2), 130 ka (D/E) and 30 ka (both E/F and F/G).

5.2.5. Link to geological history

Whereas the distribution of early and middle Cenozoic sediments along the western Barents Sea - Svalbard margin closely reflects the history of opening of the Norwegian-Greenland Sea, the late Cenozoic sediments were deposited in response to the glacial history of the margin, as is clearly demonstrated by the individualisation of huge depocentres at the mouth of the large glacially-eroded troughs on the shelf. The base of the wedge is time-transgressive from south to north, corresponding to the northward migration of seafloor spreading in the adjacent oceanic basin. As Svalbard probably was glaciated before the Barents shelf, the glacial/pre-glacial facies boundary is supposed to show a diachronous character in the opposite direction (Vogt 1986).

Several authors have related the deposition of each of their units to different phases of the geological history of the margin. Not surprisingly (the young age of a large part of the wedge was only recently revealed), the glacial aspect has long been underestimated.

Spencer et al. (1984) and Vorren et al. (1990, 1991) both attributed the deposition of their lowermost unit, unit I respectively unit TeA, to the earliest phase of seafloor spreading south of the Greenland-Senja Fracture Zones, between late Paleocene and early Eocene. These units are largely restricted to the landward side of the OCT. Base-unit II/TeB is correlated to the northward propagation of the spreading ridge in the early Eocene. This event also resulted in the reactivation of some earlier generated faults. Unit II/TeB was thus deposited west of the Stappen High during rifting and early seafloor spreading NE of the Senja FZ. Deposition of the westwards prograding units III and IV / units TeC-TeE is linked to the thermal and isostatic subsidence following termination of shear movements along the Hornsund FZ, and subsequent spreading along the entire margin, since Oligocene times. The Svalbard area was probably uplifted during deposition of unit TeD, as suggested by a southward shift of the depocentre. Whereas it is suspected (Vorren et al. 1991) that much of unit TeD was deposited already in a glaciomarine environment, unit IV/TeE accumulated during the Plio-Pleistocene when the Barents shelf was repeatedly glaciated.

This scenario was slightly modified by Richardsen et al. (1991), who inferred that their unit R (older part of TeB) was deposited contemporaneously with the early phase of seafloor spreading SW of the Greenland-Senja FZ. Unit B (younger part of TeB), which is related to a second period of uplift and faulting, is interpreted as a syn-rift unit related to rifting prior to a second phase of seafloor spreading NE of the Senja FZ. Base-unit TeC is thought to represent the break-up unconformity, created when seafloor spreading got underway all along the margin. The intermediate stage of spreading would thus have been of minor importance.

The northern part of the sediment wedge, in front of the Hornsund FZ, was mainly deposited onto oceanic crust, implying that all these sediments post-date the early Oligocene initiation of seafloor spreading along the Svalbard margin (Myhre et al. 1982). Unit SPI-II has been interpreted to result from the uplift of Svalbard since app. Miocene times, whereas SPI-I was deposited under the influence of a glacial regime (Myhre et al. 1982).

In view of the revolutionary new age datings discussed in section 5.2.4, a lot of these interpretations need to be revised however, especially with respect to the proportion of glaciogenic sediments in the wedge: it has become clear now that the upper half of the Cenozoic wedge accumulated during Plio-Pleistocene glaciations of the shelf. Sættem et al. (1994) gave an account of geological evolution and related sedimentation for a limited area SW of Bear Island, without establishing a link with the stratigraphies discussed above, though. The relation between stratigraphy and glacial evolution will be discussed for megasequences GI-GIII in section 7 at the end of this chapter, whereas the relation of the older unit G0 with the tectonic evolution will be outlined below (section 5.3.3).

5.3. A detailed seismic stratigraphy of the northern half of Bear Island Cone

5.3.1. Introductory notes

The seismic reflection data used in the present study are roughly comprised between latitudes 73° and 75° N and longitudes 10° and 16° E. Compared to previous studies (e.g. Vorren et al. 1990, 1991; Richardsen et al. 1991, 1992; Knutsen et al. 1992) the network extends far more seaward, allowing for a more comprehensive investigation of the northern half of Bear Island Cone. Because of the complementary location of the seismic profiles and the overlapping frequency spectrum of the two different data sets a relatively fine-scale stratigraphic analysis could be conducted over the entire vertical extent of the sedimentary column. Dip lines, oriented east-west, disclose the lateral outbuilding of the margin at different latitudes (Fig. 20), whereas north-south oriented strike lines (Fig. 21) give a good overview of the lateral thickness and facies variations, particularly with respect to the more northwards located Storfjorden Cone.

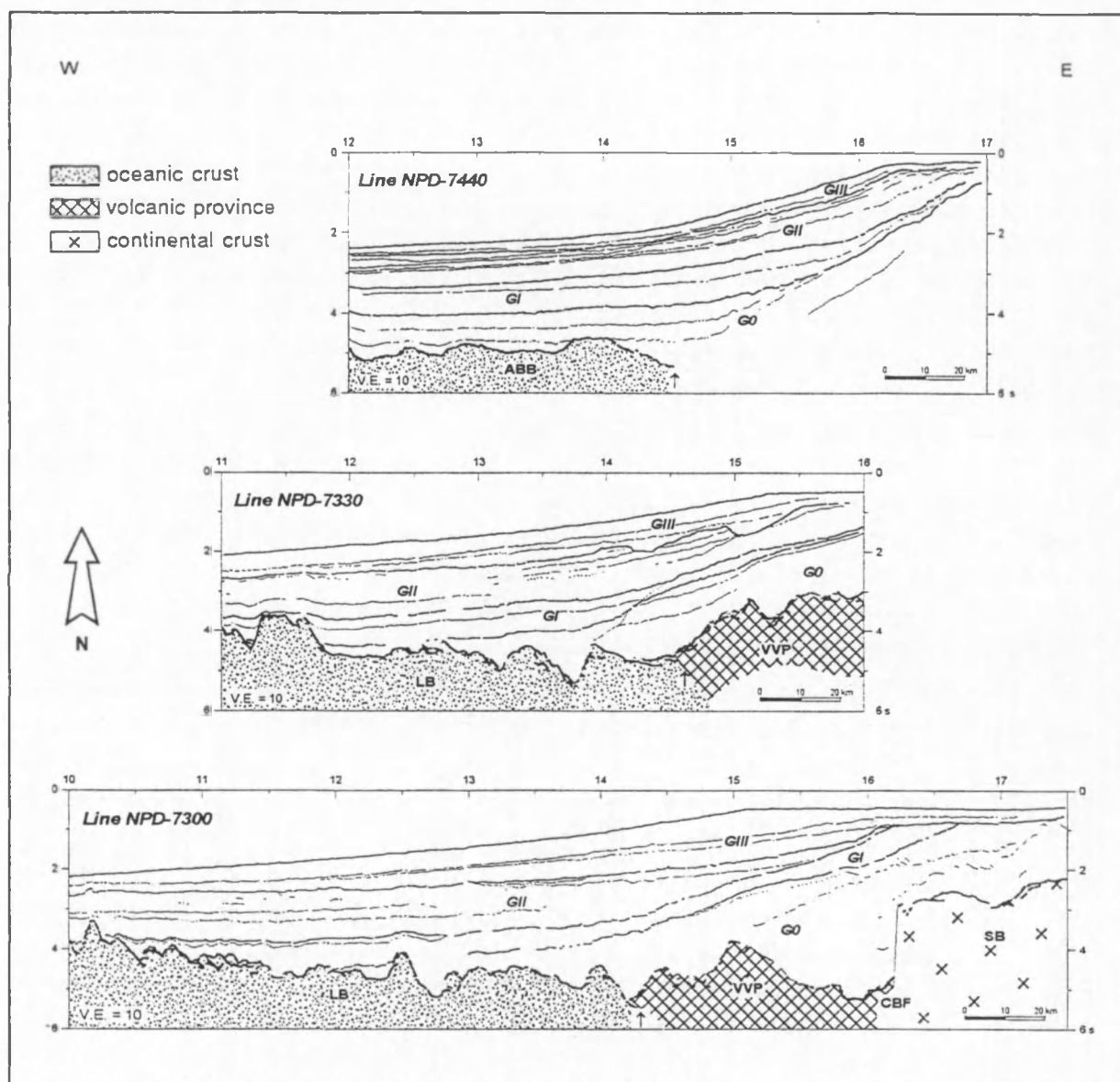


Fig. III.20 - Interpreted dip line sections, showing first-order stratigraphic units (megasequences G0-GIII) and most important seismic horizons. ABB = "Anti-Boreas Basin", CBF = continental boundary fault, LB = Lofoten Basin, SB = Sørvestsnaget Basin, VVP = Vestbakken volcanic province. Arrows mark the landward limit to where oceanic crust can be identified.

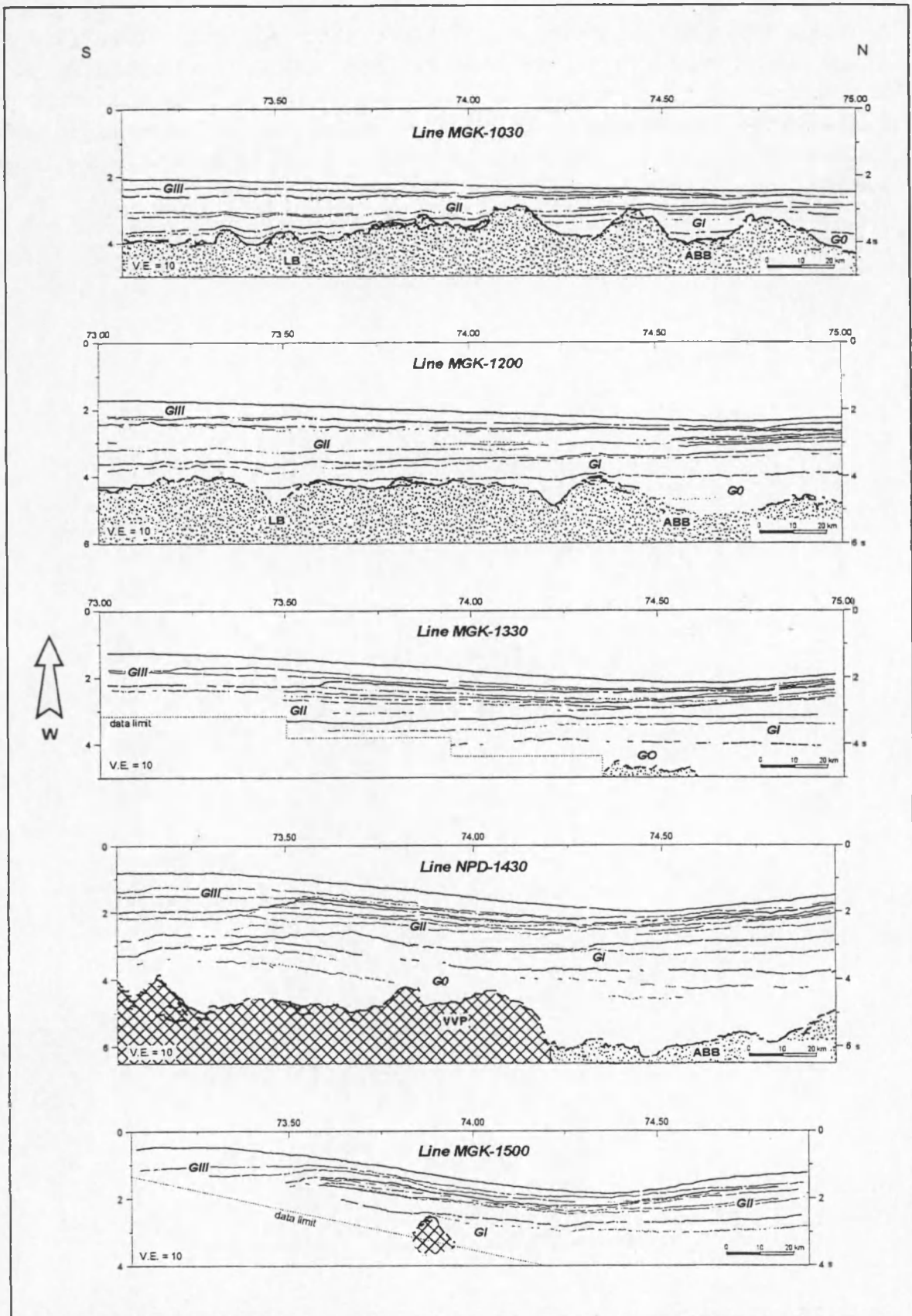


Fig. III.21 - Interpreted strike line sections, showing first-order stratigraphic units (megasequences G0-GIII) and most important seismic horizons. ABB = "Anti-Boreas Basin", LB = Lofoten Basin, VVP = Vestbakken volcanic province. Arrows mark the landward limit to where oceanic crust can be identified. Symbols follow legend in Fig. 20.

Higher-resolution studies (e.g. Sættem et al. 1991, 1992; Laberg & Vorren, in press a) have sure enough achieved more detail, but were necessarily restricted to the upper sedimentary section, whereas the results of this study can be directly fitted within the margin-wide stratigraphic framework of Faleide et al. (in press). In addition, this study is intended to bridge the gap between two other local seismic stratigraphic studies, one on the Bear Island Cone by Fiedler & Faleide (in press), and another on the Storfjorden Cone by Hjelstuen et al. (in press).

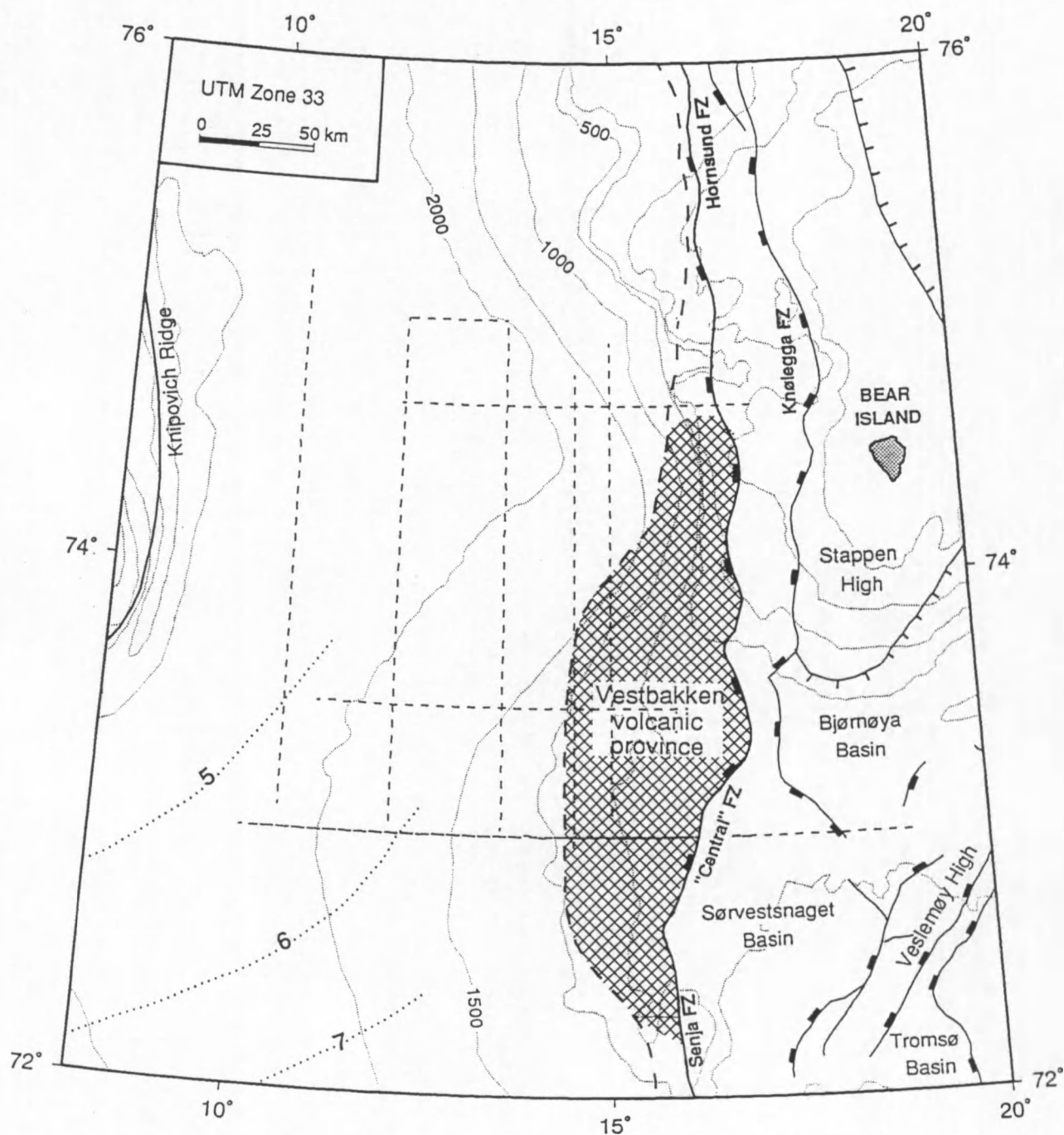


Fig. III.22 - Structural map of the study area, showing fault zones and structural lineaments (full lines), magnetic anomalies (dotted lines), bathymetric contours (faint dotted lines) and seismic grid (dashed lines). Adapted from Faleide et al. (1993).

The study area extends from the outer continental shelf, over the slope, and onto the continental rise, to just short of the mid-oceanic spreading ridge. Structurally, the area includes the continental Sørvestsnaget Basin in the south-east, the Vestbakken volcanic province in the centre, and the oceanic Lofoten and “anti-Boreas” Basins to the west (Fig. 22). It is thus entirely located along the rifted margin segment (informal “Central Fault Zone”), comprised between the Senja Fracture Zone and the Hornsund Fault Zone.

The maximum sediment thickness in the area of investigation amounts to 4.5 s TWT, as observed just seaward of the main continental boundary fault on line NPD-7300 (Fig. 20). Thinning occurs abruptly landward of this fault and more gradually in westward direction. On the westernmost end of line 7300 the sediments are still 1.5 s thick. The stratigraphy of the deposits appears to be very complex, and is for one severely disturbed by various kinds of mass wasting features. The seismic sections show reflectors that are fairly parallel and, except for an extensive and notoriously chaotic interval in the south and west of the region, have good lateral continuity. The overall geometry is characterised by complex sigmoid-oblique offlap in seaward direction, reflecting the lateral outbuilding of the margin. Unconformities are in general not very pronounced, but gain character up-slope. Up to 37 reflectors have been identified, all corresponding to surfaces that are to some extent unconformable in nature and that can be traced over large portions of the area. They have been labeled r1 (oldest) to r37 (youngest)⁴; the acoustic basement reflector is denoted as r0 and the seafloor as r38. The correlation with the regional reflectors defined by Faleide et al. (in press) was fairly well established by close comparison of both interpretations. A summary is in Table 4.

Major units	Seismic horizons	
	Faleide et al. (subm.)	this work
GIII	R0	r38
	R1	r30
GII	R2	r27
	R3	r26
	R4	r23 or r25
	R5	r15
GI	R6	r13
	R7	r8

Table III.4 - Correlation of reflectors identified in this study with the regional unconformities R1-R7 of Faleide et al. (in press).

Not all of the regional reflectors are recognised as important horizons in the study area. On the other hand, reflectors have been identified which are locally more significant than some of the regional reflectors. The first-order partition of the sediment pile into four distinct major units or “megasequences” (G0, GI, GII and GIII) is quite manifest here as well, however. The important

⁴ Small characters *r**n* are used to avoid confusion with the regional reflectors *R**n* defined by Faleide et al. (in press). Note that reflectors in this study are numbered from the bottom upwards, i.e. opposite to the numbering of Faleide et al. (in press).

seismic boundaries identified on the northern portion of Bear Island Cone are: r6, r8, r15, r25, r30 and r35. Reflectors of secondary importance are: r13, (r18), r20, r26, r27 and r34. The line drawings of Figs. 20 and 21 depict these reflectors only. More detailed line drawings, including windows zooming in on selected seismic sections, can be found in separate fold-outs in annexe. They will be referred to in the description and discussion following below. As the present stratigraphic study does not claim to be strictly sequence stratigraphic in nature, the units comprised between two successive boundaries are not believed to correspond to sequences *sensu* Posamentier et al. (1988), except perhaps in the uppermost unit GIII.

In the following pages the stratigraphy, stratal geometry, seismic facies and thickness variations will be described, and the geological implications discussed, for each of the megasequences. A separate section is dedicated to the acoustic basement reflector. Isopach maps have been constructed for the three youngest megasequences GI - GIII, constituting the main prograding wedge. Due to highly irregular basement topography, such a map could not be drawn for G0, and consequently not for the entire sediment pile either, on basis of the limited data set. The isopach map for the combined interval GI-GIII will be presented later, in section 7.

5.3.2. Acoustic basement reflector (r0)

Structurally, the study area is underlain by three types of basement (cf. Fig. 22):

- oceanic crust of the Lofoten and “anti-Boreas” Basins (south and north of about 74° N, respectively) in the west;
- strongly tectonised continental crust east of the Central Fault Zone;
- subaerial volcanic flows of the Vestbakken volcanic province (VVP) associated with the ocean-continent transition.

Thanks to the large seismic penetration, the structural basement on most profiles coincides with an acoustic basement reflector, defining the base of the sedimentary succession. This is particularly true for the NPD-lines, whereas on the MGK-lines the structural basement is masked by strong seafloor reverberations in the eastern half of the region, where no acoustic basement can be identified. The different types of basement can be distinguished on ground of dissimilar acoustic signatures.

Oceanic crust

Where the acoustic basement corresponds to oceanic crust, it is characterised by a broad and high-amplitude reflector, often associated with abundant diffraction hyperbolae reflecting the rough morphology of this surface (Windows 1, 3). The amplitude appears to decrease with increasing depth of burial. Near the OCT the oceanic crust is overlain by a maximum of 4.5 s of sediments. The elevation of the oceanic basement varies strongly over short distances (Fig. 23), but in a general sense increases from about 5.4 s near the OCT in the south-east, to app. 4.5 s in the north-western corner of the study area, concurrently with declining age in that direction, from 36 - 26 Ma (between magnetic anomalies 13 and 7) to less than 10 Ma (anomaly 5). The average depth is 5 ± 0.5 s, quite deep for oceanic crust of this age⁵, but that may be largely due to the weight of the overlying sedimentary depocentre.

⁵ Depths of 3670 m and 4250 m are predicted for oceanic crust 10 Ma and 25 Ma old, respectively, by the empirical age/depth relationship $d(t) = 6400 - 3200 e^{-t/62.8}$ derived by Parsons & Sclater (1977) for the North Atlantic.

The basement surface exhibits strongly varying relief, generally in the order of 300 to 600 ms, but in some places up to 1 s. Due to sparsity of data a contour map could not be drawn for this surface; the irregular relief is adequately visualised in the fence diagram of Fig. 23 however. The relief is most pronounced in the north-west, within a reach of 75 km from the actively spreading Knipovich Ridge. Several basement highs measuring up to 1 s are observed (Window 39); their shape (mounds or ridges?) and eventual strike cannot be determined. Information may be obtained from bathymetric data however. Eldholm et al. (1990) have reported on bathymetric lineaments striking app. parallel to the inferred flow lines of the Knipovich Ridge, and possibly reflecting fossil and active transform faults (cf. section 4.1.1). Several such lineaments are evident west of the southern Knipovich Ridge (Fig. 24); the bathymetry on the eastern flank is much smoother however, as a result of larger sediment thicknesses here. It is suggested that the observed basement highs are the eastern counterparts of these lineaments, thus striking app. in WNW-ESE direction. They were buried by overwhelming sediment input from the Barents Sea margin.

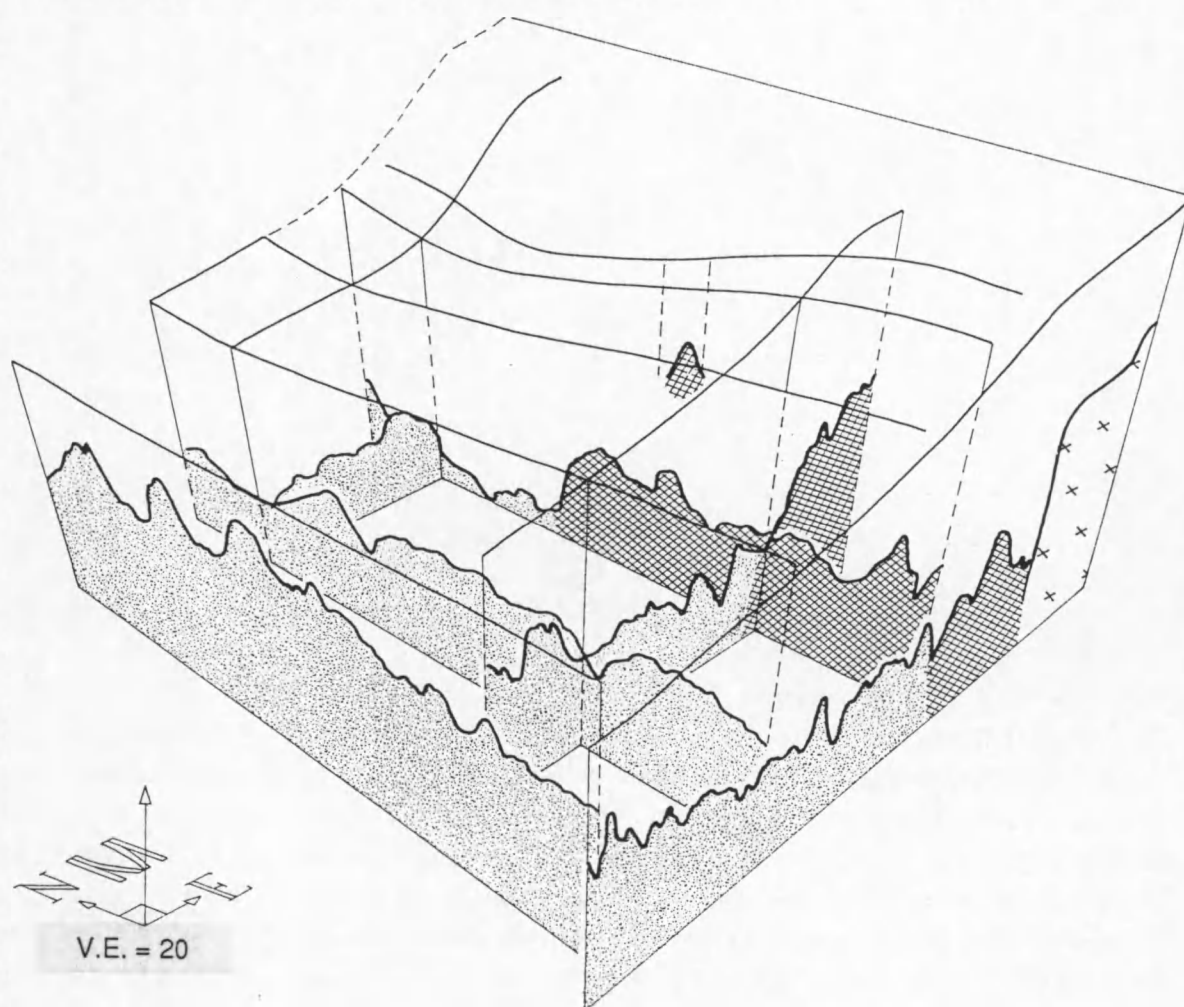
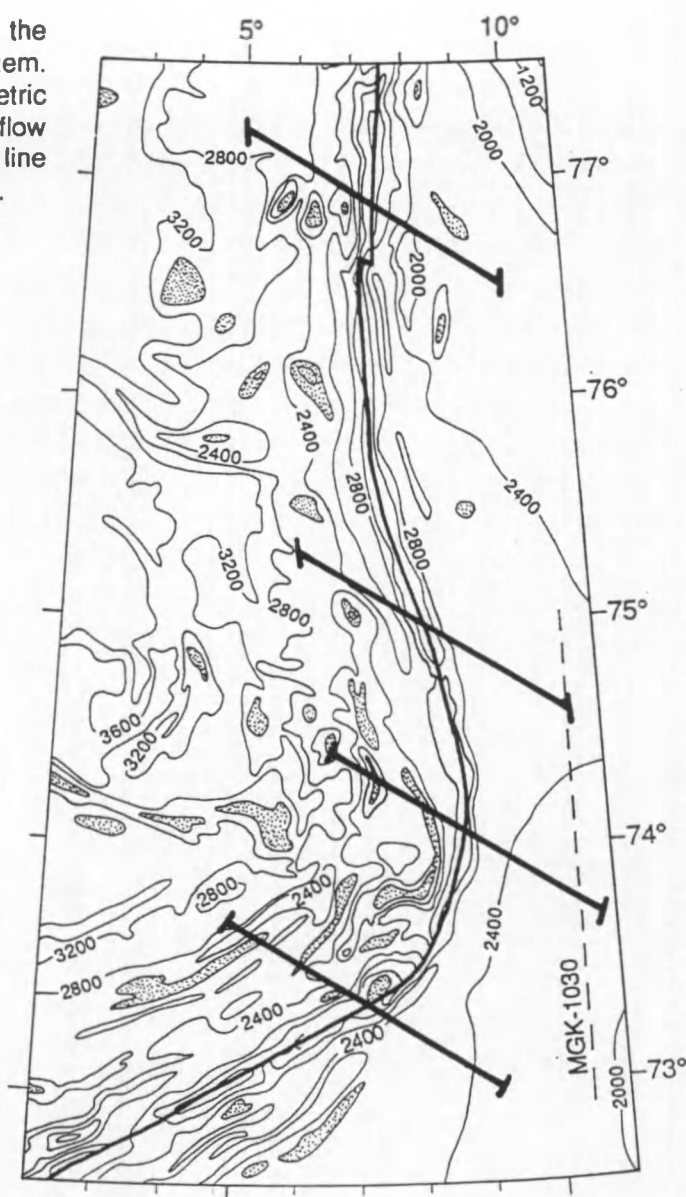


Fig. III.23 - Fence diagram depicting the morphology of the acoustic basement reflector, and the spatial distribution of the three types of structural basement. 3D visualisation by Geofox (Verschuren 1992).

Fig. III.24 - Bathymetric map of the Mohns/Knipovich Ridge spreading system. Stippled areas represent bathymetric highs, cross-bars indicate the inferred flow lines, dashed line marks position of line MGK-1030. After Eldholm et al. (1990).



Vestbakken volcanic province (VVP)

The marginal high of the Vestbakken volcanic province is mainly confined to the south-eastern part of the study area, east of 14°30' E and south of 74°15' N. The acoustic character of this type of basement is very similar to that of oceanic crust, but generally of lower amplitude (Window 6), making it more difficult to identify. The frequent observation of intra-basement reflectors closely below the main reflector suggests that several generations of basement are present, consistent with the interpretation of volcanic flows extruded subaerially during the early stages of break-up in the Early Eocene (Faleide et al. 1988). The volcanic province clearly occupies an elevated position with respect to the adjacent oceanic crust (Fig. 23), but the precise contact is poorly defined. The landward limit to where oceanic crust can be identified with confidence is marked with arrows on the line drawings in Figs. 20 and 21. The VVP is itself downfaulted from the main continental block to the east. The OCT is thought to be located a short distance seaward of the fault zone (Eldholm et al. 1987).

On line MGK-1500 (Window 19) an isolated volcanic mound is seen to rise to a depth of 3 s (1.25 s measured from the seafloor). This feature was described earlier by Faleide et al. (1988), and

interpreted as a volcanic peak penetrating the volcanic flows below, and with a relief of more than 1 km. The mound is clearly onlapped by sediments at least as old as r8; due to severe interference with the seafloor multiple, the termination pattern further down cannot be determined. The upward curvature of overlying strata can be explained by differential compaction effects, and is thus no evidence for vertical movements induced by the volcanic mound. Faleide et al. (1988) have suggested an early Oligocene age for this feature, whereas Sættem et al. (1994) related the volcanic mounds to a Late Pliocene phase of volcanism evidenced by volcanoclastic material of this age (cf. Mørk & Duncan 1993), drilled immediately below the base of the clastic wedge (r8) in the Vestbakken volcanic province.

Continental crust

The observation of continental crust is limited to the easternmost end of line NPD-7300. This third type of basement is characterised by a medium- to low-amplitude and medium-frequency reflector, locally affected by faults (Window 9). In comparison to the other basement types its reflection is more continuous and coherent, and exhibits far more regular relief (longer wavelength). A broad depression on line NPD-7300 with maximum depth of 500 ms below base level corresponds to the northern edge of the Sørvestsnaget Basin, formed during Cretaceous and early Tertiary times along the outer Barents Sea margin (Faleide et al. 1993). The basement reflector corresponds to the top of the pre-break-up sediments, and is overlain by more than 2 s of post-rift deposits, thinning in landward direction.

The continental platform is bounded to the west by a main continental boundary fault (CBF) with a throw of almost 2 s, and accompanied by a small number of secondary faults with offsets of 200 to 300 ms. This fault zone represents the central rifted segment linking the Senja Fracture Zone in the south to the Hornsund Fault Zone more northwards. It is informally denoted as Central Fault Zone (Sættem et al. 1994). Attenuated continental crust may be present to some distance west of the fault zone, but is now hidden below the volcanic flows of the VVP (Eldholm et al. 1987).

5.3.3. Megasequence G0 (r0 - r8)

5.3.3.1. General characteristics

Megasequence G0 is observed in its entirety on the NPD-lines only. The sediments overlie the three types of basement over most of the study area. Of the four major units that were identified G0 is volumetrically the most important, attaining a maximum thickness of > 3 s just seaward of the main continental boundary fault (Fig. 20). The unit pinches out towards the south-west by termination of its upper boundary r8 onto the oceanic crust. G0 has the overall shape of a wedge, effectively smoothening out the strong relief of the underlying basement. The unit is also inferred to represent the longest span of time in the depositional history of the margin, from the Early Eocene opening of the Norwegian-Greenland Sea to the Late Pliocene onset of large-scale northern hemisphere glaciations (see later).

5.3.3.2. Description of individual reflectors and units

The most important seismic markers within G0 are r1, r4 and r6. Only those will be discussed here. The units that are bounded by these reflectors are correlated with depositional units described in literature, as indicated in Table 5.

	This work	Vorren et al. (1990)	Richardsen et al. (1991)	Fiedler & Faleide (subm.)
	r8			
	B2	TeB	B	Te3 - Te4
	r6			27 Ma
	B1			Te2
	r4			36 Ma
	R		R	Te1
	r1			55 Ma
	TeA	TeA		
	r0			

Table III.5 - Stratigraphic correlation table for Megasequence G0.

Reflector r1 constitutes the top of a set of rotated fault blocks observed over the continental basement on the eastern part of line NPD-7300 (Window 9). The reflector probably terminates near the main continental boundary fault of the Central Fault Zone. The underlying unit, which is thought to correlate to unit TeA of Vorren et al. (1990), would thus be restricted to the landward side of the OCT. The unit thickens in eastward direction on the shelf to > 1 s in the Sørvestsnaget Basin. Apart from some high-amplitude reflectors below and parallel to r1, no clear reflections are evident. The geometry of this unit is strikingly similar to that indicated on a dip line at 72° N published by Vorren et al. (1990), where unit TeA is seen to pinch out near the Senja Fracture Zone (Fig. 16e). This strongly suggests that the Senja Fracture Zone and the Central Fault Zone came into existence more or less at the same time in response to the initiation of seafloor spreading at c. 54 Ma, supporting the model of continental break-up depicted in section 4.2.

Reflector r4 marks the top of a second set of rotated fault blocks extending seaward of the CFZ. The reflector is believed to correlate to the R/B boundary of Richardsen et al. (1991).

The underlying unit R does not extend seaward of c. 14° E, pinching out onto oceanic crust (lines NPD-7300 and NPD-7440) or truncated by reflector r6 (line NPD-7330, Window 12). Its thickness becomes maximal (up to 3 s, or almost 90 % of the entire unit G0 !) at the foot of the main continental boundary fault on line NPD-7300. Landward of this fault unit R is only 800 ms thick, gradually thinning to 300 ms east of the Sørvestsnaget Basin. The seismic facies of unit R varies from irregular on line NPD-7300 to almost transparent on line NPD-7330. Geometry and facies suggest that the sediments of this unit were dumped on an immature slope during and just after

downfaulting of the Vestbakken volcanic province along the Central Fault Zone (cf. Faleide et al. 1988), contemporaneously with the early stages of regular seafloor spreading along this margin segment, from c. 51 Ma onwards (Eldholm et al. 1987). This is in good agreement with the ages (Table 5) obtained by Fiedler & Faleide (in press) by observing termination of reflectors onto oceanic basement of known age in the Lofoten Basin.

The overlying unit B exhibits thickness variations quite opposite to those of unit R. The thickness minimum (c. 200 ms) is located over the Central Fault Zone. East of this fault it thickens to a maximum of 1 s in the Sørvestsnaget Basin, before being truncated by the upper regional unconformity (r30). West of the CFZ the thickness increases again to a maximum of 1.2 s over irregular basement lows. The seismic facies of unit B is commonly identical to that of unit R, but differentiates towards the north. Here, in the Storfjorden area, reflector r4 marks a clear change in reflector style, from continuous high-amplitude and low-frequent cycles below (unit R), to less low-frequent and disrupted reflectors above (unit B).

Reflector r6 is a seismic horizon dividing unit B in a lower and an upper part, here denoted as units B1 and B2, respectively. The main characteristic of r6 is the profound erosion evidenced on line NPD-7330 (Window 12), where the reflector appears to truncate unit B1 and the entire unit R, a sediment package of c. 1.4 s. Tracing of this boundary to the north along NPD-1430 proves to be problematic, as is the case for r4 too. The unconformity is not very pronounced in this part of the area, and is itself eroded by the top-G0 reflector r8 in landward direction.

Unit B1 develops a rather uniform thickness of max. 500 ms on lines NPD-7330 and NPD-1430. Its facies is identical to that of unit R, but becomes chaotic in the north of the study area. In the south, on line NPD-7300, unit B1 markedly thins towards the CFZ. Whether the unit pinches out or continues further eastward is not clear, however.

Unit B2 is generally thin (< 200 ms), but thickens to c. 400 ms and locally even to 1 s over the basement lows on line NPD-7330. The unit is entirely removed by erosion towards the east on line NPD-7440, and towards the south of the study area. On the southernmost line NPD-7300 unit B2 reappears and probably thickens east of the CFZ. The seismic facies is again largely reflection-free, changing to chaotic in the north.

The entire unit B was probably deposited after the CFZ became inactive. Correlation with the stratigraphy of Fiedler & Faleide (in press) indicates a maximum age of 36 Ma for this event, i.e. around the time of the early Oligocene change in relative plate motion and the ultimate opening of the northern Greenland Sea (Myhre et al. 1982). The contrasting thicknesses of units B1 and B2 east and west of the fault zone may suggest two phases of deposition, in which the depocentre shifted up-slope and a more mature continental slope was established. The B1/B2 boundary r6 extends northwards into unambiguously oceanic domain, created when seafloor spreading was well underway in the Greenland Sea. Fiedler & Faleide (in press) infer a maximum age of 27 Ma for this boundary, more or less correlating to the upper limit of an Early Oligocene to Early Miocene hiatus identified by Sættem et al. (1994) in shallow drillholes on the Barents shelf. This hiatus may be in part controlled by the global mid-Oligocene sea level fall, but the authors also showed evidence of tectonic uplift.

5.3.4. Megasequence GI (r8 - r15)

5.3.4.1. Basal unconformity r8

The base of megasequence GI is defined by reflector r8, which corresponds to R7 of Faleide et al. (in press). This boundary has a clear erosive character, both in upper slope and deep-sea paleoenvironments, and displays high amplitudes; in the western half of the study area it is generally the deepest strong reflector that is seen to overlie the oceanic basement. The surface morphology of r8 is depicted in the "isochron" map⁶ of Fig. 25. West of c. 12° E reflector r8 terminates by south-westward downlap onto oceanic basement (Window 3); this occurs more or less at the location of anomaly 6 on line NPD-7300, and about half-way between anomalies 5 and 6 on line NPD-7330. Up-slope, on the Barents shelf, r8 is truncated by the upper regional unconformity (r30) east of 16°30' (line NPD-7300, Window 8). At this position the base of GI is developed as a foreset dipping more steeply (c. 3.5°) than the current upper slope which has an angle of c. 1.2°. Overlying strata onlap the boundary in landward direction and show downlap in WSW direction, towards the deep-sea. More importantly, r8 marks the onset of strong progradation, particularly on line NPD-7300. The reflector thus defines the base of the prograding part of the wedge, above which the depocentres of the Bear Island and Storfjorden Cones developed (cf. Fig. 14 in section 5.2).

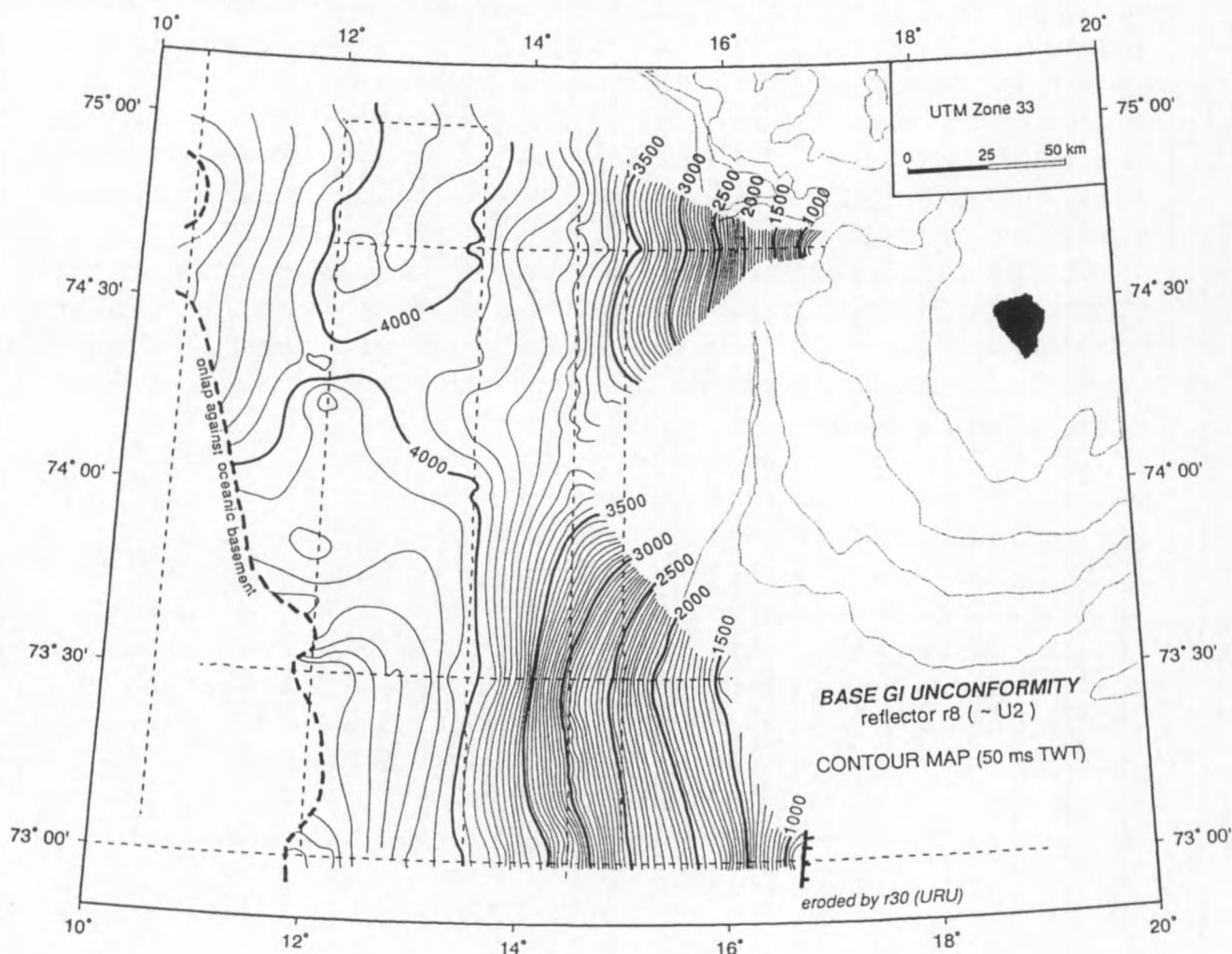


Fig. III.25 - Water-depth corrected contour map, in ms TWT, of base GI unconformity r8. The dashed lines represent the seismic grid. Gridded using Geotix (Verschuren 1992).

⁶ All surface contour maps presented here are in ms two-way travel time, but corrected for water depth.

5.3.4.2. Thickness distribution and description

On the upper slope, megasequence GI is best developed on line NPD-7300, where it has the appearance of a prism, 500 - 700 ms thick and composed of a set of prograding units that are separated by distinct high-amplitude foresets (Window 8). These foresets are all truncated by the upper regional unconformity below the app. position of the respective paleo-shelf edge, and are also the steepest dipping reflectors that are observed in the study area: the angle gradually increases from 3.5° at the base of the prism to 4° at the top. This upward steepening concurs with a gradual evolution of the foresets into more characteristic clinoforms, indicating that the truncated ends more and more approximate the position of the paleo-shelf edge. The different prograding units probably correspond to sequences C1-C6 identified by Richardsen et al. (1992); these sequences have not been described west of 15° E and north of 74° N, however. In each of these sequences the authors recognised a downslope complex of mounded strata, overlain by more proximal offlapping strata. Due to the limitations of the data set this configuration could not be confirmed here; on the other hand, striking chaotic intervals were recognised both at the base and at the top of the prism.

The isopach map of Fig. 26 indicates that the prograding prism is probably a local depocentre, confined to the axial mouth of Bear Island Trough, where its weight has resulted in local downwarping of the basal unconformity r8. The thickness of the upper slope sediments drastically decreases northward, to only 100 ms on line NPD-7330 and slightly increasing again to 300 ms on line NPD-7440. Furthermore, the prograding prism is more or less detached from thick sediments on the lower slope by an intermediate zone of thinning over the middle slope.

The main accumulation within GI has taken place on the lower slope, where thicknesses are generally between 500 and 750 ms, culminating in a major northerly depocentre (> 1 s), which represents the influence of the Storfjorden Trough region as sediment provenance area. Near the basement highs in the west and north-west of the study area (lines MGK-1030 and NPD-7330) the entire unit GI is locally absent. In the southernmost part of the area, the detachment of the lower slope sediments from the prograding prism may indicate that these sediments were derived from further north, and actually constitute an outlier of the depocentre further north. This is also supported by the isopach map.

On the lower slope and rise a series of high-amplitude, low-frequency reflectors is identified (r9 - r14), which in the Storfjorden area are locally disturbed and typically separate discontinuously stratified to vaguely chaotic intervals (line NPD-7440, Window 15). The facies becomes better stratified more distally on line NPD-7440, and further north on line MGK-7500; to the south and west it is overall transparent. The reflectors r9 to r14 have no further significance as angular unconformities, and cannot be otherwise correlated to the reflectors recognised within the upper slope prograding prism on line NPD-7300. The most prominent reflector is certainly r13, corresponding to R6 of Faleide et al. (in press). In the Storfjorden depocentre the reflector constitutes the boundary between a lower chaotic and an upper stratified part (Window 15). This differentiation of GI becomes obscured towards the south, however. Reflector r13 is cut by the top-GI reflector r15 towards the south-east, on the northern flank of the Bear Island Cone (lines NPD-7300 and NPD-1430; Fig. 27). The chaotic reflection style between r8 and r13 is the continuation of a pattern initiated well earlier, probably around r4 time (cf. section 5.3.3.2), on the Storfjorden Cone. It is interpreted to result from high accumulation rates of sediment derived from the Stappen High, which is located in the present-day Storfjorden Trough area. This is in agreement with the thickness distribution of GI (Fig. 26), which indicates that the Storfjorden Cone was much more active than

the Bear Island Cone during this period of time. This conforms to the results of Vorren et al. (1990, 1991) and Richardsen et al. (1991), who have identified the Stappen High as the main source of sediment for their unit TeC, correlative to GI.

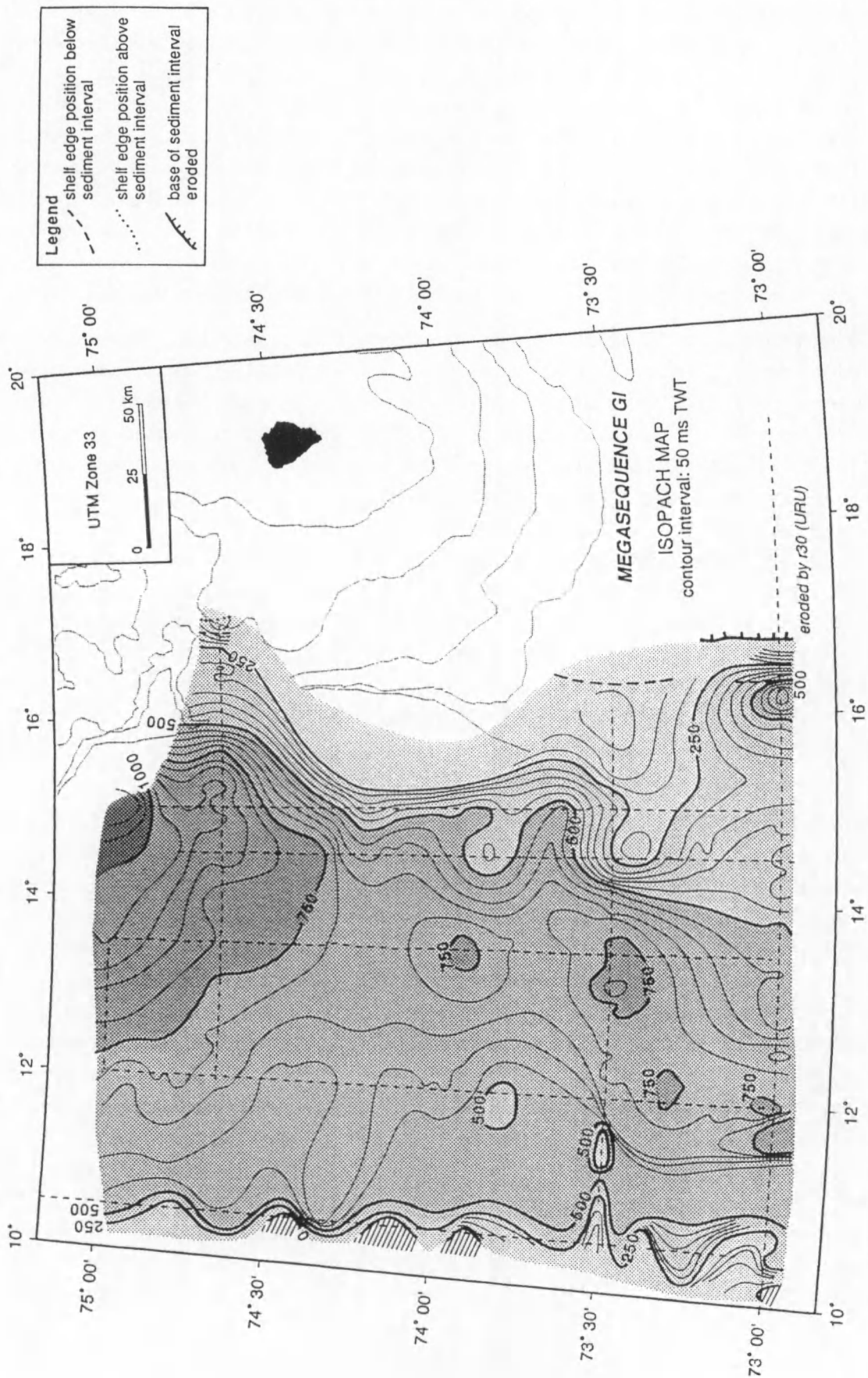


Fig. III.26 - Isopach map of Megasequence GI. Contour interval is 50 ms TWT, except in the extreme west of the study area, where thickness variations are larger due to irregular basement relief. Gridded using Geofox (Verschuren 1992).

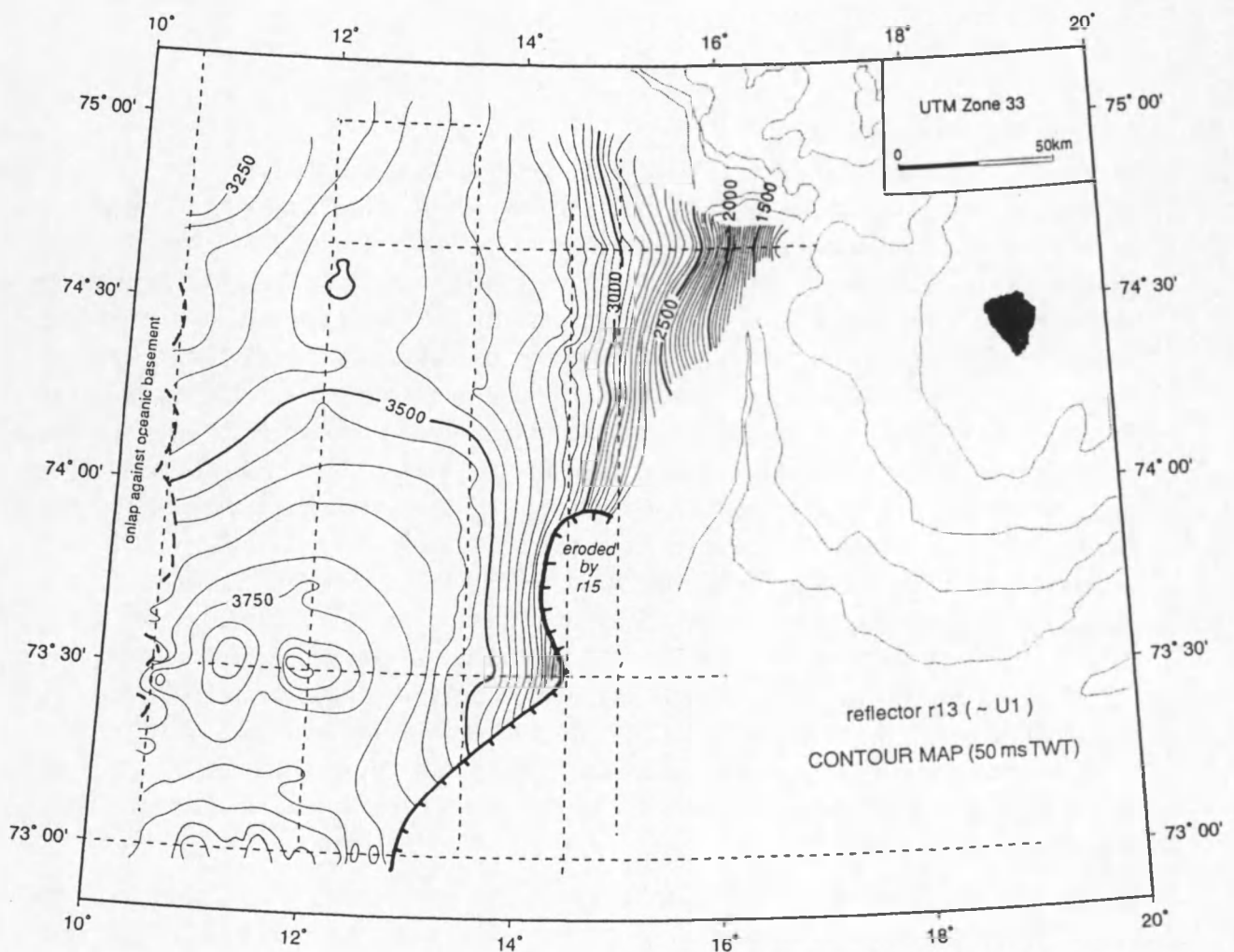


Fig. III.27 - Water-depth corrected contour map, in ms TWT, of reflector r13, illustrating the truncation of this horizon on the upper and middle slope of Bear Island Cone. Gridded using Geofox (Verschuren 1992).

5.3.4.3. Summary of GI

Megasequence GI is best developed on the lower continental slope, where its thickness averages 500 to 750 ms, wedging out against the highest peaks of the oceanic basement in the west. A maximal thickness of over 1 s is observed in the north of the study area, which points to the relatively higher sediment supply from the Storfjorden area. In addition, the sediments in this area are characterised by a chaotic seismic facies, which is thought to indicate deposition by large-scale mass movements, caused by a significant increase of sedimentation rates on the paleo-upper continental slope. Reflector r13 (~R6) is a conspicuous horizon, marking the transition between chaotic facies below, and acoustically stratified facies above. This differentiation loses distinction towards the south, however, while on the flank of Bear Island Cone, r13 is eroded by the base-GII unconformity r15 (~R5). Megasequence GI strongly thins on the upper slope, except in a localised depocentre in front of the axial mouth of present-day Bear Island Trough. Individual sequences within this depocentre display a pronounced progradation (18 km in total), with steeply dipping foresets that are all truncated up-slope by the reflector defining the base of GIII. Base-GI reflector r8 (~R7) and top-reflector r15 are truncated as well, resulting in the absence of the entire megasequence from the Barents shelf.

5.3.5. Megasequence GII (r15 - r30)

5.3.5.1. Basal unconformity r15

Reflector r15, the equivalent of R5 of Faleide et al. (in press), represents the base of megasequence GII. It is in several respects the most remarkable horizon identified above r8. First, r15 marks an important erosional surface in the study area. Most of its erosional characteristics were already reported above (section 5.2.3). The reflector is strongly erosive on the paleo-upper slope in the Storfjorden area (Hjelstuen et al., in press), but also in more deep-water contexts, as is particularly evidenced by truncation of the secondary reflector r13 on the northern flank of the Bear Island Cone (lines NPD-7300 and NPD-1430). In addition, a distinct erosional scarp was identified on the central part of line NPD-1430. This suggests that multiple mechanisms are responsible for generating this surface, acting both on the outer shelf / upper slope and on the lower slope / rise. Secondly, r15 is easily recognisable as it coincides with the top of a series of high-amplitude reflectors over most of the area. The highest amplitudes are observed in the north (north of 74°20' N on lines MGK-1330 and NPD-1430; Window 29) and in the west (west of 12°30' E on line NPD-7330), and in an area centred around 73°40' N on line NPD-1430 (Window 22). In the latter case, r15 is clearly updoming and also affected by faults (Window 21). This may be indicative of local tectonic uplift at the time of r15. Contemporaneous uplift of the shelf and adjacent land areas was indirectly inferred by Richardsen et al. (1991) and Vorren et al. (1991) from a southward shift of depocentre of unit TeD (\pm corresponding to GII) with respect to older units. And thirdly, the sediments overlying r15 are over large parts of the study area characterised by extensive acoustically chaotic intervals. This is further elaborated in section 5.3.5.3.

Like the base-GI reflector r8, r15 is truncated as a foreset by the upper regional unconformity on the Barents shelf, near the inferred position of the paleo-shelf break (line NPD-7300, Window 9; Fig. 28). Its dip here (c. 3°) is slightly less than that of the foresets within the underlying prograding prism (cf. section 5.3.4.2). Downslope, the reflector terminates by onlap onto oceanic basement highs in the extreme west of the study area. Overlying sediments onlap the basal unconformity in eastern and north-eastern direction; onlap is most pronounced on line NPD-7300, where the depositional pinch-out of an up to 1 s thick interval is implied (Window 7). More seaward, downlap towards the south-east becomes the dominant stratal termination pattern.

5.3.5.2. Thickness distribution

The isopach map of GII in Fig. 29 shows two pronounced and clearly separated depocentres, occupying different physiographic positions. In the Storfjorden area in the north the unit reaches maximum thicknesses of 1000 ms in a relatively small depocentre located on the paleo-upper slope. Whereas the southern half of the area is dominated by an extensive depocentre (over 1000, and up to 1250 ms thick) over the lower slope and rise. A notorious observation is the virtual absence of GII on the upper slope of line NPD-7300, strongly contrasting to the situation on other lines. This is the result of pronounced onlap at this location, as discussed in the previous section.

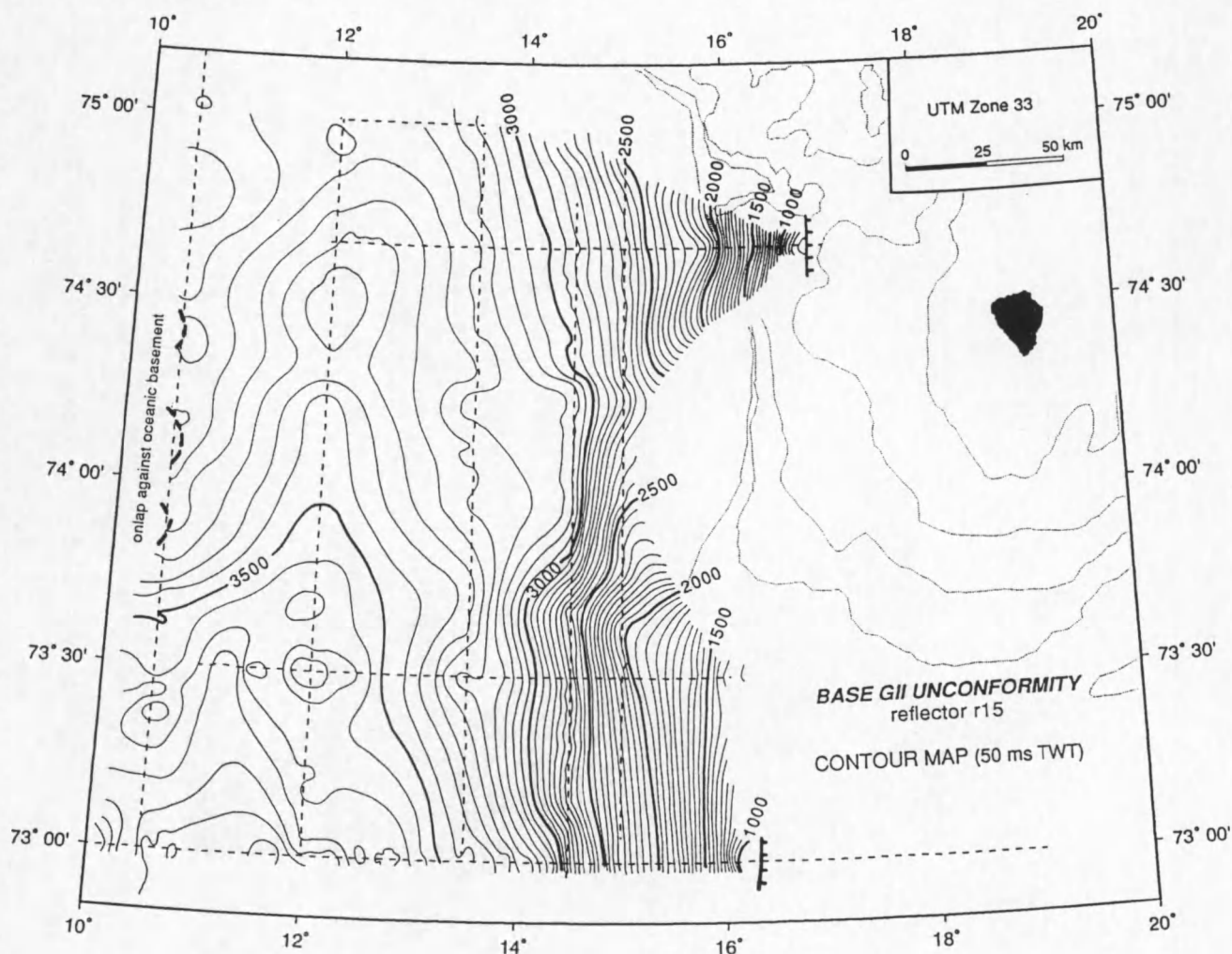


Fig. III.28 - Water-depth corrected contour map, in ms TWT, of base GII unconformity r15. Gridded using Geofox (Verschuren 1992).

5.3.5.3. General seismic facies characteristics

The most conspicuous characteristic of megasequence GII is its seismic facies, which varies between chaotic and transparent in the south and west, but becomes stratified towards the north-east. This chaotic facies imposes major limitations on the tying of internal reflectors around the network.

The chaotic facies is composed of numerous diffraction hyperbolae and acoustic noise. The diffraction hyperbolae are attributed to a disruption of the original stratification; a more transparent facies is interpreted to indicate a higher degree of homogenisation, and thus stronger deformation. On the other hand, a lower degree of deformation is suggested in some places (e.g. around the intersection of lines NPD-7300 and MGK-1330, Windows 5, 25), where faulted blocks can be recognised in the chaotic facies. In other cases discontinuous reflectors can be observed, abruptly disappearing laterally into the chaos. Often the seismic facies is chaotic both above and below these reflector segments.

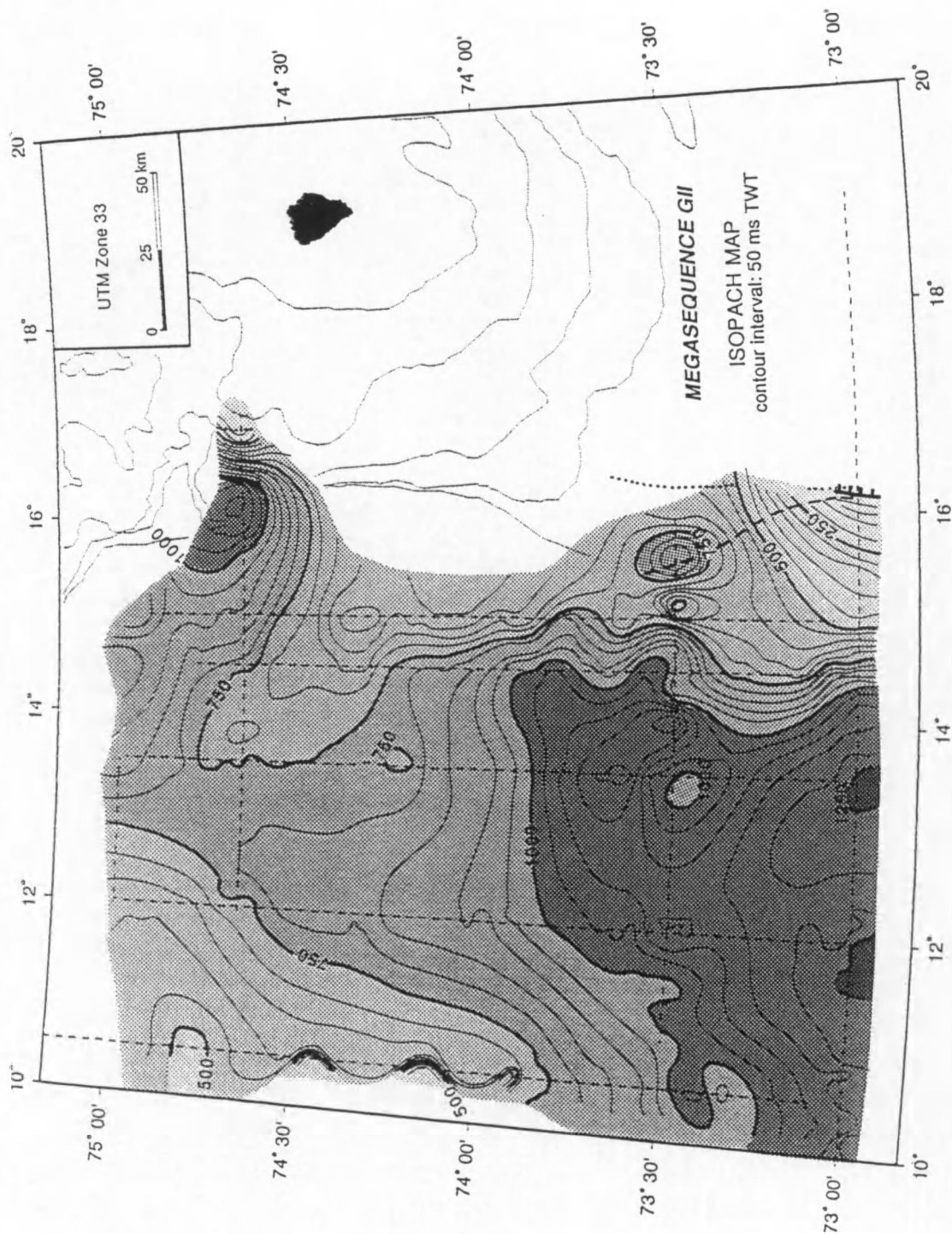


Fig. III.29 - Isopach map of Megasequence GII. Contour interval is 50 ms TWT. Legend as in Fig. III.26. Gridded using Geofax (Verschuren 1992).

The distribution of the chaotic facies within GII is extremely complex, as illustrated by the fence diagram in Fig. 30. Chaos occurs at several levels, but there is generally one dominant chaotic interval (in the following referred to as the “main chaotic interval”), which in the south-east is locally developed over the entire vertical extent (± 1 s) of GII (Windows 11, 21); locally (NPD-1430) even the base-GII reflector r15 is affected. The main chaotic interval gradually thins to c. 200 ms in the north-western corner of the area, where it becomes confined between the reflectors r26 (~R3) and r27 (~R2) (line MGK-1200, Window 34). This is in part the result of a jump of the base of the chaotic interval to stratigraphically higher levels. A more striking basal jump occurs in the south-

west of the study area (line NPD-7300, Window 4), where the interval becomes limited to the upper third (< 500 ms) of unit GII; the lower two thirds of GII become apparently stratified, but often the chaotic facies is seen to extend some distance between reflectors below the base of the main chaotic interval (Window 2). The abrupt thinning of the chaotic interval may indicate that it disappears a short distance south-west of the study area.

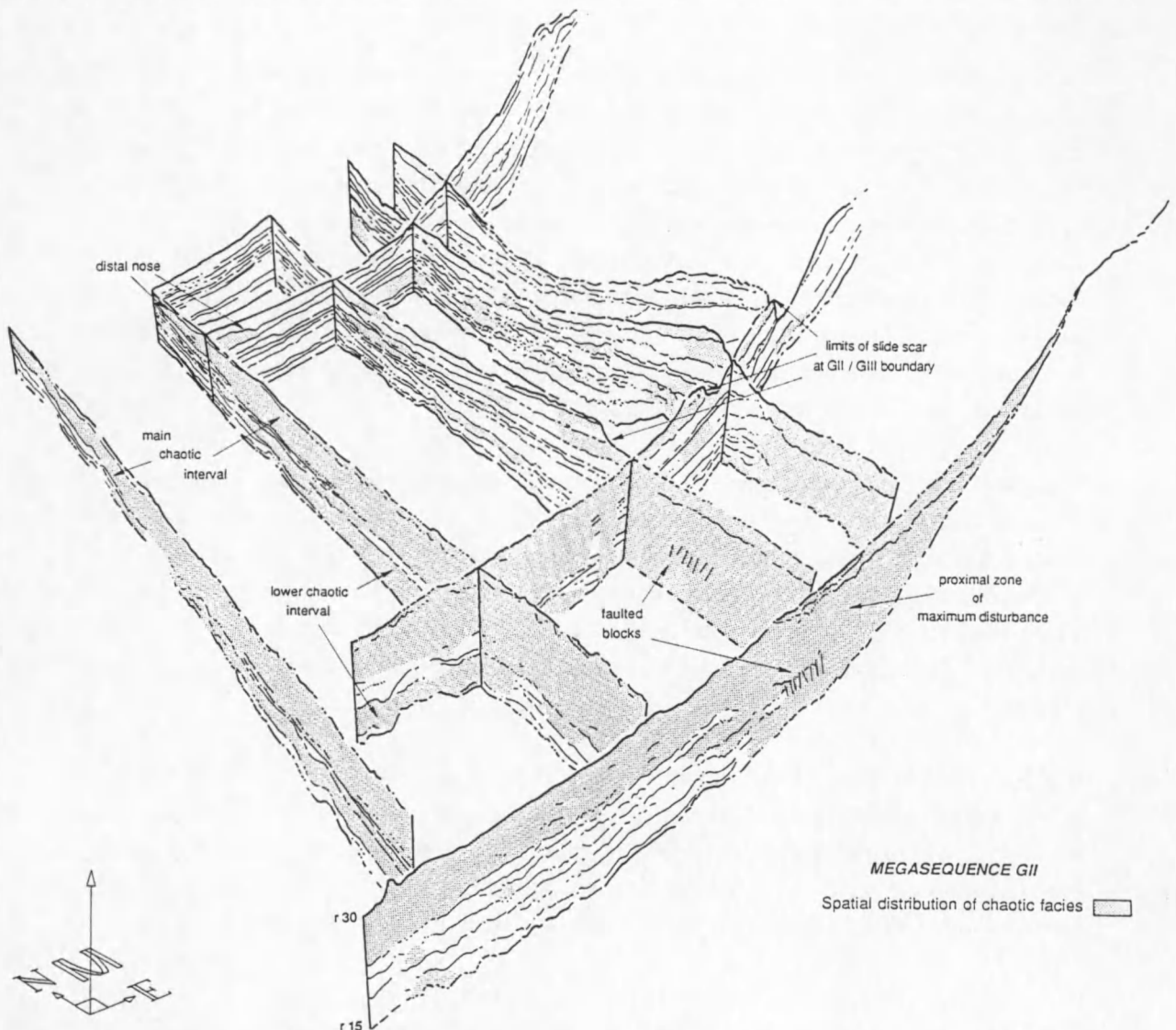


Fig. III.30 - Fence diagram demonstrating the distribution of acoustically chaotic facies in Megasequence GII. 3D visualisation by Geofox (Verschuren 1992).

More frequently, however, several levels of chaotic facies are observed. In the south-east the main chaotic level is divided into two levels by r25 (Window 7), whereas in the west the main interval is separated from a lower and more transparent interval by the more or less continuous reflector r20 (Windows 32, 37). In addition, several smaller chaotic intervals have been identified in the east.

In the north-east of the study area the seismic facies of megasequence GII becomes predominantly stratified, grading from regularly stratified on the lower slope, to irregularly and diffusely stratified on the upper slope. The transition chaotic/stratified is of two kinds. In the extreme north-west, at the intersection of lines NPD-7440 and MGK-1200 the transition is smooth: the main chaotic unit

gradually thins and at the same time becomes restricted to a stratigraphically narrower interval, between r26 and r27. At a certain limit more abrupt thinning takes place in the form of a toe- or snout-shaped edge, beyond which acoustic stratification emerges (Windows 14, 34). Just short of this limit, a stack of several discontinuous reflectors is observed, standing more than 100 ms high above the base of the chaotic interval (r26); part of the chaotic interval continues above it. The interpretation of this feature has major implications for the nature and scale of the process that has created the chaotic interval (see section 6.3).

East of about 13° E the transition chaotic/stratified is much more drastic: centred around 73°30' N a marked lateral facies change occurs between the 750 - 1000 ms thick main chaotic interval, in which only one reflector (r25) can be recognised, and an equally thick succession in which several reflectors (r16 - r28) are observed (Windows 11, 21). However, some intervals within the apparently layered succession are characterised by chaotic facies as well, and in fact the entire unit GII between 73°30' and 74°40' N displays a very complex stratigraphy, in which numerous horizontal and vertical facies transitions take place. In addition, complex stratal termination patterns are localised to an area overlying the updoming of r15 (line NPD-1430, around 73°40' N); this may be indicative of continuing uplift in the Vestbakken volcanic province, at least until r23 time. From latitude 74°40' N northwards the facies is more uniformly stratified.

- Recapitulating, the chaotic facies in GII is most extensively developed in the south-east of the study area, i.e. centrally off the mouth of Bear Island Trough. The main chaotic interval gradually thins towards the north-west, its basal boundary jumps to stratigraphically higher levels towards the south-west, and to the north-east an abrupt transition takes place into a complex stratified facies, which becomes more regularly stratified in the extreme north and east. In the western half of the study area the chaotic facies splits into a lower, transparent unit and an upper, chaotic unit, separated by r20.

5.3.5.4. *Description of individual reflectors and units*

In the section below the most important characteristics are described of the reflectors identified within GII, and of the respective underlying units. The reader is notified here that reading of this purely descriptive section is not fully obligatory to keep track of the headlines of this chapter. A summary of the stratal termination patterns will be presented in Fig. 34 at the end of section 5.

- Reflector r16 is a relatively high-amplitude reflector close above the GI/GII boundary, onto which it onlaps in landward direction (line NPD-7330) or laps out (onlap or downlap) towards the north. On line NPD-1430, r16 terminates against an erosional scarp described above (section 5.3.5.1). In the south-east of the area, the reflector is lost into the main chaotic unit.

Unit r15-r16 is best developed in the extreme south-west of the area (line NPD-7300), and locally on line NPD-1430 where it fills in erosional relief in the base-GI horizon. Thicknesses up to 200 ms are recorded. In some locations, the unit has a distinct mounded aspect. Its facies varies between chaotic and transparent.

- Reflector r17 is a little pronounced seismic horizon that is truncated by r18 everywhere in the centre of the study area. The reflector constitutes a foreset on the upper slope, but disappears in the chaotic unit in the south-east as well.

Unit r16-r17 is generally thicker in the south (c. 100 ms) than in the north (c. 50 ms), and also thickens on the upper slope. The facies is predominantly stratified, particularly in the north, but locally develops into a transparent to chaotic facies.

- Reflector r18 is a high-amplitude erosional unconformity, truncating r17 on the middle and lower slope, and in one location (southern part of line NPD-1430) even eroding into r16. The reflector is recognised as a prograding foreset on the upper slope of lines NPD-7330 and NPD-7440, thus not showing landward onlap. As with most reflectors identified within GII, r18 is interrupted by the main chaotic interval in the south-east of the study area; additional disruption occurs on the lower slope, near the intersection of lines NPD-7330 and MGK-1200, by the lower transparent to chaotic interval topped by r20.

The thickness of the r17-r18 interval is usually less than 100 ms, in the north hardly exceeding 50 ms. The thickness maximum, up to 200 ms, is observed on the upper slope in both the south (NPD-7330) and north (NPD-7440). The seismic facies is weakly stratified, grading into transparent towards the west (MGK-1030). It never becomes chaotic, except for the upper slope portion of line NPD-7330.

- Reflector r19 is a distinct seismic horizon that is identified north of about 74°15' N only. The reflector is seen to downlap onto r18 towards the south, and appears to be truncated by r20 towards the upper slope on line NPD-7440.

Unit r18-r19 is commonly over 100 ms thick, pinching out to the south, however. The facies of the unit is predominantly stratified, but develops into a chaotic facies on the lower slope portion of line NPD-7440, where the unit also reaches its maximum thickness of c. 200 ms.

- Reflector r20 does not appear to be an angular unconformity, except for the upper slope portion of line NPD-7440, where it cuts r19. Probably r20 is itself eroded by r21 on the central part of line NPD-1430. In the western part of the area the reflector gains in significance, as it defines the top of an almost 400 ms thick and extensive transparent to chaotic unit, encompassing the entire interval r15-r20 (Windows 32, 37). On the central parts of MGK-1200 and MGK-1330, r20 is itself interrupted by a chaotic zone, and in the south-east it is entirely entrained within the main chaotic unit: the two most extensive chaotic intervals are merged here.

Unit r18/r19-r20 is more not than often recognised. The unit is generally less than 100 ms thick, and is again thicker south than north. With a thickness maximum located in the south-west and zero thicknesses on the upper slope, the unit has the typical appearance of a base-of-slope unit. The seismic facies is predominantly transparent, but becomes more clearly stratified to the north. The development into the thick, transparent and locally chaotic interval is closely linked to the disturbance of underlying reflectors.

- Reflector r21 is again a prominent reflective surface. Its unconformable character is obvious only in the south-east, near the intersection of NPD-1430 and NPD-7330, where it truncates r20. In about the same location, and also towards the upper slope, r21 is itself eroded by r23. Erosion by r23 is also observed in the south-west. Furthermore, the reflector is absent from a large area in the south, being disrupted by the main chaotic interval.

Where the unit r20-r21 is preserved, its facies is unmistakably chaotic and in places disrupts the lower boundary r20 (see above). More northward the unit is stratified. The thickness is again greatest (100 - 200 ms) on the southern lower slope, thinning to less than 50 ms in the north. On the upper slope the unit is not observed, due to truncation.

- Reflector r22 is a rather unobvious horizon that is restricted to the south-east of the area, near 73°30' N. The reflector downlaps onto r21 towards the north, is truncated by r23 on the upper slope (NPD-7330), and is entrained into the main chaotic interval to the south and west.

Unit r21-r22 is maximum 100 ms thick, and its seismic facies is not very clear.

- Reflector r23 is a relatively weak reflector, which becomes more distinct on the lower slope portion of line NPD-7300. This horizon truncates r21 in the eastern part of the area (MGK-1330 and NPD-1430), and both r21 and r22 towards the upper slope. Reflector r23 is inferred to be eroded itself by r25 near the intersection of lines NPD-7330 and NPD-1430, but this geometrical relationship is obscured by local canyon-like incision of the GII/GIII boundary into both reflectors (Window 13). Otherwise, it is missing over large parts of the southern area, related to the extensive development of the main chaotic interval.

The interval r22-r23 has a very limited occurrence: it has only been observed in a small area centred around 73°30' N and 14°30' E. The unit pinches out in northward direction, is eroded on the upper slope to the south-east, and is incorporated in the main chaotic interval towards south and west. The seismic facies is mostly transparent.

- Reflector r24 is mostly a high-amplitude reflector, showing little unconformable character. It is eroded by r25 to the south-east. The most important characteristic of this reflector is that it can be recognised as the uppermost more or less continuous reflector locally (near the south-western edge of the area, line NPD-7300) defining the base of the main chaotic unit (Window 2); north and east of this location r24 terminates into the chaotic facies.

Unit r23-r24 obtains a maximum thickness of c. 150 ms on the middle slope portion of line NPD-7330. The unit is eroded on the upper slope, and thins to 100 ms downslope. More northward the unit is generally less than 50 ms thick. The facies ranges between transparent and clearly chaotic; the latter facies is particularly observed on line NPD-7300, where unit r23-r24 merges into the main chaotic interval. The facies probably becomes stratified in the north.

- Reflector r25 is a high-amplitude seismic marker, and an important unconformity in the south-eastern region, where it truncates r24 and r23 towards the upper slope. On line NPD-1430 the reflector is interpreted to deeply incise down to r22 in a similar fashion and location as the younger major incision at the GII/GIII boundary r30 (Window 21). On the northern end of line MGK-1200 the reflector may be eroded by r26. Reflector r25 is particularly striking in the south-east, where it stands out as a seemingly continuous reflector within the upper third of the main chaotic interval; the facies both above and below this boundary is chaotic here (Windows 7, 26). To the west r25 is gradually disrupted, and finally disappears in the chaotic facies. Towards the north it continues as one of the many reflectors. Another important characteristic is the conspicuous landward onlap of r25 onto the GI/GII boundary on line NPD-7300, implying the depositional pinch-out of the entire and up to 1 s thick r15-r25 interval. On the more northerly dip lines this notorious termination pattern is not observed, and r25 can in fact be traced as a slope foreset continuing onto the paleo-shelf, where it is eventually truncated by r30 (NPD-7330) or r27 (NPD-7440). Finally, r25 is also locally incised by the GII/GIII boundary near the intersection of NPD-7330 and MGK-1500.

Where it is preserved as an individual unit, the r24-r25 interval is everywhere less than c. 75 ms thick. The unit could not be identified in the entire south-western half of the study area, however. The seismic facies follows the general trend: transparent to chaotic, and becoming stratified to the north. On the northern part of line MGK-1330, and partly of MGK-1200 as well, the unit exhibits a prominent mounded shape, with associated chaotic facies, locally disrupting its base reflector (r24); faint bi-directional downlap onto the base may also be suggested on the seismic sections (Window 27). A smaller such feature occurs more southward. Their interpretation will be discussed later in section 6.4.

- Reflector r26, the equivalent of R3 of Faleide et al. (in press), has most significance in the north-west of the area as the base of the northward thinning main chaotic interval, confined in its distal parts between r26 and r27 (Windows 14, 34). The boundary has only weak erosional expression in this region, probably cutting locally into r25. South of about 74° N the reflector dissolves, as from there onward the chaotic facies extends stratigraphically deeper (Window 32). In the eastern half of the study area r26 still constitutes a high-amplitude reflector, no longer separating strongly contrasting facies above and below, however. The horizon is eroded to the south-east by the prominent incision at the GII/GIII boundary near 73°30' N (Windows 21, 26), which also aborts continuation of the reflector onto the upper slope. In contrast, on the more northerly dip line NPD-7440, r26 can be traced up-slope to the app. position of the paleo-shelf edge, where it appears to be truncated by r27 (Window 16). In a very restricted area on the middle slope section of this line, r26 shows evidence for erosion of underlying internal reflectors.

The r25-r26 interval is quite thick (100 - 150 ms) in both the south and north, but much thinner (c. 50 ms) in the central part of the study area. The greatest thickness (> 300 ms) is recorded on the upper slope portion of line NPD-7440, whereas on the southerly dip lines the unit is absent in this location. The facies varies between transparent and weakly stratified, the latter character being more expressed in the north. Only on the southernmost part of line NPD-1430, where the basal unconformity r25 is interpreted to form a large incision, the facies is clearly chaotic.

- Reflector r27 corresponds to R2 of Faleide et al. (in press), and like r26 it is especially distinguished in the north-west, as the distal top of the main chaotic interval. The facies contrast disappears in southern (proximal) direction, however, as the overlying facies becomes chaotic as well (Fig. 30, Window 33); at the same time r27 gradually loses continuity, and ultimately ends up as disrupted pieces closely below the GII/GIII boundary (Window 32), which effectively takes over as the new top of the main chaotic unit. Eastward of this location the main chaotic unit gradually passes into a predominantly stratified facies, making all facies contrasts vanish (Window 14). Reflector r27 accordingly loses distinction, though on the northern end of line MGK-1330 it shows up as a striking onlap surface for overlying internal reflectors, including r28 (Window 28). This observation is limited to this location, because only here the r27-r28 interval is reasonably developed. The northwards onlap of overlying strata gives some indication on the activity of the Bear Island and Storfjorden depocentres, relatively to each other (see sections 7.3 and 7.4). Further south-east, r27 is locally eroded by the GII/GIII boundary on line NPD-1430, and completely cut off by the major incision exhibited by this boundary near 73°30' N (Window 26); the reflector no longer exists southward and up-slope from this erosional escarpment. In the northern area, however, r27 continues as a foreset onto the upper slope, and develops into a prominent topset showing erosional relief in the form of a trough on the outer shelf (Window 16).

Unit r26-r27 is beyond doubt the most conspicuous interval identified within GII. It coincides with the main chaotic interval in the north-west, and probably constitutes the major part of this interval over the remaining part of the area. Within the chaotic facies between r26 and r27, the existence of one or two heavily disturbed reflectors may be suspected by the local alignment of diffraction hyperbolae (Window 33). Unit r26-r27 has a thickness distribution typical of a base-of-slope unit; the largest thicknesses occur on the lower continental slope and rise, and are characteristically associated with a chaotic facies. A maximum thickness of 300 ms is observed on the central parts of lines MGK-1030 and MGK-1200. The unit probably thickens towards its source area in the south, but this is difficult to prove as both r26 and r27 become intensely disturbed in that direction. Unit r26-r27 gradually thins to some 200 ms in northward direction; near the intersection of lines MGK-1200 and NPD-7440 abrupt thinning takes place, from 200 ms to 75 ms, in the form of a snout- or toe-shaped edge facing approx. north-east (Windows 14 and 34). The edge is furthermore associated with a marked lateral facies transition, from chaotic in the south and west to uniformly stratified beyond the edge. Implications of these features will be discussed in section 6.3. In the eastern half of the area the facies of unit r26-r27 displays complex variations between chaotic, transparent and stratified, the latter becoming dominant towards the north. Its thickness drops below 150 ms up-slope, but in the south further original thinning may be obscured due to erosion by the GII/GIII boundary. Minimum thicknesses of c. 50 ms are found on the lower and middle slope portions of line NPD-7440, and between 74°15' and 74°35' N on lines MGK-1330 and NPD-1430, i.e. in between the influence spheres of both depocentres.

- Reflector r28 is a relatively high-amplitude reflector which has only been identified on the central portion of line MGK-1330, between 73°30' and 74°40' N. The horizon onlaps onto r27 towards the north (Window 28), and is erosionally truncated by the GII/GIII boundary incision to the south. The reflector does not exhibit unconformable character.

Reflector r29 has not been defined.

The interval r27-r30 is seen to consist of the two separate intervals r27-r28 and r28-r29 on part of line MGK-1330 only. The two intervals are almost equal in thickness; unit r27-r28 has a maximum thickness of 150 ms, pinching out to the north (Window 28), whereas unit r28-r30 is up to 120 ms thick over the site of pinch-out of underlying unit r27-r28, thins to below 50 ms towards the north, and is increasingly eroded in southward direction. Both intervals are predominantly stratified in this location, locally disturbed by a chaotic facies. The interval r28-r29 is particularly noted for the occurrence of contorted internal reflectors. Everywhere else only the combined interval r27-r30 is observed. It is speculated that it essentially corresponds to unit r27-r28, and that the other interval r28-r30 is eroded. The thickness does generally not exceed 100 ms, except in a limited area on line NPD-7440, around the intersection with MGK-1330, where the two intervals are probably present, but not individually observed due to the lower resolution of the NPD-line with respect to the MGK-line. Thinning takes place to the north-west, and up-slope in eastern direction. The facies of the combined unit r27-r30 is clearly chaotic in the west and south-west of the study area, but grades into stratified facies to the north-west, concurrently with the increasing continuity of the basal boundary r27 (see above). The northern region is again stratified, according to the overall trend in megasequence GII, and in the east the facies is commonly transparent to chaotic.

5.3.5.5. Summary of GII

Megasequence GII is bounded at its base by reflector r15 (~R5), a pronounced seismic marker exhibiting erosion over the entire area, but which is itself cut near the offlap break by the base of GIII in the outer Bear Island Trough. Similar to GI, megasequence GII is therefore absent from most of the southern Barents shelf. Two individual depocentres are recognised on the isopach map: a smaller depocentre of 1 s max. on the upper continental slope in front of Storfjorden Trough, and a more extensive depocentre (up to 1250 ms) occupying the lower slope and rise in the southern half of the area. The latter depocentre clearly demonstrates the increased influence of the Bear Island Trough area; northward onlap of strata against reflector r27 suggests that the Bear Island depocentre even starts overwhelming the Storfjorden depocentre in the upper part of megasequence GII. Upslope from the Bear Island depocentre, GII strongly thins by the notable landward onlap of reflector r25 against the GI/GII boundary, and by the consequent pinch-out of an up to 1 s thick interval. The single most striking characteristic of megasequence GII is its predominantly chaotic to transparent seismic facies, which is most extensively developed (over the entire vertical extent of GII) on the middle slope in front of present-day Bear Island Trough. Often, however, several chaotic intervals can be discerned, separated by more continuous reflectors. The main chaotic interval thins in northwestern direction, towards the distal portion of the Storfjorden Cone, where it becomes confined between the reflectors r26 (~R3) and r27 (~R2). This thinning occurs both gradually and by the sudden appearance of new base and top reflectors. An abrupt lateral transition shifts the chaotic facies to the northeast into a complexly stratified seismic facies, which becomes more regularly stratified towards the Storfjorden area. The chaotic facies is thought to reflect a strong disturbance of the original stratigraphy, resulting from several phases of large-scale mass wasting. This severely hampers the correlation of seismic horizons through the study area. In addition, very complex stratal termination patterns are observed over a local upward bulge, associated with faulting, of the base-GII reflector r15 in the Vestbakken volcanic province; this points to a tectonic uplift of this area, at least until r23 time.

5.3.6. Megasequence GIII (r30 - seafloor)

5.3.6.1. Basal unconformity r30

Reflector r30, corresponding to the uppermost regional reflector R1 defined by Faleide et al. (in press), can be regarded as the most outstanding seismic marker identified in the study area. Its most important aspects were already briefly described earlier, in section 5.2.3. In the outer Bear Island Trough on the Barents shelf, r30 corresponds to the so-called URU or upper regional unconformity (Solheim & Kristoffersen 1984), which in landward direction successively truncates all seaward-sloping reflectors in megasequences GII and GI, and partly erodes into G0 (Window 8). Overlying this unconformity are mainly horizontal shelf strata. In the Storfjorden Trough area to the north, the pronounced unconformable character of r30 is strongly reduced, as the URU in this area occurs somewhat deeper in the stratigraphy, coinciding with r26 or R3 (Faleide et al., in press); moreover, r30 appears to be cut itself here on the outer shelf by reflector r36.

But the most notorious characteristic of reflector r30 undoubtedly is the featuring of a huge incision at this boundary in the south-eastern corner of the study area. The incision commences just downslope of the paleo-shelf edge and has affected large parts of the upper slope. On strike lines the limits of the incision are recognised as southward facing erosional escarpments (Windows 21, 26),

centred around $73^{\circ}30'$ N. The sinuous trajectory of this limit (Fig. 31) is the reason for the appearance of two seemingly separate and canyon-like incisions on line NPD-7330 (Window 13). The relief of the escarpment is max. 300 ms and gradually decreases downslope, fading out somewhere between 12° and $13^{\circ}30'$ E. On dip lines the incision limit can be distinguished as a concave-upward curvature of reflector r30. This is distinctly observed on line NPD-7300, just beyond the position of the paleo-shelf break (Window 8), indicating that the incision extends at least as far south as 73° N. The entire upper slope south of $73^{\circ}30'$ N thus appears to have been eroded, to an average depth of about 185 ms (Fig. 32). The entire feature is interpreted as a buried slide scar, similar in shape to the more recent scar near 72° N which still has expression in the present-day seafloor morphology (Kristoffersen et al. 1978; see Fig. 5). On the upper slope, reflector r30 dips at an angle of c. 1.5° , as measured just downslope of the concave-upward relief.

Outside the incision-affected part of the area, r30 generally constitutes an erosional and high-amplitude reflector, which locally has a contorted character on line MGK-1330, incidentally the location where erosion appears to be minimal. Over almost the entire western half of the study area r30 furthermore coincides with the top of the main chaotic interval identified within megasequence GII (section 5.3.5.3). Here, the horizon exhibits hummocky relief, and is locally even disrupted (Windows 1, 30, 35), but becomes level again where the underlying unit turns acoustically stratified.

The geometrical relationship of overlying GIII reflectors with respect to r30 is mostly downlap in WNW direction, and infilling onlap in the incisional area.

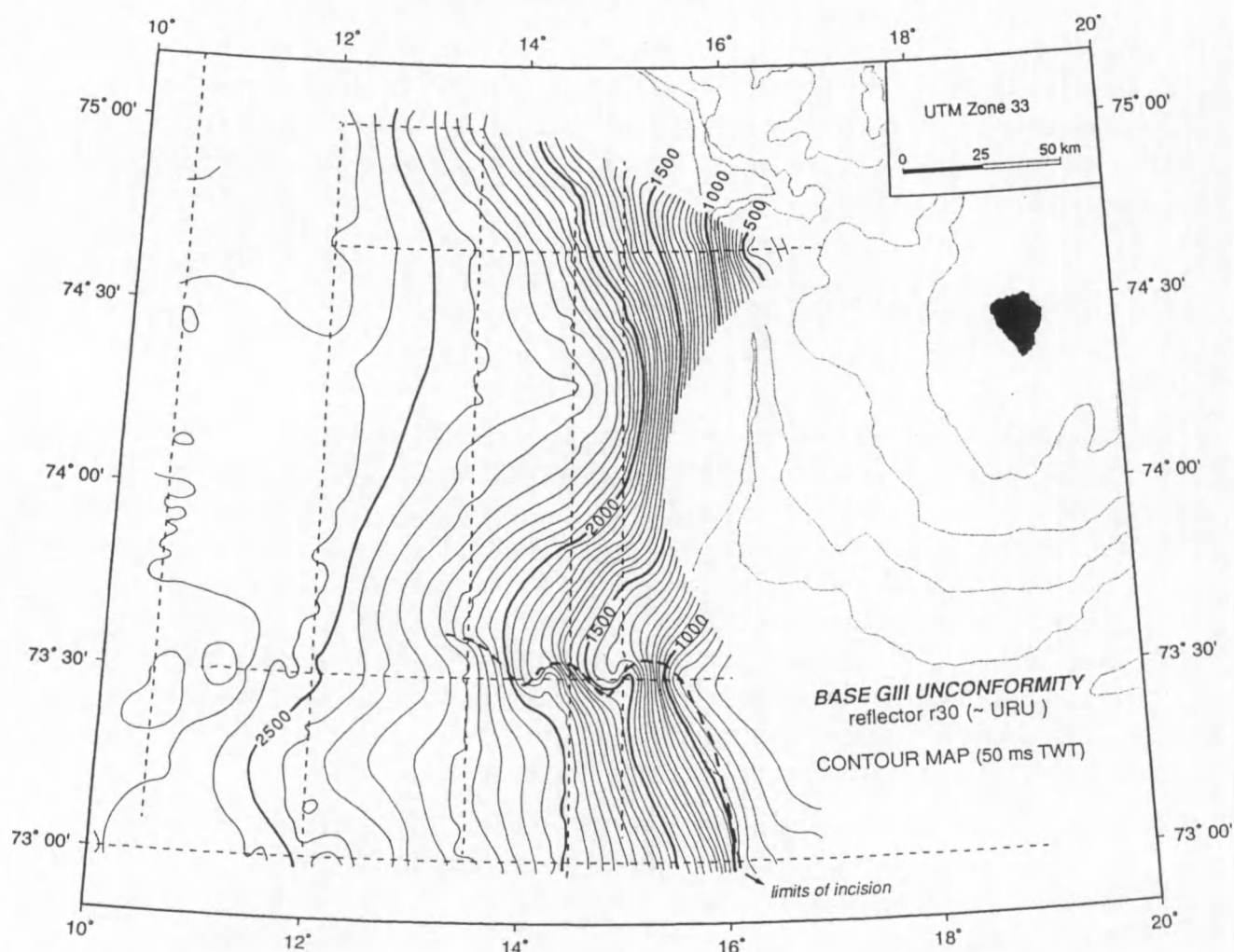


Fig. III.31 - Water-depth corrected contour map, in ms TWT, of base GIII unconformity r30. The thick dashed line marks the limits of the upper slope incision. Geofax by Verschuren (1992).

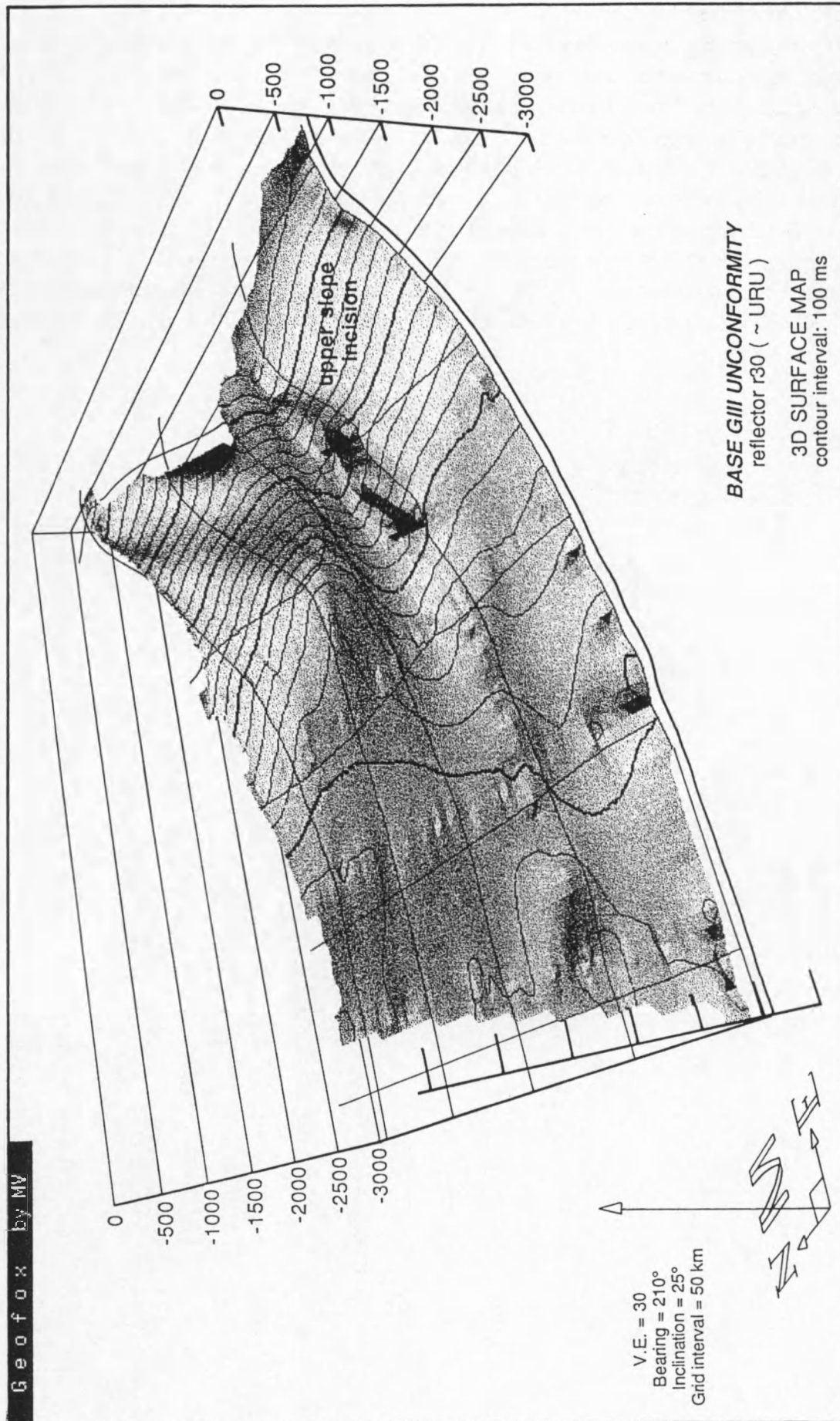


Fig. III.32 - 3D surface map of base GIII unconformity r30, visualising the pronounced incision on the upper slope of the Bear Island Cone. Gridded using Geofox (Verschuren 1992).

5.3.6.2. Thickness distribution

The isopach map of megasequence GIII (Fig. 33) is relatively simple, showing a single very prominent depocentre with thicknesses over 500 ms and dominating at least the southern half of the area, if not more. The thickness even greatly increases to between 750 and 1000 ms over the slide-affected area on the upper slope south of 73°30' N. A maximum thickness of 1250 ms is achieved below the present shelf break at 73° N. Internally, a distinction can be made between lower units (r30 - r34) which are mainly confined to the area of incision and pinch out in north-westward direction, and overlying units (r34 - seafloor) with obvious progradational character. Particularly noteworthy is that this southern depocentre occupies a more up-slope position than its precursor in megasequence GII (compare with Fig. 29). Being the only one of the three youngest megasequences that extends on the continental shelf in the Bear Island Trough area, GIII is also characterised by significant aggradation.

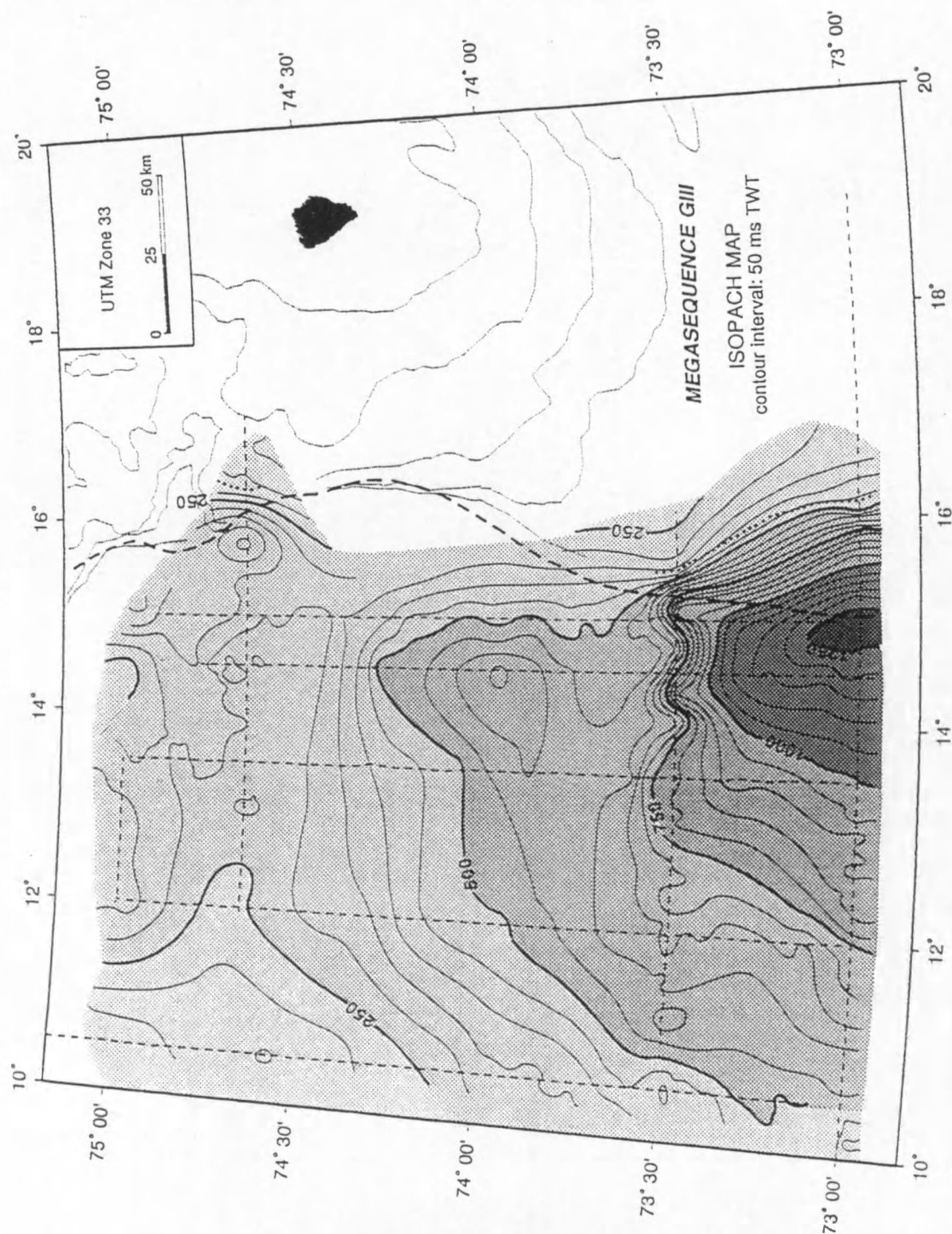


Fig. III.33 - Isopach map of Megasequence GIII. Contour interval is 50 ms TWT. Legend as in Fig. III.26. Gridded using Geofox (Verschuren 1992).

In contrast to preceding intervals, there is no obvious depocentre in the Storfjorden area: the sediments in the northern part of the area have a rather uniform thickness of less than 300 ms. There are indications, however, that the GIII sediments get somewhat thicker northward of the study area.

The large discrepancy between the Bear Island and Storfjorden depocentres is also evidenced by the amount of progradation: progradation is very pronounced on line NPD-7300, where it totals more than 30 km. Further north, values decrease to less than 5 km on line NPD-7440.

5.3.6.3. General seismic facies characteristics

The acoustic facies of megasequence GIII is hard to describe: it occupies the twilight zone between stratified, transparent and chaotic facies, and in addition appears slightly different on the two data sets, which have different resolution. The lower units, infilling the r30 incision, are unambiguously chaotic in nature, their facies not much diverging from that of megasequence GII (Window 13). The facies of the overlying units is mainly weakly stratified on the MGK-lines (Window 31), but rather transparent on the NPD-lines (Window 21). Common to both data sets is the local association with diffraction hyperbolae, especially in the south-eastern part of the study area. This “semi-chaotic” facies is distinctly different from the chaotic facies characterising GII. The observed diffraction hyperbolae, for one, are individually developed and not overlapping, and there is almost everywhere some evidence of stratification, which was completely absent from the main chaotic intervals within GII. This facies is interpreted to indicate a lesser degree of disturbance than was inferred for GII. In a general sense, the stratified character becomes more pronounced towards the north and west. On the upper slope portion of line NPD-7440, stratification is more irregular and diffuse.

5.3.6.4. Description of individual reflectors and units

The same warning applies here as the one issued in section 5.3.5.4.

- Reflectors r31, r32 and r33 are three discontinuous, locally high-amplitude reflectors onlapping the escarpment which delimits the huge incision at the GII/GIII boundary (r30) in the south-eastern part of the area (Window 26). Reflector r31 downlaps onto the GII/GIII boundary in western and northern direction. Reflectors r32 and r33 can essentially be traced to the western border of the study area, but are truncated by r34 or, where this horizon is itself eroded, by r35. None of the reflectors r31-r33 are observed in the north-east, however.

The units bounded by these reflectors are most extensively developed in the south-east, obtaining a maximal combined thickness of 350 ms in the incisional area. The units pinch out against, or greatly thin beyond the erosional escarpment delimiting the incision; complete pinch-out takes place further north. In western direction thinning occurs more gradually, to c. 100 ms. The seismic facies of the r30-r31 interval is clearly chaotic, whereas the units r31-r33 have a less well-defined facies, weakly stratified to reflection-free, and specked with local chaotic zones. The chaotic facies, with unmistakable diffraction hyperbolae, is again best developed where it is infilling the slide scar.

- Reflector r34 is mostly a medium- to low-amplitude reflector, which becomes more pronounced over the incision-affected area on the south-eastern upper slope. In this location the reflector has a higher amplitude, and makes a conspicuous facies boundary, separating chaotic facies below from transparent facies above (Window 13). On the dip lines NPD-7300 and NPD-7330, r34 onlaps the GII/GIII boundary near the apparent position of the offlap break, creating the false impression of erosional truncation of the latter horizon by r34 (Window 8). For this reason r34 has long been

regarded as an important boundary (it corresponds to base-unit IV of Spencer et al. 1984, and to base-TeE of Vorren et al. 1990, 1991), and as the downslope projection of the upper regional unconformity. On strike lines, r34 is seen to extend northward over and beyond the erosional escarpment shouldering the large incision at the level of the GII/GIII boundary (Window 26). Except for line MGK-1500, where the horizon laps out against r30, r34 is everywhere eroded by r35 towards the north and west. The reflector can therefore not be observed north of 74°20' N and west of 11°30' E. In one instance (line MGK-1330) it cuts itself into r33.

Unit r33-r34 is again best developed (c. 150 ms) in the incisional area, attaining maximum thicknesses of 200 ms in the canyon-like incisions near the limits of this feature on line NPD-7330. The unit abruptly thins to some 50 ms north of 73°30' N, pinching out entirely further north, and is also inferred to thin downslope. The facies of unit r33-r34 is almost everywhere chaotic, to a higher degree than in the underlying interval r31-r34. The chaotic facies is most pronounced in one of the canyon-like incisions on NPD-7330 (Window 13); it grades downslope into a more stratified facies. On the westernmost line MGK-1030 a similar but smaller-scale snout-shaped termination of chaotic facies (Window 38) is observed as has been described for the interval r26-r27 further north.

- Reflector r35 is the most important reflector identified within the entire GIII megasequence. It is the oldest significant reflector that is developed as a typical prograding clinoform, with a distinct offlap break. The topset section is only partly preserved, as r35 is truncated on the outer shelf by r37 (Bear Island Trough) or by r36 (Storfjorden area). The horizon erodes r34 on the middle and lower slope towards the north-west; towards the west both reflectors probably merge without significant erosion. The erosive character is particularly expressed on the northern end of line MGK-1200, in a channel-like incision (Window 34) which erodes some 50 ms below the base level of r35, and truncates down to r32. The large spacing of the seismic grid does, unfortunately, not allow to determine the up- and downslope extension of this feature. Overlying reflectors downlap the boundary in north-westward direction. The most conspicuous characteristic of r35 is observed on the upper to middle slope in the extreme south-east of the region, however. Lines MGK-1330 and NPD-1430 both show the development of an escarpment, centred around 73°10' N (Windows 20, 24). This escarpment has smaller relief (75 - 100 ms) and is also smoother, but otherwise has the same aspect as the above described escarpment at the level of r30, which occurs c. 45 km further north. Although the erosive nature of the scarp is less obvious (the underlying unit has a transparent facies), the feature is similarly interpreted as the buried scar of a slope failure. Concave-upward relief, indicated near 15°30' E on dip line NPD-7300, suggests that the scar extends southward of the limits of the study area, where a complementary escarpment is likely to occur.

Unit r34-r35 is the oldest unit blanketing the outer continental shelf, where its thickness amounts to 150 ms. A maximum thickness between 150 and 200 ms is recorded on the upper slope in the south-east of the region. The unit gradually thins, commonly to pinch-out, in northern and western direction. Drastic thinning by 100 ms to the south is an effect of the overlying escarpment. Thinning is also observed between 13°30' and 14° E on line NPD-7300, caused by local updoming of base reflector r34. The r34-r35 interval is horizontally stratified on the shelf. On the upper slope, however, the unit is typically transparent with isolated diffraction hyperbolae on the NPD-records, whereas it appears to be generally weakly stratified on the MGK-lines. Stratification becomes more prominent downslope and towards the north.

- Reflector r36 is mostly a discontinuous and medium- to low-amplitude reflector which loses distinction towards the north and downslope. The seismic horizon is most prominently developed on the upper slope portion of line NPD-7300, whereas it is extremely disrupted in the same location on line NPD-7330 (Window 13). Reflector r36 is cut by r37 in the outer Bear Island Trough on the continental shelf. On the continental rise (line MGK-1030) it locally onlaps against r35.

Unit r35-r36 is up to 350 ms thick on the middle slope in the southernmost part of the region (NPD-7300), where it overlies the important incision at the level of r35. In this location the interval even represents the thickest unit within the entire GIII megasequence. North of the r35 escarpment a more representative thickness of 150 ms is observed, gradually decreasing to 50 ms to the north. In downslope direction, however, the unit hardly thins: on the southern end of line MGK-1200 the interval still has a thickness between 150 and 200 ms. In contrast, unit r35-r36 does not extend far on the continental shelf in Bear Island Trough, as both its top and base reflectors are towards the east eroded by r37. The facies of the r35-r36 interval is typically transparent to weakly stratified on the NPD-records, but clearly stratified on the MGK-lines. Non-overlapping diffraction hyperbolae are often observed on both types of records; they are mainly concentrated to the area overlying the r35 incision. A distinct high-amplitude reflector at the base of the unit onlaps the foot of the ramp that delimits this incision. A marked lateral facies change occurs towards the upper slope: the facies here can best be described as highly irregular, complex and noisy (Window 17).

- Reflector r37 is the uppermost seismic horizon recognised below the seafloor. It constitutes a prominent unconformity on the outer shelf in Bear Island Trough, where it truncates the reflectors r36 and r35. The reflector can be traced at least as far landward as 17°30' E on line NPD-7300 without being truncated by the seafloor. These geometries cannot be confirmed on the shelf further north, as the seismic grid does not extend far enough eastward. On the continental slope and rise, r37 displays an overall conformable character.

The thickness of the r36-r37 interval follows approximately the same trends as the interval below. The unit is about 200 ms thick on the middle and lower slope in the south, and gradually thins to less than 75 ms towards the north and on the continental rise. It pinches out on the outer shelf in Bear Island Trough as well, due to the mergence of the top and base reflectors towards the east. The facies of unit r36-r37 is irregularly stratified to stratified on the NPD-lines, and definitely stratified on the MGK-lines. Usually the stratified character is more pronounced than that of the underlying unit. The upper slope is also dominated by the dark irregular facies described for the unit below (Window 17).

- The seafloor behaves slightly erosive with respect to internal reflectors, but is nowhere seen to erode down to the unit boundary r37. On the upper slope north of Bear Island Trough (line MGK-1500, Window 18), the seafloor is intersected by a number of small erosional channels, less than 50 ms deep and c. 1 km wide. These features do not appear to extend far downslope, as they are not observed on the adjacent line NPD-1430, some 15 km westward of this location. Their origin is discussed in section 6.1. Disturbance of the seafloor is furthermore indicated just beyond the shelf break on line NPD-7330 (Window 13). This is thought to be the result of a relatively recent slope collapse event, similar but much smaller in scale than the process that has shaped the buried slide scars at the level of r30 and r35. A last peculiarity concerns the occurrence of a brusque convex-upward curvature on the northern end of line MGK-1330 (Window 28), on the middle to lower slope. The extension of this feature can again not be determined, but it seems to be depositional in nature.

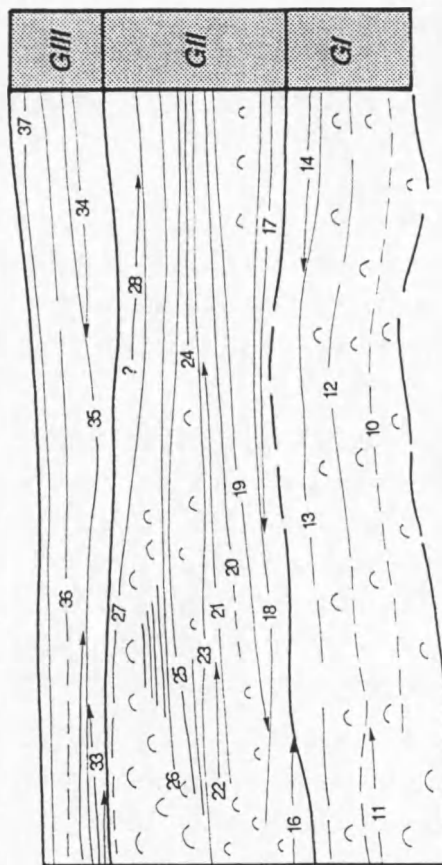
The interval between r37 and the seafloor extends over the entire outer shelf in the Bear Island Trough region, obtaining a maximal thickness of 150 ms below the shelf break, and slowly thinning in landward direction. Beyond the shelf break the thickness rapidly drops below 100 ms and gradually decreases to a mere 50 ms downslope and in northern direction. The seismic facies of this upper interval is horizontally stratified on the shelf, and stratified on the upper slope at 73° N. More northward, near 73°30' N it has a more transparent appearance, and is associated with some diffraction hyperbolae. Further downslope and northward the facies can no longer be discerned, due to insufficient resolution.

5.3.6.5. Summary of GIII

Megasequence GIII is the youngest of the four identified first-order stratigraphic entities. Its base is defined by reflector r30 (~R1), probably the most striking seismic horizon in the area of investigation. In the outer Bear Island Trough, r30 truncates all seaward dipping foresets of successively GII and GI, a characteristic from which it derives the name "upper regional unconformity" (URU). Overlying sediments are mainly horizontal and parallel stratified. The unconformable character of r30 is strongly reduced in the Storfjorden Trough, however. A huge incision in the upper slope in front of the mouth of Bear Island Trough undoubtedly constitutes the most conspicuous feature of the GII/GIII boundary. The incision forms a semi-circular depression, its open end downslope, and surrounded by pronounced erosional escarpments which are up to 300 ms in height. The entire feature is interpreted as a buried slide scar, resulting from a major collapse of the paleo-upper slope. The thickness distribution of GIII is characterised by a single depocentre dominating the entire southern half of the study area. Its thickness exceeds 500 ms, and even amounts to more than 1 s over the area of incision. This depocentre clearly occupies a higher position on the slope than the equivalent GII depocentre, while in contrast to the older two megasequences, no depocentre has developed at the mouth of Storfjorden Trough. Within the main depocentre, a clear bipartition is noted of the composing sediments. Lower units (r30-r34) are restricted to the confines of the slide-affected area, onlapping onto, or just beyond the encircling escarpments; they represent an initial phase of preferential infilling of the slide scar. The upper units (r34-seafloor) extend beyond the limits of incision and over the entire area, thus reflecting a situation in which the scar was "healed", and the slope had again attained its original profile. Individual units display pronounced progradation (over 30 km at the mouth of Bear Island Trough), but also significant aggradation (almost 500 ms in outer Bear Island Trough), which makes them the first units within the GI-GIII interval reaching onto the continental shelf. Some of these units are eroded towards the inner shelf, however. The seismic facies of megasequence GIII is described as semi-chaotic (transparent to weakly stratified, with non-overlapping diffraction hyperbolae), distinctly different from the unambiguously chaotic facies of GII. It is inferred to indicate disturbance by smaller-scale mass wasting features than in GII. Reflector r35, the most important horizon within GIII, shows evidence of a slide scar, similar to but smaller than that at the GII/GIII boundary, whereas the present-day seafloor is locally to a small degree collapsed on the upper slope.

Stratal geometry and distribution of acoustically chaotic facies in GI - GIII, for both the Bear Island and the Storfjorden areas, are summarised in the idealised stratigraphic columns in Fig. 34.

STORFJORDEN CONE
(southern half)



BEAR ISLAND CONE
(northern half)

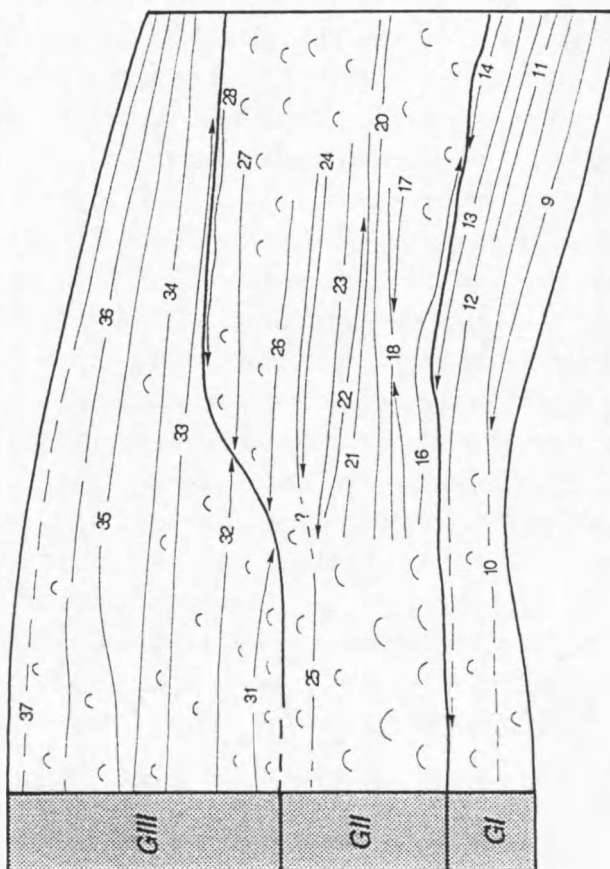


Fig. III.34 - Conceptual stratigraphic diagram ("type section") illustrating the stratal geometry and distribution of chaotic seismic facies in megasequences G1 - GIII, distinguishing between Bear Island and Storfjorden Cones.

6. Sediment remobilisation processes on the Bear Island Cone

6.1. Introduction

Most of the Bear Island Cone appears to have been emplaced on the lower continental slope and rise by sediment remobilisation processes, moving downslope sediments that were originally deposited on the outer shelf and upper slope. Original deposition mainly involved glacial and glaciomarine processes, and will be discussed elsewhere, in relation with the glacial history of the margin (section 7.4).

Buried slope failure scars, disrupted reflectors, and the massive occurrence of an acoustically chaotic facies, interpreted to indicate disturbed stratification, form abundant evidence that large-scale mass wasting processes have dominated deposition in this remarkable environment. The importance of smaller-scale mass movements such as turbidity currents is more difficult to assess, since the resulting deposits basically fall below the resolution of the seismic tool. It is clear, however, that stable, long-term action of turbidity currents has not prevailed, as the stacking of turbidite facies should show up as intervals of well-defined and continuous stratification on the seismic sections.

Apart from purely gravity-driven transport, sediment can also be redistributed by water currents. Downslope transport of sediment by episodic thermohaline currents may be evidenced in the form of erosional gullies (Fig. 35a) observed in the seafloor on the upper slope at the northern mouth of Bear Island Trough. These gullies are relatively small features, less than 1 km wide and 50 m deep, and do not extend far downslope: they are observed on line MGK-1500, in water depths of 640 to 900 m, but can no longer be detected on the adjacent line NPD-1430 where corresponding water depths are between 940 and 1010 m. This is in accordance with findings of Bugge (1983) and Vorren et al. (1989) on the upper slope south of the mouth of Bear Island Trough, where gullies of similar size occur (Fig. 35b), many of them starting at the shelf edge and continuing down to water depths of 1000 m. Vorren et al. (1989) suggested that they are eroded by thermohaline currents, which lose bed contact at a depth where their density equals that of the surrounding deep-sea water, thus becoming interflows. Some of these gullies continue to greater depths, however, and the asymmetric convex-upward feature observed on line MGK-1330 (Window 28), in a water depth of c. 2100 m, may have been deposited as a levee by similar downslope currents flowing along the bathymetric divide between the Bear Island and Storfjorden Cones. Alternatively, the gullies could be explained as relict features, formed by ice-marginal processes during periods of glaciation (Bugge 1983; Laberg & Vorren, in press b). At any rate, the local occurrence, limited downslope extent and restricted preservation in the geological record, strongly suggest that the process that has shaped the gullies, had no significant contribution to the total sediment budget of the Bear Island Cone. The same applies to the influence of contour currents. The seismic lines show no evidence of major contourite drift deposits, conforming to the fact that no important contour current activity is documented in this part of the Norwegian-Greenland Sea (Coachman & Aagaard 1974). Yoon & Chough (1993) have reported some indications for sedimentation from contour currents on the southern flank of Bear Island Cone, but their observations are limited to the upper few metres of the sedimentary column. These contour currents would be driven by exchange of water masses with the North Atlantic Ocean.

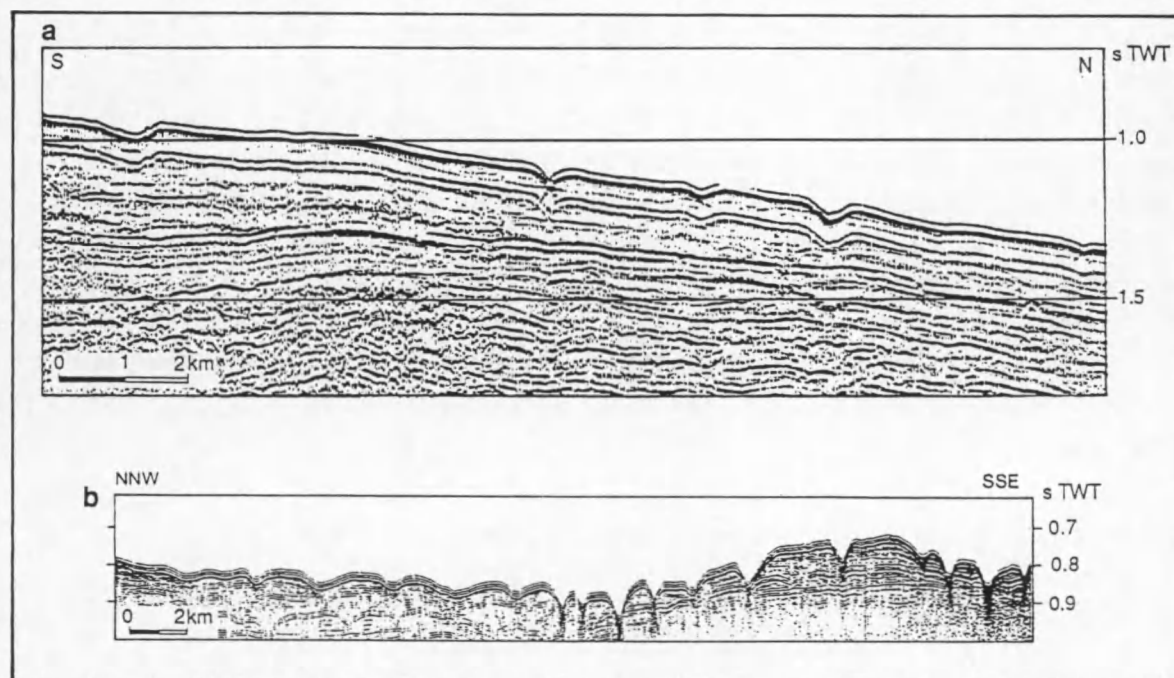


Fig. III.35 - [a] Small-scale gullies eroding the seafloor on the upper slope north of the axial mouth of Bear Island Trough (line MGK-1500). [b] Similar features on the upper slope south of the axial mouth of Bear Island Trough (sparker record from Vorren et al. 1989).

6.2. Submarine mass movements — a short overview

The seismic sections show abundant evidence of several kinds of mass wasting. In order to comprehend the processes that shaped the Bear Island Cone, full understanding of the different types of mass wasting and their range of dimensions is indispensable. A short overview is therefore given first.

Mass movement can be defined as the gravity-driven downslope transport of sediment moving *en masse*, as a result of slope instability. It is a widespread phenomenon in a wide variety of environments, but particularly the continental slope is known to be the site of all sorts of mass movement. Large features involving sediment volumes between 0.001 and several 100 km³ have caught most attention, but smaller-scale displacements, ranging between 10³ and 10⁶ m³, may well be of equal importance (Field & Clarke 1979; Einsele 1991). In contrast to subaerial analogues, submarine slope instabilities can develop on extremely low-angle slopes, of even less than 1° (Prior & Coleman 1984).

The first-order classification of submarine mass movements (Table 6) is based on the mechanical behaviour during downslope transport (Dott 1963; Nardin et al. 1979), which is reflected in the degree of internal deformation within the resulting deposit. Creep, rockfall and sliding are elastic processes, in which sediment moves rigidly, without significant internal deformation. Plastic behaviour, implying irreversible internal deformation, is exhibited by debris flows. In fluidal flows, finally, the mass no longer moves as a solid, but as a viscous fluid. Anelastic transport mechanisms are jointly referred to as sediment gravity flows or mass flows, as it is often difficult to determine whether plastic or fluid behaviour has dominated during transport, and both mechanisms may even

have acted together in a single flow. Mass flows are further subdivided (Table 6) according to the dominant coarse-particle support mechanism operative during sediment transport (Middleton & Hampton 1976; Lowe 1979): in cohesive debris flows and mud flows, clasts are supported by cohesive strength, provided by a matrix containing varying proportions of mud; grain flows are characterised by frictional strength, arising from direct grain-to-grain interactions which maintain a dispersive pressure against gravity; in fluidised and liquefied flows sediment is, respectively, fully and partly supported by upward escaping pore fluids; and in turbidity currents sediment is supported by the upward component of fluid turbulence. Natural flows probably exist throughout a continuum between these conceptual end members. In addition, many mass flows evolve from steady laminar to fully turbulent systems (Einsele 1991). The only long-distance transport mechanisms are debris flows and turbidity currents (Nardin et al. 1979).

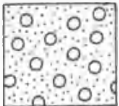
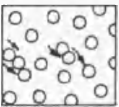

Mechanical behaviour	Mass transport processes				
<i>rigid</i>	CREEP				Coarse-particle support mechanism
	ROCKFALL				
	SLIDE	SLIDE s.s.		 cohesion (matrix strength)	
		SLUMP			
<i>plastic</i>	SEDIMENT GRAVITY FLOW	DEBRIS FLOW	DEBRIS FLOW s.s.		 friction (grain interaction)
			MUD FLOW		
<i>viscous fluid</i>	or MASS FLOW	GRAIN FLOW		 upward intergranular flow	
		LIQUEFIED FLOW			
		FLUIDISED FLOW			
		TURBIDITY CURRENT			

Table III.6 - Classification of submarine mass movements, based on mechanical behaviour and coarse-particle support mechanism. Adapted from Nardin et al. (1979).

Creep

Creep refers to the slow downslope movement of sediment without failure (Pickering et al. 1989). Though stability modelling indicates that creep may be widespread and significant, no deposits have been unambiguously attributed to this slope process (Prior & Coleman 1984).

Rockfall

Rockfall includes the free fall of individual rock masses or clasts along steep, near-vertical slopes (Prior & Coleman 1984). The transport distance is thus very limited, and the resulting deposits commonly form a talus cone at the base of these slopes.

Slides and slumps

A slide (Fig. 36a) involves the downslope translocation of large coherent or semi-coherent sediment masses along discrete shear or slip planes (Nardin et al. 1979). The basal slip plane corresponds to a plane of weakness, usually a bedding surface parallel to the regional slope (Prior & Coleman 1984). Towards the head of the slide the shear surface becomes concave-upward, intersecting the contemporaneous seafloor; the exposure of the shear surface is expressed as a scarp-bounded depression, known as the slide scar (Lewis 1971). The length between the frontal scarp (or headwall) and the displaced mass is a measure of the minimum transport distance, which is usually rather short. In plan view, slide scars are typically arcuate, open towards the downslope end (Prior & Coleman 1982). The “toe” of the slid mass may show irregular topography and internal contortion, reflecting compressional folding and thrusting at the leading edge of the slide (Lewis 1971). Sliding is considered the most widespread type of submarine slope instability, and typically occurs on low-angle slopes ($< 5^\circ$); their dimensions are often much larger than those of terrestrial slides (Prior & Coleman 1984). Some extremely large slides are documented, with volumes between 1000 and 20,000 km³ (Table 7).

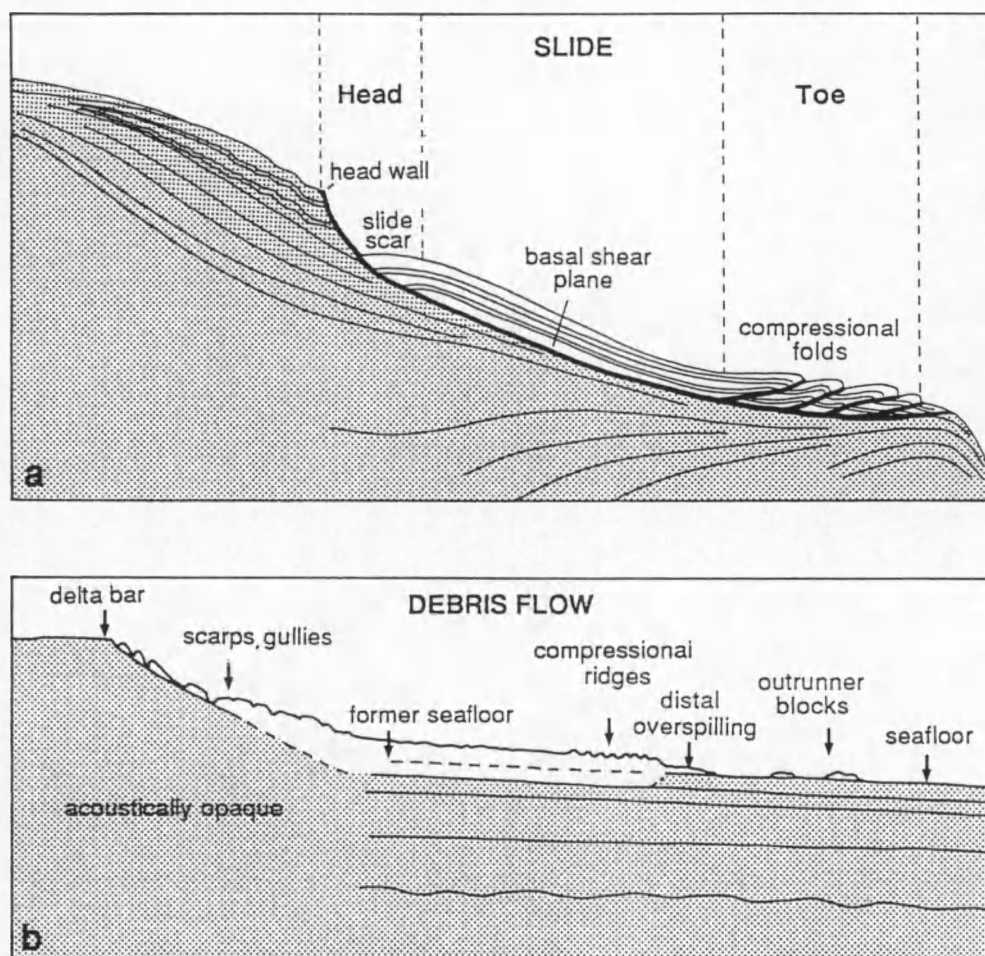


Fig. III.36 - Morphological characterisation of submarine mass deposits. [a] Slide (Lewis 1971). [b] Debris flow (Prior et al. 1984).

Type of mass movement	Location	Slope angle (°)	Extent (km)	Thickness (m) average/max.	Area (km ²)	Volume (km ³)	Reference
SLIDES	Agulhas slide, S. Africa	n.d.	750	255/375	79,448	20,331	listed in Prior & Coleman (1979, 1984)
	Storegga slide, Norway	0.6	800	114/280 (st. 1) 160/430 (total)	34,000	3,880 (st. 1) 5,580 (total)	Bugge et al. (1987)
	Grand Banks slide, Newfoundland	3 - 4	160	- /365	27,500	760	listed in Prior & Coleman (1979, 1984)
	Rockall slide, NE Atlantic	2	160	136/330	2,200	300	listed in Prior & Coleman (1979, 1984)
	Kidnappers slide, New Zealand	4	11	20/50	250	8	Lewis (1971)
FLOW-SLIDE ?	Rhône Fan, NW Mediterranean	n.d.	170	33/160	5,100	170	Bellaiche et al. (1990)
DEBRIS FLOWS	Canaries debris flow, NW Africa (W. Sahara)	1.5	700	20/-	30,000	600	Embley (1976)
	Orphan Basin debris flows, Newfoundland	1.5	15 - 65	9 - 37/50	60 - 1,000	1 - 27	Aksu & Hiscott (1992)
	Baffin Bay debris flows, Canadian Arctic	1.5 - 2	8 - 15	15 - 25/-	43 - 1,000 (3,869)	0.3 - 7.7 (36.7)	Hiscott & Aksu (1994)
	South Pass mud flows, Mississippi Delta	1.5	50	5 - 15/35	770	11.2 (?)	Coleman & Garrison (1977)
	Kitimat fjord debris flow, British Columbia, Canada	8	5	8/-	7.5	0.055	Prior et al. (1984)
MEGA-TURBIDITES	Grand Banks turbidite, Newfoundland	n.d.	600 (1 m) - > 1,000	- /1	100,000 - 400,000	160	Heezen & Ewing (1952), Piper et al. (1985)
	Black Shell turbidite, Hatteras Abyssal Plain	n.d.	500	- /4	44,000	100	Elmore et al. (1979)

Table III.7 - Figures illustrating the wide range of dimensions of various types of submarine mass movements. n.d. = no data, st. = stage.

The term “slump” has been used to indicate either slides with a rotational component (Dingle 1977; Nardin et al. 1979), or slides showing considerable internal deformation and often evolving into debris or mud flows (Einsele 1991). In rotational slumps, multiple concave-upward shear planes are observed in between which individual blocks are rotated backward; at depth these curved failure planes coalesce into one planar basal glide plane (Prior & Coleman 1979). Prior & Coleman (1984) argue, however, that the vertical exaggeration of seismic data tends to magnify the curvature of failure planes in appearance, and that the rotational component is often insignificant. The more general definition of Einsele (1991) will therefore be applied here.

A further morphological distinction has been made by Prior & Coleman (1984) between shallow rotational slides with more or less circular slip planes, and the more common translational slides, in which the basal failure surface is planar and more or less parallel to the surface. In this classification scheme a special position is reserved for bottleneck slides, which are composed of an arcuate, depressed source region, a narrow neck and a widespread depositional lobe; they involve both sliding and flowing, and can therefore be characterised as flow-slides.

Debris flows

In debris flows the shear stress is distributed throughout the entire mass, rather than concentrated along a limited number of well-defined slip planes (Nardin et al. 1979). This results in a laminar flow, resembling that of wet concrete, and which is composed of a relatively dense and cohesive mixture of fine sediment and interstitial fluid, capable of supporting larger blocks (Einsele 1991). Debris flows are sometimes regarded as transitional between slides and turbidity currents (Prior & Coleman 1984), and represent the most important flow type in the oceans. They can be quite mobile, even on very gentle slopes of 0.1 to 1° (Embley 1976). The flow probably exhibits erosive power only when confined to linear depressions (Aksu & Hiscott 1992), or when sediments at the seafloor are very soft (Prior et al. 1984). Deposition from debris flows occurs by rapid “freezing” when the excess pore water dissipates (Einsele 1991). There is no sharp boundary between debris flows s.s. and mud flows. Debris flows s.s. consist of a medium- to fine-grained matrix and a varying proportion of clasts or blocks that can reach the size of a house or more; mud flows have a muddy matrix with a high silt content and contain only a small amount of clasts (Einsele 1991).

The resulting deposits are called debrites or olistostromes. They are composed of pebbly mud, with textures strongly resembling tillite deposits (Kennett 1982). The high degree of homogenisation is reflected in the typical lack of stratification (Einsele 1991). Debrites form finger-shaped depositional lobes, with the longest axis oriented downslope (Fig. 37). Their thickness can total some tens of metres (Table 7). Further morphological characteristics were described by numerous authors (e.g. Embley 1976; Coleman & Garrison 1977; Prior et al. 1984; Hesse 1992; Hiscott & Aksu 1994), and are shown in Fig. 36b: debrites terminate abruptly, laterally and in the downflow direction, in bullet- or snout-shaped margins, and have a mounded upper surface forming a positive relief above the contemporaneous seafloor. They tend to fill in pre-existing morphology, which results in a shingled configuration when deposited on top of one another (Aksu & Hiscott 1992). The basal contact is in most cases not apparently erosive.

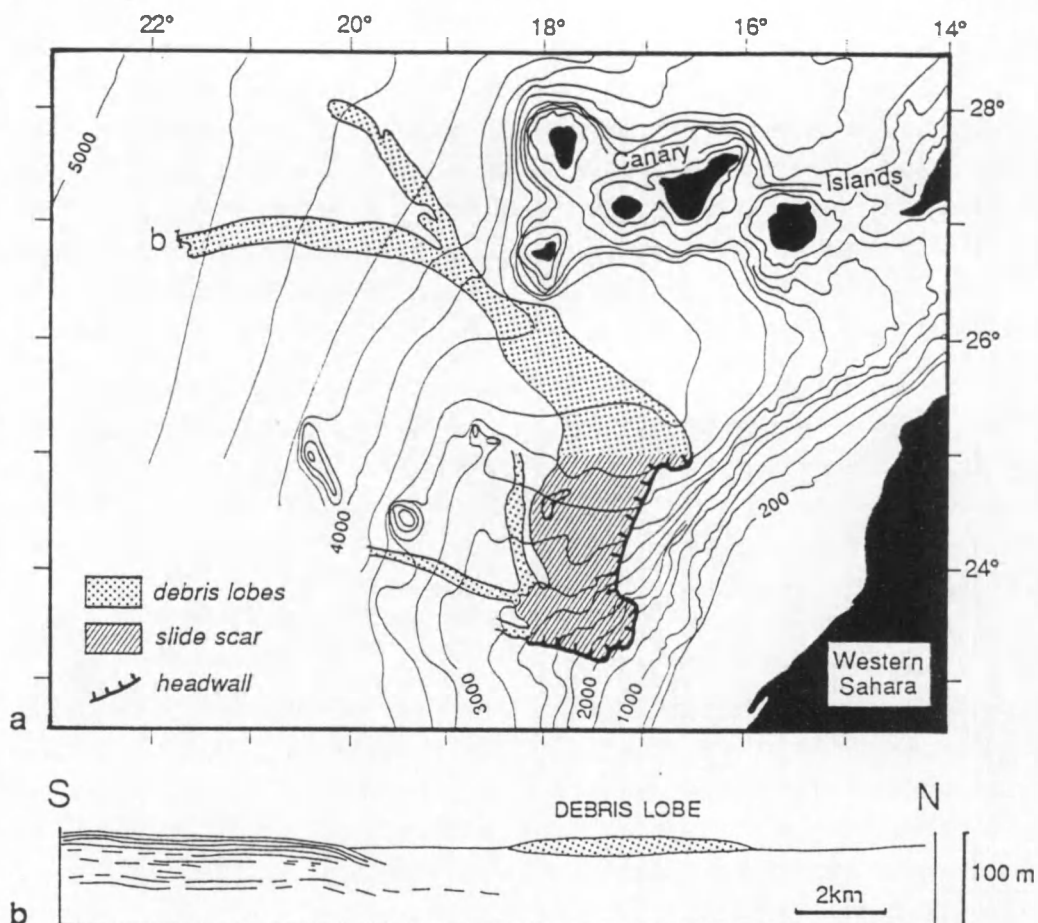


Fig. III.37 - [a] Plan view of a typical finger-shaped debris flow, exemplified by the Canaries debris flow. [b] Cross-section through distal debris lobe. From Embley (1976).

Grain flows

Grain flows specifically involve pure and uniformly-sized sand, and can only be maintained on slopes greater than about 20° (Lowe 1979). They are generally less than 5 cm thick (Lowe 1976), and the travel distance is short (Einsele 1991). The effects of grain flows are therefore localised.

Turbidity currents

Turbidity currents are very widespread and significant processes which have built up large portions of the world's continental rises and abyssal plains. Several mechanisms can lead to the generation of turbulent suspensions (Prior & Coleman 1984; Einsele 1991): failure of unstable submarine sediment accumulations, evolution from high-density mass movements such as slumps or debris flows by the uptake of additional water, or continuous underflow of dense sediment plumes at the mouths of heavily charged rivers and glaciers; the latter process cannot be considered a true slope instability process, however. A distinction is made between high- and low-density turbidity currents (Einsele 1991). High-density currents can carry relatively coarse-grained sand, and even gravel as bed load. They reach high velocities, can travel over long distances, and have the capacity to erode cohesive muds on the seafloor. Low-density turbidity currents flow slowly and can therefore keep only silt- and clay-sized material in suspension. Their erosional capacity is limited. They can attain

considerable flow thicknesses (up to several hundred metres) and distribute their suspended load as a thin bed over wide areas. Turbidites, i.e. sediments deposited from suspension currents, commonly have mm- to cm-scale; in rare cases ("megaturbidites") metre-scale thicknesses are attained (Table 7). Turbidites are moderately sorted, and display a typical vertical succession of sediment properties and structures (Bouma 1962), known as the Bouma sequence. The development of this type of graded bedding is governed by the vertical variation in flow regime of the turbidity current.

Acoustic signature of mass deposits

Most gravity deposits that can be recognised on seismic records of a resolution comparable to the lines used in this study, probably fall in the category of slide/slump masses and of debris or mud flow deposits. Other types are generally of a scale too small to have seismic expression, unless the stacking of several such deposits combines into a recognisable reflection pattern. This is particularly known for turbidite sequences, which appear as thick and regularly stratified mound-shaped intervals (Fig. 38d), e.g. in submarine fans.

Slide masses (Fig. 38a and b) show up on seismic records as slope- or base-of-slope units with well-defined internal reflectors which are only slightly deformed (Nardin et al. 1979). Local contortion, associated with a hummocky topography, may be evident, especially at the toe, where deformation is most pronounced (Lewis 1971). In slump masses a higher amount of internal deformation is indicated by the presence of diffraction hyperbolae, and discontinuous or even absent internal reflectors, resulting in an overall chaotic facies. The front of each slide mass is defined by a concave-upward unconformity (the shear plane), cutting into underlying slope reflectors and turning down-dip into a more conformable (and hence less conspicuous) reflector defining the base of the slided mass. Internal reflectors sometimes exhibit inverse dip towards the upward curving basal unconformity, which reflects backward rotation during slope failure (Nardin et al. 1979).

Large debris flow or mud flow deposits (Fig. 38c) are typically expressed as chaotic to transparent lenses or mound-shaped units with few or no coherent internal reflectors (e.g. Embley 1976). The lack of internal structure is the result of destruction of the original stratification, and concurrent deformational homogenisation of the sediment mass (Nardin et al. 1979). Indistinct internal reflections may sometimes indicate a composite origin of deposits that accumulated from successive separate flows (Hesse 1992), whereas in other cases individual lenses are more clearly separated by a veneer of acoustically stratified sediments (Hiscott & Aksu 1994). Debris flow units are usually characterised by low-amplitude, prolonged bottom echoes (Nardin et al. 1979) that may show evidence of erosion (Prior et al. 1984; Bellaiche et al. 1990; Aksu & Hiscott 1992). On high-resolution records the debris flow units are opaque, masking underlying strata (Prior et al. 1984). The lateral and frontal margins are typically sharp and distinct, shaped as a snout or toe which is elevated with respect to the more distal contemporaneous seafloor (e.g. Coleman & Garrison 1977). The top surface of a debris flow deposit is commonly undulating, occasionally associated with diffraction hyperbolae, and especially near the distal edge becoming irregular and hummocky (Prior et al. 1984). Other morphological characteristics were described above.

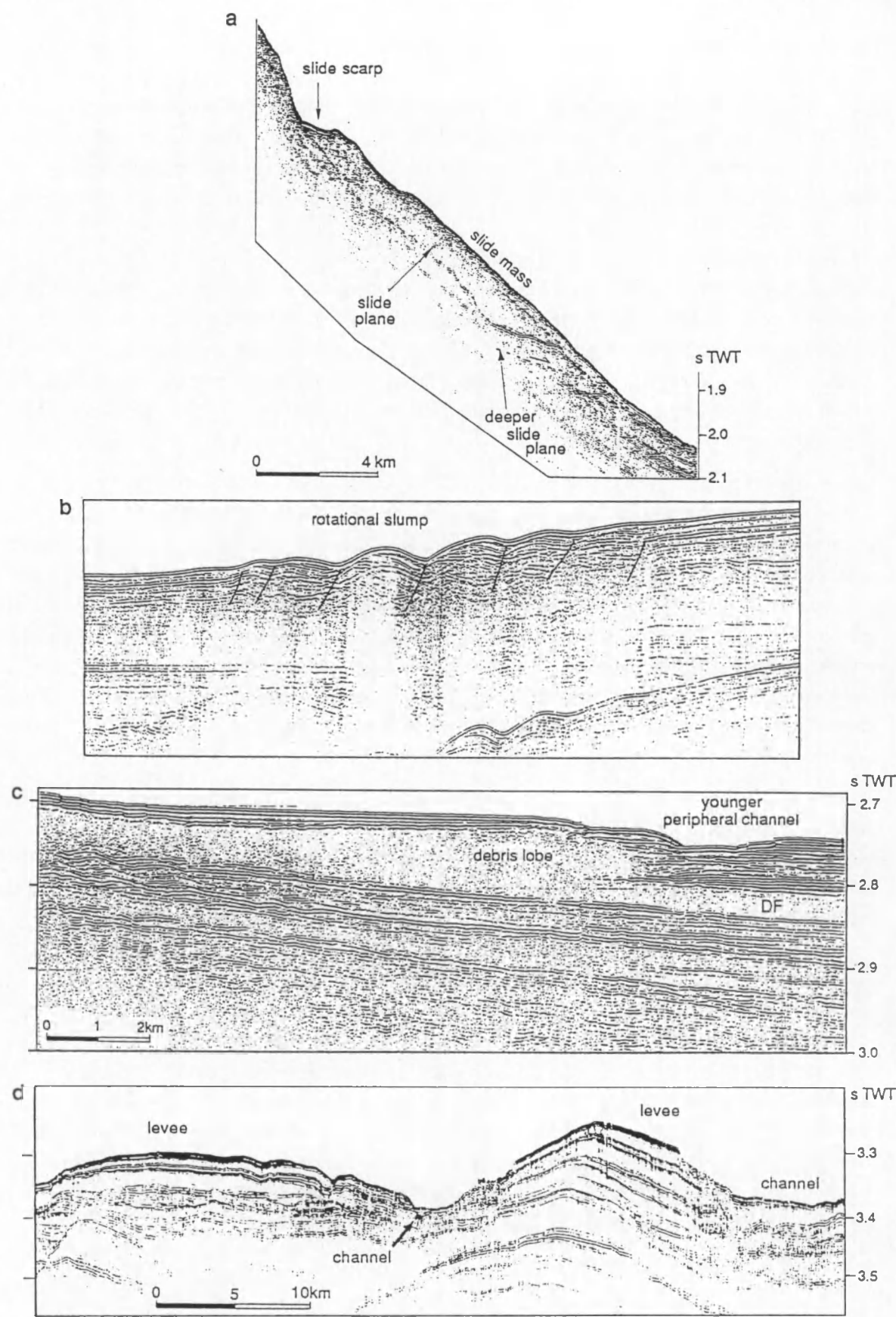


Fig. III.38 - Acoustic signature of different types of submarine mass deposits. [a] Slide (Hiscott & Aksu 1994). [b] Rotational slump (Hart 1993). [c] Debris flow deposit (Hiscott & Aksu 1994). [d] Turbidites stacked into a channel/levee system (Hesse 1992).

6.3. The slide scar at the GII/GIII boundary

Certainly one of the most prominent manifestations of large-scale mass wasting on the seismic records is the huge incision identified at the GII/GIII boundary in the south-eastern part of the region (cf. section 5.3.6.1; Fig. 39). The incision occupies a paleo-upper slope position in front of the axial mouth of Bear Island Trough, and is characterised by erosional ramps surrounding a (towards the sea) open-ended semi-circular area from which a substantial volume of sediment has been removed. The landward limit of the incision is defined by a concave-upward curvature of the r30 horizon (Fig. 39d), probably cutting c. 300 ms down into contemporaneous upper slope sediments that can be recognised up-slope from the feature; whether this basal slide surface becomes subparallel to the older stratification further downslope cannot be confirmed, since these sediments are essentially chaotic in nature. The northern limit is outlined by a sharp escarpment or “shoulder” (Fig. 39b and e), with elevation between 260 ms (NPD-1430) and 120 ms (MGK-1330), but disappearing downslope towards line MGK-1200. The development of two seemingly separate canyon-like incisions on dip line NPD-7330 (Fig. 39c) appears to be the result of the sinuous trajectory of this escarpment (Fig. 39a). A southern limit could not be observed on the seismic lines, indicating that the incision extends a fair distance south of the study area.

Knutsen et al. (1992) were the first to report on the feature described here, but did not realise its full extent. Mainly based on the appearance on line NPD-7330, they put forward the idea of two large submarine canyons. Kuvaas & Kristoffersen (in press) on the other hand, interpreted the whole incision as the youngest (“yellow”) of a series of five slide scars, and attributed the undulating nature of the northern limit to tributary scars. An erosional escarpment complementary to the ramp further north forms the southern limit of the slide scar, extending as far south as 72°30' N (Fig. 39a). This is also indicated on maps published by Laberg & Vorren (in press a) (their slide “B”). The observations made in the present study and summarised above, support the interpretation of the incision as a huge slide scar with a width between 100 and 120 km. The surface area of the scar in the study area is estimated at 5500 km²; combined with the observations of Kuvaas & Kristoffersen (in press) and of Laberg & Vorren (in press a) a total area of c. 9500 km² is inferred. Taking an average of 185 m for the depth of incision, the volume of the removed sediment in the study area would total c. 1020 km³. Comparison of these values with Table 7 in the preceding section shows that the slide on the central Bear Island Cone ranks amongst the largest such artefacts known. In fact, its dimensions are quite comparable to two other large-scale slides that have been identified further south, on the southern flank of the Bear Island Cone, and on the mid-Norwegian margin (the Storegga slide), respectively. Relevant parameters for these features are summarised in Table 8.

There is, however, some disagreement regarding the exact mechanism of mass wasting, and the amount of sediment involved. Kuvaas & Kristoffersen (in press) suggest that most of the sediments filling in the slide scar, almost up to the reflector they regard as URU (but which in fact corresponds to r34), were entrained in a slide or slump characterised by very little deformation and a small travel distance. Better coverage of the middle and lower slope, and the use of data of intermediate resolution, prompts for a revision of this concept. First, r34 is indeed the uppermost reflector onlapping the slide head, but further west it is seen to spill over the escarpment (line MGK-1330); the top of the escarpment is here onlapped by r32. This indicates that at least the interval r32-r34 has an origin not related to the slope failure. And secondly, several units can be discerned in the deposits filling in the slide scar depression, some with distinct chaotic facies. The alternation of continuous reflectors and intervening chaotic facies does not concede with a single displacement of the entire

interval. Rather, it is suggested here that only the lower unit r30-r31 (shaded in Fig. 39), though volumetrically the least important of these intervals, represents the material wasted by the failure.

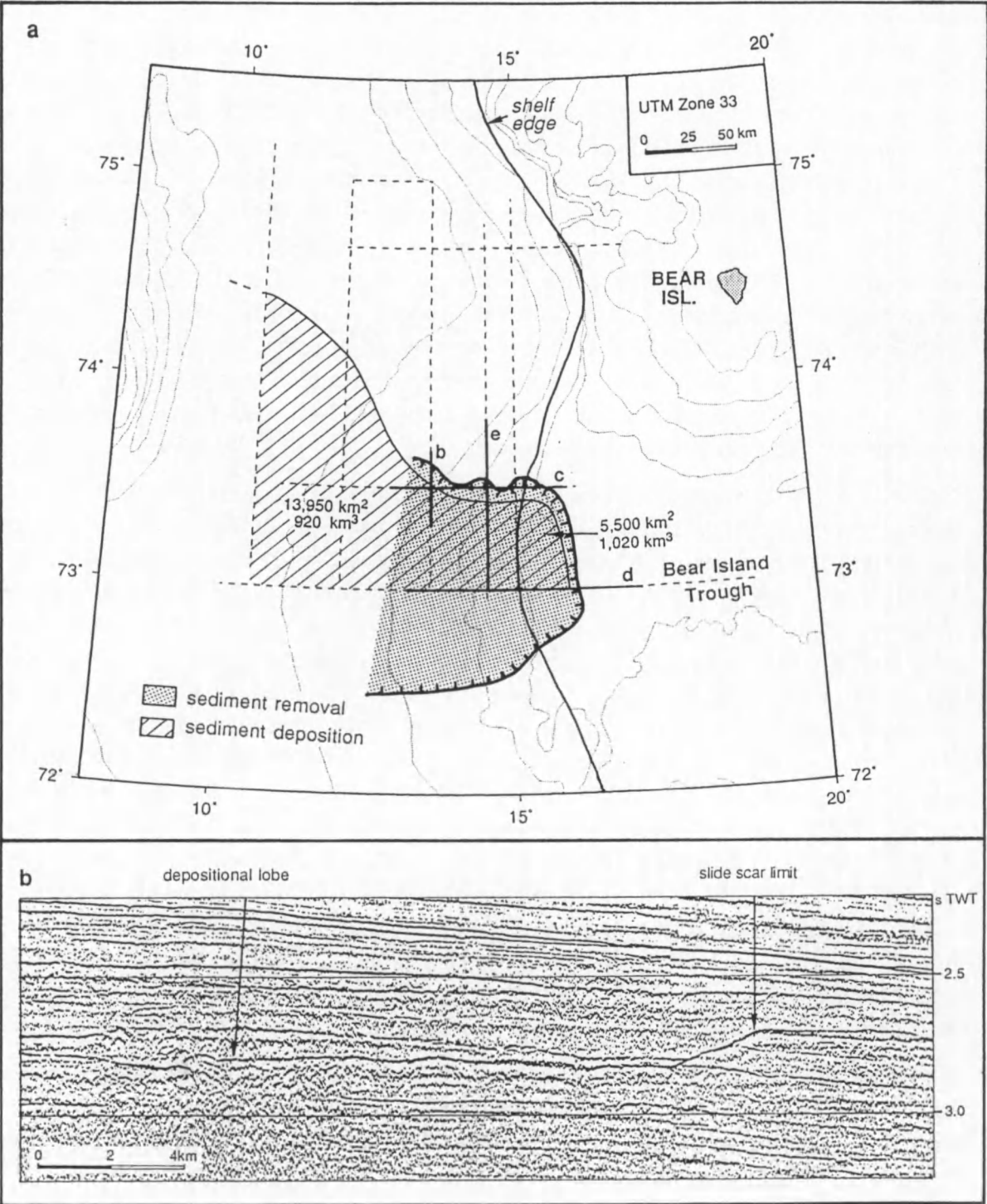
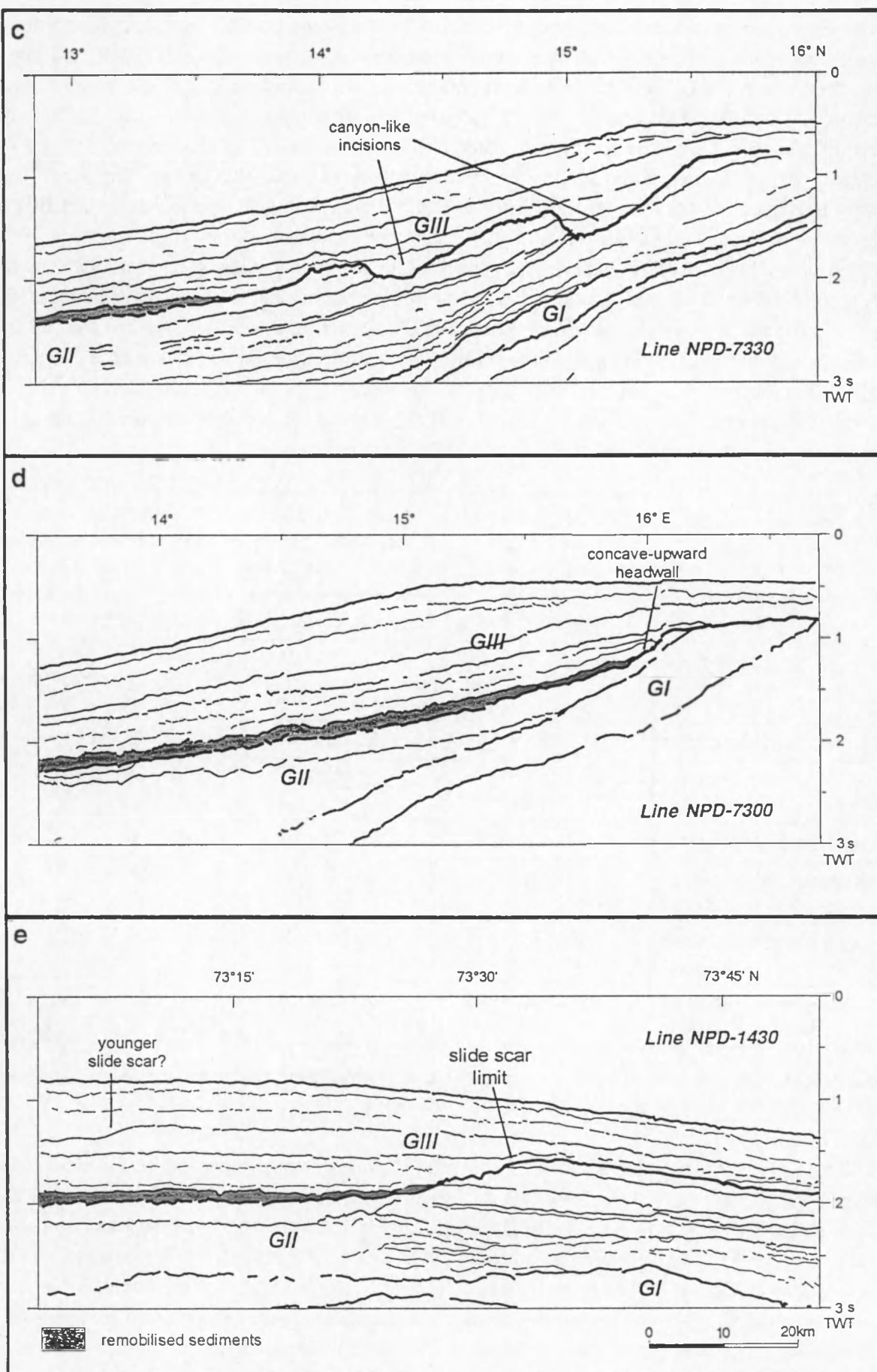


Fig. III.39 - The slide scar at the GII/GIII boundary. [a] Areal map of zones of sediment removal and sediment deposition. Location of headwall south of 73° N is taken from Kuvaas & Kristoffersen (in press) and Laberg & Vorren (in press b). [b] Seismic cross-section (line MGK-1330) showing erosional ramp and depositional lobe. [c] Line drawing of section near the limit of incision (line NPD-7330). The slide scar appears as two seemingly separate canyon-like incisions. [d] Line drawing of longitudinal section through the slide (line NPD-7300). The headwall is characterised by concave-upward relief. [e] Line drawing of cross-section through northern half of the slide scar (line NPD-1430).



The other units would thus have been deposited at a later stage, possibly by mass movements as well. This conclusion is confirmed by geometry and facies considerations: [i] unit r30-r31 is entirely confined within the limits of the slide scar, and spreads out downslope (Fig. 39a); [ii] its seismic facies is more unambiguously chaotic than that of the other units filling the scar; [iii] the unit displays an overall mounded shape; and finally, [iv] its top surface r31 in some instances (Fig. 39b) clearly dips back towards the foot of the escarpment bounding the slide scar to the north. Unit r30-r31 is max. 150 ms, and generally less than 100 ms thick. Estimates of the volume of sediment contained within the unit are necessarily very rough, but the outcome gives at least an idea of the order of magnitude: using average thicknesses of 80 ms in the slide scar and 60 ms in the depositional lobe in front of it, a total volume of 920 km³ is calculated within the confines of the study area, which is comparable to the estimate of the amount of material that is removed; of this volume, c. 320 km³ is left in the slide scar itself. Note that the actual values for the entire displaced mass are probably about double. Following this interpretation, the GII/GIII boundary should more correctly be placed at the r31 horizon instead of at r30, but this has not been implemented due to the more obvious distinction of the latter reflector on the seismic sections.

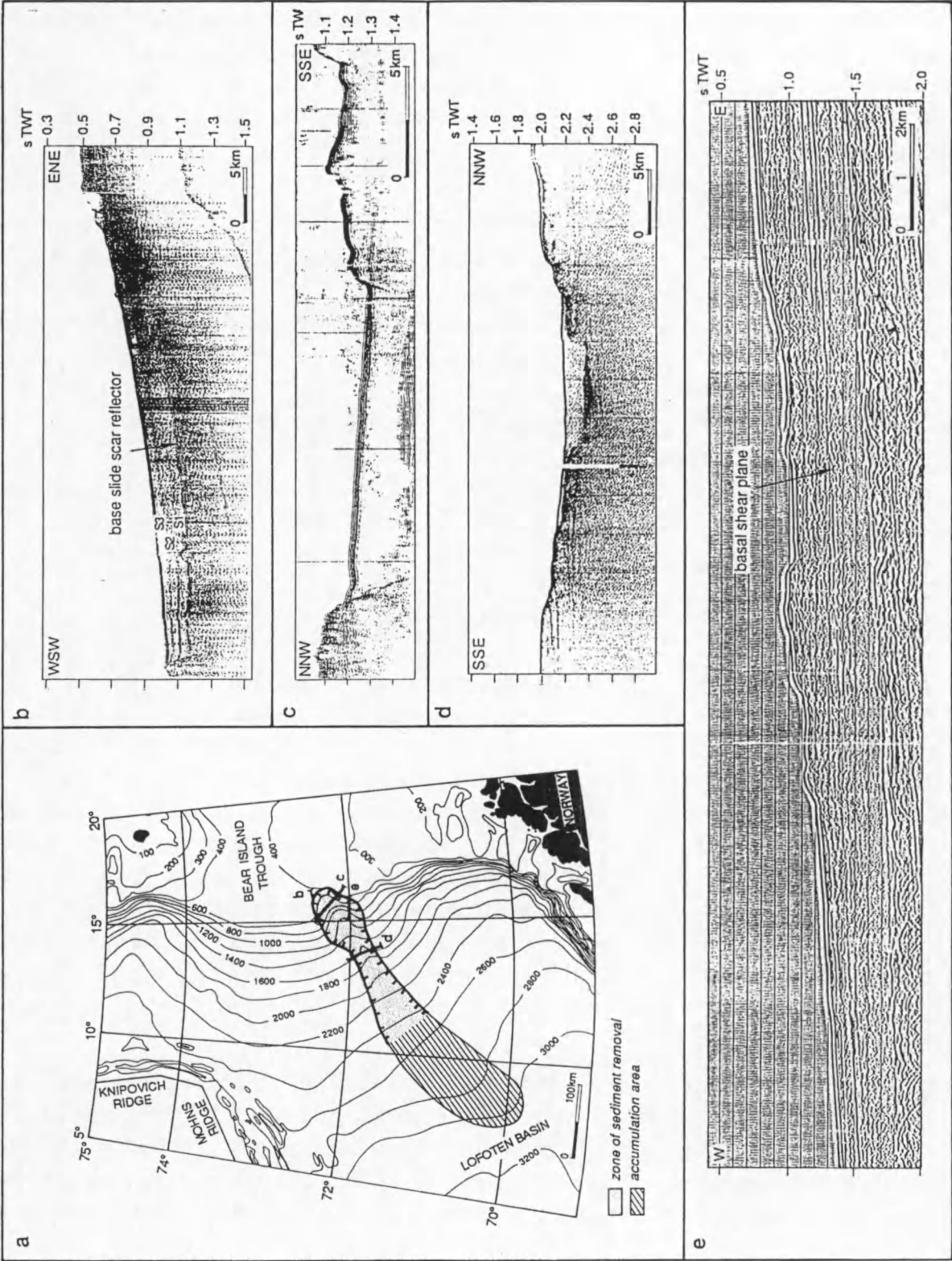
	Storegga Slide, mid-Norwegian margin	Recent slide on southern flank Bear Island Cone	Buried slide on central Bear Island Cone
Reference	Bugge et al., 1987	Laberg & Vorren, 1993	this study
Slope gradient	< 0.6°	< 0.7°	< 1.5° (not corrected for post- depositional tilting)
Width of slide scar	85 - 235 km	20 - 50 km	100 - 120 km
Area occupied by slide scar	34,000 km ² (1st stage)	12,500 km ²	9,500 km ²
Area of deposition	34,000 km ²	n.d.	14,000 km ² (x 2)
Average thickness of displaced sediments	114 m	60 - 70 ms	60 - 80 ms
Volume of displaced sediments	3880 km ³ (1st stage)	1100 km ³	1750 km ³
Volume of deposits left in slide scar	400 km ³	n.d.	320 km ³ (x 2)

Table III.8 - Comparison of relevant parameters for three large-scale slope failures along the Norwegian and Barents Sea margins. n.d. = no data.

Further support for the interpretation of unit r30-r31 comes from comparison with a similar, but more recent slide scar on the southern flank of Bear Island Cone, near 72° N (cf. section 2.1). This slide scar was first described by Kristoffersen et al. (1978), and discussed in more detail by Laberg & Vorren (1993). It bears many similarities to the feature described here, as shown in Fig. 40. The scar exhibits relief up to 400 m, and is filled with max. 160 m of sediment. Examination of low-resolution records (Fig. 40e) reveals that a large mass deficiency in the slide-affected area persists to the present day. Laberg & Vorren (1993) have recognised three predominantly transparent seismic units, each max. 60-70 ms thick, filling in the scar (Fig. 40b). Only the lower of these units,

exhibiting a more clearly chaotic character, is thought to contain sediments originating from the slope failure event (J.S. Laberg, pers. comm. 1995); the overlying units probably mainly comprise hemipelagic sediments deposited after the slide occurred.

Fig. III.40 - The more recent slide scar on the southern flank of Bear Island Cone. [a] General extension of the feature. [b, c, d] High-resolution seismic cross-sections. [e] Low-resolution seismic cross-section through the head of the slide (line NPD-7200). a, b and d are taken from Laberg & Vorren (1993), c is from Vorren et al. (1989).



At any rate, all these observations point to a much greater mobility of the mass movement than envisaged by Kuvaas & Kristoffersen (in press). Mainly based on morphological criteria, Laberg & Vorren (1993) have classified the slide on the southern flank of Bear Island Cone as a bottleneck slide, following the terminology of Prior & Coleman (1979). A same classification is favoured for the buried slide on the central Bear Island Cone, but on different grounds. Bottleneck slides are characterised by an arcuate, depressed source region, a narrow neck and a widespread depositional lobe; they involve both sliding and flowing (Prior & Coleman 1984). Besides the evident geometry of the slide scar, the large travel distance, strong deformation and fan-like geometry of the displaced sediment mass closely match such a hybrid process. It should be kept in mind, however, that there is a substantial difference in scale with the bottleneck slides originally described by Prior & Coleman (1978) on very low-angle slopes ($0.3 - 0.4^\circ$) in inter-distributary bays of the Mississippi Delta: these features vary in length from 150 to 600 m, and the depth of their shear plane below the seafloor does not exceed 12 m.

The most important conclusions with respect to this feature can be summarised as follows:

- the GII/GIII boundary (r30) is affected by a huge slide scar, evident as a prominent incision, on the upper slope off central Bear Island Trough;
- the slide scar has dimensions comparable to two more recent failures along the eastern margin of the polar North Atlantic, and can in fact be reckoned among the largest such features presently on record;
- the deposits resulting from the failure were largely funnelled out of the scar area, and now form a widespread depositional lobe in front of the scar;
- a greater mobility and deformation is implied for the mass wasting event than previously thought; the process probably involved both sliding and flowing.

6.4. Seismic evidence for mass wasting in megasequence GII

It has been shown in section 5.3.4.3 that megasequence GII is to a large extent dominated by a chaotic to transparent seismic facies. The distribution of this facies in three dimensions appears to be very complex, not restricted to a single interval (cf. Fig. 30). Locally, however, and particularly in the south-eastern part of the study area, the chaotic facies extends over the entire vertical extent of GII. Abundant diffraction hyperbolae, the occurrence of disrupted reflectors, and in one place even of intraformational faults, all point towards an intense disorganisation of the original stratification, here interpreted to result from large-scale mass movements. This is amongst other things supported by the downslope position occupied by these sediments, and by the observation of a typical snout-shaped distal margin to the main chaotic interval (see further). The buried slide scar at the GII/GIII boundary, discussed in the previous section, and a more recent such feature, described by Laberg & Vorren (1993), proves that large-scale slope failures indeed have occurred several times in the depositional environment of the Bear Island Cone.

The conspicuous chaotic facies of megasequence GII has been noted before, e.g. by Knutsen et al. (1992). These authors, strongly hampered by poor seismic control west of 15° E and north of $73^\circ 45'$ N, attributed the entire chaotic interval to a single mass wasting event affecting a major portion of GII. In particular, an average sediment thickness of 430 m, and up to as much as 970 m, would have been displaced by a process of sliding or slumping, accompanied by debris or mud

flows. With minimum estimates of 12,000 km² for the affected area, and 5100 km³ for the volume of the displaced sediments, the feature would figure amongst the absolutely largest on record (cf. Table 7), and especially its immense thickness is stunning. Knutsen et al. (1992) further reported that the surface continuing up-slope from the slip surface at the base of the slide mass, i.e. the contemporaneous seafloor, passes into two large submarine canyons around 73°30' N, and even suggested that these might have been generated simultaneously with the slide event; the present study provides clear evidence that these canyon-like features, described in the previous section, are positioned stratigraphically higher (r30) than the reflector believed by Knutsen et al. (1992) to represent the contemporaneous seafloor (r25) to the slide scar. It will further be argued that the entire chaotic interval in GII cannot be accounted for by a single mass wasting event, and that a significant amount of mass wasting occurred above the r25 horizon as well.

The interpretation of a single mass movement was earlier challenged by Kuvaas & Kristoffersen (in press), who have discerned five separate phases of slumps and slides, two of which (the “blue” and “green” slope failures) are contained within megasequence GII; the youngest “yellow” slope failure coincides with the GII/GIII boundary (see above), and the other “orange” and “red” slope failures are probably older than GII. The blue and green slope failures appear to correlate more or less to the base-GII and r25 horizons, respectively. Based on a better seismic coverage of the lower slope and rise, it will be shown below that even this scenario is minimalistic, and that GII is most likely composed of still more individual large-scale mass deposits, with smaller dimensions, however, than put forward by Knutsen et al. (1992) or Kuvaas & Kristoffersen (in press). Smaller dimensions are also supported by comparison with the limited thickness of the deposits resulting from the major mass wasting event at the GII/GIII boundary, after all one of the largest slope failures ever reported.

Evidence that several phases of mass movements have occurred, is provided [i] by the recognition of several, more or less continuous reflectors, dividing the chaotic facies into different levels, [ii] by the occurrence of several chaotic levels in the predominantly stratified zone which is laterally correlative to the main chaotic unit, and [iii] by the lack of acoustic expression of the basal boundary of the chaotic facies, in contrast to the slide scar at the GII/GIII boundary, which can in all places be recognised as an individual reflector cutting into the deeper stratigraphy. The latter point is illustrated by segments of line NPD-7300 where the base of the chaotic facies is seen to jump to a shallower level (Fig. 41). Knutsen et al. (1992) have interpreted this as a ramp connecting two slip surfaces at different depths. The ramp does, however, not reflect any acoustic energy, and — perhaps a more convincing argument — closer examination reveals that the basal reflector is gradually disrupted and entrained within the chaos before jumping to a deeper stratigraphic level; the chaotic facies may also in part extend below the disrupted reflector, and thus below the main chaotic interval. The difference between the two interpretations is indicated in Fig. 41.

More clues to the nature and scale of the processes that have created the chaotic facies are embodied within the interval r26-r27. This interval is best defined distally, on the continental rise of the Storfjorden Cone. The reflectors r26 and r27 can be traced southwards, to app. 74° N, as respectively the base and top of the main chaotic interval. Further south r26 terminates as the chaotic facies extends deeper in the stratigraphy, while r27 is broken up into discontinuous segments entirely surrounded by chaotic facies, the top of which is now defined by the GII/GIII boundary (see Fig. 30). The latter observation is considered conclusive evidence for the compound nature of the chaotic facies: reflector r27, which marks the top of a mass deposit (see below), was entrained in a succeeding mass wasting event, and hereby disrupted over most of its extent; the reflector has

remained intact only in the most distal locations, where the mass flow probably had strongly reduced erosive power, or even completely dissolved (as witnessed by a transition into more stratified facies). Though these stratal patterns are nowhere seen as clearly, such a process of amalgamation can probably be extrapolated to the entire chaotic interval in GII.

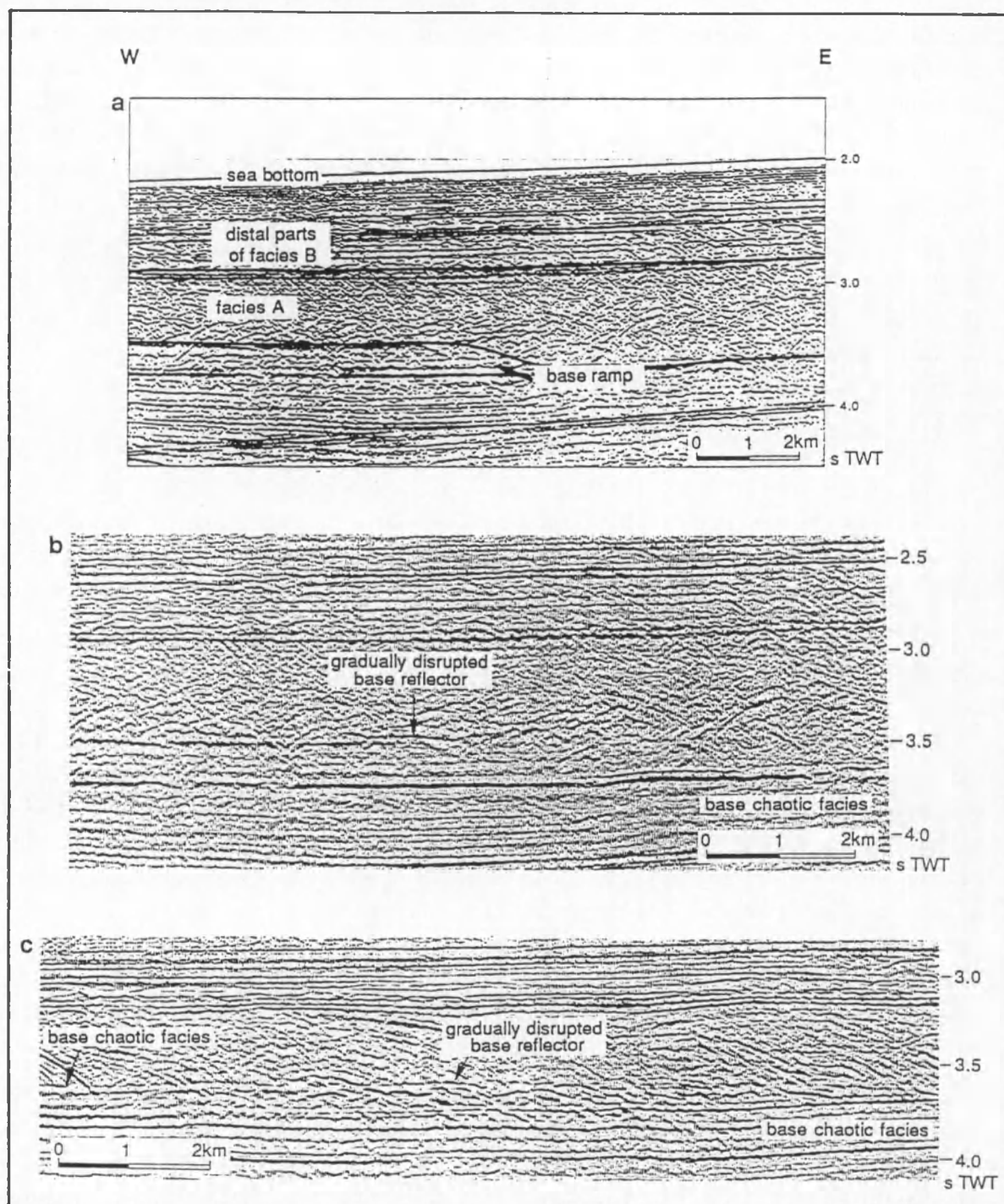


Fig. III.41 - Upward shift of the base of the chaotic facies in GII (line NPD-7300). **[a]** Upward jump of a basal slip plane, as interpreted by Knutsen et al. (1992). **[b]** The same, uninterpreted, section as in **[a]**, showing that the incisional ramp is not associated with an acoustic reflection. **[c]** Similar situation more westward, clearly demonstrating how the base of the chaotic interval is gradually disrupted and entrained within the chaos; beyond that, a deeper reflector defines the new base level of the chaotic interval.

As described in more detail in sections 5.3.5.3 and 5.3.5.4, the interval r26-r27 also exhibits a distinct snout-shaped distal margin, beyond which the unit strongly thins and becomes acoustically stratified. The resemblance of this feature to the frontal nose of a debris or mud flow, and associated transition into turbidites, is striking (Fig. 42), keeping in mind again that the dimensions are much bigger than described in literature (refer to section 6.2). The characteristic undulating character of the top reflector (compare with Fig. 44a), commonly attributed to compression at the front of a mass flow, further adds to the similarity. Such frontal snout seems to preclude an origin of the unit as a slide or slump, but instead indicates a greater mobility and higher degree of deformation. The large scale and fan-shaped distribution of the chaotic facies (Fig. 43) suggest that the mass movement developed as a flow-slide, analogous to the mode of displacement inferred for the slope failure at the GII/GIII boundary (see preceding section), and evolved distally into smaller-scale debris or mud flows and turbidites. The local alignment of diffraction hyperbolae within the chaotic to transparent facies provides some evidence for the existence of one or two heavily disturbed reflectors within unit r26-r27 (Window 33). This in turn may indicate that the interval, which is about 300 ms thick in a position that is not even proximal to the source region (Fig. 43), is in fact composed of two to three separate mass flow deposits of about 100 ms thick, comparable in size to the deposits resulting from the flow-slide at the GII/GIII boundary. This would also explain a peculiarity observed just proximal of the frontal snout: amidst the chaotic facies, a stack of several discontinuous reflectors stands more than 100 ms high above base reflector r26; part of the chaotic interval continues above. The most plausible explanation, depicted in Fig. 44c, is that the reflector "island" is laterally equivalent to the distal stratified facies of the lower two mass flows, as a result of a local indentation of their frontal margin, and was overrun by a third mass flow whose margin has a more rectilinear trajectory. The — at first sight more obvious — interpretation of this feature as an upward jump of the slip surface at the base of a slide (Fig. 44b), is not supported by the characterisation of the mass movement as a flow-slide, and by the absence of prominent compressional structures, which would be expected to accompany such a jump in this distal portion of the mass deposit.

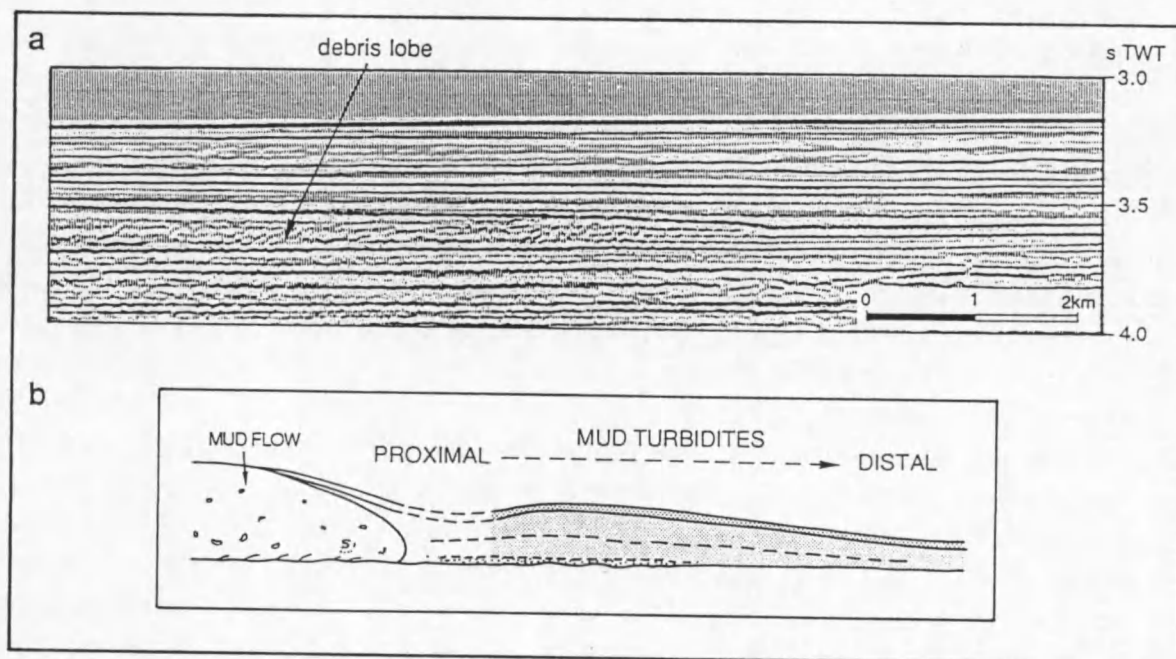


Fig. III.42 - [a] Distal snout-shaped edge of the main chaotic interval, associated with distinct thinning and transition into acoustically stratified facies (line NPD-7440). [b] Possible analogue: distal transition of a mud flow into mud turbidites (redrawn from Einsele 1991).

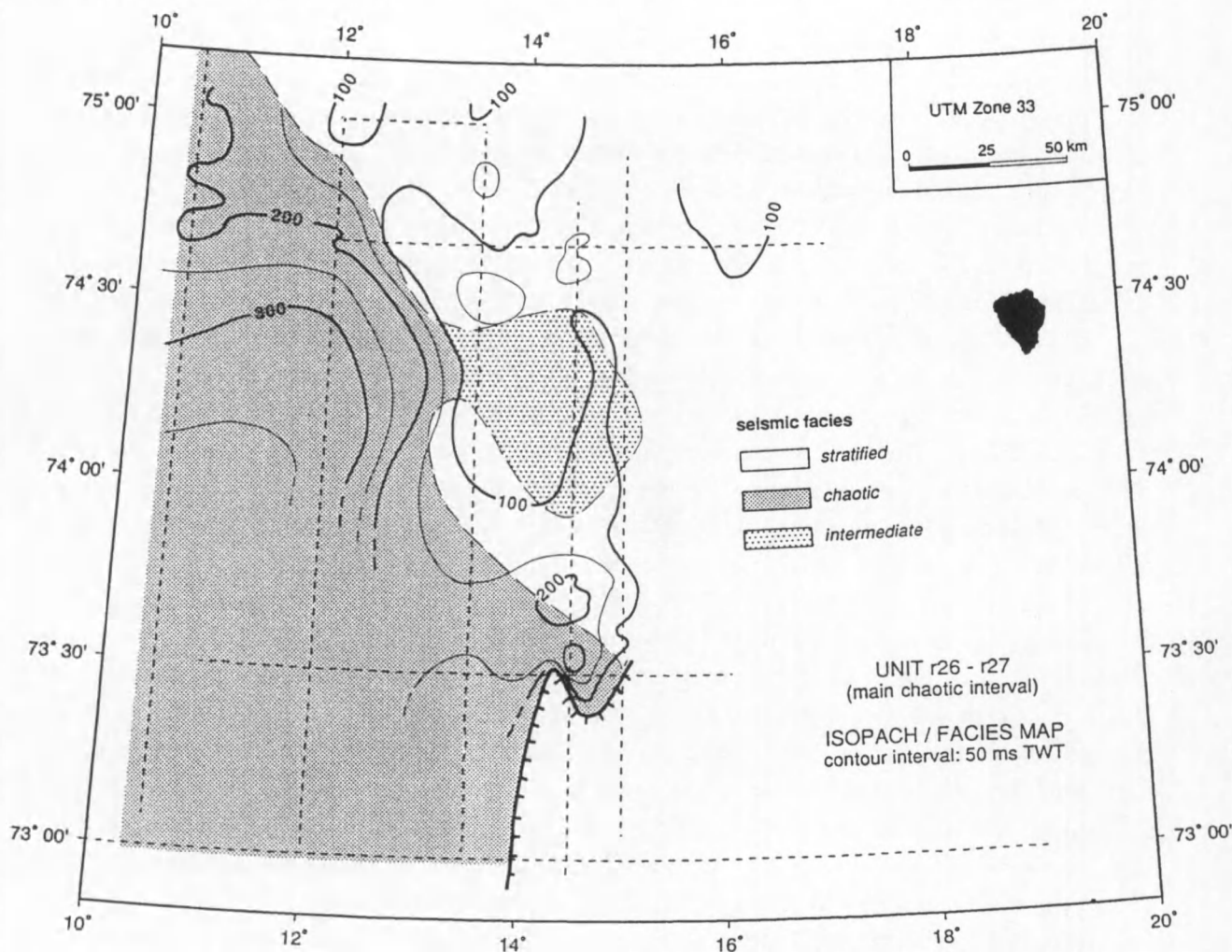


Fig. III.43 - Combined isopach and facies map of the chaotic interval confined between reflectors r26 and r27. The interval has the shape of a fan spreading out from its source area on the upper slope off the axial Bear Island Trough mouth. Gridded using Geofox (Verschuren 1992).

The distribution of the chaotic facies, as shown in the fence diagram of Fig. 30, and the external shape of especially the r26-r27 interval (Fig. 43), indicate that the majority of the mass movements in GII was sourced from the upper slope off the central axis of present-day Bear Island Trough. This is also evidenced by the downward shift of sediment accumulation, which is nowhere as spectacular as in this location: on line NPD-7300, the upper slope equivalent of GII is virtually absent because of the notorious pinch-out against the GI/GII boundary of an up to 1 s thick sediment interval bounded by r25, in an approximate paleo-middle slope position (Window 7). Quite interesting, but hard to explain, is that the GI/GII boundary itself does not (or only negligibly, e.g. line NPD-1430) appear to be affected by the numerous slope failures which must have occurred in this location. The focused provenance of all these mass movements in an area centred around 73° N can also provide an explanation for two additional observations (Fig. 30): [i] the occurrence of faulted blocks limited to an area around 73° N and 13°30' E is probably the result of more rigid deformation, particularly of the earliest mass movements, close to the source region; and [ii] the local development of the chaotic facies over almost the entire vertical extent of GII in more or less the same area may indicate more extensive reworking, related to repeated incision by slide scars, and maybe also to a greater erosive power of the flow-slides in their proximal portion. Beyond this heavily disturbed area, the

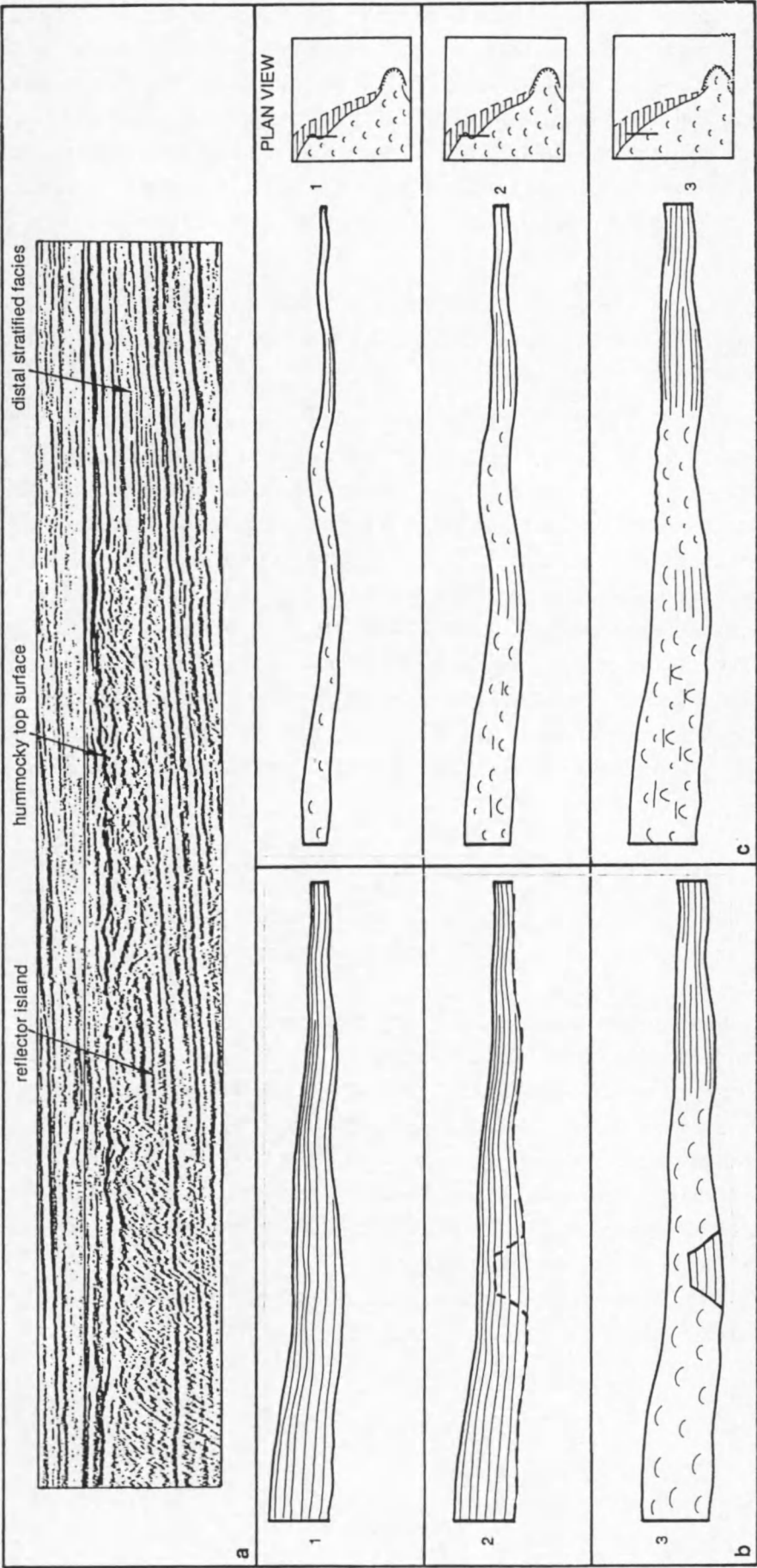


Fig. III.44 - Cartoon sketch of the development of the peculiar reflector "island" within the chaotic interval r26-r27. [a] Detailed seismic section of distal portion of the chaotic interval (line MGK-1200). [b] Evolution as a single failure event, with upward jump of basal shear plane. [c] Superposition of two or three individual flow-slides — the favoured interpretation; the reflector island is laterally equivalent to the distal stratified facies in the lower two mass deposits, as indicated in plan view.

mass flows appear to have spread out broadly to form a fan-shaped depositional lobe. The farthest traveled of these flows are those contained within the interval r26-r27, and extend as far north as 75° N on line MGK-1030, i.e. a distance of c. 270 km! This, of course, does not indicate the actual transport distance. Being the uppermost level of mass wasting that could be identified with confidence within GII, the interval r26-r27 is also best preserved, as demonstrated by the identification of a typical snout-shaped margin at its distal end. This peculiar feature, pointing in up-slope direction on line NPD-7440 (Window 14), precludes a provenance from the Storfjorden Trough region.

Exceptional sourcing from another area may, however, be evidenced by the mounded lobes present in unit r24-r25 (Window 27); these features were probably emplaced by a different mechanism as well, perhaps in the form of huge debris flows.

The present study has failed to resolve the exact amount of mass wasting events that has occurred throughout deposition of GII on the Bear Island Cone. It has in particular proved impossible to recognise any slide scars in the source region, with the possible exception of one such feature at the level of r25, which is inferred to occur closely below the GII/GIII slide scar on line NPD-1430, and may correspond to the green slope failure of Kuvaas & Kristoffersen (in press). This setback may be due to poor seismic control on the upper slope, but is also in part caused by the heavy disturbance resulting from repeated failure in always the same area. Trying to identify base and top reflectors of individual mass deposits turned out to be unrealistic as well. Some reflectors appear to define both the top of an underlying mass deposit, and the base of a subsequent one. Careful tying of reflectors around the network has delimited at least six chaotic to transparent intervals, separated in places by more or less continuous reflectors. The best constrained of these intervals, unit r26-r27, is likely to have formed in two or three separate events.

The following points summarise the most important conclusions concerning the origin of the chaotic facies in megasequence GII:

- the widespread chaotic facies in GII is most likely the result of repeated and large-scale mass wasting processes;
- most of these mass movements can probably be characterised as flow-slides, comparable in size to the flow-slide identified at the GII/GIII boundary;
- the farthest traveled and best preserved of these flow-slides are contained within unit r26-r27, which displays a characteristic snout-shaped margin representing the distal termination of the flow-slide, and associated transition into smaller-scale mass flows;
- the majority of the mass movements was initiated in the south-eastern part of the study area, on the upper slope off Bear Island Trough, where vertical extent of the chaotic facies appears to be maximal, and internal deformation minimal;
- the various mass movement processes have removed much of the stratigraphical significance of the GII succession.

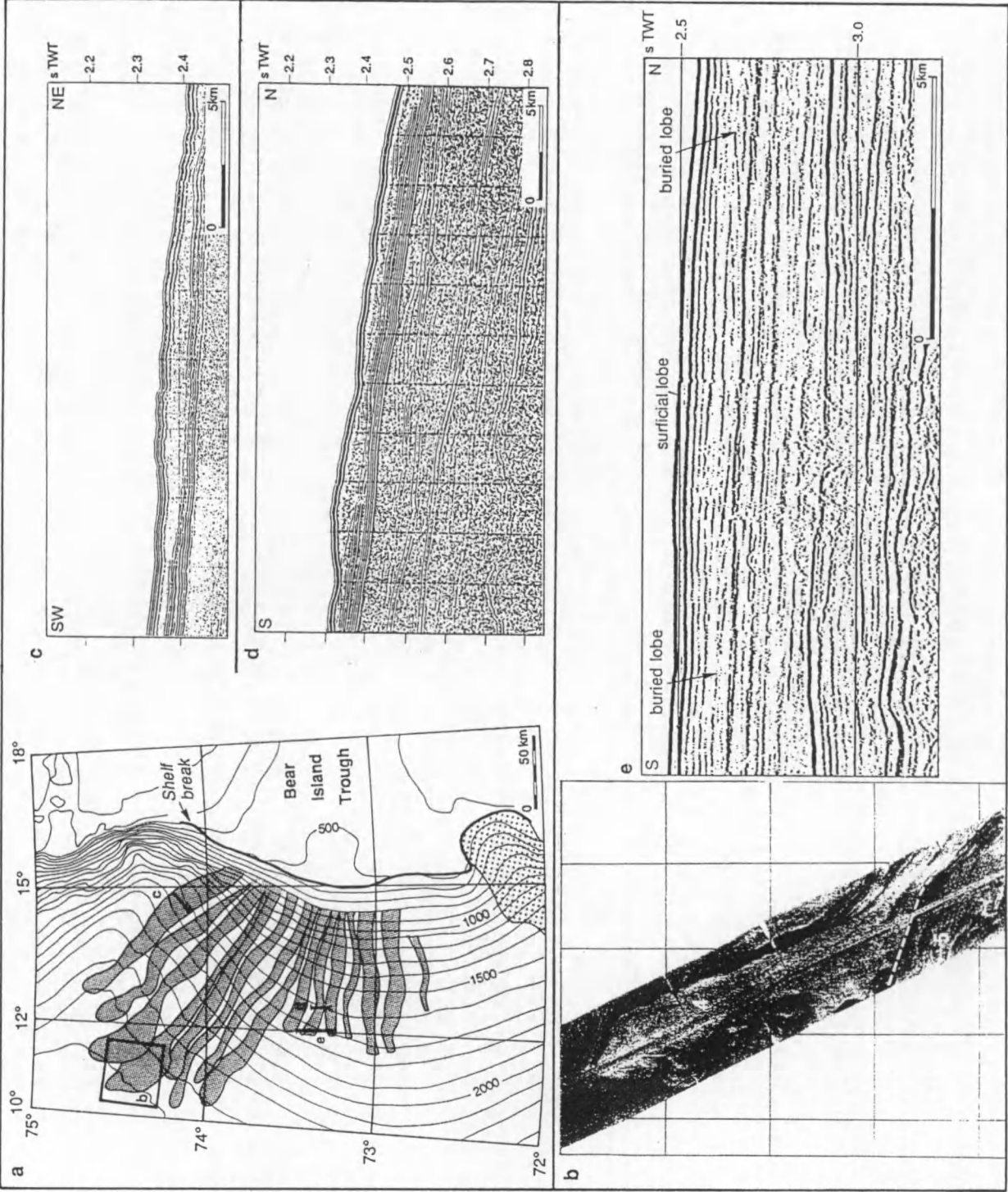
6.5. Mass wasting styles in megasequence GIII

Though more limited than in GII, there is evidence for mass wasting in megasequence GIII as well (Figs. 45, 46). The seismic facies, described in section 5.3.6.3, is varying between chaotic, transparent and stratified. The chaotic facies, associated with individually developed diffraction hyperbolae, particularly dominates in the sediments infilling the slide scar at the GII/GIII boundary. The chaotic to transparent facies is again taken as indicative of mass deposits, but involving much smaller scales than in the GII megasequence. Massive and extensive chaotic lobes of comparable size to those preserved in e.g. the r26-r27 interval have nowhere been observed in the study area. Individual mass wasting events were thus probably not as extensive as the flow-slides dominating GII. Most disturbance seems to have taken place in the area of the former large-scale slope failure at the level of r30, and was probably in part related to the locally increased relief at the edges of this feature, until the scar was “healed” by preferential infilling of the depression. The seismic facies generally becomes more stratified downslope and towards the north. It should be realised, however, that acoustic stratification, especially on the intermediate- to low-resolution lines used in this study, does not necessarily reflect stratification on outcrop scale: mass deposits with dimensions less than 10 - 20 m are equally imaged as predominantly stratified facies.

Other evidence for mass wasting in GIII includes local failure of the present-day upper slope on line NPD-7330, and a more extensive slide scar at the level of r35, both described in section 5.3.6.4. The former feature (Window 13) has very small dimensions, not at all comparable to the giant failures at the GII/GIII boundary or at the seafloor further south, at 72° N; it is probably representative for the instability processes that have governed deposition of megasequence GIII. The slide scar at the r35 horizon (Windows 20, 24), in contrast, has a relatively large scale, and is estimated to slightly less than half of its predecessor at the level of r30. It is expressed by a south-facing erosional ramp, shifted c. 45 km to the south with respect to the very much similar escarpment bounding the r30 scar. Both failures thus occurred in more or less the same location, at the mouth off central Bear Island Trough. As was also the case for the r30 scar, a complementary ramp forming the southern limit of the incision, is expected to intersect the upper slope at some distance south of 73° N. A high-amplitude reflector onlapping the foot of the escarpment is thought to represent the top of the sediment mass displaced by the slope failure; this unit is too thin to be analysed in more detail, however. It is suspected that the whole feature represents one of the largest mass wasting events that has taken place throughout deposition of GIII in the study area.

Higher-resolution seismic reflection studies by Vorren et al. (1989) and Laberg (1994) have revealed that the upper sediment section on both the Bear Island and Storfjorden Cones is composed of numerous stacked debris lobes, with thicknesses ranging between 10 and 30 m, to max. 50 m. These debris lobes are very elongated, generally not more than 20 km wide and over 100 km long; their shape and dimensions are thus fundamentally different from the fan-like lobes identified as flow-slides in megasequence GIII. The volume of displaced sediments in one such lobe averages 18 km³, and is maximum 32 km³. The debrites on the Storfjorden Cone have in general smaller dimensions than those on the Bear Island Cone. Debris lobes within the same seismic unit appear to radiate from the mouth of Bear Island Trough (Fig. 45a); this is confirmed for the lobes presently at the seafloor by recent side-scan sonar imaging (Fig. 45b; Vogt et al. 1993; Dowdeswell & Kenyon 1995). The debris flows probably resulted from small-scale slope failures as exemplified by the present seafloor at 73°30' N (see above).

Fig. III.45 - Mass wasting styles in megasequence GIII. [a] Radiating pattern of youngest set of debris lobes out from the mouth of Bear Island Trough (Laberg & Vorren, in press b). [b] SeaMARC II side scan sonar image of debris lobe termination (Vogt et al. 1993). [c, d] Appearance of debris lobes on high-resolution seismic sections. From Laberg & Vorren (in press a+b). [e] Appearance of debris lobes on intermediate-resolution seismics used in this



On the high-resolution seismics the debris lobes are imaged as acoustically transparent lenses with distinct lateral and frontal terminations (Fig. 45c and d). On the low-resolution seismics their presence may sometimes be indicated by uneven or wavy reflections overlying thin transparent intervals, and by mounded features on the seafloor (Fig. 45e). The tendency for smaller debris flow deposits on the Storfjorden Cone is reflected on the lower-resolution records by an overall increase of stratified character to the north. The depositional architecture of shingled debris lobes in GIII strongly resembles that of similar (glacial) settings along the Canadian Atlantic margin, in particular in areas off transverse shelf troughs on the Newfoundland slope (Aksu & Hiscott 1992) and in Baffin Bay (Hiscott & Aksu 1994).

The findings for megasequence GIII can be summarised as follows:

- ➔ megasequence GIII is probably also to a large extent composed of mass deposits;
- ➔ the scales of these mass deposits are an order of magnitude smaller than those in GII; they mostly originated as debris flows instead of flow-slides;
- ➔ a relatively large slide scar at the r35 horizon, about half the size of the scar at the GII/GIII boundary, is thought to represent the largest mass wasting event affecting GIII;
- ➔ a small collapse of the seafloor on the upper slope is probably representative for the scale of instability processes that have acted throughout GIII time;
- ➔ it seems probable that the same scale of processes has acted throughout GII time as well, but was overprinted by frequent large-scale events.

Fig. 46 summarises the differences in mass wasting style among the three youngest megasequences GI-GIII.

6.6. Causes behind mass wasting

Slope failure takes place if the shear stress exceeds the shear strength of the sediment at a given depth below the seafloor. The shear stress increases with the slope angle and with depth below the seafloor, while the shear strength usually increases with burial depth, thus counteracting the effect of increasing shear stress. The most widely cited factors contributing to slope instability are:

Factors enhancing shear stress:

- earthquake shocks (Heezen & Ewing 1952; Lewis 1971; Bugge et al. 1987; Mosher et al. 1994);
- depositional or erosional oversteepening of the existing slope (Lewis 1971);
- tectonic uplift or diapirism (Nardin et al. 1979);
- sea level falls (Embley 1976);
- surface wave perturbation of sea bottom sediments in shallow water (Prior & Coleman 1982; Aksu & Hiscott 1992).

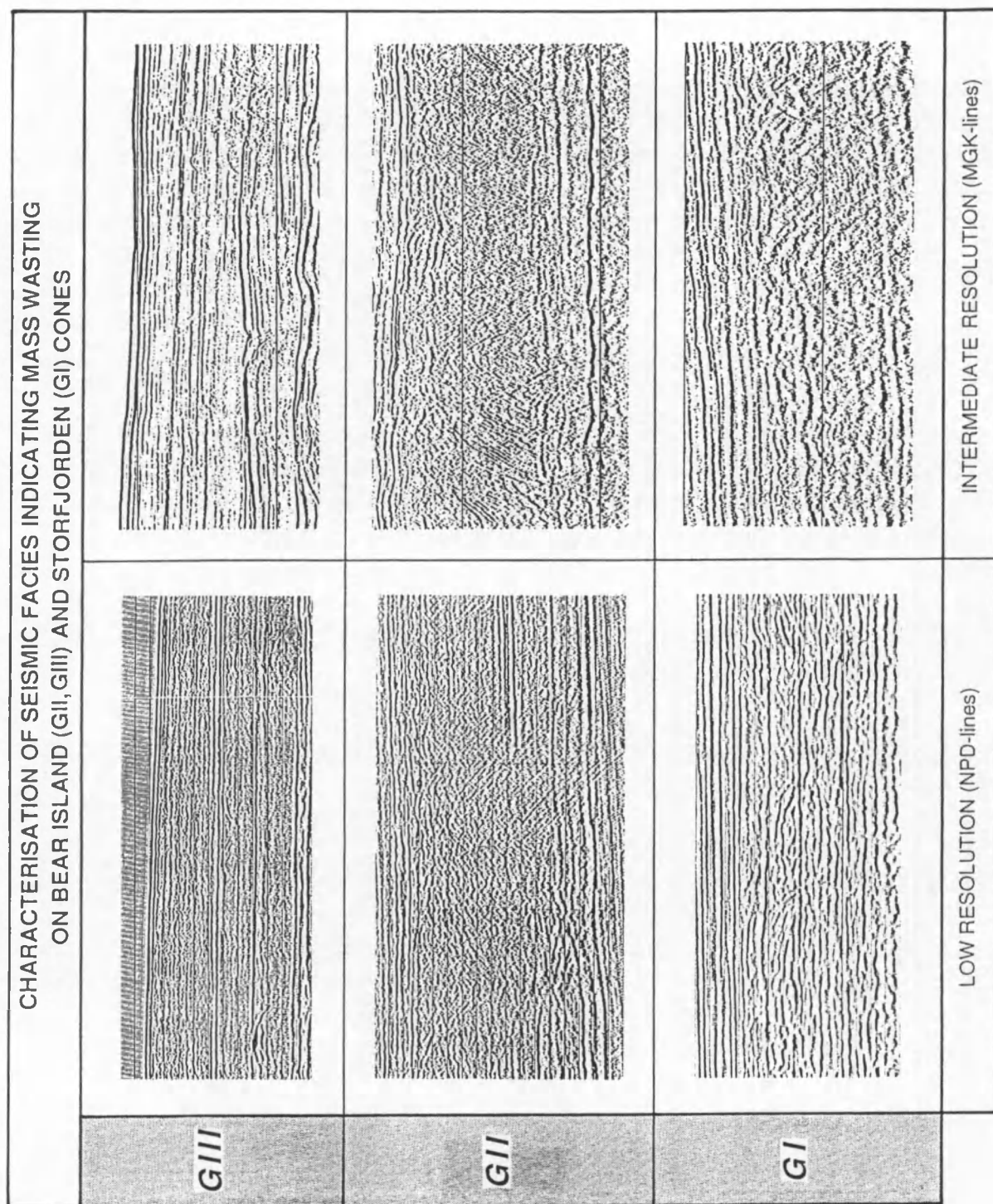


Fig. III.46 - Varying aspect of chaotic facies in megasequences GI, GII and GIII.

Factors reducing shear strength, all involving increased pore water pressures:

- underconsolidation by rapid accumulation of fine-grained sediments (Lewis 1971; Coleman & Garrison 1977);
- undrained external loading (Prior & Coleman 1978; Einsele 1991);
- release of gas by in situ decomposition of organic material in the uppermost tens of metres, or by phase transition from crystallised gas hydrates (Prior & Coleman 1978, 1982; Bugge et al. 1987).

Furthermore, it has been recognised (Kurtz & Anderson 1979; Bugge et al. 1987; Aksu & Hiscott 1992; Mosher et al. 1994) that glaciated continental margins constitute specific environments favourable for mass wasting: conditions of rapid sedimentation have existed during repeated large glaciations, when major ice outlets supplied vast amounts of sediment directly to the upper slope; peak sedimentation rates during glacial retreat probably even enhanced this. Additionally, advancing ice sheets have imposed a burden on outer shelf sediments, and resulted in isostatic vertical movements; these two contributions to instability of the slope are considered minor, however.

The preceding sections have provided abundant evidence that the Bear Island Cone has been the site of numerous mass wasting events. Triggering mechanisms for a certain failure are seldom uniquely identified, and in the case of the Barents Sea margin too, several factors appear to have combinedly made for an environment that is exceptionally susceptible to slope instability:

- The Barents shelf, which has acted as the source area for the Bear Island Cone, was a glaciated environment from at least GII, and possibly GI time on (see section 7.2). High sedimentation rates prevailed on the upper slope at the mouth of Bear Island Trough at times of glacial maximum. In the light of the young ages found for most of the cone by recent datings (cf. section 5.2.4), the effect of high accumulation rates, in the order of 1 m/ka in the long term, seems even more important than previously recognised. Faleide et al. (in press) have calculated average sedimentation rates of 37 cm/ka (GI), 172 cm/ka (GII), and 44.5 cm/ka (GIII) (Fig. 47). Actual sedimentation rates must even have been larger, as deposition took place intermittently, during the intervals when ice sheets were positioned at the shelf edge (cf. Laberg & Vorren, in press b).
- The substrate eroded by the ice is dominated by late Paleozoic to Mesozoic sedimentary rocks (section 4.1.3). Such rocks are much less resistant to mechanical erosion than e.g. crystalline rocks, so that most of the sediment supplied to the upper slope is probably relatively fine-grained in nature. This is confirmed by gravity cores penetrating the uppermost debris lobes (Laberg & Vorren, in press b), and which have recovered a massive diamicton (gravelly, sandy mud), strongly resembling sediments presently at the sea bed on the outer shelf.
- The sediments on the shelf are often characterised by overconsolidation (few hundreds of kNm^{-2}), as they were probably deposited from grounded ice; the degree of overconsolidation in general decreases towards the outer shelf and upper slope, however, concurrently with a decrease in ice sheet thickness in that direction (Solheim & Kristoffersen 1984). Sættem et al. (1992) have even identified levels of glacial sediment with a consolidation as low as 20 kNm^{-2} , probably indicating a situation of undrained loading with strongly reduced porewater drainage. These observations imply that sediments on the outer shelf and upper slope are not insensitive to slope instability.
- Studies of recent seismicity (Kvamme & Hansen 1989) have revealed relatively high activity along older fault systems, especially along the Senja Fracture Zone, which is seated below the southern half of the Bear Island Cone. Seismic activity along the spreading ridge (Géli 1993) is considered too remote (c. 200 km), however, to trigger mass movements on the Bear Island Cone. Mosher et al. (1994) argue that the relatively small-scale failures (c. 5.75 km^3) observed on the Scotian slope require magnitude 5.0 earthquakes or greater within 40 km of the site, or magnitude 6.7 for an earthquake centred 100 km from the site.
- Finally, Knutsen et al. (1992) and Laberg & Vorren (1993) have reported some indications for the presence of gas and/or mud diapirism on the Bear Island Cone. Both features could enhance slope instability.

The results of the present study clearly demonstrate a significant difference in scale between mass deposits in GII and GIII. This trend runs markedly parallel with the variation of sedimentation rate through geologic time, as reported by Faleide et al. (in press) (Fig. 47): during deposition of megasequence GII, the average sedimentation rate is inferred to have been up to 4.5 times higher than during GIII time. The correlation between higher accumulation rates and larger-scale mass movements confirms that this parameter exerts primary control on the instability of the slope on the Bear Island Cone. The occurrence of a huge slide on the southern flank of the cone, relatively late in the deposition of GIII (Laberg & Vorren 1993), indicates that the difference in scale is in fact related to a decreased frequency of large-scale mass wasting events during GIII.

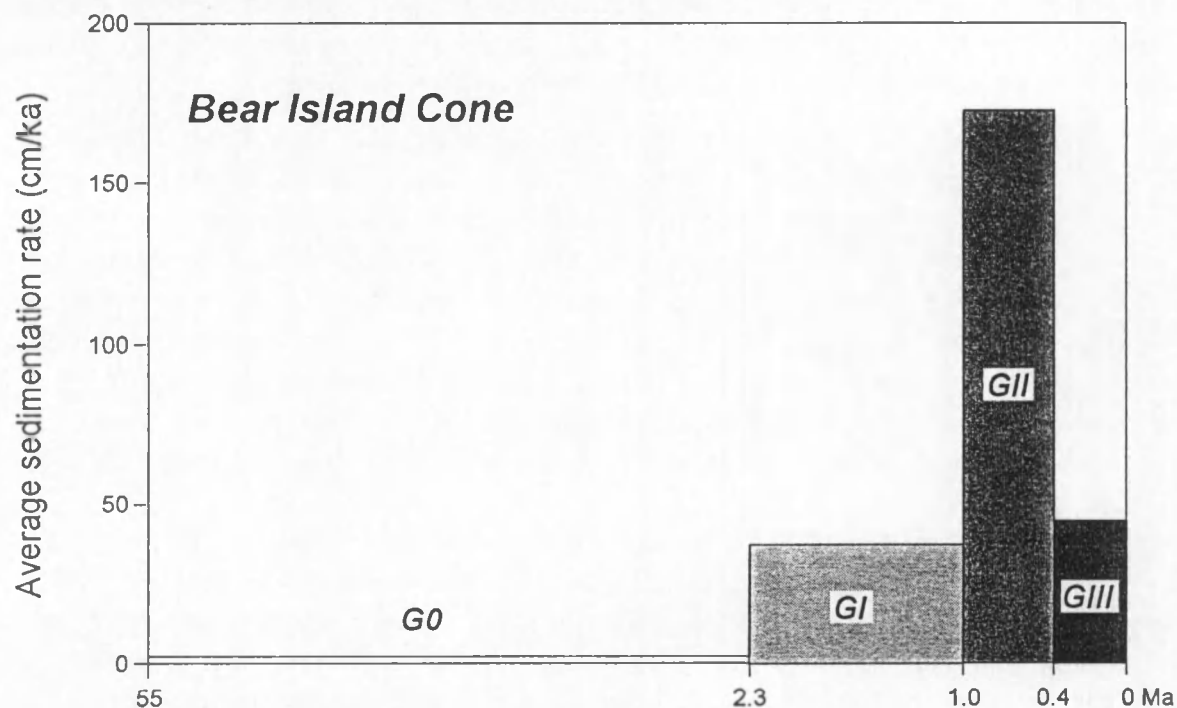


Fig. III.47 - Averaged sedimentation rates for megasequences G0 - GIII on Bear Island Cone. Redrawn from Faleide et al. (in press).

Detailed seismic stratigraphic analysis made it possible to isolate another important factor: tectonic uplift appears to have affected part of the Vestbakken volcanic province during at least the first half of GII time (r15 - r23), and may thus have initiated a period of extensive mass wasting. Furthermore, activity of the Senja Fracture Zone may help explain why most of the large-scale mass movements originated on more or less the same portion of the upper slope in the south-east of the study area. The large dimensions of the mass movements that have affected the Bear Island Cone, are to some extent also related to the very low-angle profile of the Barents Sea slope. As the shear stress generally increases with the slope angle and depth below the seafloor, the shear stress deep below a gentle slope can be as high as on a steep slope at shallow depth, as depicted in Fig. 48. For this reason, there is a tendency for thick (but less frequent) mass movements to develop on gentle slopes, whereas steep slopes are characterised by thinner, but more frequent mass movements (Einsele 1991).

Conforming to previous studies (Laberg & Vorren 1993; Kuvaas & Kristoffersen, in press) the evidence presented above supports high accumulation rates of fine-grained sediment, combined with

tectonic activity, as the main causes for mass wasting on the Bear Island Cone. When comparing with other rapidly accumulating depositional settings such as the Mississippi Delta, there still remains a scale problem, however. Sedimentation rates on the Mississippi Delta (from 1 m/a near the mouths of distributaries to a few tens of cm/a in 50 m water depth, Prior & Coleman 1982) exceed the inferred accumulation rates on the Bear Island Cone, and yet no mass wasting features with dimensions comparable to those described here, have been reported from that area (e.g. Coleman & Garrison 1977; Prior & Coleman 1978). It thus seems likely that additional instability is imposed by the specific glacial processes by which the sediments are originally deposited. The mode of deposition is strongly dependent on the behaviour and thermal regime of the ice sheets or ice streams. The Barents Sea ice sheet was most probably a relatively short-lived and wet-based ice sheet (see section 7.4), depositing sediments by deformation of basal till and/or suspension settling. No conclusive evidence has yet been presented for either one of those mechanisms (it seems improbable that they have acted simultaneously at a given point of time), but in both cases the deposited sediment is likely to have a high water content (30 - 40 %). In combination with the high sedimentation rates at the ice front, this results in underconsolidated sediments, highly prone to instability.

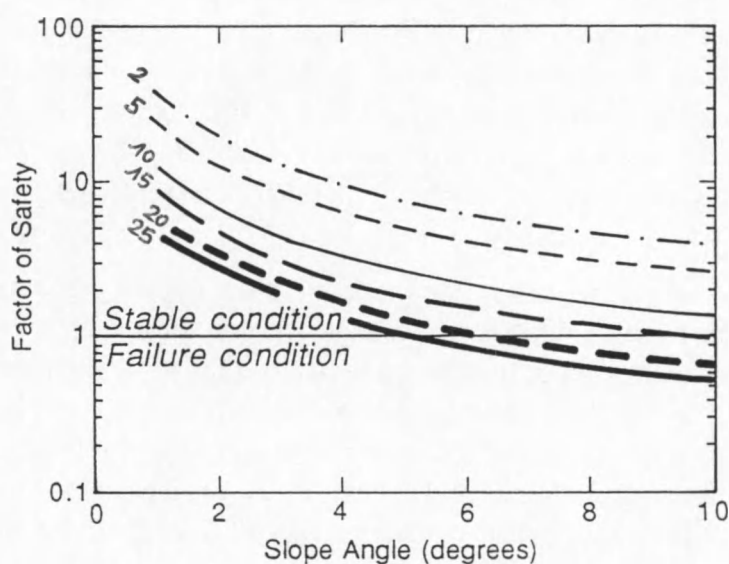


Fig. III.48 - Plot of stability (safety factor) versus slope angle for different thicknesses of sediment (in m). From Mosher et al. (1994).

6.7. The Bear Island Cone: a submarine fan?

The Bear Island Cone defines a large depocentre extending over more or less the entire continental slope at the mouth of a glacially eroded transverse shelf trough, the Bear Island Trough. It constitutes an area of enhanced progradation with respect to adjacent portions of the margin, and has been essentially built up by the action of large-scale mass wasting processes such as flow-slides and debris flows, perhaps with a minor contribution of turbidity currents. The overall internal organisation is chaotic, and significant development of leveed channel systems has nowhere been observed, nor has it been reported by other workers.

Vorren et al. (1988, 1989) originally introduced their concept of “trough mouth fans” based on the Bear Island Cone example. They stated that “the continental slope of the SW Barents Sea contains a large fan situated in front of the Bear Island trough” and that “similar types of fans at the mouth of transverse shelf troughs exist on most glaciated shelves, and we refer to them as trough mouth fans”. There is some confusion inherent in this definition, however, linked to the term “fan”. Nelson et al. (1991) noted that not just any sediment cone can be called a fan. Throughout the last two decades, a large number of sedimentologists have intensively investigated several large deep-sea fans (e.g. specific volumes edited by Bouma et al. 1985, and by Weimer & Link 1991). As a result, a rather narrow sense was attributed to the word “fan”, which has been defined as e.g.:

- radial to elongate cones of sediment deposited on marine or lacustrine basin floors by channelised fan valley systems (Nelson & Nilson 1984);
- channel and lobe (or sheet sand) complexes formed from sediment gravity flows in the deep-sea environment, commonly beyond the continental shelf (Shanmugam & Moiola 1988);
- sediment bodies characterised by proximal channelised facies and distal depositional lobe environments (Nelson et al. 1991).

Clearly, none of these definitions applies to the Bear Island Cone, which exhibits virtually none of the essential features outlined in section 1.2.2 of chapter I. Damuth (1978), probably one of the first authors to describe the sedimentation processes on this depocentre, already noted that the surface morphology and surficial acoustic character are not typical of other deep sea fans. In particular, he noticed the absence of a large, leveed central channel or fan valley, of a system of radiating distributary channels, and of a suprafan lobe. These differences were attributed to a diverging mode of deposition.

The recognition of submarine fans s.s. downslope of some major prograding depocentres at the mouth of glacial shelf troughs (i.e. trough mouth fans) considerably adds to the existing confusion. Such a configuration is exemplified by at least three fan systems along glaciated continental margins: Laurentian Fan, located off the Laurentian Channel on the Atlantic margin of Canada (Stow 1981; Normark et al. 1983; Piper et al. 1985), Cray Fan, located off Cray Trough in the south-eastern Weddell Sea (Kuvaas & Kristoffersen 1991; Moons 1992), and a presently unnamed submarine fan off Gyldenloves Trough south of the Angmagssalik fjord in East Greenland (L. Clausen, pers. comm. 1994). The trough mouth fan concept of Vorren et al. (1988, 1989) can thus not be considered as the high-latitude counterpart of the normal river- or canyon-fed submarine fan model, as put forward by Laberg (1994). Rather, it is proposed here that the term “trough mouth fan” be reserved to those fan systems proper, located further downslope. Fig. 49 demonstrates the difference in slope morphology between such a trough mouth fan (the Laurentian Fan) and Bear Island Cone.

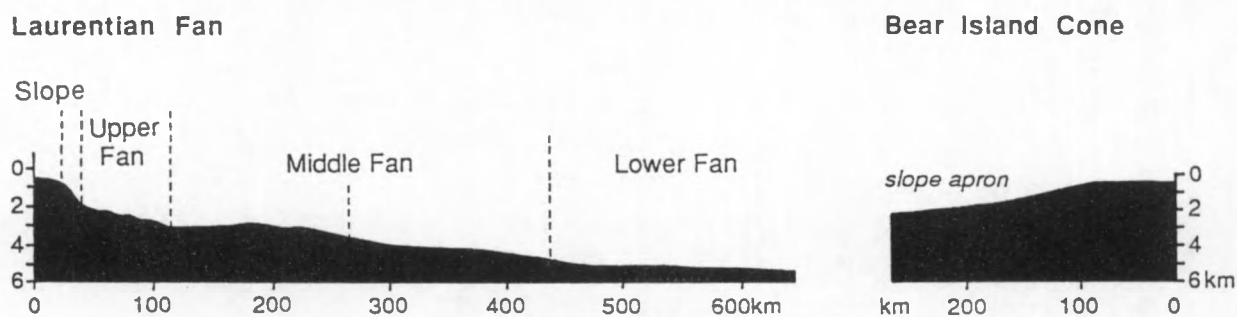
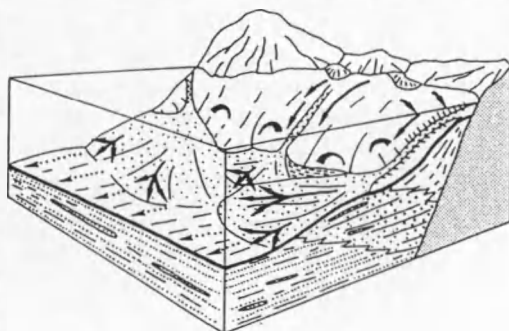


Fig. III.49 - Silhouette of [a] Laurentian Fan (Stow 1981) versus that of [b] Bear Island Cone.

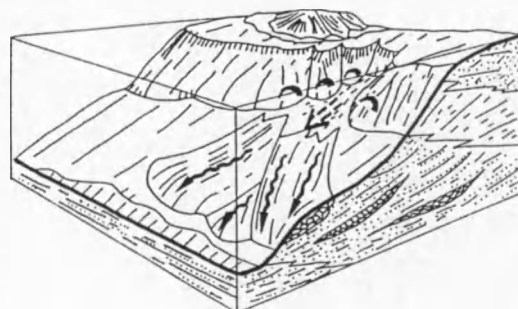
The sediment cones directly off the mouth of glacial troughs, at least off Bear Island Trough, closely match the definition of slope aprons, or debris aprons, in which non-channelised fan-like facies organisations are classified (Nelson & Nilson 1984; Stow et al. 1985; Nelson et al. 1991). Such aprons are characterised by [i] multiple sediment failures in the source area, [ii] deposition from numerous unconfined mass flows, and [iii] lack of significant channelling (Nelson et al. 1991). Two end-members are recognised: sand-rich aprons (Fig. 50a) with rhythmic sand and gravel sheets that distally grade into basin-plain turbidites, and mud-rich aprons (Fig. 50b) composed of chaotic mass flow lobes and typically lacking distal gradation.

- Sand-rich aprons usually form small (few km in length), single or coalesced, radial cones at the base of steep slopes or fault scarps in tectonically active regions. They are sourced by multiple, closely spaced debris chutes, possess a regular geometry and internal bedding, and wedge out distally;
- Mud-rich aprons are much larger systems (several tens of km in length), and have a more elongate shape. They are most common in thick prograded sequences along mud-draped passive margins. Sediment sourcing occurs by multiple failures in a broad zone (up to 100 km), i.e. a short line source. They are characterised by irregular geometry and a lack of internal organisation. There is no evidence for lateral or vertical gradation of facies, and the distal end typically remains thick.

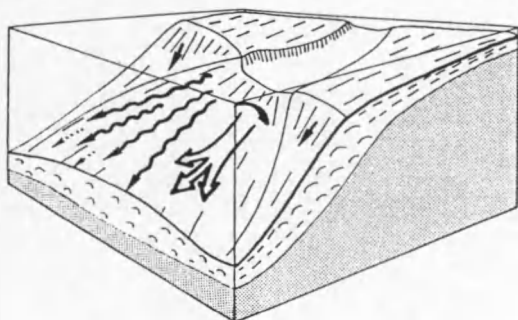
A. SAND-RICH BASE-OF-SLOPE APRON



B. MUD-RICH BASE-OF-SLOPE APRON



C. (GLACIOGENIC) MUD-RICH SLOPE APRON



PROCESSES


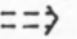

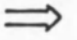
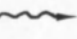
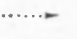

-  unconfined sediment gravity flows
-  sediment bypassing
-  slope failure
-  sliding / slumping
-  unconfined debris flows
-  distal turbidites
-  small-scale mass wasting

Fig. III.50 - Generalised block diagrams of [a] sand-rich and [b] mud-rich base-of-slope aprons (Nelson et al. 1991), and of [c] glaciogenic mud-rich slope aprons, as exemplified by the Bear Island Cone.

The Bear Island Cone has a lot of characteristics in common with mud-rich aprons, including the large dimensions, broad source area, feeding mechanism, and disorganised internal structure (Fig. 50c). A mud-dominated composition of the sediments is confirmed by gravity core samples of the uppermost debris lobes in GIII (Laberg & Vorren, in press b), and by the undulating character of the GII/GIII boundary in the western part of the study area (Windows 1, 30, 35), which is interpreted as diapiric upwellings related to the dewatering of fine-grained material composing the underlying chaotic unit. The only occurrences described to date in modern siliciclastic environments are base-of-slope aprons (Nelson et al. 1991). The Bear Island Cone, however, is not detached from the slope (Fig. 49). This configuration may to a large degree be determined by the exceptionally low gradient ($< 1^\circ$) of the continental slope. Another slight deviation from the mud-rich apron type example, is that some indications have been found for a distal lateral gradation of facies, e.g. in the r26-r27 interval (see sections 5.3.5.4 and 6.4). Nevertheless, it is concluded that large cones fed by numerous slope failures in glaciogenic sediment along the short line source represented by the mouth of a glacial shelf trough, should more correctly be addressed as “trough mouth aprons”, “glaciogenic slope aprons” or, a term adopted from Hambrey et al. (1991), as “diamict aprons”. Judging from the available literature, this also applies to the depocentres further north, off Storfjorden Trough (Laberg 1994; Hjelstuen et al., in press), and off the Isfjorden and Bellsund fjords in Svalbard (Andersen et al. 1994). It makes little sense to compare these aprons with the well-known low-latitude submarine fans such as the Bengal Fan, Mississippi Fan or Amazon Fan.

7. Glacial evolution

7.1. General outline

The sediments composing the Bear Island and Storfjorden Cones have been divided into four large-scale units, “megasequences” G0-GIII, their boundaries marking major changes in depositional style (section 5.3). The recent absolute dating of base GI unconformity r8 at c. 2.3 Ma (Mørk & Duncan 1993; section 5.2.4) favours correlation of this reflector to the onset of major northern hemisphere glaciation, for which oxygen isotope and IRD studies (Shackleton et al. 1984; Jansen et al. 1988, 1990; Thiede et al. 1989) indicate an age of 2.5 - 2.6 Ma. It appears that the main depocentres of the Bear Island and Storfjorden Cones were initiated in response to this event, and a vast volume of glacially-influenced sediment was thus deposited during this relatively short span of time (Fig. 51).

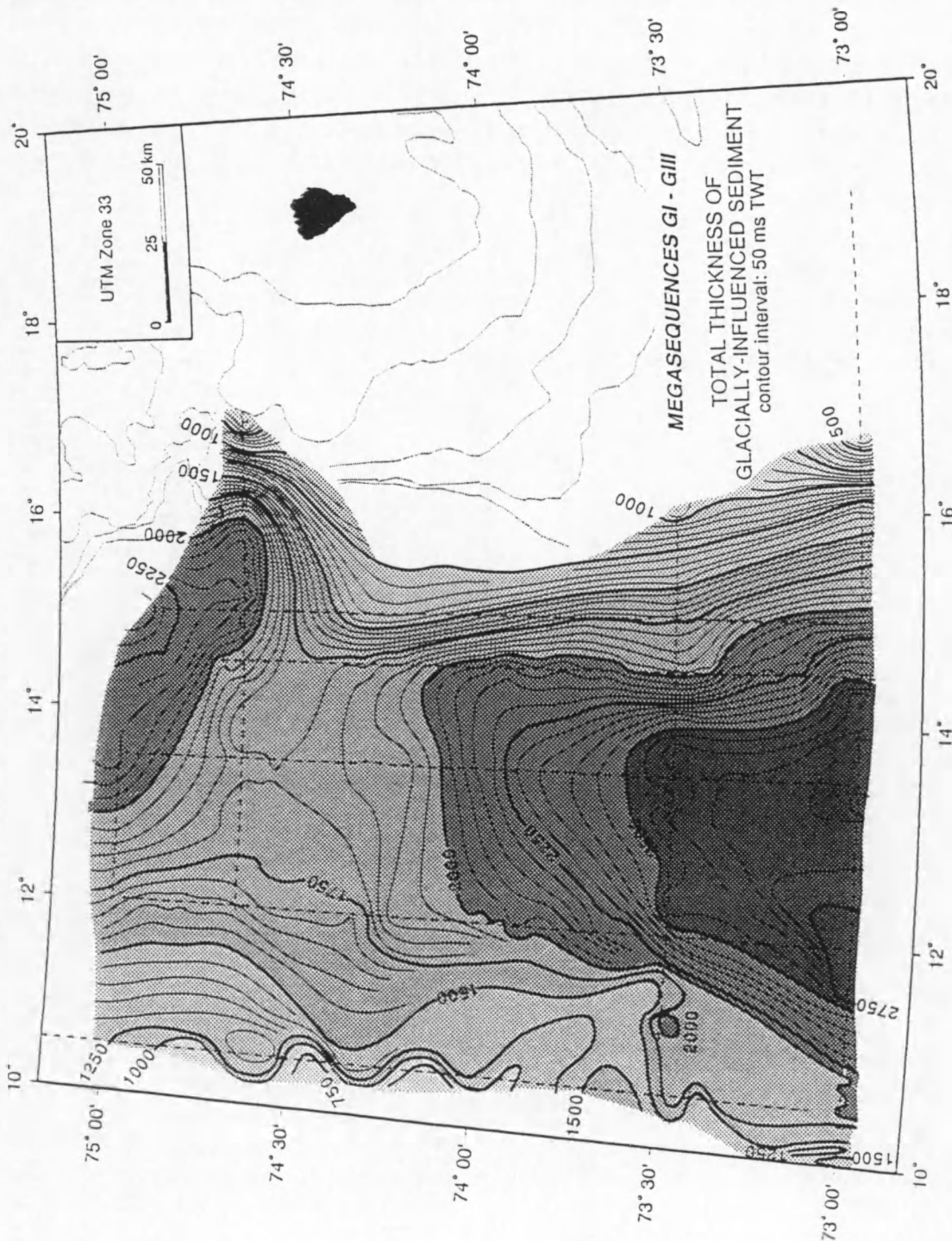


Fig. III.51 - Isopach map of the combined megasequences GI - GIII, i.e. the glacially-influenced portion of the sediment wedge. Contour interval is 50 ms TWT, except in the extreme west of the area, where thickness variations are larger due to irregular basement relief. Gridded using Geofox (Verschuren 1992).

Eidvin et al. (1993) noted the significant presence of sub-angular gravel-sized clasts, interpreted as IRD, in the sediments overlying this boundary, indicating that in the Svalbard - Barents Sea area, too, sizeable glaciers existed. This is in agreement with the recovery of an entirely glaciomarine succession in DSDP Site 344 on the distal Storfjorden Cone (Talwani, Udintsev et al. 1976), which penetrated well into megasequence GI (section 5.2.4). Sættem et al. (1994) even found IRD in sediments just below the base GI unconformity, which represents the stratigraphically deepest indication of glacial influence in the area to date. Further reconstructions of the glacial history mainly focused on the outer shelf portion of GIII (Solheim & Kristoffersen 1984; Vorren et al. 1990b; Sættem et al. 1991, 1992), and more specifically on the uppermost glacial unit (e.g. Vorren et al. 1988; Solheim et al. 1990; Elverhøi et al. 1990, 1994). The intervening period, spanning the deposition of GI and GII, is much more difficult to address, however, mainly due to the poor well control. Correlation, therefore, has to rely on comparison with more distal records from the deep sea. The most continuous and long-term (last 6 Ma) assessment of the glacial evolution in the Nordic Seas is probably provided by the ODP Leg 104 drillholes on the Vøring Plateau along the mid-Norwegian continental margin (Fig. 52a), though it should be kept in mind that these records in the first place provide a proxy to the Fennoscandian Ice Sheet. From studies of oxygen isotope, carbon isotope and IRD content (Fig. 52b) in these cores, the following three-phased glacial evolutionary model has emerged (Thiede et al. 1989; Jansen et al. 1988, 1989; Jansen & Sjøholm 1991; Henrich & Baumann 1994):

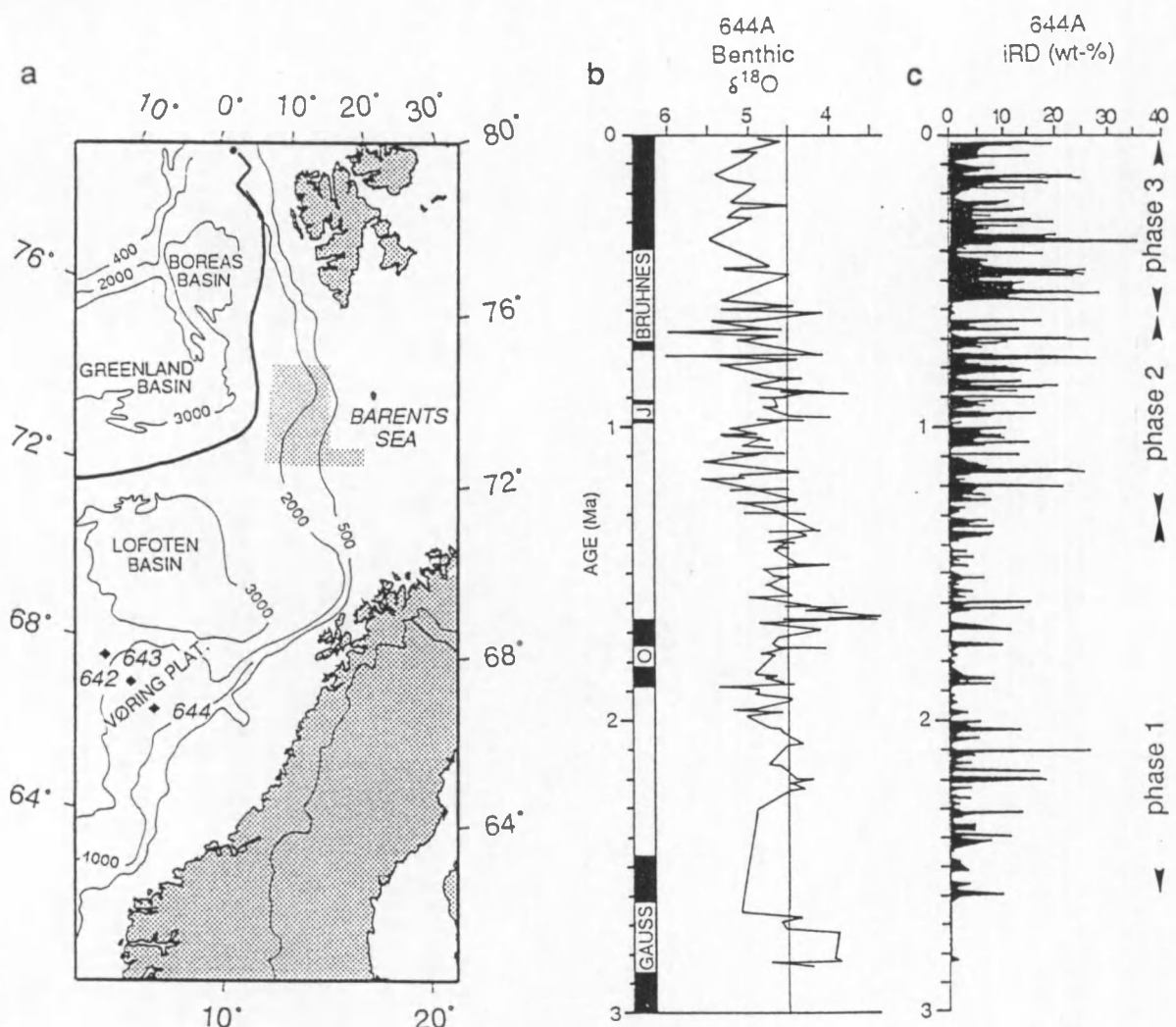


Fig. III.52 - [a] Location of ODP Leg 104 drillholes with respect to the western Barents Sea margin. [b] Magnetostratigraphy and benthic oxygen isotope record of site 644A (Jansen et al. 1988). [c] IRD-record of site 644A (Henrich & Baumann 1994).

Glacial lead-in phase

Minor but significant IRD peaks occur as far back as 5.5 Ma (Late Miocene), indicating the intermittent presence of a modest ice cover, large enough to reach the coastline along the Norwegian Sea. Perhaps the ice was only present in the form of mountain, valley and fjord glaciers in Fennoscandia, but a more extensive cover of the high alpine relief in Svalbard cannot be excluded. Cold deep-water masses were being formed within the Arctic Ocean and/or Norwegian-Greenland Sea during most of the time;

Glacial phase 1 (2.6 - 1.2/1.0 Ma)

A general increase in IRD flux by two to three orders of magnitude at 2.57 Ma is thought to signal the onset of repetitive glacial events in the regions surrounding the Nordic Seas. A stable glacial environment was established, characterised by the continuous presence of medium-sized ice caps. At 2.6 Ma a major expansion of the Fennoscandian Ice Sheet is inferred to have taken place to coastal areas. Relatively severe glacials appeared until c. 2 Ma; between 2 and 1.2 Ma the glaciations were rather small. Interglacials were not clearly developed, and stable conditions prevailed, with cold surface waters, reduced surface salinities and less influx of the warm North Atlantic Current. This indicates that the thermal gradient between the Norwegian Sea and the North Atlantic was much stronger than at present, such that the climatic system was much more zonal, as opposed to the modern meridionality. Deep-water masses were formed in the Norwegian-Greenland Sea and Arctic Ocean, and persistently exchanged with the North Atlantic. Ventilation of the deep-water masses was reduced, without leading to anoxic conditions, however.

Glacial phase 2 (1.2/1.0 - 0.6 Ma)

At approximately 1.2 (1.0) Ma a rapid increase in the deposition of coarse IRD documents a new intensification of glaciation. A shift to larger climatic variation occurred, resulting in more extensive glacials and warmer interglacials. In contrast to the preceding period, ice sheets now regularly expanded from the coastline onto the continental shelf. Glacial phase 2 is regarded as a transitional period, during which a gradual shift occurred towards longer cycles (from 41 ka to dominant 100 ka cycles, cf. Ruddiman et al. 1986) and larger ice volumes. This enabled the growth of progressively larger ice sheets, and glacial expansion towards the south, into the more temperate regions of northern Europe. Glacial/interglacial contrasts became increasingly larger, reflecting a strengthening of the Norwegian Current during interglacials. During this phase also a major transition in the mode of deep-water production took place, with strong fluctuations between an almost stagnant, quiet situation during glacials, and a situation of rapid deep-water renewal, resulting in deep-sea erosion and increased benthic activity during interglacials.

Glacial phase 3 (0.6 Ma - present)

The general trend initiated in glacial phase 2 was further amplified during this final phase of climatic variation. IRD inputs further increased, peaking to maximum concentrations at about 0.4 Ma, and decreasing again afterward. Only in the last 0.6 Ma modern conditions were established in the climatic and oceanographic system of the Norwegian-Greenland Sea, with the culmination of glacial/interglacial contrasts. An alternation occurred between short, but somewhat warmer interglacials than before, with a broad development of the Norwegian Current, deep-water formation and carbonate accumulation, and between extended glacials characterised by larger ice sheets extending onto the continental shelf, and seasonally variable sea ice cover and iceberg drift. The climatic system became overall meridional.

The three-fold subdivision of the glacially influenced sediments of the Bear Island Cone, based on the recognition of major changes in depositional style across the megasequence-bounding unconformities, suggests an evolution of this particular environment in three phases as well. The history that can be reconstructed from an analysis of stratal geometries, lateral and vertical variation of seismic facies (especially those facies indicating mass movements), rates of sediment accumulation (Fig. 53), and temporal and spatial distribution of depocentres (witnessing the relative activity of the Bear Island and Storfjorden Cones), to a high degree matches the evolutionary model depicted above. The correlation of the identified megasequences GI - GIII with the respective glacial phases 1 - 3, is therefore tentatively proposed (cf. Faleide et al., in press), grossly in accordance with the available chronology.

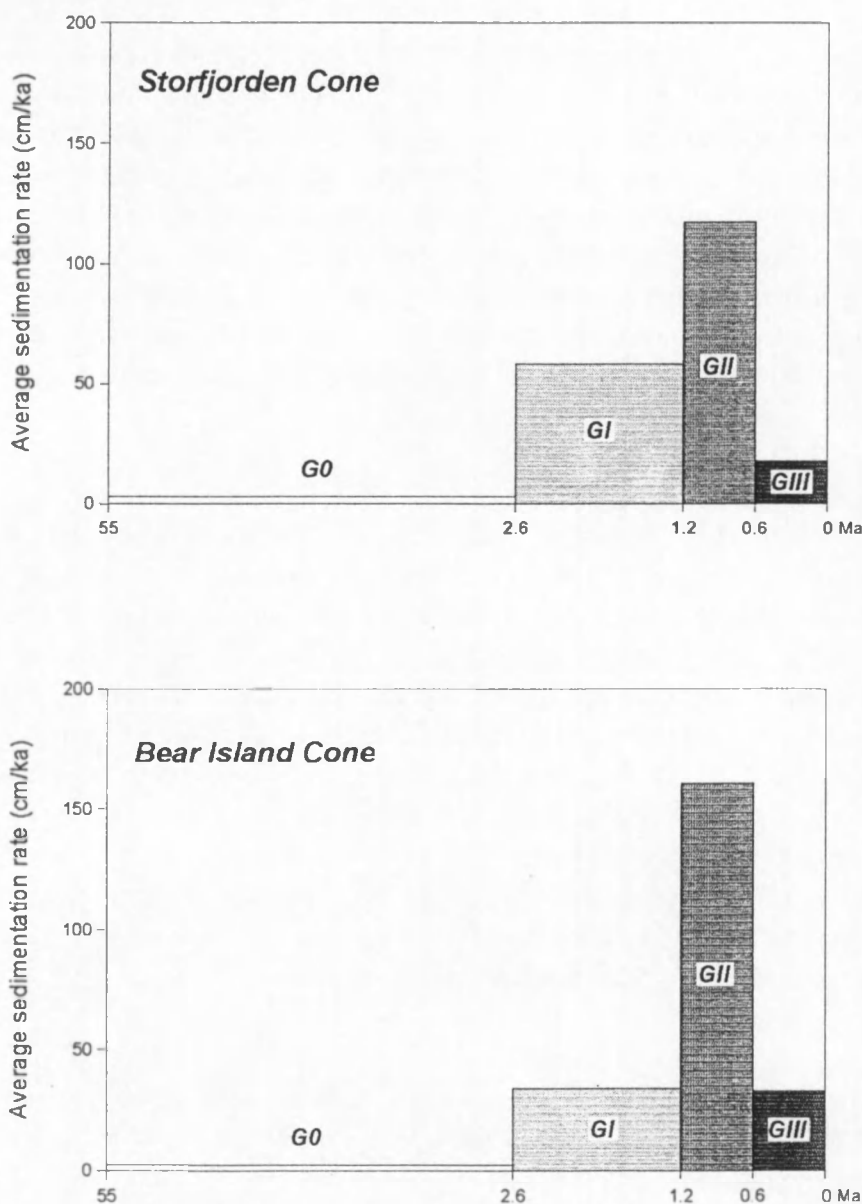


Fig. III.53 - Averaged sedimentation rates during pre-glacial (G0) and glacial (GI - GIII) episodes on [a] Storfjorden Cone and [b] Bear Island Cone. Adapted from Faleide et al. (in press), by using a slightly different time frame.

7.2. GI : initial glacial advances (2.6 - ~1.2 Ma)

It has been argued in the preceding section that the base-GI unconformity roughly coincides with the major onset of northern hemisphere glaciation at c. 2.6 Ma. The IRD found in sediments underlying this boundary probably reflects the minor preceding glaciations during the Late Miocene to Early Pliocene (Sættem et al. 1994). It has been suggested by several authors (e.g. Eidvin et al. 1993; Sættem et al. 1994) that glaciation nucleated in the high alpine areas of Svalbard, probably as the combined effect of climatic deterioration and Late Pliocene tectonic uplift of the Svalbard Platform. The first ice sheet expansions may thus have been confined to the rather narrow Svalbard shelf and the north-western Barents Sea; the remainder of the Barents shelf, which was most likely emergent at this time (Eldholm et al. 1987; Riis & Fjeldskaar 1992) but had gentle relief, was probably not yet fully glaciated (Fig. 54a). Support for such a configuration comes from the thickness distribution and seismic facies of megasequence GI. The isopach map (Fig. 26) indicates that during this first period a large depocentre individualised in the north, dominating the lower slope in the entire study area. Conforming to similar interpretations for the portion of the margin further north (Schlüter & Hinz 1978), the chaotic reflection pattern of these deposits is thought to reflect massive downslope remobilisation caused by rapid rates of accumulation (cf. Faleide et al., in press). High sedimentation rates (Fig. 53) were probably brought about by the first large ice sheets expanding from Spitsbergen into the area of the present-day Storfjorden Trough. Gradual build-out of the continental margin occurred in the ice-proximal regions during these initial glacial advances.

South of Bear Island, the base-GI unconformity marks the onset of strong progradation of the upper slope. This upper slope progradational depocentre, with relatively steep foresets dipping at 3.5 - 4°, appears to have only a local extent, however. Isopach maps published for the region immediately south of the study area (Fiedler & Faleide, in press) indicate that it is constrained in this direction as well. A shape like this strongly suggests the influence of a point source, by a small river system, possibly draining from an immature Barents Sea Ice Sheet further eastward (Fig. 54a). In the same area, Sættem et al. (1991, 1992) have discovered up to 150 m deep erosional channels, filled with gravelly sand, within their correlative outer shelf unit A₀. They interpreted these channels as glaciofluvial or glacial erosion features, formed at the margin of Late Pliocene ice caps that may have extended to a position on the outer shelf. Both observations are thus in accordance in as much that they suggest the less extensive development of ice sheets over the Barents Sea compared to the area further north, but leave the question open whether the main sediment transport agent assumed the form of a proglacial (or subglacial?) meltwater-fed river system, or, alternatively, of narrow ice streams intermittently protruding in the area of the present-day Bear Island Trough. Downslope remobilisation of sediment was far less important than in the Storfjorden depocentre, and in fact most of the sediments on the lower slope may have been sourced from the Storfjorden area or from more southerly portions of the margin.

7.3. GII : intensified glaciations (~1.2 - ~0.6 Ma)

Base-GII unconformity r15 constitutes a very important stratigraphical boundary, defining the lower limit of a prominent chaotic unit over most of the southern and western parts of the study area. It has been demonstrated in section 6.4 that the thick chaotic unit is the result of repetitive phases of extensive mass wasting, probably in the form of huge flow-slides and/or slumps, mostly initiated on the upper slope off the present-day Bear Island Trough. The onset of large-scale mass movements marks an important turn-over in the depositional history of this part of the margin, and is attributed to a major increase of sediment input, probably in response to the general intensification of polar North Atlantic glaciations around 1.2 (or 1.0) Ma (Fig. 52b). The average sedimentation rates calculated for the period of time represented by GII (Fig. 53, Faleide et al., in press), indeed indicate a marked increase in the sediment supply to the margin, though some uncertainty remains due to the poor age control of particularly the lower boundary. The values are about the same for the Storfjorden and Bear Island Cones, but the increase was most pronounced on the Bear Island Cone. This suggests that the intensified glaciations resulted primarily in a growth of the Barents Sea Ice Sheet, gradually eroding the Barents shelf to below sea level. This is again in good agreement with the results of Sættem et al. (1992), who interpret the base and top of their correlative unit A to have been formed by glacial erosion, indicating that south of Bear Island, glaciers reached the outermost contemporaneous continental shelf by this time (Fig. 54b). The authors further inferred that this unit was deposited during several glacial cycles.

The isopach map for GII (Fig. 29) further illustrates the paleogeographical situation: two coexisting depocentres developed during this period. The Storfjorden depocentre takes in a position slightly upslope from the situation in GI, corresponding with a further outbuilding of the margin. The Bear Island depocentre, on the other hand, is located on the lower slope. Apparently the period of large-scale mass wasting effectively shifted the sedimentation downslope, so that the net, long-term, progradation of this part of the margin was annihilated. Mass wasting processes took place repeatedly, and were so extensive that several mass deposits have in places amalgamated into a single very thick chaotic unit. A lot of these mass deposits even extend into the Storfjorden depocentre, which probably has some implications for the relative activity of the two sediment supply systems as deduced from volumetric calculations, as well as for the rates of erosion estimated for the Storfjorden Trough area (Hjelstuen et al., in press); the latter are probably somewhat overestimated. In addition to the increased sedimentation rates, slope instability may have been promoted by local tectonic uplift in the Vestbakken volcanic province (Fig. 54b), which partly underlies the main area of initial accumulation, in front of present-day Bear Island Trough. This uplift is different in space (more southerly) and time (younger) from the Late Pliocene uplift reported for the Svalbard Platform by Sættem et al. (1994). Probably the uplift also accounts for the strongly erosional character of the base-GII unconformity in this area. Alternatively, this erosion may be explained by a major turn-over in the bottom water regime, involving the more vehement renewal of deep-water masses, which is indicated to have occurred during glacial phase 2 (Henrich & Baumann 1994; see section 7.1). Towards the end of the GII interval, the influence of the Storfjorden Cone started to dwindle with respect to the Bear Island Cone, as indicated by the progressive northward onlap of strata derived from the latter depocentre onto reflector r27 (R2).

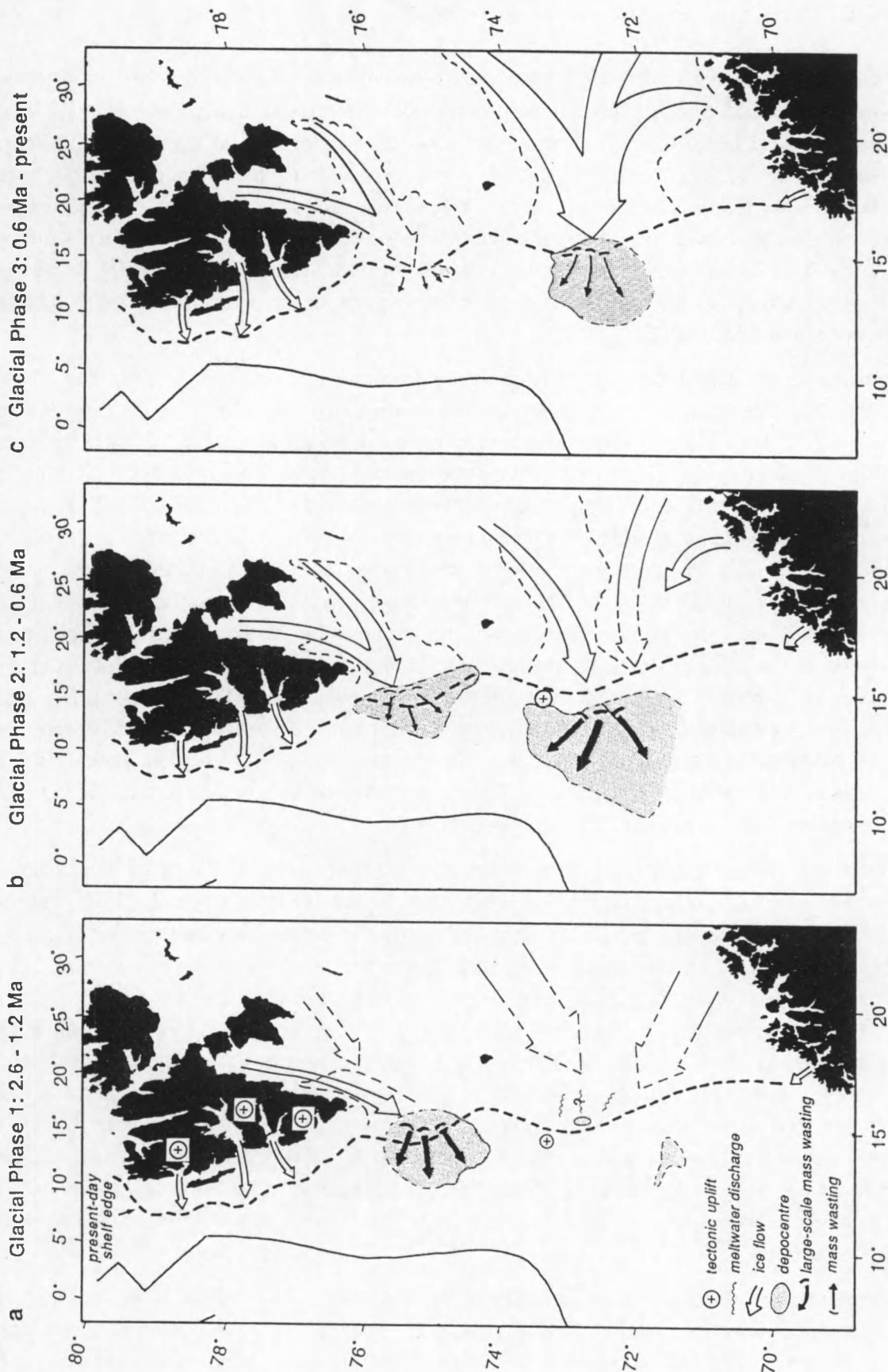


Fig. III.54 - Conceptual model for glacial evolution of the western Barents Sea margin in three phases, depicting variations in the relative activity of the two main depocentres, scale and influence of mass wasting processes, and tentative ice flow patterns. Dashed depocentre outlines are from Hjelstuen et al. (in press) for the Storfjorden Cone, and from Fiedler & Faleide (in press) for the Bear Island Cone.

7.4. GIII : modern glacial conditions (~0.6 Ma - present)

Base-GIII unconformity r30, defining the boundary between large-scale mass deposits below (flow-slides) and more medium-sized debris flow deposits above, represents the last major depositional change on the Bear Island Cone. It implies either a reduction in scale of the operating gravitational processes, or a decrease in frequency of the larger-scale events, or a combination of both. The large slope failure at the GII/GIII boundary is the last large-scale mass wasting event that has affected the study area. Another failure with comparable dimensions is recorded higher in GIII on the southern flank of the Bear Island Cone, indicating that this scale of mass wasting occurred twice during the last 600 ka, whereas this must have been much more frequent, in the order of once per 100 ka or higher, during deposition of GII.

Sedimentation rates during the GIII period generally dropped with respect to the preceding glacial phase (Fig. 53). This decrease was most pronounced on the Storfjorden Cone, and the isopach map (Fig. 33) shows that the Bear Island Cone is effectively overwhelming the Storfjorden Cone. The Bear Island depocentre also clearly occupies a more up-slope position compared to the situation in GII. Initial sedimentation acted to preferentially fill in the slide scar at the GII/GIII boundary, due to the evident location of this feature close to the main sediment supply. When the sediment deficiency was balanced again, and the slide scar "healed", sedimentation on the Bear Island Cone was shifted into a strongly progradational mode. The shelf break at the axial mouth of Bear Island Trough moved at least 35 km seaward. Not unimportantly, this progradation was accompanied by significant aggradation of shelf strata (Fig. 55a), which is responsible for the typical appearance of the upper regional unconformity on the Barents shelf. URU is most likely a polycyclic erosional surface that was mainly excavated by several glacial advances during the preceding period; the glacial advance at the GII/GIII transition was thus not necessarily more extensive than earlier advances. Following this time, erosion was considerably reduced, except at the level of r37, which is seen to truncate successively the horizons r36 and r35 in landward direction.

The sediments overlying the upper regional unconformity have been described in several high-resolution seismic stratigraphic studies (Solheim & Kristoffersen 1984; Vorren et al. 1990b; Sættem et al. 1991, 1992), which have identified four to five mostly transparent units which are separated by erosional surfaces that are continuous to the shelf break. The lithology of these units consists of massive muddy diamicton, interpreted as till deposited from grounded ice (Sættem et al. 1991, 1992). For the upper unit, a glacial origin has more or less been established by the recognition of [i] glacial flutes in the inner parts of Bear Island Trough (Solheim et al. 1990) and farther west (Elverhøi et al. 1994) (Fig. 56), [ii] sediment ridges possibly representing end moraines at the mouth of the trough (Vorren et al. 1990b, Elverhøi et al. 1992) (Fig. 56), and [iii] the (partly) overconsolidated nature of the shelf diamicton (Elverhøi et al. 1990, 1994). In combination, these observations provide evidence for multiple episodes of full glaciation in the Barents Sea during GIII time, with ice sheets extending at least four, and possibly five times far out to the mouth of Bear Island Trough.

The most detailed work so far was presented by Sættem et al. (1991, 1992), who were able to identify seven units in the post-URU section of the outer Bear Island Trough, some of which were dated by the amino acid method (Fig. 55). One of these (unit E) is a thin acoustically stratified unit comprising Eemian bioturbated marine sediments and Lower - ?Middle Weichselian glaciomarine deposits. Four older units (B, C, D₁ and D₂), and two younger ones (F and G) are inferred to be

glacial in origin. The results from the lower-resolution seismic records used in the present study can without problem be correlated to the stratigraphy established by Sættem et al. (1991, 1992), though the units C, E and F appear to be too thin to be resolved on these records. Comparison of identical lines located along the 73° N and 73°30' N parallels (Fig. 55) indicates that the intervals r34-r35, r35-r36, r36-r37 and r37-seafloor correspond to units B, C-D₁, D₂ and E-F-G, respectively. According to the datings by Sættem et al. (1991, 1992) these intervals would roughly represent the four latest 100 ka cycles (Table 9). The older interval r30-r34, which is mainly restricted to the area of the slide scar, was not recognised by these authors, however. It is therefore suggested (cf. section 5.2.4.3) that the base-GIII unconformity, which is equivalent to URU, may well be older than 440 ka — the amino acid age of the oldest sediments in the overlying unit B. Megasequence GIII is probably closely related to the latest phase of polar North Atlantic evolution (see section 7.1), and thus a tentative age of c. 600 ka is put forward. This is also suggested by Laberg & Vorren (in press a), who by simple back-counting of oxygen isotope stages, obtained an age of 622 ka, the beginning of isotope stage 16. Such an approximation is not unambiguous, however, as indicated by the correspondence of the two upper units F and G with isotope stage 2.

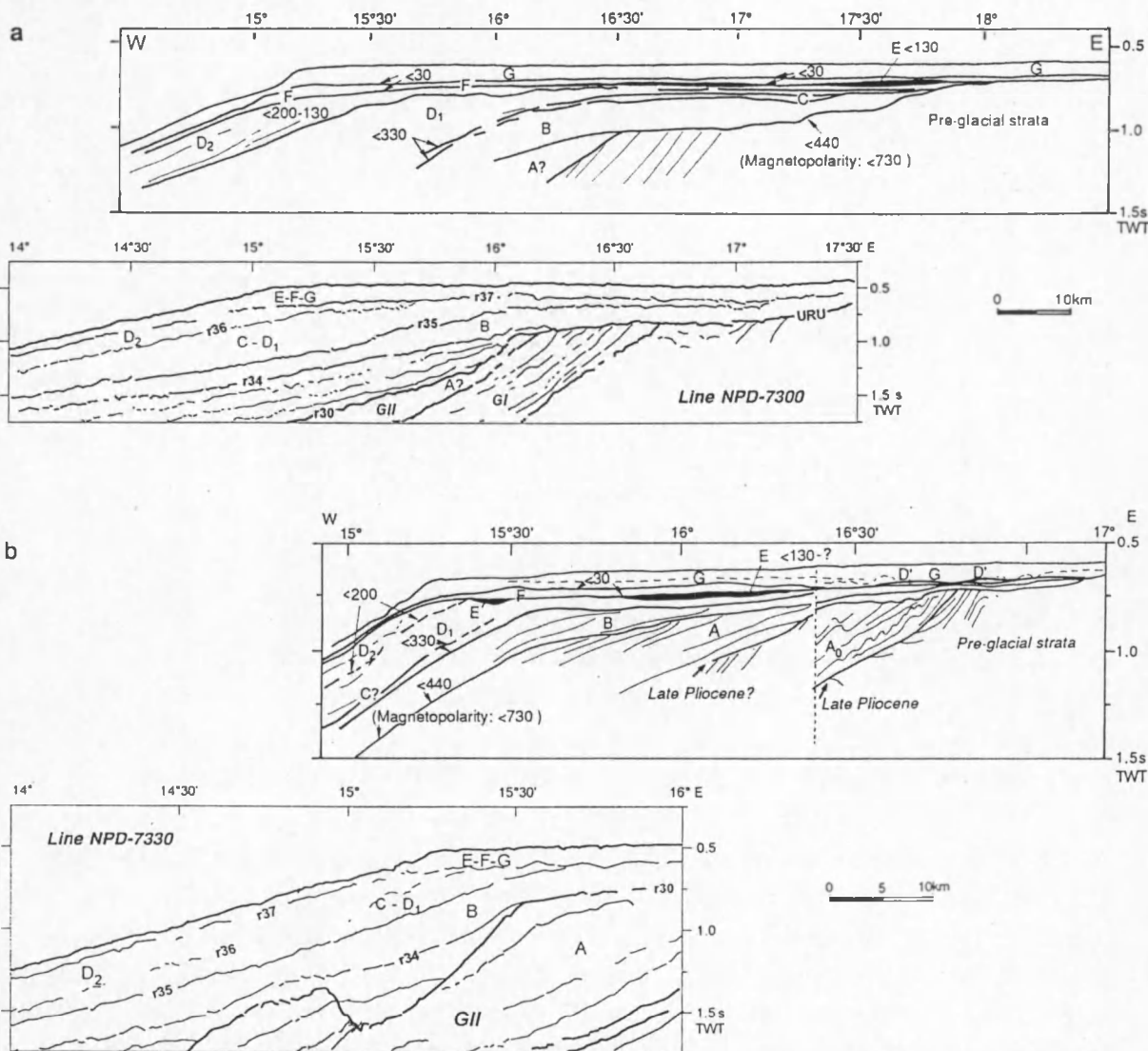


Fig. III.55 - Comparison of line drawings from high-resolution records of Sættem et al. (1991, 1992) with the low-resolution records used in this study, for lines located [a] along 73° N and [b] along 73°30' N. Numbers indicate amino-acid ages of certain horizons.

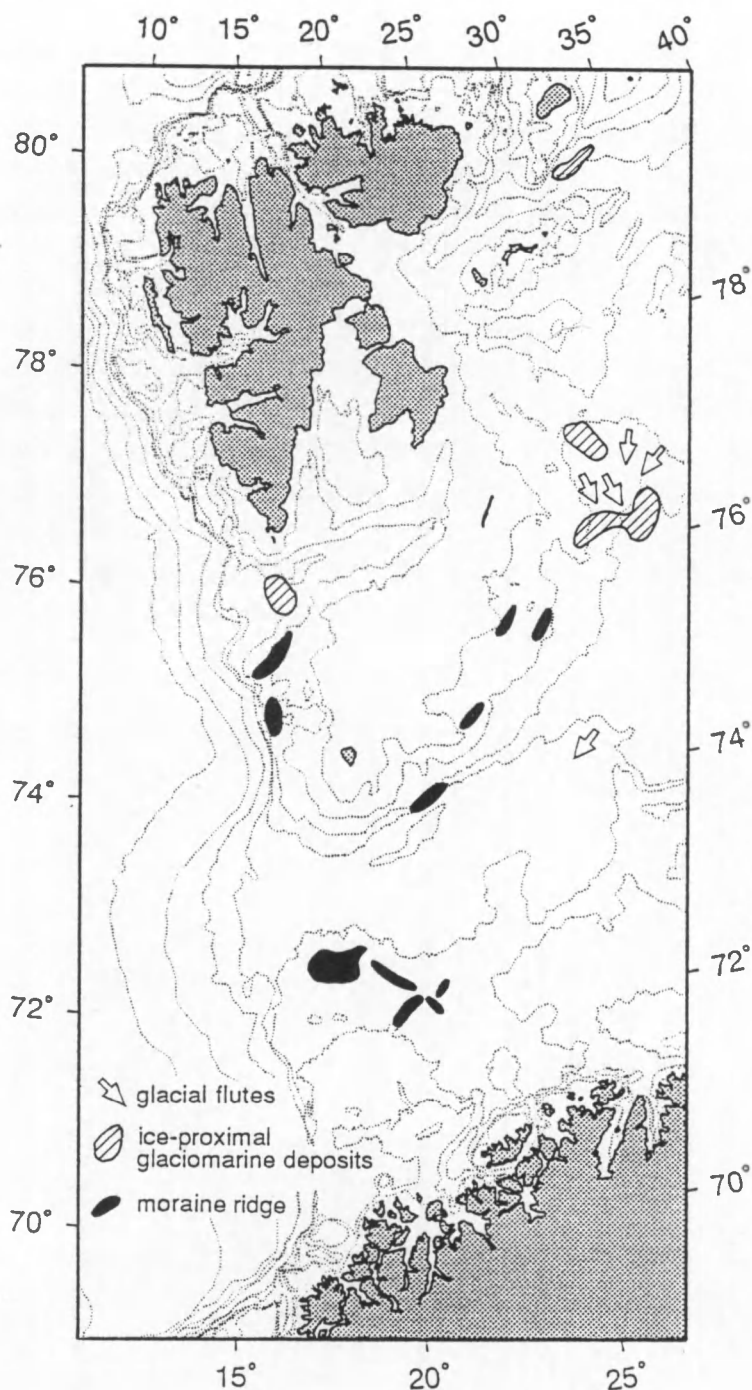


Fig. III.56 - Distribution of important glacial features (glacial flutes, moraine ridges, ice-proximal glaciomarine deposits) in the western Barents Sea. From Elverhøi et al. (1992, 1994).

The correlation of these upper units with the Late Weichselian is fairly well established by datings of 28 ka by Vorren et al. (1990b) and of 30 ka by Sættem et al. (1991, 1992). The latter authors pointed out that the erosional F/G boundary is not necessarily related to a second Late Weichselian glacial advance, but may equally well reflect a change in the ice flow regime. The correlation suggests that no Early and Middle Weichselian deposits are preserved in the outer Bear Island Trough. This is in contrast to the three separate glacial advances that are recognised on the Svalbard margin (Mangerud & Svendsen 1992), but in accordance with the situation in northern Norway (Olsen 1989).

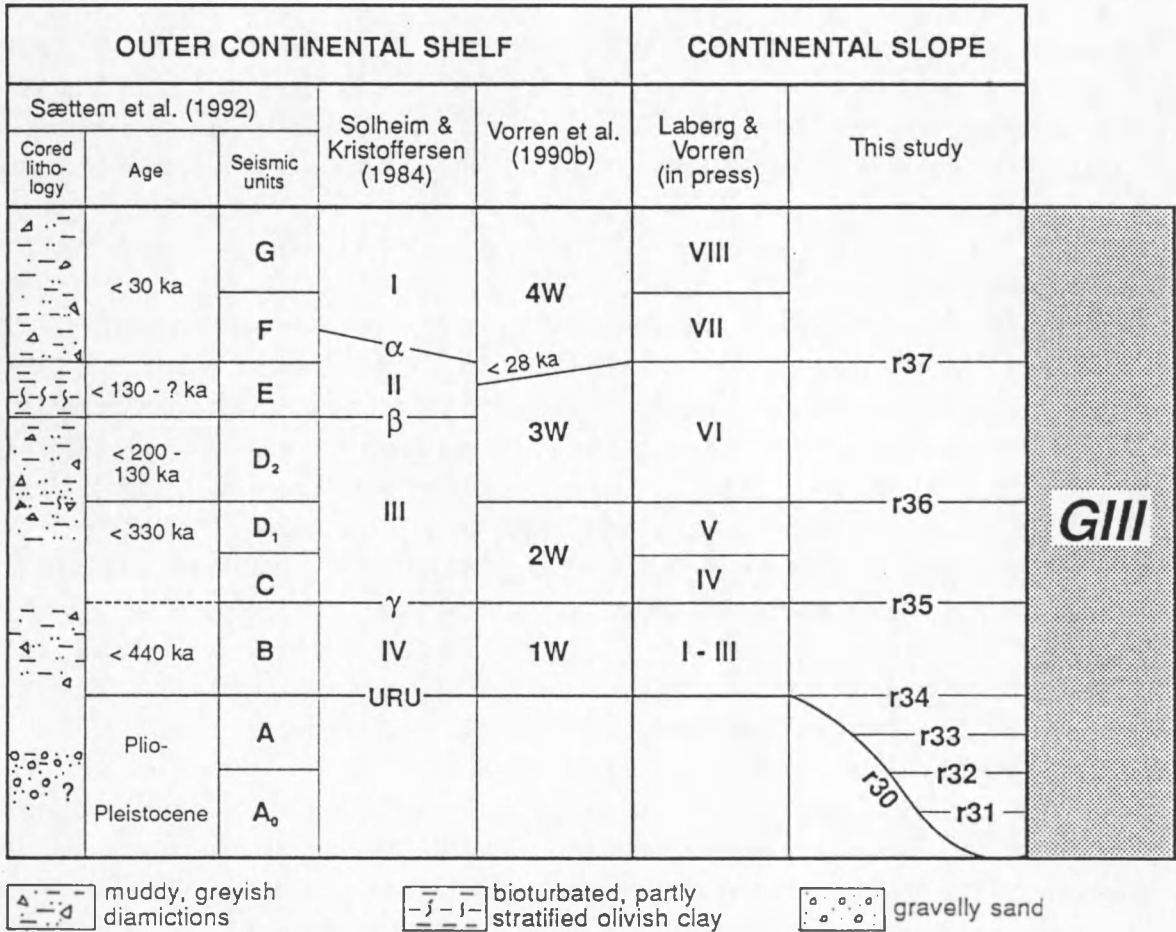


Table III.9 - Correlation of seismic units (sequences?) recognised within GIII with stratigraphies and chronologies established by various authors.

An Early and/or Middle Weichselian extension of ice streams into the outer Bear Island Trough cannot be ruled out, however, since the base of the upper sequence (r37) appears to be strongly erosive on the seismic records; this is in fact the strongest erosional surface that is recognised on the shelf within megasequence GIII. It is quite possible that these earlier advances had a more erosional character, or that their deposits were obliterated by the Late Weichselian glaciation. Datings of shell fragments and foraminifera from the central Barents Sea indicate that marine conditions prevailed until 23 - 22 ka BP (Hald et al. 1990), which in turn suggests that the Barents Sea Ice Sheet did not advance until fairly late in the Weichselian (Elverhøi et al. 1992, 1994). The last glacial maximum was probably achieved around 18 ka BP. Deglaciation was initiated at an early stage, as indicated by the re-establishment of the warm Norwegian Current between 15 and 13 ka BP (Jones & Keigwin 1988), by the radiocarbon dating of a shell fragment in the southern Barents Sea at c. 13 ka BP (Vorren & Kristoffersen 1986), and also by isostatic modelling (Elverhøi et al. 1992). The distribution of ice-proximal deposits in the Barents Sea (Fig. 56) suggests that initial deglaciation encompassed most of the Barents Sea deeper than the present-day 300 m contour, including the major part of the Bear Island Trough, whereas final deglaciation of the shallower northern Barents Sea may not have been completed until 10 ka (Elverhøi et al. 1990, 1992, 1994). The total residence time of the ice sheet at the shelf break was thus very short (Fig. 57).

Lining up all the observations regarding megasequence GIII invokes a number of apparent contradictions. On the one hand, the reduction in scale of mass wasting processes on the Bear Island Cone, the general drop of sediment accumulation rates, and the prevalence of deposition over erosion on the continental shelf could all be taken as indicative of less severe glaciations, characterised by ice sheets with reduced erosive power. On the other hand, the margin off Bear Island Trough has never been built out as strongly as during GIII, the IRD-record monitoring the activity of the Fennoscandian Ice Sheet (Fig. 52, Jansen et al. 1988, 1990) is suggesting peak glacial conditions during the latest phase of climate variation, and the oxygen isotope record indicates that late Pleistocene ice sheets attained larger sizes than before, but the latter mainly reflects ice expansion into lower latitudes (Ruddiman et al. 1986). A change in ice stream dynamics may provide the key to this dilemma, however. Evidently, the Storfjorden and Bear Island Troughs have acted as the major conduits along which the ice expanded and most of the sediment was transported. The morphology of URU, which comprises a wide channel underlying the present Bear Island Trough (Vorren et al. 1990b), and the presence of several shelfal units filling in the trough but greatly thinning beyond its limits, indicate that an overdeepened proto-Bear Island Trough had developed already by the beginning of GIII time, under the influence of converging ice flow from Svalbard and Fennoscandia. The generation of an entirely marine-based ice sheet in the Barents Sea, and especially in Bear Island Trough which is presently over 400 m deep, remains hard to explain, however. Elverhøi et al. (1992, 1994) have proposed a mechanism of small ice caps nucleating on the shallow bank areas in the Barents Sea, when these were gradually exposed by glacio-eustatic sea level lowering; the gradual expansion of these ice caps, combined with an expansion of ice sheets from surrounding land masses, may have finally resulted in a continuous ice sheet covering the Barents Sea. Fast-flowing ice streams converging in Bear Island Trough and reaching out to the shelf break, may thus have formed at the very latest stage in the glacial cycle, and were probably also the first to disappear again. The short-lived position of the ice margin at the mouth of Bear Island Trough is in particular demonstrated by the reconstructions for the Late Weichselian discussed above (Fig. 57), and is thought to be generally representative for the earlier GIII glaciations as well. It is considered likely that the gradual overdeepening of Bear Island Trough played a major role in the establishment of this regime, and that the resulting ice stream dynamics were quite different from the situation in GII. Ice occupancy in the trough was probably much shorter, implying a relatively thin ice sheet (cf. Elverhøi et al. 1994). In combination with the large water depths, an only moderate ice burden is therefore inferred, which probably to a large extent accounts for the observed decline in erosive power of the ice sheet. An accompanying reduced effect of glacio-isostatic rebound may have contributed to a greater stability of the upper slope sediments, compared to the preceding period GII.

A final consideration concerns the mode of deposition of outer shelf and upper slope sediments from the ice. Both suspension settling in front of meltwater outlets (e.g. Solheim & Kristoffersen 1984; Elverhøi et al. 1989; Laberg & Vorren, in press b) and subglacial traction in a deformable till layer (e.g. Sættem et al. 1992; Elverhøi et al. 1994; Laberg & Vorren, in press b) have been suggested as the dominant sedimentation process, but evidence is limited and can hardly discriminate between the two. Both processes imply a wet-based ice sheet, but are probably mutually exclusive (free flow versus advective transport of basal meltwater, cf. Alley et al. 1989), at least during a given time window. It is not impossible, however, that both processes were operating during different stages of the glacial cycle. The inferred rapid, surge-like advance of ice streams in Bear Island Trough at a late stage of the glacial cycle was probably lubricated by a deformable till layer, enabling faster flow rates. Large volumes of meltwater may have been released during the subsequent deglaciation,

provided that the retreat did not occur catastrophically (cf. Henrich 1991). The unstable, marine-based Barents Sea Ice Sheet was probably one of the first ice masses to disappear following climatic amelioration, and may thus have retreated in a gradual fashion, rather than abruptly breaking up in response to a sudden glacio-eustatic sea level rise. Wet-based ice sheets, which are known to yield more sediment than dry-based ice sheets (e.g. Powell & Molnia 1989), could explain the extraordinary large sediment volumes observed on the western Barents Sea margin. The sediment resulting from both suspension settling and subglacial deformation would be an unconsolidated and water-saturated glaciomarine mud (Alley et al. 1989; Boulton 1990), which is highly prone to instability when this rapidly deposited.

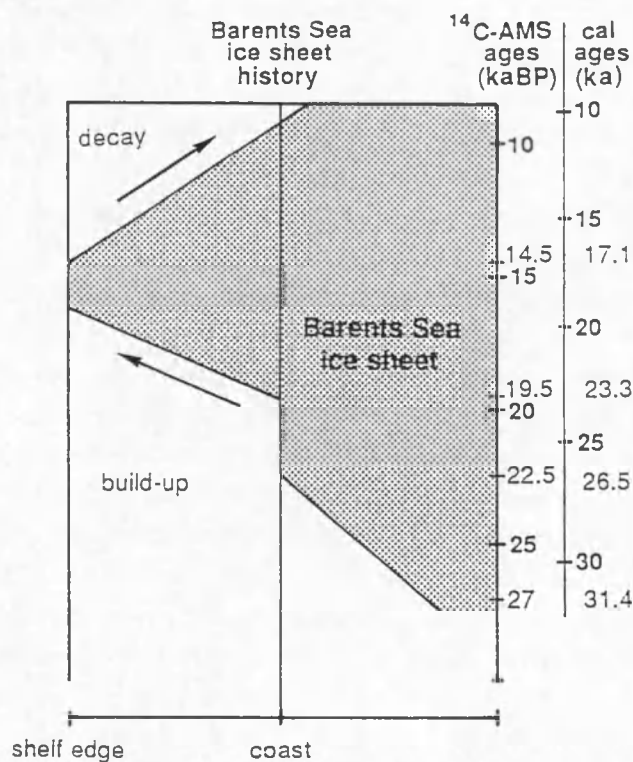


Fig. III.57 - Reconstruction of the growth and decay of the Barents Sea Ice Sheet during the latest glaciation in the Late Weichselian. Adopted from Hebbeln et al. (1994).

7.5. Conclusions

- The glacially-influenced section along the western Barents Sea margin can be divided into three first-order units, megasequences GI-GIII, which are characterised by distinct changes in stratal geometry, accumulation rate, relative activity of major depocentres (Storfjorden and Bear Island Cones), and scale of mass wasting. The depositional history, summarised in Fig. 54, closely matches a three-step model for the glacial evolution of the polar North Atlantic, which was earlier reconstructed from the deep-sea record.
- Deposition of Megasequence GI is characterised by the individualisation of the Storfjorden Cone, which was accompanied by significant mass movements transporting sediments downslope. This unit was probably deposited during the initial phase of large-scale glaciation, when ice caps covering high alpine areas like Svalbard, grew large enough to expand onto the narrow adjacent continental shelf. The Barents Sea Ice Sheet was most probably not yet fully developed at this time.
- Megasequence GII documents the coexistence of two major depocentres, on the Storfjorden and Bear Island Cones. Overall sedimentation rates leaped upward, and the Bear Island Cone now became the focus of large-scale mass wasting processes that shifted the centre of accumulation considerably downslope. Slope instability may have been enhanced by local uplift in the area of main initial sediment accumulation. GII is thought to witness a second phase of glaciation, with ice sheets periodically reaching the shelf edge in the western Barents Sea as well. The Barents shelf area was hereby gradually submerged, and a proto-Bear Island Trough started to form in the convergence zone of the Svalbard and Fennoscandian Ice Sheets.
- During deposition of Megasequence GIII sedimentation rates drop again to, or below, the level of GI. Whereas the Storfjorden Cone is dwindling, the margin at the mouth of Bear Island Trough is built out farther than ever. Slope accumulation is still dominated by mass movements, though at smaller scales than before. GIII thus monitors the final phase of climatic variation, which is speculated to have involved a major change in ice stream dynamics, possibly in part related to the overdeepening of Bear Island Trough. As has been constrained for the Late Weichselian, glaciations were probably characterised by short-lived, fast-flowing ice streams expanding from the Barents Sea Ice Sheet into Bear Island Trough, at a fairly late stage in the glacial cycle. The erosive power of these ice streams was significantly reduced, and deposition prevailed within and at the mouth of the trough.
- Though mass wasting was undeniably related to the increased sedimentation rates resulting from glaciation, it is not likely that there is a strict correlation between episodes of mass movements and the different glacial cycles. In addition, large-scale mass wasting processes have annihilated much of the significance of the stratigraphic record, particularly in Megasequence GII. This would imply that the potential of especially Bear Island Cone for reconstructing the climatic history of the Barents Sea area in greater detail, is limited. The Storfjorden Cone, which was far less disturbed, may provide a better archive, however.

References cited

- Aksu A.E. & Hiscott R.N. (1992) — Shingled Quaternary debris flow lenses on the north-east Newfoundland Slope. *Sedimentology*, 39, pp. 193-206.
- Alley R.B., Blankenship D.D., Rooney S.T. & Bentley C.R. (1989) — Sedimentation beneath ice shelves : The view from Ice Stream B. In: Powell R.D. & Elverhøi A. (Eds.), *Modern Glacimarine Environments: Glacial and Marine Controls of Modern Lithofacies and Biofacies*. *Marine Geology*, 85, pp. 101-120.
- Andersen E.S., Solheim A. & Elverhøi A. (1994) — Development of a glaciated arctic continental margin : Exemplified by the western margin of Svalbard. In: Thurston D.K. & Fujita K. (Eds.), *Proceedings of the International Conference on Arctic Margins*, Anchorage, Alaska, 1992. U.S. Department of the Interior, Mineral Management Service, Alaska Outer Shelf Region, OCS Study, pp. 155-160.
- Bellaiche G., Coutellier V., Droz L. & Le Cann C. (1990) — Les glissements en masse du glaciais provençal. *Oceanologica Acta*, 13(1), pp. 121-126.
- Berggren W.A., Burckle L.H., Cita M.B., Cooke H.B.S., Funnell B.M., Gartner S., Hays J.D., Kennett J.P., Opdyke N.D., Pastouret L., Shackleton N.J. & Takayanagi Y. (1985) — Towards a Quaternary time scale. *Quaternary Research*, 13, pp. 277-302.
- Blindheim J. (1989) — Cascading of Barents Sea bottom water into the Norwegian Sea. *Rapports et Proces-Verbaux des Réunions Conseil International pour l'Exploration de la Mer*, 188, pp. 49-58.
- Bonatti E. & Crane K. (1984) — The geology of oceanic transform faults. *Scientific American*, 250(5), pp. 40-51.
- Boulton G.S. (1990) — Sedimentary and sea level changes during glacial cycles and their control on glacimarine facies architecture. In: Dowdeswell J.A. & Scourse J.D. (Eds.), *Glacimarine Environments: Processes and Sediments*. Special Publication, 53, The Geological Society, London, pp. 15-52.
- Bouma A.H. (1962) — *Sedimentology of Some Flysch Deposits : A Graphic Approach to Facies Interpretation*. Elsevier Scientific, Amsterdam, 167 pp.
- Bouma A.H., Normark W.R. & Barnes N.E. (Eds.) (1985) — *Submarine Fans and Related Turbidite Systems*. Springer-Verlag, New York.
- Bugge T. (1983) — Submarine slides on the Norwegian continental margin, with special emphasis on the Storegga area. Publication, no. 110, Continental Shelf Institute, 152 pp.
- Bugge T., Befring S., Belderson R.H., Eidvin T., Jansen E., Kenyon N.H., Holtedahl H. & Sejrup H.-P. (1987) — A giant three-stage submarine slide off Norway. *Geo-Marine Letters*, 7, pp. 191-198.
- Coachman L.K. & Aagaard K. (1973) — Physical oceanography of Arctic and Subarctic Seas. In: Herman Y. (Ed.), *Marine Geology and Oceanography of the Arctic Seas*. Springer-Verlag, New York, pp. 1-72.
- Coleman J.M. & Garrison L.E. (1977) — Geological aspects of marine slope stability, northwestern Gulf of Mexico. *Marine Geotechnology*, 2, pp. 9-44.
- Crane K., Sundvor E., Foucher J.-P., Hobart M., Myhre A.M. & LeDouaran S. (1988) — Thermal evolution of the western Svalbard margin. *Marine Geophysical Researches*, 9, pp. 165-194.
- Damuth J.E. (1978) — Echo character of the Norwegian-Greenland Sea : Relationship to Quaternary sedimentation. *Marine Geology*, 28, pp. 1-36.
- Dingle R.V. (1977) — The anatomy of a large submarine slump on a sheared continental margin (S.E. Africa). *Journal of the Geological Society*, 134, pp. 293-310.
- Dott R.H. (1963) — Dynamics of subaqueous gravity depositional processes. *American Association of Petroleum Geologists Bulletin*, 47, pp. 104-128.
- Dowdeswell J.A. & Kenyon N.H. (1995) — Long-range side-scan sonar investigations of the polar North Atlantic : Patterns and processes of sedimentation on a glaciated passive continental margin. Cruise report, University of Wales, Aberystwyth, 50 pp.
- Eidvin T., Jansen E. & Riis F. (1993) — Chronology of Tertiary fan deposits off the western Barents Sea : Implications for the uplift and erosion history of the Barents Shelf. *Marine Geology*, 112, pp. 109-131.
- Eidvin T. & Riis F. (1989) — Nye dateringer av de tre vestligste borehullene i Barentshavet : Resultater og konsekvenser for den Tertiære hevingen. NPD Contribution 27, Oljedirektoratet, Stavanger, Norway, 44 pp.
- Einsele G. (1991) — Submarine mass flow deposits and turbidites. In: Einsele G., Ricken W. & Seilacher A. (Eds.), *Cycles and Events in Stratigraphy*. Springer-Verlag, Berlin, pp. 313-339.

- Eldholm O., Faleide J.I. & Myhre A.M. (1987) — Continent-ocean transition at the western Barents Sea/Svalbard continental margin. *Geology*, 15, pp. 1118-1122.
- Eldholm O., Karasik A.M. & Reksnes P.A. (1990) — The North American plate boundary. In: Grantz A., Johnson L. & Sweeney J.F. (Eds.), *The Arctic Ocean Region. The Geology of North America*, Vol. L, The Geological Society of America, Boulder, Colorado, pp. 171-184.
- Eldholm O., Sundvor E., Myhre A.M. & Faleide J.I. (1984) — Cenozoic evolution of the continental margin off Norway and western Svalbard. In: Spencer A.M. et al. (Eds.), *Petroleum Geology of the North European Margin*. Graham & Trotman for the Norwegian Petroleum Society, London, pp. 3-18.
- Eldholm O. & Talwani M. (1977) — Sediment distribution and structural framework of the Barents Sea. *Geological Society of America Bulletin*, 88, pp. 1015-1029.
- Elmore R.D., Pilkey O.H., Cleary W.J. & Curran H.A. (1979) — Black Shell Turbidite, Hatteras abyssal plain, western Atlantic Ocean. *Geological Society of America Bulletin*, 90, pp. 1165-1176.
- Elverhøi A., Fjeldskaar W., Solheim A., Nyland-Berg M. & Russwurm L. (1994) — The Barents Sea Ice Sheet : A model of its growth and decay during the last ice maximum. *Quaternary Science Reviews*, 12, pp. 863-873.
- Elverhøi A., Nyland-Berg M., Russwurm L. & Solheim A. (1990) — Late Weichselian ice recession in the central Barents Sea. In: Bleil U. & Thiede J. (Eds.), *Geological History of the Polar Oceans: Arctic versus Antarctic*. NATO ASI Series C, Mathematical and Physical Sciences, 308, Kluwer, Dordrecht, pp. 289-307.
- Elverhøi A., Pfirman S.L., Solheim A. & Larssen B.B. (1989) — Glaciomarine sedimentation in epicontinental seas exemplified by the northern Barents Sea. In: Powell R.D. & Elverhøi A. (Eds.), *Modern Glaciomarine Environments: Glacial and Marine Controls of Modern Lithofacies and Biofacies*. *Marine Geology*, 85, pp. 225-250.
- Elverhøi A., Solheim A., Nyland-Berg M. & Russwurm L. (1992) — Last interglacial-glacial cycle, Western Barents Sea. In: Möller P., Hjort C. & Ingólfsson Ó (Eds.), *Weichselian & Holocene Glacial and Marine History of East Svalbard: Preliminary Report on the PONAM Fieldwork in 1991*. *Lundqua Report*, 35, pp. 17-24.
- Embley R.W. (1976) — New evidence for occurrence of debris flow deposits in the deep sea. *Geology*, 4, pp. 371-374.
- Faleide J.I., Gudlaugsson S.T. & Jacquart G. (1984) — Evolution of the western Barents Sea. *Marine and Petroleum Geology*, 1, pp. 123-150.
- Faleide J.I., Myhre A.M. & Eldholm O. (1988) — Early Tertiary volcanism at the western Barents Sea margin. In: Morton A. & Parson L.M. (Eds.), *Early Tertiary Volcanism and the Opening of the NE Atlantic*. *Geological Society of London Special Publication*, 39, Blackwell Scientific Publications, Oxford, pp. 135-146.
- Faleide J.I., Solheim A., Fiedler A., Hjelstuen B.O., Andersen E.S. & Vanneste K. (in press) — Late Cenozoic evolution of the western Barents Sea-Svalbard continental margin. In: Solheim A. et al. (Eds.), *Impact of Glaciations on Basin Evolution: Data and Models from the Norwegian Margin and Adjacent Areas*. *Global and Planetary Change, Special issue*.
- Faleide J.I., Våagnes E. & Gudlaugsson S.T. (1993) — Late Mesozoic - Cenozoic evolution of the southwestern Barents Sea. In: Parker J.R. (Ed.), *Petroleum Geology of Northwest Europe: Proceedings of the 4th Conference*. The Geological Society, London, pp. 933-950.
- Faleide J.I., Våagnes E. & Gudlaugsson S.T. (1993b) — Late Mesozoic - Cenozoic evolution of the southwestern Barents Sea in a regional rift-shear tectonic setting. *Marine and Petroleum Geology*, 10(3), pp. 186-214.
- Fiedler A. (1992) — Kenozoisk sedimentasjon i Lofotenbassenget langs vestlige Barentshavmarginen. Unpublished Cand. scient. thesis, Universitetet i Oslo, 114 pp.
- Fiedler A. & Faleide J.I. (in press) — Cenozoic sedimentation along the southwestern Barents Sea margin in relation to uplift and erosion of the shelf. In: Solheim A. et al. (Eds.), *Impact of Glaciations on Basin Evolution: Data and Models from the Norwegian Margin and Adjacent Areas*. *Global and Planetary Change, Special issue*.
- Field M.E. & Clarke S.H., Jr. (1979) — Small-scale slumps and their significance for basin slope processes, southern California borderland. In: Doyle L.J. & Pilkey O.H. (Eds.), *Geology of Continental Slopes*. *Special Publication*, 27, Society of Economic Paleontologists and Mineralogists, pp. 223-230.

- Géll L. (1993) — Volcano-tectonic events and sedimentation since Late Miocene time at the Mohs Ridge, near 72° N, in the Norwegian-Greenland Sea. *Tectonophysics*, 222, pp. 417-444.
- Hald M., Sættem J. & Nesse E. (1990) — Middle and Late Weichselian stratigraphy in shallow drillings from the southwestern Barents Sea: Foraminiferal, amino acid and radiocarbon evidence. *Norsk Geologisk Tidsskrift*, 70, pp. 241-257.
- Hambrey M.J., Ehmann W.U. & Larsen B. (1991) — The Cenozoic glacial record of the Prydz Bay continental shelf, East Antarctica. In: Barron J., Larsen B. et al. (Eds.), *Proceedings of the Ocean Drilling Program, Scientific Results*, 119. College Station, TX, pp. 77-132.
- Hanisch J. (1984) — West Spitsbergen Fold Belt and Cretaceous opening of the Northeast Atlantic. In: Spencer A.M. et al. (Eds.), *Petroleum Geology of the North European Margin*. Graham & Trotman for the Norwegian Petroleum Society, London, pp. 187-198.
- Haq B.U., Hardenbol J. & Vail P.R. (1987) — Chronology of fluctuating sea levels since the Triassic. *Science*, 235, pp. 1156-1167.
- Harland W.B. (1965) — The tectonic evolution of the Arctic-north Atlantic region. *Royal Society of London Philosophical Transactions*, 258, pp. 59-75.
- Hart B.S. (1993) — Large-scale in situ rotational failure on a low-angle delta slope : The Foreslope Hills, Fraser Delta, British Columbia, Canada. *Geo-Marine Letters*, 13, pp. 219-226.
- Hebbeln D., Dokken T., Andersen E.S., Hald M. & Elverhøi A. (1994) — Moisture supply for northern ice-sheet growth during the Last Glacial Maximum. *Nature*, 370, pp. 357-360.
- Heezen B.C. & Ewing M. (1952) — Turbidity currents and submarine slumps and the 1929 Grand Banks earthquake. *American Journal of Science*, 250, pp. 849-873.
- Henrich R. (1991) — Cycles, rhythms, and events on high input and low input glaciated continental margins. In: Einsele G., Ricken W. & Seilacher A. (Eds.), *Cycles and Events in Stratigraphy*. Springer-Verlag, Berlin, pp. 751-772.
- Henrich R. & Baumann K.-H. (1994) — Evolution of the Norwegian Current and the Scandinavian Ice Sheets during the past 2.6 m.y. : Evidence from ODP Leg 104 biogenic carbonate and terrigenous records. *Palaeogeography, Palaeoclimatology, Palaeoecology*, 108, pp. 75-94.
- Hesse R. (1992) — Continental slope sedimentation adjacent to an ice margin I : Seismic facies of Labrador slope. *Geo-Marine Letters*, 12, pp. 189-199.
- Hinz K. (1981) — A hypothesis on terrestrial catastrophes : Wedges of very thick oceanward dipping layers beneath passive continental margins. *Geologisches Jahrbuch, Reihe E*, 22, pp. 3-28.
- Hiscott R.N. & Aksu A.E. (1994) — Submarine debris flows and continental slope evolution in front of Quaternary ice sheets, Baffin Bay, Canadian Arctic. *American Association of Petroleum Geologists Bulletin*, 78(3), pp. 445-460.
- Hjelstuen B.O. (1993) — Sen-kenozoisk utvikling av Storfjordvifla, basert på reproseserte multikanals data. Unpublished Cand. scient. thesis, Universitetet i Oslo, 111 pp.
- Hjelstuen B.O., Elverhøi A. & Faleide J.I. (in press) — Cenozoic erosion and sediment yield in the drainage area of the Storfjorden fan. In: Solheim A. et al. (Eds.), *Impact of Glaciations on Basin Evolution: Data and Models from the Norwegian Margin and Adjacent Areas*. *Global and Planetary Change, Special issue*.
- Houtz R. & Windisch C. (1977) — Barents Sea continental margin sonobuoy data. *Geological Society of America Bulletin*, 88, pp. 1030-1036.
- Jansen E., Bleil U., Henrich R., Kringstad L. & Slettemark B. (1988) — Paleoenvironmental changes in the Norwegian Sea and the Northeast Atlantic during the last 2.8 Ma : DSDP/ODP Sites 610, 642, 643 and 644. *Paleoceanography*, 3(5), pp. 563-581.
- Jansen E. & Sjøholm J. (1991) — Reconstruction of glaciation over the past 6 Myr from ice-borne deposits in the Norwegian Sea. *Nature*, 349, pp. 600-603.
- Jansen E., Sjøholm J., Bleil U. & Erichsen J.A. (1990) — Neogene and Pleistocene glaciations in the northern hemisphere and late Miocene - Pliocene global ice volume fluctuations : Evidence from the Norwegian Sea. In: Bleil U. & Thiede J. (Eds.), *Geological History of the Polar Oceans: Arctic versus Antarctic*. NATO ASI Series C, Mathematical and Physical Sciences, 308, Kluwer, Dordrecht, pp. 677-705.
- Johannessen O.M. (1986) — Brief overview of the physical oceanography. In: Hurdle B.G. (Ed.), *The Nordic Seas*. Springer-Verlag, New York, pp. 103-127.

- Jones G.A. & Keigwin L.D. (1988) — Evidence from Fram Strait (78° N) for early deglaciation. *Nature*, 336, pp. 56-59.
- Kennett J. (1982) — *Marine Geology*. Prentice-Hall, Englewood Cliffs, 813 pp.
- Knutsen S.-M, Richardsen G. & Vorren T.O. (1992) — Late Miocene - Pleistocene sequence stratigraphy and mass-movements on the western Barents Sea margin. In: Vorren T.O., Bergsager E., Dahl-Stamnes Ø.A., Holter E., Johansen B., Lie E. & Lund T.B. (Eds.), *Arctic Geology and Petroleum Potential*. Norwegian Petroleum Society Special Publication, 2, Elsevier, Amsterdam, pp. 573-606.
- Kristoffersen Y., Elverhøi A. & Vinje T. (1978) — Barentshavprosjektet : Marin geofysikk, geologi og havis. Unpublished report, Norsk Polarinstitut, Oslo, 81 pp.
- Kurtz D.D. & Anderson J.B. (1979) — Recognition and sedimentologic description of recent debris flow deposits from the Ross and Weddell Seas, Antarctica. *Journal Sedimentary Petrology*, 49, pp. 1159-1170.
- Kuvaas B. & Kristoffersen Y. (1991) — The Crary Fan : A trough-mouth fan on the Weddell Sea continental margin, Antarctica. *Marine Geology*, 97, pp. 345-362.
- Kuvaas B. & Kristoffersen Y. (in press) — Mass movements in glaciomarine sediments on the Barents Sea continental slope. In: Solheim A. et al. (Eds.), *Impact of Glaciations on Basin Evolution: Data and Models from the Norwegian Margin and Adjacent Areas*. Global and Planetary Change, Special issue.
- Kvamme L.B. & Hansen R.A. (1989) — The seismicity in the continental margin areas of Northern Norway. In: Gregersen S. & Basham P.W. (Eds.), *Earthquakes at North-Atlantic Passive Margins: Neotectonics and Postglacial Rebound*. Kluwer Academic Publishers, Dordrecht, pp. 429-440.
- Laberg J.S. (1994) — Late Pleistocene evolution of the submarine fans off the western Barents Sea margin. Unpublished Ph. D. thesis, University of Tromsø.
- Laberg J.S. & Vorren T.O. (1993) — A Late Pleistocene submarine slide on the Bear Island Trough Mouth Fan. *Geo-Marine Letters*, 13, pp. 227-234.
- Laberg J.S. & Vorren T.O. (in press a) — The Middle and Late Pleistocene evolution of the Bear Island Trough Mouth Fan. In: Solheim A. et al. (Eds.), *Impact of Glaciations on Basin Evolution: Data and Models from the Norwegian Margin and Adjacent Areas*. Global and Planetary Change, Special issue.
- Laberg J.S. & Vorren T.O. (in press b) — Late Weichselian submarine debris flow deposits on the Bear Island Trough Mouth Fan. *Marine Geology*.
- Larsen H.C. (1990) — The East Greenland Shelf. In: Grantz A., Johnson L. & Sweeney J.F. (Eds.), *The Arctic Ocean Region. The Geology of North America*, Vol. L, The Geological Society of America, Boulder, Colorado, pp. 185-210.
- Lewis K.B. (1971) — Slumping on a continental slope inclined at 1° - 4°. *Sedimentology*, 16, pp. 97-110.
- Lowe D.R. (1976) — Subaqueous liquefied and fluidized sediment flows and their deposits. *Sedimentology*, 23, pp. 285-308.
- Lowe D.R. (1979) — Sediment gravity flows : Their classification and some problems of application to natural flows and deposits. In: Doyle L.J. & Pilkey O.H. (Eds.), *Geology of Continental Slopes*. Special Publication, 27, Society of Economic Paleontologists and Mineralogists, pp. 75-82.
- Mangerud J. & Svendsen J.I. (1992) — The last interglacial-glacial period on Spitsbergen, Svalbard. *Quaternary Science Reviews*, 11, pp. 633-664.
- Middleton G.V. & Hampton M.A. (1976) — Subaqueous sediment transport and deposition by sediment gravity flows. In: Stanley D.J. & Swift D.J.P. (Eds.), *Marine Sediment Transport and Environmental Management*. Wiley, New York, pp. 197-218.
- Moons A. (1992) — Gedetailleerde seismo- en sequentiestratigrafische studie van de Crary Fan, zuidoostelijke Weddell Zee, Antarctica. Unpublished Ph. D. thesis, Universiteit Gent, 174 pp.
- Mørk M.B.E. & Duncan R.A. (1993) — Late Pliocene basaltic volcanism on the Western Barents Shelf margin : Implications from petrology and ⁴⁰Ar-³⁹Ar dating of volcanoclastic debris from a shallow drill core. *Norsk Geologisk Tidsskrift*, 73, pp. 209-225.
- Mosby H. (1968) — Surrounding seas. In: Sømme A. (Ed.), *A Geography of Norden*. Cappelen, Oslo, pp. 18-26.
- Mosher D.C., Moran K. & Hiscott R.N. (1994) — Late Quaternary sediment, sediment mass flow processes and slope stability on the Scotian Slope, Canada. *Sedimentology*, 41, pp. 1039-1061.

- Mutter J.C. (1985) — Seaward dipping reflectors and the continent-ocean boundary at passive continental margins. *Tectonophysics*, 114, pp. 117-131.
- Myhre A.M. & Eldholm O. (1988) — The Western Svalbard margin (74°-80° N). *Marine and Petroleum Geology*, 5, pp. 134-156.
- Myhre A.M., Eldholm O. & Sundvor E. (1982) — The margin between Senja and Spitsbergen Fracture Zones : Implications from plate tectonics. *Tectonophysics*, 89, pp. 33-50.
- Nardin T.R., Hein F.J., Gorsline D.S. & Edwards B.D. (1979) — A review of mass movement processes, sediment and acoustic characteristics, and contrasts in slope and base-of-slope systems versus canyon-fan-basin floor systems. In: Doyle L.J. & Pilkey O.H. (Eds.), *Geology of Continental Slopes*. Special Publication, 27, Society of Economic Paleontologists and Mineralogists, pp. 61-73.
- Nelson C.H., Maldonado A., Barber J.H. Jr. & Alonso B. (1991) — Modern sand-rich and mud-rich siliciclastic aprons : Alternative base-of-slope turbidite systems to submarine fans. In: Weimer P. & Link M.H. (Eds.), *Seismic Facies and Sedimentary Processes of Submarine Fans and Turbidite Systems*. Springer-Verlag, New York, pp. 171-190.
- Nelson C.H. & Nilson T.H. (1984) — Modern and ancient deep sea-fan sedimentation. Short Course, no. 14, Society of Economic Paleontologists and Mineralogists, Tulsa, Oklahoma, 404 pp.
- Normark W.R., Piper D.J.W. & Stow D.A.V. (1983) — Quaternary development of channels, levees, and lobes on Middle Laurentian Fan. *American Association of Petroleum Geologists Bulletin*, 67(9), pp. 1400-1409.
- Olsen L. (1989) — Weichselian till stratigraphy and glacial history of Finnmarksvidda, north Norway. *Quaternary International*, 3/4, pp. 101-108.
- Parsons B. & Sclater J.G. (1977) — An analysis of the variation of ocean floor bathymetry and heat flow with age. *Journal of Geophysical Research*, 82, pp. 803-827.
- Perry R.K. (1986) — Bathymetry. In: Hurdle B.G. (Ed.), *The Nordic Seas*. Springer-Verlag, New York, pp. 211-234.
- Pickering K.T., Hiscott R.N. & Hein F.J. (1989) — Deep Marine Environments : Clastic Sedimentation and Tectonics. Unwin Hyman, London, 416 pp.
- Piper D.J.W., Stow D.A.V. & Normark W.R. (1985) — Laurentian Fan, Atlantic Ocean. In: Bouma A.H., Normark W.R. & Barnes N.E. (Eds.), *Submarine Fans and Related Turbidite Systems*. Springer-Verlag, New York, pp. 137-142.
- Posamentier H.W., Jervey M.T. & Vail P.R. (1988) — Eustatic controls on clastic deposition I : Conceptual framework. In: Wilgus C.K., Hastings B.S., Kendall C.G.St.C., Posamentier H.W., Ross C.A. & Van Wagoner J.C. (Eds.), *Sea Level Changes: An Integrated Approach*. Special Publication, 42, Society of Economic Paleontologists and Mineralogists, Tulsa, Oklahoma, pp. 109-124.
- Powell R.D. & Molnia B.F. (1989) — Glacimarine sedimentary processes, facies and morphology of the south-southeast Alaska shelf and fjords. In: Powell R.D. & Elverhøi A. (Eds.), *Modern Glacimarine Environments: Glacial and Marine Controls of Modern Lithofacies and Biofacies*. *Marine Geology*, 85, pp. 359-390.
- Prior D.B., Bornhold B.D. & Johns M.W. (1984) — Depositional characteristics of a submarine debris flow. *Journal of Geology*, 92, pp. 707-727.
- Prior D.B. & Coleman J.M. (1978) — Disintegrating retrogressive landslides on very-low-angle subaqueous slopes, Mississippi Delta. *Marine Geotechnology*, 3(1), pp. 37-60.
- Prior D.B. & Coleman J.M. (1979) — Submarine landslides : Geometry and nomenclature. *Zeitschrift für Geomorphologie N.F.*, 23(4), pp. 415-426.
- Prior D.B. & Coleman J.M. (1982) — Active slides and flows in underconsolidated marine sediments on the slopes of the Mississippi Delta. In: Saxov S. & Nieuwenhuis J.K. (Eds.), *Marine Slides and Other Mass Movements*. Plenum Publishing Corporation, pp. 21-49.
- Prior D.B. & Coleman J.M. (1984) — Submarine slope instability. In: Brunsden D. & Prior D.B. (Eds.), *Slope Instability*. John Wiley & Sons, pp. 419-455.
- Richardson G., Henriksen E. & Vorren T.O. (1991) — Evolution of the Cenozoic sedimentary wedge during rifting and seafloor spreading west of the Stappen High, western Barents Sea. *Marine Geology*, 101, pp. 11-30.

- Richardson G., Knutsen S.-M., Vail P.R. & Vorren T.O. (1992) — Mid - Late Miocene sedimentation on the southwestern Barents Shelf margin. In: Vorren T.O., Bergsager E., Dahl-Stamnes Ø.A., Holter E., Johansen B., Lie E. & Lund T.B. (Eds.), *Arctic Geology and Petroleum Potential*. Norwegian Petroleum Society Special Publication, 2, Elsevier, Amsterdam, pp. 539-571.
- Riis F. & Fjeldskaar W. (1992) — On the magnitude of the Late Tertiary and Quaternary erosion and its significance for the uplift of Scandinavia and the Barents Sea. In: Larsen R.M., Brække H., Larsen B.T. & Talleraas E. (Eds.), *Structural and Tectonic Modelling and its Application to Petroleum Geology*. Norwegian Petroleum Society Special Publication, 1, Elsevier, Amsterdam, pp. 163-185.
- Rønnevik H.C. (1981) — Geology of the Barents Sea. In: Illing L.V. & Hobson G.D. (Eds.), *Petroleum Geology of the Continental Shelf of North-West Europe*. Heyden & Son Ltd. on behalf of the Institute of Petroleum, London, pp. 395-406.
- Rønnevik H.C. & Jacobsen H.-P. (1984) — Structural highs and basins in the western Barents Sea. In: Spencer A.M. et al. (Eds.), *Petroleum Geology of the North European Margin*. Graham & Trotman for the Norwegian Petroleum Society, London, pp. 19-32.
- Ruddiman W.F., Raymo M. & McIntyre A. (1986) — Matuyama 41,000-year cycles : North Atlantic Ocean and northern hemisphere ice sheets. *Earth and Planetary Science Letters*, 80, pp. 117-129.
- Sættem J., Bugge T., Fanavoll S., Goll R.M., Mørk A., Mørk M.B.E., Smelror M. & Verdenius J.G. (1994) — Cenozoic margin development and erosion of the Barents Sea : Core evidence from southwest of Bjørnøya. *Marine Geology*, 118, pp. 257-281.
- Sættem J., Poole D.A.R., Ellingsen L. & Sejrup H.P. (1992) — Glacial geology of outer Bjørnøyrønna, southwestern Barents Sea. *Marine Geology*, 103, pp. 15-51.
- Sættem J., Poole D.A.R., Sejrup H.P. & Ellingsen K.L. (1991) — Glacial geology of outer Bjørnøyrønna, western Barents Sea : Preliminary results. *Norsk Geologisk Tidsskrift*, 71, pp. 173-177.
- Schlüter H.-U. & Hinz K. (1978) — The continental margin of West Spitsbergen. *Polarforschung*, 48, pp. 151-169.
- Shackleton N.J., Backman J. & Shipboard Scientific Party (1984) — Oxygen isotope calibration of the onset of ice rafting and history of glaciation in the North Atlantic region. *Nature*, 307, pp. 620-623.
- Shanmugam G. & Moliola R.J. (1988) — Submarine fans : Characteristics, models, classification, and reservoir potential. *Earth-Science Reviews*, 24, pp. 383-428.
- Sobczak L.W. (1975) — Gravity anomalies and passive continental margins. In: Yorath C.J., Parker E.R. & Glass D.J. (Eds.), *Canada's Continental Margins and Offshore Petroleum Exploration*. Memoir, 4, Canadian Society of Petroleum Geologists, Calgary, pp. 743-761.
- Solheim A. & Kristoffersen Y. (1984) — Sediments above the Upper Regional Unconformity : Thickness, seismic stratigraphy and outline of the glacial history. *Norsk Polarinstitutt Skrifter*, 179B, 26 pp.
- Solheim A., Russwurm L., Elverhøi A. & Nyland-Berg M. (1990) — Glacial geomorphic features in the northern Barents Sea : Direct evidence for grounded ice and implications for the pattern of deglaciation and late glacial sedimentation. In: Dowdeswell J.A. & Scourse J.D. (Eds.), *Glacimarine Environments: Processes and Environments*. Special Publication, 53, The Geological Society, London, pp. 253-268.
- Solheim A., Andersen E.S., Elverhøi A. & Fiedler A. (in press) — Late Cenozoic depositional history of the western Svalbard continental shelf, controlled by subsidence and climate. In: Solheim A. et al. (Eds.), *Impact of Glaciations on Basin Evolution: Data and Models from the Norwegian Margin and Adjacent Areas*. *Global and Planetary Change*, Special issue.
- Spencer A.M., Home P.C. & Berglund L.T. (1984) — Tertiary structural development of the western Barents shelf : Troms to Svalbard. In: Spencer A.M. et al. (Eds.), *Petroleum Geology of the North European Margin*. Graham & Trotman for the Norwegian Petroleum Society, London, pp. 199-209.
- Steel R.L., Gjelberg J., Nøttvedt A., Helland-Hansen W., Kleinspehn K. & Rye-Larsen M. (1985) — The Tertiary strike-slip basins and orogenic belt of Spitsbergen. *Society of Economic Paleontologists and Mineralogists*, Special Publication, 37, pp. 339-359.
- Stow D.A.V. (1981) — Laurentian Fan : Morphology, sediments, processes, and growth pattern. *American Association of Petroleum Geologists Bulletin*, 65, pp. 375-393.
- Stow D.A.V., Howell D.G. & Nelson C.H. (1985) — Sedimentary, tectonic, and sea-level controls. In: Bouma A.H., Normark W.R. & Barnes N.E. (Eds.), *Submarine Fans and Related Turbidite Systems*. Springer-Verlag, New York, pp. 15-22.

- Sundvor E. & Eldholm O. (1979) — The western and northern margin off Svalbard. *Tectonophysics*, 59, pp. 239-250.
- Swift J.H. (1986) — The Arctic waters. In: Hurdle B.G. (Ed.), *The Nordic Seas*. Springer-Verlag, New York, pp. 129-153.
- Talwani M. & Eldholm O. (1977) — Evolution of the Norwegian-Greenland Sea. *Geological Society of America Bulletin*, 88, pp. 969-999.
- Talwani M., Udintsev G. et al. (1976) — Site 344. In: Talwani M., Udintsev G. et al. (Eds.), *Initial Reports of the Deep Sea Drilling Project*. Vol. 38, U.S. Government Printing Office, Washington D.C., pp. 389-401.
- Thiede J., Eldholm O. & Taylor E. (1989) — Variability of Cenozoic Norwegian-Greenland Sea paleoceanography and northern hemisphere paleoclimate. In: Eldholm O., Thiede J., Taylor E., et al. (Eds.), *Proceedings of the Ocean Drilling Program. Scientific Results*, Vol. 104, The Ocean Drilling Program, College Station, TX, pp. 1067-1118.
- Vail P.R., Mitchum R.M. Jr. & Thompson S. III (1977) — Seismic stratigraphy and global changes of sea level. In: Payton C.E. (Ed.), *Seismic Stratigraphy: Applications to Hydrocarbon Exploration*. Memoir, 26, American Association of Petroleum Geologists, Tulsa, Oklahoma, pp. 83-97.
- Verschuren M. (1992) — An integrated 3D approach to clay tectonic deformation, and the development of a new 3D surface modelling method. Unpublished Ph. D. thesis, Universiteit Gent, 359 pp.
- Vinje T.E. (1985) — Drift, composition, morphology and distribution of the sea ice fields in the Barents Sea. *Norsk Polarinstitutt Skrifter*, 179(C), 26 pp.
- Vogt P.R. (1986) — Seafloor topography, sediments, and paleoenvironments. In: Hurdle B.G. (Ed.), *The Nordic Seas*. Springer-Verlag, New York, pp. 237-410.
- Vogt P.R., Crane K. & Sundvor E. (1993) — Glacigenic mudflows on the Bear Island submarine fan. *EOS Transactions American Geophysical Union*, 74, pp. 449, 452-453.
- Vogt P.R., Feden, R.H., Eldholm O. & Sundvor E. (1978) — The ocean crust west and north of the Svalbard Archipelago : Synthesis and review of new results. *Polarforschung*, 48, pp. 1-19.
- Vorren T.O., Hald M. & Lebesbye E. (1988) — Late Cenozoic environments in the Barents Sea. *Paleoceanography*, 3(5), pp. 601-612.
- Vorren T.O. & Kristoffersen Y. (1986) — Late Quaternary glaciation in the south-western Barents Sea. *Boreas*, 15, pp. 51-59.
- Vorren T.O., Lebesbye E., Andreassen K. & Larsen K.-B. (1989) — Glacigenic sediments on a passive continental margin as exemplified by the Barents Sea. In: Powell R.D. & Elverhøi A. (Eds.), *Modern Glacimarine Environments: Glacial and Marine Controls of Modern Lithofacies and Biofacies*. *Marine Geology*, 85, pp. 251-272.
- Vorren T.O., Lebesbye E. & Larsen K.B. (1990b) — Geometry and genesis of the glacigenic sediments in the southern Barents Sea. In: Dowdeswell J.A. & Scourse J.D. (Eds.), *Glacimarine Environments: Processes and Sediments*. Special Publication, 53, The Geological Society, London, pp. 269-288.
- Vorren T.O., Richardsen G., Knutsen S.-M. & Henriksen E. (1990) — The western Barents Sea during the Cenozoic. In: Bleil U. & Thiede J. (Eds.), *Geological History of the Polar Oceans: Arctic versus Antarctic*. NATO ASI Series C, Mathematical and Physical Sciences, 308, Kluwer Academic Publishers, Dordrecht, pp. 95-118.
- Vorren T.O., Richardsen G., Knutsen S.-M. & Henriksen E. (1991) — Cenozoic erosion and sedimentation in the western Barents Sea. *Marine and Petroleum Geology*, 8, pp. 317-340.
- Wadhams P. (1986) — The ice cover. In: Hurdle B.G. (Ed.), *The Nordic Seas*. Springer Verlag, New York, pp. 21-84.
- Weimer P. & Link M.H. (Eds.) (1991) — *Seismic Facies and Sedimentary Processes of Submarine Fans and Turbidite Systems*. Springer-Verlag, New York.
- Wessel P. & Smith W.H.F. (1991) — Free software helps map and display data. *EOS Transactions American Geophysical Union*, 72, pp. 441, 445-446.
- Yoon S.H. & Chough S.K. (1993) — Sedimentary characteristics of Late Pleistocene bottom-current deposits, Barents Sea slope off northern Norway. *Sedimentary Geology*, 82, pp. 33-45.

CHAPTER IV

Comparing the seismic reflection geometries on the different glacial margins

1. Introduction

In the preceding two chapters the regional stratigraphy was delineated of two Plio-Pleistocene depocentres along opposite margins of the polar North Atlantic: the central East Greenland margin off Scoresby Sund, and the western Barents Sea margin off Bear Island Trough, respectively. Both sites are located off major glacial outlets, active conduits for converging ice flow during former glaciations. Bear Island Trough is a broad transverse shelf trough, its one end terminating at the shelf break, but its other end apparently not connected to a fjord system on land. Central East Greenland, by contrast, is transected by the Scoresby Sund fjord system — one of the largest fjord systems in the world — which does not seem to continue into a pronounced trough on the continental shelf, however. Common to both glacial outlets is, that they are fronted by seaward-convex bulges in the bathymetry of outer shelf and upper slope, outlining the shape of large depocentres that are thought to have mainly accumulated in response to repeated glacial extensions onto the shelf.

A comparison can now be made of the stratigraphy and stratal architecture of the two margins, as revealed by seismic reflection records. This should in the first place shed new light on the long-term glacial and climatic evolution of the regions bordering the polar North Atlantic Ocean. And secondly, it will be possible to assess the different processes that have governed accumulation on both glaciogenic depocentres; a particular challenge is to determine whether build-up of these depocentres can be described by a cyclic, sequence stratigraphic model, analogue to that developed for lower-latitude margins by Posamentier et al. (1988) and Posamentier & Vail (1988). To that purpose, the observations will be extended to a third glacial margin, located in the southern hemisphere, but very similar otherwise: the SE Weddell Sea, Antarctica.

2. Glacial evolution of the polar North Atlantic

In contrast to the increasing constraints for the ice situation during the last glacial maximum, the long-term climatic evolution of the polar North Atlantic, and in a more general sense of the northern hemisphere, still remains to a large degree enigmatic. The record preserved on land and in fjords is discontinuous and fragmentary at best, and the majority of those deposits can be attributed to the last glacial/interglacial cycle. The individual imprint of older ice ages is very difficult to recognise,

however, as most of their deposits have been obliterated by succeeding glaciations. It appears that most erosional products have been transported to the outer continental shelf and upper slope at times when the ice sheets advanced out to the shelf edge. At points of more focused or efficient ice flow, large sediment cones have accumulated along glaciated continental margins. Such glaciogenic depocentres thus hold an important archive of the long-term history of glaciation that is not observed on land. Seismic reflection, in combination with deep sea drilling, constitutes the most powerful tool to investigate the thick successions that are preserved here. Unfortunately, drilling efforts have so far not specifically addressed these particular depositional environments, partly because of harsh ice conditions (especially on the Greenland side), and partly also due to the difficulties commonly encountered in drilling and dating glacial successions. Scientific interest is rising, however, and this summer (1995) an ODP site is scheduled on a sediment cone along the western Svalbard margin, and possibly another one on the sediment cone off Scoresby Sund. For the time being, the seismic data can only be correlated in a general sense to more distal drillholes in the Norwegian-Greenland Sea, in casu the ODP Leg 104 sites on the Vøring Plateau.

The seismic evidence seems to indicate that the two opposing margins of the polar North Atlantic went through a rather parallel evolution during the Plio-Pleistocene. For both study areas a three-step glacial evolution has been proposed, deduced from the variation of stratal geometry patterns, and in good agreement with the three different glacial phases recognised in paleoceanographic records of the above-mentioned drillholes (see section 7.1 in chapter III). On the central East Greenland margin, the glacial succession obtains a maximum thickness of about 1 s TWT, and is subdivided into three units on basis of varying amounts of progradation and aggradation (Fig. 1a): a lower unit III-A characterised by moderate shelf edge progradation, a middle unit III-B marked by peak amounts of progradation, and an uppermost unit III-C which is almost purely aggradational in nature. On the Bear Island Cone along the western Barents Sea margin, a similar three-fold division is made of the glacial section which is up to three times as thick here, however (Fig. 1b): the lower unit GI is characterised by local initial progradation and limited downslope sediment remobilisation; the middle unit GII is marked by very extensive mass wasting which halted the net progradation of the margin; and the youngest unit GIII exhibits both strong progradation and aggradation, and a significant reduction in scale of mass wasting processes.

A notable contrast in glacial sediment thickness thus exists along the two margins: max. 1 s on the central East Greenland margin, opposed to max. 3 s on the western Barents Sea margin. The amount of shelf edge progradation, on the other hand, is quite comparable for both margins, totalling 45 km off Scoresby Sund and 52.5 km off Bear Island Trough. The large divergence in sediment volume may in part be the result of differences in texture of the eroded hinterland of the two margins: the central East Greenland margin is dominated by crystalline rocks that are strongly resistant to erosion, whereas the lithified sediments subcropping beneath the Barents shelf provide a more easily erodable substratum. It may, however, also in part reflect differences in the thermal regime of the two ice sheets: since wet-based ice sheets are known to yield more sediment than dry-based ones, it is suspected that the Barents Sea Ice Sheet had a more wet-based character compared to the Greenland Ice Sheet. This would also be supported by the more widespread occurrence of mass flows on the western Barents Sea margin, which probably implies a lower consolidation, and thus a higher water content, in the sediments deposited here. This is commonly related to an overall fine-grained sediment composition (e.g. water mantle around mud-sized particles), and/or high sedimentation rates, which may in turn be determined by specific depositional processes (e.g. settling from suspension, or deformation of subglacial till).

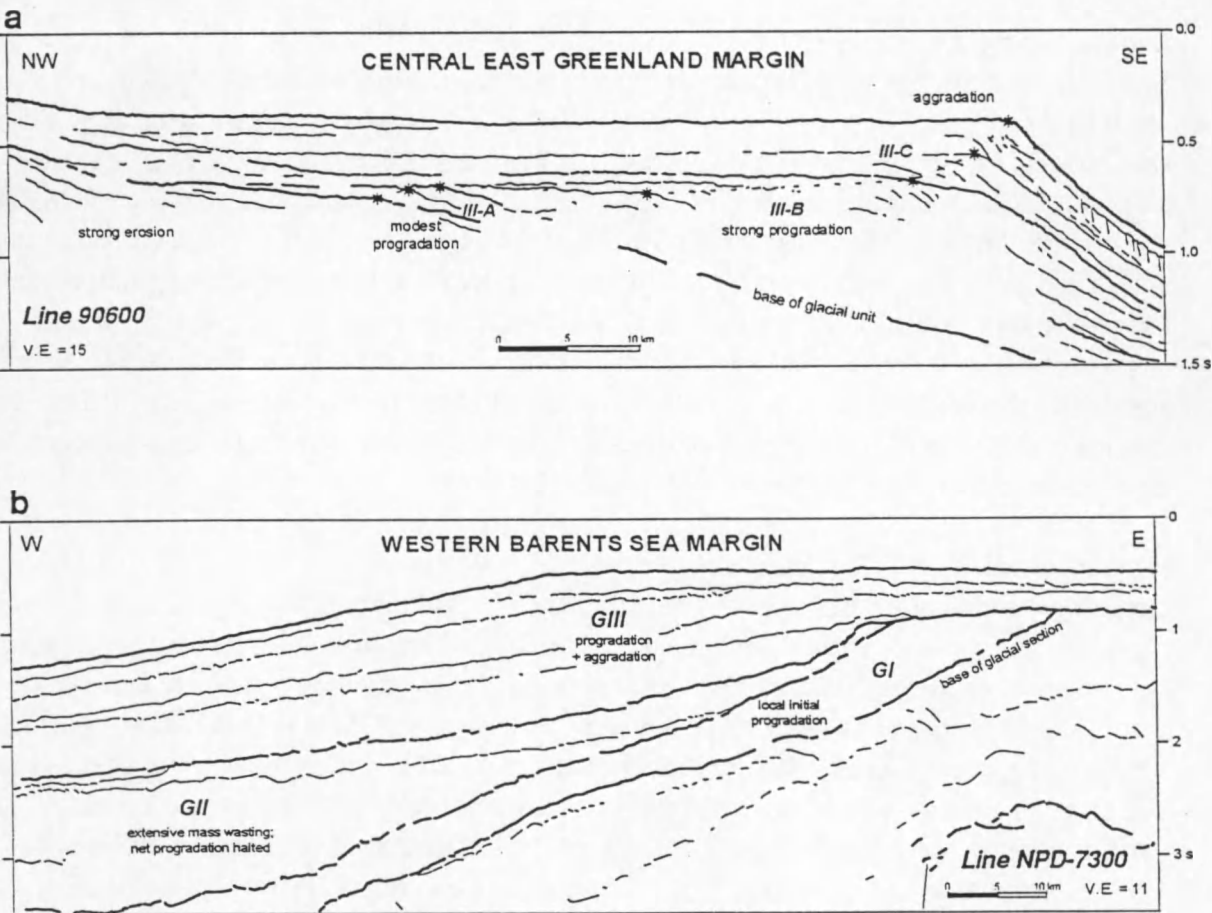


Fig. IV.1 - Three-fold division of glacial sediments on [a] the central East Greenland margin, and [b] the western Barents Sea margin. Note the different scales.

These significant differences left aside, the stratal geometry patterns of the two margins seem to match the following generalised model for the glacial evolution of the polar North Atlantic region (Table 1): [i] an initial phase of modest glaciations of the continental shelves, [ii] a second phase of markedly intensified glaciations, and [iii] a final phase of which the nature is as yet poorly understood, but which probably involved an important turn-over of ice flow dynamics.

CENTRAL EAST GREENLAND MARGIN	GENERAL POLAR NORTH ATLANTIC EVOLUTION	WESTERN BARENTS SEA MARGIN
Unit III-C distinct aggradation	Glacial phase 3 change in ice stream dynamics ? ~0.6 Ma ?	Unit GIII both pro- and aggradation; smaller-scale mass wasting
Unit III-B enhanced progradation	Glacial phase 2 intensification of glaciation 1.2 / 1.0 Ma	Unit GII large-scale mass wasting; no net progradation
Unit III-A moderate progradation	Glacial phase 1 initial phase of modest glaciation 2.56 Ma	Unit GI local initial progradation; limited mass wasting

Table IV.1 - Reconstruction of generalised long-term glacial evolution from the correlation of major depositional units on opposite margins of the polar North Atlantic Ocean. Ages are tentative and follow Jansen et al. (1988) and Henrich & Baumann (1994).

Glacial phase 1

Following the onset of major northern hemisphere glaciation, initial ice sheets advancing onto the continental shelf were likely to be rather medium-sized, as indicated by the modest amounts by which both margins were built out during this period. Ice sheets expanding from high alpine land masses such as Greenland or Svalbard were thus able to traverse narrow portions of the adjacent continental shelves. The broad and low-gradient platform of the Barents Sea area, on the other hand, was, though emergent, most probably not yet fully glaciated; localised high rates of progradation along the western Barents Sea margin are thought to be the result of a proglacial (or possibly subglacial?) meltwater system draining from an ice front located further inland. This first glacial phase is correlated to the period 2.6 - 1.2 Ma, which was characterised by moderate inputs of IRD at the location of ODP Leg 104, indicating the existence of medium-sized ice caps in the areas surrounding the Norwegian-Greenland Sea (Jansen et al. 1988, 1990).

Glacial phase 2

Increasingly strong progradation on the central East Greenland margin (38 km of a total of 45 km during the Plio-Pleistocene), and the massive occurrence of large-scale mass wasting processes on Bear Island Cone are both interpreted to indicate a significant increase of sedimentation rates (by about an order of magnitude), as a result of intensified glaciation. This observation shows a striking analogy to the marked increase in IRD deposition at about 1.2 Ma (Jansen et al. 1988, 1990). From that time on, progressively larger ice sheets are inferred to have repeatedly extended out to the contemporaneous shelf edge along the entire central East Greenland and western Barents Sea - Svalbard margins. The large variations in stratal geometry between the two margins are mainly the result of differences in the stability of the slope in response to the increased sedimentation rates. Maybe it is also in part related to a different mode of deposition, as could have been brought about by the gradual excavation of the Barents Sea area below sea level, which is thought to have had a significant impact on glacial dynamics. From that time on, the Barents Sea Ice Sheet was probably largely controlled by sea level rather than by insolation fluctuations (Elverhøi et al. 1994).

Glacial phase 3

The latest phase of deposition is characterised by aggradational geometry on the central East Greenland margin, and by both pronounced progradation (32.5 km of a total of 52.5 km during the Plio-Pleistocene) and aggradation on the Bear Island Cone. The main phase of progradation on Bear Island Cone is thus notably delayed with respect to the central East Greenland margin, but that may be mainly due to differences in slope stability as mentioned above. A significant aggradational component appears to be common to both locations, however. The possible correlation of this geometry with a final variation of climate, as recognised by Jansen et al. (1988) and Henrich & Baumann (1994), is not well constrained. This latest phase in the glacial evolution would have started about 0.6 Ma ago, and resulted in the establishment of modern glacial conditions, among other things characterised by larger interglacial/glacial contrasts; IRD input further increased, while the global oxygen isotope curve for this period indicates larger ice volumes and a dominance of longer, 100 ka cycles (Ruddiman et al. 1986), a trend which was already initiated during the preceding glacial period. This primarily reflects the expansion of ice sheets into more temperate latitudes (Ruddiman et al. 1986), however, and thus not necessarily an enlargement of polar ice masses; the somewhat decreasing sedimentation rates in both study areas indeed seem to indicate an opposite trend. As suggested by the odd number of sequences identified on both margins, a large asymmetry may have existed most of the time between a rather stable continental Greenland Ice

Sheet on one side of the ocean, and a strongly fluctuating marine-based Barents Sea Ice Sheet on the other side. This is particularly well illustrated by the last (Late Weichselian) glacial cycle: the available evidence indicates that the Greenland Ice Sheet did not extend far beyond the coastline in central East Greenland, while the Barents Sea Ice Sheet probably extended all the way to the shelf edge. But whereas the Barents Sea Ice Sheet has entirely disintegrated during the present interglacial, Greenland remains largely covered by Inland Ice to the present day.

Origin of late Pleistocene aggradation

It is of particular interest to understand how the glacial regime could have developed into a latest phase characterised by aggradational geometries. This is not an isolated observation, for one: not only does aggradation of upper shelf sequences appear in the stratigraphic record of the central East Greenland and western Barents Sea margins (Fig. 1), but also can it be recognised on a variety of other glaciated continental margin segments, including southern hemisphere margins (Fig. 2).

- a similar transition from uniform progradation to a combination of progradation and aggradation is observed in the upper sequences at the mouth of Kangerdlugssuaq Channel on the SE Greenland shelf (B. Larsen 1994) (Fig. 3a), but age estimates are not available;
- in the Home Bay transverse trough in Baffin Bay (Canadian Arctic), Hiscott & Aksu (1994) noted a distinct change in the geometry at a certain seismic horizon R0b, which is dated at c. 0.8 Ma: steeply dipping prograding foresets below this boundary are truncated, while overlying clinoforms are more gently inclined and show well developed topset sections (Fig. 3b);
- at the mouth of Crary Trough in the Weddell Sea, Antarctica, significant aggradation is shown by the youngest two sequences of an otherwise prograding wedge which is believed to be Plio-Pleistocene in age (Moons 1992) (Fig. 4a);
- in the Bellingshausen Sea, West Antarctica, an increasing amount of aggradation is evident in the upper portion of a progradational section which is tentatively dated as Plio-Pleistocene (Nitsche et al., *subm.*) (Fig. 4b).

There is thus evidence from at least six different high-latitude continental margins for a shift from predominantly progradational to a more aggradational shelf development, probably around the Middle/Late Pleistocene transition. This may be a global trend for glaciated margins, though it did not necessarily develop contemporaneously in the different locations. The overall poor age constraints make this difficult to establish. Most evidence seems to indicate, however, that the trend is significantly younger than the Plio-Pleistocene aggradation within the “global stratigraphic signature of the Neogene”, which has been recognised on both high-latitude (the Ross Sea) and lower-latitude margins (Bartek et al. 1991).

A vertical stacking pattern of shelf strata is commonly attributed to an increase of the accommodation space by a relative sea level rise, either eustatically or tectonically induced. The SPECMAP curve (Imbrie et al. 1984), which can be regarded as a proxy to eustatic sea level, does not indicate a consistent rise over the last 600 ka, however. The thermal subsidence rates for a mature passive margin, in the order of 1 to max. 10 m per 100 ka (Stow et al. 1985), are also too small to explain the observed aggradation of 200 m and more, whereas tectonic influences are unlikely to have affected several of the world's glaciated margins simultaneously. Quantitative stratigraphic modelling of several basins around the northern Atlantic has revealed a significant deviation from the predicted subsidence curve in the late Neogene (Cloetingh et al. 1992).

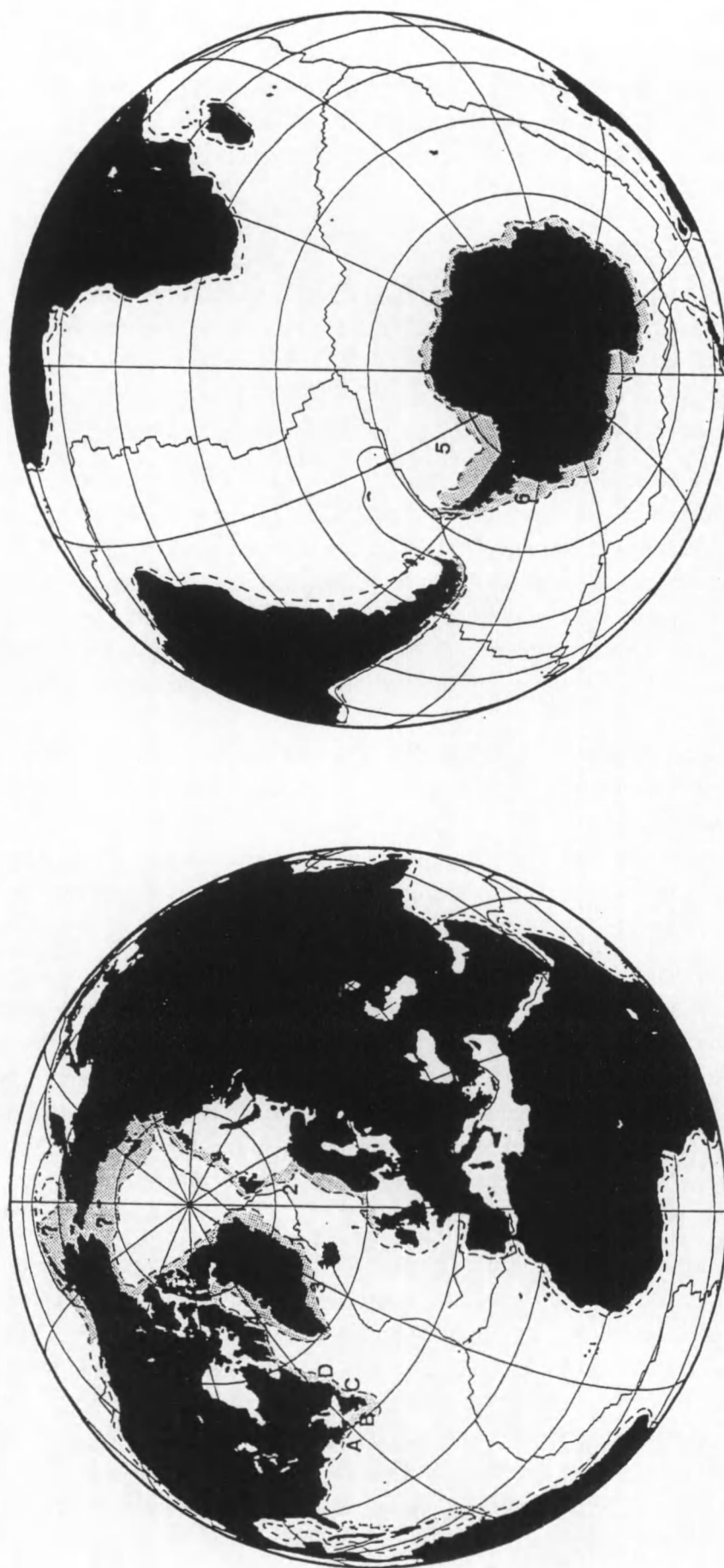


Fig. IV.2 - Location of glaciated margins characterised by a latest (late Pleistocene?) phase of aggradation: [1] central East Greenland margin (Fig. 1a), [2] western Barents Sea margin (Fig. 1b), [3] SE Greenland margin south of Kangerdlugssuaq fjord (Fig. 3a), [4] western Baffin Bay margin (Fig. 3b), [5] SE Weddell Sea margin (Fig. 4a), [6] Bellinghousen Sea, West Antarctica (Fig. 4b). Also indicated are adjacent portions of the Canadian Atlantic margin along which a gradual transition of lower slope and rise sedimentation is observed: [A] Scotian margin, [B] Laurentian Fan south of Newfoundland, [C] Newfoundland margin, [D] Labrador slope.

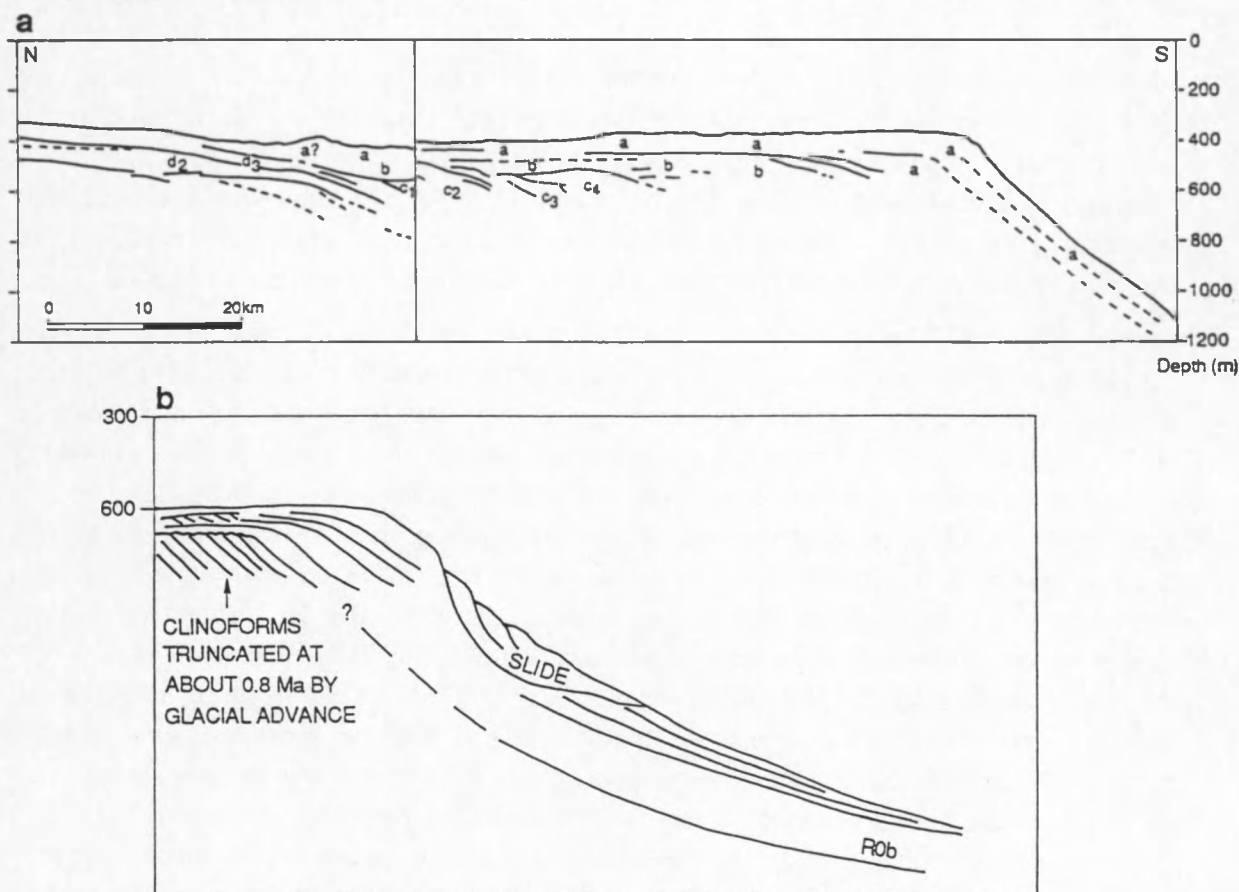


Fig. IV.3 - Line drawings revealing a latest phase of aggradation on [a] the SE Greenland margin south of Kangerdlugssuaq (from Larsen 1994), and [b] off the Home Bay transverse trough along the western Baffin Bay margin (after Hiscott & Aksu 1994).

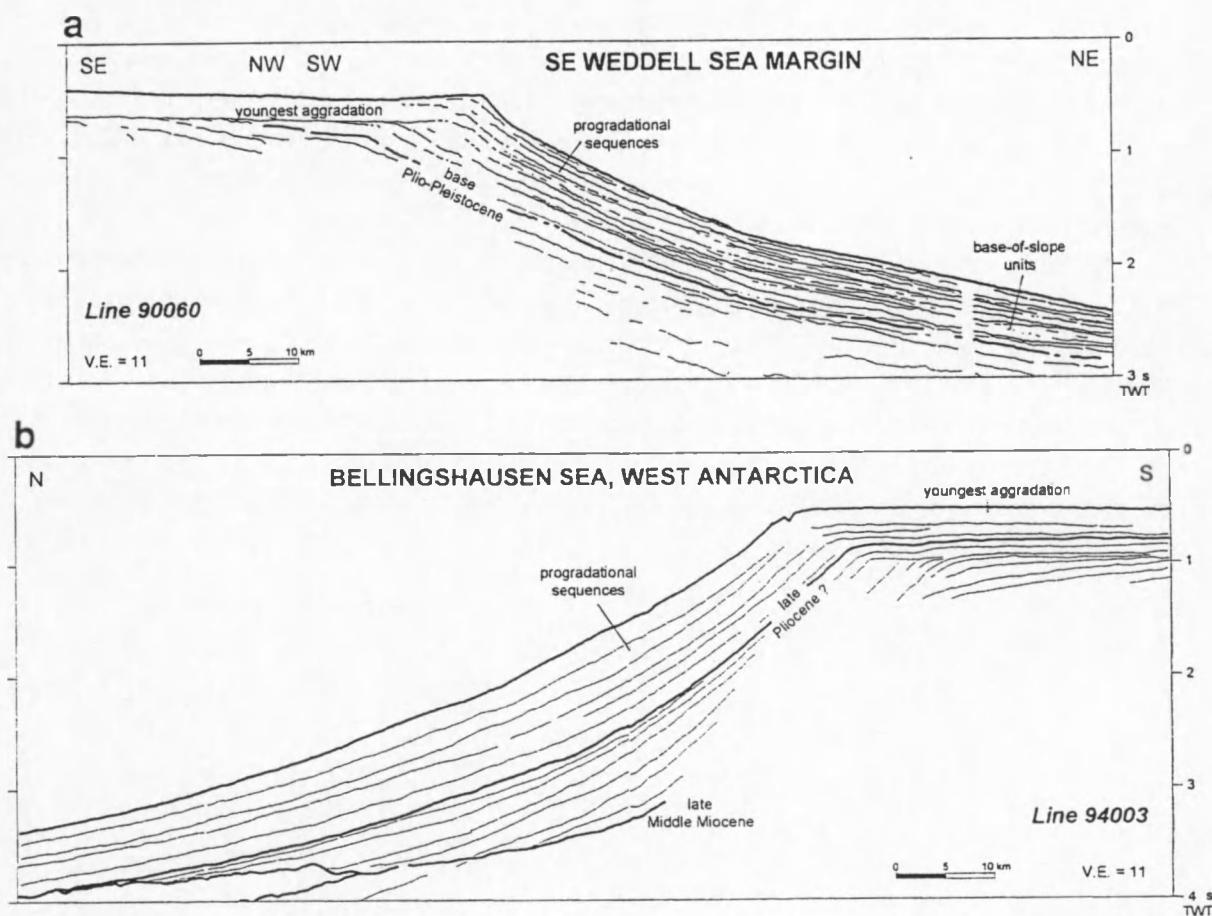


Fig. IV.4 - Water-depth corrected line drawings illustrating outer shelf and slope stratal geometries on [a] the SE Weddell Sea margin off Cray Trough, and [b] in the Bellingshausen Sea, West Antarctica. Scales are identical to that of Fig. 1b. Both lines courtesy of AWI & RCMG.

This acceleration of subsidence was well initiated before the onset of glaciation, however, and can thus not explain the observed geometries of presumed late Pleistocene age. In addition, simple variations in accommodation space are not believed to exert direct control on the stratal geometry as in the case of a low-latitude margin: during glacial periods the accommodation space is mostly occupied by grounded ice, whereas during interglacials not enough sediment is supplied to fill in the large accommodation space provided by the commonly overdeepened bathymetry of the shelf.

Hiscott & Aksu (1994) linked the aggradational sequences in Baffin Bay to proglacial sedimentation, possibly under an ice shelf, in front of ice sheets that did not ground as far as the shelf edge. In the preceding chapters, a glacial origin has been suggested for the aggradational sequences, however. For the central East Greenland margin, this was inferred from internal reflection patterns and the low Holocene sedimentation rates reported by Stein et al. (1993); on the western Barents Sea margin, a glacial origin of the upper aggradational unit is strongly suggested by the coring of massive diamicton believed to be subglacially deposited till (Sættem et al. 1992), and can with a higher level of confidence be put forward for the youngest sequence by the association with clearly glaciomorphological features in the Barents Sea (e.g. Solheim et al. 1990, Elverhøi et al. 1994). A further observation is that the aggradation seems to be greatly reduced outside glacial shelf troughs. On the Antarctic Peninsula Pacific margin, Bart & Anderson (1994, in press) have shown that the aggradational (and also the progradational) component of a given glacial sequence can strongly vary in a lateral direction. Both observations clearly demonstrate the significant influence of ice stream dynamics on the patterns of erosion and deposition on the shelf. It is therefore speculated that a distinct change in glacial dynamics, involving a reduced erosional capacity, was at the origin of the shift from prograding to mainly aggrading depositional styles. Hind-lying causes may include a global change of climate and/or the overdeepening of glacial shelf troughs below a certain threshold. The oxygen isotope record documents longer glacial cycles and larger ice volumes during the late Pleistocene, but this primarily reflects the expansion of ice sheets into more temperate latitudes (Ruddiman et al. 1986); the effect on high-latitude ice sheets is not exactly known, however. The progressive overdeepening of shelf troughs in response to continuing glaciation may have had a profound impact on glacial dynamics as well. This is in a way similar to what Bartek et al. (1991) have suggested to explain the Early Miocene aggradation in the Ross Sea, Antarctica. Larger water depths must have rendered it increasingly difficult for ice sheets to ground in these troughs. As a possible result, ice streams may have advanced into the troughs later in the glacial cycle, and the total residence time of the ice at the shelf edge may consequently have been much shorter. This is most extremely exemplified by the Late Weichselian evolution in the Barents Sea (Elverhøi et al. 1994; Hebbeln et al. 1994). Fast-flowing ice streams would thus have had lower profiles than before (cf. Elverhøi et al. 1994), resulting in a markedly reduced loading, and thus erosional capacity. It may also have resulted in a different mechanism of glacial advance, involving a larger preservation potential of sediments deposited during glacial advance and preceding retreat, but this cannot be assessed with the available data set.

3. Towards a sequence stratigraphic model for glaciated margins ?

The cyclic nature of glaciations, with repetitive advances of grounded ice and subsequent retreat, is very likely to have imposed a distinct cyclicity on the pattern of deposition on a glaciated margin, more or less the same way sea level does on a lower-latitude margin. In order to more closely address the issue of a cyclic depositional model for glaciated margins, in particular regarding accumulation on the lower slope and continental rise, an additional seismic section has been investigated from a third high-latitude margin, located in the southern hemisphere: the SE Weddell Sea, Antarctica. The available profile, line 90060 (Fig. 5), runs from the mouth of the prominent, glacially eroded Crary Trough on the outer shelf, down the continental slope and rise. The margin shows considerable variation from the other studied examples, in that it is dominated by a huge submarine fan system, Crary Fan, situated at the foot of the continental slope. The general architecture of the fan was disclosed by Kuvaas & Kristoffersen (1991), and further refined by Moons et al. (1992). The fan is composed of three major elongate fan systems that are laterally shifted with respect to each other. Each of these fan systems appears to consist of a number of stacked channels and their associated levee deposits. Individual channels have lengths of more than 200 km and widths of several tens of kilometres; they are flanked by up to hundreds of meters thick levees. The oldest fan system (system 1) was probably already initiated in Mid-Oligocene time (Moons 1992). Within the youngest system (system 3) a distinct transition is noted, from stable vertical stacking into a pattern of back-and-forth switching of channels and levees (Moons 1992) (Fig. 5). This is attributed to the development of higher-frequency glacial cycles in the Plio-Pleistocene, as the Antarctic ice was more and more controlled by eustatic sea level variations imposed by the appearance of northern hemisphere ice masses, which are much more climate-sensitive. The reflector across which this transition takes place, is thus regarded as late Pliocene (c. 2.6 Ma) in age. Overlying this reflector — and thus clearly post-dating the main phase of fan activity — is an up to 1 s thick wedge consisting of prograding slope-attached strata, the distal parts of which are interbedded with transparent base-of-slope units interpreted by Moons (1992) as isolated levees; also interbedded are more chaotic units, probably representing mass deposits, that in some cases extend onto the upper slope.

3.1. Outer shelf and upper slope geometries

The most consistent characteristic of the three examined glacial continental margins is the manifest progradational geometry of outer shelf and upper slope sequences. This feature has long been recognised by most investigators (e.g. Boulton 1990; Cooper et al. 1991; Kuvaas & Kristoffersen 1991; Larter & Cunningham 1993; Vorren et al. 1989), and is generally attributed to the grounding of ice sheets all the way to the shelf edge at times of glacial maximum. Progradation is most prominent at the mouth of broad transverse shelf troughs, which are thought to represent the preferential glacial outlets where fast-flowing ice streams tended to converge. The troughs thus also acted as the preferred conduits for sediment transport, and large volumes of sediment were deposited at the trough mouths, as the ice streams released most of their load in delta-like bodies close to the grounding line, by either one of the mechanisms discussed in chapter I. Continuous foresets developed over the continental slope by the intermittent occurrence of numerous small-scale mass wasting processes (cf. Larter & Cunningham 1993), with an additional component of debris raining out from drifting icebergs. The result are the prominent depocentres, evident as bulges in the bathymetry, and representing sites of enhanced build-out with respect to adjacent, inter-trough portions of the margin.

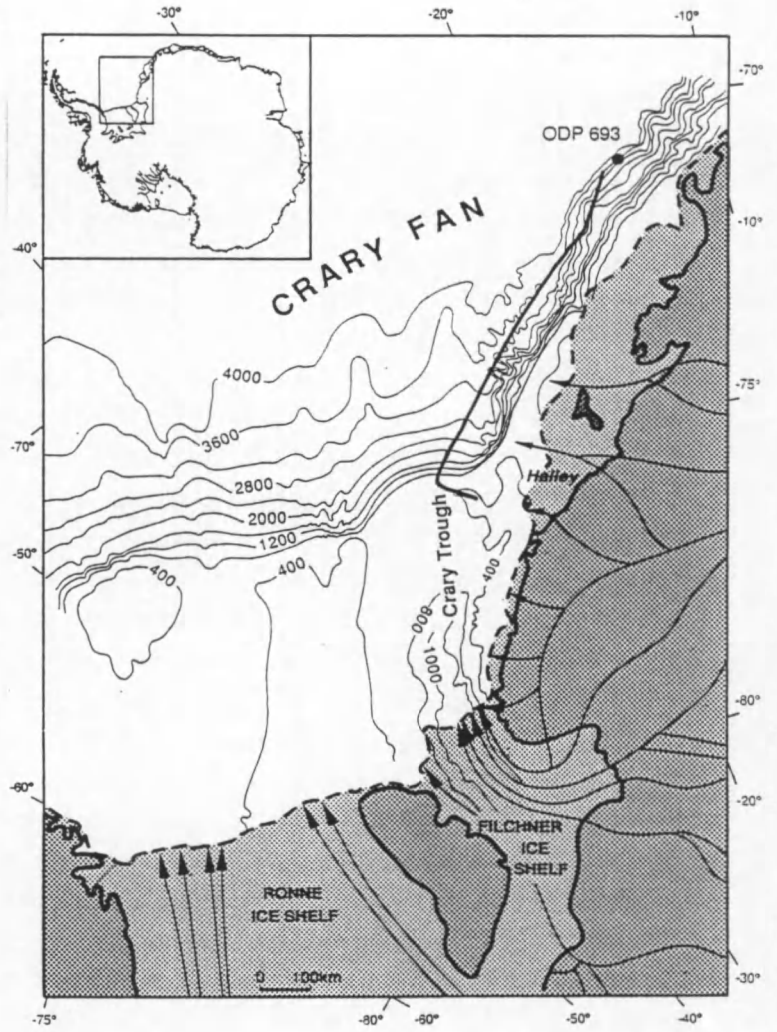
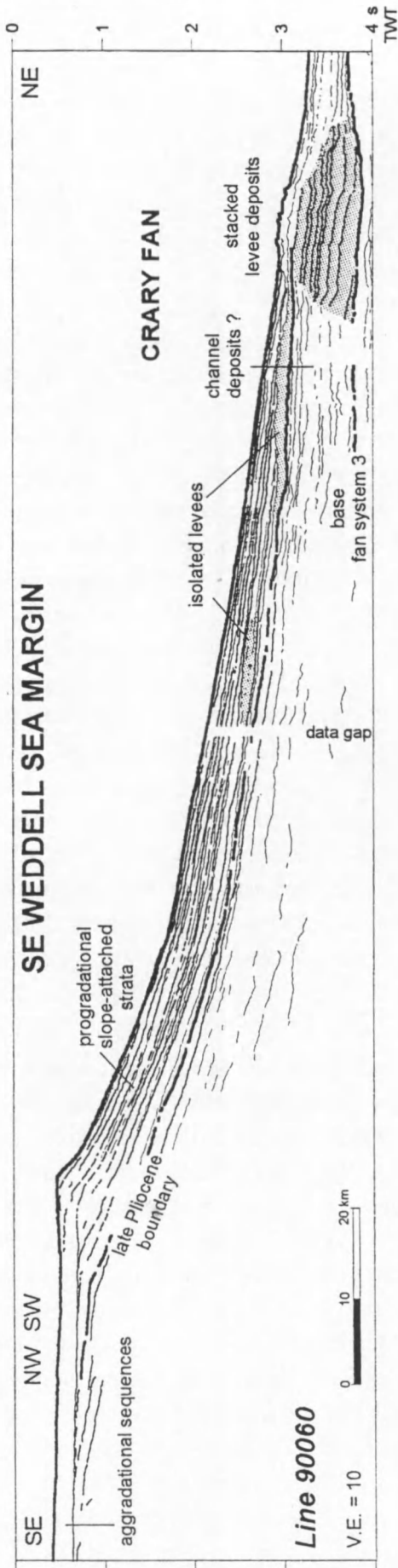


Fig. IV.5 - Water-depth corrected line drawing of entire line 90060 in the SE Weddell Sea off Crary Trough, demonstrating the relation of the Plio-Pleistocene progradational wedge with respect to fan system 3 further downslope. Levee deposits are gray-shaded. Re-interpreted from Moons (1992).

The present study clearly demonstrates that glaciated margin sequences can also have a significant vertical component in their outer shelf portion. Aggradational sequences are observed in all three examples, where they represent the youngest sequences recognised. It was argued above that these aggradational shelf sequences are equally deposited during glacial maximum. Possibly they reflect a situation of less prolonged residence of the ice sheet near the shelf edge, and/or of decreased ice sheet thickness, resulting in an overall reduced erosion and net deposition, thus favouring the development of thicker topset sections.

3.2. Lower slope and continental rise geometries

The lower continental slope and rise constitute a large domain which has not been frequently addressed in the investigation of glaciated margins. Despite the distal location, sedimentation here is still to a large extent influenced by ice front oscillations on the shelf. The validity of a sequence stratigraphic model for glaciated margins should therefore extend into this domain as well.

In contrast to the relative uniformity met on the outer shelf and upper slope, the three investigated margins show considerable variation in build-up of their downslope portions. The central East Greenland margin can be regarded as mostly ("macroscopically") stable: there is some limited evidence for relatively small-scale slumping in the youngest slope sediments; otherwise, the slope is characterised by continuous slope-attached prograding foresets, which only in the two uppermost sequences are seen to downlap onto more or less transparent base-of-slope units onlapping the lower sequence boundary. The western Barents Sea margin, on the other hand, is entirely dominated by large-scale mass wasting processes, which have disturbed a good deal of the stratigraphy and shifted the centre of accumulation significantly downslope. These mass movements have been so extensive, however, that individual mass deposits are seldom recognised and are in places even amalgamated into one thick chaotic unit. Nowhere could the geometric relation of these masses with eventual prograding foresets be established. Finally, and strongly in contrast to the other two examples, a typical submarine fan has developed at the foot of the continental slope along the SE Weddell Sea margin adjacent to Crary Trough. The latest, Plio-Pleistocene phase of deposition on Crary Fan has been characterised by less stable fan development, however, and a prevalence of upper slope progradation (in a large clastic wedge at the mouth of Crary Trough) over accumulation on the continental rise. The distal parts of slope-attached prograding strata are seen to downlap onto isolated levee units, which were identified by Moons (1992) (Fig. 5). There is also a significant contribution from more large-scale mass deposits to the total stratigraphic column, on the lower slope and rise as well as on the upper slope. These deposits, evident as chaotic units, are observed both at the base and at the top of the stratigraphic entities that are thought to represent glacial sequences.

When comparing these three specific high-latitude margins with other examples published in literature, it appears that they can be regarded as representatives of three main categories, grossly grouping all known glaciated margins on basis of the dominant mode of deposition on the lower slope and rise (Fig. 6): [i] mostly stable margins like the central East Greenland margin off Scoresby Sund, [ii] notoriously unstable margins as the western Barents Sea margin off Bear Island Trough, and [iii] fan-dominated margins like the SE Weddell Sea margin off Crary Trough. A margin that can be classified into the first category, is the Antarctic Peninsula Pacific margin, as described by Larter & Cunningham (1993), and perhaps also the West Antarctic margin in the Bellingshausen Sea (Fig. 4b); the second category includes margins like the Newfoundland margin (Aksu & Hiscott 1992) and the western Baffin Bay margin (Hiscott & Aksu 1994), whereas the Laurentian Fan south

of the Grand Banks of Newfoundland (Normark et al. 1983; Piper et al. 1985), and the SE Greenland margin off Gyldenloves shelf trough, south of Angmagssalik (L. Clausen, pers. comm. 1994) fit into the third category. This should not be envisaged as a rigid classification scheme, but rather as a ternary diagram allowing mutual overlap between each of the idealised end members. The Labrador margin, for example, shows characteristics common to both unstable and fan-dominated margins (Hesse 1992), while several gradations may exist between a mostly stable and a mostly unstable margin. Gradual transitions can also be noted in a lateral sense, between adjacent stretches of a given margin, as is particularly illustrated by the following succession, from south to north along the Canadian Atlantic margin (marked A-D on Fig. 2): Scotian slope (relatively small-scale mass wasting, Mosher et al. 1994) - Laurentian slope (submarine fan development, Normark et al. 1983) - Newfoundland slope (widespread mass wasting, Aksu & Hiscott 1992) - Labrador slope (both channel-levee deposition and mass wasting, Hesse 1992). A given margin can also evolve towards another category through geologic time, as illustrated by the SE Weddell Sea margin, which originally had all the characteristics of a purely fan-dominated situation, but is showing increasing influence of mass wasting during its latest, Plio-Pleistocene phase of development.

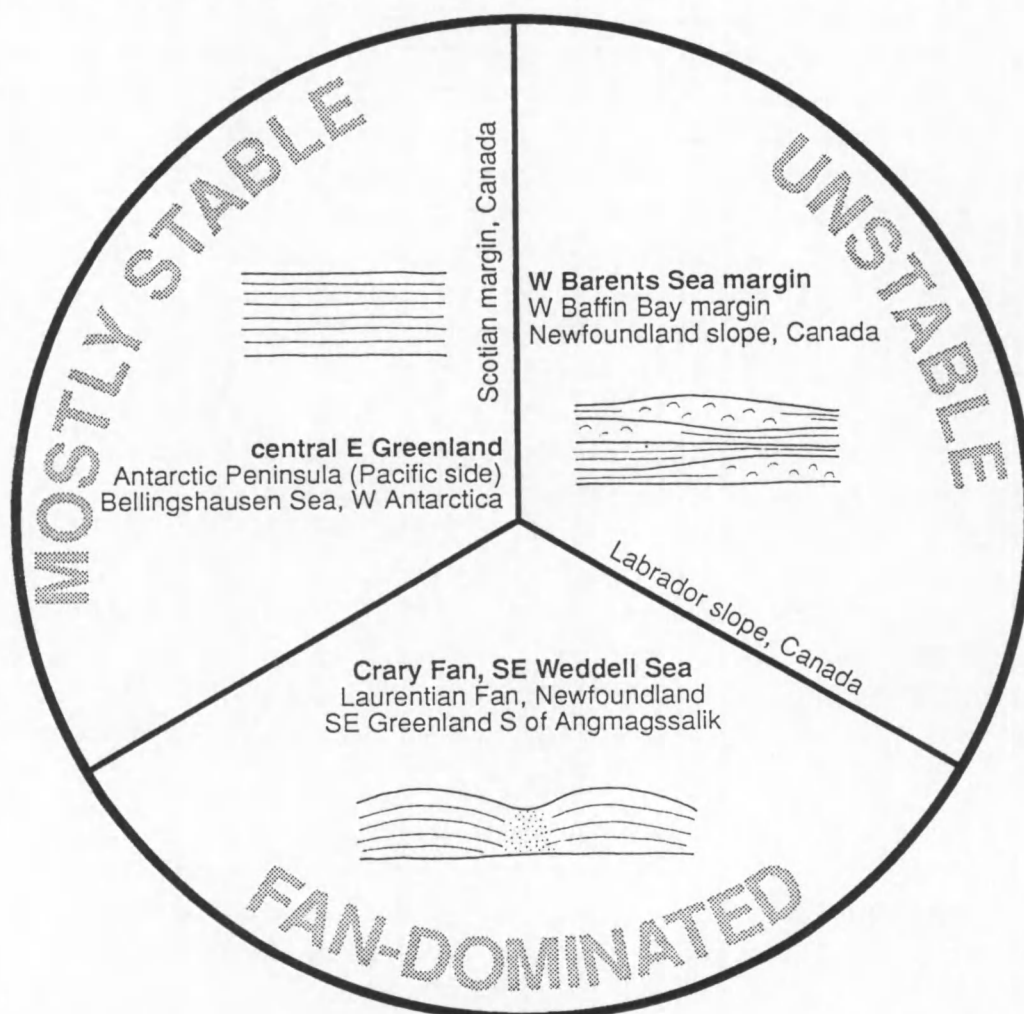


Fig. IV.6 - Qualitative ternary classification diagram for glaciated margins, based on the dominant depositional style of lower slope and rise.

Two final questions can be raised, however: [i] what are the conditions controlling the development of stable slope aprons versus unstable slope aprons or submarine fans along a glaciated margin?, and [ii] do the driving processes of mass wasting and channel-levee deposition operate in a specific interval of the glacial cycle?

It is not the purpose of the present study to provide the ultimate answer to these questions — a more detailed and multidisciplinary approach is required for that — but nevertheless it seems to be possible to isolate certain factors that show considerable variation amongst the investigated margins (Table 2), and which may have influenced the observed differences in depositional style on the respective continental slopes and rises. These factors include:

- the lithology of the eroded hinterland: a more easily erodable substratum, such as the sediments underlying the Barents Sea (opposed to e.g. the predominantly crystalline rocks on East Greenland), would result in the generation of larger volumes of sediment, with overall smaller grain sizes, which would in turn have serious implications for the stability of the slope;
- the nature of the ice sheet (partly or fully marine-based) and the morphology of the shelf (width, depth, presence of a pronounced shelf trough, foredeepened character) strongly influence the glacial dynamics, and the mode of glacial retreat (gradual or catastrophical, see below), both affecting the character (water content, consolidation) of the deposited sediment;
- the thermal regime at the base of the ice sheet determines the amount of sediment that is generated, as well as the mode of deposition and thus the properties of the sediment;
- the slope angle exerts control on the stability factor, including the thickness of mass that is eventually displaced in one event;
- the mode of retreat is of relevance to the way remaining debris is released from the waning ice sheet: the gradual retreat of an ice front is likely to sustain the discharge of sediment-laden meltwater plumes, whereas rapid retreat would cause iceberg calving, and thus the longer-distance transport of significant amounts of sediment (Henrich 1991). This probably largely depends on whether the ice sheet in question is more sensitive to insolation or sea level variations, respectively, but remains difficult to evaluate. The Barents Sea ice sheet e.g., is undoubtedly very sensitive to sea level (Elverhøi et al. 1994), but poor dating control makes it difficult to determine whether its disappearance actually occurred in response to the main glacio-eustatic sea level rise, or was leading it. The Antarctic ice sheets, on the other end of the spectrum, are solely retreating in response to the large sea level rise caused by the interglacial disappearance of northern hemisphere ice masses (J.B. Anderson, Erasmus intensive course, 1993).

These elements are to some degree interrelated, and they all seem to affect, in one way or another, the stability of the sediments deposited on the upper slope during glacial advances. Large-scale mass wasting processes are likely to occur in places where sedimentation rates are high, and where sediments are rich in mud and have a high water content. A lower slope angle would promote the failure of larger masses of sediment: on Bear Island Cone e.g., the slope angle is only 1°. The conditions favouring the development of a submarine fan are much less constrained, however. This requires the long-term generation of turbidity currents on a spot of focused sediment input, a condition that may be met at the mouth of some glacial troughs, possibly those where a more sand-rich sediment composition and a relatively steep slope restricts the size of mass movements to relatively small dimensions: the slope angles in the SE Weddell Sea, on the Newfoundland slope

south of the Grand Banks (Piper et al. 1985) and on the Labrador slope (Hesse 1992) are all in the order of 3° or greater. The pre-existence ("inheritance") of slope-transecting morphological features such as canyons or channels probably plays an important role in the confinement of the flows, which may be considered a prerequisite for the development of channel-levee systems. It may also be that the development of a submarine fan along a glaciated margin is dependent on specific depositional processes linked to the dynamics of the ice sheet, e.g. the direct generation of turbidity currents by underflow of sediment-laden turbid meltwater (Henrich 1991; Kuvaas & Kristoffersen 1991), but the occurrence of such a process has not yet been convincingly demonstrated.

Whether accumulation on the lower slope and rise is related to a specific part of the glacial cycle, can be assessed by the recognition of the geometric relationship between upper slope and lower slope strata. Though mass wasting is often triggered by essentially random earthquakes, frequent failures to produce slumps or debris flows are favoured by high sedimentation rates on the upper slope, and may thus occur in relation to the glacial cycle. The stratal patterns on Bear Island Cone are so heavily disturbed, however, that it is not possible to determine the sequence stratigraphic position of the mass deposits. Vorren et al. (1989) have suggested that they occur during periods of maximum glaciation, when an ice sheet is positioned at the shelf edge. Observations from the central East Greenland margin and from the SE Weddell Sea have revealed chaotic units onlapping and/or being downlapped by units consisting of progradational strata. This would indicate that periods of extensive mass wasting may lead or lag the main phase of margin build-out by a certain period of time. It is therefore believed here, conform to the model proposed by Boulton (1990), that mass movements preferentially, but not exclusively, operate towards the end of the glacial maximum, when slope instability is growing as a result of the large volume of sediment that has already accumulated, and when initial retreat results in a new increase of sedimentation rates and in small isostatic adjustments that can enhance the destabilisation effect.

The deposition of a submarine fan by confined turbidity currents is probably limited to certain periods of the glacial cycle as well. For the Cray Fan, Kuvaas & Kristoffersen (1991) have suggested that fan growth mainly occurred during glacial maximum, i.e. at the same time as outbuilding of the margin is supposed to take place. In the youngest section of the fan, however, isolated channel-levee complexes appear to be interbedded between the distal parts of some of the prograding slope-attached deposits (cf. Moons 1992), which would indicate an out-of-phase relationship between upper slope progradation and fan growth. Note that this does not necessarily reflect the situation during the main phase of fan deposition prior to the Plio-Pleistocene. Several processes may be responsible for the generation of turbidity currents contributing to deposition on the fan: repetitive small-scale slope failures, meltwater suspension underflows, or downslope thermohaline water currents. It was argued above that the first process tends to occur more frequently in late glacial times; underflows may be initiated during gradual retreat of the ice sheet, when increased sediment release and meltwater generation (Henrich 1991) could lead to the direct underflow of dense sediment suspensions; whereas thermohaline downslope currents typically develop during interglacials, linked to the seasonal formation of sea ice (Elverhøi et al. 1989). The effect of the latter process on the total sediment budget of the lower continental slope is thought to be negligible, however (cf. Kuvaas & Kristoffersen 1991; section 6.1 of the previous chapter). It is therefore speculated that the other two processes are more significant, and that submarine fans have a greater tendency to develop during late glaciation, in agreement with the observed stratal geometries and analogous to the main phase of lower slope accumulation on unstable glaciated margins.

	CENTRAL EAST GREENLAND MARGIN	WESTERN BARENTS SEA MARGIN	SE WEDDELL SEA MARGIN
Morphological features			
shelf width	c. 100 km	> 800 km (along trough axis)	> 600 km to Filchner ice shelf
shelf trough	not pronounced	Bear Island Trough	Crary Trough
water depth at shelf edge	395 m	495 m	495 m
slope angle	3.8°	1.1°	3.0°
Tectonic setting			
type of margin	passive margin since E. Miocene (23-20 Ma)	sheared/rifted margin passive since E. Eocene (51-47 Ma)	mature passive margin since late M. Jurassic (c. 155 Ma)
nature of eroded hinterland	mainly crystalline basement	sedimentary basins	crystalline basement
Glacial setting			
nature of ice sheet	continental ice cap	fully marine-based ice sheet disappearing during interglacials	ice sheet remaining as floating ice shelf during interglacials
basal thermal regime	dry-based ?	wet-based ?	dry-based ?
mode of retreat	?	rapid disintegration following sea level rise	in several abrupt steps; not yet complete
onset of large-scale glaciation	late Pliocene (L. Miocene?)	late Pliocene	Middle Oligocene (Miocene?)
Glaciogenic sediments			
max. Plio-Pleistocene thickness	1 km	> 3 km	1 km
Plio-Pleistocene progradation	45 km	52.5 km	16.5 km
dominant sedimentation process on lower slope and rise	small-scale mass wasting	large-scale mass wasting (slides, slumps, debris flows)	fan deposition (channelised turbidity currents)

Table IV.2 - Comparison of key parameters for the three investigated glacial continental margins.

3.3. A tentative cyclic depositional model for glaciated margins

If anything, the three investigated margins illustrate that a unified sequence stratigraphic model for glaciated margins does probably not exist. Particularly on the lower slope and rise depositional patterns are strongly diverging between different localities. Three basic types of glaciated margins have been discerned: mostly stable margins, unstable margins, and fan-dominated margins. The models presented in chapter I largely reflect individual glaciated margins, with limited applicability towards other regions. Combining elements from these different settings, the following multiple-case scenario can be constructed (Fig. 7):

- during glacial advance sedimentation is restricted to a zone proximal to the migrating ice front, while erosion dominates in the more up-stream portions of the ice sheet on the inner shelf. The sediments that are thus deposited on the outer shelf are subsequently remoulded when the ice sheet continues to advance;
- during glacial maximum, when the ice sheet is grounded all the way to the shelf edge, sedimentation is focused on the upper slope at the mouth of broad glacial troughs, resulting in a typical progradation of the margin in these locations; intermittent small-scale mass wasting processes distribute the sediment downslope, resulting in the development of continuous macro-scale foresets over the continental slope. Depending on ice stream dynamics significant aggradation may or may not take place in the outer shelf portion of the troughs;
- during deglaciation the instability of the upper slope tends towards a maximum, and the main phase of gravity-driven downslope sediment remobilisation is inferred to take place (though it may have initiated well before this time), either by unconfined mass movements on slope aprons or by channelised turbidity currents on submarine fans. Progradation of the margin thus comes to an end. Discontinuous patches of sediment are deposited on the shelf in places where the ice front temporarily halts during its retreat. Calving icebergs can strongly scour and rework the sediments on the shelf (cf. Dowdeswell et al. 1994);
- during interglacials the ice sheet has retreated to a position landward of the coastline (northern hemisphere) or to the inner shelf (large embayments in Antarctica). Ice-proximal sediments are trapped within the deep inner shelf or fjord basins, and the outer shelf, slope and rise become essentially sediment-starved; the condensed horizons that are thus formed, are thought to be characterised by higher impedance contrasts, resulting in the higher-amplitude reflectors that are intuitively picked on seismic sections. Limited remobilisation processes may be induced by the establishment of deep-reaching oceanic currents over the outer shelf, and of thermohaline currents moving down the continental slope (e.g. Vorren et al. 1989).

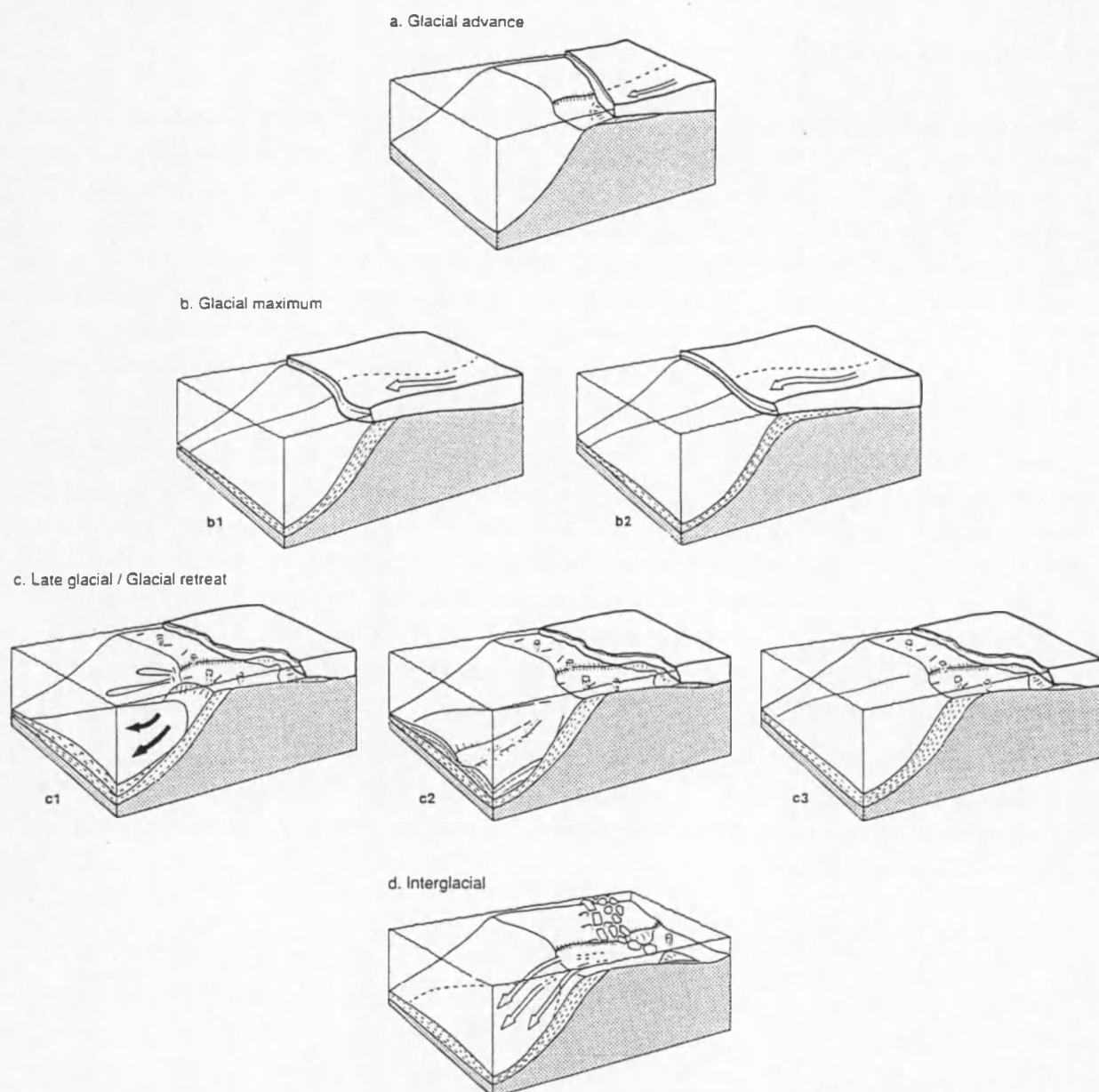


Fig. IV.7 - Tentative cyclic model for glaciated margin deposition. **[a]** Glacial advance: sediments are deposited in front of the migrating ice front, and subsequently remoulded. **[b]** Glacial maximum: ice sheet is positioned at shelf edge, and pronounced progradation takes place at the mouth of glacial shelf troughs (b1), possibly accompanied by aggradation on the outer shelf (b2); erosion dominates on the inner shelf. **[c]** Late glacial and glacial retreat: main phase of downslope sediment remobilisation, either by small-scale mass flows (mostly stable margins, c1), large-scale mass wasting (unstable margins, c2), or channelised turbidity currents (fan-dominated margins, c3); glaciomarine sediments accumulate on the shelf in places where retreating ice front temporarily halts; scouring iceberg keels rework sediment on outer shelf. **[d]** Interglacial: outer shelf, slope and rise become essentially sediment-starved; limited sediment input occurs through biogenic production, and through the reworking of shelf and slope sediments by re-established long-shelf oceanic currents, and by seasonal downslope thermohaline currents.

4. Future research scopes

The present study is undoubtedly biased towards the Barents Sea side of the polar North Atlantic ocean, as only limited information was available from the central East Greenland margin. Future work should therefore concentrate on obtaining additional intermediate-resolution seismic data from the East Greenland margin, in order to establish a tie with the SE Greenland shelf region more south (Angmagssalik and Kangerdlugssuaq regions), where the Geological Survey of Greenland has recently acquired an extensive and high-quality data set, and where a series of new ODP sites has been drilled. This way, a regional stratigraphic framework may be established, similar to that developed for the western Barents Sea - Svalbard margin, which would also allow to better assess the lateral variability along the margin.

Along the western Barents Sea - Svalbard margin, an ODP leg is scheduled for this summer 1995, which may signify a break-through in the development of a chronology for the margin, and provide more proximal and more detailed records of the history of glaciation than presently available. Calibration of the existing seismic stratigraphic framework should make it possible to extend the drilling results from the site west of Svalbard to the Storfjorden and Bear Island Cones further south, in order to finally date the major changes in depositional style identified on these depocentres, and to investigate what glacial variations may have caused them. This will also make clear to what extent the current correlation with proxy records of the Fennoscandian Ice Sheet is valid.

Finally, the further development of a glacial sequence stratigraphic model will certainly require the comparison of more data, from a wider variety of glaciated margins. Higher-resolution studies are indispensable to obtain a better insight in the depositional processes acting on a glaciated margin, and in the factors controlling them.

References cited

- Aksu A.E. & Hiscott R.N. (1992) — Shingled Quaternary debris flow lenses on the north-east Newfoundland Slope. *Sedimentology*, 39, pp. 193-206.
- Bart P.J. & Anderson J.B. (1994) — Glacial history of the Antarctic Peninsula continental shelf. *Terra Antarctica*, 1(2), pp. 263-264.
- Bart P.J. & Anderson J.B. (in press) — Seismic expression of depositional sequences associated with expansion and contraction of ice sheets on the northwestern Antarctic Peninsula continental shelf. In: De Batist M.A.O. & Jacobs P. (Eds.), *Geology of Siliciclastic Shelf Seas*, Special Publication, The Geological Society, London.
- Bartek L.R., Vail P.R., Anderson J.B., Emmet P.A. & Wu S. (1991) — Effect of Cenozoic ice sheet fluctuations in Antarctica on the stratigraphic signature of the Neogene. *Journal of Geophysical Research*, 96, pp. 6753-6778.
- Boulton G.S. (1990) — Sedimentary and sea level changes during glacial cycles and their control on glacial marine facies architecture. In: Dowdeswell J.A. & Scourse J.D. (Eds.), *Glacial Marine Environments: Processes and Sediments*. Special Publication, 53, The Geological Society, London, pp. 15-52.
- Cloetingh S., Reemst P., Kooi H. & Fanavoll S. (1992) — Intraplate stresses and the post-Cretaceous uplift and subsidence in northern Atlantic basins. *Norsk Geologisk Tidsskrift*, 72, pp. 229-235.
- Cooper A.K., Barrett P.J., Hinz K., Traube V., Leitchenkov G. & Stagg H.M.J. (1991) — Cenozoic prograding sequences of the Antarctic continental margin : A record of glacio-eustatic and tectonic events. *Marine Geology*, 102, pp. 175-213.
- Dowdeswell J.A., Whittington R.J. & Marienfeld P. (1994) — The origin of massive diamicton facies by iceberg rafting and scouring, Scoresby Sund, East Greenland. *Sedimentology*, 41, pp. 21-35.
- Elverhøi A., Fjeldskaar W., Solheim A., Nyland-Berg M. & Russwurm L. (1994) — The Barents Sea Ice Sheet : A model of its growth and decay during the last ice maximum. *Quaternary Science Reviews*, 12, pp. 863-873.
- Elverhøi A., Pfirman S.L., Solheim A. & Larssen B.B. (1989) — Glaciomarine sedimentation in epicontinental seas exemplified by the northern Barents Sea. In: Powell R.D. & Elverhøi A. (Eds.), *Modern Glacial Marine Environments: Glacial and Marine Controls of Modern Lithofacies and Biofacies*. *Marine Geology*, 85, pp. 225-250.
- Hebbeln D., Dokken T., Andersen E.S., Hald M. & Elverhøi A. (1994) — Moisture supply for northern ice-sheet growth during the Last Glacial Maximum. *Nature*, 370, pp. 357-360.
- Henrich R. (1991) — Cycles, rhythms, and events on high input and low input glaciated continental margins. In: Einsele G., Ricken W. & Seilacher A. (Eds.), *Cycles and Events in Stratigraphy*. Springer-Verlag, Berlin, pp. 751-772.
- Henrich R. & Baumann K.-H. (1994) — Evolution of the Norwegian Current and the Scandinavian Ice Sheets during the past 2.6 m.y. : Evidence from ODP Leg 104 biogenic carbonate and terrigenous records. *Palaeogeography, Palaeoclimatology, Palaeoecology*, 108, pp. 75-94.
- Hesse R. (1992) — Continental slope sedimentation adjacent to an ice margin I : Seismic facies of Labrador slope. *Geo-Marine Letters*, 12, pp. 189-199.
- Hiscott R.N. & Aksu A.E. (1994) — Submarine debris flows and continental slope evolution in front of Quaternary ice sheets, Baffin Bay, Canadian Arctic. *American Association of Petroleum Geologists Bulletin*, 78(3), pp. 445-460.
- Imbrie J., Hays J.D., Martinson D.G., McIntyre A., Mix A.C., Morley J.J., Pisias N.G., Prell W.L. & Shackleton N.J. (1984) — The orbital theory of Pleistocene climate : Support from a revised chronology of the marine $\delta^{18}\text{O}$ record. In: Berger A.L., Imbrie J., Hays J.D., Kukla G. & Saitzman B. (Eds.), *Milankovitch and Climate*. NATO ASI Series C, Mathematical and Physical Sciences, 126, Kluwer, Dordrecht, pp. 269-305.
- Jansen E., Bleil U., Henrich R., Kringstad L. & Slettemark B. (1988) — Paleoenvironmental changes in the Norwegian Sea and the Northeast Atlantic during the last 2.8 Ma : DSDP/ODP Sites 610, 642, 643 and 644. *Paleoceanography*, 3(5), pp. 563-581.
- Jansen E., Sjøholm J., Bleil U. & Erichsen J.A. (1990) — Neogene and Pleistocene glaciations in the northern hemisphere and late Miocene - Pliocene global ice volume fluctuations : Evidence from the

- Norwegian Sea. In: Bleil U. & Thiede J. (Eds.), *Geological History of the Polar Oceans: Arctic versus Antarctic*. Kluwer Academic Publishers, Dordrecht, pp. 677-705.
- Kuvaas B. & Kristoffersen Y. (1991) — The Crary Fan : A trough-mouth fan on the Weddell Sea continental margin, Antarctica. *Marine Geology*, 97, pp. 345-362.
- Larsen B. (1994) — Morphology and seismic stratigraphy of the East Greenland shelf in the Denmark Strait area compared to the Prydz Bay, Antarctica. *Terra Antarctica*, 1(2), pp. 427-430.
- Larter R.D. & Cunningham A.P. (1993) — The depositional pattern and distribution of glacial-interglacial sequences on the Antarctic Peninsula Pacific margin. *Marine Geology*, 109, pp. 203-219.
- Mariénfeld P. (1991) — Holozäne Sedimentationsentwicklung im Scoresby Sund, Ost-Grönland. *Berichte zur Polarforschung*, no. 96, Alfred-Wegener Institut für Polar- und Meeresforschung, Bremerhaven, 162 pp.
- Moons A. (1992) — Gedetailleerde seismo- en sequentiestratigrafische studie van de Crary Fan, zuidoostelijke Weddell Zee, Antarctica. Unpublished Ph. D. thesis, Universiteit Gent, 174 pp.
- Moons A., De Batist M., Henriët J.-P. & Miller H. (1992) — Sequence stratigraphy of the Crary Fan, Southeastern Weddell Sea. In: Yoshida Y., Kaminuma K. & Shiraishi K. (Eds.), *Recent Progress in Antarctic Earth Science*. Terra Scientific Publishing Company, Tokyo, pp. 613-618.
- Mosher D.C., Moran K. & Hiscott R.N. (1994) — Late Quaternary sediment, sediment mass flow processes and slope stability on the Scotian Slope, Canada. *Sedimentology*, 41, pp. 1039-1061.
- Nitsche F.O., Gohl K., Vanneste K. & Miller H. (submitted) — Indication of glacially deposited sequences in the Bellingshausen and Amundsen Seas, West Antarctica : first results of a regional seismic survey. In: Cooper A. et al. (Eds.), *Geology and Acoustic Stratigraphy ... (Vol. B)*, Antarctic Research Series, American Geophysical Union.
- Normark W.R., Piper D.J.W. & Stow D.A.V. (1983) — Quaternary development of channels, levees, and lobes on Middle Laurentian Fan. *American Association of Petroleum Geologists Bulletin*, 67(9), pp. 1400-1409.
- Piper D.J.W., Stow D.A.V. & Normark W.R. (1985) — Laurentian Fan, Atlantic Ocean. In: Bouma A.H., Normark W.R. & Barnes N.E. (Eds.), *Submarine Fans and Related Turbidite Systems*. Springer-Verlag, New York, pp. 137-142.
- Posamentier H.W., Jervey M.T. & Vail P.R. (1988) — Eustatic controls on clastic deposition I : Conceptual framework. In: Wilgus C.K., Hastings B.S., Kendall C.G.St.C., Posamentier H.W., Ross C.A. & Van Wagoner J.C. (Eds.), *Sea Level Changes: An Integrated Approach*. Special Publication, 42, Society of Economic Paleontologists and Mineralogists, Tulsa, Oklahoma, pp. 109-124.
- Posamentier H.W. & Vail P.R. (1988) — Eustatic controls on clastic deposition II : Sequence and systems tract models. In: Wilgus C.K., Hastings B.S., Kendall C.G.St.C., Posamentier H.W., Ross C.A. & Van Wagoner J.C. (Eds.), *Sea Level Changes : An Integrated Approach*. Special Publication, 42, Society of Economic Paleontologists and Mineralogists, Tulsa, Oklahoma, pp. 125-154.
- Ruddiman W.F., Raymo M. & McIntyre A. (1986) — Matuyama 41,000-year cycles : North Atlantic Ocean and northern hemisphere ice sheets. *Earth and Planetary Science Letters*, 80, pp. 117-129.
- Sættem J., Poole D.A.R., Ellingsen L. & Sejrup H.P. (1992) — Glacial geology of outer Bjørnøyrønna, southwestern Barents Sea. *Marine Geology*, 103, pp. 15-51.
- Solheim A., Russwurm L., Elverhøi A. & Nyland-Berg M. (1990) — Glacial geomorphic features in the northern Barents Sea : Direct evidence for grounded ice and implications for the pattern of deglaciation and late glacial sedimentation. In: Dowdeswell J.A. & Scourse J.D. (Eds.), *Glacimarine Environments: Processes and Environments*. Special Publication, 53, The Geological Society, London, pp. 253-268.
- Stein R., Grobe H., Hubberten H., Mariénfeld P. & Nam S. (1993) — Latest Pleistocene to Holocene changes in glaciomarine sedimentation in Scoresby Sund and along the adjacent East Greenland continental margin: preliminary results. *Geo-Marine Letters*, 13, pp. 9-16.
- Stow D.A.V., Howell D.G. & Nelson C.H. (1985) — Sedimentary, tectonic, and sea-level controls. In: Bouma A.H., Normark W.R. & Barnes N.E. (Eds.), *Submarine Fans and Related Turbidite Systems*. Springer-Verlag, New York, pp. 15-22.
- Vorren T.O., Lebesbye E., Andreassen K. & Larsen K.-B. (1989) — Glacigenic sediments on a passive continental margin as exemplified by the Barents Sea. In: Powell R.D. & Elverhøi A. (Eds.), *Modern Glacimarine Environments: Glacial and Marine Controls of Modern Lithofacies and Biofacies*. *Marine Geology*, 85, pp. 251-272.

List of frequently used abbreviations

a.s.l.	above sea level
AWI	Alfred Wegener Institut
BLKS	Blosseville Kyst shelf
BP	Before Present
CBF	continental boundary fault
CFZ	Central Fault Zone
DSDP	Deep-Sea Drilling Project
EGC	East Greenland Current
FZ	Fracture Zone, or Fault Zone
GGU	Grønlands Geologiske Undersøgelse
GPS	Global Positioning System
GRIP	Greenland Ice-core Project
GSDW	Greenland Sea Deep Water
IKU	Institutt for Kontinentalsokkelundersøkelser
IRD	ice-rafted debris
LGM	last glacial maximum
LILS	Liverpool Land shelf
MCS	multi-channel seismics
MGK	Marine Geophysik Kiel
NEAS	North-Eastern shelf
NPD	Norwegian Petroleum Directorate
NSDW	Norwegian Sea Deep Water
NWABW	North-West Atlantic Bottom Water
OCT	ocean-continent transition
ODP	Ocean Drilling Program
PONAM	Polar North Atlantic Margins
RCMG	Renard Centre of Marine Geology
SEAS	South-Eastern shelf
TMF	trough mouth fan
TWT	two-way travel time
URU	upper regional unconformity
VVP	Vestbakken volcanic province

List of Tables

CHAPTER II

Table II.1 - Overview of seismic lines shot during the ARK VII/3b survey.	43
Table II.2 - Recording parameters of digitally recorded profiles.	47
Table II.3 - Comparison of the main characteristics of the East Greenland shelf provinces (compiled from H.C. Larsen 1984, 1985, 1990).	68
Table II.4 - Summary of the terrestrial record of glaciation in Greenland (compiled from Funder 1971, 1984, and PONAM comm. 1993; Funder et al. 1991; Weidick 1976). YD = Younger Dryas.	76
Table II.5 - Sequence stratigraphic correlation table for line 90600, summarising reflector configurations and thickness variations for each individual sequence, along with a tentative age correlation and interpreted geological significance.	119

CHAPTER III

Table III.1 - Length of individual seismic profiles.	135
Table III.2 - Key acquisition and recording parameters of the two data sets.	135
Table III.3 - Key data for drillholes available on the western Barents Sea - Svalbard margin. DSDP = Deep Sea Drilling Project, IKU = Institutt for Kontinentalsokkelundersøkelser.	170
Table III.4 - Correlation of reflectors identified in this study with the regional unconformities R1-R7 of Faleide et al. (in press).	177
Table III.5 - Stratigraphic correlation table for Megasequence G0.	182
Table III.6 - Classification of submarine mass movements, based on mechanical behaviour and coarse-particle support mechanism. Adapted from Nardin et al. (1979).	208
Table III.7 - Figures illustrating the wide range of dimensions of various types of submarine mass movements. n.d. = no data, st. = stage.	210
Table III.8 - Comparison of relevant parameters for three large-scale slope failures along the Norwegian and Barents Sea margins. n.d. = no data.	218
Table III.9 - Correlation of seismic units (sequences?) recognised within GIII with stratigraphies and chronologies established by various authors.	247

CHAPTER IV

Table IV.1 - Reconstruction of generalised long-term glacial evolution from the correlation of major depositional units on opposite margins of the polar North Atlantic Ocean. Ages are tentative and follow Jansen et al. (1988) and Henrich & Baumann (1994).	261
Table IV.2 - Comparison of key parameters for the three investigated glacial continental margins.	273

List of figures

CHAPTER I

Fig. I.1 - Distribution of present-day glacially-influenced continental margins in the world.	18
Fig. I.2 - Conceptual sketch model of an idealised glacial continental margin, showing prograding upper slope depocentres at the mouth of broad transverse shelf troughs. Upper slope depocentres may be associated with a submarine fan lower on the slope.	20
Fig. I.3 - Conceptual sketch model of a submarine fan at the foot of the continental slope (from Weimer & Link 1991). The upper fan is characterised by a leveed fan valley which divides into numerous distributary channels on the middle fan. The middle fan usually has a convex-upward profile and lobate shape (suprafan lobe).....	20
Fig. I.4 - First-order depositional processes on a glaciated margin: subglacial melt-out, squeeze and push, settling from meltwater plumes, and release of ice-rafted debris; also indicated is the accumulation of biogenic products.	21
Fig. I.5 - Relationship between sedimentation rate and distance from the glacier for suspension settling and iceberg rafting (Boulton 1990).	23
Fig. I.6 - Secondary sedimentation processes on a glacial margin: [a] iceberg scouring, [b] gravitational mass transport, [c] downslope thermohaline circulation, and [d] winnowing by long-shelf currents. Partly adopted from Henrich et al. (1989). Not to scale.	24
Fig. I.7 - Sequence stratigraphic model for low-latitude continental margins: [a] lowstand systems tract: lowstand fan, [b] lowstand systems tract: lowstand wedge, [c] transgressive systems tract, [d] highstand systems tract, [e] shelf margin systems tract. After Posamentier et al. (1988) and Posamentier & Vail (1988).	26
Fig. I.8 - Model for the development of a glacial margin sequence, proposed by Larter & Barker (1989): [a] early stage of ice sheet advance: deposition of an intergrounding subsequence (IGS) on shelf and slope, [b] initial grounding, [c] glacial maximum: ice sheet is eroding and compacting shelf sediments and is depositing a grounding subsequence (GS) on the slope, [d] early stage of glacial retreat: hiatus on outer shelf ends and deposition of next IGS begins.	29
Fig. I.9 - Schematic model of the main sedimentary processes on the outer shelf and upper slope during glacials and interglacials, proposed by Vorren et al. (1989).	29
Fig. I.10 - A model of glaciomarine facies architecture for different portions of the continental margin through one glacial cycle, proposed by Boulton (1990). The relative sea level changes appropriate to each zone are shown as well.	31
Fig. I.11 - Two views regarding the origin of shelf edge progradation: [a] in the till tongue model of King & Fader (1986) and King et al. (1987) lodgement till deposited at the base of a grounded ice sheet forms the topset beds of a glacial sequence, whereas glaciomarine sediment deposited below a floating ice shelf build the foresets; [b] in the deformable till layer concept of Alley et al. (1989) remoulded till is dragged along by the movement of the overlying ice, and where the ice becomes gradually decoupled from the till by a mm thick film of water, a till delta develops. The active till layer and the delta are on the order of a few metres and a few tens of metres thick, respectively. Vertical scales in a and b are different.	33
Fig. I.12 - Bathymetry map of the polar North Atlantic Ocean (from Perry 1986), outlining the location of the two different study areas: the central East Greenland margin off Scoresby Sund, and the western Barents Sea margin off Bear Island Trough.	35

CHAPTER II

- Fig. II.1** - Location of the study area around Scoresby Sund (shaded box) in Greenland. KG = Kangerdlugssuaq fjord, A = Angmagssalik fjord.40
- Fig. II.2** - Location of the seismic lines 90500 and 90600 on the East Greenland continental shelf. HB = Hochstetter Bugt, SS = Scoresby Sund.....44
- Fig. II.3** - Location of low-resolution seismic profiles in Scoresby Sund. KB = Kap Brewster.45
- Fig. II.4** - Location of higher-resolution lines in the outer fjord region of Scoresby Sund. KB = Kap Brewster.46
- Fig. II.5** - Data processing schemes for ARK VII/3b lines.49
- Fig. II.6** - Physiographic map of the East Greenland shelf, showing sea floor morphology in 500 m intervals (from IHO/IOC/CHS 1984), oceanic current patterns (The Open University 1989), and thickness contours of the Greenland Ice Sheet; small arrows represent the most important outlet glaciers (after Reeh 1985). Accentuated 500 m contour marks approximate position of the shelf edge. EGC = East Greenland Current, HB = Hochstetter Bugt, IC = Irminger Current, LC = Labrador Current, NWABW = North-West Atlantic Bottom Water, SS = Scoresby Sund, WGC = West Greenland Current.51
- Fig. II.7** - Physiographic map of the Scoresby Sund fjord region, showing distribution of ice and rivers (after Henriksen 1986), and summer surface water circulation (from Koch 1945).....53
- Fig. II.8** - Rough outline of the main geological units recognised in Greenland and surrounding land areas (from Escher & Watt 1976).55
- Fig. II.9** - [a] Simplified geological map of the Scoresby Sund area (after Henriksen 1986). Numbers represent the zonation described in the text: (1) tectonic window complexes, (2) Vestfjord - Hinks Land gneiss and schist zone, (3) Gåsefjord - Stauning Alper migmatite and granite zone, (4) Jameson Land basin, (5) Liverpool Land, (6) Geikie Plateau. KB = Kap Brewster. [b] Geological cross-section through the northern part of the region (after Henriksen 1989).57
- Fig. II.10** - The Jameson Land (JL) basin as the southernmost part of a larger Mesozoic sedimentary basin in central East Greenland (after Henriksen 1989).58
- Fig. II.11** - Geological and tectonic map of the East Greenland margin, showing the location of the different shelf provinces (after H.C. Larsen 1990). GFZ = Greenland Fracture Zone, JMFZ = Jan Mayen Fracture Zone, SPFZ = Spar Fracture Zone, TFZ = Tjörnes Fracture Zone; b-d mark location of cross-sections presented in Fig. II.12.62
- Fig. II.12** - Cross-sections through different shelf provinces (from north to south). Location is indicated in Fig. II.11. [a] North-East Greenland shelf at 76° N (hypothetical), [b] Liverpool Land shelf, [c] Blossville Kyst shelf, and [d] South-East Greenland shelf. After H.C. Larsen 1984 (d), 1985 (a-c).63
- Fig. II.13** - Four steps in the sea floor spreading history of the NE Atlantic (H.C. Larsen 1988). GIR = Greenland-Iceland Ridge, GSFZ = Greenland-Senja Fracture Zone, IFR = Iceland-Faeroe Ridge, JMFZ = Jan Mayen Fracture Zone, JMR = Jan Mayen Ridge, KnR = Knipovich Ridge, KoR = Kolbeinsey Ridge, PJMFZ = proto - Jan Mayen Fracture Zone.64
- Fig. II.14** - Schematic evolution of wedges of seaward dipping reflectors, formed by extensive volcanism along a subaerial spreading axis. The dip of lava flows towards the spreading centre is post-depositional, acquired through rapid differential subsidence under the weight of younger flows in the central rift zone [a-c]. When the spreading centre drops below sea level, the lava flow lengths dramatically reduce, and the normal chaotic structure of the upper oceanic crust is created [d]. Modified from Mutter (1985).65

- Fig. II.15** - [a] Thickness contour map of the Greenland Ice Sheet (from Weidick 1976), with black dots indicating known sites of pre-Holocene glacial sediment (Funder 1984). [b] Cross-section and temperature profile through the central part of the Inland Ice. Arrows indicate general ice flow direction. From Weidick (1976).70
- Fig. II.16** - Coarse-fraction record for the last 3 Ma in ODP Site 644A on the Vøring Plateau (Jansen et al. 1988).....72
- Fig. II.17** - Results of ODP Leg 152. [a] Location of ODP Sites 914, 915, 916 and 917 in the transverse trough on the SE Greenland shelf south of Angmagssalik, and Sites 918 and 919 in the oceanic Irminger Basin. [b] Interpreted line drawing of seismic profile connecting the drill sites. [c] Simplified lithologic log of the most complete Miocene - Pleistocene record, obtained at Site 918. From H.C. Larsen et al. (1994).....73
- Fig. II.18** - The continuous $\delta^{18}\text{O}$ record of the GRIP ice core in Summit (location in Fig. II.15a), plotted linearly in function of core depth (note the two sections). The non-linear scale in the middle is a time scale based on counting of annual layers back to 14.5 ka BP, and on ice flow modelling beyond that. From Dansgaard et al. (1993).74
- Fig. II.19** - Past and present ice cover in Scoresby Sund (from Henriksen 1989).77
- Fig. II.20** - Interpolated bathymetric contour map of Hall Bredning. Contour interval is 100 m. Shaded areas represent local minima. Dashed boxes surround areas for which more detailed maps were drawn (Figs. II.29 and II.39). KS = Kap Stevenson, KL = Kap Leslie.80
- Fig. II.21** - Bedrock geology and structural map of Hall Bredning, constructed from the available seismic data. Location is indicated of seismic sections presented in the corresponding figure numbers. SF = Schuchert Flod.82
- Fig. II.22** - [a, b] Seismic signature and morphology of Mesozoic sediments in the southern part of Hall Bredning (location of profiles in Fig. II.21), compared to an outcrop photograph from the southern Jameson Land coast [c]. The elevation on b is the subaqueous extension of Kap Stevenson. Mz = Mesozoic strata, QS = Quaternary sediments.83
- Fig. II.23** - [a] Seismic signature and morphology of Caledonian metamorphics in the SW part of Hall Bredning (location of seismic line in Fig. II.21), compared to an outcrop photograph from Nordvestfjord [b]. Note the faulted nature of the Mesozoic sediments close to the contact. CM = Caledonian metamorphics, Mz = Mesozoic strata, QS = Quaternary sediments.84
- Fig. II.24** - [a] Seismic signature and morphology of Caledonian intrusives close to the NE coast of Milne Land (location in Fig. II.21), compared to an outcrop photograph from the same area [b]. Note the differences in character with respect to the adjacent Caledonian metamorphics. CI = Caledonian intrusives, CM = Caledonian metamorphics, QS = Quaternary sediments.85
- Fig. II.25** - Seismic signature and morphology of facies units of supposedly basaltic nature along Volquart Boon Kyst [a] and at the mouth of Vikingebugt [b], compared to an outcrop photograph from Gåsefjord [c]. Location of seismic lines in Fig. II.21. Mz = Mesozoic strata, QS = Quaternary sediments, TB = Tertiary basalts.87
- Fig. II.26** - Graben system near the entrance of Nordvestfjord into Hall Bredning. Location of line in Fig. II.21. Symbolic notations follow the conventions used in Figs. II.22 - II.25.88
- Fig. II.27** - Seismic profile showing the small area in the northern part of Hall Bredning where Caledonian metamorphics underlie a thin layer of Mesozoic strata. Location of line is given in Fig. II.21. Symbolic notations follow the conventions used in Figs. II.22 - II.25.88
- Fig. II.28** - [a] Positive flower structure identified west of the graben system depicted in Fig. II.26, compared to a schematic representation [b]. Location of line in Fig. II.21. Symbolic notations follow the conventions used in Figs. II.22 - II.25.89
- Fig. II.29** - Detailed bathymetry map delineating the elongated trough along the Milne Land coast. Contour interval is 50 m. Shaded area represents maximum depression.90

- Fig. II.30** - Three different cross-sections through the elongated fault-controlled trough along the Milne Land coast: [a] N-S section, [b] E-W section, [c] E-W section crossing a smaller depression carved in Mesozoic sediments in the southern continuation of the trough. Location of lines in Fig. II.29. Symbolic notations follow the conventions used in Figs. II.22 - II.25.91
- Fig. II.31** - Small graben structure cutting Caledonian intrusives in the SW arm of Scoresby Sund. Location in Fig. II.21. Symbolic notations follow conventions used in Figs. II.22 - II.25.92
- Fig. II.32** - Watergun line 90300 showing the contact zone between Mesozoic sediments and Caledonian terrain near the entrance of Gåsefjord. Location indicated in Fig. II.21.93
- Fig. II.33** - Typical appearance of the thin unconsolidated sediment drape in Hall Bredning. Location of line in Fig. II.34.95
- Fig. II.34** - Distribution map of Quaternary sediments in and around Hall Bredning. Thicknesses are calculated using a seismic velocity of 1.6 km/s. Distribution on land is from Henriksen (1986). Position is indicated of seismic sections presented in the corresponding figure numbers.96
- Fig. II.35** - Some examples of local sediment accumulations in Hall Bredning: [a] along Volquart Boon Kyst, at the mouth of Vikingebugt, [b] along the rims of a presumed basaltic outlier SW of Milne Land, [c] in the trough along the Milne Land coast, [d] in a large basinal area in the north of Hall Bredning and [e, f] in front of some river mouths along the Jameson Land coast. Location of seismic lines is indicated in Fig. II.34. Symbolic notations follow the conventions used in Figs. II.22 - II.25.97
- Fig. II.36** - Floating iceberg containing basal debris layers, photographed during ARK VII/3b survey in 1990.99
- Fig. II.37** - 1985 Landsat image of the outer fjord region, showing turbid meltwater plumes discharged from glacier fronts and rivers (from Dowdeswell et al. 1994).99
- Fig. II.38** - Vikingebugt — view towards Bredegletscher.101
- Fig. II.39** - Detailed bathymetry map of the area around Vikingebugt. Contour interval is 50 m.102
- Fig. II.40** - Morphology of the glacially eroded bedrock surface in Vikingebugt, calculated using seismic velocities of 1.46 km/s in the water column and 1.6 km/s for the Quaternary sediments. Contour interval is 50 m.102
- Fig. II.41** - Inferred deflection of Bredegletscher by the main eastward moving fjord glacier during the last glacial maximum.103
- Fig. II.42** - Distribution map of Quaternary sediments in and around Vikingebugt. Sediment thicknesses are based on a seismic velocity of 1.6 km/s. Location is indicated of seismic sections presented in the corresponding figure numbers.104
- Fig. II.43** - Watergun line 90561, crossing Vikingebugt from head to mouth. Indicated are facies units and features discussed in text. Location in Fig. II.42.105
- Fig. II.44** - Watergun lines 90563 - 90565, crossing Vikingebugt obliquely. Indicated are facies units and features discussed in text. Note that deformation of the seafloor sediments is much less pronounced above the lens-shaped transparent deposit. Location in Fig. II.42.106
- Fig. II.45** - Location of line 90600 on the East Greenland shelf in front of Scoresby Sund. Bathymetric contours (solid lines) are superposed on a tectonic sketch map of the region, showing location of the East Greenland Escarpment (EGE), ocean-continent transition (OCT), and magnetic anomaly lineations (dashed lines). The 500 m isobath approximately represents the shelf break. Adapted from H.C. Larsen (1990). Bathymetry from IHO/IOC/CHS 1984.110
- Fig. II.46** - Common-offset plot of line 90600, displaying identified unconformities and specific features discussed in the text. Note that seismogram is in two sections.111

- Fig. II.47** - Stacked seismic section, outlining in more detail the sediment wedge on the continental slope and pseudo-escarpment. Note how suppression of the seismic multiple improved the continuity of reflectors R3 and R6 and of the acoustic basement.112
- Fig. II.48** - Removal of the velocity pull-up effect: [a] original time section, [b] time/depth conversion curve published by H.C. Larsen (1985) for the Blosseville Kyst shelf region, [c] interval velocities (thin line) and average velocity (thick line) calculated from b, [d] depth section resulting from the application of the interval velocities in c.114
- Fig. II.49** - Three-step model for the evolution of the pseudo-escarpment along the subaerially spreading Knipovich Ridge (KR).116
- Fig. II.50** - Water-depth corrected line drawing of line 90600, illustrating the first-order division of the sediment wedge into three units. NWABW = North-West Atlantic Bottom Water, PE = pseudo-escarpment.117
- Fig. II.51** - Detailed, water-depth corrected line drawing illustrating the stratal geometries on the continental shelf. Based on the variation of progradational and aggradational components, glacial unit III can further be divided into three subunits A-C.121
- Fig. II.52** - Line 90600 compared to three other seismic sections published for the surrounding area: [a] line BGR 76-11 (from Hinz & Schlüter 1980), [b] line GGU 82-12 (from H.C. Larsen 1990), [c] line AWI-RCMG 90600, and [d] line GGU 82-28 (from H.C. Larsen 1990). BGR = Bundesanstalt für Geowissenschaften und Rohstoffe, GGU = Grønlands Geologiske Undersøgelse.122
- Fig. II.53** - Cartoon showing evolution of line 90600 in 7 stages. [a] Initial phase of subaerial spreading, sediment input from E Greenland proceeds by rivers. [b] increase of magma production along subaerial spreading ridge, leading to the formation of a pseudo-escarpment. [c] submergence of spreading ridge below sea level. [d] two depocentres coalesce, resulting in sedimentation all over the profile. [e] initial moderate glaciations of the continental shelf. [f] intensification of glaciation, resulting in strong progradation and deepening of the shelf. [g] latest glacial phase of aggradational development. Basement depth in g partly taken from maps of H.C. Larsen (1985).125
- Fig. II.54** - Proposed correlation of the seismic stratigraphy with oxygen isotope stages (Imbrie et al. 1989), coarse fraction record of ODP Site 644A, and general northern hemisphere glacial evolution (Jansen et al. 1988).127

CHAPTER III

- Fig. III.1** - Location of the available seismic grid along the western Barents Sea margin.134
- Fig. III.2** - Idealised process flow for MGK-lines.136
- Fig. III.3** - Location and generalised bathymetry of the Barents Sea. Shaded areas represent shelf depressions deeper than 300 m.137
- Fig. III.4** - Generalised bathymetry of the western Barents Sea margin. Contour interval is 100 m on the shelf, and 500 m on the slope and in the deep-sea.138
- Fig. III.5** - Detailed bathymetry in the area of investigation. Contour interval is 100 m (full lines), and 20 m on the shelf (dashed lines). Bathymetric data courtesy of Norsk Polarinstitutt (the Norwegian Polar Institute).140
- Fig. III.6** - 3D seafloor morphology visualising the major cone-shaped depocentres at the mouth of deep shelf troughs along the western Barents Sea margin. Based on bathymetric data from the Norwegian Polar Institute. Gridded using Geofox (Verschuren 1992).141
- Fig. III.7** - Location of polar front and main surface water currents in the Barents Sea. From Johannessen (1986).142

- Fig. III.8** - Structural setting of the western Barents Sea margin. BB = Bjørnøya Basin, CB = Central Basin, GFZ = Greenland Fracture Zone, HB = Harstad Basin, HfB = Hammerfest Basin, KE = Knipovich Escarpment, KFZ = Knølegga Fracture Zone, LH = Loppa High, MR = Molloy Ridge, SB = Sørvestsnaget Basin, SH = Stappen High, SpFTB = Spitsbergen Fold and Thrust Belt, Sp FZ = Spitsbergen Fracture Zone, TB = Tromsø Basin, VH = Veslemøy High, VVP = Vestbakken volcanic province. Dotted lines represent magnetic anomaly lineations. From Myhre & Eldholm (1988) and Faleide et al. (1993).....145
- Fig. III.9** - Free-air gravity map of the western Barents Sea margin. Contour interval is 25 mgal, shaded areas mark gravity maxima > 75 mgal. From Myhre & Eldholm (1988).....149
- Fig. III.10** - Early Cretaceous plate reconstruction prior to opening of the North Atlantic ocean. FB = Faeroe Basin, GB = Grand Banks, MB = Møre Basin, RHB = Rockall-Hatton Basin, RT = Rockall Trough, VB = Vøring Basin. From Faleide et al. (1993b).....151
- Fig. III.11** - Plate tectonic evolution of the western Barents Sea margin during the early Tertiary. Simplified from Eldholm et al. (1987) and Faleide et al. (1993b).....152
- Fig. III.12** - Schematic model for the development of a “leaky” fracture zone along an oblique shear margin (Eldholm et al. 1987).....153
- Fig. III.13** - Schematic model for the development of an asymmetric spreading centre by oblique impact with a pre-existing continental shear zone (Crane et al. 1988).....155
- Fig. III.14** - Location of main depocentres along the western Barents Sea margin. The sediment thickness contours refer to the glacial part of the wedge only. From Faleide et al. (in press).....157
- Fig. III.15** - General correlation table of important stratigraphic boundaries on the western Barents Sea and Svalbard margins. Abbreviations used: NH = Northern Hemisphere, sfs = seafloor spreading.159
- Fig. III.16** - Representative cross-sections through the western Barents Sea margin, illustrating the build-up of the margin, and the widely diverging stratigraphies used by different authors; [a,c] from Myhre & Eldholm (1988), [b] from Schlüter & Hinz (1978), [d] from Rønnevik (1981), [e] from Vorren et al. (1990), [f] from Spencer et al. (1984).160
- Fig. III.17** - [a] Cross-section of outer Bear Island Trough along 73°30' N, outlining the stratigraphic units identified by Sættem et al. (1991, 1992). [b] Line drawing of low-resolution seismic profile NPD-7330 along the same latitude, illustrating the eastward pinch-out of a significant interval against URU.165
- Fig. III.18** - Long seismic transect parallel to the western Barents Sea - Svalbard margin, demonstrating the regional stratigraphic framework developed by Faleide et al. (in press), and chaotic facies occurrences.166
- Fig. III.19** - Location of drillholes along the western Barents Sea - Svalbard margin, relative to the available seismic grid.....171
- Fig. III.20** - Interpreted dip line sections, showing first-order stratigraphic units (megasequences G0-GIII) and most important seismic horizons. ABB = “Anti-Boreas Basin”, CBF = continental boundary fault, LB = Lofoten Basin, SB = Sørvestsnaget Basin, VVP = Vestbakken volcanic province. Arrows mark the landward limit to where oceanic crust can be identified.174
- Fig. III.21** - Interpreted strike line sections, showing first-order stratigraphic units (megasequences G0-GIII) and most important seismic horizons. ABB = “Anti-Boreas Basin”, LB = Lofoten Basin, VVP = Vestbakken volcanic province. Arrows mark the landward limit to where oceanic crust can be identified. Symbols follow legend in Fig. 20.175
- Fig. III.22** - Structural map of the study area, showing fault zones and structural lineaments (full lines), magnetic anomalies (dotted lines), bathymetric contours (faint dotted lines) and seismic grid (dashed lines). Adapted from Faleide et al. (1993).....176

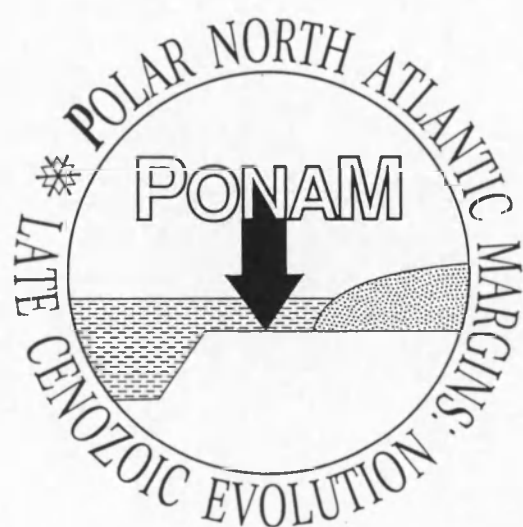
- Fig. III.23** - Fence diagram depicting the morphology of the acoustic basement reflector, and the spatial distribution of the three types of structural basement. 3D visualisation by Geofox (Verschuren 1992).179
- Fig. III.24** - Bathymetric map of the Mohns/Knipovich Ridge spreading system. Stippled areas represent bathymetric highs, cross-bars indicate the inferred flow lines, dashed line marks position of line MGK-1030. After Eldholm et al. (1990).180
- Fig. III.25** - Water-depth corrected contour map, in ms TWT, of base GI unconformity r8. The dashed lines represent the seismic grid. Gridded using Geofox (Verschuren 1992).184
- Fig. III.26** - Isopach map of Megasequence GI. Contour interval is 50 ms TWT, except in the extreme west of the study area, where thickness variations are larger due to irregular basement relief. Gridded using Geofox (Verschuren 1992).186
- Fig. III.27** - Water-depth corrected contour map, in ms TWT, of reflector r13, illustrating the truncation of this horizon on the upper and middle slope of Bear Island Cone. Gridded using Geofox (Verschuren 1992).187
- Fig. III.28** - Water-depth corrected contour map, in ms TWT, of base GII unconformity r15. Gridded using Geofox (Verschuren 1992).189
- Fig. III.29** - Isopach map of Megasequence GII. Contour interval is 50 ms TWT. Legend as in Fig. III.26. Gridded using Geofox (Verschuren 1992).190
- Fig. III.30** - Fence diagram demonstrating the distribution of acoustically chaotic facies in Megasequence GII. 3D visualisation by Geofox (Verschuren 1992).191
- Fig. III.31** - Water-depth corrected contour map, in ms TWT, of base GIII unconformity r30. The thick dashed line marks the limits of the upper slope incision. Geofox by Verschuren (1992).198
- Fig. III.32** - 3D surface map of base GIII unconformity r30, visualising the pronounced incision on the upper slope of the Bear Island Cone. Gridded using Geofox (Verschuren 1992).199
- Fig. III.33** - Isopach map of Megasequence GIII. Contour interval is 50 ms TWT. Legend as in Fig. III.26. Gridded using Geofox (Verschuren 1992).200
- Fig. III.34** - Conceptual stratigraphic diagram ("type section") illustrating the stratal geometry and distribution of chaotic seismic facies in megasequences GI - GIII, distinguishing between Bear Island and Storfjorden Cones.205
- Fig. III.35** - [a] Small-scale gullies eroding the seafloor on the upper slope north of the axial mouth of Bear Island Trough (line MGK-1500). [b] Similar features on the upper slope south of the axial mouth of Bear Island Trough (sparker record from Vorren et al. 1989).207
- Fig. III.36** - Morphological characterisation of submarine mass deposits. [a] Slide (Lewis 1971). [b] Debris flow (Prior et al. 1984).209
- Fig. III.37** - [a] Plan view of a typical finger-shaped debris flow, exemplified by the Canaries debris flow. [b] Cross-section through distal debris lobe. From Embley (1976).212
- Fig. III.38** - Acoustic signature of different types of submarine mass deposits. [a] Slide (Hiscott & Aksu 1994). [b] Rotational slump (Hart 1993). [c] Debris flow deposit (Hiscott & Aksu 1994). [d] Turbidites stacked into a channel/levee system (Hesse 1992).214
- Fig. III.39** - The slide scar at the GII/GIII boundary. [a] Areal map of zones of sediment removal and sediment deposition. Location of headwall south of 73° N is taken from Kuvaas & Kristoffersen (in press) and Laberg & Vorren (in press b). [b] Seismic cross-section (line MGK-1330) showing erosional ramp and depositional lobe. [c] Line drawing of section near the limit of incision (line NPD-7330). The slide scar appears as two seemingly separate canyon-like incisions. [d] Line drawing of longitudinal section through the slide (line NPD-7300). The headwall is characterised by concave-upward relief. [e] Line drawing of cross-section through northern half of the slide scar (line NPD-1430).216

- Fig. III.40** - The more recent slide scar on the southern flank of Bear Island Cone. [a] General extension of the feature. [b, c, d] High-resolution seismic cross-sections. [e] Low-resolution seismic cross-section through the head of the slide (line NPD-7200). a, b and d are taken from Laberg & Vorren (1993), c is from Vorren et al. (1989).219
- Fig. III.41** - Upward shift of the base of the chaotic facies in GII (line NPD-7300). [a] Upward jump of a basal slip plane, as interpreted by Knutsen et al. (1992). [b] The same, uninterpreted, section as in [a], showing that the incisional ramp is not associated with an acoustic reflection. [c] Similar situation more westward, clearly demonstrating how the base of the chaotic interval is gradually disrupted and entrained within the chaos; beyond that, a deeper reflector defines the new base level of the chaotic interval.222
- Fig. III.42** - [a] Distal snout-shaped edge of the main chaotic interval, associated with distinct thinning and transition into acoustically stratified facies (line NPD-7440). [b] Possible analogue: distal transition of a mud flow into mud turbidites (redrawn from Einsele 1991).223
- Fig. III.43** - Combined isopach and facies map of the chaotic interval confined between reflectors r26 and r27. The interval has the shape of a fan spreading out from its source area on the upper slope off the axial Bear Island Trough mouth. Gridded using Geofox (Verschuren 1992).224
- Fig. III.44** - Cartoon sketch of the development of the peculiar reflector "island" within the chaotic interval r26-r27. [a] Detailed seismic section of distal portion of the chaotic interval (line MGK-1200). [b] Evolution as a single failure event, with upward jump of basal shear plane. [c] Superposition of two or three individual flow-slides — the favoured interpretation; the reflector island is laterally equivalent to the distal stratified facies in the lower two mass deposits, as indicated in plan view.225
- Fig. III.45** - Mass wasting styles in megasequence GIII. [a] Radiating pattern of youngest set of debris lobes out from the mouth of Bear Island Trough (Laberg & Vorren, in press b). [b] SeaMARC II side scan sonar image of debris lobe termination (Vogt et al. 1993). [c, d] Appearance of debris lobes on high-resolution seismic sections. From Laberg & Vorren (in press a+b). [e] Appearance of debris lobes on intermediate-resolution seismics used in this study (line MGK-1200).228
- Fig. III.46** - Varying aspect of chaotic facies in megasequences GI, GII and GIII.230
- Fig. III.47** - Averaged sedimentation rates for megasequences G0 - GIII on Bear Island Cone. Redrawn from Faleide et al. (in press).232
- Fig. III.48** - Plot of stability (safety factor) versus slope angle for different thicknesses of sediment (in m). From Mosher et al. (1994).233
- Fig. III.49** - Silhouette of [a] Laurentian Fan (Stow 1981) versus that of [b] Bear Island Cone.234
- Fig. III.50** - Generalised block diagrams of [a] sand-rich and [b] mud-rich base-of-slope aprons (Nelson et al. 1991), and of [c] glaciogenic mud-rich slope aprons, as exemplified by the Bear Island Cone.235
- Fig. III.51** - Isopach map of the combined megasequences GI - GIII, i.e. the glacially-influenced portion of the sediment wedge. Contour interval is 50 ms TWT, except in the extreme west of the area, where thickness variations are larger due to irregular basement relief. Gridded using Geofox (Verschuren 1992).237
- Fig. III.52** - [a] Location of ODP Leg 104 drillholes with respect to the western Barents Sea margin. [b] Magnetostratigraphy and benthic oxygen isotope record of site 644A (Jansen et al. 1988). [c] IRD-record of site 644A (Henrich & Baumann 1994).238
- Fig. III.53** - Averaged sedimentation rates during pre-glacial (G0) and glacial (GI - GIII) episodes on [a] Storfjorden Cone and [b] Bear Island Cone. Adapted from Faleide et al. (in press), by using a slightly different time frame.240

- Fig. III.54** - Conceptual model for glacial evolution of the western Barents Sea margin in three phases, depicting variations in the relative activity of the two main depocentres, scale and influence of mass wasting processes, and tentative ice flow patterns. Dashed depocentre outlines are from Hjelstuen et al. (in press) for the Storfjorden Cone, and from Fiedler & Faleide (in press) for the Bear Island Cone.243
- Fig. III.55** - Comparison of line drawings from high-resolution records of Sættem et al. (1991, 1992) with the low-resolution records used in this study, for lines located [a] along 73° N and [b] along 73°30' N. Numbers indicate amino-acid ages of certain horizons.245
- Fig. III.56** - Distribution of important glacial features (glacial flutes, moraine ridges, ice-proximal glaciomarine deposits) in the western Barents Sea. From Elverhøi et al. (1992, 1994).246
- Fig. III.57** - Reconstruction of the growth and decay of the Barents Sea Ice Sheet during the latest glaciation in the Late Weichselian. Adopted from Hebbeln et al. (1994).249

CHAPTER IV

- Fig. IV.1** - Three-fold division of glacial sediments on [a] the central East Greenland margin, and [b] the western Barents Sea margin. Note the different scales.261
- Fig. IV.2** - Location of glaciated margins characterised by a latest (late Pleistocene?) phase of aggradation: [1] central East Greenland margin (Fig. 1a), [2] western Barents Sea margin (Fig. 1b), [3] SE Greenland margin south of Kangerdlugssuaq fjord (Fig. 3a), [4] western Baffin Bay margin (Fig. 3b), [5] SE Weddell Sea margin (Fig. 4a), [6] Bellingshausen Sea, West Antarctica (Fig. 4b). Also indicated are adjacent portions of the Canadian Atlantic margin along which a gradual transition of lower slope and rise sedimentation is observed: [A] Scotian margin, [B] Laurentian Fan south of Newfoundland, [C] Newfoundland margin, [D] Labrador slope.264
- Fig. IV.3** - Line drawings revealing a latest phase of aggradation on [a] the SE Greenland margin south of Kangerdlugssuaq (from Larsen 1994), and [b] off the Home Bay transverse trough along the western Baffin Bay margin (after Hiscott & Aksu 1994).265
- Fig. IV.4** - Water-depth corrected line drawings illustrating outer shelf and slope stratal geometries on [a] the SE Weddell Sea margin off Crary Trough, and [b] in the Bellingshausen Sea, West Antarctica. Scales are identical to that of Fig. 1b. Both lines courtesy of AWI & RCMG.265
- Fig. IV.5** - Water-depth corrected line drawing of entire line 90060 in the SE Weddell Sea off Crary Trough, demonstrating the relation of the Plio-Pleistocene progradational wedge with respect to fan system 3 further downslope. Levee deposits are gray-shaded. Re-interpreted from Moons (1992).268
- Fig. IV.6** - Qualitative ternary classification diagram for glaciated margins, based on the dominant depositional style of lower slope and rise.270
- Fig. IV.7** - Tentative cyclic model for glaciated margin deposition. [a] Glacial advance: sediments are deposited in front of the migrating ice front, and subsequently remoulded. [b] Glacial maximum: ice sheet is positioned at shelf edge, and pronounced progradation takes place at the mouth of glacial shelf troughs (b1), possibly accompanied by aggradation on the outer shelf (b2); erosion dominates on the inner shelf. [c] Late glacial and glacial retreat: main phase of downslope sediment remobilisation, either by small-scale mass flows (mostly stable margins, c1), large-scale mass wasting (unstable margins, c2), or channelised turbidity currents (fan-dominated margins, c3); glaciomarine sediments accumulate on the shelf in places where retreating ice front temporarily halts; scouring iceberg keels rework sediment on outer shelf. [d] Interglacial: outer shelf, slope and rise become essentially sediment-starved; limited sediment input occurs through biogenic production, and through the reworking of shelf and slope sediments by re-established long-shelf oceanic currents, and by seasonal downslope thermohaline currents.275





UNIVERSITEIT GENT

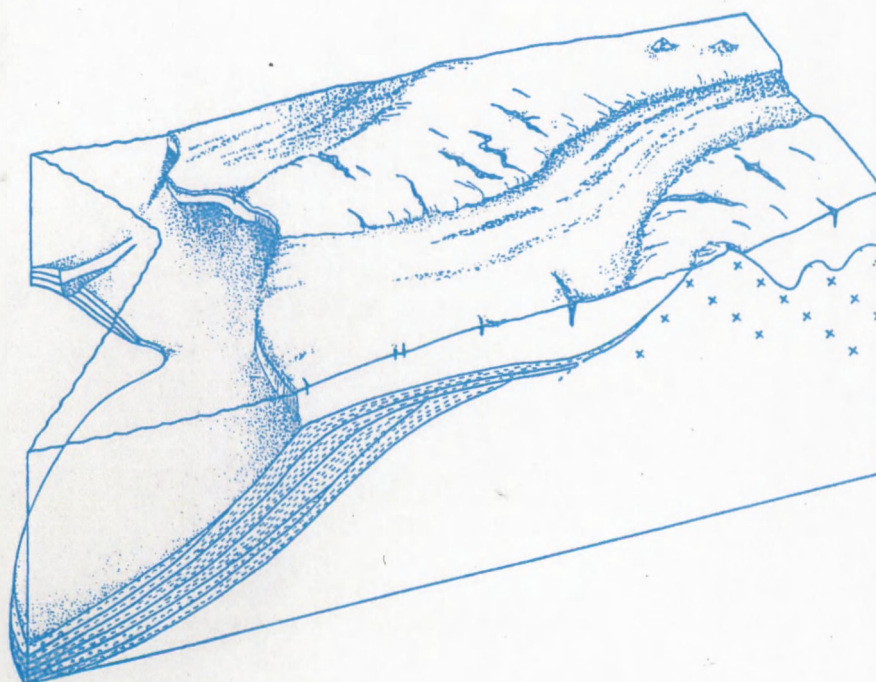
Faculteit Wetenschappen
Vakgroep Geologie en Bodemkunde

A comparative seismic stratigraphic study of major Plio-Pleistocene glaciogenic depocentres along the polar North Atlantic margins

Vergelijkend seismostratigrafisch onderzoek van
grootschalige Plio-Pleistocene glacigene sedimentkegels
langs de randen van de polaire Noord-Atlantische Oceaan

ANNEXE

Kris Vanneste



Academiejaar 1994-1995

ANNEXE

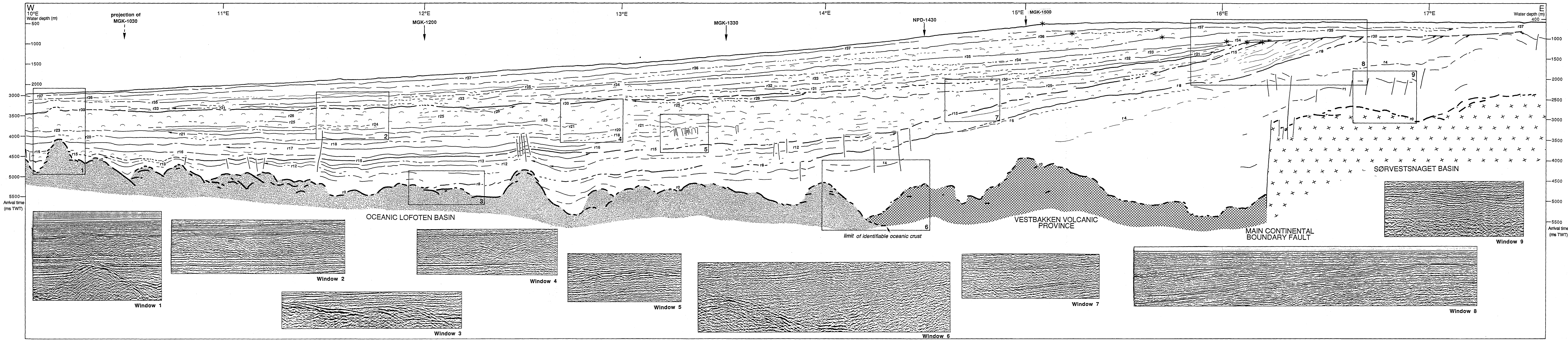
Barents Sea interpreted sections

Dip-oriented lines (from south to north)

- | | |
|----------------|-----------------|
| 1. NPD-7300 | (Windows 1-9) |
| 2. NPD-7330-77 | (Windows 10-13) |
| 3. NPD-7440-77 | (Windows 14-16) |
| 4. MGK-7500 | |

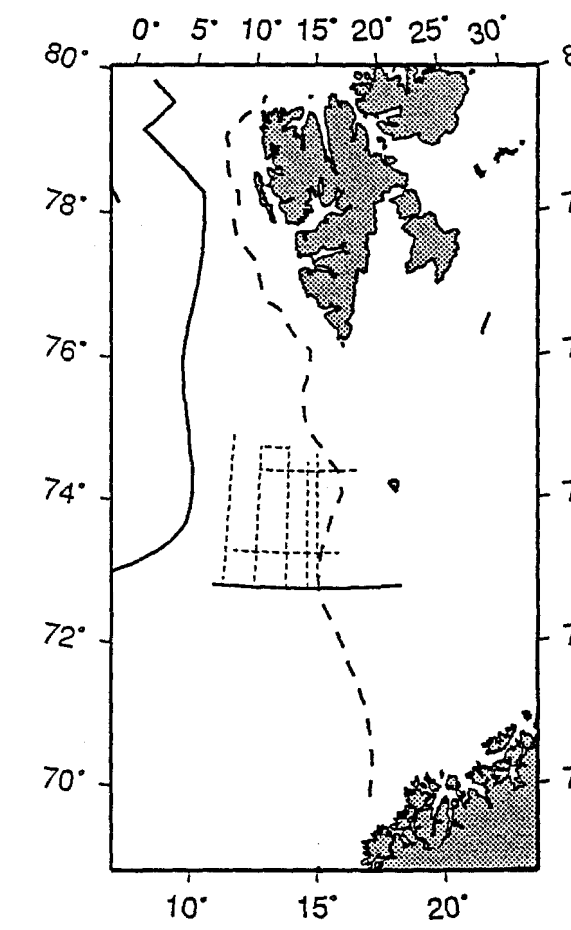
Strike-oriented lines (from east to west)

- | | |
|----------------|-----------------|
| 5. MGK-1500 | (Windows 17-19) |
| 6. NPD-1430-77 | (Windows 20-23) |
| 7. MGK-1330 | (Windows 24-29) |
| 8. MGK-1200 | (Windows 30-34) |
| 9. MGK-1030 | (Windows 35-39) |



Line NPD-7300

INTERPRETED SECTION

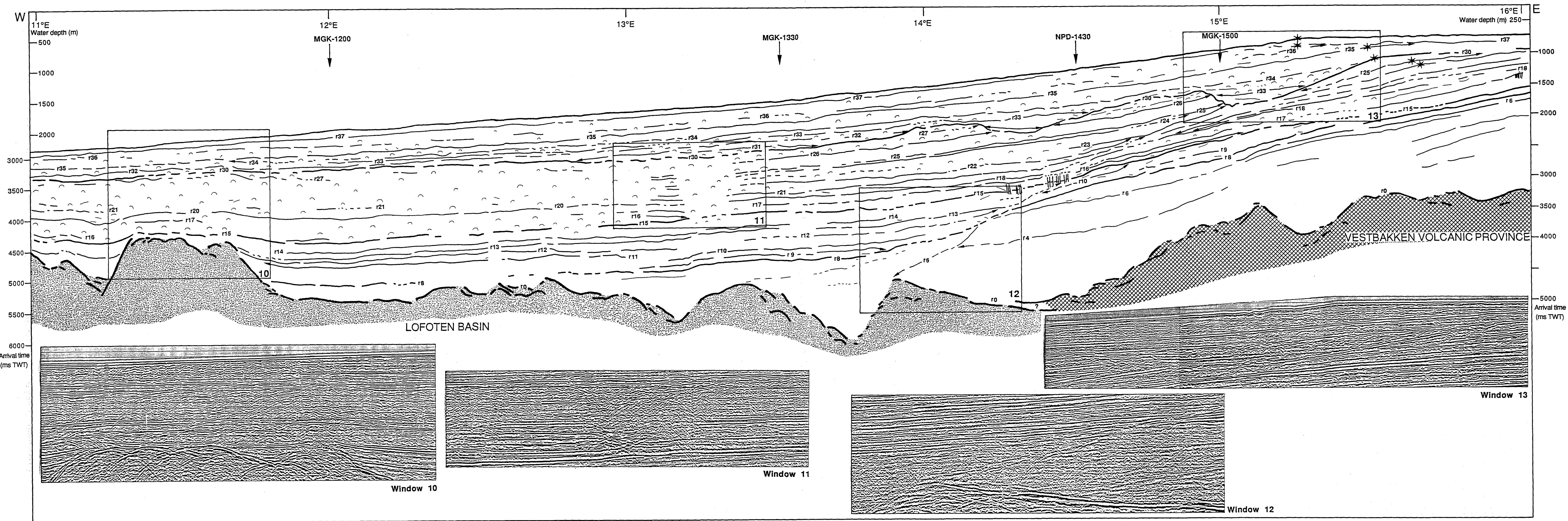


Horizontal scale :
V.E. ~ 15

Horizontal scale :
V.E. ~ 5

0 5 10 km

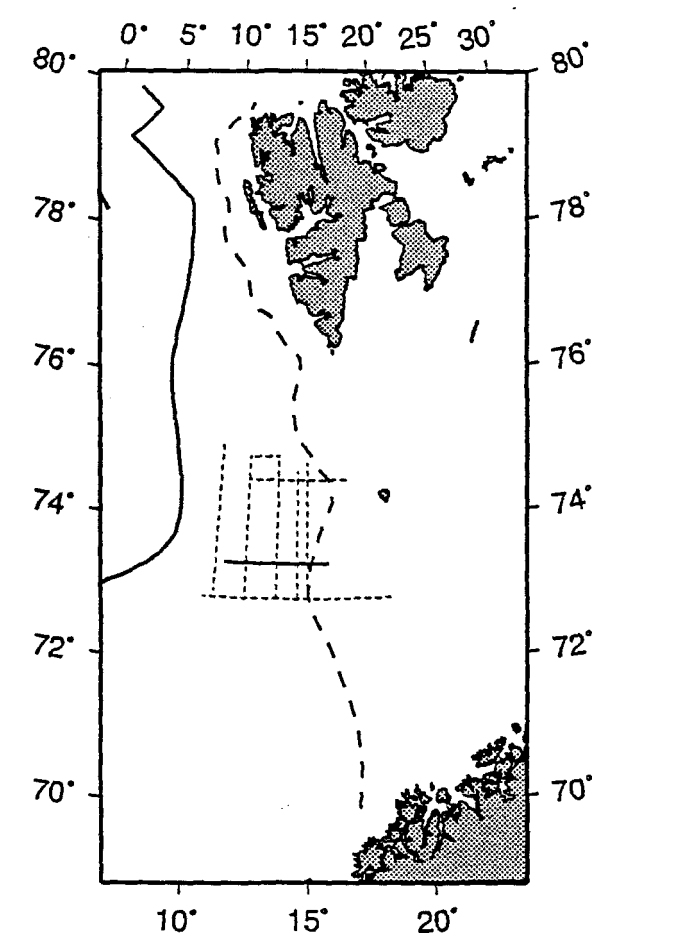
0 1.5 3 km



Norwegian Petroleum
Directorate

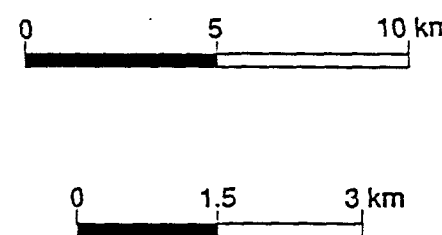
Line NPD-7330-77

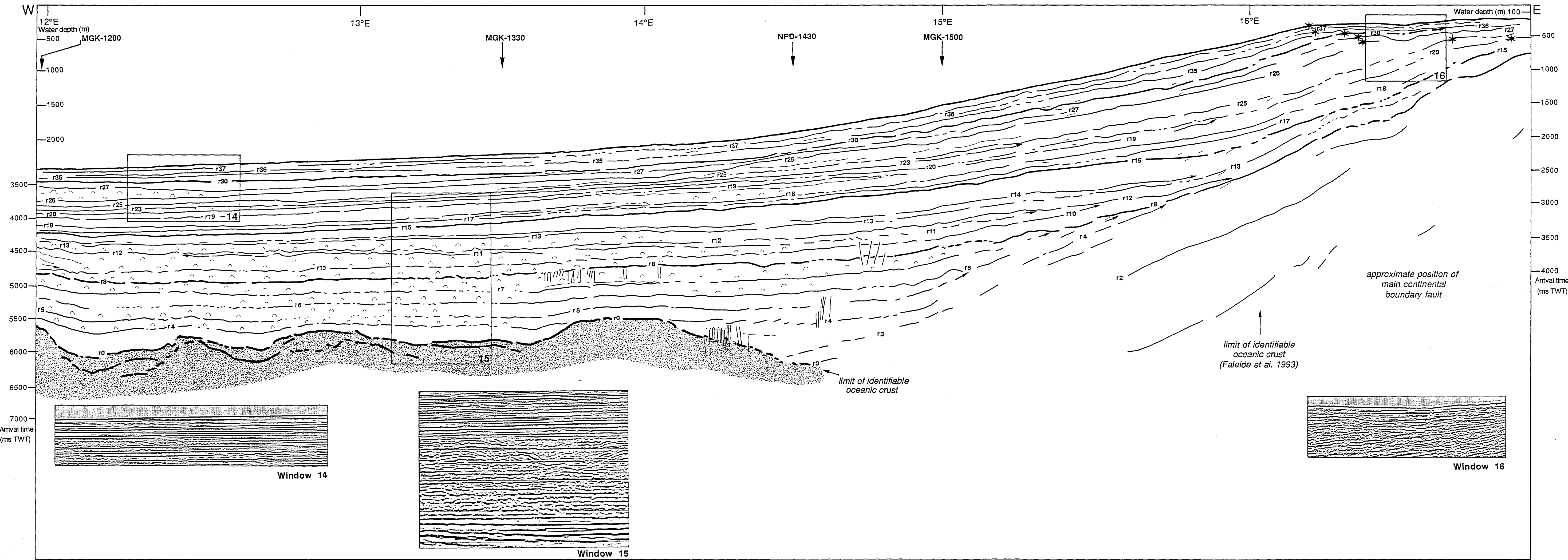
INTERPRETED SECTION



Horizontal scale :
V.E. ~ 15

Seismic windows :
Horizontal scale :
V.E. ~ 5

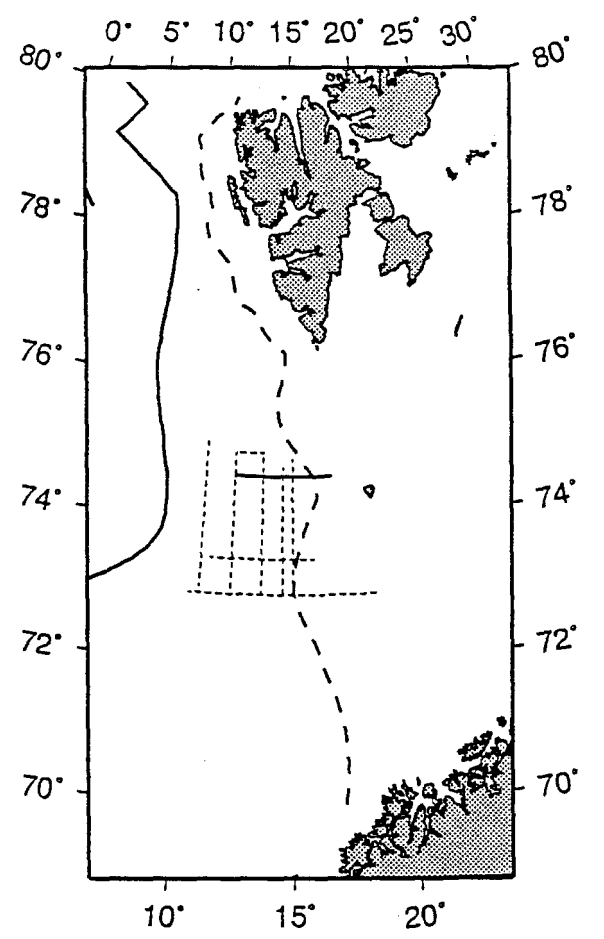




Norwegian Petroleum Directorate

Line NPD-7440-77

INTERPRETED SECTION



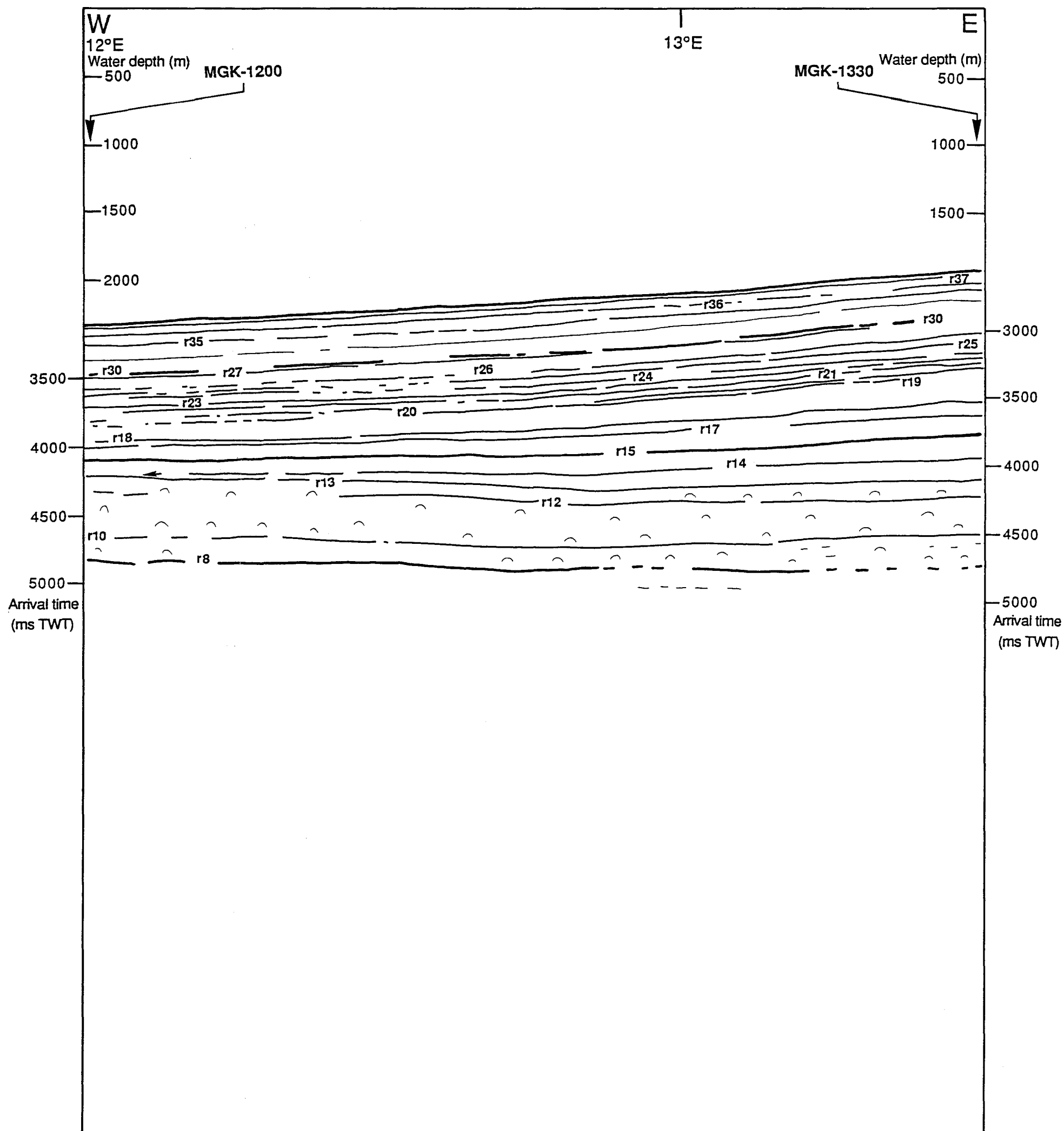
Horizontal scale :
V.E. ~ 15

0 5 10 km

Seismic windows :

Horizontal scale :
V.E. ~ 5

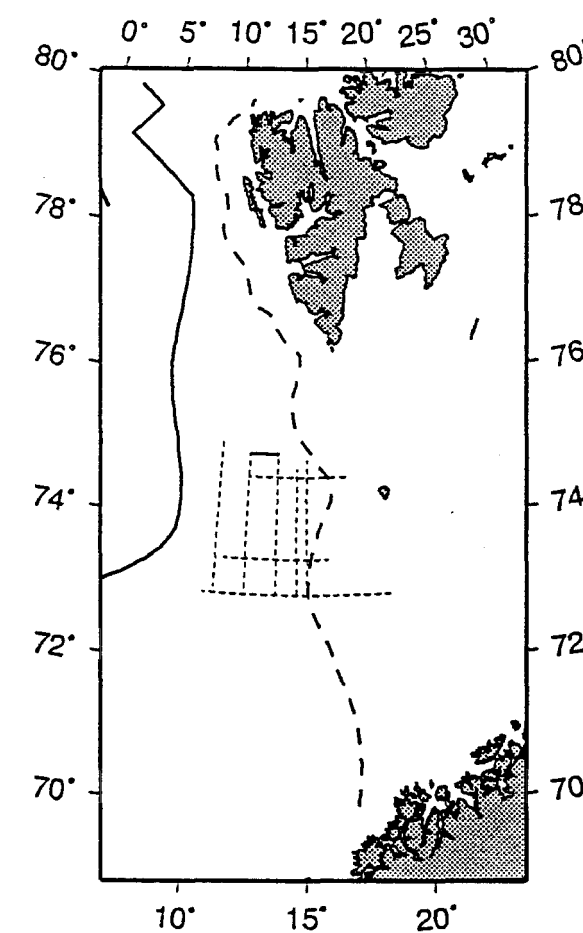
0 1.5 3 km



Marine Geophysik
Kiel

Line MGK-7500 (BEAR-VI)

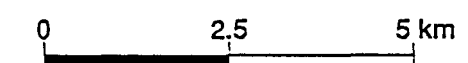
INTERPRETED SECTION

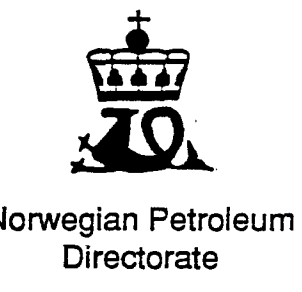
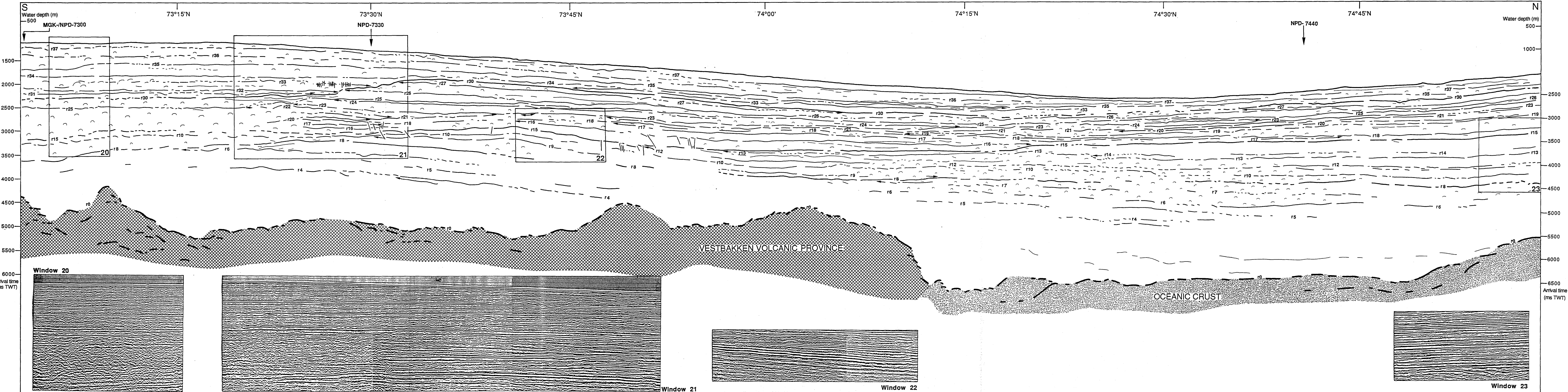


Horizontal scale :
V.E. ~ 15

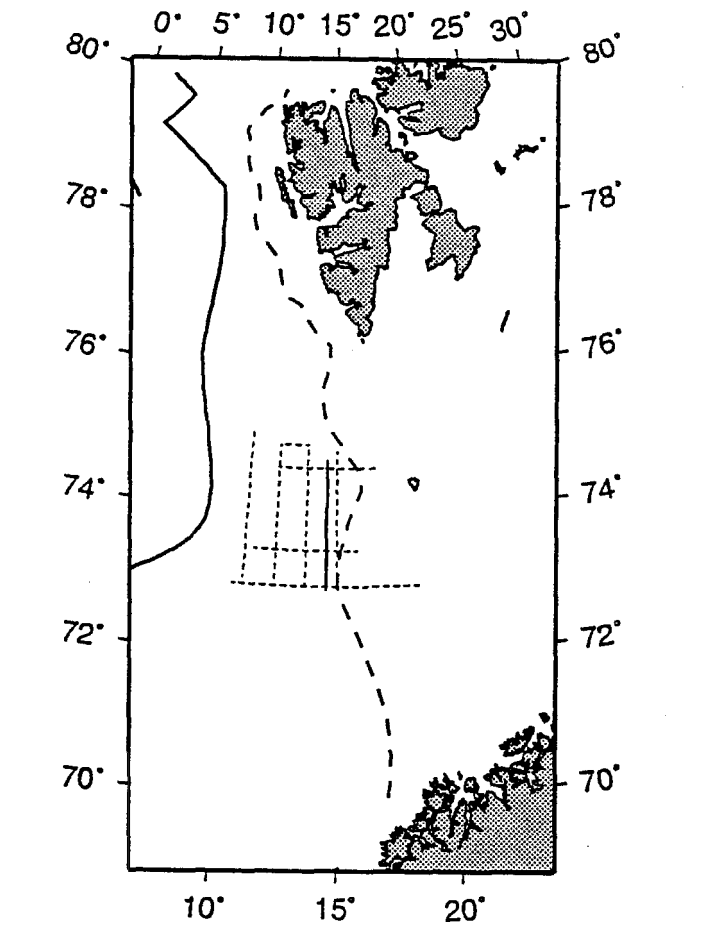


Seismic windows :
Horizontal scale :
V.E. ~ 8



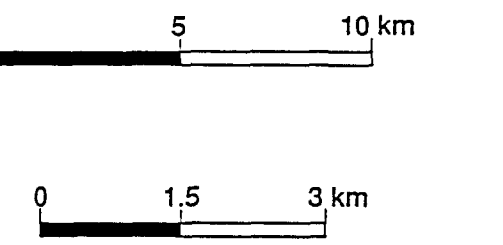


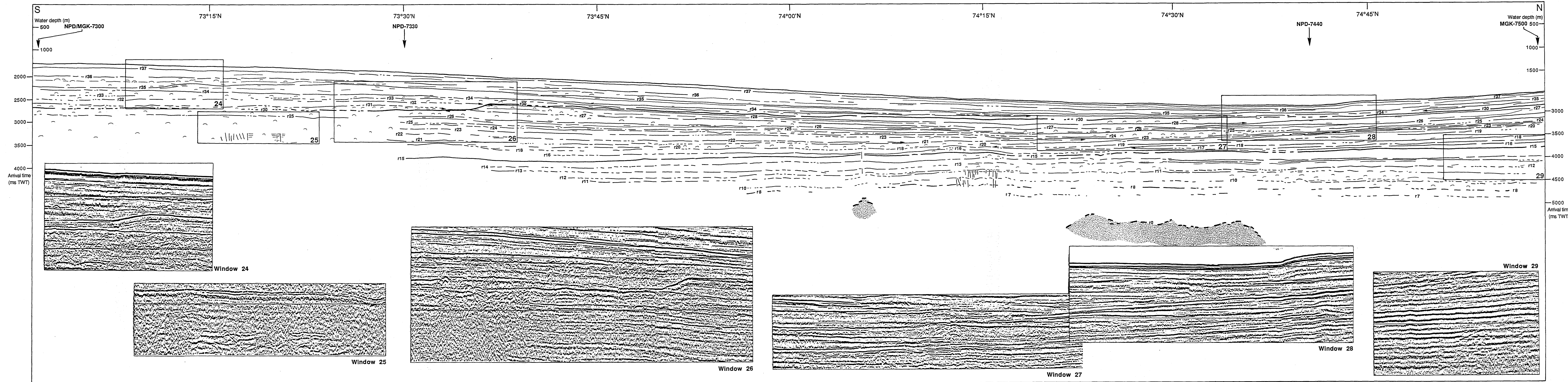
Line NPD-1430-77
INTERPRETED SECTION



Horizontal scale :
V.E. ~ 15

Seismic windows :
Horizontal scale :
V.E. ~ 5

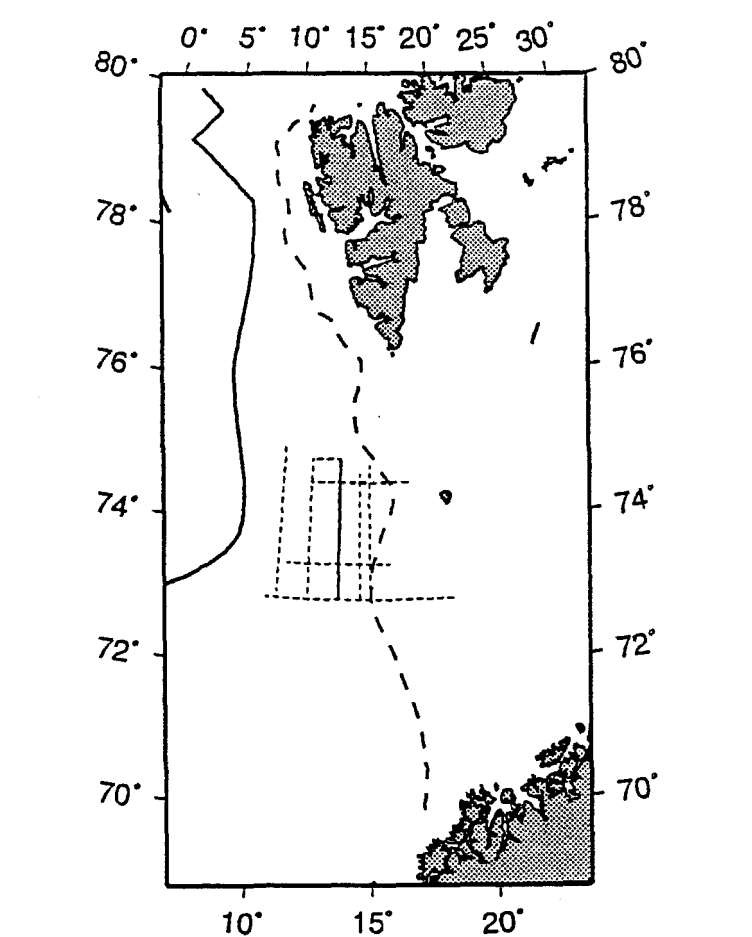




Marine Geophysik
Kiel

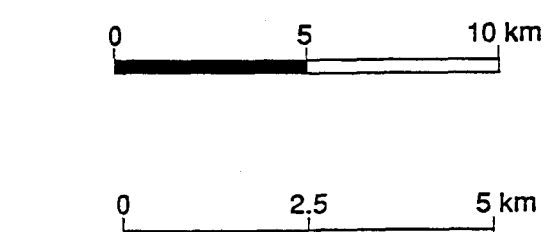
Line MGK-1330 (BEAR-V)

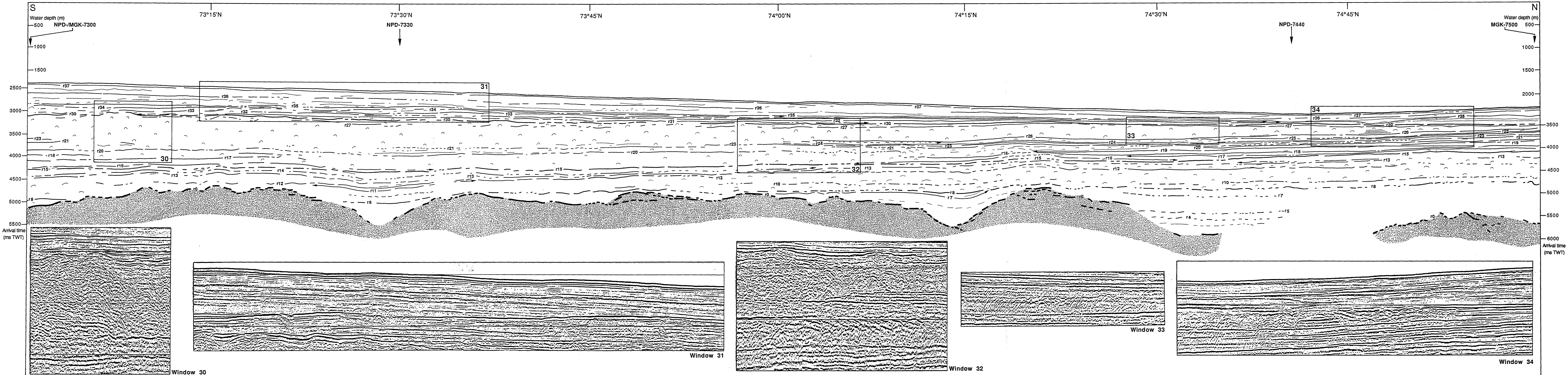
INTERPRETED SECTION



Horizontal scale :
V.E. ~ 15

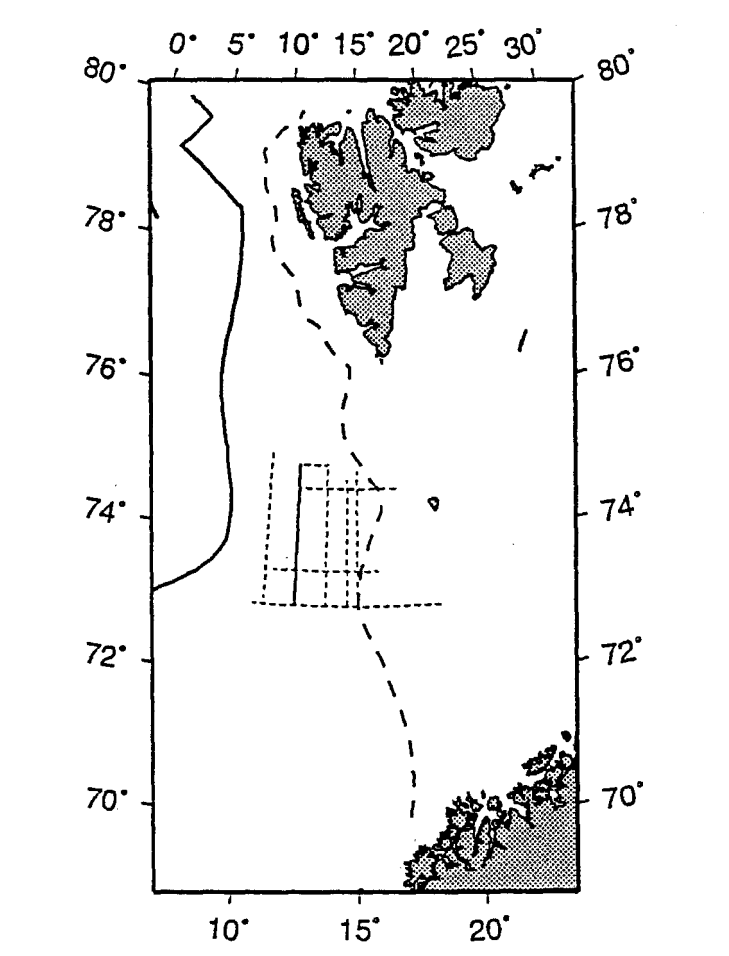
Seismic windows :
Horizontal scale :
V.E. ~ 8





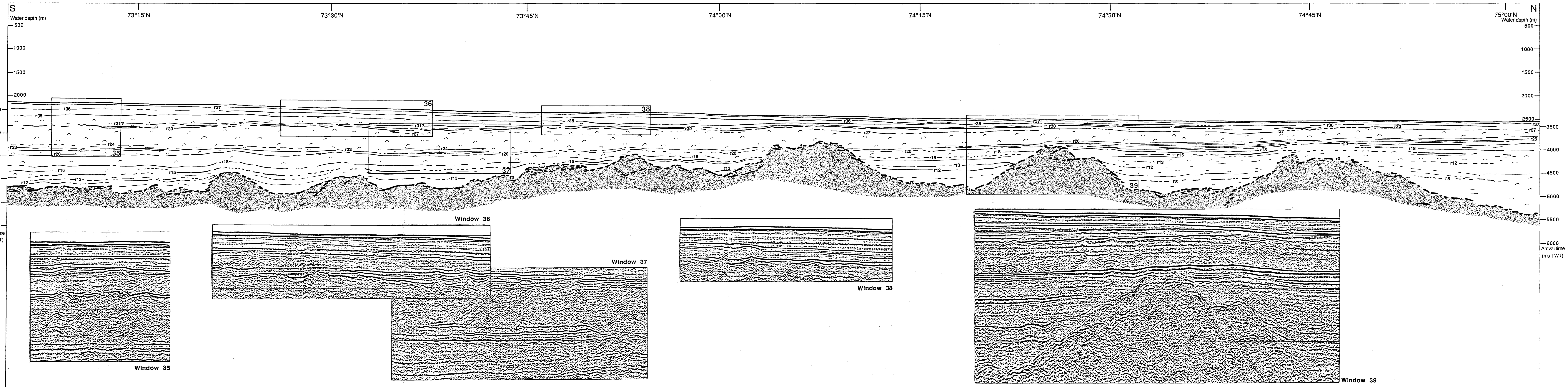
Line MGK-1200 (BEAR-VII)

INTERPRETED SECTION



Horizontal scale :
 V.E. ~ 15
 0 5 10 km

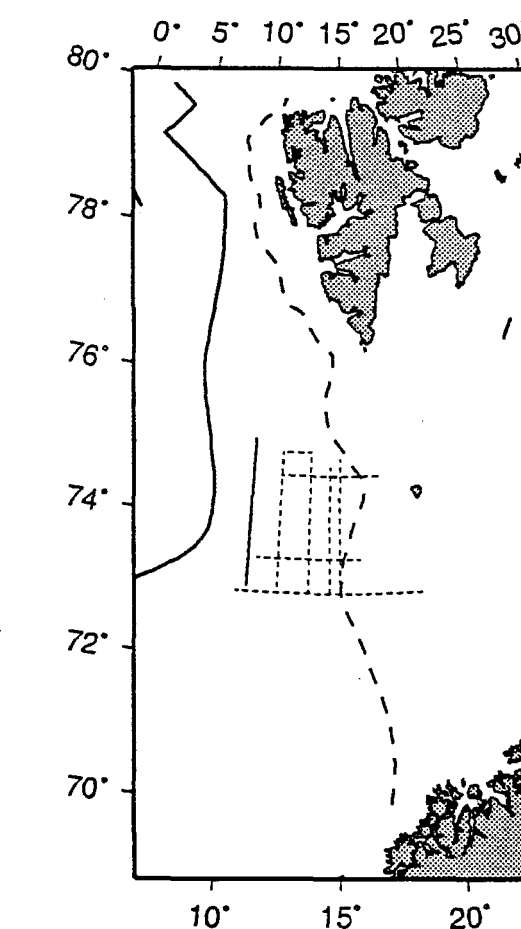
Seismic windows :
 Horizontal scale :
 V.E. ~ 8
 0 2,5 5 km



Marine Geophysik
Kiel

Line MGK-1030 (BEAR-II)

INTERPRETED SECTION



Horizontal scale :
V.E. ~ 15

Horizontal scale :
V.E. ~ 8